# University of Florida Health Science Center

## 2010 Annual Report
of the
McKnight Brain Institute
& Institute on Aging

*Prepared for the McKnight Brain Research Foundation*

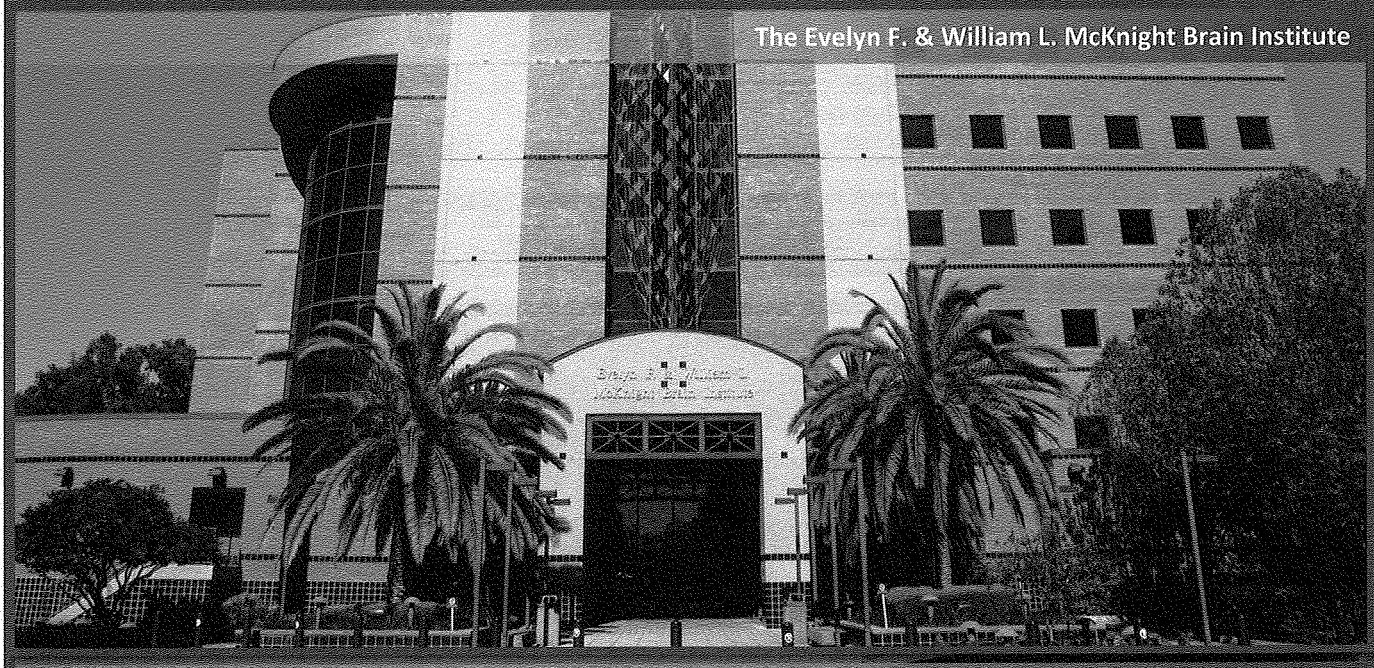

The Evelyn F. & William L. McKnight Brain Institute

Artist Rendering of the New Institute on Aging & CTSI Building

# TABLE OF CONTENTS

**Letter from David S. Guzick, M.D., Ph.D.** ..... 1
**Letter from Dean Michael L. Good, M.D.** ..... 3

**McKnight Brain Institute (MBI)** ..... 5

Letter from Tetsuo Ashizawa, M.D. ..... 7
Annual Report from MBI ..... 11-15
Projected Budget ..... 17
Annual Report prepared by Thomas C. Foster, Ph.D. ..... 19-24

**Institute on Aging (IOA)** ..... 25

Letter from Marco Pahor, M.D. ..... 27
Projected Budget ..... 29
Candidates for CAM Director ..... 31-32

**UF Foundation Endowment Reports** ..... 33

Evelyn F. McKnight Chair for Brain Research in Memory Loss (F007889) ..... 35
Evelyn F. McKnight Brain Research Grant (F008057) ..... 36
Transfer Summary Report ..... 37
McKnight Fund Report Summary ..... 38
UFICO Report ..... 39-44

**Faculty Biography/Curriculum Vitae** ..... 45
*Alphabetical Order*

Ashizawa, Tetsuo ..... 47-49
Bizon, Jennifer ..... 51-55
Foster, Thomas ..... 57-60
Leeuwenburg, Christiaan ..... 61-64
Omerod, Brandi ..... 65-69
Pahor, Marco ..... 71-74
Sarkisian, Matthew ..... 75-80
Steindler, Dennis ..... 81-83

**Articles** ..... 85-213

**Contact Information** ..... 215

UF | UNIVERSITY of FLORIDA

**Office of the Senior Vice President, Health Affairs**
President, UF&Shands Health System

1515 SW Archer Road, Suite 23C1
Gainesville, FL 32608
PO Box 100014
Gainesville, FL 32610-0014
352-733-1700 Tel
352-733-1701 Fax

January 15, 2011

The McKnight Brain Research Foundation
The SunTrust Bank
Mail Code FL-ORL-2160
300 South Orange Ave., Suite 1600
Orlando, FL 32801

Dear Trustees:

I would like to express my great appreciation to the McKnight Brain Research Foundation for its generous support of the University of Florida McKnight Brain Institute. Funds from the McKnight Brain Research Foundation have been critical in advancing our efforts to understand the mechanisms of age-related memory loss and to aid in its prevention.

As Senior Vice President of the UF Health Science Center, in September 2010, I appointed Dr. Tetsuo Ashizawa, Chair of the Department of Neurology, to take the position of Executive Director of the McKnight Brain Institute (MBI) at University of Florida. Chairs of Departments of Neurology, Neurosurgery, Psychiatry and Neuroscience serve on the Steering Committee of MBI, along with and Dr. Marco Pahor, Director of UF Institute on Aging, and two MBI faculty. Thus, MBI is well positioned to promote interdisciplinary research on age-related memory loss. I also established Neuromedicine Interdisciplinary Clinical and Academic Program (ICAP) as one of the four ICAPs in The UF&Shands Health System. In the Neuromedicine ICAP, the four Departments are integrated to deliver our cutting-edge care for neurological health. Under the leadership of Dr. William Friedman, who is Chair of the Department of Neurosurgery, the Neuromedicine ICAP will also support the MBI mission of age-related memory loss.

The enclosed report provides information on the past year's accomplishments. I strongly believe that we will further strengthen the McKnight Brain Institute with the new administrative changes described above. We look forward to continuing our productive partnership with the McKnight Brain Research Foundation to promote research that will lead to a clear understanding of age-related memory loss and its prevention.

Sincerely,

David S. Guzick, M.D., Ph.D.
Senior Vice President, Health Affairs
President, UF&Shands Health System

UF | UNIVERSITY of FLORIDA

**Dean, College of Medicine**
Folke H. Peterson Dean's Distinguished Professor

PO Box 100215
Gainesville, FL 32610-0215
352-273-7500 Tel
352-273-8309 Fax

January 15, 2011

The McKnight Brain Research Foundation
The SunTrust Bank
Mail Code FL-ORL-2160
300 South Orange Ave., Suite 1600
Orlando, FL 32801

Dear Trustees:

I would like to express my sincere gratitude to the Foundation for the continuous support of the Everlyn F. & William L. McKnight Brain Institute (MBI) of the University of Florida (UF) over the past 10 years. This year's report includes new changes at MBI. I was charged by Senior Vice President Dr. David Guzick to chair the review committee to assess governance and leadership of the MBI. We made recommendations which we believe will significantly enhance the accomplishments and impact of the MBI, locally, regionally, and nationally. On September 1, 2010 Dr. Guzick appointed Dr. Tetsuo Ashizawa, Chair of the Department of Neurology, College of Medicine as the new Executive Director of the MBI. He has formed the MBI Steering Committee which consists of key UF leaders in research on age-related memory loss research, including Drs. Marco Pahor (Director, Institute on Aging; Chair, Department of Aging and Geriatrics), Thomas Foster (McKnight Chair for Research on Aging and Memory), William Friedman (Chair, Department of Neurosurgery; Director, Neuromedicine Program), Mark Gold (Chair, Department of Psychiatry), Lucia Notterpek (Chair, Department of Neuroscience) and Todd Golde (Director, Center for Translational Research in Neurodegenrative Disease).

The new MBI leadership aims to develop multi-disciplinary synergistic programs on age-related memory loss, and to increase collaborations with other McKnight Brain Institutes and Center. Thanks to your Foundation's support, the College of Medicine was able to recruit Dr.Jennifer Baizon, a prominent neruobehavioral researcher who investigates mouse models of age-related memory loss. She has relocated from Texas A&M University to UF as a faculty of our Neuroscience Department, and has already started her research in the MBI. In collaboration with UF Institute on Aging, we are working on recruitment of Director and Associate Director of the Cognitive Aging and Memory

Clinical Translational Research Program (CAM-CTRP). We have outstanding candidates who are keenly interested in these positions.

The UF College of Medicine researchers in the MBI have conducted innovative, cutting-edge basic and clinical scientific research on age-related memory loss, using funds generated by endowments given by your Foundation. The UF College of Medicine has significantly increased its research portfolio, including NIH funding, in the past year. The MBRF's generous endowments have significantly contributed to this advancement, and we are determined to become one of the country's premier institutions for academic medicine. In this account, we are truly grateful for your support. We look forward to continuing our fruitful partnership to promote the research that will lead to a clear understanding and prevention of age-related memory loss.

Sincerely,

M L Good, MD

Michael L. Good, M.D.
Dean, College of Medicine
Folke H. Peterson Dean's Distinguished Professor

# University of Florida Health Science Center

**2010 Annual Report**
of the
McKnight Brain Institute
& Institute on Aging

*Prepared for the McKnight Brain Research Foundation*

# McKnight Brain Institute Report

UF UNIVERSITY of FLORIDA

**Evelyn F. and William L. McKnight Brain Institute**

PO Box 100015
Gainesville, FL 32610-0015
352-273-8500 Tel.
352-846-0185 Fax
www.mbi.ufl.edu

January 7, 2011

McKnight Brain Research Foundation
Foundations & Endowments Specialty Practice
SunTrust Banks, Inc.
Mail Code FL-ORL-2160
300 South Orange Ave., Suite 1600
Orlando, FL 32801
Attn: Tiffany Ahlfield

Dear McKnight Brain Research Foundation Trustees:

Below please find my initial report to the McKnight Brain Research Foundation regarding our activities and progress in 2010. First, please allow me to introduce myself. I am the new Executive Director of the University of Florida Evelyn F. & William L. McKnight Brain Institute (hereafter, MBI). Dr. David S. Guzick, Senior Vice President of Health Affairs (SVPHA), and President, UF&Shands Health System appointed me to this position on September 1, 2010. I moved from Galveston, Texas to Gainesville to chair the Department of Neurology in the College of Medicine at this University on April 1, 2009. I continue my responsibility as Chair of Neurology while I direct the MBI. My clinical and scientific training have been in clinical neurology, neurochemistry and then neurogenetics. I must be clear that I have not targeted research on age-related memory loss in the past but the topic has keenly interested me since I moved to Gainesville. I am excited about being a part of the team.

1. The Age Related Memory Loss (ARML) Program

We have successfully recruited Dr. Jennifer Bizon as a major scientific investigator in the ARML Program at the MBI. She moved from Texas A&M University on July 1, 2010. We are currently nearing completion of extensive renovations in the MBI animal facility to support and promote her research program. Her main research program is designed to examine the role of basal forebrain in cognitive aging via innovative behavioral animal experiments using molecular and pharmacological interventions. This project is currently funded by NIA. The ARML Program has also provided funding for the revised Village Wellness Study, which is a clinical trial that is designed to evaluate the benefit of combined cognitive-physical exercise in normal elders. The study design has been significantly improved to address earlier critiques by NIH Study Section reviewers. Dr. Dawn Bowers is PI of the project, and the investigators are now actively enrolling subjects at the AvMed SantaFe Village. The ARML Program also awarded a grant to Dr. Brandi Ormerod to conduct studies on Biomarkers of Cognitive Decline. In December of 2010, the ARML Program issued a

request for application (RFA) directed at junior faculty with interests in age-related memory loss. Details of these projects are in the report attached to this letter and the report of Dr. Thomas Foster who is Chair of the ARML Program Committee. In the same report, Dr. Foster describes his own scientific and administrative accomplishments. I am also pleased to report to you that Dr. Matt Sarkisian has made an interesting observation related to age-related memory loss. The attached paper entitled "Failed cytokinesis of neural progenitors in Citron kinase deficient rats leads to multi-ciliated neurons" is a developmental paper that laid the foundation for his subsequent study that targets age-related memory loss directly. In collaboration with Dr. Foster, Dr. Sarkisian investigated age-related changes of neuronal cilia. Cilia have been implicated in memory, and are a hot topic in neuroscience. These correlative and descriptive data provide a new research area of interest in age-related memory loss.

2. The Cognitive Aging and Memory Clinical and Translational Research Program (CAM-CTRP)

There are currently no scientific publications from the CAM-CTRP. However, the CAM-CTRP has been actively seeking a Director and an Associate Director. This recruitment is the foremost urgent goal of the CAM-CTRP and the MBI. Under the direction of Dr. Thomas Foster who chairs the national search committee for these positions, nine high caliber candidates have been interviewed despite a limited pool of qualified candidates. One of the major obstacles has been a lack of a functional magnetic resonance imaging (fMRI) core and a positron emission tomography-computer tomography (PET-CT) facility that are easily accessible to researchers. We failed to recruit a promising candidate early in the search because of this lack of adequate human *in vivo* imaging capability on our campus. In a three-way collaboration involving the Clinical and Translational Science Institute (CTSI, Dr. David Nelson, Director), College of Medicine Research Office (Dr. Steve Sugrue, Senior Associate Dean of Research) and the MBI, we are in the final stage of establishing the user-friendly fMRI core within the MBI. We are about to start a search for the fMRI core director, whose salary will be supported by the CTSI for the next three years. The MBI has ordered upgrading equipment for the current 3T whole body MRI scanner in the Advanced Magnetic Resonance Imaging and Spectroscopy (AMRIS) facility in the MBI. The cost for this upgrade from 16-channel to 32-channel scanning capability is $300,000, which will be paid from the State of Florida General Fund awarded to the MBI. The State Fund will also support a Ph.D. physicist who will assist the fMRI core director in managing the magnet coils and protocols. We predict that the fMRI core will open in the late spring of 2011. A full-scale research PET-CT facility has a price tag of approximately $10,000,000, and the MBI currently has no fund to establish it. I have entered into an agreement with the Department of Radiology (Dr. Anthony Mancuso, Chair) to buy out research scan time in advance for the new PET-CT imaging. The new PET-CT equipment will primarily be used for clinical care of Shands Hospital inpatients. The deal is far from optimal from a research perspective, but it is a good start. We are currently in final negotiations with Shands for this arrangement, and it is likely that the new PET-CT will become available partly for research in the Shands Hospital South Tower as early as summer 2011. Cutting-edge human brain *in vivo* imaging capability is essential for human research on age-related memory loss, and without it the research will be significantly compromised.

The current top candidate for the CAM-CTRP Director is Dr. Keith Josephs of Mayo Clinic, Rochester, MN and for Associate Director is Dr. Madhav Thambisetty of the National Institute of Aging. Both are highly qualified and use human *in vivo* brain imaging. We expect to finalize our negotiations with them by February 2011. It should be noted that both Dr. Josephs and Dr. Thambisetty need the fMRI core, and the search for the fMRI core director is important for the recruitment of CAM-CTRP Director/Associate Director.

I strongly feel that developing a synergistic program of age-related memory loss by a seamless collaboration between ARML and CAM-CTRP is critical. Through the recruitment efforts and resource sharing, we have found that this will become our new strength. Dr. Pahor and I are increasing our collaborations between the Institute of Aging (IOA) and the MBI, and between the Department of Geriatrics and Aging and Department of Neurology. When we have the key recruitment accomplished, I expect a full-scale collaboration in human clinical and translational studies on age-related memory loss.

3. Establishing Unsurpassed Research Environment

Renovating the animal facility to accommodate Dr. Bizon's behavioral studies of age-related memory loss and upgrading the fMRI for establishing the user-friendly human *in vivo* brain imaging core are examples of our efforts to create an unsurpassed research environment. The MBI has other cores, including the Cell Sorter Core and Cell and Tissue Analysis Core (CTAC), which has been serving MBI investigators with state-of-the-art technologies. In 2010 the Computing Information and Technology Services (CITS) at MBI was restructured and incorporated into the Information Technology Center of the University of Florida (UF) Health Science Center (HSC). The restructure provided better IT services to the MBI while eliminating administrative redundancy. We are planning to conduct similar reorganizations of other cores, including merging the Cell Sorter Core with the Interdisciplinary Center for Biotechnology Research (ICBR, Dr. Robert Ferl, Director) and the MBI Animal Facility with the HSC Animal Resources Center (Dr. Gus Battles, Director). The MBI Animal Facility is currently undergoing major renovation for Dr. Bizon's research. In the process it will be of primary importance to ensure that these services to the MBI investigators improve without any significant compromise. For example, the CTAC, which is currently run well, shares resources with the Molecular Pathology Core (MPC) of the Department of Pathology.

Additionally, we plan to renovate the administrative office space on the fifth floor to create a MBI faculty lounge and the new headquarters for the UF Center for Smell and Taste (Dr. Barry Ache, Director). The faculty lounge will have two rooms with the northwest view and a foyer partitioned from the Smell and Taste Center by a glass wall and a glass door. It will be furnished so that the MBI faculty have a place to discuss various issues over coffee. The lack of such a space for free communication in the MBI building may have contributed to silos of laboratories with limited interactions. The lounge will improve communications and facilitate collaborations among our faculty members.

4. Reorganizing the Administration Office

In addition to the planned changes in core administration, I have reduced the redundancy of the MBI administration office. There were six personnel in the administrative office on the fifth floor. With advice from the SVPHA office, this overstaffing was eliminated by delegating administrative responsibilities to Departments within the MBI. For example, the MBI awards grants to faculty but currently keeps these grants in the MBI account, providing post-award services such as human resources and purchasing. The MBI can transfer the grant to the Department of the awarded investigators, and the Department can manage the grant. Equipment purchased by investigators with MBI grants can also be managed by the Department. The MBI will require quarterly financial reports and annual full reports from the Department. This way, MBI grants are more readily accessible to investigators. The office reorganization also involves hiring a new high-level administrator who can assist me in the development of dynamic scientific programs at the MBI.

5. Programmatic Development at MBI

While age-related memory loss is a priority for programmatic development, the MBI also receives funds from the State of Florida to promote other brain and spinal cord research. Examples include the Brain and Spinal Cord Injury Research Trust Fund (BSCIRTF) and the Florida Center for Brain

Tumor Research (FCBTR) grant. We also have basic, translational and clinical research strengths in many areas such as neurodegenerative disorders, movement disorders, neurovascular disorders, epilepsy, neurogenetic disorders, neurobehavioral disorders, neuromuscular disorders, brain and spinal cord injuries, addictive disorders, and pain disorders. Investigating mechanisms of these diseases is not directly relevant to the age-related memory loss research that is supported by the MBRF. However, as the history of science indicates, we can acquire an enormous amount of information about physiological brain and neuronal functions by studying the neurobiology of diseases. Strategic development of research in some of these disease areas may provide serendipitous and synergetic benefit for research of age-related memory loss.

There has also been strong research momentum in restoration of damaged brain at the MBI. The restoration strategies are based on molecular interventions, neuroplasticity-based treatments, stem cell technologies and bioengineering brain prosthetics. These technologies will be applicable to age-related memory loss when we understand the mechanism of age-related memory loss better.

6. Neuromedicine Interdisciplinary Clinical and Translational Program (NICAP)

Dr. Guzick established four Interdisciplinary Clinical and Academic Programs (ICAP). The Neuromedicine ICAP or NICAP is one of them and involves Departments of Neurosurgery, Neurology, Psychiatry and Neuroscience. The NICAP initiative led by Dr. William Friedman (Chair, Department of Neurosurgery) is transforming the four Departmental silos into a single dynamic organization. Research activities of the MBI largely overlap with those of the NICAP, yet the MBI also has research activities involving investigators outside the NICAP. The impact of establishing the NICAP has been strongly positive, and I predict that it will make clinical research on age-related memory loss more productive, with a greater impact on the field.

Best regards,

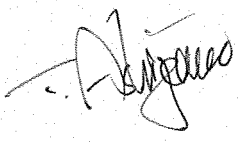

Tetsuo Ashizawa, M.D.
Executive Director, McKnight Brain Institute
Melvin Greer Professor of Neurology
Chair, Department of Neurology

**Annual Report**
**McKnight Brain Research Foundation**
**Sponsored Institutes and Research Programs**
***(Include activity of all McKnight supported faculty and trainees)***
**Report Period: January 2010 – January 2011**

*Some gift agreements require both Institute reports and Chair reports. If applicable, please clearly state whether a particular response relates to a Chair or Institute.*

Any capitalized terms used on the template are intended to have the same meaning as the term is defined in the Gift Agreement.

**Institution Report**

1. **Summary of scientific achievements since last report**

**Dr. Jennifer Bizon**
Aged individuals are often less impulsive in their choices than their young adult counterparts, demonstrating an increased ability to wisely forgo immediate in favor of delayed rewards. Such "wisdom" is usually characterized as a consequence of lifelong learning. In an attempt to isolate the effects of biological aging on decision-making from experiential factors, Dr. Bizon tested Fischer rats and found that aged rats were able to maintain a preference for the large reward regardless of delays. Neurobiology of Aging 31:853-862, 2010.

She also found that age-dependent learning defects are confounding effects in a mouse model of Alzheimer's disease. Relevant to this observation, she found that removing cholinergic input from basal forebrain (that mimics Alzheimer's disease) decreases protein kinase A-glucocorticoid receptor signaling in the hippocampus of aging rats. These two papers are in press.

**Dr. Brandi K. Ormerod**
Recent work demonstrates that cognition declines in some aged rodents and hippocampal neurogenesis declines with age. Dr. Ormerod's group found that daily exposure to an enriched environment, such as novel environments, social interactions, and motor activity, protected neurogenesis and memory from the effects of age.

**Dr. Matthew Sarkisian**
Dr. Sarkisian has characterized functions of cilia in neurons in different experimental and developmental animal models. Cilia have been implicated in memory and other neuronal functions, and have been attracting increasing attention in neuroscience. In collaboration with Dr. Foster, he found age-related changes in cilia, raising a question regarding a possible role of cilia in age-related memory loss.

**Dr. Dennis Steindler**
Dr. Steindler's group contributed to the discovery that stem cell capacity to divide and mature in the hippocampusis correlated with memory dysfunction in humans. The result suggests that age-related memory loss may be related to the functional capacity of hippocampal stem cells.

2. **Publications in peer reviewed journals**

Roland Coras, Florian A. Siebzehnrubl, Elisabeth Pauli, Hagen B. Huttner, Marleisje Njunting, Katja Kobow, Carmen Villmann, Eric Hahnen, Winifred Neuhuber, Daniel Weigel, Michael Buchfelder, Hermann Stefan, Heinz Beck, **Dennis A. Steindler**, Ingmar Blumcke (2010) Low proliferation and differentiation capacities of adult hippocampal stem cells correlate with memory dysfunction in humans. BRAIN 2010: 133; 3359-3372/3359.

Sara B. Anastas, Dorit Mueller, Susan L. Semple-Rowland, Joshua J. Breuing, **Matthew R. Sarkisian** (2010) Failed Cytokinesis of Neural Progenitors in *Citron Kinase*-Deficient Rats Leads of Multiciliated Neurons. Cerebral Cortex doi: 10.10963

Rachel. B. Speisman, Ashok Kumar, Asha Rani, Jessica M. Pazstoria, Jamie E. Severance, **Brandi K. Ormerod**, Thomas C. Foster (In preparation). New granule neuron number relates to mnemonic performance in control but not all enriched rats.

Nicholas W. Simon, Candi L. LaSarge, Karienn S. Montgomery, Matthew T. Williams, Ian A. Mendez, Barry Setlow, **Jennifer L. Bizon** (2010) Good things come to those who wait: Attenuated discounting of delayed rewards in aged Fischer 344 rats. Neurobiology of Aging 31 (2010) 853-862.

K.S. Montgomery, R.K. Simmons, G. Edwards III, M.M. Nicolle, M.A. Gluck, C.E. Myers, **J.L. Bizon** (in press). Novel age-dependent learning defects in a mouse model of Alzheimer's disease: Implications for translational research.

Chol Seung Lim, Youn Jung Kim, Yoo Kyeong Hwang, Christina Banuelos, **Jennifer L. Bizon**, Jung-Soo Han (in press). Decreased Interactions in Protein Kinase A-Glucocorticoid Receptor Signaling in the Hippocampus After Selective Removal of the Basal Forebrain Cholinergic Input.

3. **Publications (other)**
None

4. **Presentations at scientific meetings**

**Dr. Matthew Sarkisian:**

Poster at 3rd Inter-Institutional Meeting of the McKnight Brain Research Foundation at Univ. of Florida on April 28-30, 2010. Title 'Effects of Aging on Primary Neuronal Cilia" G. O. Fonseca Filho, S. M. Guadiana, A. Kumar, T. Foster, **M.R. Sarkisian**

Fonseca GF, Guadiana S, Kumar A, Foster T, **Sarkisian MR**. Effects of aging on primary neuronal cilia in the cerebral cortex. Soc Neurosci Abstr 2010.

Fonseca GF, Guadiana S, Kumar A, Foster T, **Sarkisian MR**. Effects of aging on primary neuronal cilia. Poster at 3rd Inter-Institutional Meeting of the McKnight Brain Research Foundation. 2010.

Poster at 2010 SFN Meeting in San Diego CA Nov 16, 2010, Title 'Effects of aging on primary neuronal cilia in the cerebral cortex". G. O. Fonseca Filho, S. M. Guadiana, A. Kumar, T. Foster, **M.R. Sarkisian**

R. B. Speisman, A. Kumar, A. Rani, J. E. Severasnce, T. C. Foster, **B. K. Omerod** (2010). Enrichment concomitantly improves hippocampal neurogenesis and spatial memory in aged rats. Society for Neuroscience Abstr Vol 35. 710.10.

C. Banuelos, C.L. Lasarge, J.J. Hartman, B.T. Ambrose, B.C. Gagliano, J.M. Graham, R.J. Gilbert, **J.L. Bizon** (2010) Immunomarkers of GABAergic basal forebrain projection neurons are selectively elevated in cognitively-impaired aged F344 rats. Society for Neuroscience Abstr.

J.A. McQuail, C. Banuelos, C.L. Lasarge, R.J. Gilbert, **J.L. Bizon**, M.M. Nicolle (2010) Baclofen-mediated GTP-binding is decreased in the prefrontal cortex, but not hippocampus, of aged F344 rats. Society for Neuroscience Abstr.

K.S. Montgomery, G. Edwards, III, D. Mathai, K. Burton, B. Setlow, **J.L. Bizon** (2010) Development of a novel, translational hippocampal-dependent learning assessment: Implications for early diagnosis of Alzheimer's Disease. Society for Neuroscience Abstr.

D. A. Murchison, K.A. Peebles, R.J. Gilbert, **J.L. Bizon**, W.H. Griffith (2010) Effects of aging on synaptic function in basal forebrain neurons of F344 rats: A possible link between calcium dysregulation and cognitive impairment. Society for Neuroscience Abstr.

I.A. Mendez, J. Damborsky, **J.L. Bizon**, U. Winzer-Serhan, B. Setlow (2010) The roles of nicotinic and muscaranic cholinergic receptors in cost-benefit decision making. Society for Neuroscience Abstr.

G. A. Edwards, III, K.S. Montgomery, S.L. Wilson, D.B. Zimmer, E. Roltsch, **J.L. Bizon** (2010) S100A-/-mice have attenuated odor detection abilities. Society for Neuroscience Abstr.

B. Setlow, N.W. Simon, B.S. Beas, K.S. Montgomery, R.J. Gilbert, M.R. Mitchell, R.P. Haberman, **J.L. Bizon** (2010) Dopamine receptor modulation of risky decision-making. Society for Neuroscience Abstr.

D.W. Dubois, A.S. Fincher, H. Wang, C. Banuelos, R.J. Gilbert, **J.L. Bizon**, G.D. Frye (2010) Are gaba mpscs of ms/db neurons distorted after early postnatal ethanol exposure followed by morris water maze training? Society for Neuroscience Abstr.

B.S. Beas, J.R. Huie, K.S. Montgomery, C.L. Lasarge, K.M. Baumbauer, J.W. Grau, **J.L. Bizon** (2010) Instrumental learning enhances levels of BDNF mRNA in spinally transected rats. Society for Neuroscience Abstr.

**Dr. Jennifer Bizon** has also presented in the following meetings without abstracts.

"Using Olfaction as an Early Detector of Age-Related Cognitive Decline", Annual Meeting for Center and Smell and Taste, University of Florida, Gainesville, FL

2010 "Development of Novel Cognitive Assessments for Age-related Neurodegenerative Disease", Alzheimer's Drug Discovery Foundation, New York, NY.

2010 "Normal and Pathological Aging Across Multiple Cognitive Domains: Insights from Cellular and Behavioral Studies", Joint Neurology/Neuroscience Grand Rounds, University of Florida College of Medicine, Gainesville, FL

5. **Presentations at public (non-scientific) meetings or events:**
   None

6. **Awards (other)**

   **Dr. Brandi Omerod's** graduate student Rachel Speisman received an NSF Graduate Research Fellowship award. Awarded $30,000/year for 3 years, 2010-2013, "Using biomarkers to predict successful versus unsuccessful aging in rats".

7. **Faculty. Please include abbreviated CV with publications for previous 12 months**
   See CV Section

8. **Trainees**

   a) Post doctoral:
      None

   b) Pre-doctoral:
      **Dr. Jennifer Bizon's Pre-doctoral students:**
      Karienn Montgomery
      Cristina Banuelos
      Blanca Sofia Beas

**Dr. Matthew Sarkisian's Pre-doctoral students:**
Sarah M. Guadianna
Gileno Fonseca Filho
Ashton Dequeira

c) Other:
**Dr. Jennifer Bizon:**
George Edwards II

**Dr. Matthew Sarkisian:**
Dorit S. Mueller

**9. Clinical/translational program**

a) New programs
None.

b) Update on existing clinical studies
The SantaFe Villege Study has been started (see attached letter from Dr. Ashizawa).

**10. Technology transfer**

a) Patents applications
None.

b) Revenue generated from technology
None.

**11. Budget update (last year's budget and actual results - with an explanation of material variances)**

a) Status of matching funds, if applicable
No change.

b) Projected budget for coming year
Attached.

c) Extramural funding
See Dr. Foster's report

**12. Educational programs focusing on age related memory loss**

a) Scientific:

**Dr. Jennifer Bizon:** Served on Advisory Panel entitled: "Guidelines for Pre-Clinical Testing with Animal Models of Alzheimer's Disease" for the Alzheimer's Drug Discovery Foundation, New York, New York.

b) Public
None.

**13. Collaborative programs with other McKnight Institutes, institutions and research programs**
None - However, we participated in the Third Inter-Institutional Meeting hosted by the MBRF on April 28-30, 2010 at the MBI at the University of Florida. Teams from the Evelyn F. McKnight Brain Institutes at the University of Alabama and at the University of Arizona and the Evelyn F. McKnight Center for Age Related Memory Loss at the University of Miami also participated in the meeting. We interacted with the participants.

Dr. Foster presented his research entitled "Linking Oxidative Stress of Aging to the Senescent Neurophysiology of Cognitive Decline" at the Second Cognitive Aging Summit held in Washington, D.C. on October 3-4, 2010.

**14. Collaborative program with non McKnight Institutes, institutions and research programs**
None.

**15. Briefly describe plans for future research and/or clinical initiatives.** No Response

16. **If applicable, please provide endowment investment results for the report period.**
    N/A

17. **Where any funds used for a Prohibited Purpose during the report period?**
    No.

18. **Do you recommend any modification to the Purpose or mandates in the Gift Agreement?**
    No.

19. **Did all activities during the report period further the Purpose?**
    Yes.

20. **Please describe any negative events (loss of personnel, space, budget, etc.) that occurred during the report period and the possible impact on carrying out the Gift Agreement.**
    None.

21. **Please provide any general comments or thoughts not covered elsewhere – a response is not required. Please respond only if you would like to add something not otherwise covered elsewhere.**
    See my letter attached to this report.

22. **Signature, date, and title of person submitting the report.**

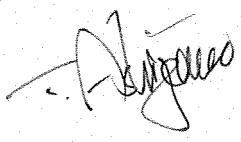

Tetsuo Ashizawa, M.D.
Executive Director
Evelyn F. & William L. McKnight Brain Institute
University of Florida

01/07/11

| | | FY 08-09 | FY 09-10 | FY 10-11 | FY 11-12 | FY 12-13 | FY 13-14 |
|---|---|---|---|---|---|---|---|
| **Spendable Income McKnight Research - (Balance after $1.6m to Aging Institute)** | | | **1,634,217** | **2,202,286** | **2,026,703** | **2,579,940** | **$ 3,161,582** |
| Current Faculty - Matthew Sarkisian | | | | | | | |
| Salary + Fringe Benefits | | $ 91,154 | $ 127,800 | $ 131,634 | $ 33,896 | | |
| Start-up | $ 850,000 | | | | | | |
| Less: Transfer | (850,000) | $ 570,604 | | $ 279,396 | | | |
| Remaining Balance | $ - | | | | | | |
| **New Recruitment** | | | | | | | |
| **Salary + Fringe Benefits Start Date July 2010** | | | | | | | |
| Dr. Jennifer Bizon | | | $ - | $ 177,706 | $ 183,037 | $ 188,528 | |
| **Start-up** | | | | | | | |
| Dr. Jennifer Bizon | | | $ 200,000 | $ 350,000 | $ 175,000 | $ 175,000 | $ 175,000 |
| **Grants#** | | | $ 45,820 | $ 182,035 | $ - | | |
| **TOTAL EXPENSES** | | | $ 373,620 | $ 1,120,771 | $ 391,933 | $ 363,528 | $ 175,000 |
| **Subtotal: (Spendable Income minus Expenses)** | | | $ 1,260,597 | $ 1,081,515 | $ 1,634,770 | $ 2,216,412 | $ 2,986,582 |
| **Projected Income** | | | | | | | |
| **Actual** | Interest Received | | $ 941,689 | $ 472,589 | | | |
| **Estimated *** | Interest **Not** Received | | $ - | $ 472,599 | $ 945,170 | $ 945,170 | $ 945,170 |
| **Net Spendable Income:** | | | **$ 2,202,286** | **$ 2,026,703** | **$ 2,579,940** | **$ 3,161,582** | **$ 3,931,752** |

#MBI McKnight Flyer Grants - These were Research Studies in place prior to the modified McKnight Gift Agreement.
*Projected Income represents half of the interest earned. The other half goes to the Aging Inst.

| Grants | Award Amount | Remaining Balance | |
|---|---|---|---|
| Manini | $ 100,000 | $ 68,996 | 9/30/2010 NC |
| Bowers | 77,855 | 77,855 * | 11/1/2009 3 yr commitment (Villages $60,000 from Santa Fe Alzheimer) |
| Omerod, B | 50,000 | 35,184 | |
| | - | | |
| | $ 227,855 | $ 182,035 | |

* Represents a grant issued to the department

**Annual Report**
**McKnight Brain Research Foundation**
**Sponsored Institutes and Research Programs**
***(Include activity of all McKnight supported faculty and trainees)***
**Report Period: January 2010 - January 2011**

*Some gift agreements require both Institute reports and Chair reports. If applicable, please clearly state whether a particular response relates to a Chair or Institute.*

Any capitalized terms used on the template are intended to have the same meaning as the term is defined in the Gift Agreement.

**Chair report**

1. **Summary of scientific achievements since last report**
This year has been a very good year for publications, with 7 publications accepted in scientific journals and two book chapters. In addition, we have received two new grants from the National Institute of Aging. Given the current funding level of the eighth percentile at NIA, we consider our funding success to be outstanding.
*Linking oxidative stress of aging to the senescent neurophysiology of cognitive decline*: Aging is associated with high levels of oxidative stress and oxidative damage. A relatively mild adjustment in oxidation can induce the reversible formation of disulfide bonds between pairs of cycteine residues, however, shifting protein function, and influencing signaling cascades. Our work in rodents shows that these highly redox sensitive cycteine residues contribute to senescent physiology of the hippocampus in two important ways: by decreasing N-methyl-D-aspartate receptor (NMDAR) responses and increasing the level of hyperpolarization during neural activity. In the case of NMDAR responses, manipulation of the intracellular redox state increased or decreased NMDAR synaptic responses in an age-dependent manner. Dithiothreitol (DTT) specifically reduces cycteine disulfide bonds and selectively enhanced NMDAR responses and the magnitude of long-term potentiation (LTP) in hippocampal slices from aged rodents. Using the relatively membrane impermeable reducing agent, glutathione, we demonstrate that the age-dependent decrease in NMDAR function was specific to intracellular redox state and dependent on CAMKII activity.

Another well-characterized biomarker of aged-memory impaired animals is an increase in the $Ca^{2+}$-dependent, potassium mediated afterhyperpolarization (AHP) observed following a burst of action potentials. The AHP is initiated by activation of voltage-gated $Ca^{2+}$ channels during the action potential. The influx of $Ca^{2+}$ from these channels binds to ryanodine receptors to release $Ca^{2+}$ from ICS, resulting in a further increase in intracellular $Ca^{2+}$. Our work shows that DTT reduces the AHP only in aged animals and the ability of DTT to influence the AHP was impaired by blockade of ryanodine receptors or depletion of $Ca^{2+}$ from intracellular $Ca^{2+}$ stores. Thus, age-related changes in redox state increase the sensitivity of the ryanodine receptors, resulting in a larger rise in intracellular $Ca^{2+}$ and a larger AHP.

It is important to note that the activation of NMDARs is dependent on cell depolarization, such that a larger AHP will inhibit NMDAR activation and impair the induction of LTP. The results indicate that a mild shift in oxidative/redox state, can act on cycteine thiol bonds and reduce NMDAR function, leading to alter $Ca^{2+}$-dependent synaptic plasticity processes that are critical in memory consolidation. Memory consolidation deficits are observed following blockade of NMDARs, supporting the idea that weakening of NMDARs underlies rapid forgetting observed during aging. We suggest that deficits in memory consolidation can be ameliorated by 1) shifting the redox state to improve NMDAR function or 2) increasing NMDAR signaling cascades in order to activate transcriptional and translational processes that mediate cell protection and memory consolidation.

*Aging and the transcriptome*: The establishment of stable memories requires that NMDARs initiate activation of transcriptional and translational processes. To examine changes in transcription linked to chronological age and biological aging (i.e. decreased memory), we have developed techniques for the analysis of massive amounts of gene expression data generated by gene microarrays. These techniques have been employed to examine the effect of caloric restriction or estrogen treatment on the aging hippocampus and the effect of antihypertensive drugs (angiotensin-converting enzyme inhibitors) on aging muscle. Our results examining the

hippocampus provide for novel hypotheses concerning the sensitivity of hippocampal regions to aging and to the compensatory mechanisms available to deal with stressors associated with aging.

**2. Publications in peer reviewed journals**

Aenlle KK, **Foster** TC (2010) Aging alters the expression of genes for neuroprotection and synaptic function following acute estradiol treatment. Hippocampus 20:1047-1060.
Bodhinathan K, Kumar A, **Foster** TC (2010a) Intracellular redox state alters NMDA receptor response during aging through Ca2+/calmodulin-dependent protein kinase II. J Neurosci 30:1914-1924.

Bodhinathan K, Kumar A, **Foster** TC (2010b) Redox sensitive calcium stores underlie enhanced after hyperpolarization of aged neurons: role for ryanodine receptor mediated calcium signaling. J Neurophysiol 104:2586-2593.

Jackson TC, Verrier JD, Semple-Rowland S, Kumar A, **Foster** TC (2010) PHLPP1 splice variants differentially regulate AKT and PKCalpha signaling in hippocampal neurons: characterization of PHLPP proteins in the adult hippocampus. J Neurochem 115:941-955.

Zeier Z, Madorsky I, Xu Y, Ogle WO, Notterpek L, **Foster** TC (2010) Gene Expression in the Hippocampus: Regionally Specific Effects of Aging and Caloric Restriction. Mech Ageing Dev. In press.

Carter, C.S., Giovaninni, S., Seo, D., DuPree, J., Morgan. D., Chung, H.Y., Lees, H., Daniels, M., Hubbard, G., Lee, S., Ikeno, Y., **Foster**, T.C., Buford, T., Marzetti, E. (2010) Differential effects of enalapril and losartan on body composition and indices of muscle quality in aged male Fischer 344 x Brown Norway rats. Age, in press.

**Foster,** T.C. (2010) Role of estrogen receptor alpha and beta expression and signaling on cognitive function during aging. Hippocampus, accepted with revisions.

**3. Publications (other)**

Aenlle, K.A. and **Foster**, T.C. (2010) Gene expression and signal transduction cascades mediating estrogen effects on memory. In J.Clelland (Ed.) Handbook of Neurochemistry and Molecular Neurobiology, Volume Number 13. Genomics, Proteomics and the Nervous System.

Guidi, M. and **Foster**, T.C. (2010) Animal model of memory and cognitive disorders. In F.H. Kobeissy (Ed.) Psychiatric disorders: Methods and Protocols, Volume *. Methods in Molecular Biology Springer, USA (Humana Press, Inc)

**4. Presentations at scientific meetings**

I was the Chairman, and Session Organizer for a session on: Altered networks in aging. In addition, I presented Redox state and altered NMDA receptor function during aging. (Feb, 2010). 22th Annual Winter Conference on Neural Plasticity, Aruba Caribbean.

Recent progress in understanding age-related memory decline (April 2010). Centers for Neuropsychological Studies Veterans Administration Hospital, Gainesville FL.

I was the organizer and moderator for a Panel Discussion on Clinical studies from trials to cohort: Moving from experimental observation to clinical trials. (April 2010). McKnight Brain Research Foundation Third Inter-Institutional Meeting. University of Florida, Gainesville, Fl.

Synaptic plasticity in the aging brain. (Sept 2010). University of Florida First Annual Society for Neuroscience Chapter Conference, Gainesville, Fl

Linking oxidative stress of aging to the senescent neurophysiology of cognitive decline. (Oct 2010). Cognitive Aging Summit II, Washington DC.

Linking oxidative stress of aging to the senescent neurophysiology of cognitive decline (Oct 2010). Florida Atlantic University, Boca Raton, FL.

K. Bodhinathan, A. Kumar, T. C. Foster (2010) Altered redox state contributes to increased afterhyperpolarization of hippocampal CA1 pyramidal neurons during senescence: role for ryanodine receptor oxidation. Soc. Neurosci. Abstr

J. Herrera, A. Kumar, A. Rani, T. C. Foster (2010) Differential influence of environmental enrichment and exercise on learning and memory, synaptic plasticity, and neuronal excitability during senescence. Soc. Neurosci. Abstr

W.H. Lee, A. Kumar, A. Rani, J. Herrera, T. C. Foster (2010) Influence of viral vector-mediated delivery of superoxide dismutase and catalase to the hippocampus on spatial learning and memory over the course of aging. Soc. Neurosci. Abstr

R.B. Speisman, A. Kumar, A. Rani, J.E. Severence, T. C. Foster, B.K. Ormerod (2010) Enrichment concomitantly improves hippocampal neurogenesis and spatial memory in aged rats. Soc. Neurosci. Abstr

5. **Presentations at public (non-scientific) meetings or events**

6. **Awards (other)**
   Associate Editor Award for work in Frontiers of Aging Neuroscience

   **NIH Funding Awards**

   *Previous*
   NIA R01 AG14979 (**Foster** PI) Mechanisms of altered synaptic function during aging, 6/01/07 to 5/31/2012, $184,500/year.

   NINDS RO1 NS041012 (Foster Co-I) Cellular events in heritable peripheral neuropathies 07/01/05 to 06/30/2010, $225,000.

   NIMH R01 MH59891 (**Foster** PI) Estrogen and cognition over the lifespan, 12/01/01 to 8/18/10. $185,000/year.

   *New*
   NIA R56 AG037984 (**Foster** PI) Estrogen and cognition over the lifespan, 9/15/2010 to 8/31/2011. $185,000.

   NIA R01AG036800 (**Foster** PI) Signaling cascades and memory deficits during aging, 10/05/2010 to 08/31/2014 $ 292,147/year.

7. **Faculty. Please include abbreviated CV with publications for previous 12 months**

8. **Trainees**

   a) Post doctoral:
      Ashok Kumar (Research Associate)

   b) Pre-doctoral:
      Travis Jackson (Graduated Ph.D. 2010)
      Karthik Bodhinathan (Graduated Ph.D. 2010)
      Wei-Hua Lee, Ph.D. program
      Xiaoxia Han, Ph.D. program
      Mike Guidi, Ph.D. program

   c) Other
      Asha Rani
      Olga Tchigrinova

**9. Clinical/translational programs**

a) New programs

b) Update on existing clinical studies

i. I am the Chair for the committee overseeing the Age-Related Memory Loss (ARML) Program. Other members of the committee include Drs. Lucia Notterpek, Tetsua Ashizawa, and Christiaan Leeuwenburg.

During the past year the ARML Program hired Dr. Jen Bizon, an Associate Professor with a history of research and funding directed at ARML. I was also a member of the search committee. Dr. Bizon is currently in the process of transitioning to the University of Florida (lab set up, establishing protocols etc). As a UF faculty member, she has been an active and valued colleague and she will represent UF as a speaker at the next Inter-Institute meeting in Miami.

The committee provided guidelines/goals for the Village Wellness Study. This study was initially approved by Dr. Steindler as the Executive Director and was under the direction of Dr. Fernandez. The project received funds from the MBRF ($30K/year for 3 years) and the SantaFe Health Alzheimer's Disease Research Center ($60K/year). Dr. Fernandez has since moved to another university and the committee approved Drs. Bowers and Marsiske as the new directors. In taking over the role of directors, Drs. Bowers and Marsiske, in consultation with the ARML Program committee, altered the scope of the project. In addition, the directors requested additional funds ($60K for 2 years) to complete the work. Conditions were set for the release of additional funds for the first year and these conditions were met (hiring a research coordinator-Kim Foli, approval of IRB – approved 8/18/2010, dedicated infrastructure for conducting the project). The funds for the first year were approved by the ARML committee and the committee indicated that subsequent funds could be made available provided that significant progress has been made on the project, along with a detailed expenditure report. We expect an update on the project in March, 2011 and the directors will provide a scientific report related to the project at the next Inter-Institutional meeting in Miami.

The committee approved funding ($50K) for several projects related to Biomarkers of Cognitive Decline to Dr. Brandi Ormerod. This funding was used for the generation of preliminary data for a National Science Foundation proposal from a graduate student in Dr. Omerod's lab. The graduate student (Rachel Speisman) received the National Science Foundation funding to continue work on Biomarkers of Cognitive Decline. A manuscript based on this research should be submitted in 2011. In addition, the funding was used to support Dr. Omerod in the re-submission of a grant proposal (24$^{th}$ percentile in the first round) to NIH. This proposal is now funded by NIA (Signaling cascades and memory deficits during aging) with Drs. Foster and Ormerod as Co-PIs. A manuscript based on this research should be submitted in 2011.

The committee felt that we should support imaging research on ARML and a request for applications (RFA) was issued in December, 2010 with proposals expected January 15, 2011. This RFA is directed at junior faculty with a history of research on ARML and/or projects that will move towards collaborations between departments at UF or UF and other MBRF sponsored institutions.

Finally, I have kept the committee updated on the CAM-CTRP searches and MBRF Inter-Institutional meetings and the committee has provided me with recommendations and suggestions related to these endeavors.

ii. I was the Chair for the Search Committee to find a Program Director and Professor for the Cognitive Aging and Memory Clinical Translational Research Program (CAM-CTRP). We interviewed five candidates. These candidates include Anna Mariya Barrett, MD; Charles DeCarli, MD; Paul A. Newhouse, M.D.; Caterina Rosano, MD, MPH; Steven L. Small, PhD, MD. Dr. Newhouse was selected as our top choice and the recommendation was sent forward.

iii. I am a member of the Search Committee to find an Assistant Program Director for the CAM-CTRP. We are several candidates have been identified and we are currently in the process of interviewing these individuals.

iv. I am a member of the Institute on Aging and Pepper Center Executive Committee.

**10. Technology transfer**

a) Patents applications: None
b) Revenue generated from technology: None

**11. Budget update (last year's budget and actual results - with an explanation of material variances)**

a) Status of matching funds, if applicable
b) Projected budget for coming year
c) Extramural funding

**12. Educational programs focusing on age related memory loss**

a) Scientific

I hosted the Third Annual McKnight Brain Research Foundation Inter-Institutional meeting in April 2010.

I was a member of the planning committee for the Cognitive Aging Summit II held Oct 2010.

I was the editor for a Special Topic issue in Frontiers in Aging Neuroscience. This Special Topic issue included 10 manuscripts which focused on mechanisms for selective vulnerability of brain regions and processes related to cognitive decline. The manuscripts include:

i. Do different neurons age differently? Direct genome-wide analysis of aging in single identified cholinergic neurons? Leonid L Moroz and Andrea B. Kohn.
ii. How do age-related changes in protein synthesis affect hippocampus-dependent memory and synaptic plasticity? Lesley Schimanski and Carol Barnes.
iii. Selective neuronal vulnerability to oxidative stress in the brain. Xinkun Wang, and Elias K. Michaelis.
iv. Selective vulnerability of NMDA receptors and subunits during brain aging. Kathy R Magnusson, Brenna L Brim, and Siba R Das.
v. The testosterone metabolite and neuroactive steroid, 3$\alpha$-androstanediol, attenuates age-related decrements in anti-anxiety and anti-depressive behavior and learning of male rats. Cheryl A Frye, Kassandra L Edinger, Edwin D Lephart, and Alicia A Walf.
vi. An epigenetic hypothesis of aging-related cognitive dysfunction. Marsha R Penner, Tania L Roth, Carol Barnes, and David Sweatt.
vii. KIBRA, a new gateway to learning and memory. Armin Schneider, Matt Huentelmann, Joachim Kremerskothen, Robert Spoelgen, and Karoly Nikolich.
viii. Age-related neuroinflammatory changes negatively impact on neuronal function. Marina A Lynch.
ix. From synaptic to intrinsic alterations with learning and aging. John Disterhoft and Matthew Oh.
x. Contribution of the d-serine-dependent pathway in cellular mechanisms underlying cognitive aging. Brigitte Potier, Fabrice R Turpin, Pierre-Marie Sinet, Emilie Rouaud, Jean-Pierre Mothet, Catherine Videau, Jacques Epelbaum, Patrick Dutar, Jean-Marie Billard.

b) Public

13. **Collaborative programs with other McKnight Institutes, institutions and research programs**
I have been investigating the possibility of generating a virus to deliver NMDA receptors to the hippocampus. This has been in collaboration with the University of Alabama.

14. **Collaborative program with non McKnight Institutes, institutions and research programs**
I have supplied virus to express estrogen receptor alpha to Dr. Jill Daniel at Tulane University.

15. **Briefly describe plans for future research and/or clinical initiatives**

a) We will continue to pursue studies that test the idea that memory consolidation deficits are an early marker of age-related cognitive decline.
b) We will continue to pursue studies that characterize early (i.e. middle-age) changes in signaling pathways from the NMDA receptor to transcription, which we hypothesis mediate the stabilization/maintenance/consolidation of memory.
c) We will continue to develop and implement the transfer of genes to reduce oxidative stress (SOD, catylase) and promote cell health, synaptic growth, and memory (estrogen receptor, NMDAR).
d) We will continue to pursue studies test the hypothesis that estrogen receptor beta is a negative regulator of estrogen receptor alpha and contributes to the reduced effects of estrogen in rejuvenating the hippocampus.

16. **If applicable, please provide endowment investment results for the report period.** N/A

17. **Were any funds used for a Prohibited Purpose during the report period?** No

18. **Do you recommend any modification to the Purpose or mandates in the Gift Agreement?**
No

19. **Did all activities during the report period further the Purpose?** Yes

20. **Please describe any negative events (loss of personnel, space, budget, etc.) that occurred during the report period and the possible impact on carrying out the Gift Agreement.**
No Response

21. **Please provide any general comments or thoughts not covered elsewhere – a response is not required. Please respond only if you would like to add something not otherwise covered elsewhere.**

22. **Signature, date, and title of person submitting the report.**

Tom Foster

Thomas Foster, Ph.D.
Professor and McKnight Chair for Research on Aging and Memory

12/14/2010

# University of Florida Health Science Center

**2010 Annual Report**
of the
McKnight Brain Institute
& Institute on Aging

*Prepared for the McKnight Brain Research Foundation*

# Institute on Aging Report

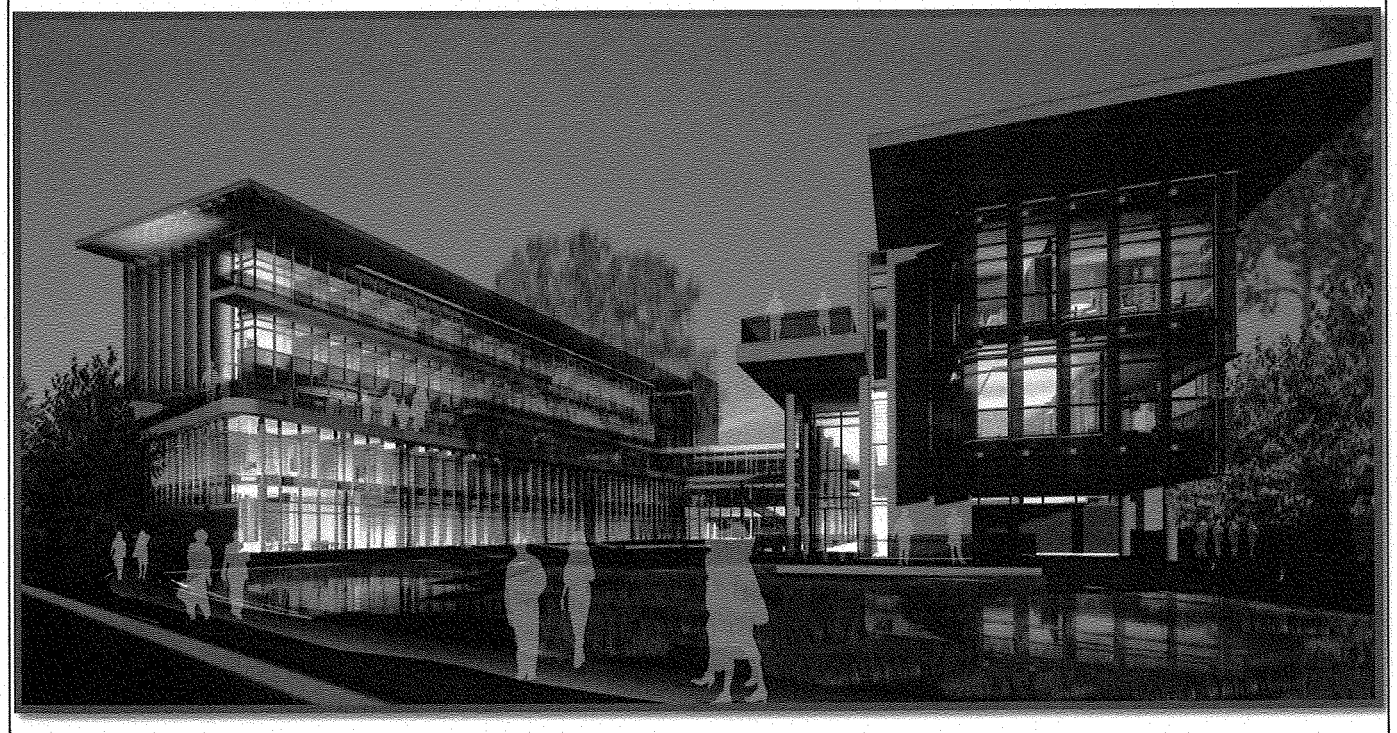

UF UNIVERSITY of FLORIDA

**Institute on Aging**
Department on Aging and Geriatric Research
College of Medicine

PO Box 100107
Gainesville, FL 32610-0107
352-265-7227
352-265-7228 Fax
www.aging.ufl.edu

January 10, 2011

McKnight Brain Research Foundation
Foundations & Endowments Specialty Practice
SunTrust Banks, Inc.
Mail Code FL-ORL-2160
300 South Orange Ave., Suite 1600
Orlando, FL 32801
Attn: Tiffany Ahlfield

Dear McKnight Brain Research Foundation Trustees:

Thank you for the opportunity to present a progress report to the McKnight Brain Research Foundation (MBRF) for the period January 1, 2010 to December 31, 2010. Activity during this timeframe has involved ongoing recruitment of the Director of the Cognitive Aging and Memory Clinical Translational Research Program (CAM-CTRP). In early October, 2009, a national search committee was established, chaired by Tom Foster, PhD. Committee members include Michael Marsiske, PhD.; Herb Ward, MD; Stephen Anton, PhD; Tony Yachnis, MD and Ken Heilman, MD. This search committee remains intact and continues its charter.

Recruiting a Director for the CAM-CTRP continues to be our highest priority. Committee members sent personal invitations to colleagues announcing the opportunity, and in addition, advertisements for the position were placed in six premier medical journals. At the recommendation of the search committee, advertisements to recruit an Associate Director were placed in these premier journals in 2010.

To date, we have identified nine (9) candidates who have demonstrated significant accomplishments in the field and who, we believe, would be an asset to the Institute. These candidates include Anna Mariya Barrett, MD; Charles DeCarli, MD; Yonas Geda, MD, MSc; Keith Josephs, MST, MD, MS; Kenneth Langa, MD, PhD; Paul A. Newhouse, M.D.; Caterina Rosano, MD, MPH; Steven L. Small, PhD, MD; and Madhav Thambisetty, MD, PhD. The attached candidate list contains more complete information including dates of interviews and status of recruitment.

Successful recruitment of the Director has been more challenging than we originally anticipated because of the highly specific position requirements, including research focus, track record in NIH

funding, career rank, and active US physician licensure. Among all the criteria, physician licensure represents the major delimiter to finding the best leader expeditiously. In fact, among approximately 120 researchers who have major active NIH grants (R01, U01, and Program grants) focused on the CAM-CTRP theme, only approximately 10% are MDs and not all of these MDs bear a US licensure. Given these challenges, we hope to recruit a highly qualified candidate in 2011.

In 2010 the NIH NCRR C06RR029852 Construction Grant for the Institute on Aging Clinical Translational Research Building was funded (Principal Investigator: Pahor, M, 4/1/2010-1/31/2015, $14,995,000), which will host the CAM-CTRP. CTRP and MBRF support played pivotal roles for the successful funding of that grant.

Please find attached a projected budget for the use of the MBRF funds. To date, we have received funding of $2,043,380. During the period of October – December 2009, we expended approximately $10,852. During the period of January 1 – December 31, 2010, we anticipate expending funds of $50,829, leaving approximately $1,981,699 unencumbered for the current reporting period. In addition we anticipate annual endowment income of approximately $470,264. The attached projected budget will be negotiated and updated once the director is successfully recruited to lead the CAM-CRTP. We anticipate substantial escalation on expenses once the program begins to take shape. You will also find attached a MBRF endowment report.

We deeply appreciate our partnership with the MBRF in the development of an interdisciplinary research program, which translates basic science discoveries regarding cognitive aging and memory into clinical applications to slow or avert the age-related cognitive decline and memory loss and to restore cognitive function.

Sincerely,

Marco Pahor, MD
Professor and Chair, Department of Aging and Geriatric Research,
College of Medicine
Director, Institute on Aging

## Budget - CAM-CTRP

**Personnel**

| Name | 10/1/09-12/31/09 Year 1 | 1/1/10-12/31/10 Year 2 | 1/1/11-12/31/11 Year 3 | 1/1/12-12/31/12 Year 4 | 1/1/13-12/31/13 Year 5 | 1/1/14-12/31/14 Year 6 | | | 10/1/09-12/31/09 Year 1 | 1/1/10-12/31/10 Year 2 | 1/1/11-12/31/11 Year 3 | 1/1/12-12/31/12 Year 4 | 1/1/13-12/31/13 Year 5 | 1/1/14-12/31/14 Year 6 | TOTALS |
|---|---|---|---|---|---|---|---|---|---|---|---|---|---|---|---|
| TBA MD | 0% | 0% | 50% | 100% | 83% | 68% | $ 274,560 | Salary | $ - | $ - | $ 141,398 | $ 291,281 | $ 250,412 | $ 210,015 | $ 893,106 |
| Program Director | | | 6 mos | | 75% | 50% | 0.2342 | Fringe | $ - | $ - | $ 33,116 | $ 68,218 | $ 58,646 | $ 49,185 | $ 209,165 |
| Professor | | | | | 2126993% | 4381606% | | Total Sal | $ - | $ - | $ 174,514 | $ 359,499 | $ 309,058 | $ 259,200 | $ 1,102,271 |
| | | | | | 8% | 18% | | | | | | | | | |
| TBA MD | 0% | 0% | 50% | 100% | 75% | 50% | $ 225,680 | Salary | $ - | $ - | $ 116,225 | $ 239,424 | $ 184,955 | $ 127,002 | $ 667,606 |
| Associate Professor | | | 6 mos | | | | 0.2342 | Fringe | $ - | $ - | $ 27,220 | $ 56,073 | $ 43,316 | $ 29,744 | $ 156,353 |
| | | | | | | | | Total Sal | $ - | $ - | $ 143,445 | $ 295,497 | $ 228,271 | $ 156,746 | $ 823,960 |
| TBA MD | 0% | 0% | 50% | 100% | 75% | 50% | $ 176,800 | Salary | $ - | $ - | $ 91,052 | $ 187,567 | $ 144,896 | $ 99,495 | $ 523,010 |
| Assistant Professor | | | 6 mos | | | | 0.2342 | Fringe | $ - | $ - | $ 21,324 | $ 43,928 | $ 33,935 | $ 23,302 | $ 122,489 |
| | | | | | | | | Total Sal | $ - | $ - | $ 112,376 | $ 231,495 | $ 178,830 | $ 122,797 | $ 645,499 |
| TBA MD | 0% | 0% | 33% | 100% | 75% | 50% | $ 42,204 | Salary | $ - | $ - | $ 14,490 | $ 44,774 | $ 34,588 | $ 23,750 | $ 117,603 |
| Post Doc Fellow | | | 4 mos | | | | 0.1825 | Fringe | $ - | $ - | $ 2,644 | $ 8,171 | $ 6,312 | $ 4,334 | $ 21,463 |
| | | | | | | | | Total Sal | $ - | $ - | $ 17,134 | $ 52,946 | $ 40,900 | $ 28,085 | $ 139,065 |
| TBA MD | 0% | 0% | 33% | 100% | 100% | 75% | $ 42,204 | Salary | $ - | $ - | $ 14,490 | $ 44,774 | $ 46,117 | $ 35,626 | $ 141,007 |
| Post Doc Fellow | | | 4 mos | | | | 0.1825 | Fringe | $ - | $ - | $ 2,644 | $ 8,171 | $ 8,416 | $ 6,502 | $ 25,734 |
| | | | | | | | | Total Sal | $ - | $ - | $ 17,134 | $ 52,946 | $ 54,534 | $ 42,127 | $ 166,741 |
| TBA | 0% | 0% | 50% | 100% | 100% | 100% | $ 45,000 | Salary | $ - | $ - | $ 23,175 | $ 47,741 | $ 49,173 | $ 50,648 | $ 170,736 |
| Admininstrative Mgr | | | 6 mos | | | | 0.3286 | Fringe | $ - | $ - | $ 7,615 | $ 15,688 | $ 16,158 | $ 16,643 | $ 56,104 |
| | | | | | | | | Total Sal | $ - | $ - | $ 30,790 | $ 63,428 | $ 65,331 | $ 67,291 | $ 226,840 |
| TBA | 0% | 0% | 25% | 25% | 25% | 20% | $ 58,000 | Salary | $ - | $ - | $ 14,935 | $ 15,383 | $ 15,845 | $ 13,056 | $ 59,218 |
| Clinical res. study mgr | | | 6 mos | | | | 0.3286 | Fringe | $ - | $ - | $ 4,908 | $ 5,055 | $ 5,207 | $ 4,290 | $ 19,459 |
| | | | | | | | | Total Sal | $ - | $ - | $ 19,843 | $ 20,438 | $ 21,051 | $ 17,346 | $ 78,678 |
| TBA | 0% | 0% | 25% | 50% | 25% | 0% | $ 40,000 | Salary | $ - | $ - | $ 10,300 | $ 21,218 | $ 10,927 | $ - | $ 42,445 |
| Res. Study Coordinator | | 6 mos | 6 mos | | | | 0.3286 | Fringe | $ - | $ - | $ 3,385 | $ 6,972 | $ 3,591 | $ - | $ 13,948 |
| | | | | | | | | Total Sal | $ - | $ - | $ 13,685 | $ 28,190 | $ 14,518 | $ - | $ 56,393 |
| Total FTE | 0% | 0% | 317% | 675% | 558% | 413% | | Salary | $ - | $ - | $ 426,066 | $ 892,162 | $ 736,912 | $ 559,592 | $ 2,614,732 |
| | | | | | | | | Fringe | $ - | $ - | $ 102,856 | $ 212,276 | $ 175,582 | $ 134,000 | $ 624,715 |
| **Personnel** | | | | | | | | Total | **$ -** | **$ -** | **$ 528,922** | **$ 1,104,438** | **$ 912,494** | **$ 693,592** | **$ 3,239,447** |

CAM-CTRP Cognitive Aging and Memory Clinical Translational Research Program v5, sheet 1

Prepared by Lauren Crump

| | | 10/1/09-12/31/09 Year 1 | 1/1/10-12/31/10 Year 2 | 1/1/11-12/31/11 Year 3 | 1/1/12-12/31/12 Year 4 | 1/1/13-12/31/13 Year 5 | 1/1/14-12/31/14 Year 6 | TOTALS |
|---|---|---|---|---|---|---|---|---|
| **Personnel** | Total | $ - | $ - | $ 528,922 | $ 1,104,438 | $ 912,494 | $ 693,592 | $ 3,239,447 |
| **Consultants** | | | | | | | | |
| External Advisory Board members (4@1500 honorarium) | | $ - | $ - | $ 6,000 | $ 6,000 | $ 6,000 | $ 6,000 | $ 24,000 |
| External Advisory Board members (4@1250 travel funds) | | $ - | $ - | $ 5,000 | $ 5,000 | $ 5,000 | $ 5,000 | $ 20,000 |
| Expert Speakers @2 per year) | | $ - | $ - | $ 5,000 | $ 5,000 | $ 5,000 | $ 5,000 | $ 20,000 |
| | **Sub Consultants** | $ - | $ - | $ 16,000 | $ 16,000 | $ 16,000 | $ 16,000 | $ 64,000 |
| **Equipment** | | | | | | | | |
| Computers/printers (8@3000) | | $ - | $ - | $ - | $ - | $ 24,000 | $ - | $ 24,000 |
| Info Services | | $ - | $ - | $ 27,000 | $ 27,000 | $ 27,000 | $ 27,000 | $ 108,000 |
| | **Sub Equipment** | $ - | $ - | $ 27,000 | $ 27,000 | $ 51,000 | $ 27,000 | $ 132,000 |
| **Travel** | | | | | | | | |
| Recruitment costs | | $ 1,089 | $ 20,018 | $ 10,000 | $ 5,000 | $ 5,000 | $ 5,000 | $ 46,107 |
| Professional Travel (specialty conferences, collaborators, etc.) | | $ - | $ - | $ 15,000 | $ 15,000 | $ 15,000 | $ 15,000 | $ 60,000 |
| | **sub travel** | $ 1,089 | $ 20,018 | $ 25,000 | $ 20,000 | $ 20,000 | $ 20,000 | $ 106,107 |
| **Supplies** | | | | | | | | |
| Software & administrative supplies | | $ - | $ - | $ 10,000 | $ 10,000 | $ 10,000 | $ 10,000 | $ 40,000 |
| Publications Cost (slides, posters) | | $ - | $ - | $ 2,500 | $ 2,500 | $ 2,500 | $ 2,500 | $ 10,000 |
| | **sub supplies** | $ - | $ - | $ 12,500 | $ 12,500 | $ 12,500 | $ 12,500 | $ 50,000 |
| **Other Cost** | | | | | | | | |
| Meals, entertainment (faculty recruitment, consultants, other mtg costs) | | $ - | $ - | $ 10,000 | $ 5,000 | $ 5,000 | $ 5,000 | $ 25,000 |
| Relocation Costs (faculty recruitment) | | $ - | $ - | $ 15,000 | $ - | $ 15,000 | $ - | $ 30,000 |
| Program supervision, coordination and administration | | $ 6,197 | $ 20,584 | $ 85,000 | $ 87,550 | $ 90,177 | $ 92,882 | $ 382,390 |
| License, insurance, dues, subscriptions | | $ - | $ - | $ 25,000 | $ 25,000 | $ 25,000 | $ 25,000 | $ 100,000 |
| Advertising | | $ 3,565 | $ 10,227 | $ 10,000 | $ 5,000 | $ 5,000 | $ 5,000 | $ 38,792 |
| Start-up Packages (faculty recruitment) | | $ - | | $ 75,000 | $ 20,000 | $ - | $ 20,000 | $ 115,000 |
| Pilot Projects | | $ - | $ - | $ 75,000 | $ 150,000 | $ 150,000 | $ 150,000 | $ 525,000 |
| | **Sub total Other** | $ 9,762 | $ 30,811 | $ 295,000 | $ 292,550 | $ 290,177 | $ 297,882 | $ 1,216,182 |
| **Total Annual Costs** | | $ 10,852 | $ 50,829 | $ 904,422 | $ 1,472,488 | $ 1,302,170 | $ 1,066,974 | $ 4,807,736 |
| Initial Transfer from UFF (50% of accumulated non-endowed funds, approx. $3.2 million) | | $ 1,634,217 | $ - | $ - | $ - | $ - | $ - | $ 1,634,217 |
| Anticipated Annual Endowment Income | | $ - | $ 470,845 | $ 470,264 | $ 470,264 | $ 470,264 | $ 470,264 | $ 2,351,901 |
| | | $ - | $ - | $ - | $ - | $ - | $ - | $ - |
| Total Transfers | | $ 1,634,217 | $ 470,845 | $ 470,264 | $ 470,264 | $ 470,264 | $ 470,264 | $ 3,986,117 |
| | diff | $ 1,623,365 | $ 2,043,380 | $ 1,609,222 | $ 606,998 | $ (224,908) | $ (821,619) | $ (1,643,237) |

## COGNITIVE AGING and MEMORY CLINICAL TRANSLATIONAL RESEARCH PROGRAM (CAM-CTRP) DIRECTOR/ASSOCIATE DIRECTOR CANDIDATES

The search for the CAM-CTRP director or associate director is actively proceeding. Among a large pool of potential candidates who have been screened, to date a total of 9 qualified candidates, who are listed below, have been interviewed for the position. The search is particularly challenging because of the position requirements, including the highly specific research focus, the track record in NIH funding, the career rank, and the active US physician licensure. Among all, the latter has represented a major limitation to find the best leader for the program and expeditiously finalize the search. In fact, among approximately 120 researchers who have major active NIH grants (R01, U01, and Program grants) focused on the CAM-CTRP theme, only approximately 10% are MDs and not all of these MDs bear a US licensure.

**Anna Mariya Barrett, MD**
Program Director, Kessler Foundation Research Center
Stroke Rehabilitation Research
Professor, University of Medicine and Dentistry
New Jersey—the New Jersey Medical School
West Orange, New Jersey
*First visit: February 22-24, 2010*

**Charles DeCarli, MD**
Director of Faculty Development in the Department of Neurology
Department of Neurology
University of California at Davis
Sacramento, CA
First visit: February 1-3, 2010

**Yonas Geda, MD, MSc**
Associate Professor of Neurology and Psychiatry
College of Medicine, Mayo Clinic
Rochester, MN
*First visit: June 21-22, 2010*
*Second visit: September 7-9, 2010*

**Keith A. Josephs, MST, MD, MS**
Associate Professor of Neurology
College of Medicine, Mayo Clinic
Rochester, MN
*Phone interview: December 16, 2010*
*To be scheduled in January or February 2011*

**Kenneth Langa, MD, PhD**
Professor, Department of Internal Medicine
Division of General Medicine
University of Michigan
*First visit: August 12-13, 2010*

**Paul A. Newhouse, MD**
Director, Clinical Neuroscience Research Unit and Brain Imaging Program
Professor, Department of Psychiatry
University of Vermont College of Medicine
Burlington, VT
*First visit: January 19-21, 2010*
*Second visit: June 10-13, 2010*

**Caterina Rosano, MD, MPH**
Associate Professor of Epidemiology
Center for Healthy Aging and Population
Graduate School of Public Health
University of Pittsburgh
Pittsburgh, PA
First visit: February 10-12, 2010

**Steven L. Small, PhD, MD**
Associate Chair for Research
Department of Neurology
The University of Chicago
Chicago, IL
First visit: November 17-19, 2009

**Madhav Thambisetty, MD, PhD**
Neurology Staff Clinician
Clinical Research Branch
National Institutes of Health
Adjunct Assistant Professor
Department of Neurology
Johns Hopkins University School of Medicine
Baltimore, MD
*First visit: September 22-24, 2010*
*Second visit: December 8-10, 2010*

University of Florida Health Science Center

**2010 Annual Report**
of the
McKnight Brain Institute
& Institute on Aging

*Prepared for the McKnight Brain Research Foundation*

# UF Foundation Endowment Reports

# Evelyn F. McKnight Chair for Brain Research in Memory Loss

The endowments of our donors form a cornerstone of success for our stellar students and faculty here at the University of Florida. Each year, the income generated by endowed funds such as yours enables the impact of their studies and research to be felt far beyond our Gainesville campus.

We are pleased to provide you with the following financial report. A spotlight of your fund may be found on the University of Florida Foundation website at: www.uff.ufl.edu/FacultyEndowments

**BOOK VALUE** **$3,995,677**
*Includes original gifts, state and company matches and additional gifts to the fund received before 09/01/10.*

**MARKET VALUE as of 09/30/10** **$4,238,754**
*Includes assets received before 09/01/10 and invested in the endowment pool on or before 10/01/10; Excludes assets not yet converted to cash.*

**PROJECTED SPENDABLE INCOME for 2010/11** **$144,118**

## ENDOWMENT MANAGEMENT

Endowment assets are invested through the University of Florida Investment Corporation (UFICO), created in 2004 to manage UF's investment portfolios. UFICO is headed by a Chief Investments Officer who reports to a volunteer Board of Directors and to the President of the University of Florida.

FOR MORE INFORMATION, CONTACT:
Thomas J. Mitchell
Vice President, Development and Alumni Affairs
(352) 392-5407 (tmitchell@uff.ufl.edu)

Cindy Belknap
Director of Stewardship and Donor Relations
(352) 846-3444 (cbelknap@uff.ufl.edu)

(Fund # 007889)

# Evelyn F. McKnight Brain Research Grant

The endowments of our donors form a cornerstone of success for our stellar students and faculty here at the University of Florida. Each year, the income generated by endowed funds such as yours enables the impact of their studies and research to be felt far beyond our Gainesville campus.

We are pleased to provide you with the following financial report. A spotlight of your fund may be found on the University of Florida Foundation website at: www.uff.ufl.edu/EndowedFunds

**BOOK VALUE** **$25,967,781**
*Includes original gifts, state and company matches and additional gifts to the fund received before 09/01/10.*

**MARKET VALUE as of 09/30/10** **$27,799,662**
*Includes assets received before 09/01/10 and invested in the endowment pool on or before 10/01/10; Excludes assets not yet converted to cash.*

**PROJECTED SPENDABLE INCOME for 2010/11** **$945,189**

## ENDOWMENT MANAGEMENT

Endowment assets are invested through the University of Florida Investment Corporation (UFICO), created in 2004 to manage UF's investment portfolios. UFICO is headed by a Chief Investments Officer who reports to a volunteer Board of Directors and to the President of the University of Florida.

FOR MORE INFORMATION, CONTACT:
Thomas J. Mitchell
Vice President, Development and Alumni Affairs
(352) 392-5407 (tmitchell@uff.ufl.edu)

Cindy Belknap
Director of Stewardship and Donor Relations
(352) 846-3444 (cbelknap@uff.ufl.edu)

(Fund # 008057)

# McKnight Brain Research Foundation

## Evelyn F. McKnight Brain Research Grant (008057/008058)

Spendable Fund Transfers since endowment inception for F008058

| | | |
|---|---|---|
| **FY 2010/2011** | **$472,589** | **(12/31/10 YTD)** |
| **FY 2009/2010** | **$941,689** | |
| **FY 2008/2009** | **$1,086,475** | |
| **FY 2007/2008** | **$1,172,824** | |
| **FY 2006/2007** | **$1,056,031** | |
| **FY 2005/2006** | **$881,347** | |
| **FY 2004/2005** | **$843,131** | |
| **FY 2003/2004** | **$729,335** | |
| **FY 2002/2003** | **$651,801** | |
| **FY 2001/2002** | **$657,852** | |
| **FY 2000/2001** | **$648,384** | |
| **TOTAL** | **$9,141,458** | |

## Evelyn F. McKnight Chair for Brain Research in Memory Loss (007889/007890)

Spendable Fund Transfers since endowment inception for F007890

| | | |
|---|---|---|
| **FY 2010/2011** | **$72,058** | **(12/31/10 YTD)** |
| **FY 2009/2010** | **$143,584** | |
| **FY 2008/2009** | **$165,660** | |
| **FY 2007/2008** | **$178,827** | |
| **FY 2006/2007** | **$161,019** | |
| **FY 2005/2006** | **$134,384** | |
| **FY 2004/2005** | **$127,813** | |
| **FY 2003/2004** | **$124,127** | |
| **FY 2002/2003** | **$125,768** | |
| **FY 2001/2002** | **$100,869** | |
| **FY 2000/2001** | **$99,417** | |
| **FY 1999/2000** | **$3,438** | |
| **TOTAL** | **$1,436,964** | |

FOR MORE INFORMATION, CONTACT:
Thomas J. Mitchell
Vice President, Development and Alumni Affairs
(352) 392-5407 (tmitchell@uff.ufl.edu)

Cindy Belknap
Director of Stewardship and Donor Relations
(352) 846-3444 (cbelknap@uff.ufl.edu)

# University of Florida Fund Report
# Prepared for the McKnight Foundation

**F007889/90 Evelyn F. McKnight Chair for Brain Research in Memory Loss**
Fund Administrator: Thomas C. Foster, Ph.D.

| | |
|---|---|
| **F007889** | |
| **Balance in Endowment** | **$4,202,724.32** |
| | |
| **F007890** | |
| **Spendable Income Beginning Balance** | **$ 107,938.49** |
| Transferred to UF | $ 0.00 |
| Endowment transfer | $ 72,058.06 |
| Investment Pool Earnings | $ 0.00 |
| **Spendable Income Balance** | **$ 179,996.55** |
| | |
| Estimated Annual Transfers | $ 144,117.63 * |

* estimated based on spending base (spending base is adjusted quarterly).

**F008057/58 Evelyn F. McKnight Brain Research Grant**
Fund Administrator: Tetsuo Ashizawa, M.D.

| | |
|---|---|
| **F008057** | |
| **Balance in Endowment** | **$27,563,365.18** |
| | |
| **F008058** | |
| **Spendable Income Beginning Balance** | **$ 2,345,972.14** |
| Transferred to UF | $ (929,396.45) |
| Transferred to F016327 | $ (470,844.50) |
| Endowment transfer | $ 472,589.27 |
| Investment Pool Earnings | $ 0.00 |
| **Spendable Income Balance** | **$ 1,418,320.46** |
| | |
| Estimated Annual Transfers | $ 945,188.52 * |

* estimated based on spending base (spending base is adjusted quarterly).

**F016327 McKnight Brain Research Foundation Cognitive Aging and Memory Program**
Fund Administrator: Marco Pahor, M.D.

| | |
|---|---|
| **F016327** | |
| Beginning balance in Fund | $1,434,216.60 |
| Transferred from 8058 on 11/30/2010 | $ 470,844.50 |
| **Current Fund balance** | **$1,905,061.10** |

Data as of 12/31/2010
*Prepared 1/10/2011*

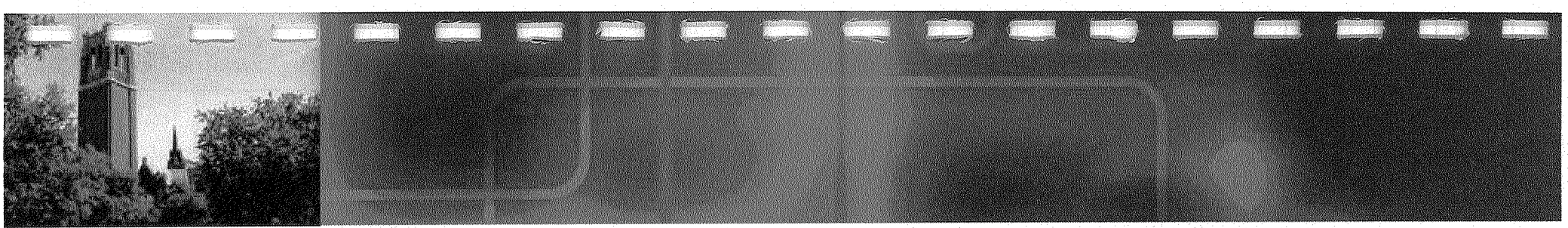

# McKnight Brain Research Foundation

## UF Investment Corporation ("UFICO") Update
## January 2011

UF | UNIVERSITY of FLORIDA INVESTMENT CORPORATION

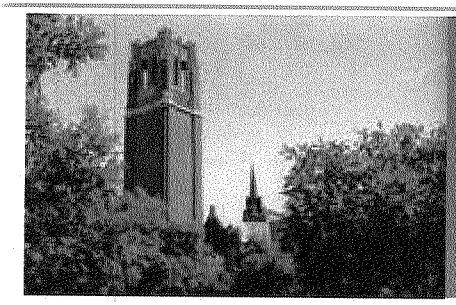

# Asset Allocation – UFF Endowment

UFF Endowment
Long-Term Strategic Target

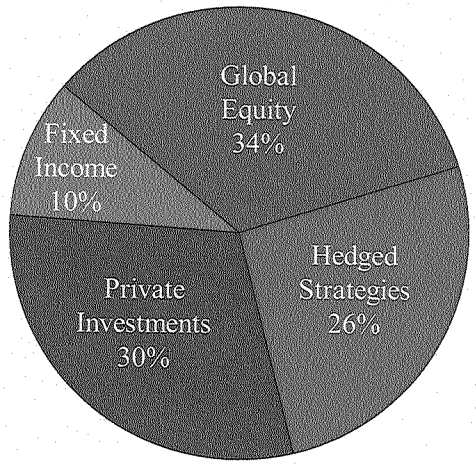


UFF Endowment
November 30, 2010

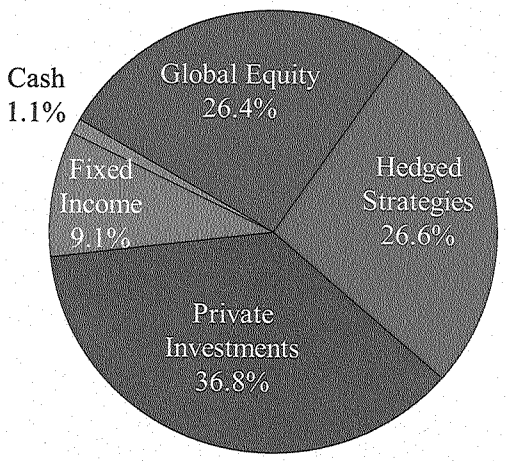


UFF Endowment
November 30, 2009

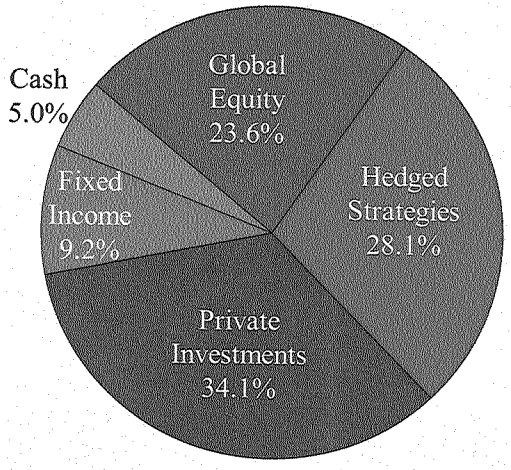

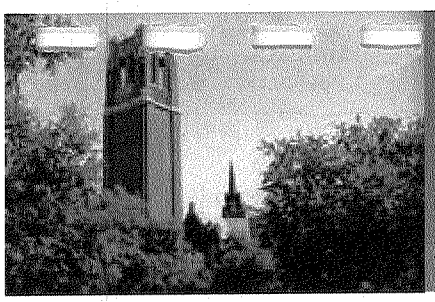

# Actual Asset Allocation – UFF Endowment

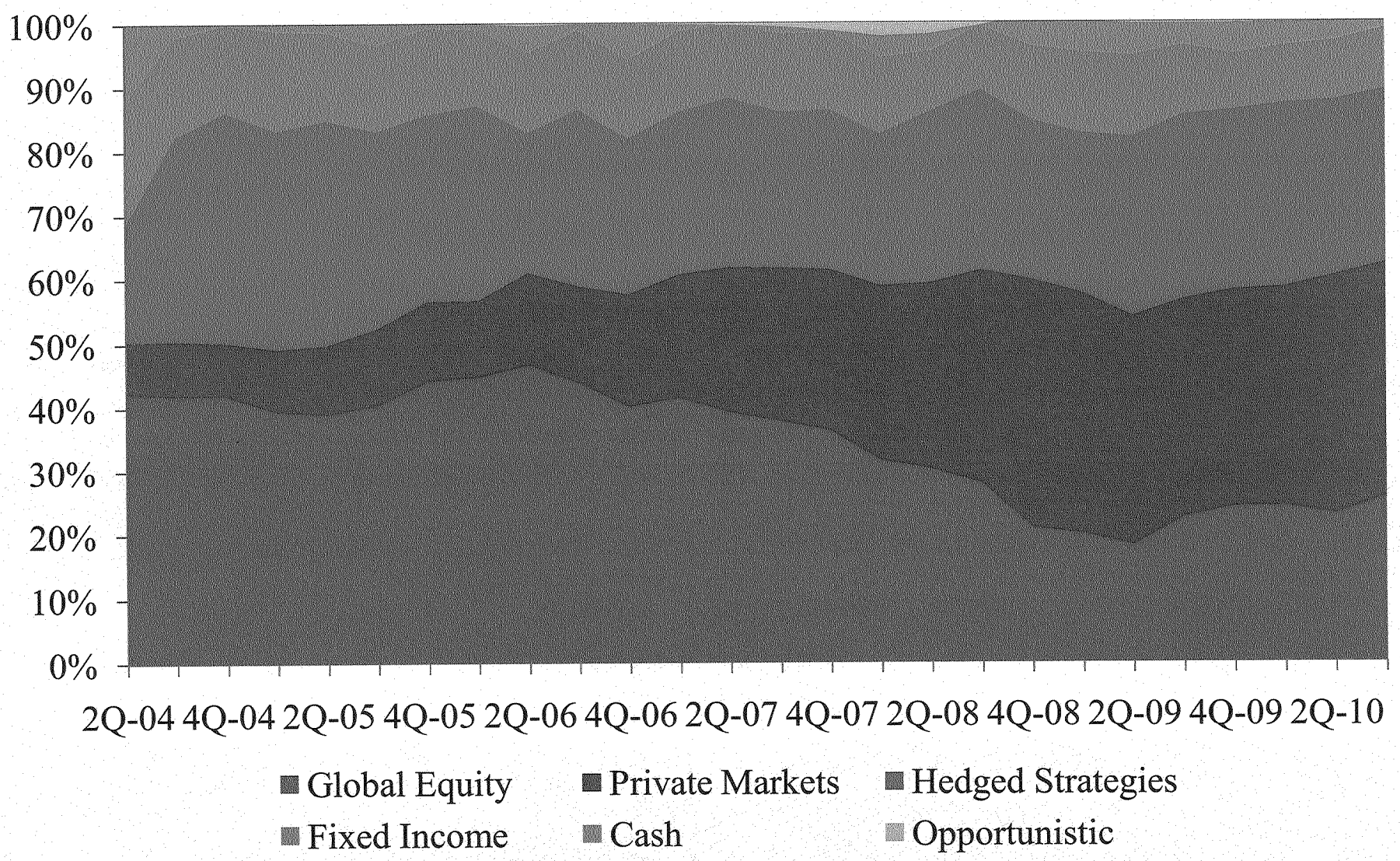

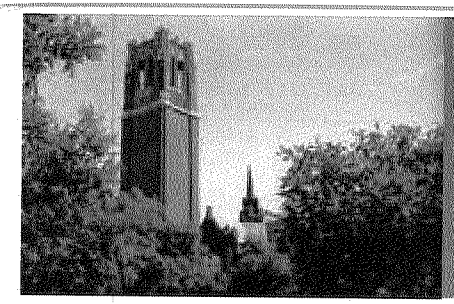

# Performance Review – UFF Endowment

## Fiscal Year 2011

**As of November 30, 2010**

| | (000's) NAV | Allocation Actual % | Allocation Target % | Last 3 Months | Fiscal YTD | Calendar YTD | 1 Year | 2 Year | 3 Year Annualized | 5 Year |
|---|---|---|---|---|---|---|---|---|---|---|
| **UFF Endowment Total Pool** | **$1,174,579** | **100.0%** | **100.0%** | **6.31%** | **7.44%** | **7.72%** | **9.00%** | **9.90%** | **-1.22%** | **5.26%** |
| *UFF Endowment Policy Benchmark* | | | | *11.46%* | *14.75%* | *7.78%* | *10.01%* | *19.05%* | *-3.42%* | *2.91%* |
| *70% Russell 3000/30% Barcap Aggregate* | | | | *9.93%* | *12.26%* | *9.40%* | *11.07%* | *16.80%* | *-0.71%* | *3.20%* |
| **Global Equity** | **$311,665** | **26.4%** | **25.0%** | **15.88%** | **18.96%** | **11.63%** | **15.51%** | **27.33%** | **-2.89%** | **4.90%** |
| *MSCI ACWI Free* | | | | *11.00%* | *15.84%* | *4.98%* | *7.16%* | *21.02%* | *-6.86%* | *2.48%* |
| **Hedged Strategies** | **$312,152** | **26.6%** | **26.5%** | **2.72%** | **3.76%** | **5.17%** | **7.59%** | **12.05%** | **-0.50%** | **5.16%** |
| *Hedged Strategies Benchmark* | | | | *4.19%* | *6.13%* | *3.96%* | *4.85%* | *9.32%* | *0.70%* | *4.81%* |
| **Fixed Income** | **$105,176** | **9.0%** | **9.5%** | **-0.82%** | **3.52%** | **8.74%** | **6.21%** | **15.90%** | **4.16%** | **5.54%** |
| *Barcap Universal* | | | | *0.17%* | *2.73%* | *8.11%* | *6.76%* | *10.40%* | *6.43%* | *6.30%* |
| **Private Investments** | **$432,112** | **36.8%** | **37.0%** | **5.05%** | **4.98%** | **8.64%** | **8.19%** | **-2.22%** | **-0.25%** | **6.88%** |
| *Private Investments Benchmark* | | | | *19.62%* | *22.52%* | *12.16%* | *16.47%* | *26.15%* | *-6.99%* | *1.07%* |
| **Opportunistic** | **$1,058** | **0.1%** | **0.0%** | *n/m* | *n/m* | *n/m* | *n/m* | *n/m* | *n/m* | *n/m* |
| **Cash** | **$12,416** | **1.1%** | **2.0%** | **0.00%** | **0.08%** | **0.27%** | **0.23%** | **0.99%** | **1.45%** | **2.80%** |
| *Citi 3 Month Treasury Bill* | | | | *0.04%* | *0.07%* | *0.12%* | *0.12%* | *0.16%* | *0.79%* | *2.36%* |

**Current Benchmark Composites**

UFF Endowment: 31% MSCI ACWI, 24% hedged strategies (2/3 (cash + 3%), 1/3 MSCI ACWI), 36% private investments (Russell 3000*1.35), 9% Barcap Universal
Hedged Strategies Benchmark (1/3 MSCI ACWI, 2/3 Cash + 3%)
Private Investments Benchmark (Russell 3000 x 1.35)

Note: Total Pool Returns are net of all fees / Asset Class Returns are gross of UFICO fees & net of manager fees

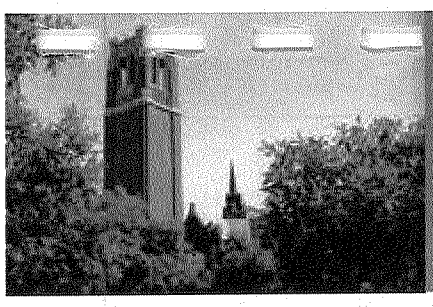

# Peer Comparison – UFF Endowment

## Rolling One-Year Percentile Rank
## Callan Midsize E&F Universe
**September 30, 2010**

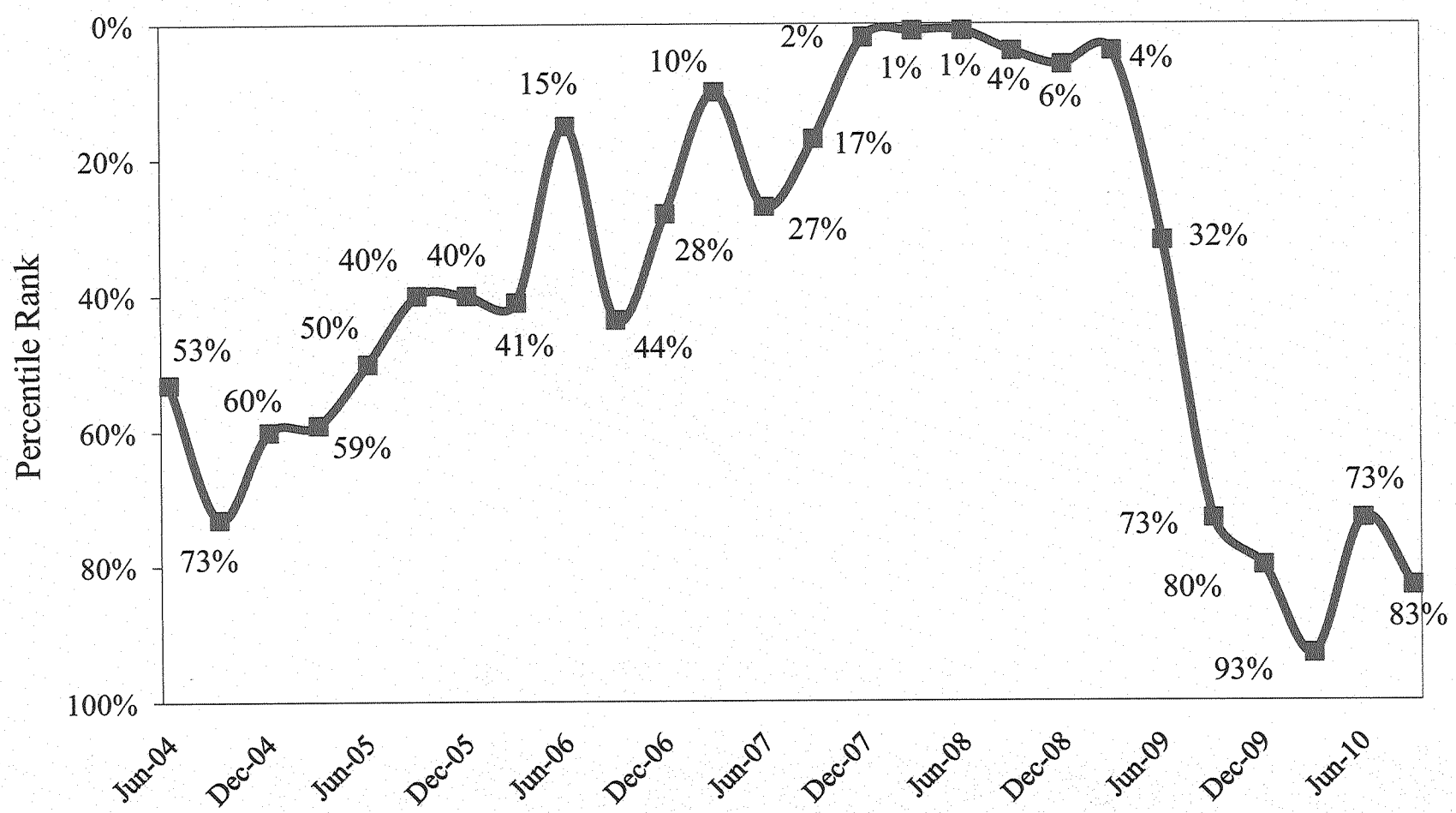

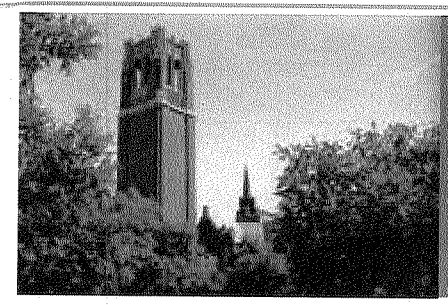

# Peer Comparison – UFF Endowment

## UFICO Inception-to-Date
## Callan Midsize E&F Universe
### September 30, 2010

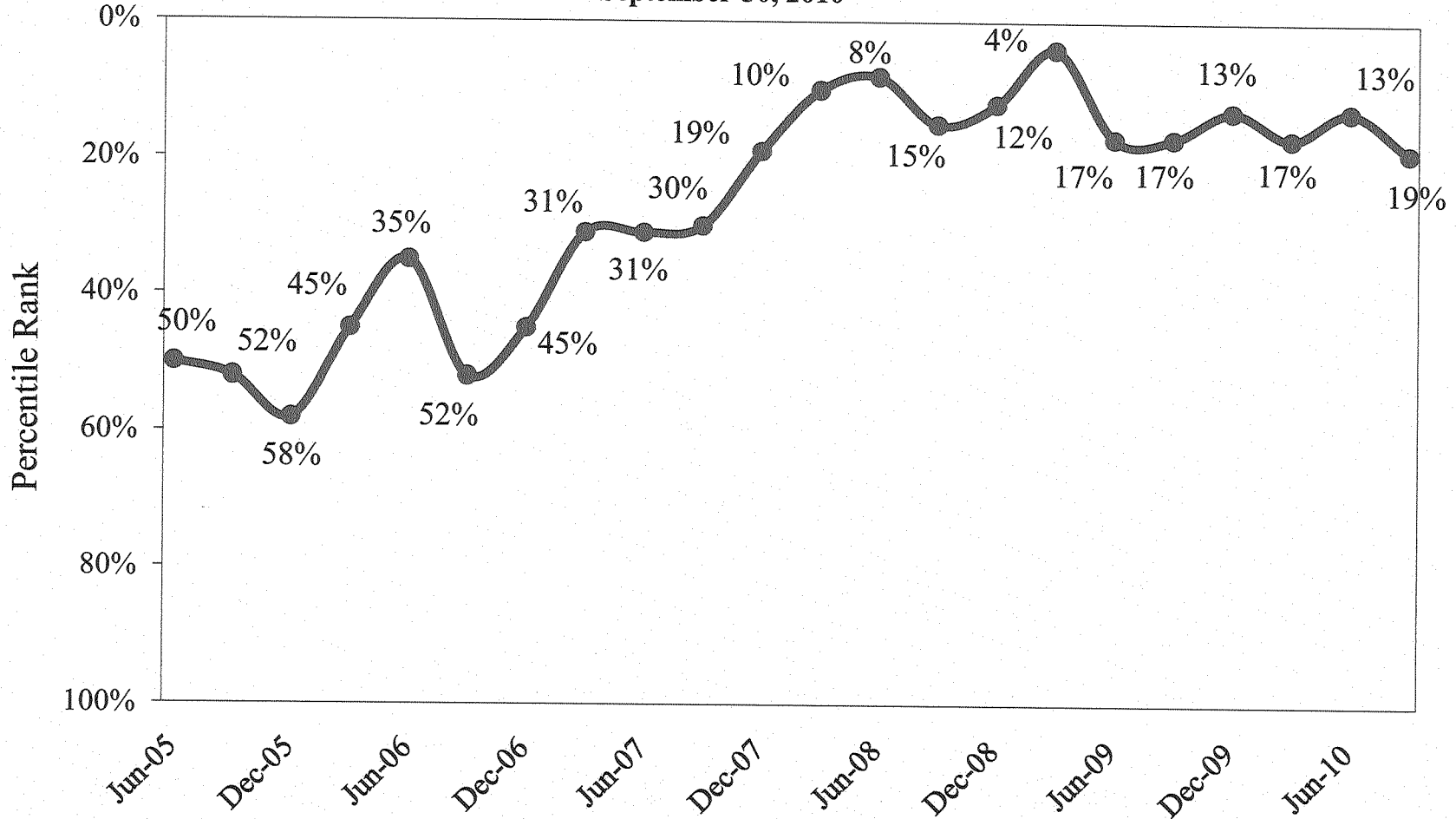

# University of Florida Health Science Center

**2010 Annual Report**
of the
McKnight Brain Institute
& Institute on Aging

*Prepared for the McKnight Brain Research Foundation*

# Faculty Biography/ Curriculum Vitae

## BIOGRAPHICAL SKETCH

Provide the following information for the Senior/key personnel and other significant contributors in the order listed on Form Page 2.
Follow this format for each person. **DO NOT EXCEED FOUR PAGES.**

| NAME | POSITION TITLE |
|---|---|
| Ashizawa, Tetsuo | Professor and Chairman |
| eRA COMMONS USER NAME (credential, e.g., agency login)<br>TEASHIZA | |

EDUCATION/TRAINING (*Begin with baccalaureate or other initial professional education, such as nursing, and include postdoctoral training.*)

| INSTITUTION AND LOCATION | DEGREE (*if applicable*) | YEAR(s) | FIELD OF STUDY |
|---|---|---|---|
| Keio University, Kanagawa, Japan | Premed | 1967-1969 | Premed |
| Keio University School of Medicine, Tokyo, Japan | M.D. | 1969-1973 | Medicine |
| U.S. Naval Hospit al, Yokosuka, Japan | Intern | 1973-1974 | Rotating Internship |
| Allegheny General Hospital, Pittsburgh, PA | Intern | 1974-1975 | Internal Medicine |
| Baylor College of Medicine, Houston, Texas | Resident | 1975-1978 | Neurology |
| Baylor College of Medicine, Houston, Texas | Fellow | 1978-1979 | Neuromuscular Disease |
| Baylor College of Medicine, Houston, Texas | Fellow | 1979-1981 | Neurochemistry |

### A. Personal Statement

The goal of the proposed research is to investigate preferential single-strand break repair in the active genes of mammalian cells focusing on establishing a direct mechanistic correlation between CAG repeat expansion and DNA repair deficiency in SCA3. This project is a great interest to me because I have been focusing on the pathogenic mechanism of spinocerebellar ataxias in my bench research with NIH funding as PI and I am PI of the Clinical Research Consortium for Spinocerebellar Ataxias (CRC-SCA) supported by NINDS and ORDR as a part of the Rare Disease Clinical Research Network (RDCRN). Results from the proposed project will provide important clue for the mechanism and evolution of the disease process. I am qualified to participate in this project because I have (1) in-depth scientific and clinical knowledge about SCAs, including SCA3, (2) an access to the patient cohort through the CRC-SCA, (3) organizational and collaborative skills to make the team work successful by assisting the PI of this project, (4) I am a qualified clinician with board certification for Neurology from ACGME, and (5) substantial knowledge about instability mechanisms of short tandem repeat DNA.

### B. Positions and Honors

**Positions and Employment**

1981-2002 Assistant Professor (1981-1992), Associate Professor with tenure (1992-1997) and Professor with tenure, Department of Neurology Baylor College of Medicine
1985-2002 Assistant Chief (1985-1987, 1988-2002) and Interim Chief (1988), Neurology Service, VA Medical Center, Houston, Texas
1994-1996 Director, Neurology Residency and Student Programs, Baylor College of Medicine
2002-2009 Professor and Chairman, Dept. of Neurology, University of Texas Medical Branch (UTMB), School of Medicine, Galveston, TX
2002-present Adjunct Professor, Department of Neurology, Baylor College of Medicine. Houston, TX
2005-2008 Co-Director, University of Texas Austin and UTMB MD-PhD Program, Galveston, TX
2009-present Professor and Chairman, Dept. of Neurology, University of Florida, Gainesville, FL
2009-present Adjunct Professor, Department of Neurology, UTMB, Galveston, TX

**Honors, Invited Membership and Awards**

1997-present Member, American Neurological Association
1998 Co-founder, International Myotonic Dystrophy Consortium (IDMC)
2001-present Member, Scientific Advisory Committee, National Registry of Myotonic Dystrophy and Facioscapulohumeral Muscular Dystrophy, (NIAMS, NINDS, P.I.: Richard Moxley III)
2002-2009 John Sealy Chair in Neurology
2005, 2006 Chair, Scientific Review Group ZNS1 SRB-R 16 1/ZNS1 SRB-A (37), NIH Gene Discovery
2005 The Team Hope Award, Huntington's Disease Society of America
2006 Medical Research Award, Myotonic Dystrophy Assistance & Awareness Support Group

| | |
|---|---|
| 2006-present | Member, Medical Research and Advisory Board, National Ataxia Foundation |
| 2007-present | Member, Scientific Advisory Board, Myotonic Dystrophy Foundation |
| 2007-present | Fellow, American Academy of Neurology |
| 2007-present | Chair, Grant Subcommittee for Center of Excellence, Huntington's Disease Society of America |
| 2007-present | Regular Member, NIH Cell Death in Neurodegeneration (CDIN) Study Section |
| 2007-present | Member, Scientific Advisory Board for A Genetic Linkage Study for GTS (TSAICG; 2U01NS040024-06A1; P.I. David Pauls) |
| 2008-present | Member, Executive Committee, Cooperative Ataxia Group |
| 2009-present | Melvin Greer Professor of Neurology |
| 2009 | The Hans Steinert Medal (for contribution to myotonic dystrophy research) by IDMC |

**C. Selected Peer-reviewed Publications**


1. Fu Y-H, Pizzuti A, Fenwick R, King J, Rajnarayan S, Dunne PW, Dubel J, Nasser GA, Ashizawa T, de Jong P, Wieringa B, Korneluk R, Perryman MB, Epstein HF, Caskey CT. An unstable triplet repeat in a gene related to myotonic muscular dystrophy. Science 1992;225:1256-1258
2. Fu Y-H, Friedman DL, Richards S, Pearlman JA, Gibbs RA, Pizzuti A, Ashizawa T, Perryman MB, Scarlato G, Fenwick RG, Jr, Caskey CT. Decreased expression of myotonin-protein kinase messenger RNA and protein in adult form of myotonic dystrophy. Science 1993;260:235-238
3. Ashizawa T, Anvret M, Baiget M, Barceló JM, Brunner H, Cobo AM, Dallapiccola B, Fenwick RG Jr, Grandell U, Harley H, Junien C, Koch MC, Korneluk RG, Lavedan C, Miki T, Mulley JC, López de Munain A, Novelli G, Roses AD, Seltzer WK, Shaw DJ, Smeets H, Sutherland GR, Yamagata H, Harper PS. Characteristics of intergenerational contractions of the CTG repeat in myotonic dystrophy. Am J Hum Genet 1994;54:414-423
4. Fu Y-H, Pearlman JA, Pizzuti A, Fenwick RG, Friedman DL, Perryman MB, Richards S, Gibbs RA, Ashizawa T, Scarlato G, Caskey CT. Muscle biochemistry and a genetic study of myotonic dystrophy. Science 1994;264:587-588
5. Krahe R, Eckhart M, Ogunniyi AO, Osuntokun BO, Siciliano MJ, Ashizawa T. *de novo* myotonic dystrophy mutation in a Nigerian kindred. Am J Hum Genet 1995;65:1067-1074
6. Tokgozoglu LS, Ashizawa T, Pacifico A, Epstein H, Zoghbi WA. Cardiac involvement in a large kindred with myotonic dystrophy:quantitative assessment and relation to expansion of CTG repeats. JAMA 1995;274:813-819
7. Zhuchenko O, Bailey J, Bonnen P, Ashizawa T, Stockton DW, Amos C, Dobyns WB, Subramony SH, Zoghbi HY, Lee CC. Autosomal dominant cerebellar ataxia (SCA6) associated with small polyglutamine expansions in the $\alpha$ 1A-voltage-dependent calcium channel. Nature Genet 1997;15:62-69
8. Matsuura T, Achari M, Khajavi M, Bachinski LL, Zoghbi HY, Ashizawa T. Mapping of the gene for a novel spinocerebellar ataxia with pure cerebellar signs and epilepsy. Ann Neurol 1999;45: 407-411 Matsuura, T., Yamagata, T., Burgess, D.L., Rasmussen, A., Grewal, R.P., Watase, K., Khajavi, M., McCall, A., Caleb F. Davis, C.F., Zu, L., Achari, M., Pulst, S.M., Alonso, E., Noebels, J.L., Nelson, D.L., Zoghbi, H.Y., Ashizawa, T. Large Expansion of ATTCT Pentanucleotide Repeat in Spinocerebellar Ataxia Type 10. Nat Genet 2000;26:191-194
9. Monckton DG, Cayuela ML, Gould FK, Brock GJR, de Silva R, Ashizawa T: Massive (CAG)n DNA repeat expansions in the sperm of spinocerebellar ataxia type 7 males. Hum Mol Genet 1999;8:2473-2478
10. Matsuura T, Fang P, Lin X, Khajavi M, Tsuji K, Rasmussen A, Grewal RP, Achari M, Alonso ME, Pulst SM, Zoghbi HY, Nelson DL, Roa BB, Ashizawa T. Somatic and germline instability of the ATTCT repeat in spinocerebellar ataxia type 10. Am J Hum Genet 2004:74;1216-1224.
11. Grewal RP, Achari M, Matsuura T, Durazo A, Tayag E, Zu L, Pulst SM, Ashizawa T. Clinical features and ATTCT repeat expansion in spinocerebellar ataxia type 10. Arch Neurol 2002;59:1285-1290.
12. Wakamiya M, Matsuura T, Liu Y, Schuster GC, Gao R, Xu W, Sarkar PS, Lin X, Ashizawa T. The role of ataxin 10 in the pathogenesis of spinocerebellar ataxia type 10. Neurology 2006;67:607-613.
13. Gatto EM, Gao R, White MC, Uribe Roca MC, Etcheverry JL, Persi G, Poderoso JJ, Ashizawa T. Ethnic origin and extrapyramidal signs in an Argentinean spinocerebellar ataxia type 10 family.

Neurology 2007; 69:216-218.
14. Teive HA, Munhoz RP, Raskin S, Arruda WO, de Paola L, Werneck LC, Ashizawa T. Spinocerebellar ataxia type 10: Frequency of epilepsy in a large sample of Brazilian patients. Mov Disord. 2010; 25:2875-2878.
15. White MC, Gao R; Xu W, Mandal SM, Lim JG, Hazra TK, Wakamiya M, Edwards SF, Raskin S, Teive HAG, Zoghbi HY, Sarkar PS, Ashizawa T. Inactivation of hnRNP K by Expanded Intronic AUUCU Repeat Induces Apoptosis via Translocation of PKCδ to Mitochondria in Spinocerebellar Ataxia 10. PLoS Genet. 2010; 6(6):e1000984.

**D. Research Support**

**Ongoing**

1. NIH/NINDS: 1RC1NS068897-01 (ARRA) 09/28/2009-09/27/2011
   Ashizawa (PI) $1,000,000 total cost
   Title: Clinical Research Consortium for Spinocerebellar Ataxias
   Effort: 1.38 calendar months
   This is an application for the Challenge Grant (RFA-OD-09-003) to establish clinical research consortium for spinocerebellar ataxias.
2. National Ataxia Foundation 07/01/2009-08/30/2011
   Subramony (PI), Ashizawa (Co-PI) $167,422 total cost
   Title: New initiative for clinical research on ataxia
   Effort: 1.2 calendar months

**Completed**

1. NIH/NINDS: 2R01NS041547-06 05/01/2006-03/30/2010
   Ashizawa (PI) $1,319,588 total cost
   Title: Pathogenic Mechanism of Spinocerebellar Ataxia Type 10.
   Effort: 2.4 calendar months
2. NIH/NINDS: 1U01NS050733-01A1 (subcontract) 09/24/2005-08/31/2010
   Newsom-Davis (PI), Ashizawa (site investigator; subcontract) $1,000 per enrollment
   Title: Thymectomy in non-thymomatous MG patients on Prednisone.
   Effort: 0.24 calendar months
3. Muscular Dystrophy Association 09/01/2009-08/31/2010
   Ashizawa (PI) $8,000
   Title: 7th Meeting of the International Myotonic Dystrophy Consortium (IDMC-7)
   Effort: 1.0 calendar month

**Invited Presentations (2010):**

2010 "Using Olfaction as an Early Detector of Age-Related Cognitive Decline", Annual Meeting for Center and Smell and Taste, University of Florida, Gainesville, FL

2010 "Development of Novel Cognitive Assessments for Age-related Neurodegenerative Disease", Alzheimer's Drug Discovery Foundation, New York, NY.

2010 "Normal and Pathological Aging Across Multiple Cognitive Domains: Insights from Cellular and Behavioral Studies", Joint Neurology/Neuroscience Grand Rounds, University of Florida College of Medicine, Gainesville, FL

**C. Selected Peer-reviewed Publications:**


1. Montgomery, K. S., Simmons, R.K., Edwards, G. 3rd, Nicolle, M. M., Meyers, C. A., Gluck, M., & Bizon, J. L. (*In Press*). Novel age-dependent learning deficits in a mouse model of Alzheimer's disease: Implications for translational research. *Neurobiol. Aging.* doi:10.1016/j.neurobiolaging.2009.08.003
2. Lim, C-S, Kim, Y-J, Hwang, Y-K, Banuelos, C, Bizon, J.L., Han, J-S Decreased Interactions in protein kinase A - glucocorticoid receptor signaling in the hippocampus after selective removal of the basal forebrain cholinergic input. *Hippocampus*.
3. Simon, N.W., LaSarge, C.L., Montomery, K.S., Williams, M.T., Mendez, I.A., Setlow, B., Bizon, J.L. (2010) Good things come to those who wait: attenuated discounting of delayed rewards in aging. *Neurobiol. Aging*, 31(5):853-62. PMCID in progress.
4. Bizon, J.L., LaSarge, C.L., Montgomery, K.S., McDermott, A.N., Setlow, B., & Griffith, W.G. (2009). Spatial Reference and working memory across the lifespan of Fischer 344 rats. *Neurobiol. Aging 30(4) 646-655.* PMCID: PMC2703480
5. LaSarge, C. L., Banuelos, C., Mayse, J. D., Bizon, J. L. (2009). Blockade of GABA(B) receptors completely reverses age-related learning impairment. *Neuroscience.* 164(3): 941-7. PMCID in progress
6. Murchison, D., Armstrong, G., Mieckowski, A. N., LaSarge, C. L., Bizon, J. L., Griffith, W. H. (2009). Cognitive performance in a spatial learning task is correlated with altered calcium homeostasis in basal forebrain neurons of aged Fischer 344 rats. *J Neurophysiol.* 102(4):2194-207. PMCID: PMC2775378
7. Simon, N.W., Gilbert, R.J., Mayse, J.D., Bizon, J.L., Setlow, B. (2009) Balancing Risk and Reward: A rat model of risky decision making. *Neuropsychopharmacology*, 43, 2208-2217. PMCID: PMC2726909
8. LaSarge, C.L., Montgomery, K.S., Tucker, C., Slaton, S.G.., Griffith, W.H., Setlow, B., & Bizon, J. L. (2007). Deficits across multiple cognitive domains in a subset of aged Fischer 344 rats. *Neurobiol. Aging,* 28(6):928-36
9. Sung, J-Y., Goo, S-E, Lee, D-E., Jin, D-Q., Bizon, J.L., Gallagher, M., Han, J-S. (2008) Learning strategy selection in the water maze and Hippocampal CREB phosphorylation differ in two inbred strains of mice. *Learning and Memory.* 15(4) 183-8. PMCID: PMC2327260
10. Montgomery, K. S., MacKey, J., Thuett, K., Ginestra, S., Bizon, J.L., Abbott, L. C. (2008) Chronic, low dose prenatal exposure to methylmercury impairs motor and mnemonic function in adult C57/B6 mice. *Behav. Brain Res.* 191(1): 55-61.
11. Bizon, J., Prescott, S., & Nicolle, M. M. (2007). Intact spatial learning in adult Tg2576 mice. *Neurobiol. Aging.* 28(2): 440-6.
12. Bizon, J.L., Gallagher, M. (2005) More is less: Neurogenesis and age-related cognitive decline in Long-Evans rats. *Science Aging Knowledge Environment. Science*. 16(7):re2.
13. Bizon, J.L., Lee, H-J, Gallagher, M. (2004) Neurogenesis in a cognitive model of aging. *Aging Cell* 3(4):227-34.
14. Bizon, J. L., Lauterborn, J, Isacson, P., Gall, C. (1996) Acidic Fibroblast growth factor is expressed by basal forebrain and striatal cholinergic neurons. *J. Comp. Neurol.,* 366: 379-389.

15. Nicolle, M., Bizon, J. L., Gallagher, M. (1996) In vitro autoradiography of ionotropic glutamate receptors in hippocampus and striatum of aged Long-Evans rats: Relationship to spatial learning. *Neuroscience*, 74 (3): 741-756.

**Abstract Presentations (2010 Only):**

1. Banuelos, C., LaSarge, C.L., Hartman, J.J., Ambrose, B.T., Gagliano, B.C., Graham, J.M., Gilbert, R.J., Bizon, J. L., Immunomarkers of GABAergic basal forebrain projection neurons are selectively elevated in cognitively-impaired aged F344 rats. . *Society for Neuroscience Abstracts,* 35.
2. Edwards III, G., Montgomery, K.S., Wilson, S.L., Zimmer, D.B., Roltsch, E., Bizon, J.L., S100A1-/- mice have attenuated odor detection abilities. *Society for Neuroscience Abstracts,* 35.
3. McQuail, J.A., Banuelos, C., LaSarge, C.L., Gilbert, R.J., Bizon, J.L., Nicolle, M.M. Baclofen-mediated GTP-binding is decreased in the prefrontal cortex, but not hippocampus of aged F344 rats. *Society for Neuroscience Abstracts,* 35.
4. Montgomery, K.S., Edwards III, G., Mathai, D., Burton, K. , Setlow, B., Bizon, J.L., Development of a noval, translational hippocampal-dependent learning assessment: Implications for early diagnosis of Alzheimer's Disease. *Society for Neuroscience Abstracts,* 35.
5. Mendez, I.A., Damborsky, J., Bizon, J.L., Winzer-Serhan, U., Setlow, B., The roles of nicotinic and muscarinic cholinergic receptors in cost-benefit decision-making. *Society for Neuroscience Abstracts,* 35.
6. Setlow, B., Simon, N.W., Beas, S., Montgomery, K.S., Giber, R.J., Mitchell, M.R., Habberman, R.P., Bizon, J.L., D2 dopamine receptor expression predicts distinct forms of impulsivity in rats. *Society for Neuroscience Abstracts,* 35.
7. Simon, N.W., Montgomery, K.S., Beas, B. S., LaSarge, C.L., Haberman, R.P., Bizon, J.L., Setlow, B.S. Dopamine receptor modulation of risky decision-making. *Society for Neuroscience Abstracts,* 35.
8. Dubois, D.W., Fincher, A.S., Wang, H., Banuelos, C., Gilbert, R.J., Bizon, J.L., Frye, G.D. Are GABA mpscs of MS/DB neurons distorted after early postnatal ethanol exposure followed by morris water maze training? *Society for Neuroscience Abstracts,* 35.
9. Beas, B.S., Huie, R, J., Mongomery, K.S., LaSarge, C.L., Baumbauer, K.M., Grau, J.W., Bizon, J.L., Instrumental learning enhances levels of BDNF mRNA in spinally transected rats. *Society for Neuroscience Abstracts,* 35.
10. Murchinson, D.A., Peebles, K.A., Gilber, R.J., Bizon, J.L., Griffith, W.H., Effects of aging on synaptic function in basal forebrain neurons of F344 rats: A possible link between calcium dysregulation and cognitive impairment. *Society for Neuroscience Abstracts,* 35.

**D. Research Support**

List both selected ongoing and completed research projects for the past three years (Federal or non-Federally-supported). *Begin with the projects that are most relevant to the research proposed in the application.* Briefly indicate the overall goals of the projects and responsibilities of the key person identified on the Biographical Sketch. Do not include number of person months or direct costs.

**Ongoing:**

R01 AG02942 (Jennifer L. Bizon, PI) 8/1/07-6/30/12 35% effort
National Institute on Aging $226,359direct/year
"Basal Forebrain and Cognitive Aging: Novel Experimental and Therapeutic Avenues"

*The goal of this project is to determine how changes in cholinergic and GABAergic basal forebrain neuron structure and function relate to cognitive decline in aging, and to ameliorate such decline by pharmacologically targeting these neurons.* No overlap.

R01-NS041548 (Grau PI, Bizon, co-I) 4/07-3/11 15% effort
National Institute of Neurological Disorder and Diseases $246,948 direct/yr
"Learning within the spinal cord: clinical implications"
*The goal of this grant is to study the role of BDNF in spinal cord learning.* No overlap.

R01 DA024671 (B. Setlow PI, Bizon co-PI) 4/1/09-3/31/14 15% effort
National Institute on Drug Abuse $205,000 direct/year
"Neural mechanisms of enduring cocaine effects on impulsive choice"
*The goal of this project is to understand the long-term effects of cocaine use on decision making and to begin to elucidate the neurobiology associated with impulsivity resulting from psychostimulant drug use.* No overlap.

F31- NS059324 (Candi Lynn LaSarge student, Bizon Sponsor) 6/1/08- 12/1/10 n/a
National Institute of Neurological Disorders and Stroke $92,123 direct/total
"The Role of Basal Forebrain in Mild Cognitive Impairment"
*The goal of the project under this training fellowship is to determine how changes in basal forebrain anatomy are related to cognitive dysfunction in aging.*

F31-AG037286-01 (Karienn Montgomery student. Bizon Sponsor) 8/1/10-8/1/13 n/a
National Institute of Aging $102,294 direct/total
Transfer Learning in Mice: Implications for improved diagnosis and treatment of Alzheimer's Disease
*The goal of this study is to design novel behavioral assessments that are very sensitive to age-related pathology and tat are highly translational.*

**Pending:**

Jennifer L. Bizon PI 5/11-5/13 15% effort
*Development of Highly Translational Cognitive Assessments and Novel Therapeutic Avenues for Alzheimer's Disease*
Alzheimer's Drug Discovery Foundation $150,000 direct/year
The goal of the project is to develop and validate novel rodent assessments for age-related memory loss in normal and pathological aging and to assess novel avenues for treatment of age-related memory loss by targeting the GABAergic system.

**Completed:**

R01-DA13188 (PJ Wellman PI, Bizon co-I) 8/01/07-6/30/10 15% effort
National Institute of Drug Abuse
"Heavy Metal and Drug Self-Administration: Mechanisms"
*The goal of this project is to determine how exposure to heavy metals (lead, cadmium) during development affects vulnerability to drug abuse during adulthood.*

R01-AA012386 (G Frye PI, Bizon co-I) 8/1/08-8/1/10 10% effort
National Institute on Alcohol Abuse and Alcoholism
"CNS Development GABAARs and Vulnerability to Ethanol"
*The goal of this project is to determine how developmental exposure to alcohol affects basal forebrain neuronal function and cognition later in life.*

F31- DA023331 (NW Simon PI, Bizon co-sponsor) 2/1/08-2/1/10 n/a
National Institute on Drug Abuse
"Long-term cocaine effects on impulsive choice and orbitofrontal cortex activity"

*The goal of the project under this training fellowship is to determine how chronic cocaine exposure affects impulsive decision-making and orbitofrontal cortex function.*

# CURRICULUM VITAE


| | |
|---|---|
| Name: | Thomas C. Foster |
| Address: | Evelyn F. & William L. McKnight Brain Institute<br>University of Florida<br>College of Medicine<br>Department of Neuroscience<br>PO Box 100244<br>Gainesville, FL 32610-0244 |
| Telephone: | (352) 392-4359 |
| Fax: | (352) 392-8347 |
| E-mail: | foster@mbi.ufl.edu |


**EDUCATION:**

B.S. (Psychology, Biology/Chemistry)
Honors and Distinction
University of Arizona
Tucson, Arizona, 1981

Ph.D. (Physiology/Pharmacology)
Bowman Gray School of Medicine
Winston-Salem, North Carolina, 1987

**PROFESSIONAL ASSOCIATIONS**

| | |
|---|---|
| 1989-present | Society for Neuroscience |
| 2006-Present | Gerontology Society of America |

**ADVISING ACTIVITIES**

Doctoral Trainees

Travis Jackson 2006-2010
Karthik Bodhinathan 2006-2010
Wei-Hua Lee 2007-present
Xiaoxia Han 2010- present
Mike Guidi 2010- present

Postdoctoral Trainees

Ashok Kumar, Ph.D. 2000-present.

**ADMINISTRATIVE ACTIVITY**

2009-present Chair for the committee overseeing the Age-Related Memory Loss (ARML) Program.

2009-present Member of the Institute on Aging and Pepper Center Executive Committee

| | |
|---|---|
| 2009-2010 | Chair for the Search Committee to find a Program Director and Professor for the Cognitive Aging and Memory Clinical Translational Research Program (CAM-CTRP). |
| 2010 | Member of the Search Committee to find an Assistant Program Director for the CAM-CTRP. |

## NATIONAL AND INTERNATIONAL PROFESSIONAL ACTIVITY

Associate Editor Frontiers in Aging Neuroscience 2009-present

Chairman, and Session Organizer for a session on: Altered networks in aging. 22th Annual Winter Conference on Neural Plasticity, Aruba Caribbean.

Organizer for McKnight Brain Research Foundation Third Inter-Institutional Meeting. University of Florida, Gainesville, Fl.

Organizer for the Cognitive Aging Summit II.

## NATIONAL AND INTERNATIONAL SPEAKING ENGAGEMENTS

International

Redox state and altered NMDA receptor function during aging. (Feb, 2010). 22th Annual Winter Conference on Neural Plasticity, Aruba Caribbean.

Linking oxidative stress of aging to the senescent neurophysiology of cognitive decline. (Oct 2010). Cognitive Aging Summit II, Washington DC.

National

Moderator for a Panel Discussion on Clinical studies from trials to cohort: Moving from experimental observation to clinical trials. (April 2010). McKnight Brain Research Foundation Third Inter-Institutional Meeting. University of Florida, Gainesville, Fl.

Recent progress in understanding age-related memory decline (April 2010). Centers for Neuropsychological Studies Veterans Administration Hospital, Gainesville FL.

Synaptic plasticity in the aging brain. (Sept 2010). University of Florida First Annual Society for Neuroscience Chapter Conference, Gainesville, Fl

Linking oxidative stress of aging to the senescent neurophysiology of cognitive decline. (Oct 2010). Cognitive Aging Summit II, Washington DC.

Linking oxidative stress of aging to the senescent neurophysiology of cognitive decline (Oct 2010). Florida Atlantic University, Boca Raton, FL.

## CURRENT EXTRAMURAL GRANT SUPPORT (2009)

**As Principal Investigator**

NIA R01 AG14979 (**Foster** PI) Mechanisms of altered synaptic function during aging, 6/01/07 to 5/31/2012, $184,500/year.

NIMH R01 MH59891 (**Foster** PI) Estrogen and cognition over the lifespan, 12/01/01 to 8/18/10. $185,000/year.

*New*
NIA R56 AG037984 (**Foster** PI) Estrogen and cognition over the lifespan, 9/15/2010 to 8/31/2011. $185,000.

NIA R01AG036800 (**Foster** PI) Signaling cascades and memory deficits during aging, 10/05/2010 to 08/31/2014 $ 292,147/year.

**As Co-Principal Investigator**
NINDS RO1 NS041012 (Notterpek PI) Cellular events in heritable peripheral neuropathies 07/01/05 to 06/30/2010, $225,000.

**As Preceptor**
NIA T32 (Meyer PI, Scarpace Co-PI) Training in Neurobiology of Aging. 5/1/06 to 4/30/11, $1,183,067 direct costs.

## PUBLICATIONS

### ARTICLES

Aenlle KK, **Foster** TC (2010) Aging alters the expression of genes for neuroprotection and synaptic function following acute estradiol treatment. Hippocampus 20:1047-1060.

Bodhinathan K, Kumar A, **Foster** TC (2010a) Intracellular redox state alters NMDA receptor response during aging through Ca2+/calmodulin-dependent protein kinase II. J Neurosci 30:1914-1924.

Bodhinathan K, Kumar A, **Foster** TC (2010b) Redox sensitive calcium stores underlie enhanced after hyperpolarization of aged neurons: role for ryanodine receptor mediated calcium signaling. J Neurophysiol 104:2586-2593.

Jackson TC, Verrier JD, Semple-Rowland S, Kumar A, **Foster** TC (2010) PHLPP1 splice variants differentially regulate AKT and PKCalpha signaling in hippocampal neurons: characterization of PHLPP proteins in the adult hippocampus. J Neurochem 115:941-955.

Zeier Z, Madorsky I, Xu Y, Ogle WO, Notterpek L, **Foster** TC (2010) Gene Expression in the Hippocampus: Regionally Specific Effects of Aging and Caloric Restriction. Mech Ageing Dev. In press.

Carter, C.S., Giovaninni, S., Seo, D., DuPree, J., Morgan. D., Chung, H.Y., Lees, H., Daniels, M., Hubbard, G., Lee, S., Ikeno, Y., **Foster**, T.C., Buford, T., Marzetti, E. (2010) Differential effects of enalapril and losartan on body composition and indices of muscle quality in aged male Fischer 344 x Brown Norway rats. Age, in press.

**Foster**, T.C. (2010) Role of estrogen receptor alpha and beta expression and signaling on cognitive function during aging. Hippocampus, accepted with revisions.

Aenlle, K.A. and **Foster**, T.C. (2010) Gene expression and signal transduction cascades mediating estrogen effects on memory. In J.Clelland (Ed.) Handbook of Neurochemistry and Molecular Neurobiology, Volume Number 13. Genomics, Proteomics and the Nervous System.

Guidi, M. and Foster, T.C. (2010) Animal model of memory and cognitive disorders. In F.H. Kobeissy (Ed.) Psychiatric disorders: Methods and Protocols, Volume *. Methods in Molecular Biology Springer, USA (Humana Press, Inc)

Carter, C.S., Marzetti1, E., Leeuwenburgh, C., Manini, T., **Foster**, T.C., Groban, L., Scarpace, P.J. and Morgan, D. Usefulness of preclinical models for assessing the efficacy of late-life interventions for sarcopenia. Journal of Gerontology, submitted.

Whidden, M. A., Kirichenkoa, N., Erdosa, B., **Foster**, T. C. and Tümer, N. Lifelong caloric restriction reverses age-induced oxidative stress in the sympathoadrenal system. Submitted.

## RECENT ABSTRACTS

K. Bodhinathan, A. Kumar, T. C. Foster (2010) Altered redox state contributes to increased afterhyperpolarization of hippocampal CA1 pyramidal neurons during senescence: role for ryanodine receptor oxidation. Soc. Neurosci. Abstr

J. Herrera, A. Kumar, A. Rani, T. C. Foster (2010) Differential influence of environmental enrichment and exercise on learning and memory, synaptic plasticity, and neuronal excitability during senescence. Soc. Neurosci. Abstr

W.H. Lee, A. Kumar, A. Rani, J. Herrera, T. C. Foster (2010) Influence of viral vector-mediated delivery of superoxide dismutase and catalase to the hippocampus on spatial learning and memory over the course of aging. Soc. Neurosci. Abstr

R.B. Speisman, A. Kumar, A. Rani, J.E. Severence, T. C. Foster, B.K. Ormerod (2010) Enrichment concomitantly improves hippocampal neurogenesis and spatial memory in aged rats. Soc. Neurosci. Abstr

## BIOGRAPHICAL SKETCH

Provide the following information for the Senior/key personnel and other significant contributors in the order listed on Form Page 2.
Follow this format for each person. **DO NOT EXCEED FOUR PAGES.**

| NAME | POSITION TITLE |
|---|---|
| Leeuwenburgh, Christiaan | Professor |
| eRA COMMONS USER NAME (credential, e.g., agency login)<br>cleeuwen | |

EDUCATION/TRAINING *(Begin with baccalaureate or other initial professional education, such as nursing, include postdoctoral training and residency training if applicable.)*

| INSTITUTION AND LOCATION | DEGREE *(if applicable)* | MM/YY | FIELD OF STUDY |
|---|---|---|---|
| University of Florida, Gainesville | BS | 1986-1988 | Applied Physiology |
| University of Florida, Gainesville | MS | 1988-1990 | Applied Physiology |
| University of Illinois, Urbana-Champaign | PhD | 1990-1995 | Biochemistry and Aging |
| University of Wisconsin, Madison | Pre-Fellow* | 1993-1995 | Biochemistry and Aging |
| Washington Univ. School of Medicine, St Louis | Post-Fellow | 1995-1998 | Biochemistry and Aging<br>Geriatrics & Gerontology |

### A. Personal Statement

The goal of the Mouse Metabolism Phenotyping Center (University of Florida) and the Mitochondria and Metabolism Core (Core C) is that it will offer novel technology platforms to assess mitochondrial biology and function. Analysis of mitochondrial function is central to the study of energy metabolism and its involvement in metabolic disorders and diseases. The Center supports the hypothesis that mitochondrial dysfunction is a major cause of metabolic diseases. Since important functional properties of mitochondria differ *in vitro* and *in vivo*, we will utilize two innovative and novel techniques to assess mitochondrial function in freshly isolated intact tissues and in living animals, respectively: 1) high-resolution respirometry; and 2) intravital multiphoton excitation laser-scanning microscopy. In addition to data obtained using these two major analytical tools, we will also offer investigators the option to obtain a select panel of standard biochemical analyses of mitochondrial function and damage (enzyme assays, HPLC-EC, and Western blot) to obtain a consistent portable data set.

I have served as the Core leader for the past 5 years overseeing research studies and career development for a Genomics and Biomarkers Core of the Institute on Aging and as the Core Leader of the Career Development Core of the NIH P30-funded Claude D. Pepper Older Americans Independence Center (UF-OAIC). In the UF-OAIC, I have guided OAIC scholars and ensured that they have received necessary scientific training and career development mentoring.

In the MMPC (UF), I will serve as both Co-PD/PI and Co-Leader of the Administrative Core (Core A) as well as the Mitochondria and Metabolism Core (Core C). In Core A, I will be responsible for working closely with Dr. Hsu to provide oversight of all Administrative Core activities as described. The Mitochondria and Metabolism Core C, provides the necessary infrastructure such as laboratory space and equipment necessary to perform translational research. In addition, Core personnel provide consultations regarding many methodologies (Confocal imaging, high resolution respiration, HPLC-EC, Western blot, etc.).

I received my PhD from the University of Illinois, Urbana-Champagne in 1995 which focused on the regulation of glutathione homeostasis (major intracellular redox regulator) during chronic glutathione deficiencies and/or supplementation. I completed my postdoctoral studies in Internal Medicine, Division of Geriatrics and Gerontology and Division of Atherosclerosis, Nutrition and Lipid Research at Washington University School of Medicine, Saint Louis with Drs John Holloszy and Jay Heinecke as major mentors. My major research focus is to better understand the molecular mechanisms of mitochondrial dysfunction, inflammation, oxidative stress, autophagy and programmed cell death (apoptosis) with disease conditions (atherosclerosis, diabetes, and with aging). I have participated in various NIH study sections, NIH workshops and have published papers in The Journal of Biological Chemistry, American Journal of Physiology, PLoS One, Journal of Gerontology, FASEB

Journal, Experimental Gerontology, Neurobiology of Aging, Rejuvenation Research, Aging Cell, Journal of Clinical Investigation and Science. Recently, we have been fortunate enough to publish papers in *Cell* and *PNAS*. Our work on the assessment of mitochondrial dysfunction, mitochondrial mediated apoptosis, and oxidative damage has been increasingly recognized and appreciated by scientist worldwide. I am also an editor for Experimental Gerontology. I have a strong background in biochemistry and physiology. As PI or co-Investigator on several university- and NIH-funded grants, my research and skill set make me the natural choice for co-leading Core C and further investigating the mechanisms of aging. In addition, I successfully administered several large projects (e.g. staffing, budget), collaborated with multiple other researchers, and produced extensive peer-reviewed publications (27 papers in 2009-2010) and therefore will have a major contribution in co-leading Core A. As a result of these experiences, I am aware of the importance of frequent communication among my staff and project leaders and of constructing a realistic research plan, timeline, and budget. Therefore, the Center and Core duties build logically on my prior work. In addition, with Drs. Jae-Sung Kim, Jinze Xu, and Anna-Maria Joseph, as co-leaders and staff we will provide added expertise in analytical chemistry, mitochondria biology, and imaging. As a scientist, my goal is to bridge the gap between basic and clinical sciences, focusing on biological mechanisms which regulate metabolisms and disease and testing translational interventions.

## B. Positions and Honors

**Positions and Employment**

| | |
|---|---|
| 1995–1998 | Washington University School of Medicine, St. Louis, Department of Internal Medicine, Divisions of Geriatrics and Gerontology, and Atherosclerosis, Nutrition and Lipid Research Postdoctoral Fellow in Internal Medicine and Geriatrics and Gerontology; Research Associate in Medicine; Adjunct Instructor; Mentors: John O. Holloszy, MD and Jay W. Heinecke, MD |
| 1998– | Faculty Associate of the Institute on Aging and Center for Gerontological Studies |
| 1998–2002 | Assistant Professor and Director of the Biochemistry of Aging Laboratory, University of Florida |
| 2002–2005 | Associate Professor and Director of the Biochemistry of Aging Laboratory, University of Florida |
| 2005–2007 | Associate Professor, College of Medicine, Department of Aging and Geriatric Research |
| 2006– | Chief, Division of Biology of Aging, Department of Aging and Geriatrics |
| 2005– | Director, Genomics and Biomarkers Core of the University of Florida Institute on Aging |
| 2005 | Joint and Affiliate Faculty, Departments of Anatomy and Cell Biology, Biochemistry and Molecular Biology |
| 2007– | Professor, College of Medicine, Department of Aging and Geriatrics, Division of Biology of Aging |

**Other Experience and Professional Memberships**

| | |
|---|---|
| 2010 | NIH Study Section CMAD. |
| 2004-Present | NIH Peer Review Committees; Special Emphasis Panels and PO1 reviews. |
| 2003- | Member, American Aging Association |
| 2003- | Member, Gerontological Society of America |
| 1997- | The American Physiological Society |
| 1995-2008 | Society for Free Radical Biology and Medicine |
| 1995-2008 | International Society for Free Radical Research |
| 2008- | Editor, Experimental Gerontology |

**Honors**

| | |
|---|---|
| 2010 | University of Florida Exemplary Teaching Award, College of Medicine |
| 2004 | Nathan W. Shock Lecture Award Winner, National Institute on Aging (Nathan W. Shock was a former scientific director of the NIA and an NIH Scientist Emeritus) |
| 2004–2005 | University of Florida Research Foundation, Professor Award |
| 2000 | American Heart Association, Young Investigator Award, FL |
| 1997–1998 | National Research Service Award, NRSA-NIH, National Institute of Aging |
| 1993–1995 | American Heart Association, Pre-doctoral Fellowship, Illinois Affiliate, completed dissertation at the University of Wisconsin. |

**C. Selected Peer-reviewed Publications** (Selected from 140 peer-reviewed publications)

**Most relevant to the current application** (1-14)


1. Seo, A.Y., Joseph, A.M., Dutta, D., Hwang, J.C., Aris, J.P., and Leeuwenburgh, C. 2010. New insights into the role of mitochondria in aging: mitochondrial dynamics and more. *J Cell Sci* 123:2533-2542.
2. Hiona, A., Sanz, A., Kujoth, G.C., Pamplona, R., Seo, A.Y., Hofer, T., Someya, S., Miyakawa, T., Nakayama, C., Samhan-Arias, A.K., et al. 2010. Mitochondrial DNA mutations induce mitochondrial dysfunction, apoptosis and sarcopenia in skeletal muscle of mitochondrial DNA mutator mice. *PLoS One* 5:e11468.
3. Someya, S., Xu, J., Kondo, K., Ding, D., Salvi, R.J., Yamasoba, T., Rabinovitch, P.S., Weindruch, R., Leeuwenburgh, C., Tanokura, M., et al. 2009. Age-related hearing loss in C57BL/6J mice is mediated by Bak-dependent mitochondrial apoptosis. *Proc Natl Acad Sci U S A* 106:19432-19437.
4. Bailey, L.J., Cluett, T.J., Reyes, A., Prolla, T.A., Poulton, J., Leeuwenburgh, C., and Holt, I.J. 2009. Mice expressing an error-prone DNA polymerase in mitochondria display elevated replication pausing and chromosomal breakage at fragile sites of mitochondrial DNA. *Nucleic Acids Res* 37:2327-2335.
5. Strong, R., Miller, R.A., Astle, C.M., Floyd, R.A., Flurkey, K., Hensley, K.L., Javors, M.A., Leeuwenburgh, C., Nelson, J.F., Ongini, E., et al. 2008. Nordihydroguaiaretic acid and aspirin increase lifespan of genetically heterogeneous male mice. *Aging Cell* 7:641-650.


**Additional publications of importance to the field**


6. Judge, S., and Leeuwenburgh, C. 2007. Cardiac mitochondrial bioenergetics, oxidative stress, and aging. *Am J Physiol Cell Physiol* 292:C1983-1992.
7. Hofer, T., Seo, A.Y., Prudencio, M., and Leeuwenburgh, C. 2006. A method to determine RNA and DNA oxidation simultaneously by HPLC-ECD: greater RNA than DNA oxidation in rat liver after doxorubicin administration. *Biol Chem* 387:103-111.
8. Kujoth, G.C., Hiona, A., Pugh, T.D., Someya, S., Panzer, K., Wohlgemuth, S.E., Hofer, T., Seo, A.Y., Sullivan, R., Jobling, W.A., et al. 2005. Mitochondrial DNA mutations, oxidative stress, and apoptosis in mammalian aging. *Science* 309:481-484.
9. Julian, D., and Leeuwenburgh, C. 2004. Linkage between insulin and the free radical theory of aging. *Am J Physiol Regul Integr Comp Physiol* 286:R20-21.
10. Drew, B., and Leeuwenburgh, C. 2003. Method for measuring ATP production in isolated mitochondria: ATP production in brain and liver mitochondria of Fischer-344 rats with age and caloric restriction. *Am J Physiol Regul Integr Comp Physiol* 285:R1259-1267.
11. Pennathur, S., Wagner, J.D., Leeuwenburgh, C., Litwak, K.N., and Heinecke, J.W. 2001. A hydroxyl radical-like species oxidizes cynomolgus monkey artery wall proteins in early diabetic vascular disease. *J Clin Invest* 107:853-860.
12. Leeuwenburgh, C., Hansen, P., Shaish, A., Holloszy, J.O., and Heinecke, J.W. 1998. Markers of protein oxidation by hydroxyl radical and reactive nitrogen species in tissues of aging rats. *Am J Physiol* 274:R453-461.
13. Tribble, D.L., Gong, E.L., Leeuwenburgh, C., Heinecke, J.W., Carlson, E.L., Verstuyft, J.G., and Epstein, C.J. 1997. Fatty streak formation in fat-fed mice expressing human copper-zinc superoxide dismutase. *Arterioscler Thromb Vasc Biol* 17:1734-1740.
14. Leeuwenburgh, C., Rasmussen, J.E., Hsu, F.F., Mueller, D.M., Pennathur, S., and Heinecke, J.W. 1997. Mass spectrometric quantification of markers for protein oxidation by tyrosyl radical, copper, and hydroxyl radical in low density lipoprotein isolated from human atherosclerotic plaques. *J Biol Chem* 272:3520-3526.
15. Someya S, Yu W, Hallows WC, Xu J, Vann JM, Leeuwenburgh C, Tanokura M, Denu JM, Prolla TA. Mitochondrial Sirt3 mediates the effects of caloric restriction on oxidative stress reduction and prevention of age-related hearing loss. *Cell* 2010 143;1-11.

## D. Research Support

**Ongoing Research Support**

2RO1 AG 17994-06 NIH (Leeuwenburgh) 7/01/2006-6/30/2011
National Institute of Health/National Institute of Aging $1,250,000
Project Title: Molecular Mechanisms of Oxidative Stress in Aging Muscle
The major goals for this project are to study mitochondrial function, energy production and oxidative stress with age in cardiac and skeletal muscle.

NIA R01AG14979-10A1 (Foster) 6/6/2007–5/31/2012
Project Title: Mechanism for altered synaptic function during aging $138,615
The aim of these studies is to investigate the molecular mechanisms of synaptic function during aging and potential interventions.
Role: Co-Investigator

1 P30 AG028740-01(Pahor) 04/01/2007-03/31/2012
NIH/NIA $630,368
Claude D. Pepper Older Americans Independence Center (OAIC)
The major goals of this program are to assess the mechanisms leading to sarcopenia and functional decline, and to develop and test interventions for the treatment and prevention of physical disability in older adults.
Metabolisms and Biomarkers Core: PI
Research Development Project #1: PI

**Completed Research Support**

RO1 AG 21042-3 Leeuwenburgh (PI) 08/01/2003-07/31/2009
National Institute of Health/National Institute of Aging $1,250,000
Project Title: Apoptosis and life-long caloric restriction
The goal of this project is to better understand the basic mechanisms of signaling transduction pathways of apoptosis with age.
Role: PI

## BIOGRAPHICAL SKETCH

| NAME | POSITION TITLE |
|---|---|
| Brandi K. Ormerod | Assistant Professor |
| eRA COMMONS USER NAME | 130 BME Building, Biomedical Engineering |
| BORMEROD | University of Florida, Gainesville, FL, 32608 |

EDUCATION/TRAINING

| INSTITUTION AND LOCATION | DEGREE *(if applicable)* | YEAR(s) | FIELD OF STUDY |
|---|---|---|---|
| Queen's University, Kingston, ON, Canada | B.Sc. | 1998 | Biopsychology |
| University of British Columbia, Vancouver, BC, Canada | Ph.D. | 2003 | Neuroscience |
| Stanford University, Stanford, California | PDF | 2006 | Stem Cell Science |

### A. Personal Statement

I have been conducting scientific research since 1996. My expertise lies in behavioral testing (water maze tasks, radial maze tasks, conditioned reward and place preference tasks, t-maze, motor behavior tasks, open field behavior, which I learned under the guidance of Dr. Richard Beninger and Dr. Liisa Galea), adult neurogenesis work (with emphasis upon how the endocrine and immune systems regulate it under the guidance of Dr. Liisa Galea and Dr. Theo Palmer) and in vitro neural progenitor cell behavior (I have established and characterized fetal, postnatal and adult lines of primate and rodent NPCs under the guidance of Dr. Theo Palmer). I have trained many students as a PhD student at the University of British Columbia, post-doctoral fellow at Stanford University and now as a professor at the University of Florida. These students have moved onto the medical school, graduate school and industry. I currently mentor or have mentored 12 undergraduate students who have received Howard Hughes Medical Institute sponsored UF Science for Life Program. Two of these students are currently in medical school and two are in graduate school. My Co-PI and outstanding colleague Dr. Khargonekar is a renowned expert in signal processing and systems and will generate the models to predict cytokine(s) that regulate adult hippocampal neurogenesis. We have personally trained the students who will work on the project. These students show excellent promise as young scientists and watching them interact in our regular lab meetings has been exciting as we forge this truly interdisciplinary, novel and promising line of research.

### B. Positions and Honors

**Positions and Employment**

1996-1998 Undergraduate Research Assistant in Dr. Beninger's Behavioral Pharm Laboratory (Queen's)
1997-1998 Undergraduate Research Assistant in Dr. Weisman's Avian Bioaccoustics Laboratory (Queen's)
1997-1998 Undergraduate Teaching Assistant for 4$^{th}$ yr Behavioral Pharmacology (Queen's University)
1998-1999 Teaching asst for 2$^{nd}$ yr Psych of Gender/Laboratory Instructor for 3$^{rd}$ yr Biopsych (UBC)
1999-2000 Teaching asst for 2$^{nd}$ yr Biopsych and Gender Psych and 4$^{th}$ yr Neuroplasticity (UBC)
2000-2001 Teaching asst for 2$^{nd}$ yr Biopsych and Gender Psych, 3$^{rd}$ yr Stats, 4$^{th}$ yr Neuroplasticity (UBC)
2001-2002 Laboratory Instructor for 2$^{nd}$ yr Biopsych/Teaching asst for 3$^{rd}$ yr Biopsych/4$^{th}$ yr Neuroplasticity
2003-2006 Postdoctoral Stem Cell Researcher, Palmer Lab, Neurosurgery Dept, Stanford University
Since 2006 Assistant Professor, Biomedical Engineering Dept, University of Florida

**Awards/Honors**

1998 Faculty of Graduate Studies Travel Award (UBC; CDN$400)
1999 Natural Sciences and Engineering Research Council of Canada Scholarship A (UBC; $34,600)
2001 Natural Sciences and Engineering Research Council of Canada Scholarship B (UBC; $38,400)
2001 Killam Predoctoral Fellowship (UBC; CDN$44,000 - $24,000 top-up accepted)
2001 Killam Predoctoral Fellowship Travel Award (UBC; CDN$1,500)
2001 Alzheimers Society of Canada Predoctoral Fellowship (UBC; CDN$44,000 – declined)
2002 Invited to introduce UBC president Dr. Martha Piper at the first Nobel Awardee Michael Smith Honorary "Women at the Frontiers of EXXcellence" Conference opening ceremony
2003 UBC Brain Research Centre "3D Microscopy of Living Cells Course" scholarship (US$2,250)
2003 Society for Neuroscience Chapters Travel Award (US$735)
2003 Michael J. Fox Foundation Postdoctoral Fellowship (US$78,000)

| | |
|---|---|
| 2003 | Natural Sciences and Engineering Research Council of Canada Fellowship (Stanford; $40,000) |
| 2003 | NIH CHOC Human Embryonic Stem Cell Course (Burnham Institute; Scholarship Bursary; $1,500) |
| 2004-2006 | Chair of the Stanford Brain Food Bimonthly Seminar Series |
| Since 2007 | UF College of Engineering Faculty Track Graduate Student Mentor |

**Committee Service**

| | |
|---|---|
| 2007 | Scientific Consultant on Aging and Cloning to the American Federation for Aging Research |
| Since 2007 | Ad Hoc Reviewer for the Maryland Funded TEDCO Stem Cell Competition |
| Since 2007 | Ad Hoc Reviewer for the University of Washington Alzheimer's Disease Research Center Competition |
| 2008/9 | UF Biomedical Engineering Faculty Search Committee |
| 2008/9 | UF Neuroscience Faculty Search Committee |
| Since 2010 | Ad Hoc Reviewer for the US-Israel Binational Science Foundation |

## B. Publications

**Peer-reviewed Publications**

1. Xu, Y., Wang R., Ormerod B.K., Ogle, W.O. (2010). Phytochemical antidepressant activity may work by protecting adult hippocampal neurogenesis from the effects of dysregulated serotonin signaling and stress responses.
2. Seifert AW[a], Ormerod BK*, Cohn MJ* (2010). Sonic hedgehog regulates cell cycle kinetics during morphogenesis. Nature Communications. 1:23. *Corresponding Authors.
3. Peltier J., Ormerod B.K. and Schaffer D.V. (2010). Isolation of adult hippocampal neural progenitors. Methods Mol Biol. 621:57-63.
4. Ormerod BK*, Hanft S[c], Lee SW[c] and Palmer TD*. (2010). Delayed memory impairment follows the interruption of adult neurogenesis by transient illness. Neuroscience. *Corresponding Authors.
5. Stratmann G, Sall JW, Rehan SA, May L, Rau V, McCulloch CE, Ormerod BK, Zusmer EJ, Bell JS, Lee, MT, Guggenheim J., Firouzian A, Dai R. (2009). Effect of hypercarbia and isoflurane on brain cell death and neurocognitive dysfunction in 7-day-old rats . Anesthesiology, 110:849-861 (JCR 2007 Impact 4.596).
6. Krevala A, Ormerod B.K., Palmer TD, Calos M (2008). Long-term gene expression in PhiC31 integrase-modified mouse neural progenitor cells. Journal of Neuroscience Methods, 173:299-305 (JCR 2007 Impact 1.884).
7. Ormerod BK., Palmer TD and Caldwell MA (2008). Stem Cells and Neurodegeneration. Philosophical Transactions of the Royal Society: Biological Sciences, 363; 153-170 (JCR 2007 Impact 5.529).
8. Buckwalter MS, Yamane M., Coleman B.S., Ormerod BK, Chin J.T., Palmer TD, Wyss-Coray T. (2006). TGF-β1 overproduction results in an age-related decrease in hippocampal neurogenesis. American Journal of Pathology, 169:154-164(JCR 2007 Impact 5.487).
9. Nagy A.I[c], Ormerod BK, Mazzucco C[c]. and Galea LAM. (2006) Estradiol-Induced Enhancement in Cell Proliferation is Mediated through Estrogen Receptors in the Dentate Gyrus of Adult Female Rats. Drug Development Research, 66; 1-8 (JCR 2007 Impact 0.976).
10. Hill MN[c], Patel S, Carrier EJ, Rademacher DJ, Ormerod BK, Hillard CJ, Gorzalka BB (2005) Downregulation of endocannabinoid signaling in the hippocampus following chronic unpredictable stress. Neuropsychopharmacology. 30:508-15 (JCR 2007 Impact 6.157).
11. Ormerod BK, Lee TT-Y[c] and Galea LAM (2004) Estradiol enhances neurogenesis in the dentate gyri of adult male meadow voles by increasing the survival of young neurons. Neuroscience, 128: 645-654(JCR 2007 Impact 3.352).
12. Ormerod BK, Falconer EM[c] and Galea LAM (2003). NMDA receptor activity and estradiol: Separate regulation of cell proliferation in the dentate gyrus of adult female meadow voles. Endocrinology, 179:155-163 (JCR 2007 Impact 5.045).
13. Ormerod BK and Galea LAM (2003). Reproductive status influences the survival but not production of new cells in the dentate gyrus of adult male meadow voles. Neurosci Letters, 346:25-28 (JCR 2007 Impact 2.045).
14. Ormerod BK, Lee TT-Y[c] and Galea LAM (2003). Estradiol enhances but subsequently suppresses (via adrenal steroids) granule cell proliferation in the dentate gyrus of adult female rats. J Neurobio, 55, 247-260 (JCR 2007 Impact 3.047).
15. Ormerod BK, Beninger RJ (2002). Water maze versus radial maze: differential performance of rats in a spatial delayed match-to-position task and response to scopolamine. Behav Brain Res, 128, 139-152 (JCR 2007 Impact 2.626).

16. Ormerod BK and Galea LAM (2001). Reproductive status regulates cell proliferation and survival in the dentate gyrus of adult female meadow voles: A possible role for estradiol. Neurosci, 102, 369-379 (JCR 2007 Impact 3.352).
17. Galea L.A.M., Wide J.K.[c], Paine T.A.[c], Holmes M.M., Ormerod B.K., and Floresco S.B. (2001). High levels of estradiol disrupt conditioned placed preference learning, stimulus response learning and reference memory but have limited effects on working memory. Behav Brain Res, 126, 115-126 (JCR 2007 Impact 2.626).
18. Beauchamp M., Ormerod BK, Jhamandas K., Boegman R.J. and Beninger R.J. (2000). Neurosteroids and reward: Allopregnanolone produces a conditioned place aversion in rats. Pharm, Biochem, Behav, 67, 29-35 (JCR 2007 Impact 2.355).
19. Galea LAM, Ormerod BK, Sampath S.[c], Kostaras X[c], Wilkie D.M. and Phelps M. (2000). Spatial working memory and hippocampal size across pregnancy in rats. Hormones and Behavior, 37, 86-95 (JCR 2007 Impact 3.401).

***Submitted or in preparation***

1. Ormerod B. K., Stephens C.S.[a], Chen Z and Palmer TD. (submitted). Harvest and expansion of primate neural stem/progenitor cells.
2. Price RO, Chang THT, Gandal MJ, Ormerod BK, Palmer TD (submitted). Interruption of fetal neurogenesis during maternal illness.
3. Chen Z., Campisi J., Lee SW., Ormerod BK., Zwierzchoniewska M, Martinez OM., Palmer TD. Non-steroidal anti-inflammatory drugs prevent major histocompatibility complex-induced inhibition of neurogenesis in stem cell autografts. (submitted).
4. Bruijnzeel A.W., Bauzo R.M., Yamada H., Ormerod B.K., Fornal C.A., Jacobs B.L. (submitted). Tobacco smoke exposure inhibits cell proliferation and cell survival in the dentate gyrus of adolescent rats.
5. Hoang-Minh L.[a], Murrow LM[c], Kelley P[b], Ormerod BK, Palmer TD (in preparation). Neural progenitor cell proliferation, differentiation and survival is affected by the circadian cycle in adult mice.
6. Stephens CL.[a], DeMarse TB, Ormerod BK (in preparation). Neural progenitor cells shift network activity in cultured cortical cells to an immature status.
7. Asokan A[a], Ormerod BK (in preparation). Neuroinflammation rapidly alters neural progenitor cell fate in the hippocampus of adult female mice.
8. Speisman RB[a], Kumar A, Ormerod BK., Foster T (in preparation). Enriched environment protects hippocampal neurogenesis from aging in rats.
9. Aditya Asokan, Alan G. Ball, Christina Laird, Linda Hermer and Brandi K. Ormerod1 (in preparation). New granule neuron maturation in the dentate gyrus of adult rats is facilitated by fast-acting desvenlafaxine versus slower-acting venlafaxine

**Book Chapters**

1. **Ormerod B.K.** and Galea L.A.M. (2001). Mechanisms and function of neurogenesis in the adult. In C. A. Shaw and J. C. McEachern (Eds.) ***Toward a Theory of Neuroplasticity***. Taylor and Francis:Philadelphia.

2. **Ormerod B.K.,** Falconer E.M. and Galea L.A.M. (2002). Neurogenesis in adult animals. In Lynn Nadel (ed.). ***Encyclopedia of Cognitive Sciences,*** Chapter 389. Macmillan Publishers Ltd (Nature Publishing Group): England.

**Published Abstracts**

1. Westly J.K., **Ormerod B.K.** and Beninger R.J. (1998). Inhibition of protein kinase in the nucleus accumbens impairs amphetamine-produced enhancement of responding for conditioned reward. Soc. Neurosci. Abstr., Vol 24, 72.8.
2. **Ormerod B.K.** and Galea L.A.M. (1999). Survival of newly born cells in the dentate gyrus of adult meadow voles, Microtus pennsylvanicus, is influenced by reproductive status. Soc. Neurosci. Abstr., Vol 25, 863.4.
3. Galea L.A.M., Paine T.A., Piaseczna M. and **Ormerod B.K.** (1999). Estradiol inhibits learning in a hippocampal-dependent task but enhances learning in a hippocampal-independent task and promotes cell survival in the dentate gyrus. Soc. Neurosci. Abstr., Vol 25, 863.5.
4. **Ormerod B.K.** and Galea L.A.M. (2000). Estradiol initially enhances but subsequently suppresses cell proliferation in the dentate gyrus of adult female meadow voles. Soc. Neurosci. Abstr., Vol 26, 847.12.
5. Hofmann C.E., Piaseczna M., **Ormerod B.K.**, Floresco S.B., Holmes M.M. and Galea L.A.M. (2000). Caudate but not hippocampus lesions impair acquisition on a cued arm task. Soc. Neurosci. Abstr., Vol 26, 650.4.

6. **Ormerod B.K.**, Witheford M. and Galea L.A.M. (2001). Estradiol enhances the survival of 6-10 day old neurons in the dentate gyrus of adult male meadow voles. P05-013 Stem Cells in the Mammalian Brain. (http://www.neuroscion.com/forum/discussions?action=browse&col=stemcells&group=stemcells.poster5&expanded=&fromthr=11&tothr=16)

7. **Ormerod B.K.**, Lee T.T-Y. and Galea L.A.M. (2001). Estradiol initially enhances but subsequently suppresses (via adrenal steroids) cell proliferation in the dentate gyrus of adult female rats. Soc. Neurosci. Abstr., Vol 27, 587.6.

8. **Ormerod B.K.**, Lee T.T-Y. and Galea L.A.M. (2002). Adult male meadow voles with estradiol-enhanced numbers of young neurons exhibit better spatial memory. Soc. Neurosci. Abstr., Vol 28, 470.10.

9. Wide J.K., **Ormerod B.K.** and Galea L.A.M. (2002). Chronic estradiol treatment does not influence cell proliferation in the dentate gyrus of adult female rats. Soc. Neurosci. Abstr., Vol 28, 470.11.

10. Nagy A.I., **Ormerod B.K.**, Mazzucco C.M. And Galea L.A.M. (2003). Estradiol-induced enhancement of granule cell proliferation is mediated via the ERa. Soc. Neurosci. Abstr., Vol 29., 348.50.

11. **Ormerod B.K.**, Falconer E.M. and Galea L.A.M. (2003). More new neurons survive in the dentate gyrus of adult estradiol- versus vehicle-treated female meadow voles. Soc. Neurosci. Abstr., Vol 29., 671.13.

12. Hill M.N., Carrier E., Patel S., **Ormerod B.K.**, Hillard C., Gorzalka B.B. (2003). Chronic stress elicits differential regulation of cannabinoid type 1 (CB1) receptor binding and expression in the hippocampus and limbic forebrain. Soc. Neurosci. Abstr., Vol 29., 829.18.

13. Price R.O., **Ormerod B.K.**, Palmer T.D. (2004). Maternal inflammation during fetal brain development disrupts cortical neurogenesis. Soc. Neurosci. Abstr Vol. 30., 831.90.

14. **Ormerod B.K.**, Hanft S., Palmer T.D. (2005). NSAID treatment protects adult hippocampal neurogenesis and hippocampus-dependent behavior from the deleterious effects of neuroinflammation. Soc Neurosci Abstr Vol 31., 141.70.

15. Meltzer L., **Ormerod B.**, Palmer T., Deisseroth K. (2005). Driving activity-dependent neurogenesis via L-Type Calcium Channels: Circuit-level and behavioral consequences. Soc Neurosci Abstr Vol 31. 141.69.

16. **Ormerod BK**., Lee SW., Cord BJ., Palmer TD (2006). Absence of monocyte chemoattractant protein-1 protects neurogenesis in response to cranial irradiation. Soc Neurosci Abstr Vol 31. 385.16.

17. Stephens CL., DeMarse TB, **Ormerod BK** (2007). Fetal and adult neural progenitor cells develop network-wide activity: a 60 channel microelectrode array analysis. Soc Neurosci Abstr Vol 32. 344.80.

18. Ferguson MC, Rani A, Kumar A, Foster TC, **Ormerod BK** (2007). Neurogenesis is enhanced in the hippocampus of young and aged rats exposed to an enriched versus impoverished environment. Soc Neurosci Abstr Vol 32. 566.70.

19. Zachrisson O, Andersson A, Isacson R, Jeldes S, Mercer A, Nielsen E, Patrone C, Ronnholm H, Wikstrom LB, Di Monte DA, McCormack AL, **Ormerod BK**, Palmer TD, Zhao M, Delfani KK, Janson Lang AM and Haegerstrand A. (2007). Neurorestorative effects of PDGF-BB in rodent models of Parkinson s disease through stimulation of cell proliferation. Soc Neurosci Abstr Vol 32. 797.1.

20. Stephens CL, DeMarse TB, Ormerod BK (2008). Neural progenitor cells influence and are influenced by the activity of primary neurons cultured on microelectrode arrays. Soc Neurosci Abstr Vol 33.

21. Asokan A, Ormerod BK (2008) A bioplex strategy for identifying candidate molecules that affect adult hippocampal neurogenesis. Soc Neurosci Abstr Vol 33.

22. Ormerod BK, Hoang-Minh L, Kelly P, Jones BE, Palmer TD (2008). Is there a circadian effect on cell production in extra-hippocampal adult brain regions? Soc Neurosci Abstr Vol 33.

23. Stephens CL, DeMarse TB, Ormerod (2009). Spontaneous activity patterns of fetal and adult neural networks are altered by the addition of adult neural progenitor cells. Soc Neurosci Abstr Vol 34, 324.13.

24. Asokan A and Ormerod BK. (2009). Lipopolysaccharide induced activation of circulating inflammatory molecules exert a negative influence on hippocampal progenitor cell differentiation in the adult brain. Soc for Neurosci Abstr Vol 34.

25. Ormerod BK, Speisman RB, Kumar A, and Foster TC. (2009) Biomarkers predict successful versus unsuccessful aging in rats. Society for Neuroscience Abstr Vol 34.

26. M. S. SANDHU, H. H. ROSS, B. J. DOUGHERTY, E. D. LAYWELL, B. K. ORMEROD, P. J. REIER, D. D. FULLER (2010). Respiratory changes following transplantation of post-natal neural precursors into high cervical hemilesions of the adult rat. Society for Neuroscience Abstr Vol 35. 469.8.

27. A. ASOKAN, M. CHANDRAN, P. P. KHARGONEKAR, B. K. ORMEROD (2010). A combined multiplex experimental and modeling approach reveals candidate neuroinflammatory cytokines that affect hippocampal progenitor cell behavior in adult mice. Society for Neuroscience Abstr Vol 35. 638.9.

28. L. B. HOANG MINH, B. K. ORMEROD (2010). Day/night variations in neurogenesis may be due to changes in cell cycle kinetics in the dentate gyrus of adult. Society for Neuroscience Abstr Vol 35. 638.19.

29. R. B. SPEISMAN, A. KUMAR, A. RANI, J. E. SEVERANCE, T. C. FOSTER, B. K. Ormerod (2010). Enrichment concomitantly improves hippocampal neurogenesis and spatial memory in aged rats. Society for Neuroscience Abstr Vol 35. 710.10.

30. C. L. STEPHENS, T. B. DEMARSE, B. K. ORMEROD (2010). Adult neural progenitor cell addition after oxygen-glucose deprivation on microelectrode arrays influences recovery of network activity. Society for Neuroscience Abstr Vol 35; 760.8.

31. V. MUNIKOTI, A. ASOKAN, B. K. ORMEROD (2010). Hippocampal neurogenesis and laminin expression are inversely regulated by lipopolysaccharide-induced neuroinflammation in adult female mice. Society for Neuroscience Abstr Vol 35; 839.15/B5

## C. Other contributions

**Additional presentations and participation**

Invited Talks - 16
Conference Presentations (not including published abstracts) – 27
Memberships in Professional Societies – 8
Ad Hoc Reviewer – 13 journals

## D. Past Support

2007 - ***UF Seed Fund*** (Frazier, Ditto, Carney, Roper, ***Ormerod – 5% CoPI***) - $100,000
Construction of the first two-photon based laser scanning epifluorescence microscope at the University of Florida: A cross-college and multidisciplinary effort.
*The major goal of this award is complete construction of a system that will stimulate cross disciplinary collaboration using techniques for imaging live cells otherwise unavailable to UF researchers.*

2007-2009 – ***McKnight Brain Institute - UF Award #FF20*** - $50,000
*The effects of chromosomal sex and developmental age on cultured and transplanted neural progenitor cells*
The major goal of this award is to determine parameters that promote optimal engraftment of stem cells into the diseased or damaged brain with emphasis on minimizing inflammation.

## Current Support

2008 – 2010 – ***Ruth K. Broad Biomedical Research Foundation Extramural Award*** - $180,000
*Neural stem cells and inflammation: Implications for Alzheimers disease*
The major goal of this award is to understand how inflammation is transduced into neuroinflammation and to identify candidate inflammatory molecules that impact neural progenitor/stem cell behavior.

2010 – 2011 – ***ARML/McKnight Brain Institute*** - $50,000
*Biomarkers of successful and unsuccessful aging*
The major goal of this award is to explore how neuroinflammation interacts with neurogenesis to produce age-related cognitive decline in rodents

2010 – 2014 **1R01 AG036800-01** ***Signaling cascades and memory deficits during aging***
National Institutes of Health – NIA
Co-PI (20% Effort) 07/1007/14 $360,425

| | |
|---|---|
| 2007-present | National Institute on Aging, Physical Exercise Task Force |
| 2008 | National Institute on Aging, National Advisory Council on Aging, review roster of the Division of Behavioral and Social Research |
| 2008-present | National Institute on Aging Clinical Trials Advisory Panel |
| 2010 | Review roster of the Geriatrics and Clinical Gerontology Program, National Institute on Aging |

**C. Selected Peer-reviewed Publications** (Selected from over 280 peer-reviewed publications)


1. **Pahor M**, Guralnik JM, Salive ME, Chrischilles EA, Brown SL, Wallace RB. Physical activity and risk of severe gastrointestinal hemorrhage in older persons. JAMA 1994;272:595-599.
2. Ferrucci L, Guralnik JM, **Pahor M**, Corti MC, Havlik RJ. Hospital diagnoses, Medicare charges and nursing home admissions in the year when older persons become severely disabled. JAMA 1997;277:728-734.
3. Penninx BW, Messier SP, Rejeski WJ, Di Bari M, Cavazzini C, Applegate WB, **Pahor M**. Physical exercise and prevention of ADL disability in older persons with osteoarthritis. Arch.Intern.Med. 2001;161:2309-2316.
4. Carter CS, Onder G, Sonntag WE, **Pahor M**. Physical performance and longevity in aged rats. J.Gerontol.A Biol.Sci.Med Sci. 2002;57:B193-B197.
5. Onder G, Penninx BW, Balkrishnan R, Fried LP, Chaves PH, Carter CS, Williamson JD, Di Bari M, Guralnik JM, **Pahor M**. ACE inhibitors use and changes in muscle strength and physical performance in older women. Lancet 2002;359:926-930.
6. **Pahor M**, Franse LV, Deitcher SR, Cushman WC, Johnson KC, Shorr RI, Tracy RP, Somes GW, Applegate WB. The Fosinopril versus Amlodipine Comparative Treatments Study (FACTS), a randomized trial to assess effects on PAI-1. Circulation 2002;105:457-461.
7. Cesari M, Penninx BW, Newman AB, Kritchevsky SB, Nicklas BJ, Sutton-Tyrrell K, Rubin S, Ding J, Simonsick EM, Harris TB, **Pahor M**. Inflammatory markers and onset of cardiovascular events: results from the Health ABC study. Circulation 2003;108:2317-2322.
8. Kritchevsky SB, Nicklas BJ, Visser M, Simonsick EM, Newman AB, Harris TB, Lange EM, Penninx BW, Goodpaster BH, Satterfield S, Colbert LH, Rubin SM, **Pahor M**. Angiotensin-converting enzyme insertion/deletion genotype, exercise, and physical decline. JAMA. 2005;294(6): 691-698.
9. Newman AB, Simonsick EM, Naydeck EM, Kritchevsky SB, Nevitt M, **Pahor M**, Satterfield S, Brach JS, Studenski SA, Harris TB. Association of long-distance corridor walk performance with mortality, cardiovascular disease, mobility limitation, and disability. *JAMA* 2006;295(17):2018-26.
10. The LIFE study investigators. Effects of a physical activity intervention on measures of physical performance: results of the Lifestyle Interventions and Independence in Elders pilot (LIFE-P) study. Journal of Gerontology: Medical Sciences 2006; 55A(2): M74-M83.
11. Verghese J, Kuslansky G, Holtzer R, Katz M, Xue X, Buschke H, **Pahor M**. Walking while talking: effect of task prioritization in the elderly. *Arch Phys Med Rehabil* 2007 January;88(1):50-3.
12. Bhasin S, Cress E, Espeland MA, Evans WJ, Ferrucci L, Fried LP, Gill TM, **Pahor M**, Studenski S, Guralnik JM, Nayfield S, Romashkan S, Eldadah BA, Suzman R, Haaqa J et al. Functional outcomes for clinical trials in frail older persons: time to be moving. *J Gerontol A Biol Sci Med Sci* 2008 February;63(2):160-4.
13. Cesari M, Kritchevsky SB, Newman AB, Simonsick EM, Harris TB, Penninx BW, Brach JS, Tylavsky FA, Satterfield S, Bauer DC, Rubin SM, Visser M, **Pahor M**. Added value of physical performance measures in predicting adverse health-related events: results from the Health, Aging And Body Composition Study. *J Am Geriatr Soc* 2009 February;57(2):251-9.
14. Harrison DE, Strong R, Sharp ZD, Nelson JF, Astle CM, Flurkey K, Nadon NL, Wilkinson JE, Frenkel K, Carter CS, **Pahor M**, Javors MA, Fernandez E, Miller RA. Rapamycin fed late in life extends lifespan in genetically heterogeneous mice. *Nature* 2009 July 16;460(7253):392-5.
15. Giovannini S, Onder G, Leeuwenburgh C et al. Myeloperoxidase Levels and Mortality in Frail Community-Living Elderly Individuals. J Gerontol A Biol Sci Med Sci 2010.


**C. Research Support**

**Ongoing Research Support**

NIH/NIA 1 UO1 AG022376-01Pahor (PI) $11,918,679 09/01/09-08/31/15

The LIFE study

The major goal of this project is to determine by conducting a Phase 3 randomized, controlled trial (RCT) whether physical exercise prevents major mobility disability in older persons.

NIH NIA U01AG022376 Pahor (PI) $1,592,446 09/01/09-08/31/11
Project title: The LIFE Study – NHLBI Supplement to assess sleep disturbances and cardiopulmonary outcomes.

NIH-NIA 1 P30 AG028740-01Pahor (PI) $461,200 03/01/07-02/28/12
Claude D. Pepper Older Americans Independence Centers
The major goals of this project are the developing, testing and dissemination of effective therapies for the treatment and prevention of physical disability.

NIH-NIA 1 P30 AG028740-03S1Pahor (PI) $219,747 09/20/09-08/31/11
Claude D. Pepper Older Americans Independence Centers Supplement
The major goal of this project is to assess the impact of mitochondrial function and fatigue on physical function and disability.

NIH-NCRR Pahor (PI) $14,985,700 01/14/10-01/13/15
Institute on Aging Clinical Translational Research Building
The goal of this project is to construct a 40,000 GSF building to host the University of Florida Clinical Translational Research Building.

NIH-NCRR Nelson(PI) $4,063,907 07/14/09-03/31/14
UF Clinical and translational science award

NIH-NIA 1 R01 AG026556-01 Pahor (PI) $225,000 12/01/06-06/30/11
Oxidative damage, disability and mortality in elders
Ancillary study to the Health, Aging and Body Composition study to evaluate the predictive value of oxidative damage, platelet activation and inflammation for incident mobility disability and mortality in older persons.

**Completed Research Support**

NIH-NIA 1 R01 AG027529 Nicklas (PI) 09/15/06-08/31/10
Exercise training and inflammatory risk factors for disability
The goal is to measure plasma concentrations of inflammatory biomarkers in blood samples collected from LIFE participants following randomization to the interventions to test our primary hypothesis that: 1) compared to a non-exercise health education intervention, a 12-month exercise training intervention will decrease concentrations of inflammatory biomarkers in elderly men and women at high risk for physical disability.

NIH-NHLBI 1 R01 HL72972-01 Pahor (PI) 09/20/03-09/19/09
The epidemiology of stress and the metabolic syndrome
The project uses epidemiological databases to explore the association between stress and the metabolic syndrome in older adults, and investigates biological mechanisms underlying this link.

NIH-NIA 1 R01-AG025119-01A1Verghese (PI) 08/01/05-06/30/10
Latent Mobility Abnormalities and Frailty
The research focus of this study is to identify latent mobility abnormalities and their biological basis in nondisabled older adults.
Role: PI, University of Florida Subcontract

NIH/NIA 1 P30 AG21332-01Pahor (PI) 10/01/02-09/30/07
Claude D. Pepper Older Americans Independence Centers
The major goals of this project are the developing, testing and dissemination of effective therapies for the treatment and prevention of physical disability from chronic diseases in later life.
Role: PI - Dr. Pahor has withdrawn from this grant on 1/31/05 when he relocated to the University of Florida

NIH-NIA RO1 AG18702-01A1 Pahor (PI) 08/01/01-07/31/06
Gene Polymorphisms and Prevention of Disability
The major goals of this project are to explore the interactions of polymorphisms of the angiotensin converting enzyme (ACE) and cytokines genes with behavior and medication use in determining physical function outcomes in older persons. Role: PI

NIH/NHLBI 1 RO1 HL68901-01 Pahor (PI) 02/01/02-01/31/07
ACE Inhibition and Novel Cardiovascular Risk Factors. The major goals of this project are to assess the effect of ACE inhibitors markers of inflammation, fibrinolysis, cell matrix degradation and endothelial function.

## BIOGRAPHICAL SKETCH

Provide the following information for the Senior/key personnel and other significant contributors in the order listed on Form Page 2.
Follow this format for each person. **DO NOT EXCEED FOUR PAGES.**

| NAME | POSITION TITLE |
|---|---|
| Matthew R. Sarkisian, Ph.D. | Assistant Professor |
| eRA COMMONS USER NAME (credential, e.g., agency login)<br>SARKISIAN01 | |

EDUCATION/TRAINING *(Begin with baccalaureate or other initial professional education, such as nursing, include postdoctoral training and residency training if applicable.)*

| INSTITUTION AND LOCATION | DEGREE *(if applicable)* | MM/YY | FIELD OF STUDY |
|---|---|---|---|
| Clemson University, Clemson, SC | B.S. | 05/95 | Biological Sciences |
| University of Connecticut, Storrs, CT | Ph.D. | 12/01 | Physiology and Neurobiology |
| Yale University, New Haven, CT | Postdoc | 02/02-10/08 | Neurobiology |

Please refer to the application instructions in order to complete sections A, B, C, and D of the Biographical Sketch.

### A. Personal Statement

The goal of my research program is to understand how mutations in genes expressed in the fetal brain lead to abnormal development and dysfunction of the cerebral cortex. Development of the cortex is a highly orchestrated process, the disruption of which sets the stage for numerous neurological disorders as well as many different types of abnormalities in learning and memory. Detailed analysis of the developing brains of animals carrying these mutations will allow us to identify the specific developmental events affected by these mutations, information that could lead to development of therapeutic strategies for these devastating neural diseases. Furthermore, our understanding of molecular mechanisms critical for establishing the plasticity of the immature brain may be useful towards protective strategies from effects of age-related memory loss. My pre- and postdoctoral training were with highly established, pioneering investigators in developmental neurobiology. This training helped me to bring new technologies and expertise to the University of Florida Neuroscience program to explore basic mechanisms of neurodevelopment and pathogenesis of the cerebral cortex.

### B. Positions and Honors

Positions and Employment

05/95-08/97 Research Technician, Children's Hospital, Harvard Medical School, Boston, MA
08/97-12/01 Graduate Student, Dept. of Physiology & Neurobiology, Univ. of Connecticut, Storrs, CT
Fall 1999 Teaching Assistant, Dept. of Physiology & Neurobiology, Univ. of Connecticut, Storrs, CT
02/02-01/08 Postdoctoral Associate/Fellow, Dept of Neurobiology, Yale Univ. School of Medicine, New Haven, CT
02/08-10/08 Associate Research Scientist, Dept of Neurobiology, Yale Univ. School of Medicine, New Haven, CT
10/2008- Assistant Professor, Dept of Neuroscience, Univ. of Florida, Gainesville, FL

Honors and Research Awards

1995 George M. Savoy Junior Fellowship Award (Savoy Foundation for Epilepsy Research)
1996,2000 Armenian Students' Assoc. of America (ASA), Inc. Academic Scholarship
1999, 2000 University Predoctoral Fellowship, awarded by the UConn Neurosciences Steering Committee
2001 ASA Scholarship
2004-2005 James Hudson Brown-Alexander Brown Coxe Postdoctoral Fellowship (Yale University)
2006-2007 Eric W. Lothman Training Fellowship (Epilepsy Foundation of America Distinguished Postdoctoral Award)
2008 Awarded Graduate Faculty Status by the University of Florida

Professional Memberships

1998- Member of the Society for Neuroscience
2000-02,06 Member of the American Epilepsy Society
2007- Member of the New York Academy of Sciences

**C. Selected Peer-reviewed Publications**


1. Tandon P, Liu Z, Stafstrom CE, **Sarkisian M**, Werner SJ, Mikati M, Yang Y, Holmes GL.(1996) Long term effects of excitatory amino acid antagonists NBOX and MK-801 on the developing brain. *Dev. Brain Res.,* 95: 256-262.
2. Liu Z, Stafstrom CE, **Sarkisian M**, Tandon P,Yang Y, Hori A, Holmes GL. (1996) Age-dependent effects of glutamate toxicity in the hippocampus. *Dev. Brain Res.,* 97: 178-184.
3. Neill JC, Liu Z, **Sarkisian M**, Tandon P, Yang Y, Stafstrom CE, Holmes GL. (1996) Recurrent seizures in immature rats: effect on auditory and visual discrimination. *Dev. Brain Res.,* 95: 283-292.
4. **Sarkisian MR**, Tandon P, Liu Z, Yang Y, Hori A, Holmes GL, Stafstrom CE.(1997) Multiple kainic acid seizures in the immature and adult brain: ictal manifestations and long-term effects on learning and memory. *Epilepsia,* 38: 1157-1166.
5. Liu Z, Stafstrom CE, **Sarkisian MR**, Yang Y, Hori A, Tandon P, Holmes GL. (1997) Seizure-induced glutamate release in mature and immature animals: and in vivo microdialysis study. *Neuroreport*, 8: 2019-2023.
6. Yang Y, Tandon P, Liu Z, **Sarkisian MR**, Stafstrom CE, Holmes GL. (1998) Synaptic re-organization following kainic acid-induced seizures during development. *Dev. Brain Res.,* 107: 169-177.
7. Bolaños AR, **Sarkisian MR**, Yang Y, Hori A, Helmers SL, Mikati M, Tandon P, Stafstrom, CE, Holmes GL. (1998) Comparison of long-term effects of valproate and phenobarbital in adolescent rats. *Neurology,* 51: 41-48.
8. Cogswell CA, **Sarkisian MR**, Leung V, Patel R., D'Mello SR, LoTurco JJ (1998) A gene essential to brain growth and development maps to the distal arm of rat chromosome 12. *Neurosci Lett,* 251: 5-8.
9. Holmes GL, **Sarkisian MR**, Ben-Ari Y, Chevassus-Au-Louis N. (1999) Mossy sprouting after recurrent seizures during development in rats. *J. Comp. Neurol*, 404: 537-553.
10. **Sarkisian MR**, Rattan S, D'Mello S, LoTurco JJ (1999) Characterization of seizures in the flathead rat: a new genetic model of epilepsy in early postnatal development. *Epilepsia*, 40: 394-400.
11. Holmes GL, **Sarkisian M**, Ben-Ari Y, Liu Z, Chevassus-Au-Louis N. (1999) Consequences of cortical dysplasia during development in rats. *Epilepsia*, 40: 537-544.
12. Liu Z, Yang Y, Silveira DC, **Sarkisian MR**., Tandon P, Huang LT, Stafstrom CE, Holmes GL (1999) Consequences of recurrent seizures during early brain development. *Neuroscience.*, 92: 1443-54.
13. **Sarkisian MR**, Holmes GL, Carmant L, Liu Z, Yang Y, Stafstrom CE. (1999) Effects of hyperthermia and continuous hippocampal stimulation on the immature and adult brain. *Brain and Dev.*, 21: 318-325.
14. Yang Y, Liu Z, Cermack JM, Tandon P, **Sarkisian MR**, Stafstrom CE, Neill JC, Blusztajn JK, Holmes GL (2000) Protective effects of prenatal choline supplementation on seizure-induced memory impairment. *J Neurosci.*, 20: RC109 (1-6).
15. **Sarkisian MR**, Frenkel M, Li W, Oborski JA, LoTurco JJ. (2001) Altered interneuron development in the cerebral cortex of the *flathead* mutant. *Cereb Cortex*, 11: 734-743.
16. Neill JC, **Sarkisian MR**., Wang, Y, Liu, Z, Yu, L, Tandon, P, Zhang, G, Holmes, GL, Geller, AI. (2001) Enhanced auditory reversal learning by genetic activation of PKC in small groups of rat hippocampal neurons. *Molec Brain Res.*, 93: 127-136.
17. Holmes GL, Yang Y, Liu Z, Cermak, JM, **Sarkisian MR**, Stafstrom CE, Neill JC, Blusztajn JK (2002) Seizure-induced memory impairment is reduced by choline supplementation before or after status epilepticus. *Epilepsy Res.*, 48: 3-13.
18. **Sarkisian MR**, Li W, Di Cunto, F, D'Mello, SR, LoTurco JJ. (2002) Citron-kinase, a protein essential to cytokinesis in neuronal progenitors, is deleted in the flathead mutant rat. *J Neurosci.*, 22: RC217 (1-5).
19. **Sarkisian MR**. (2002) Overview of the current animal models for human seizure and epileptic disorders. *Epilepsy & Behavior*, 2: 201-216.
20. LoTurco JJ, **Sarkisian MR**, Cosker L, Bai J. (2003) Citron kinase is a regulator of mitosis and neurogenic cytokinesis in the neocortical ventricular zone. *Cereb Cortex*, 13: 588-591.
21. Li MO, **Sarkisian MR***, Mehal WZ, Rakic P, Flavell RA. (2003) Phosphatidylserine receptor is required for clearance of apoptotic cells. *Science* 302: 1560-1563.

22. Chi H, **Sarkisian MR***, Rakic P, Flavell RA. (2005) Loss of mitogen-activated protein kinase kinase kinase 4 (MEKK4) results in enhanced apoptosis and defective neural tube development. *Proc. Natl. Acad. Sci. (USA)* 102: 3846-3851.
23. **Sarkisian MR**, Bartley CB, Chi H, Nakamura F, Hashimoto-Torii K, Torii M, Flavell RA, Rakic P. (2006) MEKK4 signaling regulates filamin expression and neuronal migration. *Neuron* 52: 789-801.
24. Ackman JB, Ramos RL, **Sarkisian MR**, LoTurco JJ. (2007) Citron kinase is required for postnatal neurogenesis in the hippocampus. *Dev Neurosci,* 29; 113-123.
25. Town T, Breunig J†, Sarkisian **MR**†, Spilianakis C, Ayoub AE, Liu X, Ferrandino A, Gallagher AR, Li MO, Rakic P, Flavell RA. (2008) The stumpy gene is required for mammalian ciliogenesis. *PNAS* 105: 2853-2858. †co-contributors
26. Breunig JJ, **Sarkisian MR***, Arellano JI, Morozov YM, Ayoub A, Sojitra S, Wang B, Flavell RA, Rakic P, Town T. (2008) Primary cilia regulate hippocampal neurogenesis by mediating sonic hedgehog signaling. *PNAS* 105: 13126-13131.
27. Hashimoto-Torii K, Torii M, **Sarkisian MR**, Bartley CM, Shen J, Radtke R, Gridley T, Sestan N, Rakic P. (2008) Interaction between Reelin and Notch signaling regulates neuronal migration in the cerebral cortex. *Neuron* 60: 273-284.
28. **Sarkisian MR**, Bartley CM, Rakic P. (2008) Trouble making the first move: interpreting arrested neuronal migration in the cerebral cortex. *Trends in Neurosciences* 31: 54-61.
29. Anastas SB, Mueller D, Semple-Rowland SL, Breunig JJ, **Sarkisian MR**[§]. (2010) Failed cytokinesis of neural progenitors in Citron kinase deficient rats leads to multi-ciliated neurons. *Cereb Cortex* (Epub June 4, 2010).
30. Fonseca Filho G, Guadiana S, Kumar A, Foster TC, **Sarkisian MR**[§]. (2011) Effects of aging on primary neuronal cilia in rat cerebral cortex (manuscript in preparation)

- *co-first author publication, [§]corresponding author

**D. Research Support**

Ongoing Research Support

1) Type: Start-up funds
Role: Principle Investigator
Funding period: 10/03/08-10/02/13
Amount: $850,000
Agency: McKnight Brain Research Foundation at University of Florida

2) Title: "Towards Inhibiting Ciliogenesis to Prevent Glioblastoma"
Role: Principle Investigator
Funding Period: 12/31/10-12/20/11
Amount: $30,000
Agency/Type: American Cancer Society Chris DiMarco Institutional Research Grant Junior Investigator Award

Completed Research Support

5 R01 NS014841-26 (P.I. – P. Rakic) 05/01/04 – 10/02/08
NIH/NINDS
"Neurogenetic Processes in the Fetal Brain"
The major focus of this grant is on neuronal cell proliferation, the establishment of cell phenotypes and their biochemical and structural differentiation in the embryonic mouse and primate cerebral cortex.
Role: Postdoctoral Associate

Postdoctoral Fellowship (P.I. – M. Sarkisian) 07/01/06 – 06/30/07
Epilepsy Foundation of America
"Genetic Model of Periventricular Heterotopia: Involvement of MAP Kinases"
The major goal of this fellowship is to explore the role of MAP kinases during normal and pathogenetic forebrain development. The MAP3K, MEKK4 will be tested for its role in neuronal migration and potential interaction with Filamin-A, which is known to cause cortical malformation in human.

Role: P.I.

UF UNIVERSITY of FLORIDA

**College of Medicine**
Department of Medicine
Division of Hematology/Oncology

PO Box 100278
1600 SW Archer Road
Gainesville, FL 32610-0278
352-273-7832 / 352-273-5006 Fax

January 5, 2011

Matthew Sarkisian, Ph.D.
Department of Neuroscience

Dear Dr. Sarkisian,

Congratulations! Oh behalf of the American Cancer Society Chris DiMarco Institutional Research Grant, we are happy to inform you that your proposal, "Towards Inhibiting Ciliogenesis To Prevent Glioblastoma," was selected for funding. The reviewers found your proposal to be important and worthy of support by the ACS IRG. We will be forwarding you the reviewers' comments that we hope will be helpful to you as you pursue this project.

Funding has been approved in the requested amount of $30,000 for the period 12/31/10 through 12/30/2011. The following requirements of award acceptance include:

You will be required to be part of a mentoring effort by the ACS-IRG Principle Investigator that is expected to help complement your departmental effort in helping to develop your career at this early stage. You will be contacted and scheduled to meet with Dr. May twice during the period in which this award is in force.

- If your project requires IRB (human subjects) and/or IACUC (animal) approvals, please submit a copy of the approval protocol to Ms. Maxine Rushing as soon as possible. Funds cannot be expended until this document is received.
- Complete and submit a DSR-1 form with signatures from both you and your Department Chair to Ms. Maxine Rushing. The sponsoring agency is the American Cancer Society and the date is N/A. You will then receive an Award Acceptance from the UF Division of Sponsored Research.
- Under the terms of the ACS IRG guidelines, you will be required to submit a progress report upon the completion of this grant.
- It is expected that the work that results from this award will be submitted for publication and that the awardees will seek extramural funding. The "American Cancer Society Chris DiMarco Institutional Research Grant" mechanism should be acknowledged in any and all publications.
- You may be asked to interact with the local ACS chapter and possibly give a talk to the community regarding this research project.
- You also may be asked to participate in the Topics in Cancer Cell Biology Seminar Series or the UFSCC Grand Rounds Seminar: "Presentations by the ACS Junior Investigator Recipients" in 2011(date to be determined).
- Unexpected funds will revert back to the Master Project at the end of the grant period unless a no-cost extension has been requested and approved.
- If you have not already done so, we urge you to apply for UFSCC membership

Please work with Maxine Rushing to facilitate initiation of the award. Again, congratulations on your award. We look forward to hearing about your success with this project.

Best Regards,

W. Stratford May, Jr. M.D., Ph.D.
PI: American Cancer Society Chris DiMarco Institutional Research Grant
The Henry E. Innes Professor of Cancer Research

cc: Stephen Staal, M. D.
Maureen Goodenow, Ph.D.
Maxine Rushing

## BIOGRAPHICAL SKETCH

Provide the following information for the Senior/key personnel and other significant contributors.
Follow this format for each person. **DO NOT EXCEED FOUR PAGES.**

| NAME | POSITION TITLE |
|---|---|
| Steindler, Dennis | Joseph J. Bagnor/Shands Professor of Medical Research, University of Florida |
| eRA COMMONS USER NAME (credential, e.g., agency login)<br>STEINDLER | |

EDUCATION/TRAINING *(Begin with baccalaureate or other initial professional education, such as nursing, include postdoctoral training and residency training if applicable.)*

| INSTITUTION AND LOCATION | DEGREE *(if applicable)* | MM/YY | FIELD OF STUDY |
|---|---|---|---|
| University of Wisconsin, Madison, WI | B.A. | 1973 | Zoology |
| University of California, San Francisco | Ph.D. | 1977 | Anatomy/Neurobiology |
| Max-Planck-Inst. For Biophysical Chemistry | | 1977 | Neurophysiology |

### A. Personal Statement

Dr. Steindler has worked as a developmental neurobiologist and stem cell researcher for many years, and has studied rodent and human stem/progenitor cells in many different in vitro and in vivo models. My laboratory discovered the adult human neural progenitor cell that will be further studied here, and we have great collaborations with investigators in our institute to help see the proposed cell culture and animal model experiments to a successful completion. In addition to having experience with all of the cell phenotyping and therapeutic approaches proposed here, I have been studying neural cell transplantation models as well as axonal tracing and physiological characterization of neurons and glia for many years. The goal of this R01 is to further characterize the adult human neural progenitor cell in vitro and in vivo, from brain and iPSC-derived in Huntington's Disease models; I also have worked with and published on Huntington's Disease human tissue phenotyping as well as in an animal models. The proposed studies rely on technologies and approaches well-established in my laboratory, and with a new transgenic rat model of Huntington's with an early expression of disease phenotype, we now will be characterizing the most promising human stem or progenitor cell I have ever seen, and establish its potential therapeutic application for delaying onset and potentially deterring the course of this neurodegenerative disease.

### B. Positions and Honors

**Positions and Employment**

2004-2010 Director, McKnight Brain Institute, University of Florida, Gainesville, FL
2001- Professor, Departments of Neuroscience & Neurosurgery, University of Florida, Gainesville, FL
Joseph J. Bagnor/Shands Professor Medical Research, The McKnight Brain Institute, Program In Stem Cell Biology and Regenerative Medicine, and Shands Cancer Center of the College of Medicine, University of Florida, Gainesville, FL
1991-2001 Professor, Department of Anatomy and Neurobiology, University of Tennessee, Memphis, FL
1985-1991 Associate Professor, Department of Anatomy and Neurobiology, University of Tennessee, Memphis, TN
1983-1984 Assistant Professor, Department of Anatomy and Neurobiology, University of Tennessee, Memphis, TN
1978-1983 Assistant Professor, Department of Anatomy and Neurobiology, Michigan State University, East Lansing, MI

**Other Experience and Professional Memberships**

2003-2009 Associate Editor, The Journal of Neuroscience
2001-2009 Editorial Board Member, Glia
Currently Editorial Board Member, Brain Research; Experimental Neurology,
Chair, NIH/NINDS CNNT Study Section, 10/02-6/05

Scientific Advisory Board Member, the Michael J. Fox Foundation for Parkinson's Research
Scientific & Medical Research Funding Working Group, the California Institute for Regenerative Medicine

**Honors**

| | |
|---|---|
| 1998 | Patent Technology Award, American Museum of Science and Energy |
| 1999 | Teaching Award for Medical School Neuroscience |
| 2000 | Teaching Award for Medical School Neuroscience |
| 2001 | Outstanding Lecturer Award for Medical School Neuroscience |
| 2003 | Birch Lecturer, International Neuropsychology Society |
| 2006, 2009 | Gubernatorial Appointee, Governors .Jeb Bush and Charles Crist, The Florida Center for Brain Tumor Research |
| 2008 | Atena Onlus Award, Rome, Italy, shared with Professors Gianfranco Rossi and Rita Levi Montalcini |

**C. Selected Peer-Reviewed Publications** (Selected from over 100 peer-reviewed publications)

**Five Most relevant to the current application (from 103 peer-reviewed papers):**


1. Kusakabe M, Mangiarini L, Laywell ED, Bates GP, Yoshiki A, Hiraiwa N, Inoue J, Steindler DA.Loss of cortical and thalamic neuronal tenascin-C expression in a transgenic mouse expressing exon 1 of the human Huntington disease gene. J Comp Neurol. 2001 Feb 19;430(4):485-500.PMID: 11169482 [PubMed - indexed for MEDLINE]
2. Thomas LB, Gates DJ, Richfield EK, O'Brien TF, Schweitzer JB, Steindler DA. DNA end labeling (TUNEL) in Huntington's disease and other neuropathological conditions. Exp Neurol. 1995 Jun;133(2):265-72.PMID: 7649231 [PubMed - indexed for MEDLINE]
3. Walton NM, Sutter BM, Chen HX, Chang LJ, Roper SN, Scheffler B, Steindler DA.Derivation and large-scale expansion of multipotent astroglial neural progenitors from adult human brain. Development. 2006 Sep;133(18):3671-81. Epub 2006 Aug 16.PMID: 16914491 [PubMed - indexed for MEDLINE]
4. Coras, R.*, Siebzehnrubl, F.*, Pauli, E., Huttner, H.B., Njuntig, M., Kobow, K., Villmann, C., Hahnen, E., Neuhuber, W., Weigel, D., Buchfelder, M., Stefan, H., Steindler, D.A., and I. Bluemcke. Low proliferation and differentiation capacities of adult hippocampal stem cells correlate with memory dysfunction in humans. Brain, In Press.
5. Suslov, O., V.G. Kukekov, T. Ignatova, and D.A. Steindler. Neural stem cell heterogeneity demonstrated by molecular phenotyping of clonal neurospheres in vitro. Proc. Natl. Acad. Sci. USA 99:1456-14511, 2002. PMID: 12381788 [PubMed - indexed for MEDLINE]


**Ten Additional publications of importance to the field and this proposal**


6. Laywell, E.D., P. Rakic, V.G. Kukekov, E. Holland, and D.A. Steindler. Identification of a multipotent astrocytic stem cell in the immature and adult mouse brain. Proc. Natl. Acad. Sci. USA 97:13883-13888, 2000. PMID: 11095732 [PubMed - indexed for MEDLINE]
7. Steindler, D.A. and D. Pincus. Stem cells and neuropoiesis in the adult human brain. The Lancet 359:1047-1054, 2002. PMID: 11937201 [PubMed - indexed for MEDLINE]
8. Scheffler, B., Walton, N.M., Lin, DD., Goetz, A.K., Enikolopov, G., Roper, S.N., and Steindler, D.A. Phenotypic and functional characterization of adult brain neuropoiesis. Proc Natl Acad Sci USA 102:9353-9358, 2005. PMID: 15961540 [PubMed - indexed for MEDLINE]
8. Goetz, A.K., Scheffler, B., Chen, H-X, Wang, S, Xiang, H., Brustle, O., Roper, S.N. and D.A. Steindler. Temporally restricted substrate interactions direct fate and specification of neural precursors derived from embryonic stem cells. Proc Natl Acad Sci USA 103:11063-11068, 2006. PMID: 16832065 [PubMed - indexed for MEDLINE]
10. Cogle, C., Yachnis, A., Laywell, E.D., Zander, D.S., Wingard, J.R., Steindler, D.A.*, and E.W. Scott. Bone marrow transdifferentiation in the human brain following transplantation. The Lancet 363:1432-1437, 2004. PMID: 15121406 [PubMed - indexed for MEDLINE]
11. Steindler, D.A. Redefining cellular phenotypy based on embryonic, adult and cancer stem cell biology. Brain Pathology 16:169-180, 2006. PMID: 16768757 [PubMed - indexed for MEDLINE]

12. Steindler, D.A. Stem cells, regenerative medicine, and animal models of disease. National Academy of Sciences ILAR J. 48:323-338, 2007. PMID: 17712220 [PubMed - indexed for MEDLINE]
13. Chen KA, Lanuto D, Zheng T, Steindler DA. Transplantation of embryonic and adult stem cells in the granuloprival cerebellum of the weaver mutant mouse. Stem Cells. 2009 Jul;27(7):1625-34.PMID: 19544457 [PubMed - indexed for MEDLINE]
14. Silver D. and Steindler D.A. Common astrocytic programs during brain development, injury and cancer. Trends in Neurosciences 32:303-311, 2009. PMID: 19398132 [PubMed - indexed for MEDLINE]
15. Steindler, D.A. and R.H. Bradley. N-[acetyl-3H] wheat germ agglutinin: anatomical and biochemical studies of a sensitive bidirectionally transported axonal tracer. Neuroscience 10: 219-241, 1983.

**D. Research Support**

**Ongoing Research Support**

1 R01 NS055165-04 Steindler (PI) 07/01/07-03/31/12
Total Costs $1, 259,366.00 for 5 yr
Stem/Progenitor Cell Protection for Parkinson's Disease
The major goals of this project are to study the engineering of neural and non-neural cells for the protection of at-risk dopamine neurons in Parkinson's disease.
Role: PI

No number Siebzehnrubl (PI) 2008-2010
Direct Costs $50,000
Hereditary Disease Foundation
SVZ Stem/Progenitor Cell Migration and Differentiation in HD
The major goals of this project focus on a new HD transgenic rat slice culture model.
Role: Co-Investigator

**Pending**

1 R01 NS075173-01 Steindler (PI) 07/01/11-06/30/16
Human Neural Progenitors for Brain Repair
This proposal aims to study brain-derived adult neural progenitor cells for repair of an adult rodent cortical brain injury.

**Completed Research Support**

R01 NS37556-10 Steindler (PI) 1999-2008
Studies of Adult Brain Neuropoiesis
Studies in this grant focused on the characterization of neural stem/progenitor cells and extracellular matrix involved in growth, fate choice and differentiation in vitro and in vivo.
Role: PI

1 R01 HL 70143-01 Steindler (PI) 7/01/2003-6/30/08
Altering Fate of Hematopoietic And Neural Stem Cells
This proposal focused on factors governing fate control of stem cells from blood to brain.
Role: PI

# University of Florida Health Science Center

**2010 Annual Report**
of the
McKnight Brain Institute
& Institute on Aging

*Prepared for the McKnight Brain Research Foundation*

# Articles

# Effects of Aging on Primary Neuronal Cilia

Gileno Fonseca Filho, Sarah Guadiana, Ashok Kumar, Thomas Foster, and Matthew R. Sarkisian
Dept. of Neuroscience, McKnight Brain Institute, Univ. of Florida, Gainesville, FL

#710.1

## INTRODUCTION

Most, if not all, cortical neurons extend a single, putatively non-motile cilium. The development, function and effects of aging on neuronal primary cilia have largely been overlooked and are poorly understood. In the brain, a few signaling molecules and receptors are enriched in neuronal cilia such as adenylyl cyclase III (ACIII), melanin concentrating hormone receptor 1 (MchR1), serotonin receptor subtype 6 (5-$HT_6$), and somatostatin receptor 3 (SSR3). Recently, it was demonstrated that signaling via SSR3 is important for synaptic plasticity and object recognition memory (Einstein et al., *J Neurosci* 2010). These data suggest that neuronal cilia may play an important role in learning and memory. The purpose of this study was to examine the developmental onset and effects of aging on neuronal cilia and their associated molecular components. Additionally, we examined whether or not cilia are altered in brains from memory-impaired and unimpaired animals.

## METHODS

**Animals:**
Brains of mice or rats ranging in age from embryonic day (E)11.5 to >3yrs were used for protein or immunohistochemical analysis. We also obtained some middle aged, behaviorally trained rat brains for immunohistochemical analysis. For histological analysis, brains were immersion fixed or perfused with 4% PFA, cryoprotected in 30% sucrose and cryosectioned coronally at 50µm.

**Immunohistochemistry:**
Standard procedures were followed for the following antibodies: rb anti-ACIII (1:1000; Santa Cruz), ms anti-NeuN (1:1000; Chemicon), chk anti-MAP2 (1:2000; Abcam), ms anti-pericentrin (1:200; BD Bioscences), ms anti-SMI32 (1:1000; Encore Biotech), and rb anti-SSR3 (1:500; Gramsch). Appropriate species-specific, fluorophore-conjugated secondary antibodies were used (1:400; Jackson Immuno) and sections were mounted onto glass slides and coverslipped with the Prolong Antifade Gold (with DAPI) mounting media (InVitrogen). Images of stained sections were captured using an Olympus IX81-DSU spinning disc confocal microscope. Most images displayed represent collapsed z-stacks that were collected in 0.75-1µm steps. Cilia lengths were measured from collapsed z-stacks by tracing individual ACIII+ structures in ImageJ64 (formerly NIH image).

**Western Blot Analysis:**
Fresh samples of mouse or rat cortex or hippocampus were solubilized in ice-cold 1X lysis buffer (Cell Signaling Technology) supplemented with protease and phosphatase inhibitor cocktails 1 and 2 (1:100; Sigma) and 1mM PMSF. Normalized amounts of protein lysates were boiled in 2X sample buffer (NuPAGE), loaded and run in 7.5% Bis-Tris gels (NuPAGE, InVitrogen), and transferred onto PVDF using an iBlot™ Dry Blotting System (InVitrogen). Blots were blocked for 1h in 5% NFDM in 1X Tris-buffered saline containing 0.1%Tween-20 (TBST) and incubated at 4° C o/n in 2.5% NFDM in TBST with the following antibodies (dilution; source): rabbit anti-ACIII (1:1000; (cat# S-831, Gramsch Labs), rabbit anti-BBS2 (1:200; Proteintech), goat ant-Mch1R (1:1000; (C-17) S Cruz), mouse anti-ß actin (1:10,000; Sigma); goat anti-SSR3 (1:1000; (M-18) S Cruz), rabbit anti-Kif3a (1:2000; Abcam). Appropriate HRP-conjugated secondary antibodies (1:10,000; Jackson Immuno) were detected by chemiluminescence (Pierce). Images of blots were captured and analyzed on an Alpha Innotech FluorChem Q imager (Cell Biosciences).

## 1 Cilia on Cortical Neurons

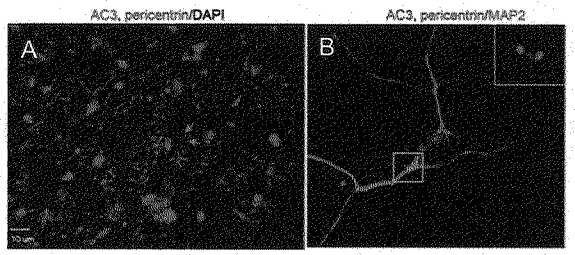


(A) Immunostaining of mouse neocortex for ACIII (green; to detect cilia axoneme) and pericentrin (red; to detect basal body). Nuclei labeled with DAPI. (B) Cilia grow off cultured neurons (MAP2 immunostaining (green)). Inset shows higher mag of cilia axoneme (blue) and basal body (red).

## 2 Cilia Develop and Elongate During Early Postnatal Ages

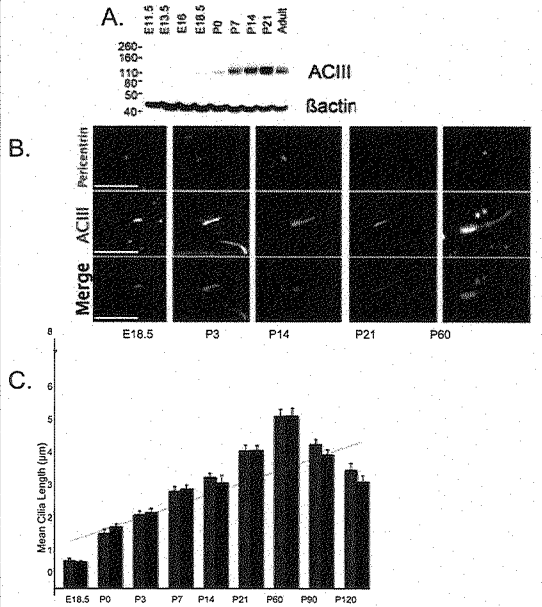


(A) Western blot detection of ACIII and SSR3 in mouse forebrain at indicates ages. E= embryonic day, P=postnatal day. ßactin is a loading control. (B) Examples of neuronal cilia basal bodies (pericentrin+) and axonemes (ACIII+) for the indicated ages. Bar =5µm. (C) Bar graph shows the average length of cilia in upper (grey) and deeper (black) of neocortex for the indicated ages. Cilia length increases significantly across age (two-way ANOVA with repeated measures) and appears to peak by P60 for both UL and DL. Nuclei are labeled with DAPI.

## 3 Cilia are Present in Aged Cortex

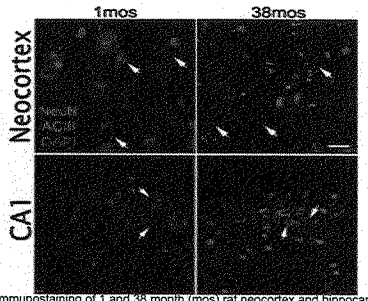


Immunostaining of 1 and 38 month (mos) rat neocortex and hippocampal region CA1 for ACIII and NeuN (red; a neuronal marker). Despite the loss of NeuN expression in aged rats, ACIII-positive cilia (arrows) are still detectable in the aged brain. Nuclei are labeled with DAPI. Bar = 10µm.

## 4 Abnormal SSR3 In Aged Cortex

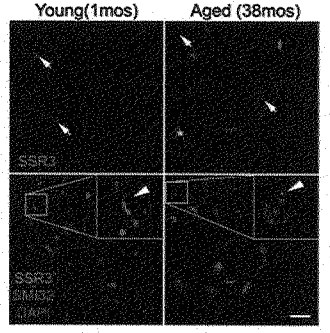


Immunostaining of young and aged rat neocortex for SSR3 (green) and neurofilament marker, SMI32 (red). Asterisk indicates lipofuscin granules common in aged brain. Higher mag insets (lower panels) show that SSR3+ cilia are detectable in young brains, however in aged cortex, SSR3 was more punctate in appearance, suggesting a loss of localization within cilia. Bar = 10µm

## 5 Altered Expression of Cilia Components in Aged Cortex

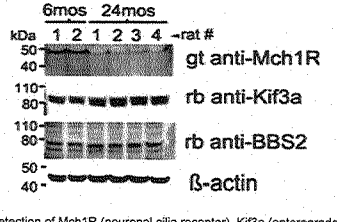


Western blot detection of Mch1R (neuronal cilia receptor), Kif3a (anterograde transporter in cilia) and BBS2 (ciliary receptor trafficking protein) in 6 and 24mos rat cortex. ßactin is a loading control. Similar to SSR3 (Fig 4), levels of Mch1R are reduced in aged cortex. In contrast, levels of Kif3a and BBS2 appear upregulated in the aged compared to young cortex. ßactin is a loading control.

## 6 Cilia Lengths From Memory-Impaired And Unimpaired Middle Aged Rats

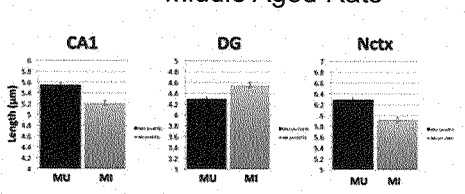


Rats (~15mos old) were behaviorally assessed in a Morris water maze task. Based on their performance, rats were grouped as either memory-unimpaired (MU) and memory-impaired (MI). We measured and quantified the lengths of ACIII+ cilia in the hippocampus (CA1 and DG subregions) and layers 2/3 of neocortex (Ntcx). Decreases in cilia length were observed in the CA1 and Nctx in MI compared to MU rats, while an increase in cilia length was observed in the DG of MI rats. N=number cilia analyzed/group. Bar graphs represent mean ± S.E.M.

## CONCLUSIONS

-Cilia develop postnatally (around birth) and appear mature by 2nd-3rd postnatal week. Cili reach peak length around P60.

-Based on ACIII labeling, cilia are still present in aged rat cortex

-Expression of SSR3 and MchR1, two receptors enriched in neuronal cilia are reduced/altered in aged cortex

-BBS2 and Kif3a, two key components of cilia transport and receptor trafficking machinery are altered with aging

-Memory-impaired rats showed differences in cilia lengths in hippocampus and neocortex.

## ACKNOWLEDGEMENTS

This work was supported in part by a National Institute on Aging grant (to T.F.) and funds from the McKnight Brain Research Foundation and the Evelyn F. and William L. McKnight Brain Institute at the University of Florida (to T. F and M.R.S.).

doi:10.1093/brain/awq215 Brain 2010: 133; 3359–3372 | 3359

BRAIN
A JOURNAL OF NEUROLOGY

# Low proliferation and differentiation capacities of adult hippocampal stem cells correlate with memory dysfunction in humans

Roland Coras,[1,*] Florian A. Siebzehnrubl,[1,2,*] Elisabeth Pauli,[3,*] Hagen B. Huttner,[3] Marleisje Njunting,[1] Katja Kobow,[1] Carmen Villmann,[4] Eric Hahnen,[5] Winfried Neuhuber,[6] Daniel Weigel,[7] Michael Buchfelder,[7] Hermann Stefan,[3] Heinz Beck,[8] Dennis A. Steindler[2] and Ingmar Blümcke[1]

1 Institute of Neuropathology, University Hospital Erlangen, 91054 Erlangen, Germany
2 Department of Neuroscience, McKnight Brain Institute, University of Florida, Gainesville, FL 32610, USA
3 Epilepsy Centre, Department of Neurology, University Hospital Erlangen, 91054 Erlangen, Germany
4 Institute for Biochemistry, Emil-Fischer-Centre, Friedrich-Alexander-University of Erlangen-Nürnberg, 91054 Erlangen, Germany
5 Institute of Human Genetics, Institute of Genetics and Centre for Molecular Medicine Cologne (CMMC), University of Cologne, 50931 Cologne, Germany
6 Department of Anatomy, Friedrich-Alexander-University of Erlangen-Nürnberg, Krankenhausstr. 9, 91054 Erlangen, Germany
7 Department of Neurosurgery, University Hospital Erlangen, 91054 Erlangen, Germany
8 Experimental Epileptology and Cognition Research, Life and Brain Centre, University of Bonn Medical Centre, 53105 Bonn, Germany

*These authors contributed equally to this work.

Correspondence to: Ingmar Blümcke,
University Hospital Erlangen,
Schwabachanlage 6,
D – 91054 Erlangen, Germany
E-mail: bluemcke@uk-erlangen.de

The hippocampal dentate gyrus maintains its capacity to generate new neurons throughout life. In animal models, hippocampal neurogenesis is increased by cognitive tasks, and experimental ablation of neurogenesis disrupts specific modalities of learning and memory. In humans, the impact of neurogenesis on cognition remains unclear. Here, we assessed the neurogenic potential in the human hippocampal dentate gyrus by isolating adult human neural stem cells from 23 surgical *en bloc* hippocampus resections. After proliferation of the progenitor cell pool *in vitro* we identified two distinct patterns. Adult human neural stem cells with a high proliferation capacity were obtained in 11 patients. Most of the cells in the high proliferation capacity cultures were capable of neuronal differentiation ($53 \pm 13\%$ of *in vitro* cell population). A low proliferation capacity was observed in 12 specimens, and only few cells differentiated into neurons ($4 \pm 2\%$). This was reflected by reduced numbers of proliferating cells *in vivo* as well as granule cells immunoreactive for doublecortin, brain-derived neurotrophic factor and cyclin-dependent kinase 5 in the low proliferation capacity group. High and low proliferation capacity groups differed dramatically in declarative memory tasks. Patients with high proliferation capacity stem cells had a normal memory performance prior to epilepsy surgery, while patients with low proliferation capacity stem cells showed severe learning and memory impairment. Histopathological examination revealed a highly significant correlation between granule cell loss in the dentate gyrus and the same patient's regenerative capacity *in vitro* ($r = 0.813$; $P < 0.001$; linear regression: $R^2_{adjusted} = 0.635$), as well as the same patient's ability to store and recall new memories ($r = 0.966$; $P = 0.001$; linear regression: $R^2_{adjusted} = 0.9$). Our results suggest that encoding new memories is related to the regenerative capacity of the hippocampus in the human brain.

Received March 8, 2010. Revised June 2, 2010. Accepted June 20, 2010. Advance Access publication August 18, 2010

Keywords: stem cells; neurogenesis; hippocampus; memory; learning; epilepsy; doublecortin

Abbreviations: BDNF = brain-derived neurotrophic factor; cdk5 = cyclin-dependent kinase 5; HPC = high proliferation capacity; IAT = intracarotid amobarbital testing; LPC = low proliferation capacity

# Introduction

Multipotent progenitor cells reside below the granule cell layer of the dentate gyrus in the adult mammalian hippocampus (Altman, 1962; Eriksson *et al.*, 1998; Gage, 2000) and give rise to newborn granule cells that mature and functionally integrate into neuronal microcircuits (van Praag *et al.*, 2002; Tashiro *et al.*, 2006; Zhao *et al.*, 2006; Jessberger *et al.*, 2008). The role of the specific regenerative capacity in the dentate gyrus, herein defined as capacity of adult hippocampal stem cells to proliferate and differentiate into neurons *in vitro*, has remained enigmatic until recent years, in which a number of studies have examined the role of the dentate gyrus in specific forms of memory and pattern processing. Particularly strong evidence is available for a role of both human and rodent hippocampus for pattern separation, which constitutes the distinct representation of similar inputs (Squire *et al.*, 2004; Leutgeb *et al.*, 2007; Bakker *et al.*, 2008; Nakashiba *et al.*, 2008). Pattern separation as a general principle may be applicable to different processing modalities both in human and in rodents and is probably a key process, important for spatial and episodic memory formation (Leutgeb *et al.*, 2007; Bakker *et al.*, 2008; Nakashiba *et al.*, 2008). More importantly, recent evidence indicates that pattern recognition is impaired if neurogenesis is reduced by irradiation (Clelland *et al.*, 2009). In addition to pattern separation, other forms of hippocampal-dependent memory tasks are also impaired when neurogenesis is experimentally reduced. For instance, hippocampus-dependent trace conditioning is impaired following pharmacological ablation of neurogenesis in the adult rat (Shors *et al.*, 2001). Transgenic inhibition of adult-born granule cells revealed deficient long-term spatial memory and further supports the notion that immature neurons that undergo maturation make an important contribution to learning and memory (Deng *et al.*, 2009; Jessberger *et al.*, 2009). Timing of neuronal differentiation plays a critical role in the functional integration of newly generated hippocampal neurons, and continuous production of neurons may be required not only for new memory acquisition, but also to use previously consolidated memories (Farioli-Vecchioli *et al.*, 2008). Taken together, these studies point to neurogenesis as a required determinant of dentate gyrus-dependent information processing and memory. Prospective studies that address the importance of neurogenesis in the human hippocampus are impossible to perform, for obvious reasons. We have taken advantage of the opportunity to obtain hippocampal specimens from epilepsy surgery to quantitatively assess the regenerative potential in the dentate gyrus in individual human subjects (Roy *et al.*, 2000; Walton *et al.*, 2006). We found two distinct groups of patients, one with a high potential for generation of neural precursors [high proliferation capacity (HPC)] and subsequent differentiation, and another with a severe deficiency in these processes [low proliferation capacity (LPC)]. As many patients with epilepsy also suffer from variable degrees of declarative learning and memory impairment (Helmstaedter and Elger, 2009), we have used these patient groups to ask if these dramatic differences in neurogenesis are reflected in altered hippocampus-dependent memory processes in human subjects.

# Materials and methods

## Human hippocampal tissue

Hippocampal specimens were obtained from 23 consecutive patients who underwent epilepsy surgery at the Erlangen Epilepsy Centre during 2006–09 (Table 1), in which drug-resistant unilateral mesial temporal lobe epilepsy was diagnosed by preoperative evaluation. Pre-surgical epilepsy monitoring included interictal and ictal video EEG monitoring, using 32–64 EEG channels, as well as MRI (1.5 Tesla Sonata Siemens, Munich, Germany) and neuropsychological evaluation. Intracarotid amytal testing (see below), PET, magnetic encephalography and intraoperative electrocorticography were applied when necessary to characterize the epileptogenic zone (Engel, 1994; Stefan *et al.*, 2004, 2009). Anti-epileptic drug treatment (at the time of surgery as well as previously administered during the course of the disease) is shown in Table 2. Mean duration of epilepsy was 24.7 years, ranging from 4 to 40 years. The average age at surgery was 36.9 years, ranging from 21 to 55 years. Tailored anterior temporal resections were performed in all patients including *en bloc* resection of the hippocampus. Available clinical data are summarized in Table 1. Informed and written consent was given by all patients included in our study for additional scientific investigations approved by the local ethics committee of the University of Erlangen. All procedures were conducted in accordance with the Declaration of Helsinki (1964).

## Human hippocampal cell culture

After surgical *en bloc* resection, the hippocampus was coronally sliced along the anterior–posterior axis. One naïve 5 mm thick section from the anteromedial body and adjacent to that used for histological analysis was available from each patient and processed for cell culture. The dentate gyrus was micro-dissected from adjacent structures (in particular from the ventricular wall) under a stereomicroscope (Olympus SZX9, Tokyo, Japan) and dissociated mechanically, followed by enzymatic digestion as described (Siebzehnrubl *et al.*, 2007). Isolated cells were plated in N5 medium (Walton *et al.*, 2006), supplemented with 20 ng/ml epithelial growth factor (CellSystems, St Katharinen, Germany), 20 ng/ml fibroblast growth factor 2 (R&D Systems, Minneapolis, MN, USA) and 10 ng/ml leukaemia inhibitory factor (Millipore, Billerica, MA, USA) onto poly-L-ornithine/laminin-coated (Sigma-Aldrich, Schnelldorf, Germany) culture plates. Growth factors were added every third day and medium was exchanged once a week. For differentiation, 20 000 cells were plated onto poly-L-ornithine/laminin-coated coverslips in N2 medium

**Table 1 Patients included in this study**

| Patient ID | Clinical history | | | | | | | |
|---|---|---|---|---|---|---|---|---|
| | Gender | First seizure (years) | Age at epilepsy onset (years) | Duration of epilepsy (years) | Age at surgery (years) | Side of resection | Seizure type | Memory (IAT) |
| P1 | F | 0 | 32 | 23 | 55 | Right | SPS, CPS, sGTCS | −2.20 |
| P2 | F | 1 | 26 | 11 | 37 | Left | SPS, CPS, sGTCS | −2.35 |
| P3 | F | 8 | 8 | 31 | 39 | Right | SPS, CPS | 0.30 |
| P4 | F | 3 | 3 | 34 | 37 | Right | SPS, CPS, sGTCS | NA |
| P5 | F | 0.5 | 14 | 23 | 37 | Left | SPS, CPS | 0.50 |
| P6 | F | 1 | 4 | 28 | 32 | Right | SPS, CPS, sGTCS | NA |
| P7 | M | 2.5 | 7 | 36 | 43 | Left | CPS, sGTCS | NA |
| P8 | F | 1 | 11 | 31 | 42 | Right | SPS, CPS, sGTCS | NA |
| P9 | M | 0.8 | 4 | 21 | 25 | Right | SPS, CPS | NA |
| P10 | F | 0.1 | 1 | 40 | 41 | Right | SPS, CPS | −1.00 |
| P11 | M | 1 | 1 | 39 | 40 | Right | SPS, CPS, sGTCS | NA |
| P12 | M | 4 | 4 | 24 | 28 | Right | SPS, CPS, sGTCS | NA |
| P13 | M | 3 | 11 | 23 | 34 | Left | CPS, sGTCS | −2.10 |
| P14 | M | 0.5 | 18 | 25 | 43 | Right | SPS, CPS, sGTCS | NA |
| P15 | F | 0.5 | 5 | 16 | 21 | Right | SPS, CPS, sGTCS | −0.70 |
| P16 | M | 42 | 42 | 4 | 46 | Right | SPS, CPS, sGTCS | NA |
| P17 | M | 2 | 3 | 32 | 35 | Left | SPS, CPS, sGTCS | NA |
| P18 | M | 2 | 20 | 7 | 27 | Left | SPS, CPS, sGTCS | −2.10 |
| P19 | F | 15 | 15 | 40 | 55 | Right | CPS, sGTCS | NA |
| P20 | M | 1.5 | 2 | 19 | 21 | Right | SPS, CPS, sGTCS | −1.40 |
| P21 | M | 5 | 26 | 25 | 51 | Right | CPS, sGTCS | NA |
| P22 | M | 7 | 7 | 25 | 32 | Right | CPS, sGTCS | NA |
| P23 | F | 18 | 18 | 10 | 28 | Right | SPS, CPS | NA |

IAT data are given as *z*-scores with normal values between 0 and −1, and severe memory impairment <−2.
CPS = complex partial seizures; F = female; IAT = Intracarotid amobarbital testing; M = male; NA = not analysed; sGTCS = secondary generalized tonic–clonic seizures; SPS = simple partial seizures.

containing 31.25 μg/ml bovine pituitary extract (Invitrogen, Karlsruhe, Germany), 1% foetal calf serum (Biochrom, Berlin, Germany); 500 ng/ml sonic hedgehog (R&D Systems), 100 ng/ml fibroblast growth factor 8 (Peprotech, Hamburg, Germany) and 1 μM suberoylanilide hydroxamic acid (Axxora, Lörrach, Germany) for 48 h. Thereafter, medium was changed to N2 supplemented with bovine pituitary extract, 1% foetal calf serum, 10 ng/ml nerve growth factor (Sigma-Aldrich) and 5 μM forskolin (Sigma-Aldrich). Cellular differentiation was immunocytochemically analysed after 14 days (see below).

## Fluorescence-immunocytochemical analysis

Immunocytochemistry of fixed cells and quantitative microscopic evaluation were performed as described earlier (Siebzehnrubl *et al.*, 2007). Primary antibodies were used at the following dilutions: mouse-anti-Map2ab (Sigma-Aldrich) 1:250, chicken-anti-MAP2 (Abcam, Cambridge, UK) 1:5.000, rabbit-anti-nestin (Millipore) 1:200, mouse-anti-nestin (Millipore) 1:200, rabbit-anti-Musashi (Millipore) 1:200, mouse-anti-Pax6 1:50 (Millipore), mouse-anti-βIII tubulin (Promega, Mannheim, Germany) 1:500, rabbit-anti-βIII tubulin (Covance, Berkeley, USA), mouse-anti-NeuN (Millipore) 1:1000, rabbit-anti-glial fibrillary acidic protein (Dako, Glostup, Denmark) 1:600, mouse-anti-glial fibrillary acidic protein (Millipore) 1:600, mouse-anti-2′,3′-Cyclic-nucleotide 3′-phosphodiesterase (Millipore) 1:200, rabbit-anti-doublecortin (Abcam) 1:500, mouse-anti-Ki67 (Dako) 1:100, rabbit-anti-brain-derived neurotrophic factor (BDNF; Abcam) 1:100, rabbit-anti-cyclin dependent kinase 5 (cdk5; Abcam) 1:100, goat-anti-Sox2 (Santa Cruz Biotechnology, Santa Cruz, CA, USA) 1:100. Secondary antibodies were obtained from Invitrogen and used in appropriate dilutions. Cellular nuclei were counterstained with Hoechst 33342 (Sigma-Aldrich). After differentiation with suberoylanilide hydroxamic acid, sonic hedgehog, fibroblast growth factor 8, forskolin and nerve growth factor, neuronal profiles were assessed *in vitro* by counting MAP2-immunoreactive cells.

## Histopathological examination

Each surgical hippocampus specimen was dissected into 5 mm thick slices along the anterior–posterior axis. Tissue from the mid-hippocampal body (see above) was fixed overnight in 10% formalin and routinely processed into liquid paraffin. All specimens were cut at 4 μm on a rotation microtome (Microm; Heidelberg, Germany) and stained with haematoxylin and eosin. Hippocampal pyramidal neurons and granule cells of the dentate gyrus were detected using immunohistochemistry for NeuN (Millipore, 1:1000) and an automated staining apparatus (Ventana, Strasbourg, France). Microwave pretreatment was applied for anti-doublecortin, anti-BDNF, anti-cdk5 and anti-Ki67 labelling of paraffin embedded tissue.

Table 2 **Anti-epileptic drug treatment in our series of 23 patients**

| Patient ID | VPA | CBZ | CLB | ESM | GBP | LTG | LEV | OXC | PB | PHT | PGB | PRM | STM | TPM | VGB | ZNS |
|---|---|---|---|---|---|---|---|---|---|---|---|---|---|---|---|---|
| P1 | N | Y | Y | N | P | N | Y | N | N | N | N | N | N | N | N | N |
| P2 | P | Y | N | N | N | P | Y | Y | N | N | N | P | N | N | N | N |
| P7 | P | Y | N | N | P | Y | P | N | P | P | N | N | N | N | N | N |
| P9 | P | N | N | N | N | N | P | Y | N | N | N | N | N | N | N | N |
| P13 | P | P | Y | N | P | P | Y | P | N | N | N | N | N | N | N | N |
| P14 | N | N | P | N | N | Y | N | N | N | N | N | N | N | N | N | N |
| P16 | P | N | N | N | N | Y | Y | N | N | N | N | N | N | N | N | N |
| P18 | N | P | N | N | N | N | Y | Y | N | N | N | N | N | N | N | N |
| P20 | P | N | N | N | N | Y | N | Y | N | N | N | N | N | N | N | N |
| P21 | P | P | Y | N | N | N | Y | Y | N | N | N | N | N | N | N | N |
| P22 | P | P | Y | N | N | N | Y | Y | N | N | N | N | N | N | N | N |
| P23 | N | P | N | N | N | Y | Y | N | N | N | P | N | N | N | N | N |
| P3 | P | P | P | N | N | Y | P | Y | N | P | P | P | N | P | N | P |
| P4 | N | N | P | P | N | Y | Y | P | N | N | N | P | N | P | P | N |
| P5 | P | N | N | N | N | Y | Y | N | N | N | N | N | N | N | N | N |
| P6 | P | N | N | N | P | Y | Y | N | N | N | P | N | N | N | N | N |
| P8 | P | P | N | N | P | P | Y | Y | N | N | P | N | N | P | N | P |
| P10 | P | P | N | N | P | N | P | Y | Y | P | N | N | N | P | N | N |
| P11 | P | P | N | N | N | Y | N | Y | P | N | N | N | N | N | N | N |
| P12 | P | P | Y | N | P | P | Y | Y | N | N | N | N | N | N | N | N |
| P15 | P | N | N | N | N | Y | P | P | N | P | N | N | Y | P | N | P |
| P17 | N | P | N | N | N | N | Y | Y | P | N | N | N | N | N | N | N |
| P19 | N | N | P | N | N | Y | N | Y | N | N | N | N | N | N | N | N |

The patient ID is the same as in Table 1, listed according to LPC (12 upper rows) and HPC (11 lower rows). Statistical analysis did not reveal any correlation between anti-epileptic drug treatment and each patient's regenerative capacity (Pearson Correlation, Table 4).
CBZ = carbamazepine medication in medical history; CLB = clobazam; ESM = ethosuximide; GBP = gabapentin; LEV = levetiracetam; LTG = lamotrigine; N = drug not obtained; OXC = oxcarbazepine; P = previously administered anti-epileptic drug medication during course of disease; PB = phenobarbital; PGB = pregabalin; PHT = phenytoin; PRM = primidon; STM = Sultiam; TPM = topiramat; VGB = vigabatrin; VPA = valproate (note that any valproate medication was stopped 3 months before surgery); Y = prescribed drug medication at time of surgery; ZNS = zonisamid.

## Neuronal cell counts

Semi-quantitative cell density measurements were obtained from all patients using 4 µm thin paraffin sections and NeuN immunohistochemistry (Wolf *et al.*, 1996). Hippocampal sectors CA1, CA2, CA3 and CA4 and the dentate gyrus were examined at ×40 objective magnification. Ten randomly placed microscopic fields were examined for each anatomical subregion. Measurements were performed with a microcomputer imaging system (ColorView II CCD camera, Soft imaging system SIS, Stuttgart, Germany) attached to a BX51 microscope (Olympus). Immunohistochemically stained neuronal cell bodies were tagged on the computer screen, counted within the region of interest and expressed as the mean number of neurons/mm$^2$ using AnalySIS imaging software (SIS) and Excel software (Microsoft, Redmond, Washington, USA). Histopathological data are summarized in Table 2. The same methodology was applied for assessing the proliferation activity *in vivo* using Ki67 immunoreactivity. The subgranular and granule cell layers were analysed in 18 patients from which sufficient material was available for preparing 10 serial 4 µm sections. We could not perform these experiments in patients P1, P2, P3, P5 and P7 (Table 1).

Nestin-, Sox2-, PAX6-, doublecortin-, BDNF- and cdk5-immunoreactive cells were semi-quantitatively estimated by the same method using fluorescence labelling. Four adjacent microscopic fields were placed into the dentate gyrus granule cell layer at ×20 objective magnification and immunoreactive cell bodies were identified using appropriate filter combinations.

## Electrophysiological recordings from human hippocampal progenitor cells

Membrane currents were measured by applying the patch-clamp technique in a whole-cell recording configuration. Current signals were amplified with an EPC-9 amplifier (HEKA, Lambrecht, Germany). Whole-cell recordings were performed after three expansion periods and induced differentiation (see above). After 14 days *in vitro*, cells with a neuronal morphology by phase contrast imaging were chosen (Fig. 2C). All cells were held at −70 mV. Following a 40 ms prepulse to −120 mV, voltage steps incremented by 10 mV were applied from −80 to +10 mV every 2 s. The external buffer consisted of 145 mM NaCl, 5 mM KCl, 2.4 mM $CaCl_2$, 1 mM $MgCl_2$, 1.8 mM glucose, 10 mM HEPES, pH adjusted to 7.4 with NaOH; the internal buffer contained 150 mM CsCl, 5 mM EGTA, 10 mM HEPES, and the pH adjusted to 7.2 using CsOH. All experiments were carried out at room temperature (~22°C). Recording pipettes were fabricated from borosilicate capillaries with open resistances of 5–6 MΩ.

## Neuropsychological examination

Intracarotid amobarbital testing (IAT; WADA) was carried out separately in both hemispheres as part of the presurgical evaluation in nine patients. The test is employed in patients in whom the risk for postoperative memory loss has to be clarified preoperatively. The greatest potential risk in surgical treatment is verbal memory loss in patients

suffering from left-sided temporal lobe epilepsy (Chelune, 1995), but suspicion of atypical memory dominance in right-sided temporal lobe epilepsy should in some cases also require examination. Thus 5 out of 6 patients with left-sided temporal lobe epilepsy and 4 out of 17 patients with right-sided temporal lobe epilepsy underwent IAT following the Erlangen Wada Test protocol. This protocol is described in detail elsewhere (Pauli *et al.*, 2006). In brief, double encodeable memory items are tested under recall and recognition conditions and the results are transformed into *z*-scores according to normative values specific for speech dominant and for non-dominant hemispheres, respectively. Since healthy control data are not available for IAT, standardization was based on values from the contralateral, non-affected left or right temporal lobes, including only those patients from our database ($n > 200$) presenting with: (i) unilateral mesial temporal lobe epilepsy; (ii) unilateral left-sided speech dominance; (iii) complete postoperative seizure freedom; and (iv) normal range IQ. IAT memory scores were transformed into *z*-values following the calculation rule: (i) if the resected hippocampus was taken from the speech dominant hemisphere: $z(\text{IAT memory}) = [(\text{Total memory score} - \text{Mean}_{left})/\text{SD}_{left}]$; and (ii) if the resected hippocampus was taken from the non-dominant hemisphere: $z(\text{IAT memory}) = [(\text{Total memory score} - \text{Mean}_{right})/\text{SD}_{right}]$. Thus, a *z*-score of 0 indicates full functional integrity of the investigated left or right hippocampal structure; i.e. indicates equality with the average score of non-affected left or right hippocampi in unilateral temporal lobe epilepsy.

## Statistical analysis

Statistical Package for the Social Sciences (SPSS, version 16) was used for statistical evaluation. The threshold for significance was set to 0.05. Correlation analysis, linear multiple regression and partial correlations were calculated to evaluate the relationship between clinical histories, histopathological data, cell culture and memory performance. Cluster analysis and discriminance analysis were used to explore neurogenesis *in vitro*. Correlation analysis (Pearson) was performed to relate (i) neurogenesis *in vitro* with clinical data (age, onset and duration of epilepsy); (ii) neurogenesis *in vitro* with cell densities in hippocampal subfields and the dentate gyrus; and (iii) neurogenesis *in vitro* with IAT memory capacity. Only variables that significantly correlated with the dependent variable were included in linear regression and partial correlation analysis. Since the multiple correlation coefficient $R$ tends to overestimate the correlation between observed and predicted values of dependent variables, adjusted $R^2$, which is thought to more closely reflect the goodness of fit of the model in a population, was calculated. $R^2_{adjusted}$ describes the proportion of variance of the dependent variable that is explained by the independent variables. To assess the relative importance of each independent variable, we applied the *t*-statistic for the linear regression coefficient and only values >2 were considered significant. To check for multicolinearity, tolerance statistics were used. In addition, partial correlation analysis was calculated to assess the correlation of the independent variable with the dependent variable after removing the linear effect of the other variables in the model. Neuropsychological parameters as well as cell densities in the hippocampal subfields were transformed into *z*-scores, representing, in standard deviation units, the amount score deviates from the mean of the population from which the score is drawn (null hypothesis). For histopathological data (cell densities in the hippocampal subfields and the dentate gyrus), standardization was based on age-matched non-epileptic autopsy controls (Blumcke *et al.*, 2007). For IAT, standardization was based on normal values from contralateral, non-affected left or right temporal lobes in unilateral temporal lobe epilepsy.

# Results

## HPC and LPC in adult human hippocampal stem cells *in vitro*

Adult hippocampal progenitor cells have the capacity for self-renewal, to generate new cells by asymmetric division and further differentiate into various cell lineages of the brain (Gage, 2000). We obtained surgical hippocampal tissue from 23 patients with drug-resistant epilepsy (Table 1). Following microdissection of the dentate gyrus, cells were dissociated and proliferated as a monolayer culture (Fig. 1A). Three cell culture passages were applied to expand the progenitor cell population ('Materials and methods' section), which were characterized by abundant expression of nestin and Musashi1 (Fig. 1B). Cluster analysis of data obtained after three cell culture passages *in vitro* from all subjects revealed two significant patterns (Fig. 1C; $F = 45.1$; $df = 1/22$; $P < 0.001$). An HPC was observed in 11 specimens, showing doubling of primarily seeded cells after 2–3 weeks and continued proliferation through further passages *in vitro* (Fig. 1D). An LPC was evident in the remaining 12 specimens. Although cell numbers increased during each passage in LPC cultures, their amount remained significantly lower after three passages *in vitro* compared with HPC specimens.

## HPC versus LPC cultures showed different propensities for neuronal differentiation

After completing our proliferation protocols, growth factor withdrawal induced spontaneous differentiation into a neuronal phenotype in most cell cultures, ranging from 0 to 6% (mean $2 \pm 2\%$) of the total cell population. Differentiation into a neuronal phenotype was significantly enhanced using suberoylanilide hydroxamic acid, an inhibitor of histone deacetylases (Hsieh *et al.*, 2004; Siebzehnrubl *et al.*, 2007), as well as sonic hedgehog and fibroblast growth factor 8 for 48 h, followed by treatment with the adenylcyclase activator forskolin and nerve growth factor for 12 days (mean $28 \pm 27\%$). Cellular phenotype was microscopically analysed after 14 days in culture and staining with antibodies directed against antigens specific for neurons, i.e. MAP2 and NeuN (Fig. 2A and B), astrocytes (glial fibrillary acidic protein, not shown) and oligodendrocytes (2′,3′-cyclic nucleotide 3′-phosphodiesterase, not shown), suggesting the maintenance of multipotent adult hippocampal stem cells in our cultures. In addition, patch-clamp recordings detected sodium inward currents of up to 300 pA (Fig. 2C) in cells with dendrite-like neuronal arborizations. These findings demonstrated that adult hippocampal stem cells can be isolated from human surgical tissue and differentiated into neurons.

There was a highly significant correlation between proliferation and the same patient's capacity to generate neurons *in vitro* ($r = 0.834$, $R^2 = 0.696$, $P < 0.001$). Linear regression analysis revealed proliferation as the only variable meeting the demands of the predictors criterion $|t| > 2$ ($T = 6.94$, $R^2_{adjusted} = 0.696$,

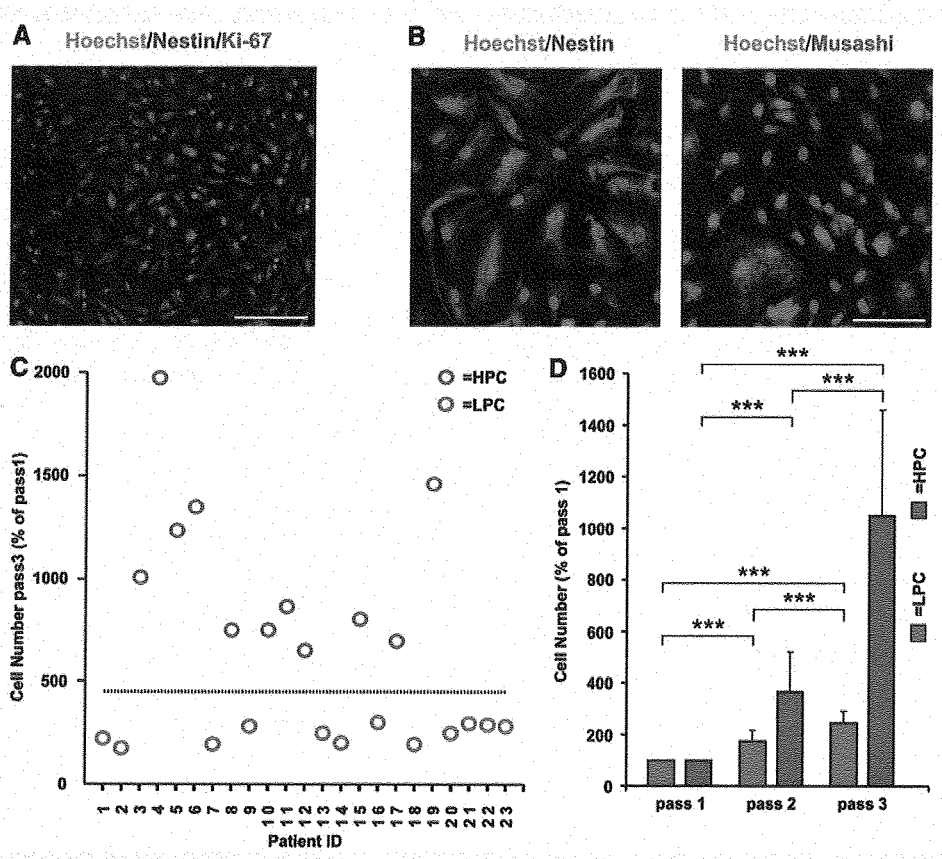


**Figure 1** Different proliferation capacities of human adult hippocampal stem cells. (**A**) Double-fluorescence immunocytochemistry of nestin (green) and Ki67 (red) epitopes confirmed proliferation activity of adult hippocampal stem cells. Hoechst nuclear staining shown in blue (also in **B**). (**B**) Fluorescence immunocytochemistry of nestin (green) and Musashi (red) confirmed stemness of the progenitor cell population. Scale bars in **A** = 50 μm and **B** = 100 μm. (**C**) Discriminance analysis of proliferation capacities obtained from all cell cultures revealed two significant growth patterns ($P < 0.001$). HPCs are indicated by blue dots, LPC by red dots. (**D**) Red bars refer to LPC culture specimens. Blue bars refer to HPC cultures, which showed a significant higher increase in cell numbers after each of the three passages (pass) *in vitro* ($P < 0.001$). ***$P < 0.001$ (*t* test).

$P < 0.001$), indicating that nearly 70% of the variance of the capacity to generate new neurons *in vitro* is explained by proliferation. HPC cell cultures showed a mean of 53 ± 13% MAP2-immunoreactive neuronal cells (compared with spontaneous neuronal differentiation of 3 ± 2% following growth factor withdrawal; Fig. 2D). In contrast, cell cultures obtained from LPC specimens failed to generate more cells with a neuronal phenotype (mean percentage of MAP2-immunoreactive cells = 4 ± 2% after targeted differentiation; Fig. 2D). In the latter cultures, expression of the neural precursor filament nestin persisted in 69 ± 12% of cells (compared with 78 ± 14% after spontaneous differentiation; Fig. 2E) and glial markers were also not significantly increased (5 ± 4% glial fibrillary acidic protein- and 2′,3′-cyclic nucleotide 3′-phosphodiesterase-immunoreactive cells after targeted differentiation compared with 3 ± 2% after spontaneous differentiation). Proliferation within the granule cell layer was studied using the Ki67-epitope in 18 patients from whom serial sections were available (Fig. 3A). These data showed a significant difference between the LPC and HPC groups ($P = 0.002$; Fig. 3B). Statistical analysis confirmed a significant correlation between the numbers of proliferating cells *in vivo* and the proliferation capacities detected *in vitro* ($P = 0.007$; Fig. 3C). Although sufficient tissue was not available for a systematic serial section analysis of additional neural stem cell marker proteins (i.e. nestin, Pax6 or Sox2), double immunofluorescence was performed in each patient and confirmed an immature phenotype of Ki67-immunoreactive, proliferating cells in the dentate gyrus (Fig. 4). These data demonstrate that patients with temporal lobe epilepsy fall into two distinct groups, with high versus low capacity for proliferation *in vivo* and *in vitro* as well as a commensurately differing capacity for differentiation.

## Patients with HPC versus LPC cultures showed different granule cell densities *in vivo*

These dramatic differences in the HPC versus LPC patient groups led us to examine whether granule cell densities were higher in the HPC group. Formalin-fixed and paraffin-embedded tissue sections from the anteromedial part of the hippocampal body were

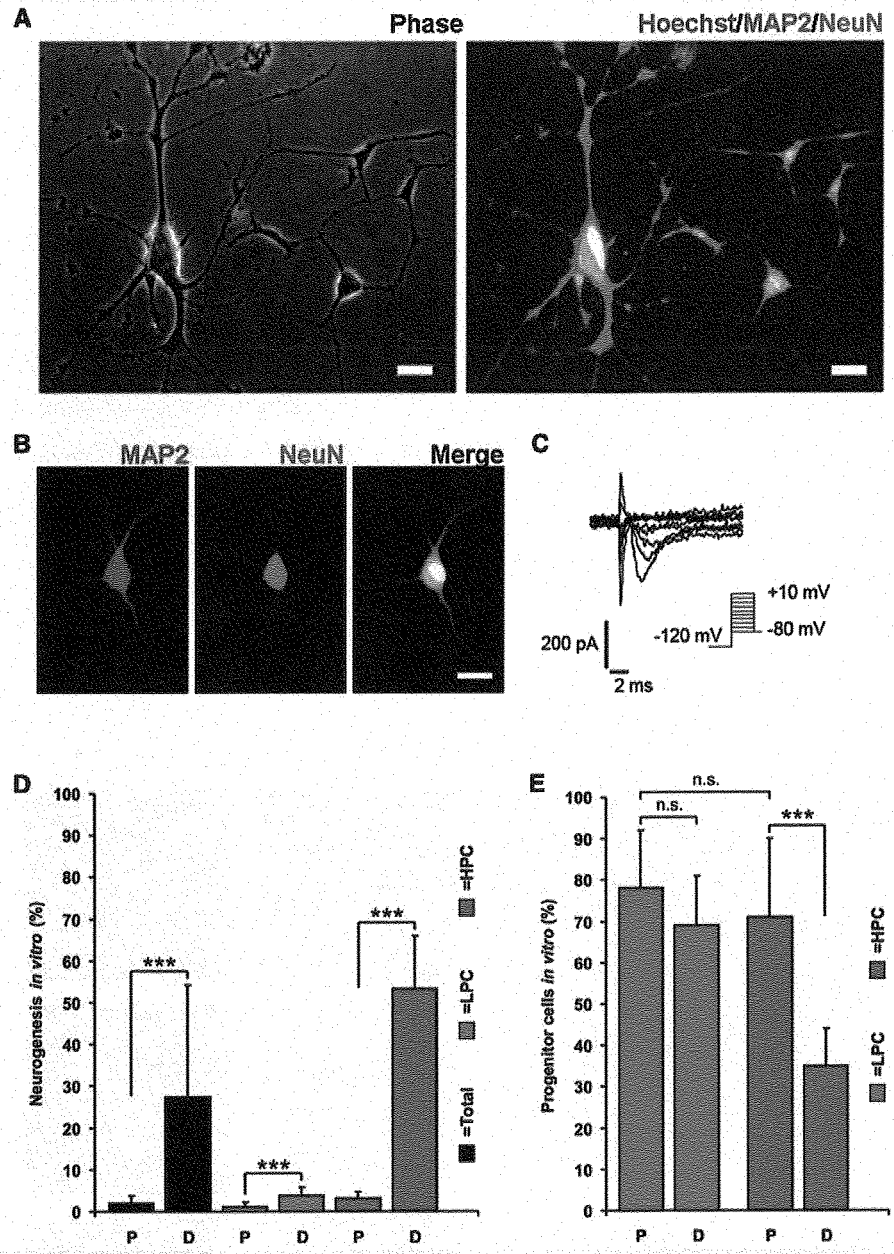


**Figure 2** Targeted neuronal differentiation of human adult hippocampal stem cells. (**A**) Following our differentiation protocol, cells with a neuronal phenotype showed elaborated process outgrowth (phase contrast) and expression of neuron-specific epitopes MAP2 (green) and NeuN (red). Coexpression of neuronal marker proteins in yellow, Hoechst nuclear staining in blue. (**B**) Single channel immunofluorescence detection from a neuron *in vitro* co-expressing MAP2 (green) and NeuN (red). (**C**) Voltage-clamp profile of adult hippocampal progenitor cells after 14 days of differentiation. This representative trace showed an inward $Na^+$ current generated following a voltage step protocol from −80 to +10 mV incremented by 10 mV every 2 s following a 40 ms prepulse to −120 mV (see inset). (**D**) After the proliferation period shown in Fig. 1D, only a few cells differentiated spontaneously into a neuronal phenotype after growth factor withdrawal (quantified by MAP2 immunoreactivity). Induction of neuronal differentiation could be achieved, however, only in HPC cultures ($P<0.001$; n.s. = not significant). (**E**) There was a significant decrease of the nestin-immunoreactive progenitor cell population after successful induction of a neuronal phenotype ($P<0.001$). Blue bars in **D** and **E** refer to HPC, red bars to LPC. Scale bars in **A** and **B** = 20 μm. ***$P<0.001$ (*t* test).

available from all surgical specimens and were adjacent to those used for cell culture experiments (Fig. 5). Neuronal cell numbers and densities were quantitatively determined in all hippocampal subfields, including the pyramidal cell layer as well as the granule cell layer of the dentate gyrus (Table 3). There was a highly significant correlation between granule cell densities and the same patient's proliferation capacity *in vitro* ($r=0.813$, $R^2=0.661$, $P<0.001$). Neuronal cell numbers obtained from hippocampal

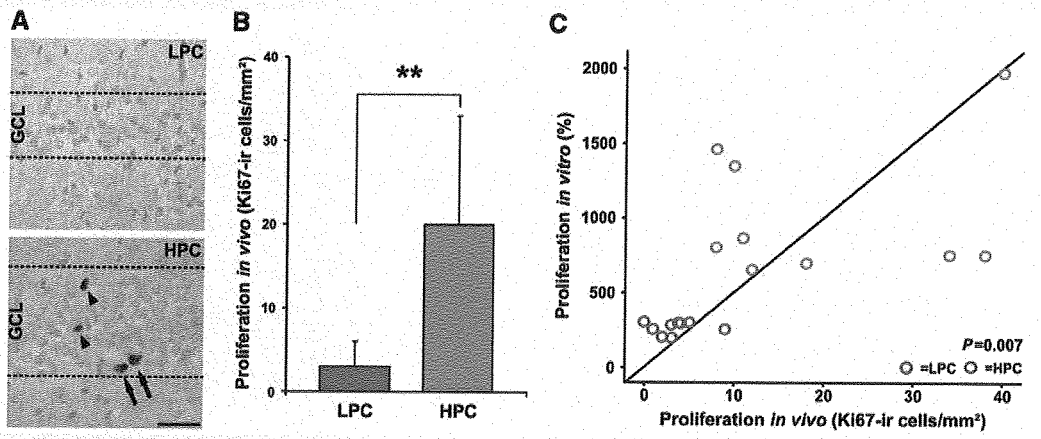


**Figure 3** Analysis of proliferating cells in the dentate gyrus of LPC and HPC patients *in vivo*. (**A**) Ki67-immunostaining. This granule cell layer depicted is from an LPC patient and revealed no Ki67-positive cell nuclei (top). Similar analysis in an HPC patient (bottom) revealed proliferating cells in the subgranular zone of the dentate gyrus (arrows) as well as in the granule cell layer (arrowheads). Scale bar = 100 μm. (**B**) The difference between *in vivo* proliferation in LPC and HPC groups reached statistical significance (numbers given are Ki67-immunoreactive cells per $mm^2$; $P = 0.002$). (**C**) There was also significant correlation between proliferation *in vivo* with the same patient's regenerative capacity *in vitro* ($r = 0.612$, $R^2 = 0.375$, $P = 0.007$, $n = 18$). LPCs are indicated by red dots and HPC by blue dots. $^{**}P < 0.01$ (*t* test).

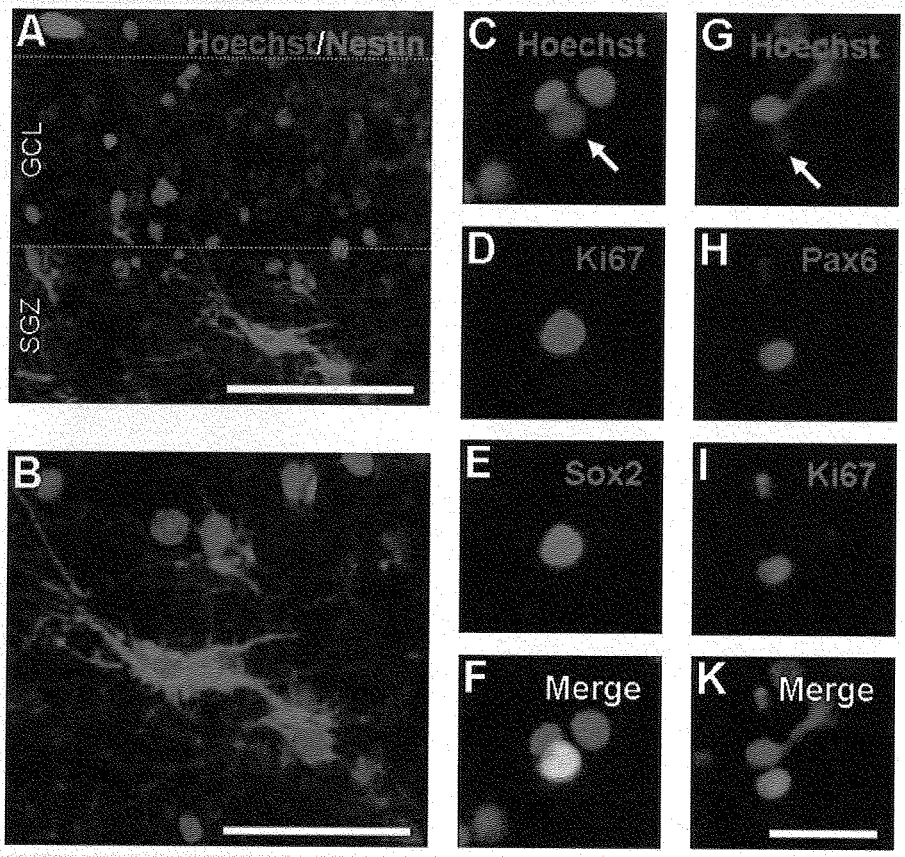


**Figure 4** Immunohistochemical characterization of precursor cells in the human dentate gyrus *in vivo*. (**A**) Nestin-immunoreactive cells were detected in the subgranular zone (SGZ) of the dentate gyrus. (**B**) Higher magnification of **A**. (**C–F**) A Ki67 positive, proliferating cell showing co-expression with Sox2 or Pax6 (**G–K**). Scale bar in **A** = 100 μm; **B** = 50 μm and **C–K** = 20 μm.

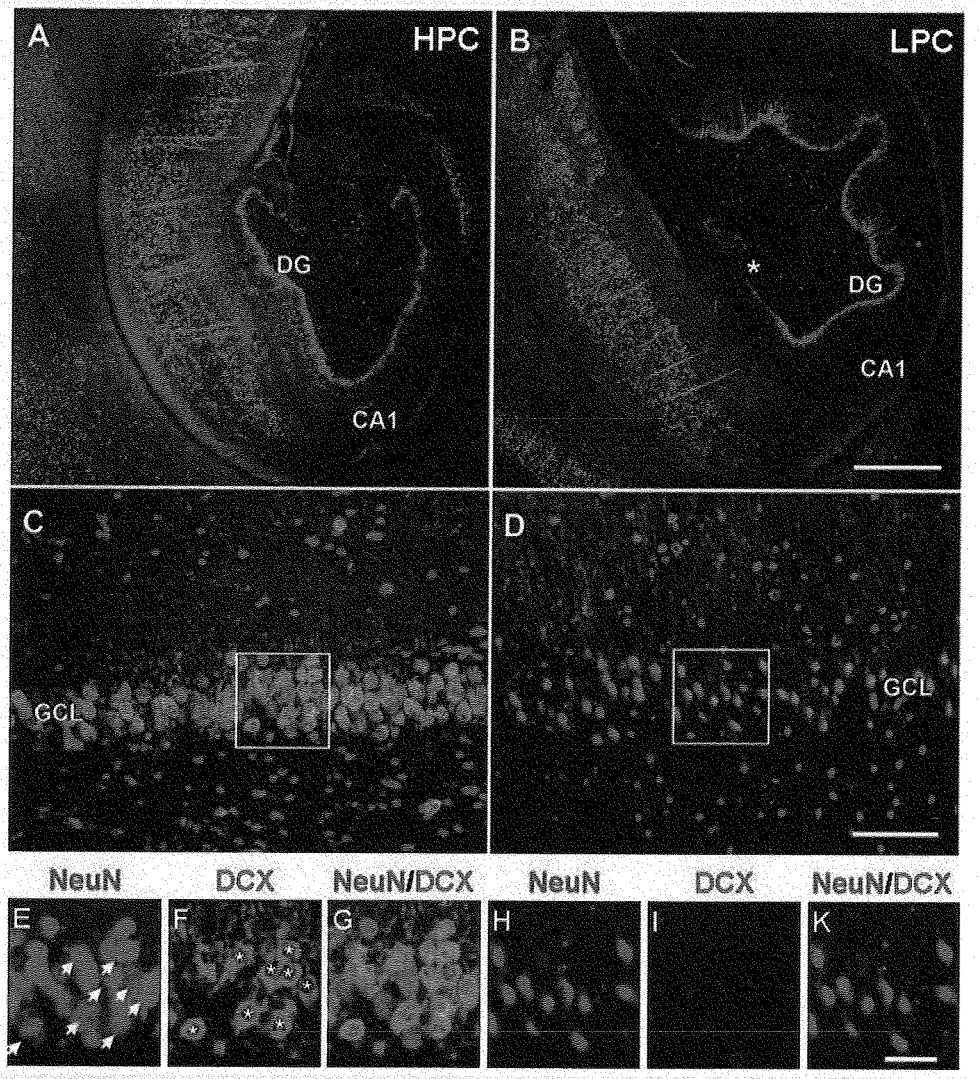


**Figure 5** Histopathological examination of surgical human hippocampus. All surgical hippocampus specimens in this study were anatomically well preserved. (**A**) All segments of the dentate gyrus (DG) showed a compacted granule cell layer in this surgical specimen (NeuN fluorescence immunohistochemistry). In contrast, CA4, CA3 and CA1 pyramidal neurons are significantly reduced, i.e. mesial temporal sclerosis type 1a (Blümcke *et al.*, 2007). (**B**) Granule cell loss is visible in various dentate gyrus segments, most prominently within the internal limb (asterisk). Pyramidal cell loss is detected in all CA segments, i.e. mesial temporal sclerosis type 1b. (**C**) Example from a surgical specimen with a densely populated granule cell layer (GCL) showing abundant doublecortin (red) and NeuN (green) co-expressing granule cells (insert refers to magnification in **E–G**). (**D**) In this severely depleted granule cell layer we observed virtually no doublecortin-immunoreactive cells (insert refers to magnification in **H–K**). (**E–G**) Arrows in **E** (granule cells with predominantly nuclear NeuN-immunoreactivity) and asterisks in **F** (granule cells with perinuclear doublecortin-staining) indicated NeuN and doublecortin double-labelled neurons. (**H–K**) NeuN-immunopositive granule cells showed no co-expression of doublecortin. **A**, **C**, **E–G** correspond to a patient from the HPC group; **B**, **D**, **H**, **I** and **K** to a patient in the LPC group. Scale bar in **A** and **B** = 500 μm; **C** and **D** = 100 μm; and **E–K** = 50 μm. Nuclear Hoechst staining in blue in **C** and **D**.

sectors CA4 ($r = 0.652$, $P = 0.001$) and CA3 ($r = 0.487$, $P = 0.040$) correlated significantly with the patient's stem cell proliferation capacity *in vitro*, although to a lower extent. Even so, there was a high intercorrelation of cell densities in the different hippocampal subfields and the dentate gyrus. Therefore, multiple linear regressions were applied to further examine these correlations and to determine the most important predictor for stem cell proliferation *in vitro*. When cell densities in CA3 and CA4 as well as granule cell density were entered stepwise into the equation, $R^2_{adjusted}$ reached 0.64, but only the granule cell density of the dentate gyrus fulfilled the predictor's criteria for relative importance ($\|t\|_{absolut} = 5.586 > 2$). Removing the effect of cell densities in CA3 and CA4 by partial correlation analysis, a significant partial correlation coefficient resulted [$R$(partial) = 0.81, $P < 0.001$], not different from the basic correlation coefficient ($r = 0.813$).

Table 3 **Quantitative histopathological analysis of human hippocampal tissue *in vivo* and neurogenesis *in vitro***

| Patient ID | Histopathological analysis (*in vivo*) | | | | | | Neurogenesis (*in vitro*) | |
|---|---|---|---|---|---|---|---|---|
| | Neuronal densities | | | | | | | |
| | CA1 | CA2 | CA3 | CA4 | DG | Diagnosis | Spontaneous (%) | Induced (%) |
| P1 | NA | NA | 100 | 56 | 1410 | MTS | 3 | 4 |
| P2 | 96 | 316 | 248 | 120 | 1330 | MTS | 0 | 2 |
| P7 | 68 | NA | NA | 128 | 370 | MTS | 1 | 4 |
| P9 | 80 | NA | NA | 112 | 1050 | MTS | 2 | 8 |
| P13 | 52 | NA | 128 | 140 | 1520 | MTS | 1 | 5 |
| P14 | 204 | 208 | 260 | 136 | 1200 | MTS | 0 | 1 |
| P16 | NA | NA | NA | NA | 1390 | no MTS | 2 | 3 |
| P18 | 68 | NA | 88 | 32 | 1590 | MTS | 0 | 2 |
| P20 | 60 | 188 | 100 | 72 | 1170 | MTS | 1 | 4 |
| P21 | 56 | 196 | 276 | 28 | 1490 | MTS | 2 | 6 |
| P22 | 80 | 256 | 96 | 56 | 1030 | MTS | 1 | 4 |
| P23 | 356 | NA | NA | 120 | 640 | MTS | 1 | 3 |
| P3 | 368 | 508 | 420 | 292 | 2930 | no MTS | 3 | 71 |
| P5 | 44 | 212 | NA | 100 | 2530 | MTS | 1 | 63 |
| P4 | 440 | 404 | 280 | 292 | 3380 | no MTS | 0 | 66 |
| P6 | 64 | NA | 240 | 184 | 2060 | MTS | 4 | 46 |
| P8 | 144 | NA | 164 | 228 | 1300 | MTS | 5 | 66 |
| P10 | 52 | 212 | 180 | 48 | 1800 | MTS | 2 | 51 |
| P11 | 52 | 216 | 316 | 180 | 2490 | MTS | 2 | 40 |
| P12 | 220 | 156 | 208 | 56 | 1810 | MTS | 3 | 31 |
| P15 | 80 | NA | NA | 304 | 1910 | MTS | 3 | 58 |
| P17 | 64 | 332 | 236 | 256 | 1810 | MTS | 4 | 51 |
| P19 | 364 | 320 | 268 | 124 | 1860 | no MTS | 6 | 44 |

CA1–CA4 = anatomical segments of the human hippocampus; DG = dentate gyrus; NA = area not available for cell counting; n (*in vitro*) = percentage of MAP2-immunoreactive cells from the entire cell population after spontaneous (withdrawal of growth factors) or induced differentiation (supplement of sonic hedgehog, suberoylanilide hydroxamic acid, forskolin, nerve growth factor and fibroblast growth factor 8); neuronal densities = NeuN-immunoreactive neurons/mm$^2$; MTS = mesial temporal sclerosis (Blümcke *et al.*, 2007).

Diagnostic evaluation of segmental neuronal cell loss patterns revealed mesial temporal sclerosis in 19 out of 23 patients, eight in the group with abundant neurogenesis *in vitro* and 11 in the group with a reduced regenerative capacity.

## Patients with HPC versus LPC cultures revealed different immunoreactivity patterns for doublecortin, brain-derived neurotrophic factor and cdk5 *in vivo*

The increased neurogenesis in the HPC patient group should be reflected in an increased proportion of neurons expressing surface markers characteristic of newly generated and integrated neurons. We carried out double-immunofluorescence labelling for doublecortin and NeuN in an additional set of experiments to address this issue (Liu *et al.*, 2008). In 12 patients with LPC, doublecortin expression was observed in 20.3 ± 8.5% of the total granule cell population. The amount of doublecortin-positive granule cells was significantly higher in the group of 11 patients with HPC *in vitro* (53.4 ± 13.6%), and correlated significantly with the proliferation rate observed *in vitro* ($r = 0.790$, $P < 0.001$; Fig. 7). These cell numbers were significantly higher compared with recently published data by Knoth *et al.* (2010) in autopsy controls and Gerber *et al.* (2009) in meningitis specimens, whereas staining patterns were similar to that reported by Jin *et al.* (2004) in the dentate gyrus of patients with Alzheimer's disease. Different antibody origin and antigen retrieval systems, as well as fixation intervals, are likely to account for these differences. Furthermore, we studied the expression of two molecules involved in the molecular signalling machinery of hippocampal neurogenesis, i.e. BDNF and cdk5 (Fig. 6). BDNF- and cdk5-expression was significantly reduced in 12 specimens with LPC *in vitro* when compared with the 11 patients with HPC *in vitro*, and the numbers correlated significantly with each patient's proliferation rate observed *in vitro* (BDNF: $r = 0.596$, $P = 0.003$; cdk5: $r = 0.596$, $P = 0.003$).

## Significant correlation between the regenerative capacity *in vitro* and the same patient's memory

We observed a striking and highly significant correlation between each patient's regenerative capacity deduced either from our cell culture assay (*in vitro*) or from histopathological characterization (*in vivo*) and the same patient's ability to acquire and recall new memories during preoperative examination. IAT memory correlated significantly with the regenerative capacity *in vitro*

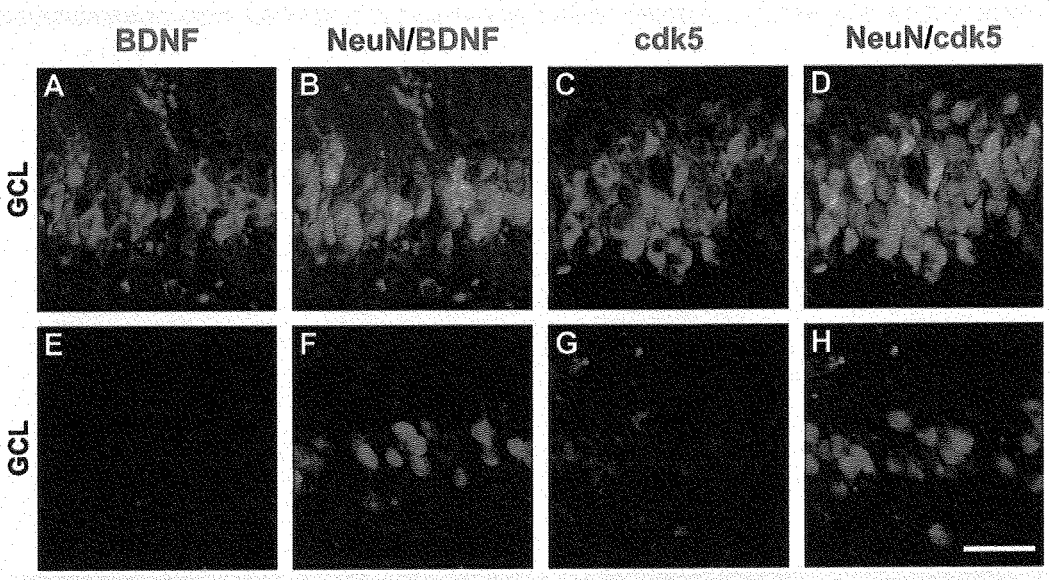


**Figure 6** Immunohistochemical characterization of BDNF and cdk5 in the human hippocampus *in vivo*. Immunohistochemical examination of the dentate gyrus in surgical hippocampus specimens showed two different patterns of BDNF and cdk5 immunoreactivities. (**A–D**) were obtained from a patient with HPC *in vitro*. (**E–H**) were obtained from a patient with LPC *in vitro*. Scale bar = 50 μm. GCL = granule cell layer.

($r = 0.966$, $R^2 = 0.933$, $P < 0.001$; Fig. 7B) and with granule cell density of the dentate gyrus *in vivo* ($r = 0.888$, $R^2 = 0.789$, $P = 0.001$; Fig. 7C). Regression analysis showed a significant linear regression when entering both variables ($R = 0.966$, $R^2_{adjusted} = 0.923$, $F = 96.976$, df = 1/7, $P < 0.001$). Using the *t*-statistic for the linear regression coefficient to assess the relative importance of each of the independent variables, the proliferation *in vitro* ($t = 9.848 > 2$) turned out to be the crucial predictor for memory capacity (Fig. 7A and B). Partial correlation analysis, to assess the correlation of both independent variables with memory and when removing the linear effect of the other variable in the model, respectively, resulted in $R$(partial) = 0.966 for regenerative capacity and $R$(partial) = 0.682 for granule cell density in the dentate gyrus.

Further analysis of the divergent regenerative capacity in the human hippocampus with clinical histories from LPC versus HPC groups of patients showed fewer females in the LPC group (Table 1; three female versus nine male patients). In contrast, female gender prevailed in the HPC group (eight female and three male patients). LPC *in vitro* was only by trend correlated to a later age at epilepsy onset ($r = -3.53$, $P = 0.098$) and positively correlated to a shorter duration of epilepsy ($r = 0.426$, $P = 0.042$), indicating that a longer seizure history is not predictive for reduced regenerative capacities *in vitro*. There was no significant correlation between age at first seizure or age at surgery. In addition, there was no significant correlation between anti-epileptic drug treatment and the regenerative capacity of the human hippocampus (Table 4).

# Discussion

Our study has demonstrated that patients with chronic, drug-resistant temporal lobe epilepsy fall into two clearly separable categories with respect to their regenerative capacity within the hippocampus. We first tested the hypothesis that the proliferation and neuronal differentiation capacity *in vitro* was correlated with each patient's memory performance prior to surgery. Animal studies have demonstrated a constitutive supply and replacement of newborn neurons as a critical mechanism for hippocampal memory consolidation (Gould *et al.*, 1999; van Praag *et al.*, 1999; Shors *et al.*, 2001; Clelland *et al.*, 2009; Deng *et al.*, 2009; Jessberger *et al.*, 2009; Kitamura *et al.*, 2009), and cognitive dysfunction is a frequent finding in subgroups of patients with temporal lobe epilepsy (Pauli *et al.*, 2006; Helmstaedter and Elger, 2009). However, this has never been experimentally addressed in humans. Our data showed a highly significant and specific correlation between the regenerative capacity *in vitro* and the same patient's ability to store and recall memories, suggesting that a similar mechanism also operates in the human hippocampus.

Is the proliferative and differentiation capacity assessed *in vitro* a good measure of the neurogenic potential *in vivo*? Our data suggest that this may be the case. We were able to show a significant correlation between the proliferation capacity *in vivo* and the regenerative capacity *in vitro*. We also studied the expression of proteins involved in the molecular signalling machinery of hippocampal neurogenesis, i.e. doublecortin, BDNF and cdk5. Doublecortin and BDNF, as well as cdk5, revealed a highly significant reduction in specimens with granule cell loss and failure of neuronal differentiation *in vitro*. BDNF is required for neurogenesis in the hippocampus (Rossi *et al.*, 2006) and long-term survival of newborn granule cells (Sairanen *et al.*, 2005). In contrast, region- or cell-specific knockdown identified cdk5 to be critically involved in the maturation process of newborn neurons during adult neurogenesis (Jessberger *et al.*, 2008, 2009; Lagace *et al.*, 2008). The observed downregulation of both important molecular factors regulating adult neurogenesis in the human dentate gyrus *in vivo*

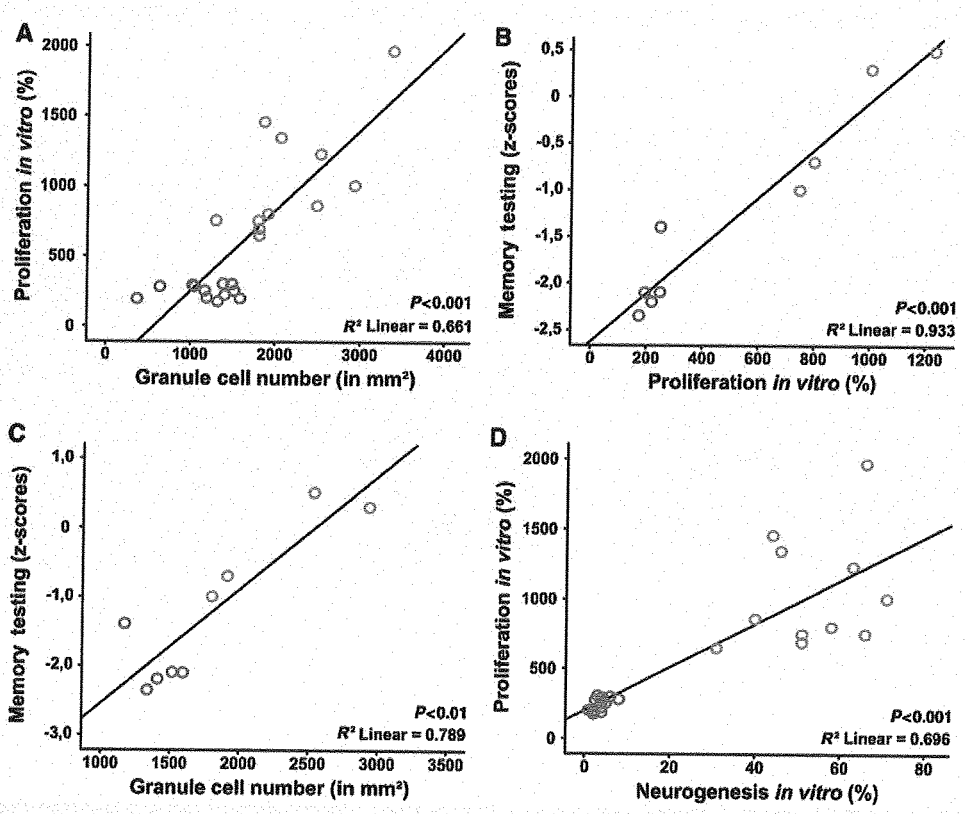


**Figure 7** Reduced proliferation capacities *in vitro* correlated with memory impairment and lower granule cell numbers *in vivo*. (**A**) Hippocampal granule cell densities *in vivo* (given as NeuN-immunoreactive granule cells per $mm^2$) correlate significantly with the same patient's regenerative capacity as determined by proliferation capacities *in vitro* ($r = 0.813$, $R^2 = 0.661$, $P < 0.001$, $n = 23$). (**B**) Proliferation capacities *in vitro* correlated significantly with neurogenesis *in vitro* ($r = 0.834$, $R^2 = 0.933$, $P < 0.001$, $n = 23$). (**C**) Memory scores were significantly related to granule cell densities *in vivo* ($r = 0.888$, $R^2 = 0.789$, $P = 0.01$, $n = 9$). *Z*-scores were calculated from intracarotid amobarbital memory testing (IAT) with normal values between 0 and −1 ('Materials and methods' section). (**D**) Correlation analysis revealed a highly significant association between the capacity to generate new neurons *in vitro* and the proliferation capacities *in vitro* ($r = 0.834$, $R^2 = 0.696$, $P < 0.001$, $n = 23$). Red dots indicate LPC patients, blue dots indicate HPC patients.

confirmed a compromised molecular machinery for hippocampal neurogenesis in the patient group with an LPC *in vitro*. This suggests that neurogenesis in the human hippocampus, first detected in five autoptic brain samples obtained from cancer patients treated with the thymidine analog bromodeoxyuridine (Eriksson *et al.*, 1998), is closely linked to the neurogenic potential *in vivo*. Finally, the close correlation of the neurogenic potential with the density of granule cells suggests that neurogenesis also regulates the granule cell numbers in human subjects.

Increased hippocampal neurogenesis has been observed in different epilepsy models (Parent *et al.*, 1997, 2006; Siebzehnrubl and Blumcke, 2008), and increased numbers of nestin-immunoreactive neural precursor cells were detected in the dentate gyrus of patients with temporal lobe epilepsy younger than 4 years at time of operation (Blumcke *et al.*, 2001). In contrast, the regenerative capacity of the hippocampus declined in chronic seizure models (Hattiangady *et al.*, 2004; Hattiangady and Shetty, 2009) and is also likely to decrease with age (Fahrner *et al.*, 2007; Ahlenius *et al.*, 2009). However, our data suggest no clear effects of early epilepsy onset, longer duration of seizures or higher age at surgery on adult neurogenesis. This may be due to the very long period of chronic seizures in all patients, far exceeding that studied in any animal model. Rather, compromised neurogenesis was observed in patients with late onset of first seizures. This observation will need further clarification. It is in line with the notion, however, that less vulnerable neuronal and stem cell populations can be detected in younger compared with older animals (Haas *et al.*, 2001; Liu *et al.*, 2003). Furthermore, nestin-expressing precursor cells persisted in cultures obtained from patients with temporal lobe epilepsy with compromised neurogenesis *in vitro* (Fig. 2E). Similar data are obtained from an animal model of temporal lobe epilepsy, showing no change in the neural precursor cell population but a dramatic decline in neuronal fate-choice decision of newly generated cells (Hattiangady and Shetty, 2009). Prolonged nestin expression at the expense of newly generated neurons was also observed in aged rats, particularly in those animals with severe spatial learning deficits during Morris Water Maze testing (Nyffeler *et al.*, 2008). Indeed, causal events in the disruption of the neurogenic fate-choice of progenitor cells may be involved and will need clarification.

There is much debate in regenerative medicine about the functional and clinical impact of hippocampal progenitor cells and

**Table 4 Statistical analysis between anti-epileptic drug treatment and neuropathological *in vivo* and *in vitro* analysis**

| | VPA | CLB | LTG | LEV | OXC |
|---|---|---|---|---|---|
| Proliferation *in vitro* | 0.550 | 0.221 | 0.118 | 0.697 | 0.489 |
| Proliferation *in vivo* | 0.850 | 0.487 | 0.859 | 0.616 | 0.746 |
| Neurogenesis *in vitro* | 0.692 | 0.160 | 0.123 | 0.760 | 0.924 |
| Memory (IAT) | 0.136 | 0.376 | 0.149 | 0.408 | 0.993 |
| Granule cell number | 0.678 | 0.536 | 0.133 | 0.688 | 0.671 |
| Doublecortin | 0.959 | 0.109 | 0.349 | 0.602 | 0.232 |
| BDNF | 0.810 | 0.633 | 0.310 | 0.760 | 0.768 |
| Cdk5 | 0.827 | 0.133 | 0.205 | 0.385 | 0.582 |

Statistical analysis did not reveal any impact of drug treatment on the proliferative capacity of adult human hippocampal stem cells or other parameters studied (as listed in left-hand column). CLB, LTG, LEV and OXC were the most commonly used anti-epileptic drugs continuously administered during 6 months prior to surgery. All numbers refer to *P*-values (Pearson correlation).
CLB = clobazam medication in clinical history; LEV = levetiracetam; LTG = lamotrigine; OXC = oxcarbazepine; VPA = valproate.

neurogenesis (Steindler and Pincus, 2002). Adult stem cells and the endogenous regenerative capacity of the human brain are promising therapeutic targets for many neurodegenerative disorders, such as Alzheimer's or Parkinson's disease (Rodriguez *et al.*, 2008; Winner *et al.*, 2009), even though the regenerative capacity may be severely compromised during a given patient's long-term disease history. Our data show evidence that neurogenesis is not necessarily affected by chronic neurological disease, as the majority of our patients suffered from a very long period of chronic seizures originating in the hippocampus. Drugs targeting the molecular machinery towards a neuronal fate-choice of hippocampal precursor cells may thus be promising therapeutic options to ameliorate learning and memory deficits associated with a variety of neurological disorders.

# Acknowledgements

We thank Dorit Müller and Birte Rings for their expert technical assistance. F.A.S. is a scholar of the German national academic foundation (Studienstiftung des deutschen Volkes e.V.).

# Funding

The European Community (LSH-CT-2006-037315 EPICURE); German Research Council (DFG Bl 421/1-2); and Bavarian Research Council (ForNeuroCell).

# References

Ahlenius H, Visan V, Kokaia M, Lindvall O, Kokaia Z. Neural stem and progenitor cells retain their potential for proliferation and differentiation into functional neurons despite lower number in aged brain. J Neurosci 2009; 29: 4408–19.

Altman J. Are new neurons formed in the brains of adult mammals? Science 1962; 135: 1127–8.

Bakker A, Kirwan CB, Miller M, Stark CE. Pattern separation in the human hippocampal CA3 and dentate gyrus. Science 2008; 319: 1640–2.

Blumcke I, Pauli E, Clusmann H, Schramm J, Becker A, Elger C, et al. A new clinico-pathological classification system for mesial temporal sclerosis. Acta Neuropathol 2007; 113: 235–44.

Blumcke I, Schewe JC, Normann S, Brustle O, Schramm J, Elger CE, et al. Increase of nestin-immunoreactive neural precursor cells in the dentate gyrus of pediatric patients with early-onset temporal lobe epilepsy. Hippocampus 2001; 11: 311–21.

Chelune GJ. Hippocampal adequacy versus functional reserve: predicting memory functions following temporal lobectomy. Arch Clin Neuropsychol 1995; 10: 413–32.

Clelland CD, Choi M, Romberg C, Clemenson GD Jr, Fragniere A, Tyers P, et al. A functional role for adult hippocampal neurogenesis in spatial pattern separation. Science 2009; 325: 210–3.

Deng W, Saxe MD, Gallina IS, Gage FH. Adult-born hippocampal dentate granule cells undergoing maturation modulate learning and memory in the brain. J Neurosci 2009; 29: 13532–42.

Engel J Jr. Epilepsy surgery. Curr Opin Neurol 1994; 7: 140–7.

Eriksson PS, Perfilieva E, Bjork-Eriksson T, Alborn AM, Nordborg C, Peterson DA, et al. Neurogenesis in the adult human hippocampus. Nat Med 1998; 4: 1313–7.

Fahrner A, Kann G, Flubacher A, Heinrich C, Freiman TM, Zentner J, et al. Granule cell dispersion is not accompanied by enhanced neurogenesis in temporal lobe epilepsy patients. Exp Neurol 2007; 203: 320–32.

Farioli-Vecchioli S, Saraulli D, Costanzi M, Pacioni S, Cina I, Aceti M, et al. The timing of differentiation of adult hippocampal neurons is crucial for spatial memory. PLoS Biol 2008; 6: e246.

Gage FH. Mammalian neural stem cells. Science 2000; 287: 1433–8.

Gerber J, Tauber SC, Armbrecht I, Schmidt H, Bruck W, Nau R. Increased neuronal proliferation in human bacterial meningitis. Neurology 2009; 73: 1026–32.

Gould E, Beylin A, Tanapat P, Reeves A, Shors TJ. Learning enhances adult neurogenesis in the hippocampal formation. Nat Neurosci 1999; 2: 260–5.

Haas KZ, Sperber EF, Opanashuk LA, Stanton PK, Moshe SL. Resistance of immature hippocampus to morphologic and physiologic alterations following status epilepticus or kindling. Hippocampus 2001; 11: 615–25.

Hattiangady B, Rao MS, Shetty AK. Chronic temporal lobe epilepsy is associated with severely declined dentate neurogenesis in the adult hippocampus. Neurobiol Dis 2004; 17: 473–90.

Hattiangady B, Shetty AK. Decreased neuronal differentiation of newly generated cells underlies reduced hippocampal neurogenesis in chronic temporal lobe epilepsy. Hippocampus 2009; 20: 97–112.

Helmstaedter C, Elger CE. Chronic temporal lobe epilepsy: a neurodevelopmental or progressively dementing disease? Brain 2009; 132: 2822–30.

Hsieh J, Nakashima K, Kuwabara T, Mejia E, Gage FH. Histone deacetylase inhibition-mediated neuronal differentiation of multipotent adult neural progenitor cells. Proc Natl Acad Sci USA 2004; 101: 16659–64.

Jessberger S, Aigner S, Clemenson GD Jr, Toni N, Lie DC, Karalay O, et al. Cdk5 regulates accurate maturation of newborn granule cells in the adult hippocampus. PLoS Biol 2008; 6: e272.

Jessberger S, Clark RE, Broadbent NJ, Clemenson GD Jr, Consiglio A, Lie DC, et al. Dentate gyrus-specific knockdown of adult neurogenesis impairs spatial and object recognition memory in adult rats. Learn Mem 2009; 16: 147–54.

Jin K, Peel AL, Mao XO, Xie L, Cottrell BA, Henshall DC, et al. Increased hippocampal neurogenesis in Alzheimer's disease. Proc Natl Acad Sci USA 2004; 101: 343–7.

Kitamura T, Saitoh Y, Takashima N, Murayama A, Niibori Y, Ageta H, et al. Adult neurogenesis modulates the hippocampus-dependent period of associative fear memory. Cell 2009; 139: 814–27.

Knoth R, Singec I, Ditter M, Pantazis G, Capetian P, Meyer RP, et al. Murine features of neurogenesis in the human Hippocampus across the lifespan from 0 to 100 years. PLoS One 2010; 5: e8809.

Lagace DC, Benavides DR, Kansy JW, Mapelli M, Greengard P, Bibb JA, et al. Cdk5 is essential for adult hippocampal neurogenesis. Proc Natl Acad Sci USA 2008; 105: 18567–71.

Leutgeb JK, Leutgeb S, Moser MB, Moser EI. Pattern separation in the dentate gyrus and CA3 of the hippocampus. Science 2007; 315: 961–6.

Liu H, Kaur J, Dashtipour K, Kinyamu R, Ribak CE, Friedman LK. Suppression of hippocampal neurogenesis is associated with developmental stage, number of perinatal seizure episodes, and glucocorticosteroid level. Exp Neurol 2003; 184: 196–213.

Liu YW, Curtis MA, Gibbons HM, Mee EW, Bergin PS, Teoh HH, et al. Doublecortin expression in the normal and epileptic adult human brain. Eur J Neurosci 2008; 28: 2254–65.

Nakashiba T, Young JZ, McHugh TJ, Buhl DL, Tonegawa S. Transgenic inhibition of synaptic transmission reveals role of CA3 output in hippocampal learning. Science 2008; 319: 1260–4.

Nyffeler M, Yee BK, Feldon J, Knuesel I. Abnormal differentiation of newborn granule cells in age-related working memory impairments. Neurobiol Aging 2008.

Parent JM, Elliott RC, Pleasure SJ, Barbaro NM, Lowenstein DH. Aberrant seizure-induced neurogenesis in experimental temporal lobe epilepsy. Ann Neurol 2006; 59: 81–91.

Parent JM, Yu TW, Leibowitz RT, Geschwind DH, Sloviter RS, Lowenstein DH. Dentate granule cell neurogenesis is increased by seizures and contributes to aberrant network reorganization in the adult rat hippocampus. J Neurosci 1997; 17: 3727–38.

Pauli E, Hildebrandt M, Romstock J, Stefan H, Blumcke I. Deficient memory acquisition in temporal lobe epilepsy is predicted by hippocampal granule cell loss. Neurology 2006; 67: 1383–9.

Rodriguez JJ, Jones VC, Tabuchi M, Allan SM, Knight EM, LaFerla FM, et al. Impaired adult neurogenesis in the dentate gyrus of a triple transgenic mouse model of Alzheimer's disease. PLoS One 2008; 3: e2935.

Rossi C, Angelucci A, Costantin L, Braschi C, Mazzantini M, Babbini F, et al. Brain-derived neurotrophic factor (BDNF) is required for the enhancement of hippocampal neurogenesis following environmental enrichment. Eur J Neurosci 2006; 24: 1850–6.

Roy NS, Wang S, Jiang L, Kang J, Benraiss A, Harrison-Restelli C, et al. In vitro neurogenesis by progenitor cells isolated from the adult human hippocampus. Nat Med 2000; 6: 271–7.

Sairanen M, Lucas G, Ernfors P, Castren M, Castren E. Brain-derived neurotrophic factor and antidepressant drugs have different but coordinated effects on neuronal turnover, proliferation, and survival in the adult dentate gyrus. J Neurosci 2005; 25: 1089–94.

Shors TJ, Miesegaes G, Beylin A, Zhao M, Rydel T, Gould E. Neurogenesis in the adult is involved in the formation of trace memories. Nature 2001; 410: 372–6.

Siebzehnrubl FA, Blumcke I. Neurogenesis in the human hippocampus and its relevance to temporal lobe epilepsies. Epilepsia 2008; 49 (Suppl. 5): 55–65.

Siebzehnrubl FA, Buslei R, Eyupoglu IY, Seufert S, Hahnen E, Blumcke I. Histone deacetylase inhibitors increase neuronal differentiation in adult forebrain precursor cells. Exp Brain Res 2007; 176: 672–8.

Squire LR, Stark CE, Clark RE. The medial temporal lobe. Annu Rev Neurosci 2004; 27: 279–306.

Stefan H, Hildebrandt M, Kerling F, Kasper BS, Hammen T, Dorfler A, et al. Clinical prediction of postoperative seizure control: structural, functional findings and disease histories. J Neurol Neurosurg Psychiatry 2009; 80: 196–200.

Stefan H, Scheler G, Hummel C, Walter J, Romstock J, Buchfelder M, et al. Magnetoencephalography (MEG) predicts focal epileptogenicity in cavernomas. J Neurol Neurosurg Psychiatry 2004; 75: 1309–13.

Steindler DA, Pincus DW. Stem cells and neuropoiesis in the adult human brain. Lancet 2002; 359: 1047–54.

Tashiro A, Sandler VM, Toni N, Zhao C, Gage FH. NMDA-receptor-mediated, cell-specific integration of new neurons in adult dentate gyrus. Nature 2006; 442: 929–33.

van Praag H, Christie BR, Sejnowski TJ, Gage FH. Running enhances neurogenesis, learning, and long-term potentiation in mice. Proc Natl Acad Sci USA 1999; 96: 13427–31.

van Praag H, Schinder AF, Christie BR, Toni N, Palmer TD, Gage FH. Functional neurogenesis in the adult hippocampus. Nature 2002; 415: 1030–4.

Walton NM, Sutter BM, Chen HX, Chang LJ, Roper SN, Scheffler B, et al. Derivation and large-scale expansion of multipotent astroglial neural progenitors from adult human brain. Development 2006; 133: 3671–81.

Winner B, Vogt-Weisenhorn DM, Lie CD, Blumcke I, Winkler J. Cellular repair strategies in Parkinson's disease. Therapeutic Advances in Neurological Disorders 2009; 2: 51–60.

Wolf HK, Buslei R, Schmidt-Kastner R, Schmidt-Kastner PK, Pietsch T, Wiestler OD, et al. NeuN: a useful neuronal marker for diagnostic histopathology. J Histochem Cytochem 1996; 44: 1167–71.

Zhao C, Teng EM, Summers RG Jr, Ming GL, Gage FH. Distinct morphological stages of dentate granule neuron maturation in the adult mouse hippocampus. J Neurosci 2006; 26: 3–11.

Cerebral Cortex Advance Access published June 4, 2010

Cerebral Cortex
doi:10.1093/cercor/bhq099

# Failed Cytokinesis of Neural Progenitors in *Citron Kinase*–Deficient Rats Leads to Multiciliated Neurons

Sara B. Anastas[1], Dorit Mueller[1], Susan L. Semple-Rowland[1], Joshua J. Breunig[2] and Matthew R. Sarkisian[1]

[1]Department of Neuroscience, McKnight Brain Institute, University of Florida, Gainesville, FL 32610-0244, USA and [2]Department of Neurobiology, Yale University School of Medicine, New Haven, CT 06510, USA

Address correspondence to email: matt.sarkisian@mbi.ufl.edu.

**Most, if not all, cortical neurons possess a single primary cilium; however, little is known about the mechanisms that control neuronal ciliogenesis. The *Citron kinase*–deficient (*Citron-K$^{fh/fh}$*) rat, a model in which failed cytokinesis during development produces cortical neurons containing multiple cellular organelles, provides a unique system in which to examine the relationship between centriole inheritance and neuronal ciliogenesis. In this study, we analyzed the cerebral cortex of these animals using immunohistochemistry, serial confocal, and electron microscopy to determine if the multinucleated neurons present in the cortex of these animals also possess multiple centrioles and cilia. We found that neurons containing multiple nuclei possessed multiple centrioles and cilia whose lengths varied across cortical regions. Despite the presence of multiple cilia, we found that perinatal expression of adenylyl cyclase III, a cilia-specific marker, and somatostatin receptor 3, a receptor enriched in cilia, were preserved in developing *Citron-K$^{fh/fh}$* brain. Together, these results show that multinucleated neurons arising from defective cytokinesis can extend multiple cilia.**

**Keywords:** cortical malformation, forebrain development, pericentrin, primary cilia, neuronal differentiation

## Introduction

Neurons of the cerebral cortex possess a single, putatively nonmotile, primary cilium (Mandl and Megele 1989; Fuchs and Schwark 2004; Whitfield 2004). Primary cilia are extended from the mother centriole as cells differentiate (Pedersen et al. 2008). During neurogenesis, the mother centriole duplicates with each round of cell division and accompanies the neural progenitor throughout the migration process. The mother centriole is a core component of the centrosome or microtubule organizing center (MTOC), which plays essential roles in neurogenesis, neuronal migration, and differentiation (for review, see Higginbotham and Gleeson 2007; Nigg and Raff 2009). During neuronal differentiation, the mother centriole docks with the plasma membrane to generate a cilium. Dysregulation of components within the centrosome/MTOC has been associated with abnormal neurogenesis and migration (Tsai et al. 2007), but it is unclear whether these defects alter cilia formation in developing neurons.

Loss of *Citron-K* function in both mouse and rat (the spontaneous *flathead* mutant or *Citron-K$^{fb/fb}$*) results in severely defective neurogenesis and massive apoptosis in the proliferative zones of the developing cortex (Di Cunto et al. 2000; Roberts et al. 2000; Sarkisian et al. 2001, 2002). Loss of these cells contributes to the abnormally small cerebral cortices observed in these animals. A hallmark of the *Citron-K* mutant cortex is the presence of a significant fraction of multinucleate neurons in the cortex that arise from defective cytokinesis in cortical progenitors (Madaule et al. 1998; Di Cunto et al. 2000; Sarkisian et al. 2002; LoTurco et al. 2003). Citron-K protein normally localizes to the cytokinesis furrows of cortical progenitors and is essential for the final cleavage of progenitor cells at the surface of the ventricular zone (Madaule et al. 1998; Sarkisian et al. 2002). The presence of multinucleate neurons in the postnatal cortex of *Citron-K*-deficient animals shows that failed cytokinesis does not automatically result in cell death and that surviving, multinucleate neural progenitors can migrate and differentiate into neurons. It is not known whether defective cytokinesis in *Citron-K*-deficient animals affects ciliogenesis during neuronal differentiation.

The unique characteristics of the *Citron-K$^{fb/fb}$* rat brain provide an opportunity to explore the cellular mechanisms that control neuronal ciliogenesis. The purpose of this study was to test the hypothesis that multinucleated neurons arising from failed cytokinesis contain multiple centrioles and develop multiple cilia. We tested this hypothesis by examining the cerebral cortices of *Citron-K*-deficient rats using immunohistochemistry, serial confocal, and electron microscopy (EM).

## Materials and Methods

### *Citron-K Wild-Type and Mutant Brain Tissue*

Wistar *Citron-K* wild-type (wt) and mutant rats were intracardially perfused with saline followed by 4% paraformaldehyde in 0.1 M phosphate buffer on postnatal day (P) 1 ($n$ = 2 wt and 2 mutant) and P14 ($n$ = 3 wt and 3 mutant). The fixed brains were removed, cryoprotected, frozen over liquid $N_2$, and sectioned on a cryostat at 50 μm in coronal and sagittal planes.

### *Immunofluorescence*

Brain sections were probed overnight at 4 °C using the following primary antibodies: rabbit anti-FoxP2 (1:100,000; Abcam), rabbit anti-adenylyl cyclase III (1:1000; Santa Cruz Biotechnology), mouse anti-NeuN (1:1000; Chemicon), rabbit anti-pericentrin (1:500; Covance), and rabbit anti-somatostatin receptor 3 (SSR3; 1:1000; Gramsch). Appropriate, species-specific, fluorescent-conjugated secondary antibodies (1:200; Jackson ImmunoResearch) were used to detect the primary antibodies. Processed sections were coverslipped using ProLong Gold Antifade media containing 4′,6-diamidino-2-phenylindole dihydrochloride (DAPI) (Invitrogen). Some sections were stained with thionin to serve as a reference for the immunostained sections and were imaged using a Leica M165 microscope and Leica software.

### *Analyses and Quantification of Cilia*

Images of immunostained sections were obtained using an Olympus IX81-DSU spinning disc confocal microscope. We collected $z$-stack images (at 1.5 μm steps) of ACIII-positive cilia and then created collapsed stacks to create maximum projection images that were saved

as tiff files, converted to black and white, and analyzed using Image J64 (http://rsbweb.nih.gov/ij/). The numbers of nuclei and cilia and the lengths of cilia per field (each field was ~15 228 $\mu m^2$) were quantified. For each genotype, we analyzed 2-3 brains and 3-6 fields/brain region. Cilia lengths were measured by manually tracing ACIII-positive structures and converting individual traces from pixels into microns. These data, which are presented as the mean ± standard error of the mean for each group, were analyzed using Student's *t*-tests (2 tailed) with statistical significance set at $P < 0.05$. For 3D rendering analyses of immunolabeled cilia, the confocal image series were imported into Reconstruct (version 1.1.0.0; http://synapse-web.org/tools/reconstruct/reconstruct.stm). 2D volumes were traced and the resulting objects were exported to 3ds max 2010 where the meshes were smoothed automatically using the turbosmooth modifier, the views were positioned, and the final images were rendered.

### *Electron Microscopy*

Somatosensory neocortex of P14 *Citron-K$^{fb/fb}$* rats and the brains of littermates that had previously been prepared for EM analysis (Sarkisian et al. 2001) were sectioned (70 nm) and stained with uranyl acetate and lead citrate. Sections were collected onto Formvar-coated grids and viewed using a Hitachi H-7600 transmission EM at 80 kV. Images were captured with a Hitachi digital camera and proprietary software.

## Results

### *Both Nuclei in Binucleate Neurons in Citron-K$^{fb/fb}$ Neocortex Appear to Be Transcriptionally Active*

In *Citron-K$^{fb/fb}$* cortex, defects in cytokinesis produce a subset of neurons that contain duplicate cellular organelles including nuclei (Sarkisian et al. 2001). Are the 2 nuclei in these neurons transcriptionally active during postnatal periods? To address this question, we immunostained P14 neocortical neurons using anti-NeuN (an antibody that stains neuronal nuclei and recently characterized as the RNA splicing factor, Fox-3 [Kim et al. 2009]) and anti-FoxP2, an antibody that recognizes the transcription factor, FoxP2, which is enriched in layer 6 of the neocortex (Ferland et al. 2003). We found that the nuclei of binucleate, NeuN-positive neurons, and those of wt neurons were comparably labeled with FoxP2 (Supplementary Fig. S1). These data suggest that the duplicated organelles in *Citron-K$^{fb/fb}$* cortex appear to remain functional.

### *Cilia in Citron-K$^{fb/fb}$ Neocortex Are Shorter than Cilia in wt Neocortex*

Cilia located in the deeper cortical layers (layers 4/5) of wt brains and the mid-cortical layers (~layer 4/5) of mutant brains were analyzed by immunostaining sections of P14 wt and *Citron-K$^{fb/fb}$* brains for ACIII, a protein that is enriched in cilia (Bishop et al. 2007). We chose to analyze these specific layers to avoid introducing the cortical progenitor loss that occurs in the mutant brain as a confounding variable in our analyses (Roberts et al. 2000). ACIII-positive cilia associated with 427 single and 452 single and multinucleated cells in wt and *Citron-K$^{fb/fb}$* neocortex, respectively, were counted and measured (Fig. 1*B*). We found that the mean number of cilia per cortical area was similar in mutant and wt cortex (ca., 75.3/field in mutant vs. 71.2/field in wt) (Table 1). Measurement of the lengths of the cilia revealed that while the lengths of the mutant cilia fell within the range of those obtained for wt cilia, the average length of the mutant cilia was shorter than the wt cilia (2.56 ± 0.07 μm in mutant vs. 4.07 ± 0.10 in wt; $P < 0.001$; Student's *t*-test [2 tailed]) (Supplementary Fig. S2 and Table 1).

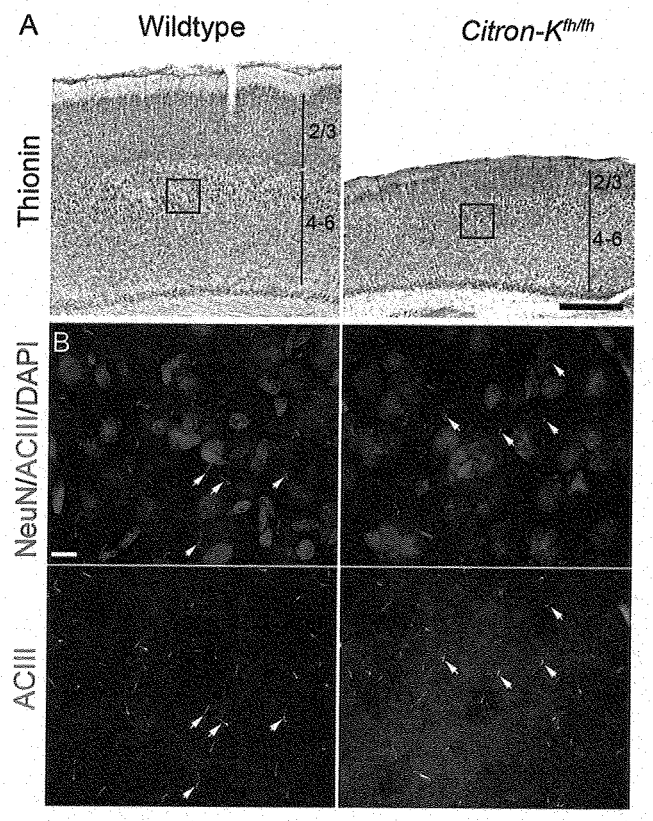


**Figure 1.** Primary cilia in P14 *Citron-K$^{fh/fh}$* are shorter than wt neocortex. (*A*) Thionin-Nissl-stained P14 wt and *Citron-K$^{fh/fh}$* rat neocortex. Boxes indicate the approximate regions that were further analyzed for cilia. (*B*) Confocal images (representing a collapsed *z*-series) of wt (left panels) and *Citron-K* mutant (right panels) neocortex immunostained for NeuN (red), ACIII (green), and nuclei (blue). ACIII-labeled cilia (arrows) were detected in the neocortex of both groups although the cilia in mutant were shorter (quantification of data shown in Table 1). Bars = 500 μm (*A*) and 10 μm (*B*).

Together, these data show that cells in *Citron-K$^{fb/fb}$* neocortex develop cilia and that, on average, these cilia are shorter than wt cilia.

### *Cilia in the CA1 Region of Citron-K$^{fb/fb}$ Hippocampus Are Shorter than wt, whereas Those in Citron-K$^{fb/fb}$ and wt Dentate Gyrus Are Indistinguishable*

In this experiment, we compared the number and lengths of cilia in the CA1 (total cilia; $n = 884$ wt and 917 mutant) and in the dentate gyrus (DG) (total cilia; $n = 1138$ wt and 318 mutant) regions of mutant and wt hippocampi (Supplementary Fig. S3). The average number of cilia/field in mutant CA1 was slightly higher than in wt CA1 (approximately 229 in mutant vs. 221 in wt), whereas the average number of cilia/field in mutant DG was significantly lower than in wt DG (approximately 106 in mutant vs. 284.5 in wt; $P < 0.001$; Student's *t*-test) (Table 1). It is likely that the reduced number of cilia in mutant DG reflects a loss of cells in this region (Ackman et al. 2007). The lengths of the cilia in mutant CA1 were slightly shorter than those in wt CA1 (2.29 ± 0.03 μm in mutant vs. 3.00 ± 0.04 in wt; $P < 0.001$; Student's *t*-test [2 tailed]). In contrast, the lengths of the cilia in mutant DG were indistinguishable from those in wt DG (2.59 ± 0.05 μm in mutant vs. 2.61 ± 0.03 μm in wt) (Table 1). These data support other observations that not all neuronal cilia are of the same length (Fuchs and Schwark

**Table 1**
Summary of cilia analyses from P14 rat cerebral cortex

| Region | Genotype | Total cilia analyzed[a] | Average number cilia/field[b] | Mean length (μm) | Mean length (μm) per animal | Cilia:DAPI+ Nuclei | #Cilia/# 3D NeuN+ cells[c] |
|---|---|---|---|---|---|---|---|
| Neocortex | wt | 427 | ~71.2 | 4.07 ± 0.10 | Rat 1 = 3.74 ± 0.15<br>Rat 2 = 4.15 ± 0.19<br>Rat 3 = 4.28 ± 0.17 | 0.90 ± 0.04 | 40/40 |
| | *Citron-K$^{fh/fh}$* | 452 | ~75.3 | 2.56 ± 0.07*** | Rat 1 = 2.39 ± 0.10<br>Rat 2 = 2.97 ± 0.12<br>Rat 3 = 2.37 ± 0.11 | 0.90 ± 0.07 | 35/31 |
| CA1 | wt | 884 | ~221 | 3.00 ± 0.04 | Rat 1 = 2.88 ± 0.05<br>Rat 2 = 3.12 ± 0.06 | ND | ND |
| | *Citron-K$^{fh/fh}$* | 917 | ~229 | 2.29 ± 0.03*** | Rat 1 = 2.42 ± 0.06<br>Rat 2 = 2.18 ± 0.04 | ND | ND |
| DG | wt | 1138 | ~284.5 | 2.61 ± 0.03 | Rat 1 = 2.73 ± 0.05<br>Rat 2 = 2.48 ± 0.04 | 0.92 ± 0.03 | ND |
| | *Citron-K$^{fh/fh}$* | 318 | ~106*** | 2.59 ± 0.05 | Rat 1 = 2.45 ± 0.06<br>Rat 2 = 2.90 ± 0.09 | 0.60 ± 0.07*** | ND |

Note: ND, not determined. Values for length and ratios are mean ± standard error of the mean.
[a]For each genotype, data were collected from 2 to 3 brains (3–6 fields per brain region).
[b]Field = ~15,228 μm$^2$.
[c]Data collected from 3D-reconstructed NeuN+ cells fully contained within a confocal z-stack.
***$P < 0.001$ (Student's *t*-test; 2 tailed) compared with wt.

2004). Why cilia lengths are differentially affected in subregions of the mutant brain requires further study.

### *Multinucleate Pyramidal Cells Possess Multiple Cilia*

Do cortical neurons with multiple nuclei generate multiple cilia? We hypothesized that if cortical binucleate cells generate a single cilium, then the ratio of cilia to nuclei in *Citron-K$^{fb/fb}$* cortex should be less than one. To test this hypothesis, we first analyzed serial, confocal sections of mutant, and wt neocortex to determine the ratios of ACIII-positive cilia to DAPI-stained nuclei. We found that the mutant and wt ratios were comparable (0.90 ± 0.07 in mutant vs. 0.90 ± 0.04 in wt) (Table 1). To further refine these analyses, we repeated these analyses but focused on determining the ratios of ACIII-positive cilia to NeuN-positive cells, thereby limiting our analyses to neocortical neurons. In wt neocortex, serial analyses of NeuN-positive cells revealed that one nucleus corresponded with a single ACIII-positive cilium (Fig. 2*A,B* and Supplementary Fig. S4*A*). We analyzed 40 3D-rendered NeuN/ACIII-positive neurons in wt cortex and found that all 40 cells extended a single cilium (Fig. 2*A* and Table 1). In contrast, in mutant neocortex, we observed binucleate neurons that appeared to have 2 distinct cilia originating from the base of the apical dendrite (Fig. 2*B,D* and Supplementary Fig. S4*B*). Examination of NeuN-positive neurons in mutant cortex with single nuclei revealed that each of these neurons possessed a single ACIII-positive cilium (Supplementary Fig. S5). We analyzed 31 3D-rendered NeuN-positive cells in *Citron-K$^{fb/fb}$* neocortex and found 25 NeuN-positive cells with single nuclei, each extending a single cilium (Fig. 2), 5 bi-nucleate neurons, each possessing 2 distinct ACIII-positive cilia originating from the base of the apical dendrite (Fig. 2), and 1 NeuN+ cell that appeared to lack ACIII positivity (data not shown).

These data show that binucleate neurons in *Citron-K$^{fb/fb}$* neocortex possess 2 cilia and suggest that there is a 1:1 relationship between neuronal nuclei number and cilia number. In addition, our analyses support previous observations that most, if not all, neurons in neocortex harbor a cilium (Mandl and Megele 1989).

### *Ultrastructural and Immunohistochemical Analyses Confirm that Multinucleate Mutant Neurons Have Multiple Cilia and Basal Bodies*

In this experiment, we examined wt and mutant neocortex at the EM level and also by immunostaining with a pericentrin antibody that recognizes centrioles and basal bodies (Delaval and Doxsey 2010). Using EM, we identified cilia in both wt and mutant somatosensory neocortex (Fig. 3), but unlike wt neocortex, mutant cells in neocortex contained multiple basal bodies and 2 cilia extending from the soma (Fig. 3*B–D*). Next, we stained wt and mutant neocortex for pericentrin. In wt neocortex, we routinely observed pairs of pericentrin-positive puncta near the base of the apical dendrite in pyramidal shaped, NeuN-positive cells (cells 1–4 in Fig. 4*A,C*). In contrast, we observed many binucleate neurons in *Citron-K$^{fb/fb}$* neocortex that appeared to have more than one pair of pericentrin-positive puncta (cells 1–6 in Fig. 4*B,C*). The pattern of pericentrin staining in mutant neurons containing a single nucleus was indistinguishable from wt neurons (cell 7 in Fig. 4*B*). Collectively, these data demonstrate the additional centrioles present in cells that fail to undergo normal cytokinesis are capable of inducing the formation of additional cilia and that the cilia that are formed are located near the base of the apical dendrite of the cell.

### *The Onset of Ciliogenesis and Cilia Receptor Trafficking Are Comparable in Citron-K$^{fb/fb}$ and wt Neocortex*

Although detailed analyses of ciliogenesis in rodent cerebral cortex have not yet been reported, immunostaining of developing rat cortex with an SSR3 antibody, a receptor that is localized to neuronal cilia (Handel et al. 1999), suggests that cilia form postmitotically and elongate between P0 and P3 (Stanic et al. 2009). In this experiment, we stained postnatal P1 and P14 mutant neocortex using ACIII and SSR3 antibodies, respectively, to determine if the onset of expression of these cilia markers in developing *Citron-K$^{fb/fb}$* cortex is comparable to that observed in wt neocortex. Though the presence of ACIII does not necessarily serve as an assay for ciliogenesis, we have observed that ACIII immunostaining strongly correlates with the onset of ciliogenesis and can be used to estimate the

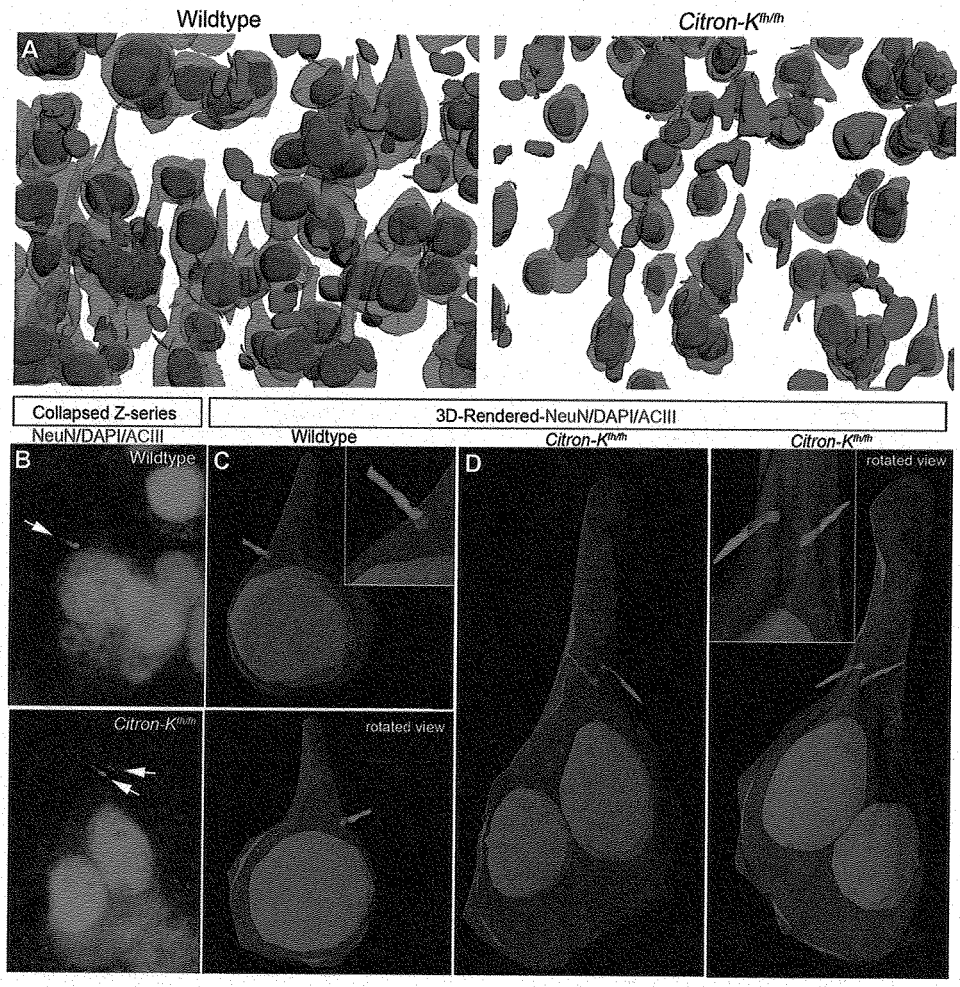


**Figure 2.** Multiple cilia arise from multinucleate neurons in P14 *Citron-K*$^{fh/fh}$ neocortex. (*A*) 3D reconstruction of confocal *z*-stacks from wt (left) and *Citron-K*$^{fh/fh}$ (right) neocortex. NeuN-positive cells are red, DAPI-labeled nuclei are blue, and ACIII-labeled cilia are green. All wt neurons had single nuclei and extended a single cilium. All multinucleate neurons extended multiple cilia. (*B*) Collapsed Z-series of confocal images shows a NeuN-positive nucleus in wt (upper) and a binucleate NeuN-positive cell in mutant (lower) neocortex. The wt neuron possessed a single ACIII-positive cilium (arrow), whereas the mutant neuron possessed a pair of ACIII-positive cilia (arrows) near the base of the apical dendrite. Complete z-series images for these cells are displayed in Figure S4. (*C*, *D*) Serial reconstructions and 3D renderings of the wt and mutant cells indicated in (*B*) revealed 1 cilium protruding from the wt cell and 2 cilia protruding from a *Citron-K*$^{fh/fh}$ cell. Rotated views of each cell are shown and the insets show higher magnification of the cilia protruding from the cell body.

lengths of primary cilia in developing mouse neocortex (JJ Breunig, MR Sarkisian, unpublished observations). Examination of P1 wt and mutant neocortices immunostained for ACIII and NeuN revealed that both tissues contained ACIII-positive neurons (Supplementary Fig. S6*A*). This observation suggests that it is unlikely that the shortened cilia observed in mutant neocortex reflect delayed cilia growth. We also examined P14 wt and mutant neocortices immunostained for SSR3 and found that both tissues contained SSR3-positive cilia (Supplementary Fig. S6*B*). Thus, the presence of SSR3 in mutant cilia suggests that the cilia associated with neurons in *Citron-K*$^{fh/fh}$ neocortex retain the ability to traffic cilia-specific receptors. It remains to be determined if these receptors are functional, enabling the neurons to respond to extracellular stimuli.

## Discussion

Collectively, our findings show that multinucleate neurons in *Citron-K*$^{fh/fh}$ neocortex that fail to undergo normal cytokinesis migrate to the appropriate lamina of the neocortex and retain multiple copies of centrioles (Fig. 5). In addition, our data suggest that multiple copies of centrioles in these cells localize to the appropriate subregion of the cell, dock with the plasma membrane, and generate multiple cilia.

### *Relationship between Cytokinesis Failure and Properties of Neuronal Cilia*

The increased number of cilia associated with *Citron-K* mutant, multinucleate neurons presumably reflects failed cytokinesis due to the absence of Citron-K, a protein that is highly expressed in cortical proliferative zones during development and is virtually absent in the postnatal cortex (Di Cunto et al. 2000; Sarkisian et al. 2002). Citron-K localizes to cleavage furrows during cytokinesis and its absence produces mitotic abnormalities along the cortical ventricular surface (Madaule et al. 1998; Sarkisian et al. 2002; LoTurco et al. 2003). Consequently, many affected cells undergo apoptosis (Di Cunto et al. 2000; Roberts et al. 2000; Sarkisian et al. 2001); however, a significant fraction of single- and multinucleate *Citron-K*-deficient cells survive and migrate into the neocortex. We found that the majority of single nucleated neurons

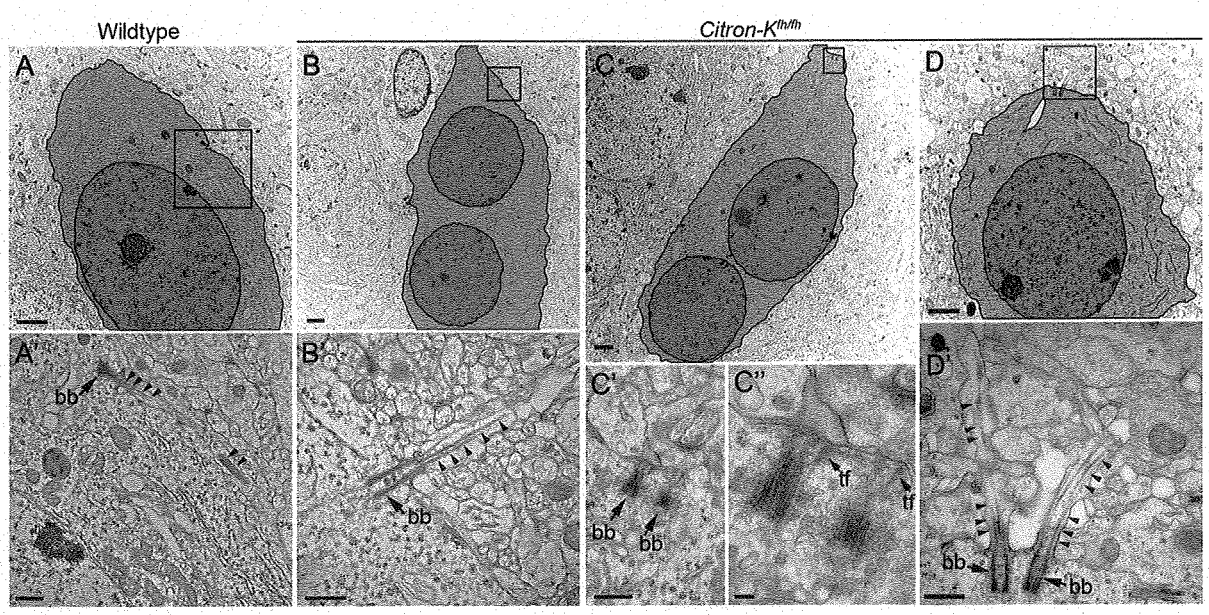


**Figure 3.** EM analysis of cilia in P14 wt and mutant somatosensory neocortex. (*A*) Low magnification view of a pyramidal-shaped cell in wt neocortex. The cell body (pink) and nucleus (blue) are roughly outlined. The boxed region shows a cilium that extends from the apical region of the cell. (*A'*) Higher magnification of the boxed region in (*A*) shows basal body (bb) and the axoneme (arrowheads) protruding out of the cell. (*B*) Example of a binucleate pyramidal shaped cell in Citron-K mutant. Higher magnification of the boxed region shows a cilium extending from this cell (*B'*). (*C*) Another example of a binucleate pyramidal-shaped cell that contains 2 basal bodies (boxed region). (*C'*, *C''*) Higher magnification of boxed region in (*C*). Two basal bodies anchored by transition fibers (tf) are localized to the apical portion of the cell and are docked at the plasma membrane. Axonemes are not visible in this plane of section. (*D*, *D'*) Example of another mutant cell with 2 axonemes extending from the soma. Scale bars = 2 μm (*A–D*), 500 nm (*A'–D'*), and 100 nm (*C''*).

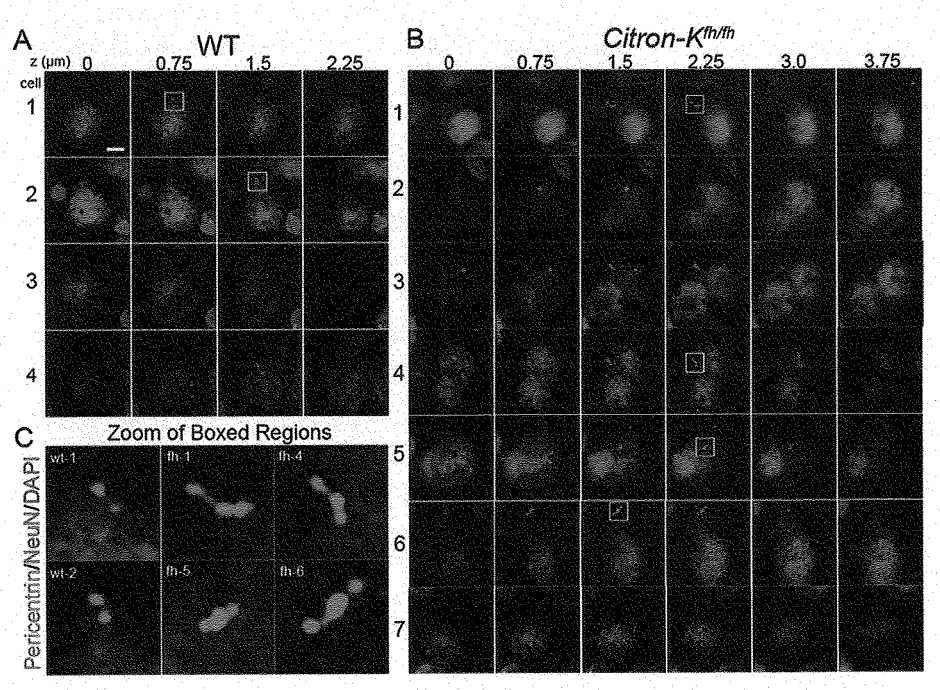


**Figure 4.** Abnormal patterns of pericentrin staining in *Citron-K* binucleate neurons. Serial confocal images (in 0.75 μm steps) through P14 neocortex immunostained for NeuN (red) and pericentrin (green). Nuclei were labeled with DAPI. (*A*) Four examples of wt NeuN+ cells. Boxed regions of cells 1 and 2 and shown in (*C*). Scale bar = 10 μm. (*B*) Examples of *Citron-K*$^{fh/fh}$ neurons. Cells 1–6 are binucleate, whereas cell 7 has a single nucleus. Boxed regions of cells 1 and 4–6 are shown in (*C*). (*C*) Higher magnifications of indicated cells (*A*) and (*B*). Pericentrin staining in wt neurons (wt—1,2) typically showed a pair of pericentrin puncta unlike mutant (fh—1, 4–6) in which there appeared to be more than a pair of pericentrin puncta.

in mutant neocortex had 1 cilium and contained 2 centrioles (Supplementary Fig. S5 and Fig. 4), whereas the binucleate neurons had 2 cilia and contained multiple centrioles (Figs 2–4). These observations suggest that the number of cilia associated with neurons depends on successful centriole segregation during cytokinesis of daughter neuroblasts.

We found that the lengths of cilia varied both across regions in *Citron-K* mutant cortex and in comparisons between

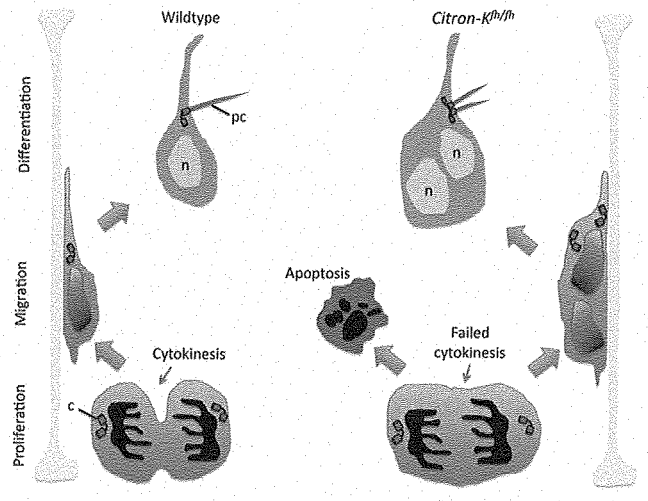


**Figure 5.** Model of ciliogenesis in *Citron-K* mutant forebrain. Under normal conditions (left), neural progenitors undergo cytokinesis that leads to the formation of 2 daughter cells. As part of the centrosome, the centrioles (c) are believed to help guide the postmitotic daughter cell's migration to the appropriate lamina of the neocortex. Once the cell reaches its cortical destination, it continues to differentiate and the mother centriole docks with the plasma membrane to form the primary cilium (pc) near the base of the apical dendrite. Based on our findings in this study, we predict that failure of cytokinesis in the developing *Citron-K*$^{fh/fh}$ cortex (right) leads to either apoptosis or production of cells containing multiple nuclei. These mutant cells migrate to the appropriate lamina of the neocortex and synthesize multiple cilia based on their inheritance of multiple centrioles.

*Citron-K* mutant and wt cortex. It is unclear what causes the shortening of mutant cilia. We found that early expression of ACIII in *Citron-K* mutant neurons is not disrupted and that the cilia that do form are in their normal subcellular location at the base of the apical dendrite of pyramidal shaped cells (Figs 2–4). These observations suggest that the trafficking mechanisms that guide the basal bodies to the base of the apical dendrite are intact in the mutant neurons and are not likely to underlie stunted growth of the cilia.

### *Factors Contributing to the Growth and Function of Neuronal Cilia*

The molecular mechanisms that regulate the growth of neuronal cilia are poorly understood. A basic, conserved program likely controls ciliary assembly as many genes implicated in ciliogenesis abnormalities in other tissues lead to loss of neuronal cilia (Davenport et al. 2007; Breunig et al. 2008; Han et al. 2008; Spassky et al. 2008; Town et al. 2008). Based on ACIII and SSR3 immunostaining at P1 and P14, respectively, it appears that the onset of ciliogenesis and ciliary receptor trafficking mechanisms are preserved in *Citron-K*$^{fh/fh}$ cortex. The question remains as to whether these cilia are able to transduce signals. Several receptors are enriched in neuronal cilia, including the G-protein–coupled receptors SSR3, the 5-HT$_6$ serotonin receptor, and the melanin-concentrating hormone receptor 1 (Mchr1) (Berbari et al. 2008a, 2008b; Handel et al. 1999). We found that SSR3 localization to cilia in *Citron-K* mutants appears to be normal (Supplementary Fig. S6*B*). SSR3 and Mchr1 are localized to neuronal cilia by Bardet-Biedl syndrome (BBS) proteins, BBS2 and BBS4 (Berbari et al. 2008b). Although we did not explore the localization or levels of BBS proteins, localization of SSR3 to cilia in *Citron-K*$^{fh/fh}$ brain suggests that BBS proteins are synthesized and functional in the mutant. In nearly every other cell type in the body, cilia communicate with nuclei, and it is tempting to speculate that neuronal cilia function in a similar manner. Indeed, we have shown that cilia are critical for Sonic hedgehog-mediated signaling in cortical astroglia (Breunig et al. 2008). The fact that many *Citron-K*$^{fh/fh}$ neurons have more than one putatively transcriptionally active nucleus (Supplementary Fig. S1) raises the questions of whether and how the cilia associated with these neurons communicate with the nuclei.

### *Relevance of Neuronal Cilia to Neurodevelopmental Disorders*

Are neuronal cilia required for normal neural development and function? Mounting evidence shows that mutations in human and rodent cilia genes are linked to various CNS abnormalities including malformations of cerebral cortex, autism, seizures, mental retardation, obesity, social, and emotional disorders (Davenport et al. 2007; Rooryck et al. 2007; Adams et al. 2008; Breunig et al. 2008; Cantagrel et al. 2008; Town et al. 2008). In humans, these disorders most often appear in neonates or early childhood. A recent study found that loss of neuronal cilia signaling may disrupt synaptic plasticity and be critical for a particular type of object recognition memory (Einstein et al. 2010). Thus, it is possible that changes in a neuron's cilium number could impact synaptic plasticity. Together, these observations support further investigation of the relationship between cilia function and neural development. Moreover, it is tempting to speculate that many other genes known to disrupt key phases of development involving centriole positioning or the MTOC (i.e., neuronal proliferation, migration, and differentiation) may produce cilia defects that contribute to or lead to cortical dysfunction.

## Supplementary Material

Supplementary material can be found at: http://www.cercor.oxfordjournals.org/


## Funding

McKnight Brain Research Foundation and the Evelyn F. and William L. McKnight Brain Institute at the University of Florida (to M.R.S.).

## Notes

We would like to thank J. LoTurco (University of Connecticut, Storrs) for providing us with control and mutant rat brain tissue for this study and for helpful comments during preparation of the manuscript. We thank G. Kasnic in the University of Florida Core EM Facility and D. Smith in the Cell Tissue and Analysis Core Facility for technical assistance. *Conflict of Interest*: None declared.


## References


Ackman JB, Ramos RL, Sarkisian MR, Loturco JJ. 2007. Citron kinase is required for postnatal neurogenesis in the hippocampus. Dev Neurosci. 29:113–123.

Adams M, Smith UM, Logan CV, Johnson CA. 2008. Recent advances in the molecular pathology, cell biology and genetics of ciliopathies. J Med Genet. 45:257–267.

Berbari NF, Johnson AD, Lewis JS, Askwith CC, Mykytyn K. 2008a. Identification of ciliary localization sequences within the third intracellular loop of G protein-coupled receptors. Mol Biol Cell. 19:1540–1547.

Berbari NF, Lewis JS, Bishop GA, Askwith CC, Mykytyn K. 2008b. Bardet-Biedl syndrome proteins are required for the localization of G protein-coupled receptors to primary cilia. Proc Natl Acad Sci U S A. 105:4242–4246.

Bishop GA, Berbari NF, Lewis J, Mykytyn K. 2007. Type III adenylyl cyclase localizes to primary cilia throughout the adult mouse brain. J Comp Neurol. 505:562–571.

Breunig JJ, Sarkisian MR, Arellano JI, Morozov YM, Ayoub AE, Sojitra S, Wang B, Flavell RA, Rakic P, Town T. 2008. Primary cilia regulate hippocampal neurogenesis by mediating sonic hedgehog signaling. Proc Natl Acad Sci U S A. 105:13127–13132.

Cantagrel V, Silhavy JL, Bielas SL, Swistun D, Marsh SE, Bertrand JY, Audollent S, Attie-Bitach T, Holden KR, Dobyns WB, et al. 2008. Mutations in the cilia gene ARL13B lead to the classical form of Joubert syndrome. Am J Hum Genet. 83:170–179.

Davenport JR, Watts AJ, Roper VC, Croyle MJ, van Groen T, Wyss JM, Nagy TR, Kesterson RA, Yoder BK. 2007. Disruption of intraflagellar transport in adult mice leads to obesity and slow-onset cystic kidney disease. Curr Biol. 17:1586–1594.

Delaval B, Doxsey SJ. 2010. Pericentrin in cellular function and disease. J Cell Biol. 188:181–190.

Di Cunto F, Imarisio S, Hirsch E, Broccoli V, Bulfone A, Migheli A, Atzori C, Turco E, Triolo R, Dotto GP, et al. 2000. Defective neurogenesis in citron kinase knockout mice by altered cytokinesis and massive apoptosis. Neuron. 28:115–127.

Einstein EB, Patterson CA, Hon BJ, Regan KA, Reddi J, Melnikoff DE, Mateer MJ, Schulz S, Johnson BN, Tallent MK. 2010. Somatostatin signaling in neuronal cilia is critical for object recognition memory. J Neurosci. 30:4306–4314.

Ferland RJ, Cherry TJ, Preware PO, Morrisey EE, Walsh CA. 2003. Characterization of Foxp2 and Foxp1 mRNA and protein in the developing and mature brain. J Comp Neurol. 460:266–279.

Fuchs JL, Schwark HD. 2004. Neuronal primary cilia: a review. Cell Biol Int. 28:111–118.

Han YG, Spassky N, Romaguera-Ros M, Garcia-Verdugo JM, Aguilar A, Schneider-Maunoury S, Alvarez-Buylla A. 2008. Hedgehog signaling and primary cilia are required for the formation of adult neural stem cells. Nat Neurosci. 11:277–284.

Handel M, Schulz S, Stanarius A, Schreff M, Erdtmann-Vourliotis M, Schmidt H, Wolf G, Hollt V. 1999. Selective targeting of somatostatin receptor 3 to neuronal cilia. Neuroscience. 89:909–926.

Higginbotham HR, Gleeson JG. 2007. The centrosome in neuronal development. Trends Neurosci. 30:276–283.

Kim KK, Adelstein RS, Kawamoto S. 2009. Identification of neuronal nuclei (NeuN) as Fox-3, a new member of the Fox-1 gene family of splicing factors. J Biol Chem. 284:31052–31061.

LoTurco JJ, Sarkisian MR, Cosker L, Bai J. 2003. Citron kinase is a regulator of mitosis and neurogenic cytokinesis in the neocortical ventricular zone. Cereb Cortex. 13:588–591.

Madaule P, Eda M, Watanabe N, Fujisawa K, Matsuoka T, Bito H, Ishizaki T, Narumiya S. 1998. Role of citron kinase as a target of the small GTPase Rho in cytokinesis. Nature. 394:491–494.

Mandl L, Megele R. 1989. Primary cilia in normal human neocortical neurons. Z Mikrosk Anat Forsch. 103:425–430.

Nigg EA, Raff JW. 2009. Centrioles, centrosomes, and cilia in health and disease. Cell. 139:663–678.

Pedersen LB, Veland IR, Schroder JM, Christensen ST. 2008. Assembly of primary cilia. Dev Dyn. 237:1993–2006.

Roberts MR, Bittman K, Li WW, French R, Mitchell B, LoTurco JJ, D'Mello SR. 2000. The flathead mutation causes CNS-specific developmental abnormalities and apoptosis. J Neurosci. 20:2295–2306.

Rooryck C, Pelras S, Chateil JF, Cances C, Arveiler B, Verloes A, Lacombe D, Goizet C. 2007. Bardet-biedl syndrome and brain abnormalities. Neuropediatrics. 38:5–9.

Sarkisian MR, Frenkel M, Li W, Oborski JA, LoTurco JJ. 2001. Altered interneuron development in the cerebral cortex of the flathead mutant. Cereb Cortex. 11:734–743.

Sarkisian MR, Li W, Di Cunto F, D'Mello SR, LoTurco JJ. 2002. Citron-kinase, a protein essential to cytokinesis in neuronal progenitors, is deleted in the flathead mutant rat. J Neurosci. 22:RC217.

Spassky N, Han YG, Aguilar A, Strehl L, Besse L, Laclef C, Ros MR, Garcia-Verdugo JM, Alvarez-Buylla A. 2008. Primary cilia are required for cerebellar development and Shh-dependent expansion of progenitor pool. Dev Biol. 317:246–259.

Stanic D, Malmgren H, He H, Scott L, Aperia A, Hokfelt T. 2009. Developmental changes in frequency of the ciliary somatostatin receptor 3 protein. Brain Res. 1249:101–112.

Town T, Breunig JJ, Sarkisian MR, Spilianakis C, Ayoub AE, Liu X, Ferrandino AF, Gallagher AR, Li MO, Rakic P, et al. 2008. The stumpy gene is required for mammalian ciliogenesis. Proc Natl Acad Sci U S A. 105:2853–2858.

Tsai JW, Bremner KH, Vallee RB. 2007. Dual subcellular roles for LIS1 and dynein in radial neuronal migration in live brain tissue. Nat Neurosci. 10:970–979.

Whitfield JF. 2004. The neuronal primary cilium—an extrasynaptic signaling device. Cell Signalling. 16:763–767.

Relevance of Cerebral Cortex manuscript to age-related memory loss.

Normal aging and memory function is dependent on maintaining a balance between neuron production and the establishment of normal connections between existing neurons. Thus, a loss of neurons or a decrease in proliferation may contribute to age related memory decline. A critical step in our understanding of neuron proliferation will be the identification of biomarkers that help us identify newly maturing neurons. A previously overlooked potential marker of this process is a cellular antennae, called the cilium. Our manuscript examined the ultrastructural detail and signaling machinery within cilia throughout the brain. Our results indicate we can discriminate different types of neurons and brain regions based on cilia parameters. Our results further suggest that the cilia are sensing organelles whose failure to grow properly may set the stage for abnormal network function. Furthermore during aging, this process could be compromised or lost.

In view of a very recent publication in which neuronal cilia have been implicated in synaptic function and memory, our findings suggest a correlation between cilia number and neuronal network function. Interestingly, our more recent discovery in collaboration with Dr. Tom Foster reveals age-related changes in neurotransmitter receptors on neuronal cilia throughout the brain (see copy of published abstract). Thus, exploring neuronal cilia biology is highly-relevant to network function (i.e. synaptic connectivity and neuron numbers) with aging.

HIPPOCAMPUS 00:000–000 (2010)

# Decreased Interactions in Protein Kinase A–Glucocorticoid Receptor Signaling in the Hippocampus After Selective Removal of the Basal Forebrain Cholinergic Input

Chol Seung Lim,[1] Youn Jung Kim,[2] Yoo Kyeong Hwang,[3] Christina Bañuelos,[4] Jennifer L. Bizon,[4] and Jung-Soo Han[3]*

**ABSTRACT:** Removal of the cholinergic innervation to the hippocampus via selective immunolesions of septohippocampal cholinergic neurons induces dysfunction of the hypothalamic–pituitary–adrenocortical (HPA) axis and decreases glucocorticoid receptor (GR) mRNA. This study examined whether removal of the cholinergic innervation decreased GR protein levels and induced changes in the interaction between GR and the cytoplasmic catalytic subunit of protein kinase A (PKAc) in the hippocampus. In lesioned animals, GR protein levels were markedly decreased in the nucleus, but not in the cytosol of hippocampal neurons, whereas mineralocorticoid receptor (MR) levels remained unchanged in both the nucleus and cytosol. PKAc levels did not differ between lesioned and control groups, but PKAc activity was reduced in lesion tissue compared with the controls. The interaction between GR and PKAc was also decreased in the hippocampus without cholinergic input. These results indicate that degeneration of septohippocampal cholinergic neurons leads to reduced PKAc activity in the hippocampus which, in turn, alters GR signaling. The altered GR signaling induced by the degeneration of basal forebrain cholinergic neurons may contribute to dysfunction of the HPA axis in aged animals and patients with Alzheimer's disease (AD) and lead to neuropsychiatric symptoms that occur throughout the course of AD. © 2010 Wiley-Liss, Inc.

**KEY WORDS:** Alzheimer's disease; HPA axis; aging; stress; 192 IgG-saporin

## INTRODUCTION

The vulnerability of neurons to disease and insult is greater at advanced ages than at earlier times in life. Degeneration of basal forebrain cholinergic neurons (BFCNs) has been figured as a factor in the cognitive decline associated with aging and Alzheimer's disease (AD) (Bartus et al., 1982; Whitehouse et al., 1982; Fischer et al., 1989; Gallagher and Colombo, 1995) because BFCN widely innervates hippocampus and cortex (De Lacalle et al., 1994).

Many studies have shown that dysregulation of the hypothalamic–pituitary–adrenocortical (HPA) axis occurs in both aging and AD, resulting in functional impairments of integrity in hippocampus and cortex (Davis et al., 1986; de Leon et al., 1988; Issa et al., 1990; Bizon et al., 2001). It is also well known that the hippocampus and cortex with cholinergic innervations from the basal forebrain are involved in regulating the HPA axis response to stress. Specifically, the hippocampus, which contains abundant glucocorticoid receptors (GRs), has been identified as a target for steroids through which negative feedback on corticosterone release is mediated. For example, in rats with damaged hippocampi, peak increases in corticosterone induced by stress are unaffected, but return to low basal levels is delayed (Sapolsky et al., 1990). It has also been reported that animals with BFCN lesions show a blunted negative feedback regulation of the HPA axis in response to stress and decreased GR mRNA levels in the hippocampus (Han et al., 2002; Helm et al., 2002).

This study was conducted to determine whether decreases in protein GR levels occur in the hippocampus without cholinergic input. Specifically, we used 192 IgG-saporin to selectively lesion the cholinergic input to the hippocampus, which has previously been shown to produce near complete removal of septohippocampal cholinergic neurons while sparing both fibers of passage and noncholinergic neurons in the septal region (Baxter and Gallagher, 1996). The results of the previous studies and this study showed that GR mRNA and nuclear protein levels of GR were decreased in the hippocampus with cholinergic lesions (Han et al., 2002).

Molecular mechanisms through which the removal of cholinergic innervations reduces nuclear GR levels in the hippocampus were also examined in this investigation. Negative regulation of GR through cross-talk mechanisms in the nucleus is well known and has been extensively studied; however, several studies have shown that GR associates with the cytoplasmic catalytic subunit of protein kinase A (PKAc) in a ligand-independent manner and that GR transcription

[1] Blanchette Rockefeller Neurosciences Institute at West Virginia University, Morgantown, West Virginia; [2] Graduate Program in Neuroscience and Institute for Brain Science and Technology, Inje University, Daejeon, South Korea; [3] Department of Biological Sciences and Center for Geriatric Neuroscience Research, IBST, Konkuk University, Seoul, South Korea; [4] Department of Neuroscience, College of Medicine, Evelyn F. and William L. McKnight Brain Institute of Florida, Gainesville, Florida

Grant sponsor: Korea Research Foundation; Grant number: KRF-313-2007-H00017 (Basic Research Promotion Fund to J.-S.H.).

*Correspondence to: Jung-Soo Han, PhD, Department of Biological Sciences, Konkuk University, 1 Hwayang-Dong, Gwangjin-Gu, Seoul 143-701, South Korea. E-mail: jshan06@konkuk.ac.kr

Accepted for publication 15 October 2010
DOI 10.1002/hipo.20912
Published online in Wiley Online Library (wileyonlinelibrary.com).

J_ID: ZA4 Customer A_ID: 10-221.R1 Cadmus Art: HIPO20912 Date: 15-NOVEMBER-10 Stage: I Page: 2



depends on PKA signaling (Haske et al., 1994; Doucas et al., 2000). Therefore, the effects of the removal of cholinergic input on PKA activity and the interaction of GR with PKAc in the hippocampus were evaluated herein.

## MATERIALS AND METHODS

### Materials and Animals

Sixty 3-month-old male Sprague-Dawley rats (SPF) obtained from Charles River Co. (Gapyeung, South Korea) were housed individually in a temperature and humidity-controlled room, with a 12:12 h light–dark cycle (lights on, 7:00 a.m. to 7:00 p.m.). Food and water were available *ad libitum*. All testing was conducted during the light cycle. Experiments were conducted in compliance with the Konkuk University's Council Directive for the use and care of laboratory animals. The 192 IgG-saporin was obtained from Advanced Targeting Systems (San Diego, CA). An enhanced chemiluminescence (ECL) kit and hyperfilm were obtained from Amersham Bioscience (Piscataway, NJ). Polyclonal anticholine acetyltransferase (ChAT), polyclonal antiphosphoserine, and polyclonal antiphosphothreonine antibodies (Abs) were obtained from Chemicon International (Temecula, CA). Polyclonal anti-GR, antimineralocorticoid receptor (MR), and horseradish peroxidase (HRP)-conjugated secondary Abs were purchased from Santa Cruz Biotechnology (Santa Cruz, CA). Polyclonal anti-PKAc and polyclonal phospho-PKAc (Thr197) Abs were obtained from Cell Signaling (Beverley, MA). PepTag Assay kits for nonradioactive detection of cyclic adenosine monophosphate (cAMP)-dependent PKA were purchased from Promega (Madison, WI). Corticosterone enzyme immunoassay (EIA) kits were obtained from Assay Designs (Ann Arbor, MI). Antiparvalbumin (PARV), monoclonal anti-β-actin Abs, and all reagents were purchased from Sigma Aldrich (St. Louis, MO), unless otherwise stated.

### Surgery

Selective cholinergic lesions of the medial septum/vertical limb of the diagonal band of Broca (MS/VDB) were made with injections of 192 IgG-saporin, as described previously (Baxter and Gallagher, 1996). The 192 IgG-saporin was dissolved in sterile 0.1 M phosphate buffered saline (PBS) at 0.25 μg/μl concentration. Rats were anesthetized with isofluorane and placed in a stereotaxic frame (Kopf Instruments, Tujunga, CA) fitted with an isofluorane gas anesthesia system and an incisor bar set at 3.3 mm below the ear bars. The scalp was then incised and retracted, and holes were drilled at appropriate locations in the skull using a dental drill. Injections of sterile PBS (control surgery, $n = 24$) or 192 IgG-saporin (lesion surgeries, $n = 36$) were made with a 28-gauge Hamilton syringe at four sites: anteroposterior (AP) + 0.45 mm, mediolateral (ML) ± 0.6 mm, and dorsoventral (DV) −7.8 mm and −6.2 mm relative to Bregma, according to the Paxinos and Watson (1986) atlas. A volume of 0.3 μl was injected into the sites DV − 7.8 mm, and a volume of 0.2 μl was injected into the sites DV − 6.2 mm. Injections were made at a rate of 0.05 μl/min, and the needle was left in place for 3–4 min after each injection.

### Immunochemistry and Acetylcholinesterase Histochemistry

Three weeks after surgery, rats used for the immunochemistry and acetylcholinesterase (AChE) histochemistry were killed by an overdose of ketamine HCl (30 mg/kg) and xylazine (2.5 mg/kg), after which they were intracardially perfused with 4% paraformaldehyde in 0.1 M phosphate buffer (pH 7.4, PB). All perfusions were conducted between 8:00 and 12:00 a.m. After fixation, the brains were removed, postfixed in PB (2 h), cryoprotected in PBS containing 20% sucrose (24 h), frozen on powdered dry ice, and sectioned (coronal plane: 40 μm) using a freezing microtome.

For lesion confirmation, basal forebrain sections were processed for either ChAT or PARV immunoreactivity, and hippocampal sections were processed for AChE histochemistry, GR, and MR. For ChAT, PARV, GR, and MR, endogenous peroxidases were blocked by 30 min incubation in 3% $H_2O_2$/10% MeOH in PBS. Sections were incubated for 1 h (room temperature, RT) in PBS with 0.3% Triton X-100, containing 10% serum followed by an 18-h incubation (4°C) in the same solution with the addition of the appropriate primary Ab (ChAT, 1:200; PARV, 1:1,000; GR, 1:200; and MR, 1:50). Sections were then incubated for 1 h in the appropriate biotinylated secondary Ab (RT; 1:200) and 1 h in ExtrAvidin peroxidase conjugate Ab (RT; 1:1,000), and then reacted using a Vector SG substrate kit (Vector Laboratories, Burlingame, CA). Sections were mounted on superfrost$^{2+}$ slides, dehydrated through ascending concentrations of alcohol, defatted in xylene, and coverslipped with Permount. The AChE staining procedure was adapted from elsewhere (Karnovsky and Roots, 1964).

### Western Blot Analysis

Three weeks after surgery, rats used for western blot, coimmunoprecipitation, and the PKA activity assay were decapitated, and the brains were removed, and a coronal cut at 2 mm posterior to the optic chiasma was made to partition the anterior portion containing BFCN from the posterior part containing the hippocampus. The anterior portion of the brains were postfixed in 4% paraformaldehyde PB (24 h), cryoprotected in PBS containing 20% sucrose (24 h), frozen on powdered dry ice, and sectioned (coronal plane: 40 μm) on a microtome. These sections were then processed for ChAT and PARV immunostaining to confirm the presence of a selective cholinergic lesion. The posterior portion of the brain was microdissected, and the hippocampus was frozen. Whole tissue and cytosolic or nuclear protein extracts were then prepared using a protein extraction method that has been described elsewhere (Murphy et al., 2002). Briefly, tissues were homogenized in





ID: subramaniank Date: 15/11/10 Time: 10:25 Path: N:/3b2/HIPO/Vol00000/100155/APPFile/JW-HIPO100155

Dounce homogenizers (five strokes; Kontes Co., Vineland, NJ) in the lysis buffer [10 mM HEPES (pH 7.9), 0.6% Nonidet P40, 150 mM NaCl, and 1 mM EDTA] containing protease and phosphatase inhibitors. Homogenates were pelleted in a microcentrifuge for 30 s, and the supernatants were incubated on ice for 5 min. Nuclei were pelleted by centrifugation at 4,000 rpm (4°C) for 5 min, and the supernatants were used as cytosolic fraction. Pellets were then resuspended in 20 mM HEPES containing 25% glycerol, 420 mM NaCl, 1.2 mM $MgCl_2$, 0.2 mM EDTA, 2 mM benzamidine, and 0.5 mM dithiothreitol supplemented with protease and phosphatase inhibitors, and incubated on ice for 20 min, and debris was pelleted for 30 s. Supernatants were collected and used for nuclear fractions. After measurement of protein concentrations by bicinchoninic acid (BCA) methods, each protein (15 μg) was separated by 8–10% sodium dodecyl sulfate-polyacrylamide gel electrophoresis (SDS-PAGE) and transferred onto a poly(vinylidene fluoride) (PVDF) membrane, which was incubated with primary Abs against GR (1:1,000), MR (1:250), actin (1:5,000), and PKAc (1:1,000), and then HRP-conjugated secondary Abs. The membranes were then visualized using an ECL system and developed onto hyperfilm.

## Coimmunoprecipitation and IP-Western Blot

Rat hippocampal tissue was homogenized in extraction buffer (10 mM Tris-HCl, pH 7.5, 5 mM EDTA, 150 mM NaCl, 1 mM sodium orthovanadate, 10 mM NaF, 1% Triton X-100, 10% glycerol, 1 mM $CaCl_2$, and 1 mM $MgCl_2$) supplemented with protease inhibitors. The extracts were then clarified by centrifugation for 10 min at 5,000*g*, and the protein concentrations in the supernatants were determined using BCA. Next, samples containing 1 mg of total protein were taken for subsequent immunoprecipitation with specific Abs against the GR or PKA catalytic domain overnight, followed by additional 3 h incubation at 4°C with protein A Sepharose beads. The immunoprecipitates were extensively washed with the same extraction buffer and then subjected to SDS-PAGE and Western blot analysis using the procedure and concentrations described above. The other primary Abs were incubated in polyclonal antiphosphoserine (1:500), polyclonal antiphosphothreonine (1:500), and polyclonal phospho-PKAc at Thr-197 (1:1,000).

## PKA Activity Assay

PKA activity was measured using a PepTag Assay kit for nonradioactive detection of cAMP-dependent PKA following manufacturer's protocol. After decapitation, the brains were microdissected and the hippocampi were frozen. Whole tissue extracts were then prepared, and the total proteins (800 μg) were immunoprecipitated using specific Ab against the PKA catalytic subunit. Ab–protein complexes were washed with PBS and used in a PKA assay. Briefly, PKA-containing samples from immunoprecipitation were incubated with fluorescent PKA-specific peptide substrate [PepTag A1 peptide, Leu-Arg-Arg-Ala-Ser-Leu-Gly (Kemptide), final 0.08 μg/μl, net charge +1] in reaction buffer [100 mM Tris-Cl, pH 7.4, 50 mM $MgCl_2$, and 5 mM adenosine triphosphate (ATP)] including cAMP as a PKA activator (1 μM). As a positive and negative control experiment, the reactions were incubated with/without purified PKA catalytic subunit (final 0.4 ng/μl). After 30 min incubation at RT, the samples were boiled for 10 min to stop the reaction and loaded onto agarose gel. Phosphated peptide, which has net charge −1 because of the addition of phosphate group by PKA, was assessed by its altered mobility to cathode direction on an agarose gel run at neutral pH. The extent of phosphorylation was determined by quantifying the amount of negatively charged peptides after scanning images of the fluorescent gels.

## Corticosterone Immunoassay

To measure the baseline levels of corticosterone, animals were scarified between 8:00 and 11:00 a.m., and trunk blood was taken. Blood serum was separated by centrifugation (3,000 rpm, 20 min) and stored at −70°C until the time of assay. Serum corticosterone concentrations were measured using corticosterone EIA kits.

## Data Analysis

The obtained data were analyzed by an independent Student's *t*-test to examine the effects of the experimental conditions (lesion vs. control) on blood corticosterone levels, MR and GR protein levels, and PKA activity levels. Any *P*-values less than 0.05 were considered significant. All data were expressed as the mean ± standard error of mean (SEM).



# RESULTS

## Histological Results for Confirmation of Cholinergic Lesions

Immunochemical analysis of the lesion sites revealed a pronounced absence of ChAT-positive neurons in all but seven lesioned rats, with no apparent loss of PARV-positive (GABAergic) neurons, confirming the selectivity of the lesion. AChE staining also revealed a marked effect of the lesion throughout the hippocampus in rats with confirmed removal of ChAT-positive cells in the basal forebrain. AChE staining revealed that the striatum, thalamus, and cortex remained intact. Rats with incomplete removal of ChAT-positive neurons ($n = 7$) were eliminated from further data analysis. Representative depictions of the histological results are shown in Figure 1. F1

## Corticosterone

Control rats ($n = 18$) and rats with confirmed cholinergic lesions ($n = 18$) were used to measure the basal levels of corticosterone (Fig. 2). Baseline values for the two groups did not differ significantly ($t(34) = -1.42$, ns). F2

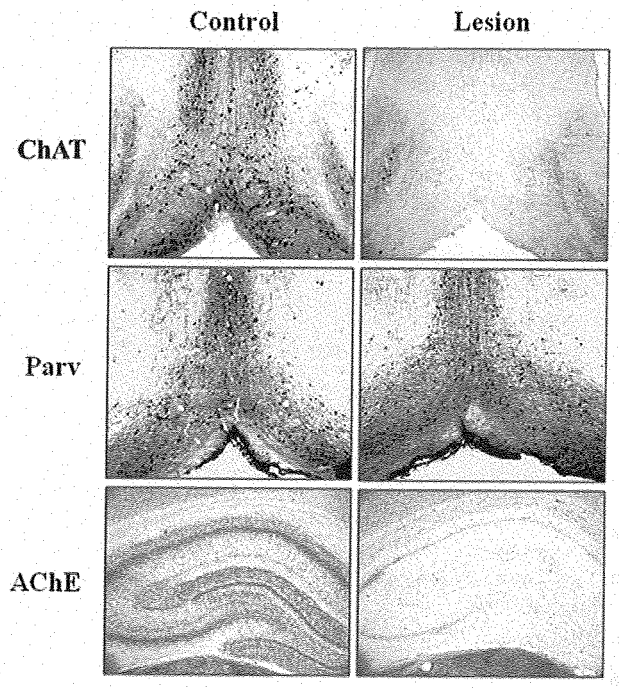


**FIGURE 1. Immunochemical (ChAT) and histochemical (AChE) depiction of lesions made with 192 IgG-saporin. Top: Bright-field photomicrographs showing immunohistochemical localization of ChAT-positive cells in the medial septum/vertical limb of the diagonal band of Broca (MS/VDB). The left panel shows labeling in saline-infused rats, and the right panel shows the relative absence of labeling in a 192 IgG-saporin-infused rat. Middle: Bright-field photomicrographs showing immunohistochemical localization of parvalbumin (PARV) immunostaining in the MS/VDB. The left and right panels show labeling in control and lesioned rats, respectively. Bottom: Hippocampal AChE staining in a control brain (left) and a lesioned rat (right) that lacks AChE staining. [Color figure can be viewed in the online issue, which is available at wileyonlinelibrary.com.]**

## GR and MR Protein Expression Levels of the Hippocampus After Lesion of Cholinergic Input

Loss of cholinergic input to the hippocampus led to a significant decrease in the 97-kDa GR band in Western blots of nuclear hippocampal extracts ($t(10) = 2.28$, $P = 0.05$), but not in cytosolic hippocampal extracts compared with the control hippocampus ($t(10) = 1.13$, ns) (Figs. 3A,B). Conversely, Western blots of hippocampi without cholinergic input showed no difference in the 102-kDa MR band of cytosolic and nuclear extracts compared with control hippocampi ($t(10) \leq 1.18$, ns) (Figs. 4A,B).

Figures 3C and 4C show localization of GR and MR protein, respectively, in the hippocampus. In agreement with previous reports describing reduced hippocampal GR mRNA in lesioned rats relative to controls (Han et al., 2002), a robust attenuation of GR protein was observed in subfields CA1 and the dentate gyrus (DG) of the hippocampus without cholinergic input relative to control animals in this study. Further, consistent with previous mRNA results (Han et al., 2002), hippocampal MR protein expression was unchanged after lesion of cholinergic input (Fig. 4).

## PKA Activity and Phosphorylation of the Hippocampus After Lesion of Cholinergic Input

To determine what causes the decrease in nuclear GR expression in the hippocampus without cholinergic input, we first measured PKA activity. PKA activity was decreased in the hippocampus of lesioned rats relative to that of control rats ($t(4) = 4.67$, $P = 0.01$) (Figs. 5A,B). We further measured PKAc levels using Western blot to determine whether the loaded amount used in the PKA activity assay was the same and found that the levels did not differ between groups (Fig. 5A).

Subsequently, we examined the status of phosphorylation at Thr197 in the activation loop of the cAMP-dependent PKAc. In the hippocampus after lesion of cholinergic input, the levels of PKAc protein were not significantly altered compared with the control (Figs. 6A,B), whereas phosphorylation of PKA at Thr197 was significantly reduced (Figs. 6C,D) ($t(4) = 4.63$, $P = 0.01$).

## Interaction Between PKAc and GR Was Attenuated in the Hippocampus After Lesion of Cholinergic Input

To determine how the interaction between PKAc and GR is altered in hippocampus without cholinergic input, the hippocampal lysates of control and lesioned rats were immunoprecipitated with anti-PKAc Ab or anti-GR Ab. The

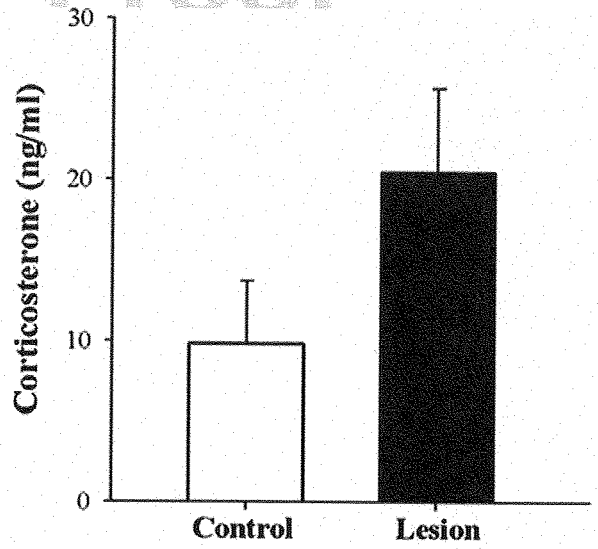


**FIGURE 2. Basal plasma corticosterone values in blood samples taken from control ($n = 18$) and lesioned rats ($n = 18$). The basal values did not differ significantly between groups. Data shown are the means ± standard error of mean (SEM).**

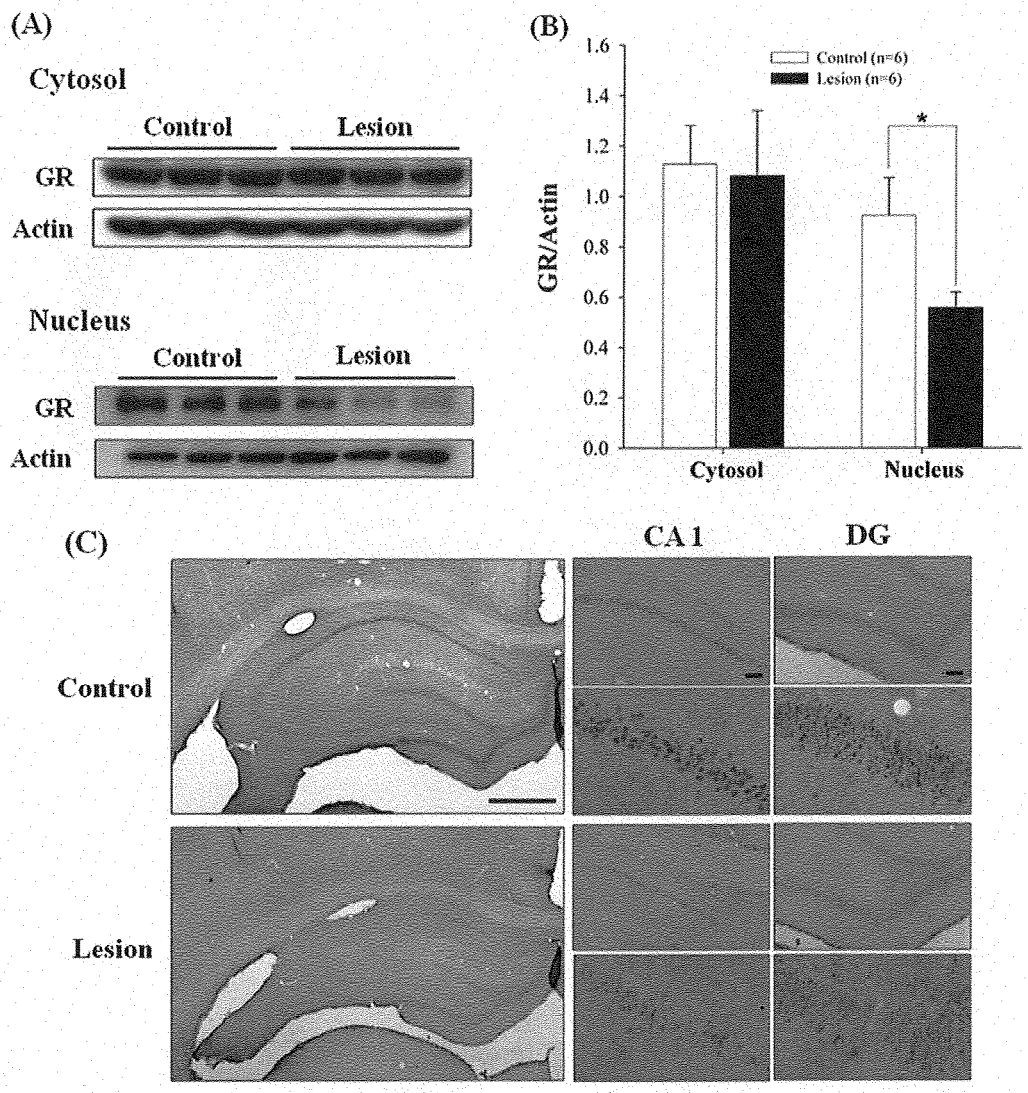


**FIGURE 3. Nuclear GR expression was decreased in the hippocampus after lesion of cholinergic input. (A) Representative Western blot of cytosolic and nuclear GR. (B) Hippocampal nuclear GR levels greatly decreased in the hippocampus with cholinergic lesions relative to those of the control hippocampus (*$P < 0.05$). Data shown are the means ± standard error of mean (SEM). (C) Photomicrograph showing the GR immunoreactivity in the hippocampus. Scale bars depicted at the top line of the photomicrographs denote 500, 100, and 25 μm from left to right.**

immunoblots incubated with anti-PKAc Ab or anti-GR Ab revealed that the interaction between PKAc and GR was significantly weaker in lesioned rats relative to controls ($t(4) \geq 3.76$, $P < 0.02$) (Fig. 7). F7

## Decreased Phosphorylation of GR in the Hippocampus After Lesions of Cholinergic Input

To elucidate the mechanism whereby GR phosphorylation is altered in the hippocampus after cholinergic denervation, hippocampal lysates of control and lesioned rats were immunoprecipitated with anti-GR Ab and immunoblots generated using antiphosphothreonine and antiphosphoserine Abs. In addition to the whole hippocampal lysates, the same experiments were conducted using cytosolic and nuclear extracts. Expression of phosphothreonine and phosphoserine on GR protein was decreased in both the whole and fractionated lysates ($t(4) \geq 2.71$, $P < 0.05$) (Fig. 8). F8

# DISCUSSION

The current data demonstrate that selective removal of septohippocampal cholinergic neurons significantly decreases GR

J_ID: ZA4 Customer A_ID: 10-221.R1 Cadmus Art: HIPO20912 Date: 15-NOVEMBER-10 Stage: I Page: 6



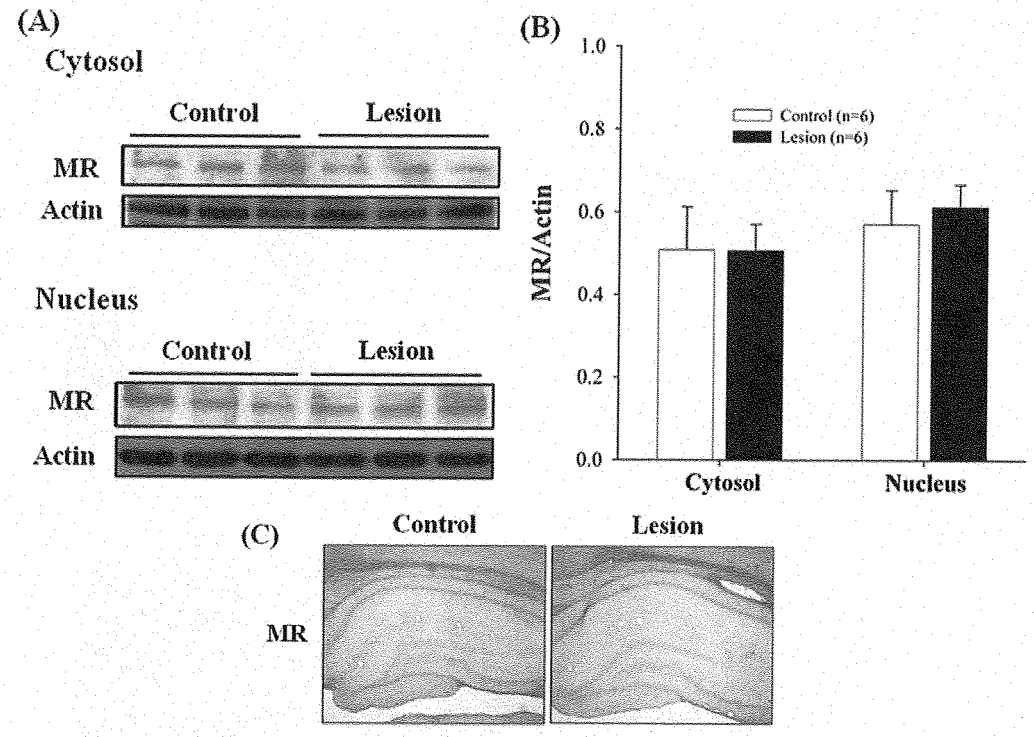


**FIGURE 4. (A) Representative Western blot of cytosolic and nuclear MR. (B) Hippocampal cytosolic and nuclear MR levels did not differ significantly between groups. Data shown are the means ± standard error of mean (SEM). (C) Photomicrograph showing the MR immunoreactivity in the hippocampus.**

but not MR protein expression in the hippocampus. These data agree with our previous reports describing selective attenuation of GR mRNA expression after removal of cholinergic afferents to hippocampus (Han et al., 2002; Helm et al., 2002). Similarly, the maintenance of basal circulating corticosterone in rats after lesion of cholinergic afferents to hippocampus agrees with our previous results (Han et al., 2002), but not that cholinergic projections from basal forebrain are important for restoring corticosterone to basal levels after an acute episode of stress (Han et al., 2002). Together, these results demonstrate that removal of BFCNs that target the hippocampus produce a change in GR expression associated with hippocampal neurons and concomitantly alters the functional regulation of the HPA axis (Han et al., 2002; Helm et al., 2002, 2004).

There is a variety of evidence supporting the finding that septohippocampal cholinergic neurons are related to hippocampal GR expression. For example, evaluation of the effects of stress on central nervous system (CNS) development revealed that cholinergic innervation of the hippocampus is highly sensitive to glucocorticoids during prenatal and postnatal development and that these septohippocampal cholinergic neurons may play an important role in the development of emotional behavior with lifelong consequences (Day et al., 1998; Takahashi and Goh, 1998). Another study of GR-conditioned knock-out mice exhibiting a CNS-specific conditional activation of the GR gene showed that the number of medial septohippocampal cholinergic neurons in mutant mice was significantly reduced during development compared with that of control littermates (Guijarro et al., 2006).

Numerous reports indicate that the integrity of BFCNs is dysfunctional late in life in both humans and rodents (Whitehouse et al., 1982; Smith and Booze, 1995). In humans, both AD and aging in the absence of AD is associated with impaired HPA function and, subsequently, greater exposure to glucocorticoids (Lupien et al., 1994; Geula, 1998). Parallel findings have been reported for aged rodents in which cognitive impairment is correlated with both a blunted feedback of HPA in response to restraint stress and decreases in hippocampal GR mRNA (Bizon et al., 2001). These results suggest that loss of BFCNs during aging contributes to the weak inhibitory control of the HPA axis by the hippocampus, resulting into overall increased glucocorticoid exposure. Such events are likely deleterious because protracted exposure to glucocorticoid levels are known to impair neural function and plasticity of the hippocampus (Sapolsky et al., 1984) and can ultimately result in hippocampal neurodegeneration observed under pathological conditions associated with aging, such as AD.

Despite these data, the molecular mechanisms by which loss of the BFCNs contribute to reduced hippocampal function and HPA axis dysregulation are poorly understood.





ID: subramaniank Date: 15/11/10 Time: 10:25 Path: N:/3b2/HIPO/Vol00000/100155/APPFile/JW-HIPO100155

J_ID: ZA4 Customer A_ID: 10-221.R1 Cadmus Art: HIPO20912 Date: 15-NOVEMBER-10 Stage: I Page: 7



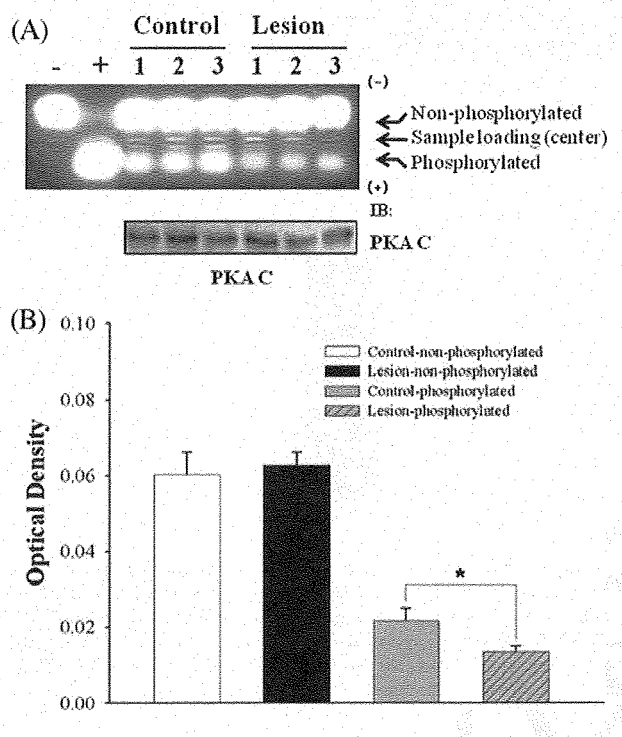


**FIGURE 5. (A) Measurement of PKA activities in the hippocampi of rats with the cholinergic lesion in the MS/VDB and control rats. PKA assay was conducted using PepTag assay protein kinase kits according to manufacturer's instructions. Phosphorylated and nonphosphorylated peptide bands were quantified by densitometry of the scanned image. (B) The density of phosphorylated peptide bands in the hippocampus with the cholinergic lesions were significantly lower than those of the control hippocampus (*$P < 0.05$), whereas the density of nonphosphorylated peptide bands showed no differences between groups. The levels of PKAc did not differ between groups. Data shown are the means ± standard error of mean (SEM) of three samples.**

Such was the focus of this study, which included characterizing GR and MR subcellular localization in the hippocampus in a rat model in which cholinergic afferents to hippocampus were selectively lesioned. Here, we report that expression levels of GR protein were selectively decreased in the nucleus, but not in the cytosol of hippocampus neurons without the cholinergic input, and, consistent with our previous work on receptor mRNA expression (Han et al., 2002; Helm et al., 2002), MR was stable after cholinergic deafferentation. Decreased translocation into nucleus of GR indicates that GR-dependent gene expression, including GR itself in nucleus, is defective (Revollo and Cidlowski, 2009) and that such dysfunction likely contributes to failed regulation of the HPA axis that is known to occur after loss of cholinergic input to hippocampus (Han et al., 2002; Helm et al., 2002).

In the last several years, cross-talk between transcriptional pathways has received a great deal of attention, and such interactions are becoming better understood (Beato et al., 1995). Cross-talk at the level of nuclear receptor-dependent transcriptional activation or through modulation of the activity of other classes of trans-activators via DNA-binding independent mechanisms may occur between GR and downstream targets, and these same mechanisms occur in the nucleus (Beato et al., 1995; Zhong et al., 1997; McKay and Cidlowski, 1998). Several studies have shown that PKAc associates with GR in a ligand-independent manner and can powerfully modulate GR-mediated transcriptional activation (Doucas et al., 2000). Moreover, GR can be phosphorylated by PKA (Haske et al., 1994), and forskolin, a PKA agonist, enhances the transcriptional activity and stability of GR mRNA (Penuelas et al., 1998).

Accordingly, we examined the PKA activity in hippocampus after lesion of cholinergic input from basal forebrain. A PepTag assay PKA assay revealed a significant reduction in PKAc phosphorylated after cholinergic deafferentation, whereas total levels of PKAc did not differ between groups. We further investigated PKAc phosphorylation at Thr197 in the two groups because post-translational autophosphorylation of Thr197 is a critical step in autoactivation of the catalytic subunit of PKA (Steinberg et al., 1993; Moore et al., 2003). Studies using IP-Western blot showed that phosphorylation of PKAc specifically at Thr197 was indeed significantly attenuated after lesion of hippocampal cholinergic afferents.

Coimmunoprecipitation demonstrated that PKAc-GR was decreased in the hippocampus without cholinergic input. In turn, phosphorylation of threonine and serine on GR were examined in the whole lysates and cytosolic and nuclear extracts of the hippocampus because the specific sites at which PKAc phosphorylates GR have not yet been reported. In both experiments, the expression of phosphothreonine and phosphoserine on GR protein was lower in the hippocampus after cholinergic lesion than in the control condition. These results, along with the previous reports of reduced GR mRNA and an increased HPA response to acute stress in lesioned rats (Han et al., 2002), suggest that changes in kinase activity that influences GR phosphorylation render the receptor differentially responsive to stress.

Cyclic AMP-dependent PKA signal pathways engage in regulation of a wide variety of biological responses, including neurotransmitter systems. For example, stimulation of serotonergic receptors and adrenergic beta receptors induces a conformational change in G protein, which activates adenyl cyclase (AC). Subsequently, AC converts ATP to cyclic AMP and activated cyclic AMP regulates translocation of GR (Nibuya et al., 1996; Pace et al., 2007). Involvement of the cholinergic system in cyclic AMP-dependent PKA signal pathways may be indicated by the results of this study and the report that septal-hippocampal cholinergic lesions with the selective neurotoxin 192 IgG-saporin caused a decrease in M1 muscarinic receptor function, resulting in the uncoupling of the receptor and G proteins (Potter et al., 1999). However, it is currently not known whether cholinergically





ID: subramaniank Date: 15/11/10 Time: 10:25 Path: N:/3b2/HIPO/Vol00000/100155/APPFile/JW-HIPO100155

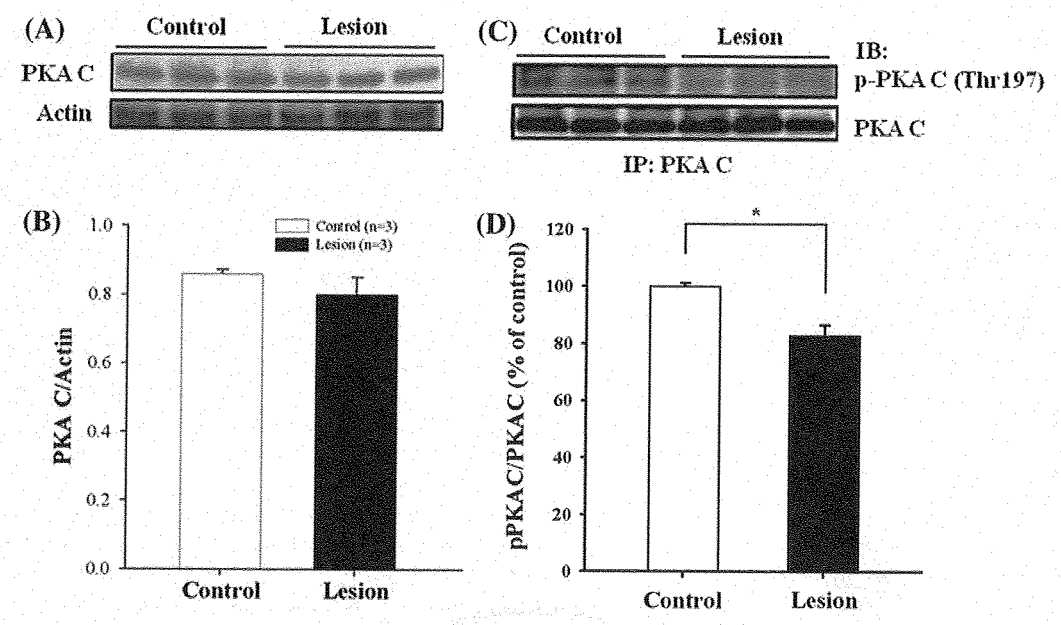


FIGURE 6. Decreased PKAc phosphorylation in the hippocampus after lesion of cholinergic input. (A) Immunoblots of hippocampal lysate from control rats and lesioned rats, conducted with PKAc and actin antibodies. (B) Densitometric analysis of the immunoblots was normalized with actin. Levels of PKAc did not differ in the hippocampus without cholinergic input relative to those of the control hippocampus. (C) Coimmunoprecipitation. Hippocampal lysate from control and lesioned rats was immunoprecipitated with anti-PKAc antibody and then subjected to immunoblot analysis for p-PKAc (Thr197). (D) Phosphorylation of PKAc at Thr197 was significantly reduced compared with the control hippocampus (*$P < 0.05$). Data shown are the means ± standard error of mean (SEM)

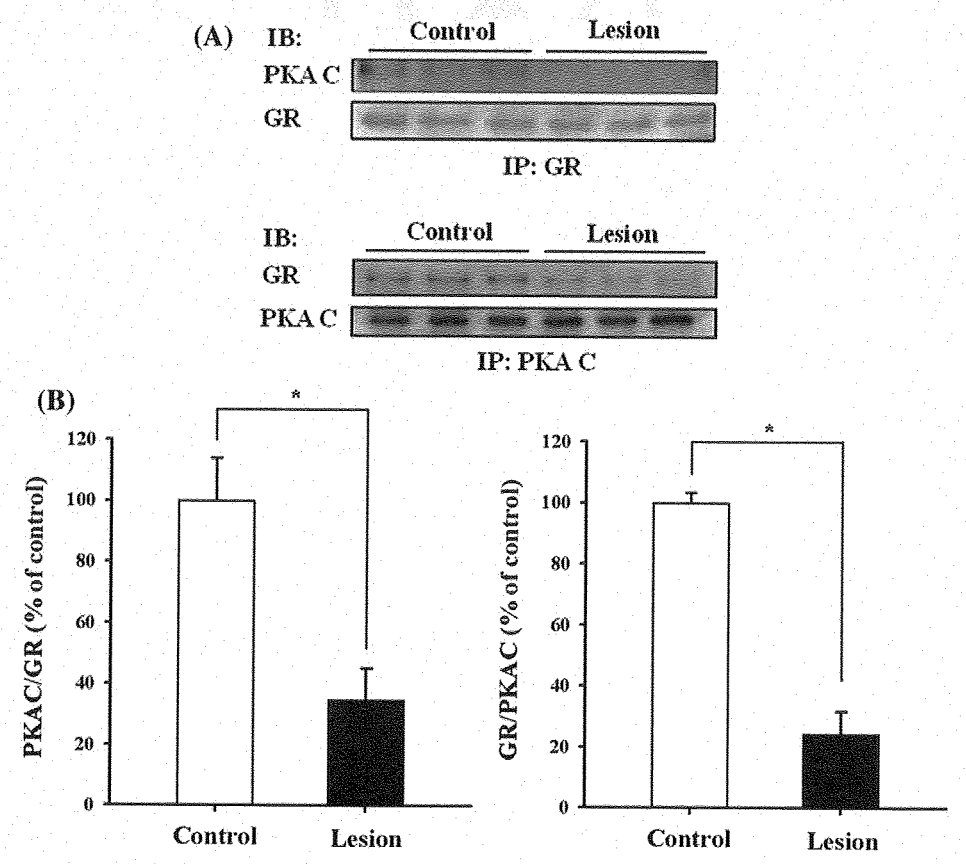


FIGURE 7. Decreased interaction between PKAc and GR in the hippocampus after lesion of cholinergic input. (A) Top: Coimmunoprecipitation. Hippocampal lysate from control rats and lesioned rats was immunoprecipitated with anti-GR antibody and then subjected to immunoblot analysis for PKAc. Interaction of GR with PKAc was decreased in the hippocampus without cholinergic input. Bottom: Coimmunoprecipitation. Hippocampal lysate from control rats and lesioned rats was immunoprecipitated with anti-PKAc antibody and then subjected to immunoblot analysis for GR. (B) Interaction of PKAc with GR was significantly decreased in the hippocampus without cholinergic input (*$P < 0.05$). Data shown are the means ± standard error of mean (SEM)

J_ID: ZA4 Customer A_ID: 10-221.R1 Cadmus Art: HIPO20912 Date: 15-NOVEMBER-10 Stage: I Page: 9



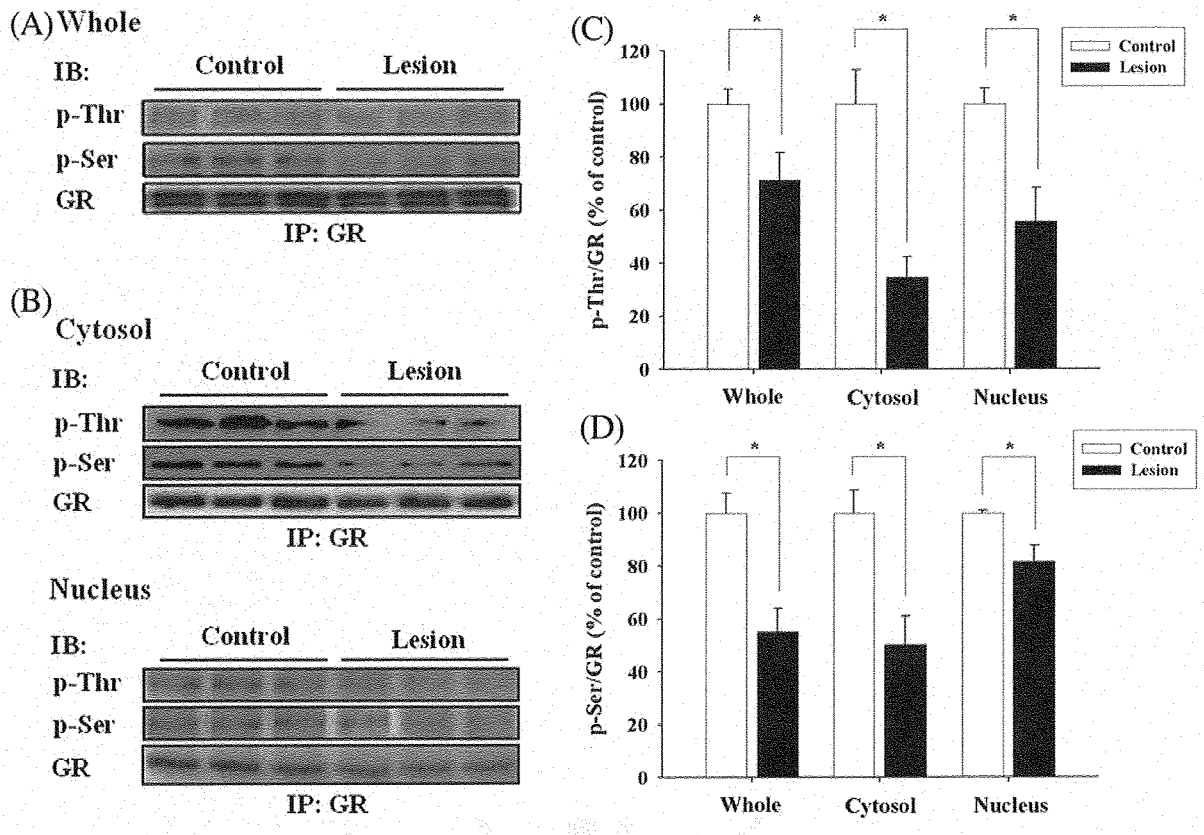


**FIGURE 8. Decreased phosphorylation of threonine and serine on GR in the hippocampus after lesion of cholinergic input. (A) IP-Western. Hippocampal lysate from control rats and lesioned rats was immunoprecipitated with anti-GR antibody and then subjected to immunoblot analysis with antiphosphothreonine and antiphosphoserine antibody. (B) IP-Western. Cytosolic and nuclear extracts of hippocampus from control rats and lesioned rats was immunoprecipitated with anti-GR antibody and then subjected to immunoblot analysis with antiphosphothreonine and antiphosphoserine antibody. (C,D) Expression of phosphothreonine and phosphoserine on GR was significantly decreased in the whole lysates and both fraction of hippocampus without cholinergic input compared with those of control (*$P < 0.05$). Data shown are the means ± standard error of mean (SEM).**

stimulated signaling pathways induce activation of the cyclic AMP-dependent PKA signal pathway and then GR activation, though it has been reported that pyramidal neurons in the rat CA1 hippocampal area have cholinergic receptor and intracellular GR receptors and that depolarizing responses to carbachol, a muscarinic agonist, were greater in a state of GR activation (Joels, 2001).

As stated above, a large body of evidence indicates that the cyclic AMP-dependent PKA signal pathway is required for GR function, and that this signal transduction system plays a key role in stress-related psychiatric disorders, including depression. Disruptions in either the cyclic AMP-dependent PKA signal pathway or GR signaling has been reported in mononuclear cells and cultured fibroblasts in patients with major depression (Shelton et al., 1996; Avissar et al., 1997) and in the brain tissue of suicide victims compared with nonpsychiatric control subjects (Dwivedi et al., 2002, 2004). An animal study of the mechanisms of action of antidepressants suggested that the cyclic AMP-dependent PKA signal pathway plays an important role as a mediator of the psychotropic effects of these agents, including serotonin- and norepinephrine-selective reuptake inhibitors (Nibuya et al., 1996). In addition, there is considerable evidence that GR signaling is impaired in patients with major depression. The most reliable supporting report is lack of suppression of adrenocorticotropic hormone (ACTH) or cortisol secretion after administration of the synthetic glucocorticoid in patients with major depression (Raison and Miller, 2003). Moreover, alteration of GR signaling in the brain tissue of suicide victims compared with matched control subjects have been reported (Lopez et al., 1998).

AD patients show neuropsychiatric symptoms throughout the course of AD, and there is evidence that a cholinergic deficit resulting from a loss of cholinergic neurons in the basal forebrain is the biological basis of these neuropsychiatric symptoms (Wynn and Cummings, 2004). Treatment of AD patients with cholinesterase inhibitors seems to stabilize neuropsychiatric symptoms. This experiment demonstrated that loss of choliner-





ID: subramaniank Date: 15/11/10 Time: 10:25 Path: N:/3b2/HIPO/Vol00000/100155/APPFile/JW-HIPO100155

J_ID: ZA4 Customer A_ID: 10-221.R1 Cadmus Art: HIPO20912 Date: 15-NOVEMBER-10 Stage: I Page: 10



gic neurons leads to alterations in the cyclic AMP-dependent PKA signal pathway and subsequent impairments in GR signaling. The results presented in this investigation along with those of previous animal studies that demonstrate a failure of regulation in response to stress in cholinergic lesioned subjects suggest that antidepressants and other pharmacological agents that can enhance cyclic AMP-dependent PKA pathway signaling may alleviate neuropsychiatric symptoms in AD.

## REFERENCES


Avissar S, Nechamkin Y, Roitman G, Schreiber G. 1997. Reduced G protein functions and immunoreactive levels in mononuclear leukocytes of patients with depression. Am J Psychiatry 154:211–217.

Bartus RT, Dean RL 3rd, Beer B, Lippa AS. 1982. The cholinergic hypothesis of geriatric memory dysfunction. Science 217:408–414.

Baxter MG, Gallagher M. 1996. Intact spatial learning in both young and aged rats following selective removal of hippocampal cholinergic input. Behav Neurosci 110:460–467.

Beato M, Herrlich P, Schutz G. 1995. Steroid hormone receptors: Many actors in search of a plot. Cell 83:851–857.

Bizon JL, Helm KA, Han JS, Chun HJ, Pucilowska J, Lund PK, Gallagher M. 2001. Hypothalamic-pituitary-adrenal axis function and corticosterone receptor expression in behaviourally characterized young and aged Long-Evans rats. Eur J Neurosci 14:1739–1751.

Davis KL, Davis BM, Greenwald BS, Mohs RC, Mathe AA, Johns CA, Horvath TB. 1986. Cortisol and Alzheimer's disease, I: Basal studies. Am J Psychiatry 143:300–305.

Day JC, Koehl M, Deroche V, Le Moal M, Maccari S. 1998. Prenatal stress enhances stress- and corticotropin-releasing factor-induced stimulation of hippocampal acetylcholine release in adult rats. J Neurosci 18:1886–1892.

De Lacalle S, Lim C, Sobreviela T, Mufson EJ, Hersh LB, Saper CB. 1994. Cholinergic innervation in the human hippocampal formation including the entorhinal cortex. J Comp Neurol 345:321–344.

de Leon MJ, McRae T, Tsai JR, George AE, Marcus DL, Freedman M, Wolf AP, McEwen B. 1988. Abnormal cortisol response in Alzheimer's disease linked to hippocampal atrophy. Lancet 2:391–392.

Doucas V, Shi Y, Miyamoto S, West A, Verma I, Evans RM. 2000. Cytoplasmic catalytic subunit of protein kinase A mediates cross-repression by NF-kappa B, the glucocorticoid receptor. Proc Natl Acad Sci U S A 97:11893–11898.

Dwivedi Y, Conley RR, Roberts RC, Tamminga CA, Pandey GN. 2002. [(3)H]cAMP binding sites and protein kinase a activity in the prefrontal cortex of suicide victims. Am J Psychiatry 159:66–73.

Dwivedi Y, Rizavi HS, Shukla PK, Lyons J, Faludi G, Palkovits M, Sarosi A, Conley RR, Roberts RC, Tamminga CA, Pandey GN. 2004. Protein kinase A in postmortem brain of depressed suicide victims: Altered expression of specific regulatory and catalytic subunits. Biol Psychiatry 55:234–243.

Fischer W, Gage FH, Bjorklund A. 1989. Degenerative changes in forebrain cholinergic nuclei correlate with cognitive impairments in aged rats. Eur J Neurosci 1:34–45.

Gallagher M, Colombo PJ. 1995. Ageing: The cholinergic hypothesis of cognitive decline. Curr Opin Neurobiol 5:161–168.

Geula C. 1998. Abnormalities of neural circuitry in Alzheimer's disease: Hippocampus and cortical cholinergic innervation. Neurology 51(1 Suppl 1):S18–S29; discussion S65–S67.

Guijarro C, Rutz S, Rothmaier K, Turiault M, Zhi Q, Naumann T, Frotscher M, Tronche F, Jackisch R, Kretz O. 2006. Maturation and maintenance of cholinergic medial septum neurons require glucocorticoid receptor signaling. J Neurochem 97:747–758.

Han JS, Bizon JL, Chun HJ, Maus CE, Gallagher M. 2002. Decreased glucocorticoid receptor mRNA and dysfunction of HPA axis in rats after removal of the cholinergic innervation to hippocampus. Eur J Neurosci 16:1399–1404.

Haske T, Nakao M, Moudgil VK. 1994. Phosphorylation of immunopurified rat liver glucocorticoid receptor by the catalytic subunit of cAMP-dependent protein kinase. Mol Cell Biochem 132:163–171.

Helm KA, Han JS, Gallagher M. 2002. Effects of cholinergic lesions produced by infusions of 192 IgG-saporin on glucocorticoid receptor mRNA expression in hippocampus and medial prefrontal cortex of the rat. Neuroscience 115:765–774.

Helm KA, Ziegler DR, Gallagher M. 2004. Habituation to stress and dexamethasone suppression in rats with selective basal forebrain cholinergic lesions. Hippocampus 14:628–635.

Issa AM, Rowe W, Gauthier S, Meaney MJ. 1990. Hypothalamic-pituitary-adrenal activity in aged, cognitively impaired and cognitively unimpaired rats. J Neurosci 10:3247–3254.

Joels M. 2001. Corticosteroid actions in the hippocampus. J Neuroendocrinol 13:657–669.

Karnovsky MJ, Roots L. 1964. A "direct-coloring" thiocholine method for cholinesterases. J Histochem Cytochem 12:219–221.

Lopez JF, Chalmers DT, Little KY, Watson SJ. 1998. A.E. Bennett Research Award. Regulation of serotonin1A, glucocorticoid, and mineralocorticoid receptor in rat and human hippocampus: Implications for the neurobiology of depression. Biol Psychiatry 43:547–573.

Lupien S, Lecours AR, Lussier I, Schwartz G, Nair NP, Meaney MJ. 1994. Basal cortisol levels and cognitive deficits in human aging. J Neurosci 14 (5 Pt 1):2893–2903.

McKay LI, Cidlowski JA. 1998. Cross-talk between nuclear factor-kappa B, the steroid hormone receptors: Mechanisms of mutual antagonism. Mol Endocrinol 12:45–56.

Moore MJ, Adams JA, Taylor SS. 2003. Structural basis for peptide binding in protein kinase A. Role of glutamic acid 203 and tyrosine 204 in the peptide-positioning loop. J Biol Chem 278:10613–10618.

Murphy EK, Spencer RL, Sipe KJ, Herman JP. 2002. Decrements in nuclear glucocorticoid receptor (GR) protein levels and DNA binding in aged rat hippocampus. Endocrinology 143:1362–1370.

Nibuya M, Nestler EJ, Duman RS. 1996. Chronic antidepressant administration increases the expression of cAMP response element binding protein (CREB) in rat hippocampus. J Neurosci 16:2365–2372.

Pace TW, Hu F, Miller AH. 2007. Cytokine-effects on glucocorticoid receptor function: Relevance to glucocorticoid resistance and the pathophysiology and treatment of major depression. Brain Behav Immun 21:9–19.

Penuelas I, Encio IJ, Lopez-Moratalla N, Santiago E. 1998. cAMP activates transcription of the human glucocorticoid receptor gene promoter. J Steroid Biochem Mol Biol 67:89–94.

Potter PE, Gaughan C, Assouline Y. 1999. Lesion of septal-hippocampal neurons with 192 IgG-saporin alters function of M1 muscarinic receptors. Neuropharmacology 38:579–586.

Raison CL, Miller AH. 2003. When not enough is too much: The role of insufficient glucocorticoid signaling in the pathophysiology of stress-related disorders. Am J Psychiatry 160:1554–1565.

Revollo JR, Cidlowski JA. 2009. Mechanisms generating diversity in glucocorticoid receptor signaling. Ann N Y Acad Sci 1179:167–178.

Sapolsky RM, Krey LC, McEwen BS. 1984. Glucocorticoid-sensitive hippocampal neurons are involved in terminating the adrenocortical stress response. Proc Natl Acad Sci U S A 81:6174–6177.

Sapolsky RM, Uno H, Rebert CS, Finch CE. 1990. Hippocampal damage associated with prolonged glucocorticoid exposure in primates. J Neurosci 10:2897–2902.






ID: subramaniank Date: 15/11/10 Time: 10:26 Path: N:/3b2/HIPO/Vol00000/100155/APPFile/JW-HIPO100155

Shelton RC, Mainer DH, Sulser F. 1996. cAMP-dependent protein kinase activity in major depression. Am J Psychiatry 153:1037–1042.

Smith ML, Booze RM. 1995. Cholinergic and GABAergic neurons in the nucleus basalis region of young and aged rats. Neuroscience 67:679–688.

Steinberg RA, Cauthron RD, Symcox MM, Shuntoh H. 1993. Autoactivation of catalytic (C alpha) subunit of cyclic AMP-dependent protein kinase by phosphorylation of threonine 197. Mol Cell Biol 13:2332–2341.

Takahashi LK, Goh CS. 1998. Glucocorticoid facilitation of cholinergic development in the rat hippocampus. Neuroscience 83:1145–1153.

Whitehouse PJ, Price DL, Struble RG, Clark AW, Coyle JT, Delon MR. 1982. Alzheimer's disease and senile dementia: Loss of neurons in the basal forebrain. Science 215:1237–1239.

Wynn ZJ, Cummings JL. 2004. Cholinesterase inhibitor therapies and neuropsychiatric manifestations of Alzheimer's disease. Dement Geriatr Cogn Disord 17:100–108.

Zhong H, SuYang H, Erdjument-Bromage H, Tempst P, Ghosh S. 1997. The transcriptional activity of NF-kappaB is regulated by the IkappaB-associated PKAc subunit through a cyclic AMP-independent mechanism. Cell 89:413–424.

ELSEVIER

Neurobiology of Aging xxx (2009) xxx–xxx

NEUROBIOLOGY OF AGING

www.elsevier.com/locate/neuaging

# Novel age-dependent learning deficits in a mouse model of Alzheimer's disease: Implications for translational research

K.S. Montgomery [a], R.K. Simmons [a], G. Edwards III [a], M.M. Nicolle [c], M.A. Gluck [d], C.E. Myers [e], J.L. Bizon [a,b,*]

[a] *Behavioral and Cellular Neuroscience, Department of Psychology, Texas A&M University, College Station, TX 77843-4235, United States*
[b] *Faculty of Neuroscience, Texas A&M University, College Station, TX 77843-4235, United States*
[c] *Internal Medicine Gerontology and Department of Physiology and Pharmacology, Wake Forest University School of Medicine, Winston-Salem, NC 27157, United States*
[d] *Center for Molecular & Behavioral Neuroscience, Rutgers University, Newark, NJ 07102-1896, United States*
[e] *Department of Psychology, Rutgers University, Newark, NJ 08854-8020, United States*

Received 23 April 2009; received in revised form 27 July 2009; accepted 3 August 2009

**Abstract**

Computational modeling predicts that the hippocampus plays an important role in the ability to apply previously learned information to novel problems and situations (referred to as the ability to generalize information or simply as 'transfer learning'). These predictions have been tested in humans using a computer-based task on which individuals with hippocampal damage are able to learn a series of complex discriminations with two stimulus features (shape and color), but are impaired in their ability to transfer this information to newly configured problems in which one of the features is altered. This deficit occurs despite the fact that the feature predictive of the reward (the relevant information) is not changed. The goal of the current study was to develop a mouse analog of transfer learning and to determine if this new task was sensitive to pathological changes in a mouse model of AD. We describe a task in which mice were able to learn a series of concurrent discriminations that contained two stimulus features (odor and digging media) and could transfer this learned information to new problems in which the irrelevant feature in each discrimination pair was altered. Moreover, we report age-dependent deficits specific to transfer learning in APP + PS1 mice relative to non-transgenic littermates. The robust impairment in transfer learning may be more sensitive to AD-like pathology than traditional cognitive assessments in that no deficits were observed in the APP + PS1 mice on the widely used Morris water maze task. These data describe a novel and sensitive paradigm to evaluate mnemonic decline in AD mouse models that has unique translational advantages over standard species-specific cognitive assessments (e.g., water maze for rodent and delayed paragraph recall for humans).


*Keywords:* Aging; AD; APP + PS1; Hippocampus; Transfer learning; Spatial learning; Cognitive decline

## 1. Introduction

Recent estimates indicate that one in ten men and one in six women who live to be 55 years will be diagnosed with Alzheimer's disease (AD, Alzheimer's Association, 2008). Despite substantial research efforts focused on uncovering the neurobiological underpinnings of this disease, there is a current lack of behavioral assays that both identify individuals at early preclinical stages and that translate well between rodent models, from which the vast majority of the neurobiological data are derived, and humans who suffer from the disease. For example, one early neuropsychological change in AD is performance on a delayed paragraph recall test. This assessment predicts with near 90% accuracy which non-demented elderly individuals will progress into subsequent cognitive decline (Kluger et al., 1999; Lowndes et al., 2008). However, it is difficult to develop analogs of such verbal tasks for use with rodent models. The development

* Corresponding author at: Behavioral and Cellular Neuroscience, Department of Psychology, Texas A&M University, College Station, TX 77843-4235, United States. Tel.: +1 979 458 3653; fax: +1 979 845 4727.
*E-mail addresses:* karienn@sbcglobal.net (K.S. Montgomery), becca.simmons@gmail.com (R.K. Simmons), getriple3@tamu.edu (G. Edwards III), mnicolle@wfubmc.edu (M.M. Nicolle), gluck@pavlov.rutgers.edu (M.A. Gluck), myers@pavlov.rutgers.edu (C.E. Myers), jbizon@tamu.edu (J.L. Bizon).

0197-4580/$ – see front matter © 2009 Elsevier Inc. All rights reserved.
doi:10.1016/j.neurobiolaging.2009.08.003

of novel assessments of hippocampal/medial temporal lobe function using non-verbal tasks that are sensitive to mild decrements in this circuitry and that are well-suited for use in rodents and humans would be of great benefit in terms of greater comparative power within and between species, and in their ability to serve as superior preclinical models in which to assess novel therapies.

Based on information from animal lesion studies (Ikonen et al., 2002), Myers, Gluck, and colleagues have generated unique computational models of hippocampal function that postulate that this structure is critically involved in encoding new information during learning so as to support the transfer of important stimulus features when familiar information is presented in novel recombinations (hereon referred to as 'transfer learning'; Gluck and Myers, 1993, 1995; Gluck et al., 2006; Johnson et al., 2008; Myers and Gluck, 1996). The prediction of the computational model that the hippocampus helps encode initial learning in such a way that it will support subsequent transfer is similar to the theoretical proposal that the hippocampus is involved in learning relations between stimuli that can be used flexibly later (Bunsey and Eichenbaum, 1996; Eichenbaum et al., 1989; Gluck and Myers, 1993, 1995, 2001). In the absence of hippocampal-region mediation, learning may still be possible, but will be restricted to simpler stimulus–response learning that does not support transfer to new contexts/recombination well. This idea finds empirical support in studies showing that individuals with bilateral hippocampal damage may "unitize" stimuli (or stimulus features) during learning (e.g., Barense et al., 2005; Quamme et al., 2007), conferring impairments when aspects of the trained stimuli are altered (see also Schacter, 1985).

Similarly, although animals with hippocampal damage often show impairments on configural learning (Sutherland and Rudy, 1989; Rudy and Sutherland, 1995) under conditions that arguably favor stimulus unitization, hippocampal-lesioned animals can learn configural tasks as well as controls (see, e.g., O'Reilly and Rudy, 2001; Moses and Ryan, 2006). The lesioned animals do not, however, perform well when the trained stimulus features are presented in novel recombinations (e.g., Eichenbaum et al., 1989).

More recently, a computer-based associative learning task was developed to assess transfer learning in humans with hippocampal damage and aged individuals at risk for cognitive decline (Myers et al., 2002, 2008a). As illustrated in Fig. 1B, this task involves a series of two item visual discrimination problems in which subjects learn via trial-and-error to choose the correct object from each pair presented. Objects have two stimulus features (shape and color) but within each pair, objects differ with respect to color or shape but not both. In other words, only one of the features (color or shape) is relevant to the correct choice within a particular pair, whereas the other feature is identical between the two items. Once a subject learns all of the discrimination pairs (presented pseudo-randomly) to criterion (learning phase), an unsignaled transfer test is given in which the irrelevant feature of each object pair is changed but the relevant features remain the same and are still predictive of

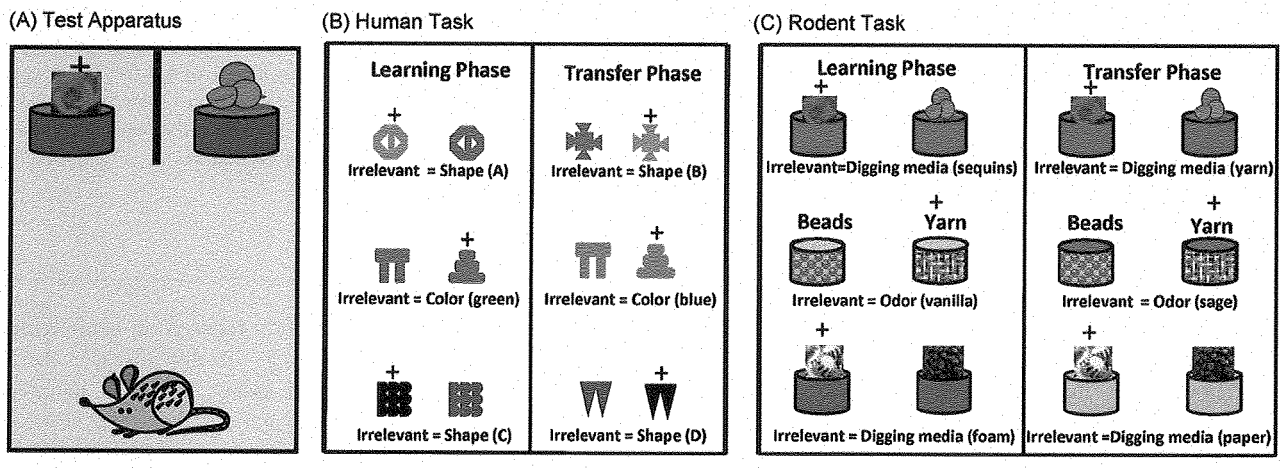


Fig. 1. Left panel shows the test apparatus for transfer learning in mice. Cylinders represent terracotta pots which were filled with a variety of digging media and scented with different odorants. In this schematic, the rose odor is positive (+) and is predictive of a food reward buried in the pot. Middle panel shows examples of visual discrimination pairs used in the human computer-based version of the transfer learning task. In each discrimination pair, either the shape or color is relevant to the correct choice (+), but not both. During both the learning and transfer phases of the task, each pair of shapes is presented sequentially and pseudo-randomly and correct choices are rewarded with a smiley face icon. After reaching criterion performance on the learning phase, without signaling, subjects are presented with the reconfigured stimuli shown under the "Transfer Phase". Note that the positive feature predictive of correct choice (+) in the learning phase remains the same but the irrelevant feature is altered. Right panel shows examples of discrimination pairs used in the mouse transfer learning task. In each pair, either the odor or digging media in the pot is relevant to the correct choice, but not both. During the learning and transfer phases of the task, each discrimination pair is presented sequentially and pseudo-randomly and correct choices are rewarded with a food reward buried in the pot (see Section 2 for details). After reaching criterion performance on the learning phase, mice were immediately presented with the reconfigured stimuli shown under the "Transfer Phase". Note that just as in the human version of the task, the positive feature (+) remained predictive of the food reward but the irrelevant feature for each discrimination problem was altered.

Please cite this article in press as: Montgomery, K.S., et al., Novel age-dependent learning deficits in a mouse model of Alzheimer's disease: Implications for translational research. Neurobiol. Aging (2009), doi:10.1016/j.neurobiolaging.2009.08.003

the correct choice (transfer phase). The model predicts that subjects with an intact hippocampus during initial learning should transfer learned information from the initial discrimination trials to the trials in which the irrelevant feature was altered. In contrast, subjects with hippocampal damage would be expected to view the altered objects as novel stimuli about which nothing is known, despite the fact that these objects retain the stimulus feature relevant to the correct choice.

This task confirmed computational predictions regarding hippocampal mediation of transfer learning in a group of amnesic patients who had bilateral hippocampal damage. These patients could learn the initial discrimination pairs normally, but performed near chance on the test of transfer learning (Myers et al., 2008a), suggesting that they treated the reconfigured stimuli as new problems and failed to transfer the relevant stimulus features of the discrimination pairs learned initially. When the same task was tested in aged subjects, elderly individuals who were non-demented but who did have mild hippocampal atrophy showed a similar pattern of performance (i.e., preserved learning of the initial discrimination pairs, followed by poor transfer learning; Myers et al., 2002). Interestingly, these individuals were not impaired relative to non-atrophied controls on delayed paragraph recall, suggesting that performance on tests of transfer learning may be a more sensitive or an earlier marker of hippocampal dysfunction. Indeed, a small-scale longitudinal study suggests that, in non-demented elderly individuals, poor performance in transfer learning may be predictive of short-term (2 years) cognitive decline (Myers et al., 2008b).

These data in human subjects suggest that transfer learning is sensitive to hippocampal/medial temporal lobe dysfunction (Johnson et al., 2008) and that this non-verbal task may be well-suited as an assessment that translates across species. The spatial version of the Morris water maze is the cognitive assessment tool most widely used to evaluate hippocampal function in aged rodents (Bizon et al., 2009; Gallagher et al., 2003; LaSarge et al., 2007; Morris et al., 1982; Squire et al., 2004). However, this task has some limitations for within-subject pharmacological intervention studies and results acquired from transgenic mouse models of AD using water maze have proven inconsistent (Bizon et al., 2007; Dumont et al., 2004; Lassalle et al., 2008; Reiserer et al., 2007). However, like humans, rodents also perform well at discriminating objects that contain more than one stimulus feature and deficits on such tasks are reliable across multiple problems (Barense et al., 2002; Bissonette et al., 2008; LaSarge et al., 2007).

The goal of the present study was to develop an analogous mouse version of the human transfer learning task developed by Gluck and Myers (1993, 1995, 2001), Myers et al. (2002). The task design was a modified version of a naturalistic odor discrimination task (Eichenbaum et al., 1989; LaSarge et al., 2007) with odors and digging media used as the two stimulus features in the discrimination problems. Double transgenic (APP + PS1) mice of different ages were assessed in this new task to determine if performance was sensitive to age-related hippocampal pathology.

## 2. Methods

### 2.1. Subjects

For all experiments, mice were individually housed in the AAALAC-accredited vivarium in the Psychology Building (Texas A&M University, College Station, TX). Mice were maintained on a 12-h light/dark cycle (lights on at 08:00) and climate controlled at 25 °C. All testing was conducted during the light cycle and mice in the study were screened daily for health problems, including but not limited to cataracts, jaundice, food and water intake, and the appearance of tumors. Sentinel mice housed in the same room as experimental mice were further screened for diseases such as pinworms, parvo virus and other pathogens. Blood work was negative for all health screens throughout testing. All animal procedures were conducted in accordance with approved institutional animal care procedures and NIH guidelines. Upon arrival, all mice were given at least two weeks to acclimate and received ad lib access to food and water. Mice continued to have free access to food and water with the exception that mice were food-restricted to 85% of their free-feeding weight prior to testing. After completion of all discrimination testing, mice were immediately returned to ad lib food.

#### 2.1.1. Experiment 1: validation of the transfer learning task

Subjects used for validation of the transfer task were C57BL/6J ($n = 5$ in each of two groups, 5 months old) female retired breeders from The Jackson Laboratory, Maine, USA.

#### 2.1.2. Experiment 2: transfer learning task with aged APP + PS1 mice

Subjects were a cohort of 12-month old, female Tg (APPswe, PSEN1dE9; APP + PS1; $n = 11$) and age-matched non-transgenic littermates of B6C3F1/J background strain (NTg; $n = 7$) obtained from The Jackson Laboratory, Maine, USA. The APP + PS1 double transgenic mice express a chimeric mouse/human amyloid precursor protein (Mo/HuAPP695swe) and the mutant human presenilin 1 (PS1-dE9). This presenilin mutation is related to the early onset of AD. The Swedish mutation (K595N/M596L), which is linked to familial AD, increases the number of Aβ deposits by stimulating the β-secretase pathway (Hardy and Selkoe, 2002). These mice develop Aβ deposits throughout the brain, including hippocampus, by 6 months of age, with numerous deposits reported by 12 months of age (Burgess et al., 2006; Chishti et al., 2001; Jankowsky et al., 2004).

#### 2.1.3. Experiment 3: longitudinal assessment of transfer learning in APP + PS1 mice

Subjects were a second cohort of female APP + PS1 ($n = 8$) and age-matched NTg littermates of B6C3F1/J background

Please cite this article in press as: Montgomery, K.S., et al., Novel age-dependent learning deficits in a mouse model of Alzheimer's disease: Implications for translational research. Neurobiol. Aging (2009), doi:10.1016/j.neurobiolaging.2009.08.003

Table 1
Odor and digging media pairs as paired in the transfer learning task.

| Discrimination pairs | Corresponding irrelevant dimension | |
|---|---|---|
| | Learning phase | Transfer phase |
| Beads × rubber string | Jasmine | Vanilla |
| Patchouli × mulberry | Pompoms | Cork |
| Paper × cut balloon | Chocolate | Watermelon |
| Jasmine × vanilla | Beads | Rubber string |
| Pompons × cork | Patchouli | Mulberry |
| Chocolate × watermelon | Paper | Cut balloon |
| Cut straws × cheese cloth | Pumpkin | Cucumber |
| Cucumber × pumpkin | Cut straws | Cheese cloth |
| Cut paper × guinea pig bedding | Lemon | Rosemary |
| Bergamot × sage | Sequins | Raffia |
| Cut bench pad × wood bedding | Lavender | Cinnamon |
| Vetiver × geranium | Yarn | Alphadri bedding |
| Raffia × sponge | Bergamot | Sage |
| Cinnamon × lavender | Wood bedding | Cut bench pad |
| Alphadri bedding × yarn | Vetiver | Geranium |

Salience and difficulty of odor and digging medium problems appeared comparable as no significant differences in performance on odor and digging media discriminations were observed in any group. Additionally, analyses of individual pairings did not result in any differences, indicating comparable salience within individual pairs.

($n = 9$). Mice were initially tested at 3 months (learning and transfer phases) and then were retested in the transfer task (learning and transfer phases) at 12 months of age using all novel stimuli.

### 2.2. Transfer learning task

#### 2.2.1. Apparatus and task parameters

The testing apparatus for the mouse transfer learning task is illustrated in Fig. 1A. It consisted of an open-topped black Plexiglas box (12 in. width; 18 in. length; 8 in. deep) with two small terra cotta flower pots (1.7 in. diameter; 1.3 in. deep) securely attached to the floor. There were two stimulus features in each discrimination problem: an odor that was applied directly to the rim of the pots and the digging media that filled the pots and hid a food reward (one chocolate-flavored food pellet, 20 mg, AIN-76A from TestDiet) placed on the bottom of the pot. Table 1 lists all complex discrimination pairs used in the study.

To disguise the odor of the reward, crushed chocolate food pellets were sprinkled over the surface of each pot. The position (left or right) of the rewarded pot varied pseudo-randomly across trials. For the first four trials of every new discrimination problem, mice were allowed to dig in both pots until they obtained the reward (i.e., they were allowed to self-correct if they dug in the incorrect pot). On these trials, only their first choice was scored (as correct or incorrect). On trials thereafter, mice were removed from the test chamber after only one dig (either correct or incorrect). A dig in a pot was scored if a mouse displaced the digging media with either its paws or nose.

Shaping took place in the box described above. Initially mice were presented with two empty pots containing a chocolate pellet in the bottom of each. The re-baiting of the pots was contingent on the mouse consuming both pellets. After 12 trials of successively retrieving both pellets, mice were then presented with two pots containing chocolate pellets in the bottom but filled with progressively more mixed digging media (12 trials per 33%, 50% and 100% full). The day after successfully retrieving both pellets with full pots, mice received one simple discrimination to habituate them to the learning aspect of the task.

In developing the mouse transfer learning task and confining it to a single behavioral session (to closely mimic the human version), satiation and motivation were initial concerns. A series of pilot experiments, in which food-restricted C57BL/6J mice were allowed free access to the chocolate food pellets used in this task, revealed that mice would consume many more pellets than were ever needed for a full testing session. Moreover, all mice shaped, learned all problems to criterion, and completed all 30 trials in the transfer portion of the task irrespective of genotype or age, suggesting that there were no motivational differences within sessions or between experimental groups.

#### 2.2.2. Testing

Just as in the human version of the transfer learning task (Gluck and Myers, 1993; Myers et al., 2002), all testing was performed within a single session. Fig. 1C and Table 2 illustrate examples of the order and sequence of presentation of the two feature stimuli in the learning and transfer phases of the task. Initially, mice were trained on a series of three concurrent discrimination problems. As in the human version of the task, new discrimination pairs were progressively introduced intermixed with learned pairs as criterion performance was reached on each pair.

For each problem, mice learned to discriminate between pots with two stimulus features (odor and digging media). One of the two pots was baited, with either the odor or the digging media as the relevant feature (Fig. 1C and Table 2). For example, if odor was the relevant feature, the pots differed in odor (with one odor always predictive of the food reward; e.g., rose+ versus citrus− as shown in Fig. 1C) but contained the same digging media (e.g., sequins) that was thus irrelevant to the correct choice. For other discrimination problems, the digging media was the relevant feature that differed between pots and predicted the reward (e.g., yarn+ versus beads− as shown in Fig. 1C), and the pots were scented with the same odor (e.g., vanilla), the irrelevant feature.

The positive and negative features in each pair and the sequence of discrimination problems were randomized across mice, although each mouse received discrimination problems in which the relevant feature was alternated between odor and digging media. As in the human task, initially several problems (2 for the mice) were presented in pseudo-random order and after criterion was reached on these problems (6 correct in a row, including 3 of each

Please cite this article in press as: Montgomery, K.S., et al., Novel age-dependent learning deficits in a mouse model of Alzheimer's disease: Implications for translational research. Neurobiol. Aging (2009), doi:10.1016/j.neurobiolaging.2009.08.003

Table 2
Representative example of the order and sequence of complex stimuli presented the mouse transfer learning paradigm.

| Discriminations: | Dimensions | | Combinations | |
|---|---|---|---|---|
| | Relevant | Irrelevant | Pot 1 (+) | Pot 2 (−) |
| Learning phase (pair 1) | Odor | Media | *O1* with M1 | O2 with M1 |
| Learning phase (pair 2) | Media | Odor | *M2* with O3 | M3 with O3 |
| Learning phase (pair 3) | Odor | Media | *O4* with M4 | O5 with M4 |
| Transfer phase (pair 1) | Odor | Media | *O1* with M5 | O2 with M5 |
| Transfer phase (pair 2) | Media | Odor | *M2* with O6 | M3 with O6 |
| Transfer phase (pair 3) | Odor | Media | *O4* with M6 | O5 with M6 |

*Abbreviations*: O, odor; M, digging media. Stimulus features predictive of reward are italicized.
Each number indicates novel stimulus.
As in the human version of the task, new discrimination pairs were progressively introduced intermixed with learned pairs as criterion performance was reached on each pair.
After reaching criterion in pair 1, the pot with *O1* remained baited and O2 unbaited but the irrelevant dimension was changed from M1 to M5.
Note that all odors and digging medias were used only once throughout training (O1–O6; M1–M6).

problem set), a third problem was introduced and the three pairs were presented in a pseudo-random fashion until mice reached criterion performance (6 correct in a row, including 2 of each problem). This design ensured that each discrimination pair was learned prior to the transfer (see Table 2).

After reaching criterion performance, mice were immediately assessed for transfer learning. The mice were presented with 30 trials in which only the stimulus feature in each discrimination pair that was irrelevant to the reward was changed, and the 3 new combinations were presented pseudo-randomly (including 10 each of the three discriminations; see Fig. 1C, Table 2). As in the human version of the task, this design affords an opportunity to assess the ability of the mice to transfer the predictive value of a previously learned relevant feature (e.g., a particular odor) to a food reward in a new context (e.g., pots containing a novel digging media).

### 2.3. Odor detection threshold testing

Anosmia has been shown to emerge as a consequence of chronological age and in Alzheimer's disease (e.g., Djordjevic et al., 2008). Thus, after evaluating transfer learning, mice in the second and third experiments (i.e., all APP + PS1 and NTg mice) were assessed for their ability to detect and respond to decreasing concentrations of odorants. Mice were tested at 13 months in cohort 2 and at 4 months in cohort 3. Odor detection threshold testing was performed in the same apparatus used for the transfer learning. First, mice were presented with a novel odor discrimination problem (sandalwood vs. mineral oil) using full strength odorant applied directly to the rims of two pots filled with mixed digging media. Sandalwood was the positive odor that predicted the food reward and mice were trained until reaching criterion performance (6 consecutive correct trials). Once achieving criterion performance, the mice were tested in a series of discrimination problems during which the sandalwood odor was systematically diluted (1/10, 1/100, 1/1000, 1/10,000). Mice were given 16 trials at each dilution and the percent error was used as the measure of performance at each dilution.

### 2.4. Reversal learning

Previous work has shown that reversal learning is impaired in the Tg2576 mouse model of AD (Zhuo et al., 2007). Thus, in Experiment 3, mice were assessed for reversal learning performance after transfer learning testing.

On a separate day, mice were presented with a novel two-odor discrimination problem with mixed digging media. After reaching criterion performance (6 consecutive correct trials), the odor–reward contingencies were reversed (such that the pot scented with the previously non-rewarded odor now contained the reward), and errors to criterion were measured.

### 2.5. Water maze assessment

The spatial reference memory version of the Morris water maze is a standard task used in rodents to assess hippocampal/medial temporal lobe function. Although these brain regions are known to be particularly vulnerable to dysfunction in aging and AD, the results from assessments of spatial learning in mouse models of AD have been mixed, with some studies reporting progressive deficits that correlate with increasing hippocampal pathology (Gordon et al., 2001; Heikkinen et al., 2004; Liu et al., 2002; Puoliväli et al., 2002), but others reporting subtle or no deficits on this task despite known widespread neuropathology in critical brain regions (Bizon et al., 2007; Dumont et al., 2004; Lassalle et al., 2008; Reiserer et al., 2007). To directly compare the sensitivity of the rodent assessment of transfer learning described here to spatial learning ability, after all other testing, the APP + PS1 and NTg mice from both cohorts (at approximately 13 months of age) were tested in hidden (hippocampal-dependent) and visible cued (non-hippocampal-dependent) versions of the Morris water maze task.

Please cite this article in press as: Montgomery, K.S., et al., Novel age-dependent learning deficits in a mouse model of Alzheimer's disease: Implications for translational research. Neurobiol. Aging (2009), doi:10.1016/j.neurobiolaging.2009.08.003

*2.5.1. Apparatus*

The water maze consisted of a 4-ft diameter circular tank filled with water (24–27 °C) made opaque by the addition of non-toxic white tempera paint. The tank was surrounded by black curtains, to which large (15 × 15 in.) white geometric cues (made with fabric) were affixed. The tank was divided into four imaginary quadrants, each with a platform position equidistant from the center to the wall. During cue training, the tank was filled to 1 cm below a black visible platform. Each mouse's swim was tracked and analyzed using a computer-based video tracking system (Water 2020, HVS Image, UK). On each trial, mice were carefully placed into the water facing the wall of the tank at one of four start points (N, S, E, or W). Throughout the experiment, mice that failed to reach the platform within 60 s were guided to it by hand. During the spatial reference memory assessment (hidden platform training), a retractable escape platform (12 cm diameter, HVS Image, UK) was located in the southwest quadrant of the maze and submerged 1.2 cm below the water's surface.

Initially, mice were trained in the non-hippocampal dependent cued version of the task in order to assess visual acuity and sensorimotor abilities, as described previously (Bizon et al., 2007; Brody and Holtzman, 2006; Montgomery et al., 2008; Puoliväli et al., 2002).

During cue training, the platform position and start positions were varied on each trial such that the platform position and extra-maze cues were made explicitly irrelevant to the mouse's escape. Training consisted of 2 days (6 trials per day). On each trial mice were given 60 s to find the visible escape platform. After finding the platform or being guided there by an experimenter, mice remained on the platform for 30 s before being removed from the tank. At the conclusion of each trial, mice were returned to a heated holding cage (about 30 °C) for a 10 min inter-trial interval.

Beginning the day immediately following completion of cue training, mice received 6 consecutive days of training (4 trials per day) to find a hidden, stationary platform, to assess hippocampal dependent spatial reference memory. The start position (N, S, E or W) was pseudo-randomly varied across trials such that mice needed to rely on the position of the platform relative to the extra-maze cues to effectively escape across trials. During each trial, mice were given 60 s to search for the hidden platform, followed by a 30 s post-trial period in which they were allowed to remain on the platform. After each trial, mice were placed in the holding cage for a 10 min inter-trial interval.

The fourth swims of days 2 and 6 of hidden platform training were probe trial, during which the platform was retracted to the bottom of the tank for the first 30 s of the 60 s trial. Rodents with a good memory for the platform location concentrate their search in that area even when the platform is removed from the tank and performance on probe trials is particularly sensitive to detecting hippocampal impairment in a variety of aging models (Bizon et al., 2007, 2009; Gallagher et al., 1993; LaSarge et al., 2007).

*2.5.2. Water maze analysis*

The water maze data were analyzed using a computer-based video tracking system, Water 2020, developed by HVS Image (Hampton, UK). Primary performance measures analyzed were path length (the total distance from the start position to the platform in centimeters) on hidden and visible training trials and percent time in the target quadrant on probe trials. Separate two-factor repeated-measures ANOVA (genotype × day) were used to evaluate differences across visible platform training trials, hidden platform training trials and probe trials. Finally, swim speed (cm/s) between groups was also analyzed using a one-factor ANOVA (genotype) on hidden and visible trials, respectively.

*2.6. Statistical analyses*

Statistics were performed as described above for each task using StatView software (version 5.01). For all discrimination learning, simple discrimination, and reversal problems, both trials and errors to criterion were analyzed. Because, in every case, data were identical by both measures, for simplicity of presentation, only errors are reported and shown. For the transfer phase and odor detection threshold testing, in which a fixed number of trials were presented, percent error was the performance measure analyzed. One-factor ANOVAs were used unless stated otherwise. In all cases $p < 0.05$ was considered significant.

## 3. Results

*3.1. Experiment 1*

The goal of Experiment 1 was to confirm that mice could learn the transfer learning task, including learning a series of concurrent discriminations (learning phase), and that mice could perceive and respond to an unsignaled recombination of stimuli in the transfer phase of the task. C57BL/B6 mice ($n = 10$) were trained on 3 concurrent discrimination problems as described above. Immediately after reaching criterion performance, half of these mice ($n = 5$) received 30 trials in which the irrelevant feature within each discrimination problem not predictive of food was altered ("test group") and half of the mice ($n = 5$) received 30 trials that were identical to those learned initially ("control group"). Assignments to control and test groups were made such that group means on initial discrimination learning were equivalent (Fig. 2A, $F(1, 8) = 00$, ns). During the transfer phase, the test group performed significantly worse than the control group (Fig. 2B, $F(1, 8) = 8.73$, $p < 0.05$). These data demonstrate that, similar to subjects in the human version of the task, mice are sensitive to alterations of the irrelevant stimulus feature.

*3.2. Experiment 2*

The goal of Experiment 2 was to determine if aged APP + PS1 mice showed impaired transfer learning perfor-

Please cite this article in press as: Montgomery, K.S., et al., Novel age-dependent learning deficits in a mouse model of Alzheimer's disease: Implications for translational research. Neurobiol. Aging (2009), doi:10.1016/j.neurobiolaging.2009.08.003

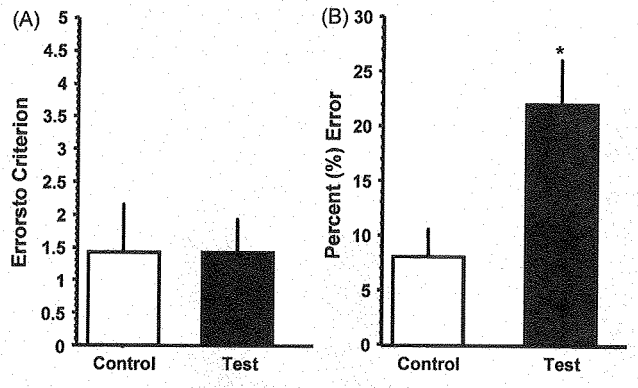


Fig. 2. Bar graphs show performance of young C57BL/6J mice ($n = 10$) during learning of three concurrent discriminations with multiple stimulus features (A; errors to criterion) and the immediate recall of those problems both with ($n = 5$; "test group"; black bar) and without ($n = 5$; "control group"; open bar) reconfiguration of the irrelevant stimuli (B; percent error). Panel A shows that although the two groups of C57BL/6J mice performed identically during the initial discrimination learning (mean errors to criterion ± S.E.M.), the "test group" (black bar) that received a change in the irrelevant stimulus feature made significantly more errors than the "control group" that received problems identical to those in the initial discriminations (percent error). See text for statistical analysis.

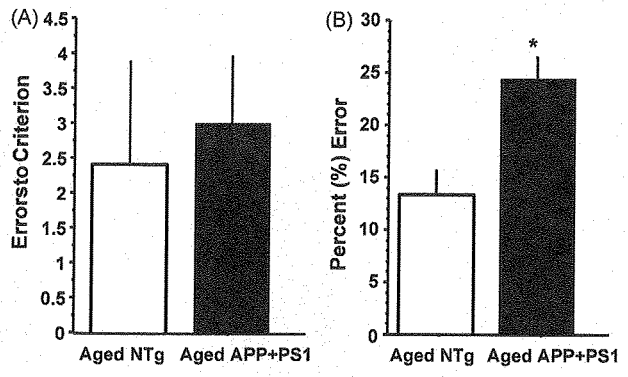


Fig. 3. Bar graphs show performance of aged (12 months) APP + PS1 (black bars) and age-matched NTg mice (open bars) on the transfer learning task. Panel (A) shows errors to criterion (mean ± S.E.M.) in the concurrent discrimination learning phase of the task and panel (B) shows percent error (mean ± S.E.M.) in the transfer phase of the task. Note that while there is no difference in performance between NTg and APP + PS1 mice in number of errors on the initial discriminations, APP + PS1 were significantly impaired relative to NTg mice on the transfer phase of the task. See text for statistical analysis.

mance relative to age-matched NTg controls, as would be expected if the mouse task is sensitive to age-related pathological changes associated with AD.

A one-factor ANOVA revealed no difference due to genotype on the initial discrimination learning phase of the task (Fig. 3A; $F(1, 17) = 0.118$, ns). However, the APP + PS1 mice were significantly impaired relative to age-matched NTg mice in their ability to perform the discrimination problems when the irrelevant feature was changed during the transfer phase of the task (Fig. 3B, main effect of genotype; $F$ (1, 17) = 12.16, $p < 0.005$).

### 3.3. Experiment 3

A second cohort of APP + PS1 and NTg mice was assessed longitudinally for transfer and reversal learning. At 3 months of age, there were no differences due to genotype on the initial discriminations (Fig. 4A; $F$ (1, 15) = 0.001, ns), nor on the transfer test (Fig. 4B, $F$ (1, 15) = 0.001, ns).

The same young cohort of APP + PS1 and NTg mice also demonstrated comparable learning in a simple odor discrimination pair presented on a separate day (Fig. 4C; $F$ (1,15) = 2.09, ns). However, in agreement with previously reported data in Tg2576 mice (Zhuo et al., 2007), the APP + PS1 mice were impaired when odors predictive of the reward were reversed (Fig. 4C, repeated-measures ANOVA; $F$ (1, 15) = 6.34, $p < 0.05$).

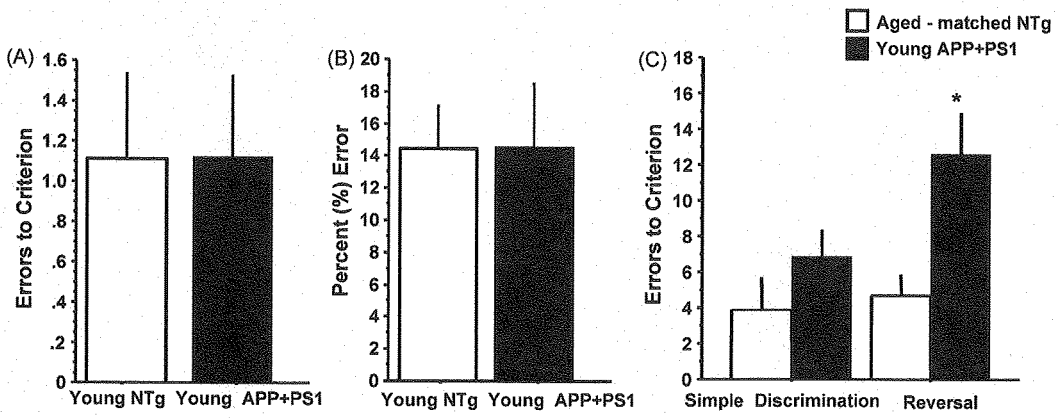


Fig. 4. Bar graphs show concurrent discrimination learning (A), transfer learning (B) and reversal learning (C) performance of young APP + PS1 (black bars) and age-matched NTg mice (open bars). No significant differences were observed in errors to criterion (mean ± S.E.M.) during initial discrimination learning (A) or in percent error (mean ± S.E.M.) during transfer learning (B). However, when subsequently tested on reversal learning, young APP + PS1 performed comparably to NTg in acquiring the new simple odor discrimination problem but were impaired when the odor predictive of reward in this new problem was reversed. See text for statistical analyses.

Please cite this article in press as: Montgomery, K.S., et al., Novel age-dependent learning deficits in a mouse model of Alzheimer's disease: Implications for translational research. Neurobiol. Aging (2009), doi:10.1016/j.neurobiolaging.2009.08.003

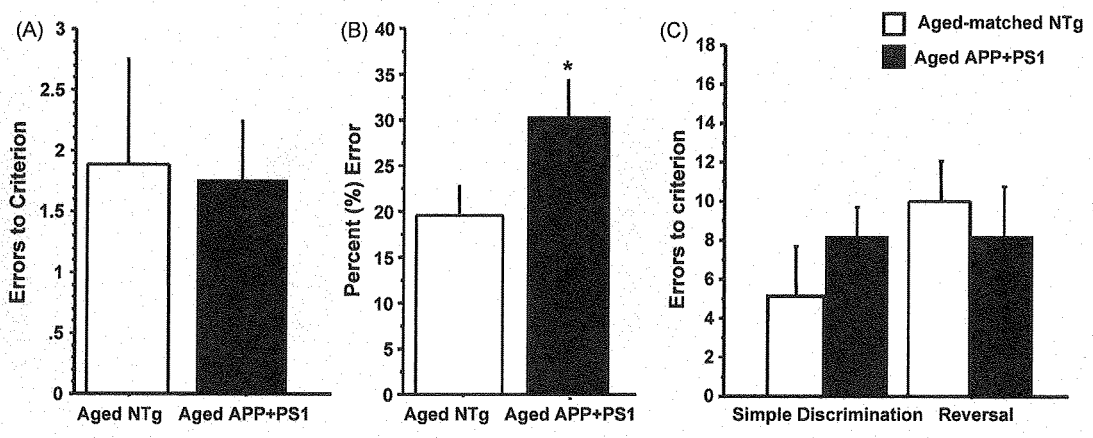


Fig. 5. Bar graphs show performance of the same APP + PS1 (black bars) and NTg mice (open bars) mice shown in Fig. 4 retested for transfer and reversal learning at 12 months. Panel (A) shows errors to criterion (mean ± S.E.M.) in the concurrent discrimination learning and panel (B) shows percent error (mean ± S.E.M.) in the transfer phase of the task. No significant differences were observed in errors to criterion (mean ± S.E.M.) during initial discrimination learning (A); however, a significant and robust deficit in transfer learning was observed in APP + PS1 mice at this age. In contrast, the reversal learning deficit observed at young ages (Fig. 4C) was not observed when aged mice were retested using a novel problem at 12 months (C). See text for statistical analyses.

These mice were retested for transfer learning at 12 months of age and data are shown in Fig. 5. As in Experiment 2, APP + PS1 mice learned the initial discriminations on par with NTg mice (Fig. 5A; $F$ (1, 15) = 0.018, ns) but the 12 months APP + PS1 mice were significantly impaired on the transfer phase of the task (Fig. 5B; $F$ (1, 15) = 4.69, $p < 0.05$). Notably, however, the deficit in reversal learning that was present at 3 months of age was absent upon retesting at 12 months (Fig. 5C; $F$ (1, 15) = 0.36, ns), nor there was a difference in learning of the novel odor pair (Fig. 5C; $F$ (1, 15) = 1.05, ns).

### 3.4. Odor detection threshold testing

In order to determine whether a decreased ability to detect odors with age and/or transgene was a factor in the transfer deficit observed in the APP + PS1 mice at 12 months of age, odor detection abilities were assessed at different ages in mice from Experiment 2 (13 months) and Experiment 3 (4 months) using identical procedures. In a separate session following transfer learning testing, mice were trained to criterion on one additional olfactory discrimination problem. Both young and aged APP + PS1 and NTg mice learned the simple discrimination problem comparably (Fig. 6A); a repeated-measures ANOVA revealed no significant differences due to age ($F$ (1,30) = 0.71, ns) or genotype ($F$ (1,30) = 0.20, ns); and, no interaction was observed between age and genotype ($F$ (1,30) = 0.77, ns). Moreover, Fig. 6B shows that the odor detection threshold did not differ across groups, with all groups showing similar declines in accuracy as concentrations of the odorant were decreased (repeated-measures ANOVA; age: $F$ (1,30) = 0.38, ns; genotype: $F$ (1,30) = 0.22, ns; age × genotype interaction: $F$ (1,30) = 0.057, ns).

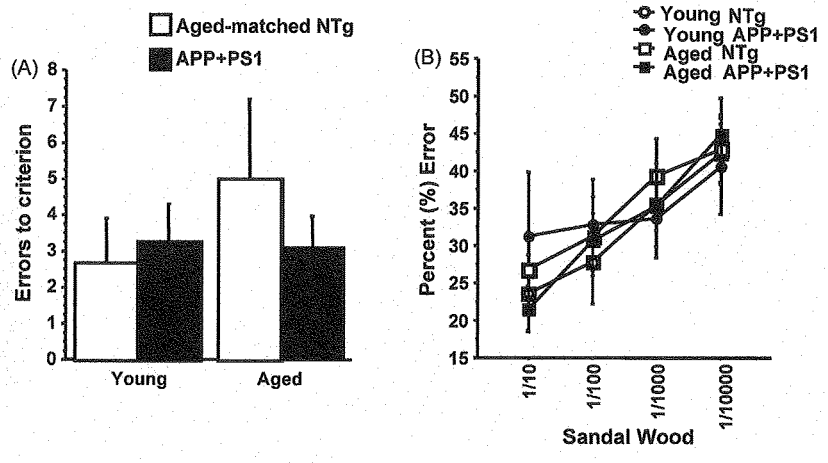


Fig. 6. Graphs show odor detection threshold testing in young and aged APP + PS1 (black bar) and NTg (open bar) mice. Errors to criterion (mean ± S.E.M.) to learn a novel odor discrimination pair are shown in (A) and percent error (mean ± S.E.M.) of responses to decreasing dilutions of the odorant (B). As expected, all groups' ability to detect the odors decreased with diminishing concentrations of the odorants, nearing chance performance at a 1:10,000 dilution of that used during training. No effects of age or genotype were observed in the ability to detect odorants. See text for statistical analysis.

Please cite this article in press as: Montgomery, K.S., et al., Novel age-dependent learning deficits in a mouse model of Alzheimer's disease: Implications for translational research. Neurobiol. Aging (2009), doi:10.1016/j.neurobiolaging.2009.08.003

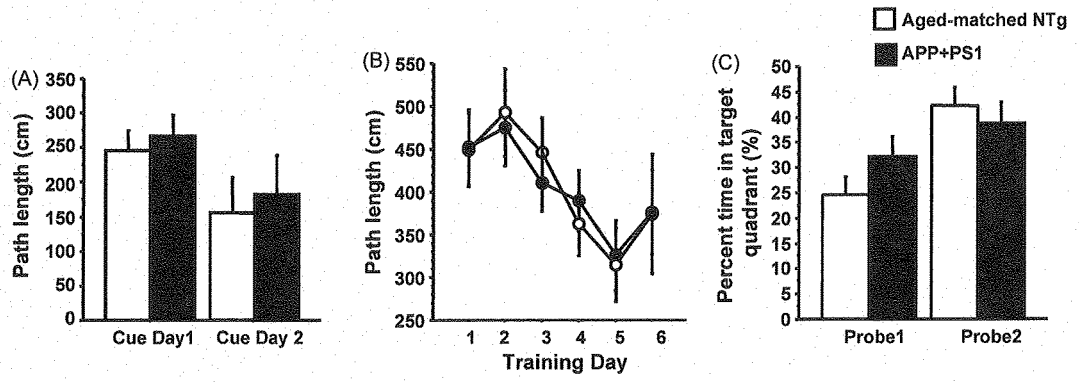


Fig. 7. Water maze performance in aged APP + PS1 (black) and NTg (open) mice. Panel (A) shows that both groups were able to find a visible platform comparably, demonstrating a lack of sensorimotor or motivational differences between groups. Panel (B) shows that the path from the start position to the stationary hidden platform decreased across the 6 training days for both groups, although there was no main effect of genotype nor any interaction of day with genotype. Panel (C) shows performance on probe trials early (probe 1) and late (probe 2) in the spatial memory version of the task. All mice spent significantly more time in the target quadrant (containing the platform) with increased training although in agreement with training trial data, no effect of genotype was observed. See text for statistical analysis.

### 3.5. Experiment 4

Following all other testing procedures, the aged mice from both Experiments 2 and 3 were trained in visible (cued) and hidden platform versions of the water maze. Repeated-measures ANOVAs were used for all analyses. As shown in Fig. 7A, aged (12 months) APP + PS1 and NTg mice showed comparable path length to reach the visible platform across days ($F$ (1, 18) = 0.083, ns) and there was no interaction between genotype and day ($F$ (1, 18) = 0.158, ns). Fig. 7B shows path length across training days 1 through 6. Both groups improved performance across training ($F$ (5, 90) = 2.921, $p < 0.05$) but there was no main effect of genotype ($F$ (1, 18) = 0.169, ns) and no interaction between day and genotype ($F$ (5, 90) = 0.563, ns). Probe trial performance is shown in Fig. 7C. Percent time in the target quadrant significantly increased for both groups from the early probe trial on day 2 and the last probe trial on day 6 ($F$ (1, 18) = 12.164, $p = 0.003$) but no main effect of genotype ($F$ (1, 18) = 0.547, ns) nor interaction between genotype and probe trial ($F$ (1, 18) = 0.260, ns) was observed.

Finally, no main effect of genotype was found on swim speed during the first trial of cue training ($F$ (1, 18) = 1.349, ns) nor on the first hidden platform training trial ($F$ (1, 18) = 2.022, ns), two measures not confounded by learning.

## 4. Discussion

The goals of the current studies were to develop a mouse analog of a computerized assessment of transfer learning and to determine if transgenic mice that have pathology associated with AD show deficits in this type of learning. First, we validated the mouse version of the transfer learning assessment. Young adult C57B6 mice counterbalanced for comparable discrimination learning abilities were sensitive to the change in the irrelevant feature. This was evident by significantly decreased accuracy of performance in a test condition during which the irrelevant feature was altered compared to recall when parameters were unchanged from the initial learning problems. Such performance in the test portion of the transfer learning task involves cognitive processes (and likely neural substrates) beyond those required for simple recall of discrimination information acquired during the learning phase of this task. Also notable from this initial experiment is that although young adult mice performed significantly worse when the irrelevant stimulus feature was altered, these mice still demonstrated relatively proficient transfer learning, providing evidence that this task should be useful for the detection of a range of decrements – mild to severe – associated with disease.

Indeed, in subsequent studies, aged (12 months) APP + PS1 mice were selectively impaired in transfer learning in comparison to age-matched NTg mice. Even at the most advanced ages tested here (12–13 months), APP + PS1 mice were able to learn three compound discriminations concurrently that included combinations across perceptual sets (i.e., on some problems odor signaled the correct choice and on others digging media signaled the correct choice). These data show that APP + PS1 mice are able to form perceptual sets across at least two stimulus features. In contrast, when the irrelevant stimulus feature was altered, aged APP + PS1 mice performed significantly worse than did NTg age-matched controls. This deficit was observed both in the initial cross-sectional study conducted on 12 months old mice (Experiment 2) and in the longitudinal study in which transfer learning in APP + PS1 mice was comparable to NTgs at young ages (3 months) but deficits of a remarkably similar magnitude as in Experiment 2 emerged in the APP + PS1 mice compared to NTgs when these groups were retested at 12 months of age (Experiment 3). As anosmia has been reported at advanced age and in AD, and odor was a key stimulus

Please cite this article in press as: Montgomery, K.S., et al., Novel age-dependent learning deficits in a mouse model of Alzheimer's disease: Implications for translational research. Neurobiol. Aging (2009), doi:10.1016/j.neurobiolaging.2009.08.003

feature in this task, mice were assessed for odor detection threshold. There were no age- or pathology-associated differences in olfactory detection abilities (Fig. 6). These data confirm that procedural aspects of the transfer task did not account for the robust age-related deficits observed in the APP + PS1 mice.

The APP + PS1 mouse strain was chosen for this study because this model exhibits significant hippocampal pathology; the presenilin mutation exacerbates the plaque pathology in mice with the APPswe mutation (Burgess et al., 2006; Hardy and Selkoe, 2002; Jankowsky et al., 2004). Similarly, these initial experiments were confined to females as Aβ pathology is reportedly greater in female than male mice in this and other AD mouse models. Indeed, epidemiological studies have reported a higher incidence of AD in women (Andersen et al., 1999; Jorm and Jolley, 1998; Schäfer et al., 2007; Xu, 2009), and female transgenic mice presenting the APP mutation develop higher plaque numbers than male mice (Bayer et al., 2003; Callahan et al., 2001; Lewis et al., 2001; Sturchler-Pierrat and Staufenbiel, 2000). Future work includes evaluating other transgenic models of AD, including those that model distinct aspects of AD (e.g., tau pathology and synaptic/neuronal loss), to determine the reliability and robustness of the transfer deficit across mouse models of AD and to define the specific genetic and neurobiological factors responsible for this deficit.

Changes in ovarian hormones, including estrogen, have been linked to cognitive changes in young and aged subjects (Green et al., 2005; Golub et al., 2008). At all ages tested here, female mice were likely cycling, but the possibility of an interaction between estrogen levels, pathology and transfer learning should be acknowledged. However, as there is no evidence to our knowledge to indicate that pathology alters entry into di- or anestrous which reportedly occurs at 14 months of age in this mouse strain (Callahan et al., 2001), it is not likely that changes in ovarian hormones alone are sufficient in 12 month APP + PS1 mice to produce transfer learning deficits observed here. Ultimately, it will be of significant interest to determine the relationship between transfer learning proficiency and levels of estrogen and other hormones that have been implicated in age-related cognitive changes.

Studies from humans tested in the analogous transfer task (see Fig. 1) strongly suggest that the age-dependent deficits in APP + PS1 mice observed here are at least in part mediated by progressive hippocampal pathology that is pervasive in the 12 months APP + PS1 mice (Burgess et al., 2006; Jankowsky et al., 2004). Specifically, humans with hippocampal damage are able to learn a series of compound discriminations on par with intact control subjects but demonstrate impaired transfer learning (Myers et al., 2008a,c). Moreover, in aged individuals, deficits selective to transfer learning correlate with hippocampal atrophy and are predictive of further cognitive decline (Myers et al., 2002, 2008b). Previous animal studies suggest that the hippocampus is important for learning of contextual information and binding of stimulus cues, sometimes called structural learning or relational learning (Aggleton et al., 2007; Chun and Phelps, 1999; Eichenbaum et al., 2007; Haskins et al., 2008; Johnson et al., 2008; Pascalis et al., 2009). Moreover, relational learning encompasses plasticity of learning and memory for relationships among stimuli, allowing for reconfiguration of these in new contexts (Aggleton et al., 2007). The nature of these stimuli is variable across these studies making a direct and reliable comparison between relational learning and transfer learning difficult, but these data further implicate the hippocampus as a critical structure mediating transfer learning. With the establishment of this new task, lesions specifically targeting the hippocampus are underway to determine the role and necessity of this structure in transfer learning.

Notably, we failed to observe deficits in the spatial reference version of the water maze in the aged APP + PS1 mice conducted after transfer learning assessment. One interpretation of these data would suggest that transfer learning is not solely dependent on the hippocampus, as hippocampal lesions dramatically impair water maze performance (Arns et al., 1999; Kirwan et al., 2005; Morris et al., 1982). However, it is notable that while deficits in water maze performance have been reported in mice with Aβ pathology (Gordon et al., 2001; Heikkinen et al., 2004; Liu et al., 2002; Puoliväli et al., 2002), many studies fail to observe such impairment (Bizon et al., 2007; Dumont et al., 2004; Lassalle et al., 2008; Reiserer et al., 2007). One possibility then is that transfer learning may assess a different aspect of potentially hippocampal-dependent cognition that is sensitive to more modest changes in pathology than is spatial reference memory.

Certainly, in addition, brain regions beyond hippocampus (e.g., prefrontal cortex, striatum, basal forebrain) may also be important for accurate transfer learning. With respect to prefrontal cortex, however, it would be expected that age/pathology associated changes in this region might largely influence the initial learning phase of the task that requires the ability to discriminate across perceptual sets, as lesions of prefrontal cortex impair this type of learning (Birrell and Brown, 2000). Notably, some deficits related to prefrontal cortical pathology were detected in young but not aged APP + PS1 mice in the current study. Despite performing on par with NTgs in transfer learning, young APP + PS1 mice were impaired in their ability to reverse the relevant contingency of a simple discrimination problem. Interestingly, this reversal deficit in APP + PS1 mice was not observed when retested at advanced age, when the transfer learning impairment was pronounced. Our reversal data agree with those from previous studies using aged rats (Schoenbaum et al., 2006) and in studies from rodents with prefrontal cortical lesions (Schoenbaum et al., 2002). In all cases, reversal learning deficits were present initially but were ameliorated with additional testing or on retests later in the lifespan. Reversal learning at least initially depends upon prefrontal cortical function, one of the earliest regions to develop Aβ plaques (Sgaramella et al., 2001; Waltz et al., 2004; Zhuo et al., 2007). Early reversal deficits in APP + PS1 mice and those reported here previously described in Tg2576 mice appear to be an

Please cite this article in press as: Montgomery, K.S., et al., Novel age-dependent learning deficits in a mouse model of Alzheimer's disease: Implications for translational research. Neurobiol. Aging (2009), doi:10.1016/j.neurobiolaging.2009.08.003

early indicator of Aβ pathology (Zhuo et al., 2007, 2008). In agreement with Schoenbaum et al. (2006), in the APP + PS1 mouse model, there appears to be a compensatory mechanism that allows such deficits to be erased later in the lifespan (compare Figs. 4C and 5C). Alternatively, as shown in rodents with orbitofrontal cortex lesions (Schoenbaum et al., 2002), while acquiring the rule of reversal learning may be impaired in the APP + PS1 mice, once acquired, the mice may simply be able to perform well on subsequent problems. As only one reversal test was performed at each age in the current study, we are unable to distinguish between these two possibilities.

It is somewhat curious that young APP + PS1 mice demonstrated deficits on reversal learning but not on the concurrent discrimination learning problems in the first phase of the transfer task, which could be conceived as having components of a set-shifting task known to depend on intact prefrontal cortical regions (Birrell and Brown, 2000). There are several possible explanations for these results. First, it may be the case that the acquisition of the initial discrimination problems, while analogous to shifting of attentional sets, does not necessarily require such abilities (i.e., the task could be learned simply as a series of discrimination problems). Second, reversal learning and the ability to shift across perceptual sets depend on two distinct neuroanatomical regions of prefrontal cortex, orbital and medial prefrontal cortex, respectively (Birrell and Brown, 2000; McAlonan and Brown, 2003; Schoenbaum et al., 2002). Again, ongoing lesion studies are directed at identifying the precise role of the orbitofrontal and medial prefrontal cortex in the rodent transfer learning task.

The current series of experiments show that we have successfully established the parameters of a rodent task to assess transfer learning, which, like the human analog of the task, is sensitive to age-related pathology. This task revealed robust deficits in cognitive function in animals that did not show deficits on more standard assessments of basal forebrain/medial temporal lobe function (i.e., the spatial reference memory version of the Morris water maze task). These data and the highly similar parameters of the human and rodent tasks provide a behavioral paradigm that should be useful for translational research between rodents and humans, resolving a high-priority need for current AD research. One of the impediments to translational research has been an inability to extend cross-sectional experimental designs traditionally used in rodent experimentation to the longitudinal experimental designs typically used in human clinical trials. Tasks such as the water maze are not easily adaptable for re-assessment due to significant savings across test sessions, even in animals with significant memory impairments (LaSarge and Nicolle, 2009; Volz et al., 2001). In contrast, the longitudinal study presented here demonstrates that the transfer learning task can be used in a within subject, test–retest manner in mice. Therefore, this new assessment should be an excellent preclinical tool for evaluation of therapeutic interventions that could halt and even reverse cognitive deficits associated with age and age-related disease.

## Conflict of interest

The authors declare no conflict of interest.

## Acknowledgements

We thank Dr. Barry Setlow, Candi Lynn LaSarge, Nicholas Simon, and Ian Mendez for comments on the manuscript. This work was supported by R01 AG029421 to J.L. Bizon and Institute for the Study of Aging (ISOA) to M.A. Gluck.

## References

Andersen, K., Launer, L.J., Dewey, M.E., Letenneur, L., Ott, A., Copeland, J.R., Dartigues, J.F., Kragh-Sorensen, P., Baldereschi, M., Brayne, C., Lobo, A., Martinez-Lage, J.M., Stijnen, T., Hofman, A., EURODEM Incidence Research Group, 1999. Gender differences in the incidence of AD and vascular dementia: the EURODEM studies. Neurology 53, 1992–1997.

Aggleton, J.P., Sanderson, D.J., Pearce, J.M., 2007. Structural learning and the hippocampus. Hippocampus 17, 723–734.

Alzheimer's Association, 2008. Alzheimer's Disease. Facts and Figures, vol. 4, issue 2.

Arns, M., Sauvage, M., Steckler, T., 1999. Excitotoxic hippocampal lesions disrupt allocentric spatial learning in mice: effects of strain and task demands. Behav. Brain Res. 106, 151–164.

Barense, M.D., Fox, M.T., Baxter, M.G., 2002. Aged rats are impaired on an attentional set-shifting task sensitive to medial frontal cortex damage in young rats. Learn. Memory 94, 191–201.

Barense, M.D., Bussey, T.J., Lee, A.C., Rogers, T.T., Davies, R.R., Saksida, L.M., Murray, E.A., Graham, K.S., 2005. Functional specialization in the human medial temporal lobe. J. Neurosci. 25, 10239–10246.

Bayer, T.A., Schafer, S., Simons, A., Kemmling, A., Kamer, T., Tepest, R., Eckert, A., Schussel, K., Eikenberg, O., Sturchler-Pierrat, C., Abramowski, D., Staufenbiel, M., Multhaup, G., 2003. Dietary Cu stabilizes brain superoxide dismutase 1 activity and reduces amyloid Abeta production in APP23 transgenic mice. Proc. Natl. Acad. Sci. U.S.A. 100, 14187–14192.

Birrell, J.M., Brown, V.J., 2000. Medial frontal cortex mediates perceptual attentional set shifting in the rat. J. Neurosci. 20, 4320–4324.

Bissonette, G.B., Martins, G.J., Franz, T.M., Harper, E.S., Schoenbaum, G., Powell, E.M., 2008. Double dissociation of the effects of medial and orbital prefrontal cortical lesions on attentional and affective shifts in mice. J. Neurosci. 28, 11124–11130.

Bizon, J.L., Prescott, S., Nicolle, M.M., 2007. Intact spatial learning in adult Tg2576 mice. Neurobiol. Aging 28, 440–446.

Bizon, J.L., LaSarge, C.L., Montgomery, K.S., McDermott, A.N., Setlow, B., Griffith, W.H., 2009. Spatial reference and working memory across the lifespan of male Fischer 344 rats. Neurobiol. Aging 30, 646–655.

Brody, D.L., Holtzman, D.M., 2006. Morris water maze search strategy analysis in PDAPP mice. Exp. Neurol. 197, 330–340.

Bunsey, M., Eichenbaum, H., 1996. Conservation of hippocampal memory function in rats and humans. Nature 379, 255–257.

Burgess, B.L., McIsaac, S.A., Naus, K.E., Chan, J.Y., Tansley, G.H., Yang, J., Miao, F., Ross, C.J., van Eck, M., Hayden, M.R., van Nostrand, W., St George-Hyslop, P., Westaway, D., Wellington, C.L., 2006. Elevated plasma triglyceride levels precede amyloid deposition in Alzheimer's disease mouse models with abundant A beta in plasma. Neurobiol. Dis. 24, 114–127.

Callahan, M.J., Lipinski, W.J., Bian, F., Durham, R.A., Pack, A., Walker, L.C., 2001. Augmented senile plaque load in aged female beta-amyloid precursor protein-transgenic mice. Am. J. Pathol. 158, 1173–1177.

Chishti, M.A., Yang, D.S., Janus, C., Phinney, A.L., Horne, P., Pearson, J., Strome, R., Zuker, N., Loukides, J., French, J., Turner, S., Lozza, G., Grilli, M., Kunicki, S., Morissette, C., Paquette, J., Gervais, F., Bergeron, C., Fraser, P.E., Carlson, G.A., George-Hyslop, P.S., Westaway, D., 2001. Early-onset amyloid deposition and cognitive deficits in transgenic mice expressing a double mutant form of amyloid precursor protein 695. J. Biol. Chem. 276, 21562–21570.

Chun, M.M., Phelps, E.A., 1999. Memory deficits for implicit contextual information in amnesic subjects with hippocampal damage. Nat. Neurosci. 2, 844–847.

Djordjevic, J., Jones-Gotman, M., De Sousa, K., Chertkow, H., 2008. Olfaction in patients with mild cognitive impairment and Alzheimer's disease. Neurobiol. Aging 29, 693–706.

Dumont, M., Strazielle, C., Staufenbiel, M., Lalonde, R., 2004. Spatial learning and exploration of environmental stimuli in 24-month-old female APP23 transgenic mice with the Swedish mutation. Brain Res. 1024, 113–121.

Eichenbaum, H., Mathews, P., Cohen, N., 1989. Further studies of hippocampal representation during odor discrimination learning. Behav. Neurosci. 3, 1207–1216.

Eichenbaum, H., Yonelinas, A.R., Ranganath, C., 2007. The medial temporal lobe and recognition memory. Annu. Rev. Neurosci. 30, 123–152.

Gallagher, M., Burwell, R., Burchinal, M., 1993. Severity of spatial learning impairment in aging: development of a learning index for performance in the Morris water maze. Behav. Neurosci. 107, 618–626.

Gallagher, M., Bizon, J.L., Hoyt, E.C., Helm, K.A., Lund, P.K., 2003. Effects of aging on the hippocampal formation in a naturally occurring animal model of mild cognitive impairment. Exp. Gerontol. 38, 71–77.

Gluck, M.A., Myers, C., 1993. Hippocampal mediation of stimulus representation: a computational theory. Hippocampus 3, 491–516.

Gluck, M.A., Myers, C.E., 1995. Representation and association in memory: a neurocomputational view of hippocampal function. Curr. Dir. Psychol. Sci. 4, 23–29.

Gluck, M.A., Myers, C.E., 2001. Gateway to Memory: An Introduction to Neural Network Models of the Hippocampus and Learning. MIT Press, Cambridge, MA.

Gluck, M.A., Myers, C.E., Nicolle, M.M., Johnson, S., 2006. Computational models of the hippocampal region: implications for prediction of risk for Alzheimer's disease in non-demented elderly. Curr. Alzheimer Res. 3, 247–257.

Golub, M.S., Germann, S.L., Mercer, M., Gordon, M.N., Morgan, D.G., Mayer, L.P., Hoyer, P.B., 2008. Behavioral consequences of ovarian atrophy and estrogen replacement in the APPswe mouse. Neurobiol. Aging 29, 1512–1523.

Gordon, M.N., King, D.L., Diamond, D.M., Jantzen, P.T., Boyett, K.V., Hope, C.E., Hatcher, J.M., DiCarlo, G., Gottschall, W.P., Morgan, D., Arendash, G.W., 2001. Correlation between cognitive deficits and Abeta deposits in transgenic APP + PS1 mice. Neurobiol. Aging 22, 377–385.

Green, P.S., Bales, K., Paul, S., Bu, G., 2005. Estrogen therapy fails to alter amyloid deposition in the PDAPP model of Alzheimer's disease. Endocrinology 146, 2774–2781.

Hardy, J., Selkoe, D.J., 2002. The amyloid hypothesis of Alzheimer's disease: progress and problems on the road to therapeutics. Science 297, 353–356.

Haskins, A.L., Yonelinas, A.P., Quamme, J.R., Ranganath, C., 2008. Perirhinal cortex supports encoding and familiarity-based recognition of novel associations. Neuron 59, 554–560.

Heikkinen, T., Kalesnykas, G., Rissanen, A., Tapiola, T., Iivonen, S., Wang, J., Chaudhuri, J., Tanila, H., Miettinen, R., Puoliväli, J., 2004. Estrogen treatment improves spatial learning in APP + PS1 mice but does not affect beta amyloid accumulation and plaque formation. Exp. Neurol. 187, 105–117.

Ikonen, S., McMahan, R., Gallagher, M., Eichenbaum, H., Tanila, H., 2002. Cholinergic system regulation of spatial representation by the hippocampus. Hippocampus 12, 386–397.

Jankowsky, J.L., Fadale, D.J., Anderson, J., Xu, G.M., Gonzales, V., Jenkins, N.A., Copeland, N.G., Lee, M.K., Younkin, L.H., Wagner, S.L., Younkin, S.G., Borchelt, D.R., 2004. Mutant presenilins specifically elevate the levels of the 42 residue beta-amyloid peptide in vivo: evidence for augmentation of a 42-specific gamma secretase. Hum. Mol. Genet. 13, 159–170.

Johnson, S.C., Schmitz, T.W., Asthana, S., Gluck, M.A., Myers, C.E., 2008. Associative learning over trials activates the hippocampus in healthy elderly but not mild cognitive impairment. Aging Neuropsychol. Cogn. 15, 129–145.

Jorm, A.F., Jolley, D., 1998. The incidence of dementia: a meta-analysis. Neurology 51, 728–733.

Kirwan, C.B., Gilbert, P.E., Kesner, R.P., 2005. The role of the hippocampus in the retrieval of a spatial location. Neurobiol. Learn. Mem. 83, 65–71.

Kluger, A., Ferris, S.H., Golomb, J., Mittelman, M.S., Reisberg, B., 1999. Neuropsychological prediction of decline to dementia in nondemented elderly. J. Geriatr. Psychiatry Neurol. 12, 168–179.

LaSarge, C.L., Montgomery, K.S., Tucker, C., Slaton, S., Griffith, W.H., Setlow, B., Bizon, J.L., 2007. Deficits across multiple cognitive domains in a subset of aged Fischer 344 rats. Neurobiol. Aging 28, 928–936.

LaSarge, C.L., Nicolle, M., 2009. Comparison of different cognitive rat models of human aging. In: Bizon, J.L., Woods, A.G. (Eds.), Animal Models of Human Cognitive Aging. Humana Press, New York, pp. 73–102.

Lassalle, J.M., Halley, H., Dumas, S., Verret, L., Francés, B., 2008. Effects of the genetic background on cognitive performances of TG2576 mice. Behav. Brain Res. 191, 104–110.

Lewis, J., Dickson, D.W., Lin, W.L., Chisholm, L., Corral, A., Jones, G., Yen, S.H., Sahara, N., Skipper, L., Yager, D., Eckman, C., Hardy, J., Hutton, M., McGowan, E., 2001. Enhanced neurofibrillary degeneration in transgenic mice expressing mutant tau and APP. Science 293, 1487–1491.

Liu, L., Ikonen, S., Heikkinen, T., Heikkilä, M., Puoliväli, J., van Groen, T., Tanila, H., 2002. Effects of fimbria-fornix lesion and amyloid pathology on spatial learning and memory in transgenic APP + PS1 mice. Behav. Brain Res. 134, 433–445.

Lowndes, G.J., Saling, M.M., Ames, D., Chiu, E., Gonzalez, L.M., Savage, G.R., 2008. Recall and recognition of verbal paired associates in early Alzheimer's disease. J. Int. Neuropsychol. Soc. 14, 591–600.

McAlonan, K., Brown, V.J., 2003. Orbital prefrontal cortex mediates reversal learning and not attentional set shifting in the rat. Behav. Brain Res. 146, 97–103.

Montgomery, K.S., Mackey, J., Thuett, K., Ginestra, S., Bizon, J.L., Abbott, L.C., 2008. Chronic, low-dose prenatal exposure to methylmercury impairs motor and mnemonic function in adult C57/B6 mice. Behav. Brain Res. 191, 55–61.

Morris, R.G., Garrud, P., Rawlins, J.N., O'Keefe, J., 1982. Place navigation impaired in rats with hippocampal lesions. Nature 297, 681–683.

Moses, S.N., Ryan, J.D., 2006. A comparison and evaluation of the predictions of relational and conjunctive accounts of hippocampal function. Hippocampus 16, 43–65.

Myers, C.E., Gluck, M.A., 1996. Cortico-hippocampal representations in simultaneous odor discrimination: a computational interpretation of Eichenbaum, Mathews, and Cohen (1989). Behav. Neurosci. 110, 685–706.

Myers, C.E., Kluger, A., Golomb, J., Ferris, S.H., de Leon, M.J., Schnirman, G., Gluck, M.A., 2002. Hippocampal atrophy disrupts transfer generalization in nondemented elderly. J. Geriatr. Psychiatry Neurol. 15, 82–90.

Myers, C.E., Hopkins, R., DeLuca, J., Moore, N., Wolansky, L.J., Sumner, J., Gluck, M.A., 2008a. Learning and generalization deficits in patients with memory impairments due to anterior communicating artery aneurysm rupture or hypoxic brain injury. Neuropsychology 22, 681–686.

Myers, C.E., Kluger, A., Golomb, J., Gluck, M.A., Ferris, S.H., 2008b. Learning and generalization tasks predict short-term outcome in nondemented elderly. J. Geriatr. Psychiatry Neurol. 21, 93–103.

Myers, C.E., Hopkins, R.O., DeLuca, J., Moore, N.B., Wolansky, L.J., Gluck, M.A., 2008c. Learning and generalization deficits in patients with mem-

Please cite this article in press as: Montgomery, K.S., et al., Novel age-dependent learning deficits in a mouse model of Alzheimer's disease: Implications for translational research. Neurobiol. Aging (2009), doi:10.1016/j.neurobiolaging.2009.08.003

ory impairments due to anterior communicating artery aneurysm rupture or hypoxic brain injury. Neuropsychology 22, 681–686.

O'Reilly, R.C., Rudy, J.W., 2001. Conjunctive representations in learning and memory: principles of cortical and hippocampal function. Psychol. Rev. 108, 311–345.

Pascalis, O., Hunkin, N.M., Bachevalier, J., Mayes, A.R., 2009. Change in background context disrupts performance on visual paired comparison following hippocampal damage. Neuropsychologia 47, 2107–2113.

Puoliväli, J., Wang, J., Heikkinen, T., Heikkilä, M., Tapiola, T., van Groen, T., Tanila, H., 2002. Hippocampal A beta 42 levels correlate with spatial memory deficit in APP and PS1 double transgenic mice. Neurobiol. Dis. 9, 339–347.

Quamme, J.R., Yonelinas, A.P., Norman, K.A., 2007. Effect of unitization on associative recognition in amnesia. Hippocampus 17, 192–200.

Reiserer, R.S., Harrison, F.E., Syverud, D.C., McDonald, M.P., 2007. Impaired spatial learning in the APPSwe + PSEN1DeltaE9 bigenic mouse model of Alzheimer's disease. Genes Brain Behav. 6, 54–65.

Rudy, J., Sutherland, R., 1995. Configural association theory and the hippocampal formation: an appraisal and reconfiguration. Hippocampus 5, 375–398.

Schacter, D., 1985. Multiple forms of memory in humans and animals. In: Weinberger, N., McGaugh, J., Lynch, G. (Eds.), Memory Systems of the Brain: Animal and Human Cognitive Processes. Guildford Press, New York, pp. 351–379.

Schäfer, S., Wirths, O., Multhaup, G., Bayer, T.A., 2007. Gender dependent APP processing in a transgenic mouse model of Alzheimer's disease. J. Neural Transm. 114, 287–394.

Schoenbaum, G., Nugent, S., Saddoris, M.P., Setlow, B., 2002. Orbitofrontal lesions in rats impair reversal but not acquisition of go, no-go odor discriminations. Neuroreport 13, 885–890.

Schoenbaum, G., Setlow, B., Saddoris, M.P., Gallagher, M., 2006. Encoding changes in orbitofrontal cortex in reversal-impaired aged rats. J. Neurophysiol. 95, 1509–1517.

Sgaramella, T.M., Borgo, F., Mondini, S., Pasini, M., Toso, V., Semenza, C., 2001. Executive deficits appearing in the initial stage of Alzheimer's disease. Brain Cogn. 46, 264–268.

Squire, L.R., Stark, C.S., Clark, R.E., 2004. The medial temporal lobe. Annu. Rev. Neurosci. 27, 279–306.

Sturchler-Pierrat, C., Staufenbiel, M., 2000. Pathogenic mechanisms of Alzheimer's disease analyzed in the APP23 transgenic mouse model. Ann. N. Y. Acad. Sci. 920, 134–139.

Sutherland, R., Rudy, J., 1989. Configural association theory: the role of the hippocampal formation in learning, memory and amnesia. Psychobiology 17, 129–144.

Volz, H.P., Nenadic, I., Gaser, C., Rammsayer, T., Häger, F., Sauer, H., 2001. Time estimation in schizophrenia: an fMRI study at adjusted levels of difficulty. Neuroreport 12 (2), 313–316.

Xu, X., 2009. γ-Secretase Catalyzes Sequential Cleavages of the AβPP Transmembrane Domain. J. Alzheimers Dis. 16, 211–224.

Waltz, J.A., Knowlton, B.J., Holyoak, K.J., Boone, K.B., Back-Madruga, C., McPherson, S., Masterman, D., Chow, T., Cummings, J.L., Miller, B.L., 2004. Relational integration and executive function in Alzheimer's disease. Neuropsychology 18, 296–305.

Zhuo, J.M., Prescott, S.L., Murray, M.E., Zhang, H.Y., Baxter, M.G., Nicolle, M.M., 2007. Early discrimination reversal learning impairment and preserved spatial learning in a longitudinal study of Tg2576 APPsw mice. Neurobiol. Aging 28, 1248–1257.

Zhuo, J.M., Prakasam, A., Murray, M.E., Zhang, H.Y., Baxter, M.G., Sambamurti, K., Nicolle, M.M., 2008. An increase in Abeta42 in the prefrontal cortex is associated with a reversal-learning impairment in Alzheimer's disease model Tg2576 APPsw mice. Curr. Alzheimer Res. 5, 385–391.

Please cite this article in press as: Montgomery, K.S., et al., Novel age-dependent learning deficits in a mouse model of Alzheimer's disease: Implications for translational research. Neurobiol. Aging (2009), doi:10.1016/j.neurobiolaging.2009.08.003

Print this Page

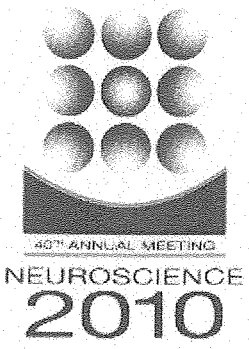


Presentation Abstract

Program#/Poster#: 710.1/NNN1

Title: Effects of aging on primary neuronal cilia in the cerebral cortex

Location: Halls B-H

Presentation Time: Tuesday, Nov 16, 2010, 1:00 PM - 2:00 PM

Authors: *G. O. FONSECA FILHO, S. M. GUADIANA, A. KUMAR, T. FOSTER, M. R. SARKISIAN;
Neurosci., Univ. of Florida Col. of Med., Gainesville, FL

Abstract: Most, if not all, cortical neurons extend a primary cilium into the extracellular environment. However, the development, function and effects of aging on neuronal primary cilia have largely been overlooked. A recent study reported that signaling through the somatostatin subtype receptor 3 (SSR3), a receptor enriched in neuronal cilia, was important for synaptic plasticity and objection recognition memory (Einstein et al., J Neurosci. 2010). The purpose of this study was to examine when neuronal cilia appear in the cerebral cortex and the effects of aging on cilia-associated molecular components. By western blot and immunostaining analyses of rodent cortex, we found that expression of adenylyl cylcase 3 (ACIII), a molecule enriched in neuronal cilia, is detectable around birth and persists into adulthood. ACIII also correlates with elongation of neuronal cilia during the first three postnatal weeks. Examination of neuronal cilia receptors, melanin concentrating hormone receptor 1 (Mchr1) and SSR3 are also detectable in the first and

second postnatal weeks. To test whether or not cilia and their associated receptors are present in aged cortex, we examined young (1mos) and aged (38mos) rat cortex. We found that although ACIII was still expressed in the aged brain, there was dramatically reduced expression of SSR3 and Mchr1. Molecular motors (e.g. Kif3a) and receptor localizing proteins (e.g., Bardet-Biedl Syndrome (BBS) proteins) are critical components for cilia function. Surprisingly, levels of Kif3a and BBS2 appeared to be significantly increased in aged cortex. Because neuronal cilia have been implicated in synaptic plasticity and memory, we examined cilia in the cerebral cortex of middle-aged rats that had been behaviorally tested and classified as memory-impaired (MI) or unimpaired (MU). We found that MI rats showed slight changes in their cilia lengths in hippocampus and neocortex compared to MU rats. Together, our data suggest that neuronal cilia elongate during the first couple postnatal weeks. Moreover cilia persist in the aged brain but may be compromised in their ability to respond to external environmental signals.

Disclosures: **G.O. Fonseca Filho**, None; **S.M. Guadiana**, None; **A. Kumar**, None; **T. Foster**, None; **M.R. Sarkisian**, None.

Keyword(s): Cilium

Somatostatin

LEARNING AND MEMORY

Support: Funds from the McKnight Brain Research Foundation and the Evelyn F. and William L. McKnight Institute at the University of Florida (to M.R.S.)

NIH Grant AG014979-09 (to T.F.) and an Evelyn F. McKnight Brain Research Grant (to T.F.)

[Authors]. [Abstract Title]. Program No. XXX.XX. 2010 Neuroscience Meeting Planner. San Diego, CA: Society for Neuroscience, 2010. Online.

ELSEVIER

Neurobiology of Aging 31 (2010) 853–862

NEUROBIOLOGY OF AGING

www.elsevier.com/locate/neuaging

# Good things come to those who wait: Attenuated discounting of delayed rewards in aged Fischer 344 rats☆

Nicholas W. Simon, Candi L. LaSarge, Karienn S. Montgomery, Matthew T. Williams, Ian A. Mendez, Barry Setlow, Jennifer L. Bizon *

*Department of Psychology, Texas A&M University, College Station, TX 77843-4235, United States*

Received 4 April 2008; received in revised form 4 June 2008; accepted 7 June 2008
Available online 26 July 2008

**Abstract**

The ability to make advantageous choices among outcomes that differ in magnitude, probability, and delay until their arrival is critical for optimal survival and well-being across the lifespan. Aged individuals are often characterized as less impulsive in their choices than their young adult counterparts, demonstrating an increased ability to forgo immediate in favor of delayed (and often more beneficial) rewards. Such "wisdom" is usually characterized as a consequence of learning and life experience. However, aging is also associated with prefrontal cortical dysfunction and concomitant impairments in advantageous choice behavior. Animal models afford the opportunity to isolate the effects of biological aging on decision-making from experiential factors. To model one critical component of decision-making, young adult and aged Fischer 344 rats were trained on a two-choice delay discounting task in which one choice provided immediate delivery of a small reward and the other provided a large reward delivered after a variable delay period. Whereas young adult rats showed a characteristic pattern of choice behavior (choosing the large reward at short delays and shifting preference to the small reward as delays increased), aged rats maintained a preference for the large reward at all delays (i.e., attenuated "discounting" of delayed rewards). This increased preference for the large reward in aged rats was not due to perceptual, motor, or motivational factors. The data strongly suggest that, independent of life experience, there are underlying neurobiological factors that contribute to age-related changes in decision-making, and particularly the ability to delay gratification.


*Keywords:* Aging; Decision-making; Choice; Impulsivity; Delay discounting; Rat

## 1. Introduction

People are faced with numerous decisions throughout their lives, the consequences (outcomes) of which significantly impact their survival and quality of life. Often such decisions include temporal considerations, in which a delay imposed between a choice and the arrival of its corresponding outcome can substantially alter the desirability of that outcome. For example, individuals will virtually always choose a large over a small reward when the delay to delivery of the large reward is short; however, as the delay to the large reward increases, its subjective value decreases, or is "discounted", making the small reward more preferable. This phenomenon, known as delay discounting, is well documented in a variety of settings, and all subjects reliably demonstrate it to some degree (Ainslie, 1975; Green et al., 1996; Rachlin and Green, 1972; Winstanley et al., 2006a). However, the degree of discounting can be modified substantially by factors including pharmacological agents, genetic background, and age (Bickel et al., 1999; Cardinal et al., 2001, 2000; Clark et al., 2004; Green et al., 1994; Kirby and Petry, 2004; Petry, 2001b; Simon et al., 2007).

Children and adolescents discount delayed rewards to a greater degree than adults (i.e. – the "impulsivity of

☆ The data in this manuscript have not been previously published (except in abstract form, Society for Neuroscience 2007), and are not and will not be considered for publication elsewhere. All animal procedures were approved by the University Laboratory Animal Care Committee at Texas A&M University, and all authors approve of the final contents of the manuscript and verify the accuracy of the data.

* Corresponding author at: Behavioral and Cellular Neuroscience, Department of Psychology, Texas A&M University, College Station, TX 77843-4235, United States. Tel.: +1 979 845 2506; fax: +1 979 845 4727.
*E-mail address:* jbizon@tamu.edu (J.L. Bizon).

0197-4580/$ – see front matter © 2008 Elsevier Inc. All rights reserved.
doi:10.1016/j.neurobiolaging.2008.06.004

youth" – (Green et al., 1994, 1996)). However, surprisingly little is known about how more advanced ages affect this component of decision-making, an issue of increasing importance as average life expectancy continues to rise (FIFARS, 2005). Anecdote suggests that aged individuals are less impulsive than their younger counterparts. Consistent with this perception, Green et al. (1994, 1996) reported that 70-year olds discount delayed rewards to a lesser extent than do 20-year olds. In contrast, behavioral economic models suggest that aged individuals should consider their reduced number of remaining years when making decisions, and therefore should discount delayed rewards to a greater extent than younger individuals (Sozou and Seymour, 2003). In agreement with such models, some aged subjects show disadvantageous choice behavior in laboratory tests of decision-making such as the Iowa Gambling Task (Denburg et al., 2005; Fein et al., 2007). Furthermore, functional studies in both animal and human subjects show that prefrontal cortical areas (particularly orbitofrontal cortex) involved in decision-making processes may be compromised at advanced ages (Lamar and Resnick, 2004; Lamar et al., 2004; Schoenbaum et al., 2006; West, 1996).

The influence of environmental factors on delay discounting (Dixon et al., 2003; Green et al., 1996; Petry, 2001a) renders comparisons between young adult and aged humans difficult to interpret. For example, among many possible interpretations, such age-related differences in delay discounting could reflect differing degrees of opportunity for learning about the benefits of waiting for rewards (i.e., learning that "patience has its virtues"), and/or even differences in socioeconomic status (Green et al., 1996). The current study was designed to minimize the influence of prior experience on decision-making in aging using a rat model of human cognitive aging in which experiential factors (prior learning, environmental history) are controlled in young adult and aged subjects. Rats were trained in a two-choice delay discounting task, which pitted choice of a small immediate reward against a large reward delivered after a delay period. Aged subjects demonstrated a strong preference for the larger reward, irrespective of delay, providing support for a neurobiological (rather than solely experiential) explanation of decision-making differences across the lifespan.

## 2. Materials and methods

### 2.1. Subjects

Male Fischer 344 rats were used for this study. Aged ($n = 8$) and young adult ($n = 8$) rats were a mean of 24.72 (S.E.M. = .16) and 6.11 (S.E.M. = .03) months old, respectively, at the onset of behavioral testing. Young adult rats of this age were chosen because it is well past the age of sexual maturity (approximately 2–3 months). Fischer 344 rats are considered "aged" at 24 months (with an average lifespan of 26.6 months and a maximum lifespan of approximately 30 months). By 24 months, a considerable proportion of the F344 population displays cognitive deficits on a range of behavioral tasks (Bizon et al., in press; Frick et al., 1995; LaSarge et al., 2007; Yu et al., 1982). Rats were obtained from the National Institute on Aging colony and housed in the vivarium in the Psychology Building at Texas A&M University. This AALAC-accredited facility was maintained at a consistent 25 °C with a 12:12 h light/dark cycle (lights on at 0800), and rats had free access to food and water except as noted below. All rats in the study were screened daily for health problems including, but not limited to, cataracts, jaundice, food and water intake, and the appearance of tumors. Sentinel rats, housed alongside the rats used in this study, were routinely health screened and found to be negative for a range of pathogens. Upon autopsy, each subject was screened for visible pituitary tumors that could impair visual acuity by impinging on the optic nerve. No subjects were excluded from the study for health reasons, although two aged rats ceased responding during the control experiments that were conducted after the completion of the delay discounting procedure in Experiment 1. These rats were removed from the study at those points and excluded from subsequent analyses (one was removed during Experiment 2 and one was removed during Experiment 3). All animal procedures were conducted in accordance with approved institutional animal care procedures and NIH guidelines.

### 2.2. Apparatus

Testing was conducted in six identical standard rat test chambers (30.5 cm × 25.4 cm × 30.5 cm; Coulbourn Instruments, Allentown, PA) with metal front and back walls, transparent Plexiglas side walls, and a floor composed of steel rods (.4 cm in diameter) spaced 1.1 cm apart. Each test chamber was housed in a sound-attenuating cubicle, and equipped with a recessed food pellet delivery trough fitted with a photobeam to detect head entries and a 1.12-W lamp to illuminate the food trough. This trough, into which the 45 mg grain-based food pellet rewards (PJAI, Test Diet: Richmond, IN) were delivered, was located 2 cm above the floor in the center of the front wall. Two retractable levers were located to the left and right of the food delivery trough, 11 cm above the floor. Experiments were controlled and data collected by a computer interfaced with the behavioral test chambers and equipped with Graphic State 3.01 software (Coulbourn Instruments).

### 2.3. Experimental procedures

The procedures for the delay discounting task have been described previously (Evenden and Ryan, 1996; Simon et al., 2007). Prior to the start of behavioral testing, rats were reduced to 85% of their free-feeding weight over the course of 1 week, and were maintained as such throughout the duration of the experiment. On the day before the start of behavioral

testing, each rat was given five 45 mg food pellets in its home cage to reduce neophobia to the food reward used in the task.

*2.3.1. Shaping*

The task began with a 64-min session of magazine training consisting of 38 deliveries of a single food pellet with an inter-trial interval (ITI) of 100 ± 40 s. On the following day, the rats were shaped to press a single lever (either left or right, counterbalanced across groups; the other was retracted during this phase of training) in order to receive a single food pellet. Once they reached a criterion of 50 lever presses during a 30-min session, they were shaped to press the opposite lever using the same schedule and criterion.

Following completion of lever press shaping, both levers were retracted, and rats were shaped to nose poke into the food trough during simultaneous illumination of the trough light and a 1.12-W house light. When a nose poke occurred, a single lever was extended, and a lever press resulted in immediate delivery of a single food pellet. Immediately following the lever press, the house and trough lights were extinguished and the lever was retracted. The left and right levers were presented an equal number of times, with no more than two consecutive presentations of the same lever. Rats were trained to a criterion of at least 60 successful trials in an hour with an ITI of 40 ± 10 s.

*2.3.2. Experiment 1: assessing age-related differences in delay discounting*

Each session in the delay discounting task consisted of 5 blocks of 12 trials each. Within each session, each of the 100-s trials began with a 10-s illumination of the food trough and house lights. A nose poke into the food trough during this time extinguished the food trough light and triggered extension of either a single lever (forced trials) or of both levers simultaneously (choice trials). Trials on which rats failed to nosepoke during this time window were scored as omissions. A press on one lever (either left or right, counterbalanced across groups) resulted in delivery of a single food pellet immediately following the lever press. A press on the other lever resulted in delivery of four food pellets after varying delays. Once either lever was pressed, both levers were retracted and the house light was extinguished until food delivery. Food delivery was accompanied by the re-illumination of both lights, which were again extinguished upon entry to the food trough to collect the food or after 10 s, whichever occurred sooner. Each of the five 12 trial blocks in a session began with two forced trials (one for each lever), followed by 10 choice trials. During the first 12-trial block, the delay to the large reward was set at 0 s. In subsequent 12-trial blocks, the delay to the large reward increased to 10, 20, 40, and 60 s. Note that because trial durations were of fixed duration, reward choice did not influence the rapidity of progress through the trials (e.g., choice of the small immediate reward did not result in sooner choice opportunities). Thus, choice of the large delayed reward was, from an objective perspective, an "optimal" choice, as it resulted in more food delivery. The percentage of trials on which rats chose the large reward lever (number of large reward lever choices/total responses) was calculated for each block as an indicator of reward preference (Cardinal et al., 2000; Simon et al., 2007). Both young and aged rats were tested in the delay discounting task for 40 sessions, at which point stable responding was observed across the final 5 sessions (36–40). Stable responding was defined by the absence of a main effect of days in a repeated measure ANOVA, accompanied by a significant main effect of delay (Cardinal et al., 2000; Simon et al., 2007).

*2.3.3. Experiment 2: reversed order of presentation of delays*

To determine whether the order of presentation of the delays across trial blocks affected choice behavior or the number of completed trials, the order of the delay blocks was reversed. Thus, the delays began at 60 s in the first block, and decreased to 40, 20, 10, and 0 s in each subsequent block of trials in a session. All other experimental conditions remained consistent with the procedures in Experiment 1. Rats were run in this condition for 13 sessions, at which point stable responding was observed across the final 5 sessions (9–13).

*2.3.4. Experiment 3: equal rewards condition*

To test for delay perception and response perseveration, the reward for each lever was equalized (1 food pellet for either choice) while the delays remained the same as in Experiment 2 (thus rendering the no delay lever the optimal choice in all blocks). Rats were run in this condition for 10 sessions.

*2.3.5. Experiment 4: no-delay condition*

To examine reward magnitude perception and to further test for response perseveration, the reward magnitudes were restored to their initial conditions (1 food pellet vs. 4 food pellets) and the delays preceding the large reward were eliminated (thus rendering the large reward lever the optimal choice in all blocks). Rats were run in this condition for 10 sessions.

*2.3.6. Experiment 5: fixed ratio responding*

As a final test of motivation to obtain food, rats were tested for five sessions in a different set of four behavioral test chambers with dimensions identical to those used in the delay discounting task but with only a single response lever fixed in place 3.5 cm above the food trough. In each 30 min session, presses on this lever resulted in delivery of a single food pellet on various fixed ratio (FR) schedules (FR1, FR3, FR10, FR20, FR40, one schedule per session).

*2.4. Data analysis*

Raw data files were exported from Graphic State software and compiled using a custom macrowritten for Microsoft Excel (Dr. Jonathan Lifshitz, Department of Anatomy and

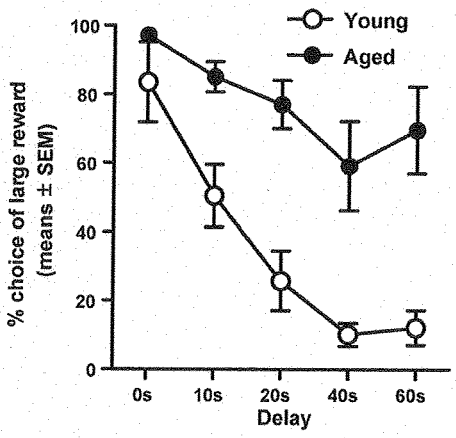


Fig. 1. Delay discounting in young adult and aged rats (Experiment 1). All rats discounted the value of the large reward (as shown by decreased preference for the large reward) as delays increased ($p < .01$). However, aged rats showed less discounting than young adults ($p < .01$).

Neurobiology, Virginia Commonwealth University). Statistical analyses were conducted in SPSS 12.0. In Experiments 1–4, data were averaged across the final five sessions in each experiment (Cardinal et al., 2000; Simon et al., 2007), and these averages were analyzed using two-factor repeated measures ANOVAs (age group X delay duration). Additional analyses (three-factor repeated measures ANOVAS; age group X delay duration X session) were performed to determine whether young adult and aged rats differed in their rates of adaptation to the changes in task contingencies between experiments (i.e., to assess differences in perseverative behavior). Data from shaping sessions and fixed ratio responding in Experiment 5 were analyzed using independent samples *t*-tests. In all cases, *p*-values less than .05 were considered significant.

## 3. Results

### 3.1. Shaping

There were no differences between young adult and aged rats in the number of sessions required to complete either of the phases of shaping (lever press or nosepoke shaping, $t_s < .80$, $p_s > .48$), indicating that both groups were able to acquire the task procedures at a similar rate (young adult mean, 13.25; S.E.M. = 2.66 and aged mean, 14.25 and S.E.M. = 2.09). Following shaping, rats were tested for a total of 78 days in Experiments 1–5.

### 3.2. Experiment 1

As shown in Fig. 1, a two-factor ANOVA (delay × age) revealed that all rats decreased their preference for the large reward as the delay to large reward delivery increased ($F_{(4,56)} = 24.16$, $p < .01$). Most importantly, however, there was a robust and significant main effect of age ($F_{(1,14)} = 20.88$, $p < .01$), as well as a significant interaction between delay and age ($F_{(4,56)} = 3.83$, $p < .01$). These data demonstrate that discounting of delayed rewards is dramatically attenuated in aged rats compared to their young adult cohorts.

It should be noted that aged rats omitted significantly more trials than young adult cohorts, particularly in the trial blocks with the longest delays, which occurred later in the session. Analysis of the number of completed trials (defined as trials with a response on either lever) across the session using a two-factor ANOVA (delay duration × age group) confirmed both a main effect of age ($F_{(1,14)} = 49.50$, $p < .01$) and an interaction between the factors of age and delay ($F_{(4,56)} = 68.70$, $p < .01$), such that aged rats completed significantly fewer trials than young adult cohorts, and this effect became larger across successive trial blocks (Fig. 2A). This difference could be due to the order of presentation of the delays, increased fatigue, or faster satiation in the aged rats. In order to assess satiation, the amount of total food consumed across trials was assessed. Indeed, despite completing fewer trials, because aged rats consistently chose the large reward more often than their young adult cohorts, both age groups consumed comparable

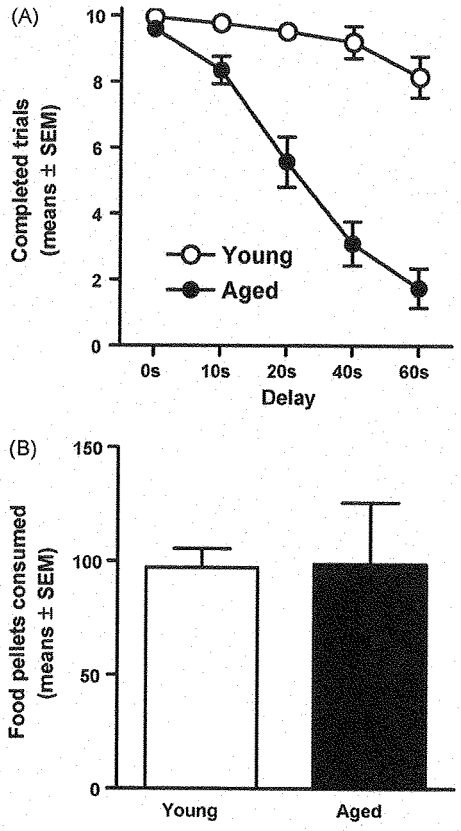


Fig. 2. Total responses and food consumed (Experiment 1). (A) Aged rats responded less frequently than young adults in later blocks of trials ($p < .01$). (B) Despite this difference in omitted trials, however, young adult and aged rats consumed equal amounts of food per session.

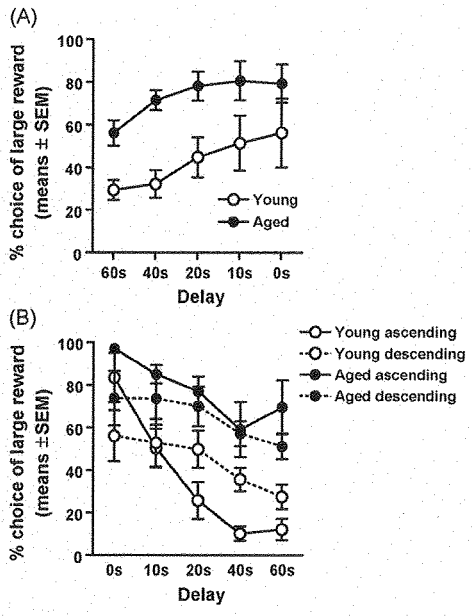


Fig. 3. Delay discounting in young adult and aged rats with order of delays reversed (Experiment 2). (A) Aged rats continued to discount the value of large rewards to a lesser degree than young adult cohorts when the order of delay presentations was reversed ($p < .05$). Thus, the effects of age on delay discounting in Experiment 1 were not due to fewer responses in aged rats at longer delays. (B) Data from Figs. 1 and 2A are re-plotted using the same *X*-axis to facilitate direct comparison of performance with ascending and descending orders of delay presentation.

amounts of food across sessions ($t_{(14)} = .16$, $p = .91$; Fig. 2B). To determine the influence of the order of delay presentations and fatigue on the age-related difference in discounting, in Experiment 2, the same subjects were tested further on the same task with the order of the delay presentations reversed.

### 3.3. Experiment 2

In this condition, the order of delay presentation was reversed, such that the longest delay to large reward delivery (60 s) was presented first, with subsequent delays to large reward delivery decreasing in order to 0 s. Rats in both groups reached stable responding in this phase of testing by day nine, and the subsequent five sessions (9–13) were analyzed. In agreement with the findings in Experiment 1, both age groups showed a decreased preference for the large reward lever with longer delays to large reward delivery (two-factor ANOVA (delay duration × age group); $F_{(4,52)} = 6.06$, $p < .01$; Fig. 3A). Importantly, there was still a significant main effect of age ($F_{(1,13)} = 7.64$, $p < .05$), such that aged rats chose the large delayed reward more often than young adult cohorts (although the interaction between the factors of delay and age was no longer significant, $F_{(4,52)} = .54$, $p = .71$). Further repeated measures ANOVAs comparing performance on the ascending (Experiment 1) and descending (Experiment 2) order of delays within each age group (Fig. 3B) revealed no main effect of age on choice behavior across these conditions ($p_s > .29$). Together, these data strongly indicate that the order of delay presentations was not solely responsible for the age-related attenuation of delay discounting.

Analyses of the number of completed trials in each trial block revealed the same pattern of results observed with the ascending order of delay presentations in Experiment 1, such that aged rats increased their number of omitted trials in blocks later in the sessions, which in this experiment were the blocks with the shortest delays (Fig. 4A). A two-factor ANOVA (delay duration × age group) revealed a main effect of age ($F_{(1,13)} = 8.05$, $p < .05$) and an interaction between delay and age ($F_{(4,54)} = 5.39$, $p < .01$). These data suggest that satiation (or possibly fatigue) in the aged rats was likely a significant factor in the low response rates of aged subjects in later blocks of trials. Indeed, as in Experiment 1, food consumption across sessions was equivalent between age groups when the delays were reversed ($t_{(13)} = .51$, $p = .62$; Fig. 4B). Most importantly, the observation that aged rats preferentially chose the large delayed reward more often than young adult rats in both conditions (ascending and descending order of delay presentations) indicates that the effects of age on delay

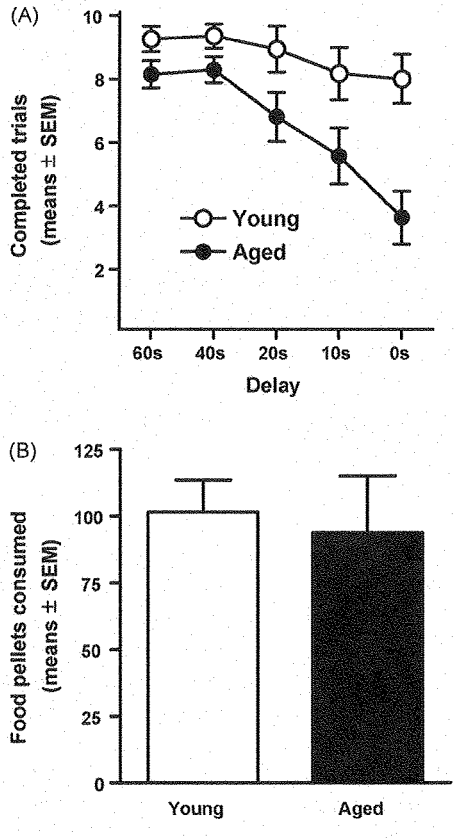


Fig. 4. Total responses and food consumed with order of delays reversed (Experiment 2). (A) Similar to Fig. 2, aged rats responded less as the session progressed ($p < .05$), even though the order of delay presentations was reversed. This indicated that the increase in trial omissions in aged rats was not a function of the order of delay presentations. (B) Young adult and aged rats consumed equivalent amounts of food per session.

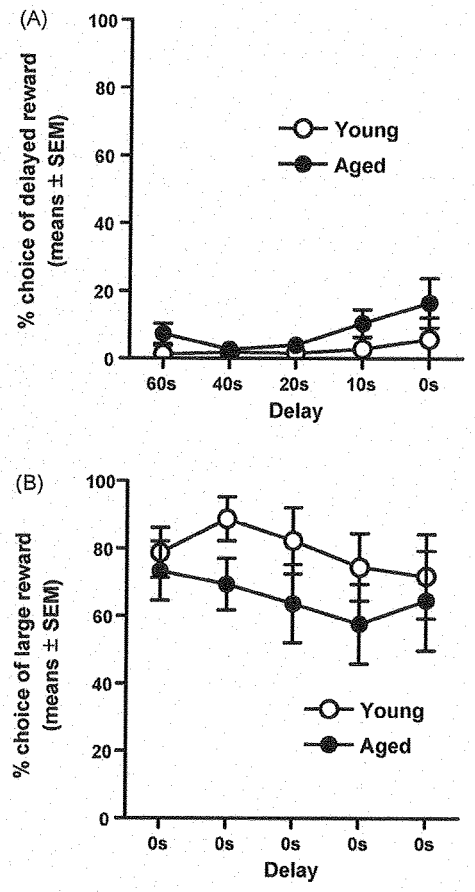


Fig. 5. Tests of delay and reward magnitude perception (Experiments 3 and 4). (A) Aged rats were able to detect and respond appropriately to the delays to the same degree as young adult rats when the delays were maintained but the reward magnitudes made equal. (B) Aged rats were able to detect and respond appropriately to the different reward magnitudes to the same degree as young adult rats when the reward magnitudes were maintained but the delays made equal.

discounting are independent of the order of presentation of the delays and number of completed trials.

### 3.4. Experiment 3

To determine whether aged rats were less sensitive than young adult cohorts to the aversive consequences of delayed reward delivery, the task contingencies were modified such that both the immediate and delayed rewards consisted of only a single food pellet. Rats performed under these contingencies for 10 sessions and stable responding was reached by session 6 for both groups. In *both* age groups, choice of the delayed reward dropped to near-zero levels (Fig. 5A). Analysis of the mean percentage of choices of the delayed reward in sessions 6–10 using a two-factor ANOVA (delay duration × age group) revealed neither a main effect nor any interactions involving age ($F_s < 1.94$, $ps > .19$). The data strongly suggest that the ability of aged rats to perceive and respond to delays was comparable to that of young adult cohorts.

### 3.5. Experiment 4

To determine whether aged rats were differentially sensitive to the different reward magnitudes compared to young adult cohorts, the task contingencies were modified such that the reward magnitudes were returned to their original condition (1 food pellets vs. 4 food pellets), but the delays to the large reward were eliminated (i.e., a zero delay was imposed across all trial blocks). Rats performed under these contingencies for 10 sessions and stable responding was obtained by session 6. Subjects in *both* age groups switched to responding on the lever with the larger reward (Fig. 5B). Analysis of the mean percentage of choices of the large reward lever in sessions 6–10 using a two-factor ANOVA (delay duration × age group) revealed neither a main effect nor any interactions involving age ($F_s < 1.46$, $p_s > .23$). These data strongly suggest that young adult and aged rats in this study were similarly sensitive to the different reward magnitudes used in the task.

### 3.6. Analyses of perseverative behavior in young adult and aged rats

To determine whether age-related differences in delay discounting could be accounted for by perseverative responding on the large reward lever, a number of additional analyses were conducted. First, a three-factor ANOVA (delay duration × age group × session) conducted across all 13 sessions of Experiment 2 (in which the order of delay presentations was reversed) revealed no interactions between age and session ($F_s < 1.32$, $p_s > .21$). These data suggest that aged rats had no more difficulty than young adult rats in altering their choice pattern from that used in Experiment 1. Moreover, in Experiment 3, when reward magnitudes were made equivalent, aged rats switched their responding to the lever that produced the immediate reward at a rate comparable to young adult cohorts (no interactions between age and session ($F_s < 1.10$, $p_s > .30$) in a three-factor ANOVA (delay duration × age group × session) conducted across all 10 sessions of the equal-reward condition). Finally, in Experiment 4, when delays were made equivalent across trials, aged rats switched their responding to the lever that produced the large food reward at a rate comparable to young adult rats (no interactions between age and session ($F_s < 1.69$, $p_s > .10$); three-factor ANOVA (delay duration × age group × session) conducted across all 10 sessions of equal-delay condition). In sum, aged and young adult rats appeared comparable in their ability to alter their choice pattern in accord with changes in task contingencies, arguing against increased perseveration being a primary factor in the marked attenuation of delay discounting in aged rats.

### 3.7. Experiment 5

To determine general motivation to work for food (particularly under conditions of high response ratios, which are necessarily correlated with delayed reward delivery),

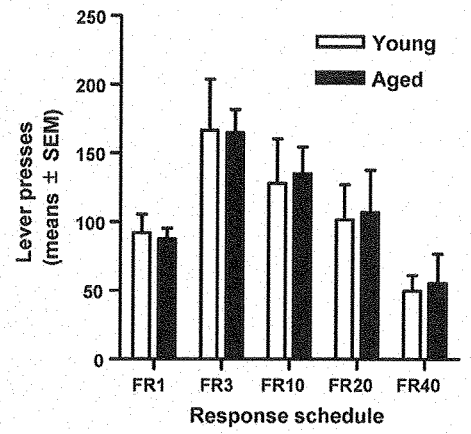


Fig. 6. Fixed ratio responding (Experiment 5). Aged rats performed comparably to young adult rats across a range of free-operant fixed ratio schedules of responding for single food pellets, suggesting that aged and young adult rats were similarly motivated to respond for and obtain the food reward used in the delay discounting task.

rats were placed in a new testing environment and given the opportunity to press a single lever (located above the food trough) to obtain food pellets. Rats were initially tested under a fixed ratio 1 (FR1) schedule, on which one lever press was required for food delivery, and the response ratio requirement was increased in subsequent daily sessions. Comparisons of the total number of lever presses in each session in young adult and aged rats revealed no differences between groups on performance under any response ratio ($t_s < .30$, $p_s > .79$), demonstrating that young adult and aged rats were similarly able and motivated to perform the lever-pressing responses involved in the delay discounting task (Fig. 6).

## 4. Discussion

The results of these experiments demonstrate that aged Fischer 344 rats show significantly attenuated discounting of delayed rewards compared to young adult cohorts (i.e., aged rats prefer large delayed over small immediate rewards to a greater extent than young adult rats). This attenuated delay discounting was not likely due to increased perseverative responding or age-related changes in motivation or perception of reward or delay magnitude, as aged rats performed comparably with young adults on several control tasks. This difference was also not likely due to especially steep delay discounting in the young adult rats. Although adolescents are reported to discount delayed rewards more steeply than adults, the young adult rats began these experiments at 6 months of age, which is well beyond the age at which rats are considered to be sexually mature (Brenhouse et al., 2008; Green et al., 1996). These findings suggest that age-related changes in decision-making observed in humans are not solely due to experiential and life-history factors, and that such changes can be effectively modeled in rodents (Denburg et al., 2005; Green et al., 1994, 1996; Lamar and Resnick, 2004).

The main finding from this series of experiments (depicted in Fig. 1) is that in comparison to young adult rats, aged rats reliably and robustly prefer a large, delayed reward over a smaller, immediate reward. Despite this clear age difference, of some initial concern was the fact that aged rats made fewer overall responses than young adult rats (i.e., had more omissions), particularly during the later trial blocks on which the greatest age differences were observed. This increase in omissions over the course of the sessions could be due to satiation, fatigue, or frustration with the long delays, which might have skewed the results to produce the observed difference in choice behavior. Two additional analyses were conducted to specifically address these possibilities. First, total food consumption per session was assessed for each group and found to be identical. Thus, although satiation earlier in the session may have caused the increased omissions in aged rats, such satiation seemed to be a consequence, rather than a cause of their choice behavior, as aged rats' satiation threshold was similar to that of young adults (at least to the extent examined here). Second, in Experiment 2 the order of presentation of the delays until large reward delivery was reversed such that the block of trials with the longest delay in Experiment 1 (during which aged rats had the most omissions) was presented first (Fig. 3). Both young adult and aged rats displayed the same patterns of omitted trials during these sessions as in Experiment 1 (i.e., increasing numbers of omissions as the session progressed), although in this reversed delay order condition, the majority of omissions occurred in blocks with the *shortest* delay. These data strongly suggest that the omissions observed at the longest delay in Experiment 1 were unrelated to the delay duration. Most importantly, the same age differences in delay discounting were observed when the order of delays was reversed, indicating that these differences were not an artifact of trial omissions. The failure of both young adult and aged rats to reach the high levels of % choice of the large reward at the 0-s delay during Experiment 2 was likely due to some perseverative choice of the small reward lever in both groups, and is consistent with the findings of Cardinal et al. (2000) under these reversal conditions.

Aging has been associated with changes in time perception, in that subjective time appears to pass more slowly for aged compared to young adult humans (Block et al., 1998). Similarly, aged rats tested in a peak interval procedure show judgments of 20 and 40 s time intervals that are longer than those of young adult rats (Lejeune et al., 1998; Meck et al., 1986). This subjectively slower passage of time associated with aging would be predicted to bias aged rats away from choice of the delayed reward (Wittmann and Paulus, 2008). However, the aged rats in the present experiments chose the delayed reward *more* frequently than young adult rats, suggesting that reported alterations in time perception in aging do not account for the altered discounting of delayed rewards. Further evidence against age-related differences in time perception is provided by the results of Experiment 3, in which

aged rats were able to detect and respond appropriately to the delays to the same degree as young adult rats when the delays were maintained but the reward sizes made equal (i.e., they consistently chose the non-delayed over the delayed reward). This control procedure suggests that gross insensitivity to delays does not account for the attenuated delay discounting in aged rats, although more subtle impairments related to time perception are possible. Indeed, the fact that young adult and aged rats differed in delay discounting task performance suggests that *some* aspect of delay processing differed across ages. Interestingly, Niv et al. (2007) have suggested that tonic dopamine levels in striatum encode the subjective value of time. By this hypothesis, decreased tonic dopamine levels would result in time being valued less, leading to a reduction in the subjective costs of choosing the large delayed reward. In support of this idea, reductions in dopaminergic markers have been reported in aged rats, suggesting that age-related alterations in dopamine signaling are one possible mechanism that could contribute to the observed results (Burwell et al., 1995).

The results of several control experiments also suggest that alterations in reward perception and/or motivation do not account for the effects of aging on delay discounting. Although delay discounting is regulated by reward magnitude, level of hunger (Bradshaw and Szabadi, 1992; Wogar et al., 1992), and food metabolism, which can be altered significantly in aging (Kiang-Ulrich and Horvath, 1984; Speakman et al., 2002), when the delays to large reward delivery were eliminated (Experiment 4), aged rats chose the large reward to the same extent as young adults. These data indicate comparable perception and reaction to these differences in reward magnitude in the two groups. Moreover, in Experiment 5, young adult and aged rats had equivalent levels of instrumental responding under various fixed ratio schedules, demonstrating equivalent motivation to work for and obtain food rewards, even under high ratios of responding which imposed substantial delays between initiation of lever-pressing and food delivery.

In the delay discounting task, learning about the relationship between the large reward lever and the delayed reward with which it is associated, and subsequent choice of that lever, would be presumed to require maintenance of some representation of the large reward outcome across the delay preceding its delivery (Hinson et al., 2003). Indeed, maintenance of such outcome representations across delays can be impaired in aging (Knuttinen et al., 2001; McEchron et al., 2004). However, impairments in the ability to learn and utilize associations between the large reward lever and the delayed reward itself would be expected to bias responding *away* from choice of the large reward. Because aged rats chose the large delayed reward more often than young adult cohorts, such impairments do not likely account for the attenuated delay discounting reported here.

Performance on this delay discounting task is mediated by a network of limbic-striatal brain structures, including orbitofrontal cortex (OFC), basolateral amygdala, ventral striatum, and subthalamic nucleus, as well as their dopaminergic and serotonergic innervation (Cardinal, 2006; Cardinal et al., 2001; Winstanley et al., 2005, 2004, 2006b). In particular, lesions of OFC can decrease discounting of delayed rewards in the task used here (although this effect may depend on pre-lesion training on the task (Mobini et al., 2002; Winstanley et al., 2004)), and OFC is compromised with age in both rats and humans (Convit et al., 2001; Lamar et al., 2004; Schoenbaum et al., 2002, 2006). One behavioral function ascribed to OFC is assignment of motivational value to rewards under conditions in which this value changes rapidly (Fellows, 2007; Kim and Ragozzino, 2005; Pickens et al., 2003; Roesch et al., 2007). Because "normal" performance in the delay discounting task involves tracking the changing reward value as the delays change across a session and modifying responses accordingly, age-related impairments in these abilities could result in increased choice of the large reward at longer delays (indeed, some evidence suggests that a subpopulation of aged humans is impaired in tracking changes in reward value (Deakin et al., 2004; Denburg et al., 2005; Fein et al., 2007; Lamar and Resnick, 2004)). Note, however, that the pattern of results in the aged rats is not consistent with simple perseverative responding on the large reward lever. There was no evidence for increased perseverative responding in aged compared to young adult rats after the order of presentation of the delays was reversed (i.e., the slopes of their performance curves are similar in Fig. 3B), and young adult and aged rats modified their choice behavior at similar rates in response to each change in the task contingencies. It should be noted, however, that although attenuated delay discounting in the aged rats was clearly advantageous under the task contingencies employed here (i.e., it resulted in more food delivery earlier in the session), it could likely prove maladaptive in other situations, particularly when behavioral flexibility provides superior advantage (Schoenbaum et al., 2002).

The results of these experiments provide strong evidence that discounting of delayed rewards is attenuated in aging. Several control procedures suggest that this attenuated discounting is not due to age-related alterations in time perception, motivation, or perseveration. These findings are consistent with the idea that aging is associated with increased ability to delay gratification (i.e., "good things come to those who wait"). The fact that these findings were obtained in laboratory rats (which, unlike humans, have limited prior opportunities to learn about the benefits of delayed gratification) suggests that attenuated delay discounting results not solely from experiential factors, but also (or instead) from fundamental age-related neurobiological changes. Of course, it is not possible even in animal subjects to rule out entirely the influence of prior experience on decision-making, as even the controlled and relatively impoverished environment of laboratory housing could conceivably provide opportunities for learning to delay gratification. Nevertheless, the results

clearly show that decision-making tasks used in humans can be effectively and robustly modeled in aged rodents, which will enable future investigation of the neural basis of altered decision-making across the lifespan.

## Conflicts of interest

None.

## Acknowledgements

We thank Atasi Bhavsar and Deepa Ramamurthi for technical assistance. Supported by AG029421 (JLB & BS), DA023331 (NWS), NS059324 (CLL), and MH65728 (IAM) from the National Institutes of Health.

## References

Ainslie, G., 1975. Specious reward: a behavioral theory of impulsiveness and impulse control. Psychological Bulletin 82, 463–496.

Bickel, W.K., Odum, A.L., Madden, G.J., 1999. Impulsivity and cigarette smoking: delay discounting in current, never, and ex-smokers. Psychopharmacology 146, 447–454.

Bizon, J.L., LaSarge, C.L., Montgomery, K.S., McDermott, A.N., Setlow, B., Griffith, W.H., in press. Spatial reference and working memory across the lifespan of male Fischer 344 rats. Neurobiology of Aging (Epub ahead of print).

Block, R.A., Zakay, D., Hancock, P.A., 1998. Human aging and duration judgments: a meta-analytic review. Psychology and Aging 1998, 584–596.

Bradshaw, C.M., Szabadi, E., 1992. Choice between delayed reinforcers in a discrete-trials schedule: the effect of deprivation level. The Quarterly Journal of Experimental Psychology 44, 1–6.

Brenhouse, H.C., Sonntag, K.C., Andersen, S.L., 2008. Transient d1 dopamine receptor expression on prefrontal cortex projection neurons: relationship to enhanced motivational salience of drug cues in adolescence. The Journal of Neuroscience 28, 2375–2382.

Burwell, R.D., Lawler, C.P., Gallagher, M., 1995. Mesostriatal dopamine markers in aged Long–Evans rats with sensorimotor impairment. Neurobiology of Aging 16 (2), 175–186.

Cardinal, R.N., 2006. Neural systems implicated in delayed and probabilistic reinforcement. Neural Networks 19, 1277–1301.

Cardinal, R.N., Robbins, T.W., Everitt, B.J., 2000. The effects of D-amphetamine, chlordiazepoxide, α-flupenthixol and behavioural manipulations on choice of signaled and unsignaled delayed reinforcement in rats. Psychopharmacology 152, 362–375.

Cardinal, R.N., Pennicot, D.R., Sugathapala, C.L., Robbins, T.W., Everitt, B.J., 2001. Impulsive choice induced in rats by lesions of the nucleus accumbens core. Science 292, 2499–2501.

Clark, L., Cools, R., Robbins, T.W., 2004. The neuropsychology of ventral prefrontal cortex: decision-making and reversal learning. Brain and Cognition 55, 41–53.

Convit, A., Wolf, O.T., de Leon, M.J., Patalinjug, M., Caraos, C., Scherer, A., Saint Louis, L.A., Cancro, R., 2001. Volumetric analysis of the prefrontal regions: findings in aging and schizophrenia. Psychiatry Research 107, 61–73.

Deakin, J.F., Aitken, M., Robbins, T.W., Sahakian, B.J., 2004. Risk taking during decision-making in normal volunteers changes with age. Journal of the International Neuropsychological Society 10, 590–598.

Denburg, N.L., Tranel, D., Bechara, A., 2005. The ability to decide advantageously declines prematurely in some normal older persons. Neuropsychologia 43, 1099–1106.

Dixon, M.R., Marley, J., Jacobs, E.A., 2003. Delay discounting by pathological gamblers. Journal of Applied Behavior Analysis 36, 449–458.

Evenden, J.L., Ryan, C.N., 1996. The pharmacology of impulsive behavior in rats: the effects of drugs on response choice with varying delays of reinforcement. Psychopharmacology 128, 161–170.

Fein, G., McGillivray, S., Finn, P., 2007. Older adults make less advantageous decisions than younger adults: cognitive and psychological correlates. Journal of the International Neuropsychological Society 13, 480–489.

Fellows, L.K., 2007. The role of orbitofrontal cortex in decision making: a component process account. Annals of the New York Academy of Sciences (Epub ahead of print).

Federal Interagency Forum on Aging-Related Statistics, September 25, 2005. Older Americans 2004: Key Indicators of Well-Being. <http://www.agingstats.gov/chartbook2004/population.html> (accessed September 25, 2005).

Frick, K.M., Baxter, M.G., Markowska, A.L., Olton, D.S., Price, D.L., 1995. Age-related spatial reference and working memory deficits assessed in the water maze. Neurobiology of Aging 16 (2), 149–160.

Green, L., Fry, A.F., Myerson, J., 1994. Discounting of delayed rewards: a life-span comparison. Psychological Science 5, 33–36.

Green, L., Myerson, J., Lichtman, D., Rosen, S., Fry, A., 1996. Temporal discounting in choice between delayed rewards: the role of age and income. Psychology and Aging 11, 79–84.

Hinson, J.M., Jameson, T.L., Whitney, P., 2003. Impulsive decision making and working memory. Journal of Experimental Psychology Learning, Memory, and Cognition 29, 298–306.

Kiang-Ulrich, M., Horvath, S.M., 1984. Age-related metabolic modifications in male F344 rats. Experimental Aging Research 10, 89–93.

Kim, J., Ragozzino, M.E., 2005. The involvement of the orbitofrontal cortex in learning under changing task contingencies. Neurobiology of Learning and Memory 83, 125–133.

Kirby, K.N., Petry, N.M., 2004. Heroin and cocaine abusers of higher discount rates for delayed rewards than alcoholics or non-drug-using controls. Addiction 99, 461–471.

Knuttinen, M.G., Gamelli, A.E., Weiss, C., Power, J.M., Disterhoft, J.F., 2001. Age-related effects in eyeblink conditioning in the F344 × BN F1 hybrid rat. Neurobiology of Aging 22, 1–8.

Lamar, M., Resnick, S.M., 2004. Aging and prefrontal functions: dissociating orbitofrontal and dorsolateral issues. Neurobiology of Aging 25, 553–558.

Lamar, M., Yousem, D.M., Resnick, S.M., 2004. Age differences in orbitofrontal activation: an fMRI investigation of delayed match and nonmatch to sample. Neuroimage 21, 1368–1376.

LaSarge, C.L., Montgomery, K.S., Tucker, C., Slaton, G.S., Griffith, W.H., Setlow, B., Bizon, J.L., 2007. Deficits across multiple cognitive domains in a subset of aged Fischer 344 rats. Neurobiology of Aging 28 (6), 928–936.

Lejeune, H., Ferrara, A., Soffie, M., Bronchart, M., Weardon, J.H., 1998. Peak procedure performance in young adult and aged rats: acquisition and adaptation to a changing temporal criterion. The Quarterly Journal of Experimental Psychology 51, 193–217.

McEchron, M.D., Cheng, A.Y., Gilmartin, M.R., 2004. Trace fear conditioning is reduced in the aging rat. Neurobiology of Learning and Memory 82, 71–76.

Meck, W.H., Church, R.M., Wenk, G.L., 1986. Arginine vasopressin innoculates against age-related increases in sodium-dependent high affinity choline uptake and discrepancies in the content of temporal memory. European Journal of Pharmacology 130, 327–331.

Mobini, S., Body, S., Ho, M.-Y., Bradshaw, C.M., Szabadi, E., Deakin, J.F.W., Anderson, I.M., 2002. Effects of lesions of the orbitofrontal cortex on sensitivity to delayed and probabilistic reinforcement. Psychopharmacology 160, 290–298.

Niv, Y., Daw, N., Joel, D., Dayan, P., 2007. Tonic dopamine: opportunity costs and the control of response vigor. Psychopharmacology 191 (3), 507–520.

Petry, N.M., 2001a. Delay discounting of money and alcohol in actively using alcoholics, currently abstinent alcoholics, and controls. Psychopharmacology 154, 243–250.

Petry, N.M., 2001b. Pathological gamblers, with and without substance use disorders, discount delayed rewards at high rates. Journal of Abnormal Psychology 110, 482–487.

Pickens, C.L., Saddoris, M.P., Setlow, B., Gallagher, M., Holland, P.C., Schoenbaum, G., 2003. Different roles for orbitofrontal cortex and basolateral amygdala in a reinforcer devaluation task. The Journal of Neuroscience 23, 11078–11084.

Rachlin, H., Green, L., 1972. Commitment, choice, and self-control. Journal of the Experimental Analysis of Behavior 17, 15–22.

Roesch, M.R., Calu, D.J., Burke, K.A., Schoenbaum, G., 2007. Should I stay or should I go? Transformation of time-discounted rewards in orbitofrontal cortex and associated brain circuits. Annals of the New York Academy of Sciences 1104, 21–34.

Schoenbaum, G., Nugent, S.L., Saddoris, M.P., Gallagher, M., 2002. Teaching old rats new tricks: age-related impairments in olfactory reversal learning. Neurobiology of Aging 13, 885–890.

Schoenbaum, G., Setlow, B., Saddoris, M.P., Gallagher, M., 2006. Encoding changes in orbitofrontal cortex in reversal-impaired aged rats. The Journal of Neurophysiology 95, 1509–1517.

Simon, N.W., Mendez, I.A., Setlow, B., 2007. Cocaine exposure causes long term increases in impulsive choice. Behavioral Neuroscience 121, 543–549.

Sozou, P.D., Seymour, R.M., 2003. Augmented discounting: interaction between ageing and time-preference behaviour. In: Proceedings of the Royal Society of London Series B: Biological Sciences, vol. 270, pp. 1047–1053.

Speakman, J.R., Selman, C., McLaren, J.S., Harper, E.J., 2002. Living fast, dying when? The link between aging energetics. The Journal of Nutrition 132, 1583S–1597S.

West, R.L., 1996. An application of prefrontal cortex function theory to cognitive aging. Psychological Bulletin 120, 272–292.

Winstanley, C.A., Theobald, D.E.H., Cardinal, R.N., Robbins, T.W., 2004. Contrasting roles of basolateral amygdala and orbitofrontal cortex in impulsive choice. The Journal of Neuroscience 24, 4718–4722.

Winstanley, C.A., Baunez, C., Theobald, D.E.H., Robbins, T.W., 2005. Lesions to the subthalamic nucleus decrease impulsive choice but impair autoshaping in rats: the importance of the basal ganglia in Pavlovian conditioning and impulse control European. Journal of Neuroscience 21, 3107–3116.

Winstanley, C.A., Eagle, D.M., Robbins, T.W., 2006a. Behavioral models of impulsivity in relation to ADHD: Translation between clinical and preclinical studies. Clinical Psychology Review 26, 379–395.

Winstanley, C.A., Theobald, D.E.H., Dalley, J.W., Cardinal, R.N., Robbins, T.W., 2006b. Double dissociation between serotonergic and dopaminergic modulation of medial prefrontal and orbitofrontal cortex during a test of impulsive choice. Cerebral Cortex 16, 106–114.

Wittmann, M., Paulus, M.P., 2008. Decision making, impulsivity and time perception. Trends in Cognitive Sciences 12 (1), 7–12.

Wogar, M.A., Bradshaw, C.M., Szabadi, E., 1992. Choice between delayed reinforcers in an adjusting-delay schedule: the effects of absolute reinforcer size and deprivation level. Quarterly Journal of Experimental Psychology B: Comparative and Physiological Psychology 45, 1–13.

Yu, B.P., Masoro, E.J., Murata, I., Bertrand, H.A., Lynd, F.T., 1982. Life span study of SPF Fischer 344 male rats fed ad libitum or restricted diets: longevity, growth, lean body mass and disease. Journal of Gerontology 37, 130–141.

Society for Neuroscience Presentation Abstract

Program#/Poster#: 710.10/NNN10

Title: Enrichment concomitantly improves hippocampal neurogenesis and spatial memory in aged rats

Location: Halls B-H

Time: Tuesday, Nov 16, 2010, 2:00 PM - 3:00 PM

Authors: ***R. B. SPEISMAN**[1], A. KUMAR[2], A. RANI[2], J. E. SEVERANCE[3], T. C. FOSTER[2], B. K. ORMEROD[1];
[1]J. Crayton Pruitt Family Dept. of Biomed. Engin., [2]Dept. of Neuroscience, McKnight Brain Inst., [3]Univ. of Florida, Gainesville, FL

Abstract: Recent work has demonstrated that cognition declines in some aged rodents and hippocampal neurogenesis declines with age. However, the relationship between these phenomena across age is only beginning to be explored. We examined whether changes in hippocampal neurogenesis across age relate to mnemonic ability in the Morris water maze, a task sensitive to age-related cognitive decline. We also explored whether daily exposure to an enriched environment protected neurogenesis and/or spatial ability from the effects of age. Young (5-8 mo; n = 14) and aged (22-24 mo; n = 16) male Fischer 344 rats (NIA colony at Harlan) were kept in standard single-housing with the exception that some rats were exposed to an enriched environment for 2h per day (n = 7 young, 9 aged) for the duration of the 10 week-long experiment. At the end of week 5, the rats were trained and tested on a short version of the Morris water maze and then given 5 daily injections of the cell synthesis marker bromodeoxyuridine (BrdU, 50mg/kg; i.p.). After 10 weeks, all rats were perfused and their hippocampal tissue processed immunohistochemically to quantify new cells (using light microscopy and stereology) and their phenotypes (using confocal microscopy). We found no effect of age and/or exposure to an enriched environment on total new (BrdU-immunoreactive) cell number. Total new neuron (BrdU- and DCX- and/or NeuN-immunoreactive) number decreased ($p = 0.00002$) and new glia (BrdU- and GFAP- or NG2-immunoreactive) number increased ($p = 0.009$) with age. However, age interacted with enrichment such that enrichment protected neurogenesis from the effects of age ($p = 0.05$). Although, strength of learning probes (conducted immediately after training trials) showed that all rats had learned the platform position similarly, older rats had trouble remembering the platform position 24h later ($p = 0.008$). However, we found a statistically significant positive correlation between new neuron number and scores on the memory probe conducted 24h after training ($p \leq 0.02$). Our data show that neurogenesis decreases and gliogenesis increases with age and that older rats exhibit poorer spatial memory after massed training trials than young rats. Daily exposure to an enriched environment protects neurogenesis from the effects of age and rats with more new neurons (regardless of age) exhibited better spatial memory. These data suggest that consideration of within-groups variability plays an important role in understanding the link between neurogenesis and performance across behavioral tasks.

Dennis A. Steindler, Ph.D.

There have been numerous studies in rodents relating the generation of new neurons, or "neurogenesis", in the hippocampus to cognition incuding memory functions. Until this study, the impact of neurogenesis on cognition in humans has remained relatively unexplored. This is the first study to look at adult human neural stem/progenitor cells, that our laboratory discovered in 2006, in patients undergoing temporal lobectomy for intractable epilepsy. These cells were isolated from surgical resection specimens from 23 patients who also underwent memory testing during the resection procedure and showed that the number of neural stem/progenitor cells and their ability to generate new neurons correlated exactly with the memory capacity of the tested subjects; e.g. patients with low neural stem/progenitor cell proliferation capacity stem cells showed severe learning and memory impairment. Even though additional studies are needed to resolve certain aspects of causality with regard to altered neurogenesis, abnormal circuitry behaviors in seizure disorders and memory functions, these findings point to a potentially highly important relationship between human neurogenesis and one's ability to acquire and recall new memories. In light of a very recent study (Pieper et al, Cell 142:39-51, 2010) reporting the discovery of a neuroprotective, pro-neurogenic compound "P7C3" that showed enhanced neurogenesis in the rodent hippocampus that appears to preserve cognitive capacity during aging, the findings presented in our paper support a notion that new pharmacological therapeutics aimed at human hippocampal neurogenesis may be useful for memory enhancement following age-related cognitive decline.

*HIPPOCAMPUS 20:1047–1060 (2010)*

# Aging Alters the Expression of Genes for Neuroprotection and Synaptic Function Following Acute Estradiol Treatment

Kristina K. Aenlle and Thomas C. Foster*

**ABSTRACT: This study used microarray analysis to examine age-related changes in gene expression 6 and 12 h following a single estradiol injection in ovariectomized mice. Estradiol-responsive gene expression at the 6 h time point was reduced in aged (18 months) animals compared with young (4 months) and middle-aged (MA, 12 months) mice. Examination of gene clustering within biological and functional pathways indicated that young and MA mice exhibited increased expression of genes for cellular components of the synapse and decreased expression of genes related to oxidative phosphorylation and mitochondrial dysfunction. At the 12 h time point, estradiol-responsive gene expression increased in aged animals and decreased in young and MA mice compared with the 6 h time point. Gene clustering analysis indicated that aged mice exhibited increased expression of genes for signaling pathways that are rapidly influenced by estradiol. The age differences in gene expression for rapid signaling pathways may relate to disparity in basal pathway activity and estradiol mediated activation of rapid signaling cascades.** © 2009 Wiley-Liss, Inc.

**KEY WORDS: estrogen; hippocampus; microarray; signaling**

## INTRODUCTION

In humans, age-related impairments in hippocampal-dependent memory begin in middle-age and cognitive weakening continues with advancing age (Small et al., 1999; Foster, 2006). Estrogen treatment in women (Sherwin, 2006), nonhuman primates (Lacreuse et al., 2002; Rapp et al., 2003), and rodents (Markham et al., 2002; Foster et al., 2003; Aenlle et al., 2009) has been shown to protect against cognitive decline. However, it is becoming apparent that estradiol treatment initiated late in life is less effective (Adams et al., 2001; Foster et al., 2003; Daniel et al., 2006; Sherwin and Henry, 2008).

The mechanism for differential estradiol effects across the lifespan is unclear. In younger animals, estradiol has numerous effects on the hippocampus that could provide a mechanism for improved cognition. For example, estradiol can rapidly activate signaling pathways for neuroprotection (Kuroki et al., 2001; Guerra et al., 2004; Wu et al., 2005; Jover-Mengual et al., 2007; Sarkar et al., 2008) and synaptogenesis (Akama and McEwen, 2003; Mukai et al., 2007) and estradiol effects on neuroprotection and synaptogenesis may be impaired in aged animals (Miranda et al., 1999; Adams et al., 2001; Brinton, 2008; Yildirim et al., 2008) suggesting a possible breakdown in estrogen signaling.

To determine whether the age differences in synaptogenesis and neuroprotection result from a weakening of the signaling pathways, we investigated differences in gene expression following an acute estradiol treatment. In vitro (Carroll et al., 2006; Schnoes et al., 2008) and in vivo studies (Fertuck et al., 2003; Naciff et al., 2007; Pechenino and Frick, 2009) have provided evidence for distinct temporal patterns of estrogen-mediated gene expression. In general, genes related to the regulation of transcription are altered within the first 2 h of treatment. Protein changes associated with this early transcription contribute to the amplification in the number of altered genes occurring between 4 and 12 h. Furthermore, this second wave of altered genes expression, between 4 and 12 h, includes genes related to the functional effects of estrogen treatment for specific cell systems. Therefore, 17β-estradiol was injected in ovariectomized mice and estradiol-responsive genes were identified by transcript profiling at 6 and 12 h after treatment. Pathway analysis of estradiol-responsive genes identified age-related differences in functional pathways related to oxidative phosphorylation, synaptic plasticity, and estrogen responsive signaling cascades.

## MATERIALS AND METHODS

### Subjects

Procedures involving animal subjects have been reviewed and approved by the Institutional Animal Care and Use Committee at the University of Florida and were in accordance with guidelines established by the U.S. Public Health Service Policy on Humane Care and Use of Laboratory Animals. Initially 85 female C57/BL6 mice were obtained from National Institute of Aging for gene array analysis, with one gene chip per animal. However, quality controls for gene arrays indicate that five chips were outliers and the data for these animals were removed from further analysis. Therefore, a total of 80 female mice (young: $n$ = 26, 4 months; middle-aged: $n$ = 26, 12 months; aged: $n$ = 28, 18 months) were

**Department of Neuroscience, McKnight Brain Institute, University of Florida, Gainesville, Florida**
Grant sponsor: NIA; Grant numbers: AG02499, AG14979; Grant sponsor: NIMH; Grant number: 059891; Grant sponsor: Evelyn F. McKnight Brain Research Foundation.
*Correspondence to: Thomas C. Foster, Department of Neuroscience, McKnight Brain Institute, University of Florida, PO Box 100244, Gainesville, FL 32610-0244. E-mail: Foster@mbi.ufl.edu
Accepted for publication 30 July 2009
DOI 10.1002/hipo.20703
Published online 29 September 2009 in Wiley Online Library (wileyonlinelibary.com).

*TABLE 1.*

*Context Sequence of Genes for RT-PCR Analysis*

| Gene symbol | Assay ID | Context sequence |
|---|---|---|
| WDFY1 | Mm00840455_m1 | GGGGTGTGATGGAATTTCACGTTT |
| GABRA2 | Mm01211683_m1 | CGGGAAGAGTGTAGTCAATGACAAG |
| NNT | Mm01298455_m1 | GCCAACATCTCTGGTTATAAGGCTG |
| PPARGC1A | Mm00447183_m1 | CGCAACATGCTCAAGCCAAACCAAC |
| ATF4 | Mm00515324_m1 | GCCATGGCGCTCTTCACGAAATCCA |
| ENTPD4 | Mm00491888_m1 | TTCCTGCCCTTGAGAGACATCCGGC |
| GAPDH | Mm99999915_g1 | GAACGGATTTGGCCGTATTGGGCGC |

employed in this study. Animals were housed three to five per cage and maintained on 12:12 light–dark cycle (lights on at 6 a.m.). Following 1-week habituation, mice were anesthetized (2 mg ketamine and 0.2 mg xylazine per 20 g of body weight) and ovaries were removed through a small midline incision on the abdomen. All mice received ad lib access to food (Purina mouse chow, St Louis, MO) and water, until the surgery when they were placed on Casein based chow (Cincinnati Lab Supply, Cincinnati, OH), which is low in phytoestrogens found in soy based chow.

## Hormone Administration

Briefly, a single injection of 17β-estradiol (Sigma Chemical Co, St Louis, MO) or mineral oil was initiated 10 days after ovariectomy (OVX) at 10 p.m. or 4 a.m. To control for time of day effects, all animal were sacrificed between 10 and 11 a.m., ~4 h after lights on and either 6 h (injection at 4 a.m.) or 12 h (injection at 10 p.m.) following the injection of estradiol or oil. Estradiol was dissolved in light mineral oil (Fisher Scientific, Pittsburgh, PA) to concentration of 0.1 mg/ml. Oil or estradiol (5 μg) in oil was injected subcutaneously at the nape of the neck in volumes of 0.05 ml. The groups included: young receiving oil and sacrificed 6 h ($n$ = 5) and 12 h ($n$ = 3) later; young receiving estradiol and sacrificed 6 h ($n$ = 10) and 12 h ($n$ = 8) later; middle-aged receiving oil and sacrificed 6 h ($n$ = 5) and 12 h ($n$ = 6) later; middle-aged receiving estradiol and sacrificed 6 h ($n$ = 9) and 12 h ($n$ = 6) later; aged receiving oil and sacrificed 6 h ($n$ = 5) and 12 h ($n$ = 7) later; aged receiving estradiol and sacrificed 6 h ($n$ = 9) and 12 h ($n$ = 7) later. To determine effectiveness of estradiol treatment, uteri were excised at the time of sacrifice and weighed immediately. An analysis of variance (ANOVA) was used to compare main effects on uterine weight.

At the time of sacrifice, each animal was anesthetized with $CO_2$ and decapitated. The brain was quickly removed and placed in ice-cold artificial cerebral spinal fluid. Both hippocampus were removed, frozen in liquid nitrogen, and stored at −80°C. RNA was isolated from each sample using Qiagen RNeasy Lipid Tissue Mini Kit (Qiagen, Germantown, MD). RNA concentration was determined using spectrophometer and a subset of samples was examined using Agilent 2,100 Bioanalyzer (Santa Clara, CA). Microarray analysis was performed for individual animals (one chip per animal).

## Microarray Hybridization and Signal Detection

An amount of 5 μg of total RNA was synthesized to cRNA using Affymetrix amplification kit following the manufacture's protocol. Hybridization of cRNA was carried out by the Interdisciplinary Center for Biotechnology Research Microarray

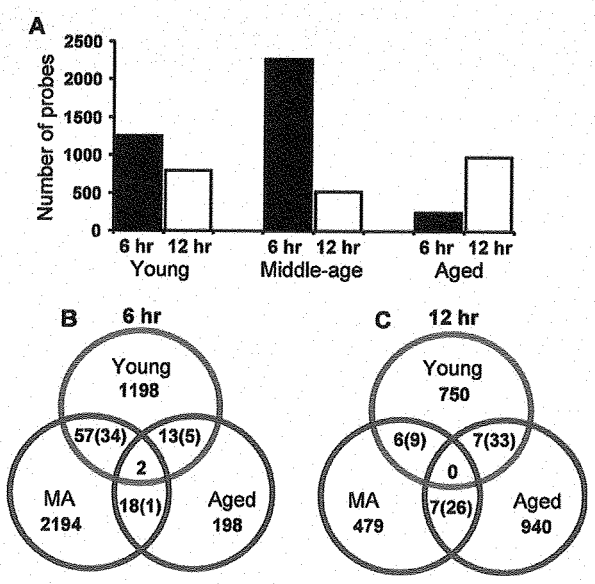


**FIGURE 1. Estradiol-responsive gene expression is altered over the course of aging. (A) Illustration of the number of probes that were increased or decreased by estradiol treatment in young (Young), middle-aged (MA), and aged (Aged) animals at 6 h (filled bars) or 12 h (open bars) after a single estradiol injection. MA animals exhibited over two times the number of altered probes at 6 h relative to the other two age groups. The number of altered probes decreased at 12 h relative to 6 h for young and MA animals. In contrast, aged animals exhibited approximately a fivefold increase in the number of estradiol-responsive probes during this time period. (B and C) Venn diagrams of the number of differentially expressed probes in response to estradiol treatment at (B) 6 h and (C) 12 h. The numbers in parentheses represent probes that changes in opposite directions.**

*Hippocampus*

*TABLE 2.*

*Synaptic Component Genes Increased at 6 h in Young and MA Mice*

| Affymetrix | Symbol | Description | *P* value | Fold |
|---|---|---|---|---|
| Young | | | | |
| 1458298_at | CADPS | $Ca^{2+}$ dependent activator protein for secretion | 1.58E-02 | 1.20 |
| 1443876_at | CAMK2A | Calcium/calmodulin-dependent protein kinase II alpha | 1.00E-02 | 1.19 |
| 1423286_at | CBLN1 | Cerebellin 1 precursor protein | 1.33E-02 | 1.53 |
| 1433607_at | CBLN4 | Cerebellin 4 precursor protein | 9.86E-03 | 1.38 |
| 1433451_at | CDK5R1 | Cyclin-dependent kinase 5, regulatory subunit (p35) 1 | 1.49E-03 | 1.26 |
| 1422887_a_at | CTBP2 | c-terminal binding protein 2 | 9.81E-03 | 1.20 |
| 1442223_at | ENAH | Enabled homolog (drosophila) | 9.46E-03 | 1.20 |
| 1455444_at | GABRA2 | Gamma-aminobutyric acid receptor, subunit alpha 2 | 1.06E-06 | 2.75 |
| 1434098_at | GLRA2 | Glycine receptor, alpha 2 subunit | 1.29E-02 | 1.34 |
| 1458285_at | GRIA1 | Glutamate receptor, ionotropic, ampa1 (alpha 1) | 5.61E-03 | 1.34 |
| 1440891_at | GRIA4 | Glutamate receptor, ionotropic, ampa4 (alpha 4) | 1.55E-02 | 1.48 |
| 1436575_at | GRIN3A | Glutamate receptor ionotropic, nmda3a | 1.35E-02 | 1.20 |
| 1435951_at | GRIP1 | Glutamate receptor interacting protein 1 | 4.60E-03 | 1.20 |
| 1437363_at | HOMER1 | Homer homolog 1 (drosophila) | 1.94E-02 | 1.19 |
| 1417376_a_at | IGSF4A | Immunoglobulin superfamily, member 4a | 1.19E-02 | 1.22 |
| 1450435_at | L1CAM | L1 cell adhesion molecule | 1.18E-02 | 1.15 |
| 1452328_s_at | PJA2 | Praja 2, ring-h2 motif containing | 1.78E-02 | 1.41 |
| Middle-age | | | | |
| 1439220_at | ANK3 | Ankyrin 3, epithelial | 1.93E-02 | 2.01 |
| 1458525_at | APP | Amyloid beta (a4) precursor protein | 2.94E-03 | 2.03 |
| 1445798_at | DLGH1 | Discs, large homolog 1 (drosophila) | 1.95E-02 | 1.74 |
| 1446585_at | DLGH2 | Discs, large homolog 2 (drosophila) | 1.32E-02 | 1.37 |
| 1429768_at | DTNA | Dystrobrevin alpha | 5.52E-03 | 1.27 |
| 1445329_at | DTNB | Dystrobrevin, beta | 5.79E-03 | 1.66 |
| 1446426_at | ENAH | Enabled homolog (drosophila) | 4.17E-03 | 1.85 |
| 1454022_at | EPHB2 | Eph receptor b2 | 9.43E-03 | 1.58 |
| 1458285_at | GRIA1 | Glutamate receptor, ionotropic, ampa1 (alpha 1) | 1.36E-02 | 1.37 |
| 1453098_at | GRIA2 | Glutamate receptor, ionotropic, ampa2 (alpha 2) | 1.27E-02 | 1.75 |
| 1443285_at | GRIA4 | Glutamate receptor, ionotropic, ampa4 (alpha 4) | 4.53E-03 | 2.08 |
| 1440602_at | GRIK2 | Glutamate receptor, ionotropic, kainate 2 (beta 2) | 6.52E-03 | 2.57 |
| 1421350_a_at | GRIP1 | Glutamate receptor interacting protein 1 | 1.69E-02 | 1.57 |
| 1458861_at | GRM7 | Glutamate receptor, metabotropic 7 | 2.12E-02 | 1.42 |
| 1440637_at | ITSN1 | Intersectin 1 (sh3 domain protein 1a) | 1.58E-02 | 1.75 |
| 1424848_at | KCNMA1 | Potassium large conductance calcium-activated channel | 9.27E-03 | 2.99 |
| 1440807_at | MAGI2 | Membrane associated guanylate kinase | 1.97E-03 | 2.90 |
| 1420171_s_at | MYH9 | Myosin, heavy polypeptide 9, nonmuscle | 1.25E-02 | 1.34 |
| 1422520_at | NEF3 | Neurofilament 3, medium | 2.28E-02 | 1.13 |
| 1447216_at | NRXN1 | Neurexin I | 1.37E-02 | 2.10 |
| 1457212_at | NRXN3 | Neurexin III | 9.69E-04 | 2.11 |
| 1444126_at | PJA2 | Praja 2, ring-h2 motif containing | 1.52E-04 | 2.07 |
| 1442620_at | PSD3 | Pleckstrin and sec7 domain containing 3 | 3.20E-04 | 2.12 |
| 1438282_at | SYT1 | Synaptotagmin I | 2.99E-03 | 2.02 |
| 1429729_at | SYT11 | Synaptotagmin 11 | 1.22E-02 | 1.88 |
| 1459009_at | UTRN | Utrophin | 2.27E-02 | 1.44 |

Core, University of Florida. Hybridization of Affymetrix Mouse 430 2.0 Arrays occurred for 17 h at 60°C in accordance with manufacture's instructions and arrays were scanned using an Affymetrix Microarray scanner. Images were analyzed using Affymetrix Gene Chip Operating System software (GCOS version 1.1) and scaled to 500. Hybridization signal intensities between GeneChips were normalized using dChip's (Li and Wong, 2001) model-based expression index with the PM-only model. The model was used to set thresholds for identify outlier probe sets. Arrays with a large number of outlier probe sets (>5% of total) were removed from further analysis. Data was then transferred into Microsoft excel for further analysis. Probe sets were annotated using Affymetrix® NetAffx™ (12/2,007).

TABLE 3.

*Estradiol-Responsive Pathways 6 h Posttreatment*

| Increasing | P value | Genes | Decreasing | P value | Genes |
|---|---|---|---|---|---|
| Young | | | | | |
| PPAR/RARa activation | 5.E-03 | 15 | Oxidative phosphorylation | 5.E-05 | 17 |
| Glutamate receptor signaling | 5.E-03 | 8 | Mitochondrial dysfunction | 1.E-03 | 14 |
| Circadian rhythm signaling | 1.E-02 | 4 | | | |
| Middle-age | | | | | |
| None | | | Oxidative phosphorylation | 1.E-05 | 24 |
| | | | Mitochondrial dysfunction | 5.E-03 | 18 |
| | | | Protein ubiquination pathway | 1.E-02 | 25 |
| Aged | | | | | |
| None | | | None | | |

## Real-Time PCR

Real-time PCR (RT-PCR) was performed to verify microarray results. RNA from each group was treated with Turbo DNAfree (Ambion, Austin, TX) to remove any remaining genomic DNA. RNA was then converted to cDNA using High Capacity cDNA Archive Kit (Applied Biosystems, Foster City, CA). Primers and probes for WDFY1, GABRA2, NNT, PPARGC1A, AFT4, ENTPD4 and GAPDH were purchased from Applied Biosystems. Briefly, 3 μg of total RNA from a single animal was incubated with appropriate reagents at 25°C for 10 min and then heated to 37°C for 120 min using 7,300 Fast Real-Time PCR System (Applied Biosystems). For relative quantification of RNA, 100 ng in 2.5 μl of cDNA was added to 12.5 μl of Taqman® Universal PCR Master Mix (2×), 1.25 μl of 20X Gene Expression Assay Mix, a probe specific primer mixture (Table 1), and 8.75 μl of nuclease-free water for a total volume of 25 μl. Thermal cycler conditions were set at 2 min at 50°C, 10 min at 95°C and cycles 15s at 95°C and 1 min at 60°C for 40 cycles. The point at which the fluorescence crosses the threshold (Ct) was determined using 7,300 Real-Time PCR System and SDS Software 1.3.1 analysis software (Applied Biosystems). Each sample was in triplicate and normalized to corresponding GAPDH values ($\Delta Ct_{sample}$) and then compared with normalized young oil ($\Delta Ct_{reference}$). The mean normalized values were compared using ΔΔCt method as described by Applied Biosystems to derive fold change (Aenlle et al., 2009), where ΔΔCt = (ΔCtsample) − (ΔCtreference).

## Statistical Analysis

Probe set filtering and initial statistical analysis was performed according to our previously published work (Blalock et al., 2003; Aenlle et al., 2009). Briefly, the number of present calls for each probe was determined across all chips and the probed was removed if fewer than 80% of the chips exhibited a present call for the probe. For all studies, differential expression was determined using two-tailed *t*-tests with the alpha level set at 0.025 in accordance with our previous studies (Blalock et al., 2003; Aenlle et al., 2009). The probes sets that exhibited an increase or decrease in expression following treatment were submitted to Ingenuity Pathway Analysis's (IPA; Ingenuity Systems). With alpha set at $P < 0.025$ we were able to obtain >800 molecules for generating networks, in accordance with IPA best practices for pathway analysis. The IPA program uses a right-tailed Fisher's exact test to compute the likelihood that the relationship between the list of submitted genes and a set of genes representing a given pathway is due to chance. A similar procedure was employed for determining overrepresentation of genes related to synaptic structure using the Expression Analysis Systematic Explorer (EASE) through the NIH DAVID Bioinformatics Resources (Hosack et al., 2003).

# RESULTS

For each age group, all animals treated with oil (young = 8, MA = 11, aged = 12) were used as controls to determine effects of treatment for age-matched animals sacrificed 6 h (young = 10, MA = 9, aged = 9) or 12 h (young = 8, MA = 6, aged = 7) after a single estradiol injection. To determine the effectiveness of the estradiol treatment uterine weight was compared across groups (young oil 20 ± 5 mg; young estradiol 6 h 54 ± 3 mg; young estradiol 12 h 50 ± 3 mg; middle-aged oil 30 ± 6 mg; middle-aged estradiol 6 h 52 ± 3 mg; middle-aged estradiol 12 h 43 ± 10 mg; aged oil 34 ± 4 mg; aged estradiol 6 h 56 ± 3 mg; aged estradiol 12 h 56 ± 4 mg). An ANOVA indicated an overall treatment effect ($P < 0.0001$) in the absence of an age differences and post hoc FLSD tests indicated a significant increase in uterine weight at 6 h ($P < 0.0001$) and 12 h ($P < 0.0001$) following treatment relative to oil treated controls.

*Hippocampus*

*TABLE 4.*

*Oxidative Phosphorylation and Mitochondrial Dysfunction Genes Altered at 6 h in Young and Middle-Aged Mice*

| Affymetrix | Symbol | Description | *P* value | Fold |
|---|---|---|---|---|
| Young | | | | |
| 1417607_at | COX6A2 | Cytochrome c oxidase subunit VIa polypeptide 2 | 4.53E-03 | −1.37 |
| 1424364_a_at | UCRC | Ubiquinol-cytochrome c reductase complex (7.2 kD) | 1.86E-02 | −1.31 |
| 1416057_at | NDUFB11 | NADH dehydrogenase (ubiquinone) 1 beta subcomplex, 11, 17.3 kDa | 1.98E-02 | −1.28 |
| 1417286_at | NDUFA5 | NADH dehydrogenase (ubiquinone) 1 alpha subcomplex, 5, 13 kDa | 9.06E-03 | −1.27 |
| 1454716_x_at | COX5B | Cytochrome c oxidase subunit Vb | 2.13E-02 | −1.25 |
| 1437680_x_at | GLRX2 | Glutaredoxin 2 | 7.65E-03 | −1.22 |
| 1423676_at | ATP5H (includes EG:10476) | ATP synthase, H+ transporting, mitochondrial F0 complex, subunit d | 2.48E-02 | −1.17 |
| 1453229_s_at | HCG 25371 | hCG25371 | 7.61E-03 | −1.16 |
| 1428360_x_at | NDUFA7 | NADH dehydrogenase (ubiquinone) 1 alpha subcomplex, 7, 14.5 kDa | 1.42E-02 | −1.16 |
| 1416526_a_at | PARK7 | Parkinson disease (autosomal recessive, early onset) 7 | 3.80E-03 | −1.16 |
| 1416495_s_at | NDUFS5 | NADH dehydrogenase (ubiquinone) Fe-S protein 5, 15 kDa (NADH-coenzyme Q reductase) | 2.01E-03 | −1.14 |
| 1428322_a_at | NDUFB10 (includes EG:4716) | NADH dehydrogenase (ubiquinone) 1 beta subcomplex, 10, 22 kDa | 3.85E-03 | −1.14 |
| 1455283_x_at | NDUFS8 | NADH dehydrogenase (ubiquinone) Fe-S protein 8, 23 kDa (NADH-coenzyme Q reductase) | 1.12E-02 | −1.14 |
| 1415980_at | ATP5G2 | ATP synthase, H+ transporting, mitochondrial F0 complex, subunit C2 (subunit 9) | 1.45E-02 | −1.13 |
| 1428075_at | NDUFB4 | NADH dehydrogenase (ubiquinone) 1 beta subcomplex, 4, 15 kDa | 3.76E-03 | −1.13 |
| 1426689_s_at | SDHA | succinate dehydrogenase complex, subunit A, flavoprotein (Fp) | 1.11E-02 | −1.11 |
| 1428179_at | NDUFV2 | NADH dehydrogenase (ubiquinone) flavoprotein 2, 24 kDa | 9.55E-03 | −1.10 |
| 1415966_a_at | NDUFV1 | NADH dehydrogenase (ubiquinone) flavoprotein 1, 51 kDa | 1.02E-02 | −1.07 |
| 1449622_s_at | ATP6AP1 | ATPase, H+ transporting, lysosomal accessory protein 1 | 1.66E-02 | −1.07 |
| Middle-age | | | | |
| 1429329_at | COX10 | COX10 homolog, cytochrome c oxidase assembly protein, heme A: farnesyltransferase (yeast) | 7.36E-04 | −1.38 |
| 1419544_at | ATP6V1C1 | ATPase, H+ transporting, lysosomal 42 kDa, V1 subunit c1 | 1.98E-02 | −1.32 |
| 1426742_at | ATP5F1 | ATP synthase, H+ transporting, mitochondrial F0 complex, subunit B1 | 9.93E-03 | −1.30 |
| 1415967_at | NDUFV1 | NADH dehydrogenase (ubiquinone) flavoprotein 1, 51 kDa | 3.37E-03 | −1.30 |
| 1428782_a_at | UQCRC1 | Ubiquinol-cytochrome c reductase core protein I | 3.35E-03 | −1.29 |
| 1455640_a_at | TXN2 | Thioredoxin 2 | 7.96E-03 | −1.29 |
| 1423711_at | NDUFAF1 | NADH dehydrogenase (ubiquinone) 1 alpha subcomplex, assembly factor 1 | 1.42E-03 | −1.27 |
| 1417799_at | ATP6V1G2 | ATPase, H+ transporting, lysosomal 13 kDa, V1 subunit G2 | 1.13E-02 | −1.25 |
| 1423737_at | NDUFS3 | NADH dehydrogenase (ubiquinone) Fe-S protein 3, 30 kDa (NADH-coenzyme Q reductase) | 5.67E-04 | −1.24 |
| 1451312_at | NDUFS7 | NADH dehydrogenase (ubiquinone) Fe-S protein 7, 20 kDa (NADH-coenzyme Q reductase) | 4.13E-03 | −1.23 |
| 1424488_a_at | PPA2 | pyrophosphatase (inorganic) 2 | 4.49E-04 | −1.23 |
| 1448331_at | NDUFB7 | NADH dehydrogenase (ubiquinone) 1 beta subcomplex, 7, 18 kDa | 8.45E-03 | −1.22 |
| 1450968_at | UQCRFS1 | Ubiquinol-cytochrome c reductase, Rieske iron-sulfur polypeptide 1 | 1.08E-02 | −1.22 |
| 1437013_x_at | ATP6V0B | ATPase, H+ transporting, lysosomal 21 kDa, V0 subunit b | 4.57E-03 | −1.21 |
| 1432264_x_at | COX7A2L | Cytochrome c oxidase subunit VIIa polypeptide 2 like | 1.44E-02 | −1.21 |
| 1448153_at | COX5A | Cytochrome c oxidase subunit Va | 2.60E-05 | −1.20 |
| 1448292_at | UQCR | Ubiquinol-cytochrome c reductase 6.4 kDa subunit | 2.33E-02 | −1.20 |
| 1448286_at | HSD17B10 | Hydroxysteroid (17-beta) dehydrogenase 10 | 4.13E-03 | −1.19 |
| 1448589_at | NDUFB5 | NADH dehydrogenase (ubiquinone) 1 beta subcomplex, 5, 16 kDa | 1.29E-03 | −1.18 |
| 1451096_at | NDUFS2 | NADH dehydrogenase (ubiquinone) Fe-S protein 2, 49 kDa (NADH-coenzyme Q reductase) | 4.95E-03 | −1.18 |
| 1428631_a_at | | ubiquinol-cytochrome c reductasecore protein II | 2.34E-02 | −1.17 |
| 1428179_at | NDUFV2 | NADH dehydrogenase (ubiquinone) flavoprotein 2, 24 kDa | 1.60E-03 | −1.16 |

*TABLE 4. (Continued).*

| Affymetrix | Symbol | Description | *P* value | Fold |
|---|---|---|---|---|
| 1416663_at | NDUFA9 (includes EG:4704) | NADH dehydrogenase (ubiquinone) 1 alpha subcomplex, 9, 39 kDa | 2.01E-03 | −1.16 |
| 1416952_at | ATP6V1D | ATPase, H+ transporting, lysosomal 34 kDa, V1 subunit D | 1.41E-02 | −1.16 |
| 1448203_at | ATP5L | ATP synthase, H+ transporting, mitochondrial F0 complex, subunit G | 7.34E-03 | −1.15 |
| 1415671_at | ATP6V0D1 | ATPase, H+ transporting, lysosomal 38 kDa, V0 subunit d1 | 1.19E-03 | −1.13 |
| 1428075_at | NDUFB4 | NADH dehydrogenase (ubiquinone) 1 beta subcomplex, 4, 15 kDa | 1.56E-02 | −1.12 |

## Age Differences in Estradiol-Responsive Genes for Synaptogenesis, and Neuroprotection 6 h After Treatment

Figure 1 illustrates the number of estradiol-responsive probes for the 6 and 12 h time points. At the 6 h time point the MA mice exhibited the greatest shift in gene expression with approximately twice as many probes exhibiting altered expression relative to young animals and approximately a 10-fold increase in the number of altered probes relative to aged mice. Age-related differences in the pattern of estradiol-responsive gene expression were also apparent. For probes that were observed to change expression at 6 h, young and MA mice exhibited increased expression for ~60% of the probes, while the majority (64%) of estradiol-responsive probes were decreased in aged animals. A few probes were altered in the same direction across the different age groups; however, in some cases estradiol effects were in the opposite direction (Fig. 1B).

To examine markers of synaptic components, estradiol-responsive genes were grouped according to age and whether the genes increased or decreased expression. The gene groups were submitted to DAVID Bioinformatics Resources to determine overrepresentation of genes related to the gene ontology classification for synapse cellular components (GO: 0045202). The results indicate that estradiol treatment was associated with increased expression of synaptic genes only for young (17 genes, $P < 0.0005$) and MA animals (26 genes, $P < 0.00005$) at the 6 h time point. Five of the genes (ENAH, GRIA4, PJA2, GRIP1, GRIA1) were increased in both age groups (Table 2). A significant clustering was not observed for synaptic component genes that decreased expression (young: four genes; MA: six genes). Furthermore, aged animals did not exhibit altered expression, increasing or decreasing, for genes related to synaptic components.

Estrogen responsive genes were submitted to IPA to determine whether expression changes were associated with gene-enrichment for signaling pathways. Table 3 shows the pathways that exhibited significant ($P < 0.01$) overrepresentation. For genes that increased expression at the 6 h time point, only young animals exhibited overrepresentation in specific signaling pathways including PPAR/RAR signaling, which has been linked to neuroprotection (Santos et al., 2005; Martin et al., 2006; Sanguino et al., 2006; Rosa et al., 2008). Interestingly, while significant gene enrichment was not observed for the PPAR/RAR pathway in MA mice, three of the six genes that increased in MA mice were common for the young group (CLOCK, GNAQ, NCOR1). For genes that decreased expression at the 6 h time point, young and MA animals exhibited clustering of genes for oxidative phosphorylation and mitochondrial dysfunction (Table 4), with two genes NDUFV1 and NDUFV2 decreased in both age groups.

## Age Differences in Estradiol-Responsive Genes 12 h After Treatment

The number of probes influenced by treatment decreased from the 6 to 12 h time points for young and MA mice. In contrast, aged animals exhibited approximately a fivefold increase in the number of estradiol-responsive probes at 12 h relative to the 6 h time point (Fig. 1A). Most of the probes (67%) for aged animals exhibited decreased expression at 12 h. When estradiol-responsive genes were compared across age groups, common probes were usually altered in the opposite direction in aged animals compared with the other two groups (Fig. 1C) and include a number of genes involved in the regulation of transcription (Table 5).

To examine overrepresentation in functional categories, the list of significantly altered genes was submitted to DAVID Bioinformatics Resources for examination of synaptic components. For all age groups, overrepresentation of synaptic component genes was not observed. Data were then submitted to IPA for determination of over representation in functional pathways ($P < 0.01$). No significant clustering was observed for genes that exhibited decreased expression, regardless of age group (Table 6). In the case of increased expression, only aged animals exhibited gene enrichment which was largely focused on signaling pathways that are rapidly influenced by estrogen including α-adrenergic signaling (Favit et al., 1991; Bowman et al., 2002; Heikkinen et al., 2002; Aydin et al., 2008), $Ca^{2+}$ signaling (Foster, 2005; Brewer et al., 2006; Zhao and Brinton, 2007), synaptic plasticity (Warren et al., 1995; Cordoba Montoya and Carrer, 1997; Smith and McMahon, 2005), and IGF-1 signaling (Azcoitia et al., 1999; Perez-Martin et al., 2003; Donahue et al., 2006). Several of the genes interact with multiple signaling pathways (Table 7). Finally, the PPAR pathway was increased at 6 h in young and 12 h in aged mice;

*TABLE 5.*

*Genes From Aged Mice Which Exhibited Expression Opposite Young or MA Mice at 12 h*

| Affy ID | Gene | Protein | *P* value | | | Fold change | | |
|---|---|---|---|---|---|---|---|---|
| | | | Y | MA | A | Y | MA | A |
| 1452369_at | MAGI1 | Membrane-associated guanylate kinase, WW and PDZ domain containing 1 | 6.3E-04 | 4.4E-01 | 3.8E-03 | −1.29 | −1.10 | 1.51 |
| 1434008_at | SCN4B | Sodium channel, type IV, beta | 2.2E-02 | 3.9E-01 | 3.9E-03 | −1.26 | −1.16 | 1.47 |
| 1419008_at | NPY5R | Neuropeptide Y receptor Y5 | 9.2E-01 | 2.1E-02 | 5.3E-05 | 1.01 | −1.52 | 1.45 |
| 1426495_at | 2410042D21RIK | Riken CDNA 2410042D21 gene | 5.2E-01 | 1.2E-02 | 1.9E-03 | 1.08 | −1.51 | 1.41 |
| 1448795_a_at | TBRG4 | Transforming growth factor beta regulated gene 4 | 6.8E-01 | 1.6E-02 | 5.3E-03 | −1.05 | −1.34 | 1.33 |
| 1427329_a_at | IGH-6 | Immunoglobulin heavy chain 6 (HEAVY CHAIN of IGM) | 5.0E-02 | 2.3E-02 | 1.3E-02 | −1.41 | −1.27 | 1.32 |
| 1455277_at | HHIP | HEDGEHOG-interacting protein | 8.4E-05 | 7.1E-01 | 1.1E-02 | −1.45 | 1.06 | 1.29 |
| 1426582_at | ATF2 | Activating transcription factor 2 | 1.4E-01 | 2.1E-02 | 2.4E-02 | 1.27 | −1.45 | 1.28 |
| 1429249_at | 4833424O15RIK | Riken CDNA 4833424O15 gene | 7.1E-01 | 1.9E-02 | 5.9E-03 | 1.04 | −1.58 | 1.27 |
| 1456904_at | EST | | 8.0E-01 | 1.0E-02 | 2.2E-02 | 1.02 | −1.18 | 1.26 |
| 1426806_at | OBFC2A | Oligonucleotide binding fold containing 2A | 2.6E-01 | 1.9E-02 | 1.9E-02 | 1.15 | −1.51 | 1.25 |
| 1428429_at | RGMB | RGM domain family, member B | 2.9E-01 | 2.2E-02 | 1.3E-02 | 1.13 | −1.43 | 1.25 |
| 1435165_at | CNTN2 | Contactin 2 | 2.1E-02 | 4.4E-01 | 1.1E-02 | −1.23 | −1.09 | 1.25 |
| 1416286_at | RGS4 | Regulator of G-protein signaling 4 | 4.9E-01 | 2.3E-02 | 5.9E-04 | 1.05 | −1.13 | 1.23 |
| 1433719_at | SLC9A9 | Solute carrier family 9 (sodium/hydrogen exchanger), isoform 9 | 2.3E-02 | 4.4E-01 | 3.5E-03 | −1.18 | −1.07 | 1.21 |
| 1455734_at | CRBN | Cereblon | 2.1E-01 | 2.4E-02 | 2.3E-03 | 1.09 | −1.15 | 1.20 |
| 1436056_at | KIF13B | Kinesin family member 13B | 7.6E-03 | 6.6E-01 | 2.4E-02 | −1.23 | 1.04 | 1.20 |
| 1419184_a_at | FHL2 | Four and a half lim domains 2 | 4.7E-03 | 5.6E-01 | 1.7E-02 | −1.17 | −1.03 | 1.20 |
| 1456967_at | TRIM66 | KIAA0298 hypothetical protein (human) | 1.2E-02 | 7.4E-01 | 1.8E-02 | −1.24 | 1.04 | 1.19 |
| 1448752_at | CAR2 | Carbonic anhydrase 2 | 7.9E-01 | 2.4E-02 | 9.7E-03 | 1.02 | −1.25 | 1.16 |
| 1449164_at | CD68 | CD68 antigen | 9.2E-01 | 1.3E-02 | 7.7E-03 | −1.00 | −1.33 | 1.15 |
| 1428903_at | 3110037I16RIK | Riken CDNA 3110037I16 gene | 9.8E-03 | 9.8E-01 | 1.2E-02 | −1.13 | −1.00 | 1.14 |
| 1423332_at | SDCBP | Syndecan binding protein | 7.4E-01 | 1.8E-02 | 1.4E-02 | 1.03 | −1.13 | 1.13 |
| 1429087_at | 1110054O05RIK | Riken CDNA 1110054O05 gene | 2.3E-02 | 4.7E-02 | 2.0E-02 | −1.20 | −1.18 | 1.13 |
| 1429227_x_at | NAP1L1 | Nucleosome assembly protein-1 | 2.1E-01 | 1.5E-02 | 2.4E-03 | 1.09 | −1.25 | 1.13 |
| 1424801_at | ENAH | Enabled homolog (Drosophila) | 3.8E-01 | 1.9E-02 | 2.5E-02 | 1.05 | −1.20 | 1.12 |
| 1416458_at | ARF2 | ADP-ribosylation factor 2 | 9.6E-01 | 1.4E-02 | 2.0E-02 | −1.00 | −1.26 | 1.12 |
| 1434440_at | GNAI1 | Guanine nucleotide binding protein, alpha inhibiting 1 | 6.2E-01 | 1.4E-02 | 2.3E-02 | 1.05 | −1.10 | 1.12 |
| 1424594_at | LGALS7 | Lectin, galactose binding, soluble 7 | 1.0E-02 | 3.1E-01 | 6.3E-03 | −1.12 | −1.05 | 1.12 |
| 1455403_at | MANEA | Mannosidase, endo-alpha | 1.8E-02 | 9.3E-01 | 2.3E-02 | −1.12 | 1.01 | 1.11 |
| 1434612_s_at | SBNO1 | SNO, strawberry notch homolog 1 (Drosophila) | 8.1E-01 | 2.2E-02 | 2.4E-02 | 1.01 | −1.17 | 1.11 |
| 1448963_at | NFYC | Nuclear transcription factor-y gamma | 1.8E-02 | 4.5E-01 | 1.9E-03 | −1.10 | −1.05 | 1.11 |
| 1455011_at | STARD4 | Riken CDNA 4632419C16 gene | 9.2E-03 | 4.4E-03 | 2.1E-02 | −1.23 | −1.17 | 1.10 |
| 1417364_at | EEF1G | Eukaryotic translation elongation factor 1 gamma | 8.8E-01 | 2.4E-02 | 1.2E-02 | −1.01 | −1.13 | 1.09 |
| 1452159_at | 2310001A20RIK | Riken CDNA 2310001A20 gene | 2.1E-04 | 2.4E-01 | 2.2E-02 | 1.17 | −1.10 | −1.10 |
| 1417252_at | NT5C | 5′,3′-Nucleotidase, cytosolic | 1.4E-03 | 1.2E-01 | 2.9E-03 | 1.32 | −1.17 | −1.12 |
| 1429048_at | BLOC1S2 | Biogenesis of lysosome-related organelles complex-1, subunit 2 | 2.1E-02 | 2.4E-02 | 1.5E-02 | 1.24 | −1.28 | −1.14 |
| 1434521_at | RFXDC2 | Regulatory factor X domain containing 2 homolog (human) | 7.8E-01 | 9.3E-03 | 7.9E-03 | −1.01 | 1.20 | −1.15 |
| 1459874_s_at | MTMR4 | Myotubularin-related protein 4 | 4.9E-03 | 1.9E-01 | 1.3E-02 | 1.22 | 1.14 | −1.16 |
| 1434745_at | CCND2 | Cyclin D2 | 1.1E-03 | 2.3E-01 | 1.5E-02 | 1.23 | −1.09 | −1.16 |

TABLE 5. (Continued)

| Affy ID | Gene | Protein | P value | | | Fold change | | |
|---|---|---|---|---|---|---|---|---|
| | | | Y | MA | A | Y | MA | A |
| *Hippocampus* | | | | | | | | |
| 1456748_a_at | NIPSNAP1 | 4-Nitrophenylphosphatase domain and nonneuronal snap25-like protein H | 1.3E-02 | 6.0E-01 | 2.2E-02 | 1.21 | 1.04 | −1.17 |
| 1426858_at | INHBB | Inhibin beta-B | 1.5E-02 | 5.6E-01 | 2.2E-02 | 1.20 | −1.05 | −1.17 |
| 1441003_at | ERCC4 | Excision repair cross-complementing rodent repair deficiency, compleme | 2.8E-01 | 2.9E-03 | 2.3E-02 | −1.14 | 1.48 | −1.19 |
| 1431890_a_at | MLLT3 | DNA segment, CHR 4, ERATO DOI 321, expressed | 6.5E-03 | 8.2E-01 | 2.5E-04 | 1.14 | 1.02 | −1.20 |
| 1455940_x_at | WDR6 | WD repeat domain 6 | 2.4E-02 | 3.6E-01 | 2.0E-02 | 1.16 | 1.14 | −1.20 |
| 1447320_x_at | RPO1-3 | RNA polymerase 1–3 | 7.7E-03 | 1.4E-01 | 1.3E-02 | 1.29 | −1.20 | −1.20 |
| 1436443_a_at | KDELC1 | KDEL (lys-asp-glu-leu) containing 1 | 7.4E-03 | 9.5E-01 | 1.6E-02 | 1.31 | −1.01 | −1.21 |
| 1448694_at | JUN | JUN oncogene | 3.4E-01 | 1.4E-02 | 2.8E-03 | −1.05 | 1.13 | −1.22 |
| 1436114_at | Rnf165 | Ring finger protein 165 | 2.3E-02 | 2.4E-01 | 1.3E-03 | 1.19 | 1.11 | −1.25 |
| 1455039_a_at | SIN3B | transcriptional regulator, sin3b (yeast) | 1.8E-02 | 6.7E-01 | 4.5E-03 | 1.23 | 1.04 | −1.30 |
| 1441727_s_at | ZFP467 | Hypothetical protein, MNCB-3350 | 1.6E-02 | 3.1E-01 | 5.6E-03 | 1.34 | 1.10 | −1.33 |
| 1456573_x_at | NNT | Nicotinamide nucleotide transhydrogenase | 2.0E-03 | 5.8E-01 | 1.7E-02 | 1.77 | 1.09 | −1.33 |
| 1434210_s_at | LRIG1 | Leucine-rich repeats and immunoglobulin-like domains 1 | 2.1E-03 | 9.9E-01 | 2.1E-02 | 1.42 | −1.00 | −1.34 |
| 1438157_s_at | NFKBIA | Nuclear factor of kappa light chain gene enhancer in B-cells inhibitoR | 1.4E-02 | 3.0E-01 | 2.4E-03 | 1.29 | 1.14 | −1.35 |
| 1439422_a_at | C1QDC2 | C1Q domain containing 2 | 2.4E-02 | 4.1E-01 | 3.2E-03 | 1.25 | −1.06 | −1.37 |
| 1429372_at | SOX11 | SRY-box containing gene 11 | 3.5E-03 | 6.7E-01 | 1.3E-02 | 1.51 | 1.06 | −1.39 |
| 1446464_at | PSME4 | Proteasome (prosome, macropain) activator subunit 4 | 9.3E-01 | 5.4E-03 | 1.5E-02 | −1.02 | 2.11 | −1.58 |
| 1454869_at | WDR40B | WD repeat domain 40B | 8.2E-01 | 2.1E-02 | 1.3E-03 | −1.07 | 1.59 | −1.74 |

however, only one gene, CHUK, was common for young 6 h and aged 12 h groups.

The increase in the number of altered genes at 12 h for aged animals suggests that gene changes observed in younger mice may have been delayed in older animals. To examine this possibility we employed the gene expression data for 6 h in young and MA mice and compared it with gene expression in aged mice at 6 and 12 h to determine the number of genes that changed in the same direction. As illustrated in Figure 1B for age mice, the number of genes that changes in the same direction at 6 h was 13 compared with young and 18 compared to MA. When we used the gene expression from age mice at 12 h, we expected to observe an increase of approximately four-fold, since the number of genes for the aged group increase from 198 to 940. However, relative to the young 6 h group we saw a small increase from 13 to 19 and relative to MA animals the number of genes decreased from 18 to 4.

Four genes that increased (WDFY1, GABRA2, NNT, PPARGC1) and two that decreased (ATF4, ENTPD4) in young mice treated with estradiol were selected for validation of microarray results using RT-PCR. These genes were selected because they exhibited altered expression in the same direction at 6 h and 12 h after treatment at $P < 0.025$, except for PPARGC1 which was increased at 12 h for $P < 0.05$. RNA isolated from oil treated mice ($n = 3$) was used as the control to calculate the fold change for mice ($n = 3$) treated 6 h earlier with estradiol. Similarly, the fold change was calculated for values on the microarray for young oil and estradiol (6 h) treated mice. Figure 2 illustrates that the direction and extent of altered transcription was similar for the microarray and RT-PCR.

## DISCUSSION

### Age Differences in Estradiol-Responsive Gene Signatures 6 h After Treatment

The current study examined altered gene expression in the hippocampus following estradiol treatment over the course of aging. The results reveal that aged animals were less responsive to estradiol treatment examined 6 h after an acute treatment. In young and MA animals, estradiol treatment reduced expression for genes involved in oxidative phosphorylation and mitochondrial dysfunction. The decreased expression may represent feedback regulation due estradiol effects on oxidative phosphorylation. Altered oxidative phosphorylation is a major outcome of estradiol treatment in young animals and recent work indicates that in the brain, estradiol can enhance mitochondrial efficiency and decrease oxidative stress (Zheng and Ramirez, 1999; Massart et al., 2002; Stirone et al., 2005; Nilsen et al., 2007; Irwin et al., 2008). It is unclear whether estradiol influences oxidative phosphorylation to the same extent in aged animals. This point is important since previous research indicates that regulation of mitochondrial function and oxidative phosphorylation may constitute a corner stone for

*TABLE 6.*

*Estradiol-Responsive Pathways 12 h Posttreatment*

| Increasing | *P* value | Genes | Decreasing | *P* value | Genes |
|---|---|---|---|---|---|
| Young | | | | | |
| None | | | None | | |
| MA | | | | | |
| None | | | None | | |
| Aged | | | | | |
| α-Adrenergic signaling | 5.E-05 | 13 | None | | |
| Calcium signaling | 1.E-04 | 16 | | | |
| Long-term depression signaling | 5.E-04 | 13 | | | |
| Long-term potentiation signaling | 1.E-03 | 12 | | | |
| G-protein coupled receptor signaling | 5.E-03 | 13 | | | |
| cAMP-mediated signaling | 1.E-02 | 11 | | | |
| IGF-1 signaling | 1.E-02 | 10 | | | |
| PPAR signaling | 1.E-02 | 7 | | | |
| Neuregulin signaling | 1.E-02 | 8 | | | |

estrogen's neuroprotective effects (Simpkins and Dykens, 2008). Thus it will be important for future studies to determine whether acute estradiol effects on oxidative phosphorylation are reduced with advanced age.

Age differences in genes that increased expression were also apparent. Estradiol treatment is associated with an increase in dendritic spines in the hippocampus of young adult rats (Gould et al., 1990; Woolley et al., 1990, 1996; Woolley and McEwen, 1992, 1993), and this process is impaired in older rats (Miranda et al., 1999; Adams et al., 2001; Yildirim et al., 2008). We observed that young and MA, but not aged mice, exhibited an increase in expression of genes related to the synapse 6 h after acute estradiol treatment. Young mice exhibited an increase in genes related to PPAR signaling. Although, MA did not exhibit a significant number of genes in this pathway, for the six genes that increased, three were common to young and MA animals. Aged animals exhibited increased expression of genes related to the PPAR pathway at 12 h post treatment suggesting that the interaction of estrogen and PPAR signaling is maintained in advanced age. The ability of estrogen to increase gene expression of this pathway may be important for hippocampal aging since PPAR signaling has been implicated in the progression of Alzheimer's disease (Dupuy et al., 2001) and neuroprotection from inflammation (Kapadia et al., 2008; Vegeto et al., 2008). Furthermore, age and sex-specific changes have been noted for hippocampal PPAR signaling (Sanguino et al., 2006), suggesting that older females may be at greater risk.

## Age Differences in Estradiol-Responsive Gene Signatures 12 h After Treatment

In contrast to young and MA mice, which exhibited a decline in the number of altered gene between 6 and 12 h, the number of genes with altered expression increased during this time in aged animals. For aged mice at the 12 h time point after an acute injection, gene expression increased in signaling pathways that are rapidly influenced by estradiol including $Ca^{2+}$ signaling (Foster, 2005; Brewer et al., 2006; Zhao and Brinton, 2007), cAMP signaling (Gu and Moss, 1996), IGF-1 signaling (Azcoitia et al., 1999), and synaptic plasticity (Sharrow et al., 2002; Foy et al., 2008). The rapid activation of these pathways by estrogen is due to membrane interactions and not the result of classic transcriptional regulation. However, there is some indication for a reciprocal interaction between rapid membrane effects of estrogen on $Ca^{2+}$, G-protein coupled receptor, and trophic factor signaling and estrogenic modulation of genes in these pathways (Foster, 2005).

## Mechanisms for Age-Related Differences in Estradiol-Responsive Gene Signatures

In the case of increased expression of genes for rapid signaling cascades, it may be important that these same signaling cascades decline during aging (Foster, 2005). Thus, aged cells may be differentially sensitive to estradiol influences due to age-related changes in baseline function and differential activation of rapid of signaling cascades by estradiol. Estradiol effects on $Ca^{2+}$ signaling provides a prime example. Estradiol rapidly influences $Ca^{2+}$ signaling (Wu et al., 2005; Sarkar et al., 2008). In turn, $Ca^{2+}$ signaling can regulate gene expression through "nonclassical" transcriptional regulation, independent of estrogen nuclear receptor mechanisms (Bading et al., 1993; Foster, 2005). Aged hippocampal neurons exhibit altered $Ca^{2+}$ homeostasis and estrogen has effects on $Ca^{2+}$-dependent processes, which are opposite that observed during aging (Foster, 2007). For example, the $Ca^{2+}$-dependent afterhyperpolarization is increased with age and estradiol reduces the afterhyperpolarization (Kumar and Foster, 2002). Furthermore, estradiol pretreatment may have a greater effect on $Ca^{2+}$ regulation in aged cells (Brewer et al., 2006, 2009). Together the results indicate that age differences in gene expression for rapid signaling

*TABLE 7.*

*Signaling Genes Altered at 12 h in Aged Mice*

| Affymetrix | Symbol | Description | *P* value | Fold | Signaling pathways | | | | | | | | |
|---|---|---|---|---|---|---|---|---|---|---|---|---|---|
| | | | | | α-Adrenergic | Calcium | LTD | LTP | G-Protein | cAMP | IGF | PPAR | Neuregulin |
| 1426585_s_at | MAPK1 | Mitogen-activated protein kinase 1 | 1.47E-02 | 1.14 | x | x | x | x | x | x | x | x | x |
| 1416351_at | MAP2K1 | Mitogen-activated protein kinase 1 | 1.08E-02 | 1.11 | x | | x | x | x | x | x | x | x |
| 1453419_at | MRAS | Muscle RAS oncogene homolog | 1.27E-02 | 1.25 | x | | x | x | x | | x | x | x |
| 1452032_at | PRKAR1A | Protein kinase, cAMP-dependent, regulatory, type I, alpha (tissue specific extinguisher 1) | 4.08E-05 | 1.12 | x | x | | x | x | x | x | | |
| 1440132_s_at | PRKAR1B | Protein kinase, cAMP-dependent, regulatory, type I, beta | 5.23E-03 | 1.14 | x | x | | x | x | x | x | | |
| 1460419_a_at | PRKCB | Protein kinase C, beta | 2.03E-02 | 1.16 | x | | x | x | x | | | | x |
| 1418754_at | ADCY8 | Adenylate cyclase 8 (brain) | 1.26E-02 | 1.24 | x | | x | x | x | x | | | |
| 1426582_at | ATF2 | Activating transcription factor 2 | 2.39E-02 | 1.28 | | x | | x | x | x | | | |
| 1433592_at | CALM1 | Calmodulin 1 (phosphorylase kinase, delta) | 3.37E-03 | 1.18 | x | x | | x | | x | | | |
| 1434440_at | GNAI1 | Guanine nucleotide binding protein (G protein), alpha inhibiting activity polypeptide 1 | 2.30E-02 | 1.12 | x | | x | | x | x | | | |
| 1450186_s_at | GNAS | GNAS complex locus | 1.96E-02 | 1.14 | x | | x | | x | x | | | |
| 1417279_at | ITPR1 | Inositol 1,4,5-triphosphate receptor, type 1 | 1.33E-02 | 1.28 | x | x | x | x | | | | | |
| 1426645_at | HSP90AA1 | Heat shock protein 90kDa alpha (cytosolic), class A member 1 | 5.62E-03 | 1.36 | | | | | | | | x | x |
| 1422103_a_at | STAT5B | Signal transducer and activator of transcription 5B | 2.07E-02 | 1.16 | | | | | | | | x | x |
| 1417091_at | CHUK | Conserved helix-loop-helix ubiquitous kinase | 1.42E-03 | 1.26 | | | | | x | | | x | |
| 1421622_a_at | RAPGEF4 | Rap guanine nucleotide exchange factor (GEF) 4 | 2.09E-02 | 1.49 | | | | | x | x | | | |
| 1416286_at | RGS4 | Regulator of G-protein signaling 4 | 5.89E-04 | 1.23 | | | | | x | x | | | |
| 1450202_at | GRIN1 | Glutamate receptor, ionotropic, *N*-methyl D-aspartate 1 | 4.12E-03 | 1.35 | | x | | x | | | | | |
| 1452533_at | RYR3 | Ryanodine receptor 3 | 1.02E-03 | 1.36 | | x | x | | | | | | |
| 1440962_at | SLC8A3 | Solute carrier family 8 (sodium/calcium exchanger), member 3 | 3.51E-03 | 1.26 | x | x | | | | | | | |
| 1450655_at | PTEN | Phosphatase and tensin homolog | 2.15E-02 | 1.28 | | | | | | | | | x |
| 1419073_at | TMEFF2 | Transmembrane protein with EGF-like and two follistatin-like domains 2 | 1.08E-02 | 1.16 | | | | | | | | | x |
| 1418099_at | TNFRSF1B | Tumor necrosis factor receptor superfamily, member 1B | 5.29E-03 | 1.26 | | | | | | | | x | |
| 1419036_at | CSNK2A1 | Casein kinase 2, alpha 1 polypeptide | 4.59E-03 | 1.11 | | | | | | | x | | |
| 1421992_a_at | IGFBP4 | Insulin-like growth factor binding protein 4 | 1.76E-02 | 1.32 | | | | | | | x | | |
| 1422313_a_at | IGFBP5 | Insulin-like growth factor binding protein 5 | 1.65E-03 | 1.57 | | | | | | | x | | |
| 1417933_at | IGFBP6 | Insulin-like growth factor binding protein 6 | 8.90E-03 | 1.35 | | | | | | | x | | |
| 1450431_a_at | NEDD4 | Neural precursor cell expressed, developmentally down-regulated 4 | 1.33E-02 | 1.10 | | | | | | | x | | |
| 1452046_a_at | PPP1CC | Protein phosphatase 1, catalytic subunit, gamma isoform | 1.95E-02 | 1.15 | | | | x | | | | | |

TABLE 7. (Continued)

| Affymetrix | Symbol | Description | *P* value | Fold | Signaling pathways: α-Adrenergic | Calcium | LTD | LTP | G-Protein | cAMP | IGF | PPAR | Neuregulin |
|---|---|---|---|---|---|---|---|---|---|---|---|---|---|
| 1420534_at | GUCY1A3 | Guanylate cyclase 1, soluble, alpha 3 | 8.46E-03 | 1.56 | | | x | | | | | | |
| 1420871_at | GUCY1B3 | Guanylate cyclase 1, soluble, beta 3 | 3.69E-03 | 1.43 | | | x | | | | | | |
| 1453260_a_at | PPP2R2A | Protein phosphatase 2 (formerly 2A), regulatory subunit B, alpha isoform | 2.23E-02 | 1.23 | | | x | | | | | | |
| 1452788_at | PPP2R5E | Protein phosphatase 2, regulatory subunit B′, epsilon isoform | 1.44E-02 | 1.87 | | | x | | | | | | |
| 1417943_at | GNG4 | Guanine nucleotide binding protein (G protein), gamma 4 | 4.75E-04 | 1.30 | x | | | | | | | | |
| 1452363_a_at | ATP2A2 | ATPase, Ca++ transporting, cardiac muscle, slow twitch 2 | 1.76E-03 | 1.15 | | x | | | | | | | |
| 1417606_a_at | CALR | Calreticulin | 2.45E-02 | 1.16 | | x | | | | | | | |
| 1434572_at | HDAC9 | Histone deacetylase 9 | 7.05E-04 | 1.35 | | x | | | | | | | |
| 1424852_at | MEF2C | Myocyte enhancer factor 2C | 6.59E-03 | 1.27 | | x | | | | | | | |
| 1450243_a_at | RCAN2 | Regulator of calcineurin 2 | 1.57E-02 | 1.50 | | x | | | | | | | |
| 1423721_at | TPM1 | Tropomyosin 1 (alpha) | 1.41E-02 | 1.13 | | x | | | | | | | |

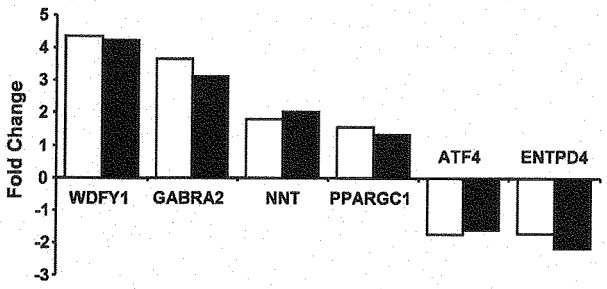


**FIGURE 2. Validation of estradiol treatment effects in young animals at 6 h for six genes using RT-PCR. The bars represent the mean fold change in gene expression for young mice 6 h following estradiol treatment compared with the mean of age-matched oil treated animals using RT-PCR (open bars) and for microarray measures (filled bars).**

pathways may relate to disparity in basal pathway activity and estrogen mediated activation of rapid signaling cascades.

In addition, to age-related changes in rapid signaling cascades, it is likely that changes in estrogen receptors contribute to differences in gene expression. In brain regions like the hippocampus that express both estrogen receptor alpha (ERα) and beta (ERβ), the magnitude and direction of gene regulation will depend on the relative expression of each receptor and the interaction of receptors (Gottfried-Blackmore et al., 2007; Gonzales et al., 2008). While it is unclear how estrogen receptor expression changes in the hippocampus of mice, aging female mice exhibit a decrease in the transcription and expression of ERβ in the cortex (Sharma and Thakur, 2006; Thakur and Sharma, 2007). In contrast, an age-related shift in the hippocampal expression of ERα splice variants may reduce the sensitivity to estrogen treatment in women (Ishunina et al., 2007). In the hippocampus of rats, expression of both ERα and ERβ declines during aging (Mehra et al., 2005) and the loss of ERα is associated with the decreased responsiveness of hippocampal synapses to estradiol (Adams et al., 2002). Indeed, previous work indicates an important role for ERα in the estrogen-mediated increase in synaptic markers (Jelks et al., 2007; Mukai et al., 2007; Morissette et al., 2008). However, several of these studies report a similar, though usually blunted effect of ERβ activation (Patrone et al., 2000; Jelks et al., 2007; Morissette et al., 2008), suggesting that ERβ may be less active but have similar effects on transcription (Lindberg et al., 2003).

An age-related change in ERα and ERβ or a decline in rapid signaling pathways could have reduced or delayed estradiol induced signaling and gene regulation. In the current study there appears to be a delay in the expression of PPAR genes. However, only one gene was common for young 6 h and aged 12 h groups. Although, gene enrichment was observed for the PPAR pathway in young and aged mice, IPA analysis indicated that many more pathways were differentially influenced between the two age groups. Similarly, synaptic component genes increased for young, but not for aged mice. Finally, examination of all genes indicated little correspondence in the gene changes between young 6 h and aged 12 h groups.

Together, the results indicate that delayed activation is not responsible for most of the age differences in altered gene expression between 6 and 12 h. The longer-term effects of estradiol on gene transcription in aged animals remain to be determined.

It is possible that gene changes observed in aged animals could act as a priming response for successive estradiol induced changes beyond the 12 h time point. For example, estradiol application to hippocampal slices rapidly increases ERK/MAPK activation and NMDA receptor function (Bi et al., 2003) and the magnitude of LTP (LTP) (Foy et al., 2008) in young, but not aged animals. In contrast, in vivo priming with estradiol 48 h before sacrifice can enhance LTP in slices from young and aged animals (Smith and McMahon, 2005; Yun et al., 2007). Previous works suggests that both estrogen receptors and rapid signaling cascades are involved in the estradiol-mediated spine growth and synaptogenesis (Murphy and Segal, 1996, 1997; Akama and McEwen, 2003; Znamensky et al., 2003; Lee et al., 2004; Mukai et al., 2007; Yildirim et al., 2008). Thus, while young mice exhibit a rapid increase in the expression of the synaptic marker synaptophysin, an increase in synaptophysin can also be observed in aged mice following treatment with estradiol over several days (Frick et al., 2002; Spencer et al., 2008). Similarly, behavioral studies suggest that a single estradiol injection delivered after training can improve memory in young and MA animals, but not aged animals (Frick, 2009), consistent with the idea that aged animals are less responsive to a single injection. Estradiol treatment for several days prior to training reliably improves memory in middle-aged animals (Foster, 2005; Frick, 2009); however, the effects in aged animals can vary across species. Treatment prior to training improves memory in mice (Frick et al., 2002; Vaucher et al., 2002; Heikkinen et al., 2004), and is less effective in aged rats (Foster et al., 2003; Savonenko and Markowska, 2003; Talboom et al., 2008). Similar differences in responsiveness are noted for estradiol effects on synaptic markers, which can be increased in aged mice (Frick et al., 2002; Spencer et al., 2008), but not in aged rats (Miranda et al., 1999; Adams et al., 2001; Yildirim et al., 2008). The difference in rats and mice may be due to differences in the expression of estrogen receptors during aging as noted above. Regardless, the results indicate that aged animals are less responsive to a single injection of estradiol, however; depending on the species, estradiol priming may rescue estrogen responsiveness. It would be enlightening to determine whether an increase in the expression of estrogen receptors or an enhancement of rapid signaling would ameliorate age-related differences in gene changes, synaptic plasticity and memory following estradiol treatment.

## REFERENCES


Adams MM, Fink SE, Shah RA, Janssen WG, Hayashi S, Milner TA, McEwen BS, Morrison JH. 2002. Estrogen and aging affect the subcellular distribution of estrogen receptor-alpha in the hippocampus of female rats. J Neurosci 22:3608–3614.

Adams MM, Oung T, Morrison JH, Gore AC. 2001. Length of post-ovariectomy interval and age, but not estrogen replacement, regulate *N*-methyl-D-aspartate receptor mRNA levels in the hippocampus of female rats. Exp Neurol 170:345–356.

Aenlle KK, Kumar A, Cui L, Jackson TC, Foster TC. 2009. Estrogen effects on cognition and hippocampal transcription in middle-aged mice. Neurobiol Aging 30:932–945.

Akama KT, McEwen BS. 2003. Estrogen stimulates postsynaptic density-95 rapid protein synthesis via the Akt/protein kinase B pathway. J Neurosci 23:2333–2339.

Aydin M, Yilmaz B, Alcin E, Nedzvetsky VS, Sahin Z, Tuzcu M. 2008. Effects of letrozole on hippocampal and cortical catecholaminergic neurotransmitter levels, neural cell adhesion molecule expression and spatial learning and memory in female rats. Neuroscience 151:186–194.

Azcoitia I, Sierra A, Garcia-Segura LM. 1999. Neuroprotective effects of estradiol in the adult rat hippocampus: Interaction with insulin-like growth factor-I signalling. J Neurosci Res 58:815–822.

Bading H, Ginty DD, Greenberg ME. 1993. Regulation of gene expression in hippocampal neurons by distinct calcium signaling pathways. Science 260:181–186.

Bi R, Foy MR, Thompson RF, Baudry M. 2003. Effects of estrogen, age, and calpain on MAP kinase and NMDA receptors in female rat brain. Neurobiol Aging 24:977–983.

Blalock EM, Chen KC, Sharrow K, Herman JP, Porter NM, Foster TC, Landfield PW. 2003. Gene microarrays in hippocampal aging: Statistical profiling identifies novel processes correlated with cognitive impairment. J Neurosci 23:3807–3819.

Bowman RE, Ferguson D, Luine VN. 2002. Effects of chronic restraint stress and estradiol on open field activity, spatial memory, and monoaminergic neurotransmitters in ovariectomized rats. Neuroscience 113:401–410.

Brewer GJ, Reichensperger JD, Brinton RD. 2006. Prevention of age-related dysregulation of calcium dynamics by estrogen in neurons. Neurobiol Aging 27:306–317.

Brewer LD, Dowling AL, Curran-Rauhut MA, Landfield PW, Porter NM, Blalock EM. 2009. Estradiol reverses a calcium-related biomarker of brain aging in female rats. J Neurosci 29:6058–6067.

Brinton RD. 2008. The healthy cell bias of estrogen action: Mitochondrial bioenergetics and neurological implications. Trends Neurosci 31:529–537.

Carroll JS, Meyer CA, Song J, Li W, Geistlinger TR, Eeckhoute J, Brodsky AS, Keeton EK, Fertuck KC, Hall GF, Wang Q, Bekiranov S, Sementchenko V, Fox EA, Silver PA, Gingeras TR, Liu XS, Brown M. 2006. Genome-wide analysis of estrogen receptor binding sites. Nat Genet 38:1289–1297.

Cordoba Montoya DA, Carrer HF. 1997. Estrogen facilitates induction of long term potentiation in the hippocampus of awake rats. Brain Res 778:430–438.

Daniel JM, Hulst JL, Berbling JL. 2006. Estradiol replacement enhances working memory in middle-aged rats when initiated immediately after ovariectomy but not after a long-term period of ovarian hormone deprivation. Endocrinology 147:607–614.

Donahue CP, Kosik KS, Shors TJ. 2006. Growth hormone is produced within the hippocampus where it responds to age, sex, and stress. Proc Natl Acad Sci USA 103:6031–6036.

Dupuy AM, Mas E, Ritchie K, Descomps B, Badiou S, Cristol JP, Touchon J. 2001. The relationship between apolipoprotein E4 and lipid metabolism is impaired in Alzheimer's disease. Gerontology 47:213–218.

Favit A, Fiore L, Nicoletti F, Canonico PL. 1991. Estrogen modulates stimulation of inositol phospholipid hydrolysis by norepinephrine in rat brain slices. Brain Res 555:65–69.

Fertuck KC, Eckel JE, Gennings C, Zacharewski TR. 2003. Identification of temporal patterns of gene expression in the uteri of immature, ovariectomized mice following exposure to ethynylestradiol. Physiol Genomics 15:127–141.

Foster TC. 2005. Interaction of rapid signal transduction cascades and gene expression in mediating estrogen effects on memory over the life span. Front Neuroendocrinol 26:51–64.

Foster TC. 2006. Biological markers of age-related memory deficits: Treatment of senescent physiology. CNS Drugs 20:153–166.

Foster TC. 2007. Calcium homeostasis and modulation of synaptic plasticity in the aged brain. Aging Cell 6:319–325.

Foster TC, Sharrow KM, Kumar A, Masse J. 2003. Interaction of age and chronic estradiol replacement on memory and markers of brain aging. Neurobiol Aging 24:839–852.

Foy MR, Baudry M, Foy JG, Thompson RF. 2008. 17beta-estradiol modifies stress-induced and age-related changes in hippocampal synaptic plasticity. Behav Neurosci 122:301–309.

Frick KM. 2009. Estrogens and age-related memory decline in rodents: What have we learned and where do we go from here? Horm Behav 55:2–23.

Frick KM, Fernandez SM, Bulinski SC. 2002. Estrogen replacement improves spatial reference memory and increases hippocampal synaptophysin in aged female mice. Neuroscience 115:547–558.

Gonzales KL, Tetel MJ, Wagner CK. 2008. Estrogen receptor (ER) beta modulates ERalpha responses to estrogens in the developing rat ventromedial nucleus of the hypothalamus. Endocrinology 149:4615–4621.

Gottfried-Blackmore A, Croft G, McEwen BS, Bulloch K. 2007. Transcriptional activity of estrogen receptors ERalpha and ERbeta in the EtC. 1 cerebellar granule cell line. Brain Res 1186:41–47.

Gould E, Woolley CS, Frankfurt M, McEwen BS. 1990. Gonadal steroids regulate dendritic spine density in hippocampal pyramidal cells in adulthood. J Neurosci 10:1286–1291.

Gu Q, Moss RL. 1996. 17 beta-Estradiol potentiates kainate-induced currents via activation of the cAMP cascade. J Neurosci 16:3620–3629.

Guerra B, Diaz M, Alonso R, Marin R. 2004. Plasma membrane oestrogen receptor mediates neuroprotection against beta-amyloid toxicity through activation of Raf-1/MEK/ERK cascade in septal-derived cholinergic SN56 cells. J Neurochem 91:99–109.

Heikkinen T, Puolivali J, Liu L, Rissanen A, Tanila H. 2002. Effects of ovariectomy and estrogen treatment on learning and hippocampal neurotransmitters in mice. Horm Behav 41:22–32.

Heikkinen T, Puolivali J, Tanila H. 2004. Effects of long-term ovariectomy and estrogen treatment on maze learning in aged mice. Exp Gerontol 39:1277–1283.

Hosack DA, Dennis G Jr, Sherman BT, Lane HC, Lempicki RA. 2003. Identifying biological themes within lists of genes with EASE. Genome Biol 4:R70.

Irwin RW, Yao J, Hamilton RT, Cadenas E, Brinton RD, Nilsen J. 2008. Progesterone and estrogen regulate oxidative metabolism in brain mitochondria. Endocrinology 149:3167–3175.

Ishunina TA, Fischer DF, Swaab DF. 2007. Estrogen receptor alpha and its splice variants in the hippocampus in aging and Alzheimer's disease. Neurobiol Aging 28:1670–1681.

Jelks KB, Wylie R, Floyd CL, McAllister AK, Wise P. 2007. Estradiol targets synaptic proteins to induce glutamatergic synapse formation in cultured hippocampal neurons: Critical role of estrogen receptor-alpha. J Neurosci 27:6903–6913.

Jover-Mengual T, Zukin RS, Etgen AM. 2007. MAPK signaling is critical to estradiol protection of CA1 neurons in global ischemia. Endocrinology 148:1131–1143.

Kapadia R, Yi JH, Vemuganti R. 2008. Mechanisms of anti-inflammatory and neuroprotective actions of PPAR-gamma agonists. Front Biosci 13:1813–1826.

Kumar A, Foster TC. 2002. 17beta-estradiol benzoate decreases the AHP amplitude in CA1 pyramidal neurons. J Neurophysiol 88: 621–626.

Kuroki Y, Fukushima K, Kanda Y, Mizuno K, Watanabe Y. 2001. Neuroprotection by estrogen via extracellular signal-regulated kinase against quinolinic acid-induced cell death in the rat hippocampus. Eur J Neurosci 13:472–476.

Lacreuse A, Wilson ME, Herndon JG. 2002. Estradiol, but not raloxifene, improves aspects of spatial working memory in aged ovariectomized rhesus monkeys. Neurobiol Aging 23:589–600.

Lee SJ, Campomanes CR, Sikat PT, Greenfield AT, Allen PB, McEwen BS. 2004. Estrogen induces phosphorylation of cyclic AMP response element binding (pCREB) in primary hippocampal cells in a time-dependent manner. Neuroscience 124:549–560.

Li C, Wong WH. 2001. Model-based analysis of oligonucleotide arrays: Expression index computation and outlier detection. Proc Natl Acad Sci USA 98:31–36.

Lindberg MK, Moverare S, Skrtic S, Gao H, Dahlman-Wright K, Gustafsson JA, Ohlsson C. 2003. Estrogen receptor (ER)-beta reduces ERalpha-regulated gene transcription, supporting a "ying yang" relationship between ERalpha and ERbeta in mice. Mol Endocrinol 17:203–208.

Markham JA, Pych JC, Juraska JM. 2002. Ovarian hormone replacement to aged ovariectomized female rats benefits acquisition of the morris water maze. Horm Behav 42:284–293.

Martin B, Mattson MP, Maudsley S. 2006. Caloric restriction and intermittent fasting: Two potential diets for successful brain aging. Ageing Res Rev 5:332–353.

Massart F, Paolini S, Piscitelli E, Brandi ML, Solaini G. 2002. Dose-dependent inhibition of mitochondrial ATP synthase by 17 beta-estradiol. Gynecol Endocrinol 16:373–377.

Mehra RD, Sharma K, Nyakas C, Vij U. 2005. Estrogen receptor alpha and beta immunoreactive neurons in normal adult and aged female rat hippocampus: A qualitative and quantitative study. Brain Res 1056:22–35.

Miranda P, Williams CL, Einstein G. 1999. Granule cells in aging rats are sexually dimorphic in their response to estradiol. J Neurosci 19: 3316–3325.

Morissette M, Le Saux M, Di Paolo T. 2008. Effect of oestrogen receptor alpha and beta agonists on brain N-methyl-D-aspartate receptors. J Neuroendocrinol 20:1006–1014.

Mukai H, Tsurugizawa T, Murakami G, Kominami S, Ishii H, Ogiue-Ikeda M, Takata N, Tanabe N, Furukawa A, Hojo Y, Ooishi Y, Morrison JH, Janssen WG, Rose JA, Chambon P, Kato S, Izumi S, Yamazaki T, Kimoto T, Kawato S. 2007. Rapid modulation of long-term depression and spinogenesis via synaptic estrogen receptors in hippocampal principal neurons. J Neurochem 100:950–967.

Murphy DD, Segal M. 1996. Regulation of dendritic spine density in cultured rat hippocampal neurons by steroid hormones. J Neurosci 16:4059–4068.

Murphy DD, Segal M. 1997. Morphological plasticity of dendritic spines in central neurons is mediated by activation of cAMP response element binding protein. Proc Natl Acad Sci USA 94: 1482–1487.

Naciff JM, Overmann GJ, Torontali SM, Carr GJ, Khambatta ZS, Tiesman JP, Richardson BD, Daston GP. 2007. Uterine temporal response to acute exposure to 17alpha-ethinyl estradiol in the immature rat. Toxicol Sci 97:467–490.

Nilsen J, Irwin RW, Gallaher TK, Brinton RD. 2007. Estradiol in vivo regulation of brain mitochondrial proteome. J Neurosci 27: 14069–14077.

Patrone C, Pollio G, Vegeto E, Enmark E, de Curtis I, Gustafsson JA, Maggi A. 2000. Estradiol induces differential neuronal phenotypes by activating estrogen receptor alpha or beta. Endocrinology 141: 1839–1845.

Pechenino AS, Frick KM. 2009. The effects of acute 17beta-estradiol treatment on gene expression in the young female mouse hippocampus. Neurobiol Learn Mem 91:315–322.

Perez-Martin M, Azcoitia I, Trejo JL, Sierra A, Garcia-Segura LM. 2003. An antagonist of estrogen receptors blocks the induction of adult neurogenesis by insulin-like growth factor-I in the dentate gyrus of adult female rat. Eur J Neurosci 18:923–930.

Rapp PR, Morrison JH, Roberts JA. 2003. Cyclic estrogen replacement improves cognitive function in aged ovariectomized rhesus monkeys. J Neurosci 23:5708–5714.

Rosa AO, Egea J, Martinez A, Garcia AG, Lopez MG. 2008. Neuroprotective effect of the new thiadiazolidinone NP00111 against oxygen-glucose deprivation in rat hippocampal slices: Implication of ERK1/2 and PPARgamma receptors. Exp Neurol 212:93–99.

Sanguino E, Roglans N, Rodriguez-Calvo R, Alegret M, Sanchez RM, Vazquez-Carrera M, Laguna JC. 2006. Ageing introduces a complex pattern of changes in several rat brain transcription factors depending on gender and anatomical localization. Exp Gerontol 41:372–379.

Santos MJ, Quintanilla RA, Toro A, Grandy R, Dinamarca MC, Godoy JA, Inestrosa NC. 2005. Peroxisomal proliferation protects from beta-amyloid neurodegeneration. J Biol Chem 280:41057–41068.

Sarkar SN, Huang RQ, Logan SM, Yi KD, Dillon GH, Simpkins JW. 2008. Estrogens directly potentiate neuronal L-type Ca2+ channels. Proc Natl Acad Sci USA 105:15148–15153.

Savonenko AV, Markowska AL. 2003. The cognitive effects of ovariectomy and estrogen replacement are modulated by aging. Neuroscience 119:821–830.

Schnoes KK, Jaffe IZ, Iyer L, Dabreo A, Aronovitz M, Newfell B, Hansen U, Rosano G, Mendelsohn ME. 2008. Rapid recruitment of temporally distinct vascular gene sets by estrogen. Mol Endocrinol 22:2544–2556.

Sharma PK, Thakur MK. 2006. Expression of estrogen receptor (ER) alpha and beta in mouse cerebral cortex: Effect of age, sex and gonadal steroids. Neurobiol Aging 27:880–887.

Sharrow KM, Kumar A, Foster TC. 2002. Calcineurin as a potential contributor in estradiol regulation of hippocampal synaptic function. Neuroscience 113:89–97.

Sherwin BB. 2006. Estrogen and cognitive aging in women. Neuroscience 138:1021–1026.

Sherwin BB, Henry JF. 2008. Brain aging modulates the neuroprotective effects of estrogen on selective aspects of cognition in women: A critical review. Front Neuroendocrinol 29:88–113.

Simpkins JW, Dykens JA. 2008. Mitochondrial mechanisms of estrogen neuroprotection. Brain Res Rev 57:421–430.

Small SA, Stern Y, Tang M, Mayeux R. 1999. Selective decline in memory function among healthy elderly. Neurology 52:1392–1396.

Smith CC, McMahon LL. 2005. Estrogen-induced increase in the magnitude of long-term potentiation occurs only when the ratio of NMDA transmission to AMPA transmission is increased. J Neurosci 25:7780–7791.

Spencer JL, Waters EM, Romeo RD, Wood GE, Milner TA, McEwen BS. 2008. Uncovering the mechanisms of estrogen effects on hippocampal function. Front Neuroendocrinol 29:219–237.

Stirone C, Duckles SP, Krause DN, Procaccio V. 2005. Estrogen increases mitochondrial efficiency and reduces oxidative stress in cerebral blood vessels. Mol Pharmacol 68:959–965.

Talboom JS, Williams BJ, Baxley ER, West SG, Bimonte-Nelson HA. 2008. Higher levels of estradiol replacement correlate with better spatial memory in surgically menopausal young and middle-aged rats. Neurobiol Learn Mem 90:155–163.

Thakur MK, Sharma PK. 2007. Transcription of estrogen receptor alpha and beta in mouse cerebral cortex: Effect of age, sex, 17beta-estradiol and testosterone. Neurochem Int 50:314–321.

Vaucher E, Reymond I, Najaffe R, Kar S, Quirion R, Miller MM, Franklin KB. 2002. Estrogen effects on object memory and cholinergic receptors in young and old female mice. Neurobiol Aging 23: 87–95.

Vegeto E, Benedusi V, Maggi A. 2008. Estrogen anti-inflammatory activity in brain: A therapeutic opportunity for menopause and neurodegenerative diseases. Front Neuroendocrinol 29:507–519.

Warren SG, Humphreys AG, Juraska JM, Greenough WT. 1995. LTP varies across the estrous cycle: Enhanced synaptic plasticity in proestrus rats. Brain Res 703:26–30.

Woolley CS, Gould E, Frankfurt M, McEwen BS. 1990. Naturally occurring fluctuation in dendritic spine density on adult hippocampal pyramidal neurons. J Neurosci 10:4035–4039.

Woolley CS, McEwen BS. 1992. Estradiol mediates fluctuation in hippocampal synapse density during the estrous cycle in the adult rat. J Neurosci 12:2549–54.

Woolley CS, McEwen BS. 1993. Roles of estradiol and progesterone in regulation of hippocampal dendritic spine density during the estrous cycle in the rat. J Comp Neurol 336:293–306.

Woolley CS, Wenzel HJ, Schwartzkroin PA. 1996. Estradiol increases the frequency of multiple synapse boutons in the hippocampal CA1 region of the adult female rat. J Comp Neurol 373:108–117.

Wu TW, Wang JM, Chen S, Brinton RD. 2005. 17Beta-estradiol induced Ca2+ influx via L-type calcium channels activates the Src/ERK/cyclic-AMP response element binding protein signal pathway and BCL-2 expression in rat hippocampal neurons: A potential initiation mechanism for estrogen-induced neuroprotection. Neuroscience 135:59–72.

Yildirim M, Janssen WG, Tabori NE, Adams MM, Yuen GS, Akama KT, McEwen BS, Milner TA, Morrison JH. 2008. Estrogen and aging affect synaptic distribution of phosphorylated LIM kinase (pLIMK) in CA1 region of female rat hippocampus. Neuroscience 152:360–370.

Yun SH, Park KA, Kwon S, Woolley CS, Sullivan PM, Pasternak JF, Trommer BL. 2007. Estradiol enhances long term potentiation in hippocampal slices from aged apoE4-TR mice. Hippocampus 17: 1153–1157.

Zhao L, Brinton RD. 2007. Estrogen receptor alpha and beta differentially regulate intracellular Ca(2+) dynamics leading to ERK phosphorylation and estrogen neuroprotection in hippocampal neurons. Brain Res 1172:48–59.

Zheng J, Ramirez VD. 1999. Rapid inhibition of rat brain mitochondrial proton F0F1-ATPase activity by estrogens:comparison with Na+, K+-ATPase of porcine cortex. Eur J Pharmacol 368: 95–102.

Znamensky V, Akama KT, McEwen BS, Milner TA. 2003. Estrogen levels regulate the subcellular distribution of phosphorylated Akt in hippocampal CA1 dendrites. J Neurosci 23:2340–2347.

Mechanisms of Ageing and Development xxx (2010) xxx–xxx

Contents lists available at ScienceDirect

Mechanisms of Ageing and Development

journal homepage: www.elsevier.com/locate/mechagedev

# Gene expression in the hippocampus: Regionally specific effects of aging and caloric restriction

Zane Zeier [a], Irina Madorsky [a], Ying Xu [b], William O. Ogle [b], Lucia Notterpek [a], Thomas C. Foster [a,*]

[a] Department of Neuroscience, McKnight Brain Institute, University of Florida, P.O. Box 100244, Gainesville, FL 32610-0244, USA
[b] Department of Biomedical Engineering, University of Florida, Gainesville, FL 32611, USA

ARTICLE INFO

*Article history:*
Received 3 February 2010
Received in revised form 13 October 2010
Accepted 21 October 2010
Available online xxx

*Keywords:*
Aging
Diet
Hippocampus
Transcription
Proteosome
Ubiquitin

ABSTRACT

We measured changes in gene expression, induced by aging and caloric restriction (CR), in three hippocampal subregions. When analysis included all regions, aging was associated with expression of genes linked to mitochondrial dysfunction, inflammation, and stress responses, and in some cases, expression was reversed by CR. An age-related increase in ubiquintination was observed, including increased expression of ubiquitin conjugating enzyme genes and cytosolic ubiquitin immunoreactivity. CR decreased cytosolic ubiquitin and upregulated deubiquitinating genes. Region specific analyses indicated that CA1 was more susceptible to aging stress, exhibiting a greater number of altered genes relative to CA3 and the dentate gyrus (DG), and an enrichment of genes related to the immune response and apoptosis. CA3 and the DG were more responsive to CR, exhibiting marked changes in the total number of genes across diet conditions, reversal of age-related changes in p53 signaling, glucocorticoid receptor signaling, and enrichment of genes related to cell survival and neurotrophic signaling. Finally, CR differentially influenced genes for synaptic plasticity in CA1 and CA3. It is concluded that regional disparity in response to aging and CR relates to differences in vulnerability to stressors, the availability of neurotrophic, and cell survival mechanisms, and differences in cell function.



## 1. Introduction

Brain aging processes are enormously complex affecting multiple systems, cell types, and cellular pathways. Gene expression studies attempt to estimate the status of critical parameters for multiple cellular processes that change with age. Examination of gene expression in brain tissue over the lifespan indicates alterations in general aging processes including inflammation, oxidative stress, $Ca^{2+}$ regulation, and cell growth/structural organization (Aenlle et al., 2009; Blalock et al., 2003; Erraji-Benchekroun et al., 2005; Prolla, 2002; Terao et al., 2002).

Caloric restriction (CR) is the most accepted approach to slow the aging process and delay or prevent many age-related diseases (Mattson and Wan, 2005; Weindruch et al., 1988). A review of transcription changes associated with CR indicates that there are no common genes or groups of genes which are influenced by CR across different species (Han and Hickey, 2005). Indeed, for studies that examine gene changes across tissues, even in the same animal, only a handful of genes may emerge as sensitive to treatment (Fu et al., 2006; Selman et al., 2006; Swindell, 2008). Differences may be related to whether the cells in the tissue are post-mitotic (Spindler and Dhahbi, 2007), the function of the tissues examined, and the effects of aging on the tissue (Weindruch et al., 2002).

While much work has focused on peripheral organs and lifespan, little is known concerning the effects of CR on the nervous system. There are some indications that CR improves motor and cognitive function in aged animals (Carter et al., 2009; Fontan-Lozano et al., 2007; Ingram et al., 1987; Pitsikas and Algeri, 1992) and in models of neurodegeneration (Bruce-Keller et al., 1999; Halagappa et al., 2007). The hippocampus is a region that is particularly sensitive to aging, resulting in impaired synaptic plasticity and memory deficits (Foster, 1999, 2007). The three main regions of the hippocampus include the CA1, CA3, and dentate gyrus (DG). These regions differ in terms of efferents, afferents and major cell types (Knowles, 1992), neurogenesis (Ormerod et al., 2008; Pawluski et al., 2009), vulnerability to stressors (Jackson and Foster, 2009; Jackson et al., 2009; McEwen, 2001), and synaptic plasticity mechanisms (Hussain and Carpenter, 2005; McBain, 2008; Zalutsky and Nicoll, 1990). In addition, differences have been noted concerning biological markers of aging within these regions, including altered synaptic function and response to stress (Foster, 2002; Jackson et al., 2009; McEwen, 2001; Patrylo and Williamson, 2007; Rosenzweig and Barnes, 2003). The current study was designed to determine whether CR had a similar effect in these

* Corresponding author. Tel.: +352 392 4359; fax: +352 392-8347.
*E-mail address:* Foster@mbi.ufl.edu (T.C. Foster).

0047-6374/$ – see front matter © 2010 Elsevier Ireland Ltd. All rights reserved.
doi:10.1016/j.mad.2010.10.006

Please cite this article in press as: Zeier, Z., et al., Gene expression in the hippocampus: Regionally specific effects of aging and caloric restriction. Mech. Ageing Dev. (2010), doi:10.1016/j.mad.2010.10.006

three closely linked regions and whether CR would act on genes related to biological markers of aging in the hippocampus such as inflammation, stress, and mitochondrial dysfunction.

## 2. Materials and methods

### 2.1. Animals

All procedures involving animals were approved by the Institutional Animal Care and Use Committee of the University of Florida. *Ad libitum* (AL) fed and calorie restricted (CR) male F344xBN rats were obtained from the National Institute on Aging (NIA) rodent colony. Reduction of calorie intake began at 14 weeks of age starting with 10%, 25%, and finally 40% restriction at 17 weeks until the end of the experiment. Animals were maintained in our facility for approximately one month prior to tissue collection. All animals had free access to water and AL fed rats had free access to NIH-31 pellets. For CR animals, the dietary regimen of 40% restriction was maintained, with food delivered at 17:00 h each evening. Animals were assessed on a weekly basis for signs of overt health problems including marked weight loss. For gene arrays, middle aged (MA) and old (O) animals (18 and 28 months (mo) of age, respectively) were employed. In general, biological variability increases with advanced age (Busuttil et al., 2007; Foster and Kumar, 2007); therefore, the number of animals in the older groups was increased in order to increase the power of the study. The groups consisted of AL-MA ($n = 3$), AL-O ($n = 6$), and CR-O ($n = 6$). Due to the limited supply of CR rats at specific ages, western blots were performed for 8 mo AL, 38 mo AL and 38 mo CR animals ($n = 3$ per group). Ubiquitin-like immunofluorescence was examined in the brains of an 18 mo AL, 38 mo AL, and 38 mo CR rat.

### 2.2. RNA isolation and gene chips

On the day of tissue collection, animals were killed using a guillotine. Brains were quickly removed and placed on an ice-cold Petri dish. Brains were then bisected, making a dorsal to ventral incision along the midline such that the two hemispheres were separated. The neocortex of each hemisphere was then resected in order to expose and remove the hippocampus using forceps and a spatula and 2–3 tissue blocks of the dorsal hippocampus were cut parallel to the alvear fibers (~1 mm thick) using a razor blade. The blocks were laid flat and the subiculum was removed. An incision was made from the CA3–CA1 border to the end of the upper and lower blades of the dentate gyrus (DG) in order to isolate the CA3 region, and an incision through the hippocampal fissure was used to separate the DG and CA1 regions. Tissue from each region was placed into separate tubes and immediately snap-frozen in liquid nitrogen. Tissue samples from three regions of the hippocampus (CA1, CA3, DG) were removed from storage at −80 °C and homogenized for 30 s in 600 μL of RLT buffer using a Rotor–stator homogenizer. Following centrifugation for 3 min at maximum speed the supernatant was transferred to a new tube and an equal volume of 70% ethanol was added, the solution was then applied to a Qiagen RNeasy mini column and isolated according to the manufacturer's protocol. Purified RNA was labeled and hybridized to RAE 230 V2.0 gene chips by the NIH core facility. The chips were scanned with an Affymtrix GeneChip Scanner 3000, and the raw data, publicly available through the NIH neuroscience microarray consortium (http://arrayconsortium.tgen.org/np2/viewProject.do?action=viewProject&projectId=522821) and the NCBI gene expression omnibus Accession No. GSE21681, were processed with Affymetrix GCOS software.

### 2.3. Data analysis

For the 15 animals (AL-MA = 3, AL-O = 6, and CR-O = 6), one chip was hybridized per region (CA1, CA3, DG) per animal, resulting in 45 arrays. Array outliers were identified by dChip and performance in leave-one-out-cross validation studies; two arrays (one CR-O for CA1 and one CR-O for CA3) were removed from the study due to poor hybridization. Probe set filtering was performed according to our previously published work (Aenlle and Foster, 2010; Aenlle et al., 2009; Blalock et al., 2003). Microarray Suite (Affymetrix) was used to determine whether a particular probe was reliably detectable (presence/absence calls). The number of present calls for each probe set was determined across all chips and the probe set was removed if fewer than 80% of the chips exhibited a present call for the probe. Normalization and computation of gene expression values were performed using the perfect-match-only method by inputting data (.cel files) into dChip (Li and Wong, 2001). Unsupervised hierarchical cluster analyses were performed with probe sets that exhibited hybridization signal intensities with a coefficient of variation of greater than 0.5 identified using algorithms implemented in dChip. Statistical algorithms implemented in BRB array tools (version 3.5.0-beta 1, developed by Richard Simon, Amy Peng Lam, Supriya Menezes, NCI and EMMES Corp.) were used to identify probe sets whose hybridization signal intensity values differed between experimental groups (alpha level set at $p < 0.001$) and calculate the false discovery rate (FDR). The ability of significant genes to distinguish between treatment groups was assessed by leave-one-out-cross-validation studies. The ability of gene expression classifiers to correctly predict the class label of the array left out of the analysis was estimated using Monte Carlo simulations. Functional pathways associated with pools of significantly altered probe sets were identified using Ingenuity Pathway Analysis (IPA, Ingenuity Systems, Redwood City, CA). Fischer's exact test was used to calculate a $p$-value determining the probability that each pathway assigned to that data set is due to chance alone. In addition, BRB array tools was used to calculate the largest observed/expected ratios in specific gene ontology (GO) categories for cellular component, molecular function, and biological process that were associated with the significantly altered probe sets.

### 2.4. Western blot analyses

For total protein analyses, the CA1, CA3, or DG regions were dissected from hippocampi. Samples were homogenized with an ultrasonic cell disrupter (Misonix Incorporated; Farmingdale, NY) in SDS sample buffer (62.5 mM Tris, pH 6.8, 10% glycerol, 3% SDS) supplemented with complete protease inhibitor (Roche, Indianapolis, IN). A BCA kit (Pierce, Rockford, IL) was used to determine the protein concentration of the supernatant. Samples were fractionated by SDS-gel electrophoresis using Ready Precast Gradient 8–16% SDS-polyacrylamide gels with 20 μg protein loaded per well. Following fractionation, proteins were transferred to a nitrocellulose (0.45 μm pore size) or a PVDF (for pUbi) (Bio-Rad, Hercules, CA) membrane overnight at 4 °C and a constant voltage of 35 V. Blots were blocked for one hour with Tris-buffered saline containing 0.05% Tween (TBST) and 5% nonfat dry milk. After blocking, the blots were incubated overnight at 4 °C with the following primary antibodies: Ubiquitin (rabbit polyclonal; Dako, Carpinteria, CA); UBE2J1 (mouse monoclonal; Santa Cruz Biotechnology Inc, Santa Cruz, CA); HSP90 (rabbit polyclonal; Cell signaling, Danvers, MA); HSP70 (rabbit polyclonal; Stressgen, Ann Arbor, MI); HSP40 (rabbit polyclonal; Stressgen); HSP27 (goat polyclonal; Santa Cruz); Glyceraldehyde-3-phosphate dehydrogenase (GAPDH) (mouse monoclonal; EnCor Biotechnology, Alachua, FL). After incubation with anti-rabbit, anti-mouse (Cell signaling), or anti-goat horseradish peroxidase conjugated secondary antibodies (Sigma-Aldrich, St. Louis, MO), membranes were reacted with an enhanced chemiluminescent substrate (Perkin Elmer Life Sciences; Boston, MA). A GS-710 densitometer (Bio-Rad Laboratories) was then used to digitally image the films. Densitometric analyses were made using the ImageJ 1.42q computer program (Wayne Rasband, National Institutes of Health, USA). Since many endogenous control markers are affected by aging and caloric restriction, fold change values for these experimental variables were calculated by normalizing to the 8 mo AL control signal, however, GAPDH staining is provided in order to illustrate consistency of gel-loading. Films were formatted for printing using Adobe Photoshop. Significant changes in western blot densitometry between groups were determined by two-tailed student's $t$-tests.

### 2.5. Immunolabeling

For examination of ubiquitin-like immunofluorescence, the brains were bisected through the central sulcus and half of each brain was immediately frozen in liquid nitrogen. Coronal cryosections (5 μm thickness) were collected on Superfrost Plus glass slides (Fisher), and allowed to air dry for 1 h. Slides were then fixed in 4% paraformaldehyde in PBS for 15 min., permeabilized in ice-cold methanol for 5 min. at −20° C, rinsed with PBS and blocked in 20% goat serum in PBS plus 0.05% Triton X-100 for 1 hour at room temperature. Sections were incubated with the indicated primary antibodies overnight at 4 °C. Bound anti-ubiquitin antibodies were detected with Alexa Fluor 594 (Molecular Probes, Eugene, OR). Hoechst dye (Molecular Probes) was included in the secondary antibody solution to visualize nuclei. Slides were mounted with cover slips using Antifade Kit (Molecular Probes). Samples were imaged with a Spot camera attached to a Nikon Eclipse E800 microscope (Melville, NY) and were formatted for printing by using Adobe Photoshop software.

## 3. Results

### 3.1. Gene expression changes induced by aging and CR indicate region-specific sensitivity

Filtering the data resulted in 24,244 probes sets in which at least 80% of the arrays exhibited a present call. To examine generalized gene expression changes throughout the hippocampus with age, we included arrays across all three regions from AL-MA and AL-O animals. This regionally combined analysis revealed 4821 probe sets (FDR = 0.005) that were altered by aging. In addition, we determine the number of probes that exhibited altered expression within each region of the hippocampus. The number of probe sets that change with age ($p < 0.001$) more than double between the DG (898, FDR = 0.027) and CA1 regions (2141, FDR = 0.01) (Fig. 1), suggesting that region CA1 may be more susceptible to the effects of age. The effect of age on region CA3 (1461, FDR = 0.016) was intermediate as compared with the other two.

To determine gene expression changes due to lifelong CR, arrays were analyzed for probe sets that differed between CR-O and AL-O

Please cite this article in press as: Zeier, Z., et al., Gene expression in the hippocampus: Regionally specific effects of aging and caloric restriction. Mech. Ageing Dev. (2010), doi:10.1016/j.mad.2010.10.006

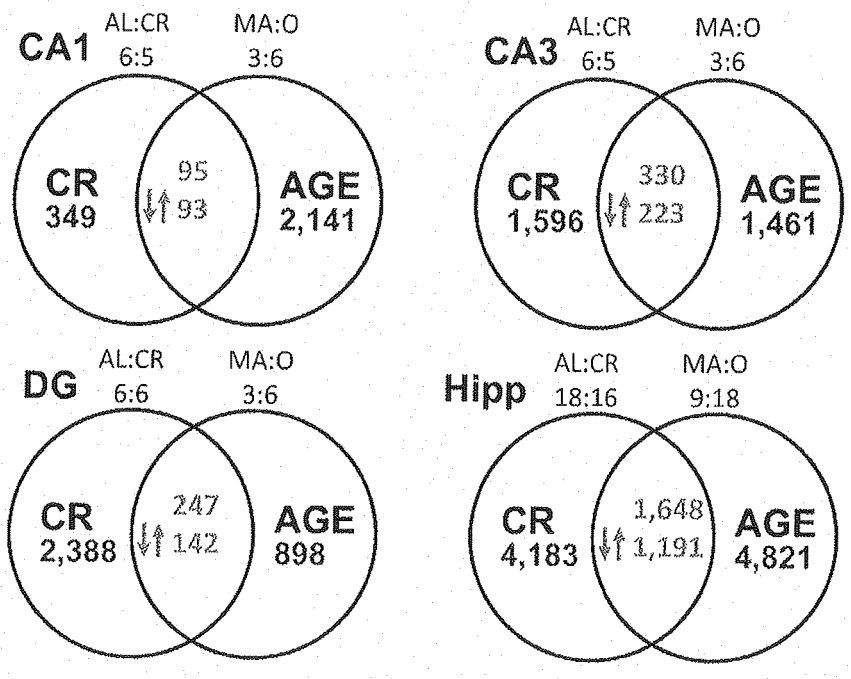


**Fig. 1.** Number of probe sets altered by CR in the hippocampus of rats aged 28 mo (AL-O versus CR-O) and across age (18 and 28 mo) in ad libitum fed rats (AL-MA versus AL-O). Numbers in the main panels (red) indicate the total probe sets altered by aging and CR in regions CA1 (upper left) and CA3 (upper right), the DG (lower left), and across all regions (Hipp, lower right). Numbers in the overlapping areas (green) indicate the number of probe sets altered by both treatments (i.e. overlapping probe sets). Arrows indicate the number of overlapping probe sets whose expression level was oppositely affected by age and CR. Above each circle is an indication of the number of arrays in each group involved in the analysis.

groups. When all regions were combined, 4183 probe sets (FDR = 0.006) were significantly ($p < 0.001$) altered by CR in the older animals (Fig. 1). Interestingly, while the number of probe sets that changed with age increased between the DG and CA1, CR effects were in the opposite direction. Specifically, CR induced a > 6-fold increase in the number of altered probe sets in the DG (2388, FDR = 0.01) relative to CA1 (349, FDR = 0.07) (Fig. 1). The number of probes altered across the diet conditions for CA3 was 1596 (FDR = 0.015). Thus, age differences, as determined by the number of altered genes, appear to be more pronounced in region CA1, whereas CR effects are magnified in the DG.

### 3.2. Pathway regulation during aging and CR

Table 1 illustrates the top GO categories for cellular component (CC), molecular function (MF), and biological process (BP), that exhibited gene enrichment in the hippocampus. In general, aging was associated with enrichment of genes in categories linked to energy homeostasis (glucose homeostasis, creatine kinase activity), oxidative stress (superoxide activity, heme oxidation, aconitate hydratase activity), and response to stress (DNA damage, MHC class II protein complex). CR was associated with an enrichment of genes for several metabolic pathways.

In order to examine age and CR influences on signaling pathways, significantly altered gene expression within each region and for the regionally combined analysis was submitted to IPA (Table 2). The results from the regionally combined analysis confirmed previous work indicating that, throughout the hippocampus, aging was associated with altered expression of genes related to inflammation, mitochondrial dysfunction, stress, and neurodegenerative diseases (Aenlle et al., 2009; Blalock et al., 2003; Prolla, 2002; Weindruch et al., 2002). CR was associated with a downregulation of inflammatory marker genes (such as antigen presentation genes) (Morgan et al., 2007; Wu et al., 2008). In addition, aging was associated with an upregulation of genes involved with the protein ubiquitination pathway, while CR resulted in a mixture of up and downregulated genes for this protein quality control mechanism.

Due to the large number of significant genes for age or CR when examined across all regions, these data sets were separated according to genes that were up or downregulated and these selective data sets were submitted to IPA. In order to limit the number of pathways examined, we selected a cut off of $p < 0.001$ for gene enrichment in the signaling pathways. The analysis indicated no significant gene clustering in pathways for downregulated genes associated with age or CR; although nucleotide excision repair and protein ubiquitination pathways for CR approached the cut off ($p = 0.0025$). An examination of upregulated genes during aging confirmed involvement of signaling for Huntington's disease, amyloid processing, mitochondrial dysfunction, NRF2-mediated oxidative stress, and protein ubiquitination. In addition, the analysis indicated gene enrichment in a number of pathways, which was likely due to the common elements in Gβγ signaling rather that increased activity in the specific signaling processes. In this case, the signaling pathways for α-adrenergic receptor, androgen receptor, tubby, FAK, and breast cancer regulation by stathmin1 exhibited an enrichment of upregulated genes. However, notably absent from these pathways was a change in the expression of the adrenergic or androgen receptor, tubby, FAK, or stathmin1. Similarly, an enrichment of upregulated genes was observed for pathways linked to the antigen presentation pathway. Gene enrichment was observed for NFAT in regulation of the immune response, IL-8, and chemokine receptor 5 (CCR5) signaling in macrophages, although, NFAT, the IL-8 receptor and CCR5 were not altered. For CR, selective analysis limited to upregulated genes confirmed an enrichment of long-term potentiation (LTP) signaling. Other pathways with gene enrichment contained elements of LTP signaling including Rac, breast cancer regulation by stathmin1, IL-3, and formyl-Met-Leu-Phe (fMLP) signaling in neutrophils. Again, while many of the elements were increased, major determinants of the pathway (rac, stathmin1, IL-3

Please cite this article in press as: Zeier, Z., et al., Gene expression in the hippocampus: Regionally specific effects of aging and caloric restriction. Mech. Ageing Dev. (2010), doi:10.1016/j.mad.2010.10.006

**Table 1**
Results of GO analysis for age and CR.

| Effect of Age | | | | Effect of CR | | | |
|---|---|---|---|---|---|---|---|
| GO category | GO ID | GO Term | Ratio | GO category | GO ID | GO Term | Ratio |
| CA1 | | | | | | | |
| CC | 42613 | MHC class II protein complex | 4.46 | CC | 5891 | voltage-gated calcium channel complex | 6.76 |
| MF | 16527 | brain-specific angiogenesis inhibitor activity | 7.14 | MF | 8191 | metalloendopeptidase inhibitor activity | 19.67 |
| BP | 45582 | positive regulation of T cell differentiation | 4.45 | BP | 19233 | sensory perception of pain | 7.07 |
| BP | 30330 | DNA damage response, signal transduction by p53 class mediator | 4.45 | | | | |
| CA3 | | | | | | | |
| CC | 30864 | cortical actin cytoskeleton | 3.24 | CC | 35253 | ciliary rootlet | 6.99 |
| MF | 16527 | brain-specific angiogenesis inhibitor activity | 10.35 | MF | 5093 | Rab GDP-dissociation inhibitor activity | 9.9 |
| MF | 4757 | sepiapterin reductase activity | 10.35 | MF | 4740 | [pyruvate dehydrogenase (lipoamide)] kinase activity | 9.9 |
| BP | 48145 | regulation of fibroblast proliferation | 4.96 | BP | 6613 | cotranslational protein targeting to membrane | 4.96 |
| DG | | | | | | | |
| CC | 5802 | trans-Golgi network | 3.88 | CC | 35253 | ciliary rootlet | 4.03 |
| MF | 4757 | sepiapterin reductase activity | 15.99 | MF | 4965 | GABA-B receptor activity | 7.23 |
| BP | 15802 | basic amino acid transport | 8.22 | MF | 4740 | [pyruvate dehydrogenase (lipoamide)] kinase activity | 7.23 |
| | | | | BP | 6596 | polyamine biosynthetic process | 4.95 |
| Hippocampus | | | | | | | |
| CC | 42613 | MHC class II protein complex | 3.34 | CC | 35253 | ciliary rootlet | 3.07 |
| CC | 30669 | clathrin-coated endocytic vesicle membrane | 3.34 | MF | 4965 | GABA-B receptor activity | 4.32 |
| CC | 30666 | endocytic vesicle membrane | 3.34 | MF | 4658 | propionyl-CoA carboxylase activity | 4.32 |
| CC | 30128 | clathrin coat of endocytic vesicle | 3.34 | MF | 4133 | glycogen debranching enzyme activity | 4.32 |
| CC | 30122 | AP-2 adaptor complex | 3.34 | MF | 4069 | aspartate transaminase activity | 4.32 |
| CC | 5666 | DNA-directed RNA polymerase III complex | 3.34 | BP | 6573 | valine metabolic process | 4.51 |
| MF | 16783 | sulfurtransferase activity | 3.35 | | | | |
| MF | 16527 | brain-specific angiogenesis inhibitor activity | 3.35 | | | | |
| MF | 8526 | phosphatidylinositol transporter activity | 3.35 | | | | |
| MF | 4965 | GABA-B receptor activity | 3.35 | | | | |
| MF | 4757 | sepiapterin reductase activity | 3.35 | | | | |
| MF | 4558 | alpha-glucosidase activity | 3.35 | | | | |
| MF | 4430 | 1-phosphatidylinositol 4-kinase activity | 3.35 | | | | |
| MF | 4392 | heme oxygenase (decyclizing) activity | 3.35 | | | | |
| MF | 4111 | creatine kinase activity | 3.35 | | | | |
| MF | 3994 | aconitate hydratase activity | 3.35 | | | | |
| BP | 19430 | removal of superoxide radicals | 3.53 | | | | |
| BP | 6788 | heme oxidation | 3.53 | | | | |
| BP | 1678 | cell glucose homeostasis | 3.53 | | | | |
| BP | 389 | nuclear mRNA 3'-splice site recognition | 3.53 | | | | |

For each category; cellular component (CC), molecular function (MF), and biological process (BP), the gene ontology groups with the largest observed/expected ratio (Ratio) are identified according to the GO ID and term.

and fMLP receptors) were not increased. Finally, enrichment was observed for clathrin-mediated endocytosis.

Regional differences associated with aging were observed in the regulation of genes for pathways related to neuroinflammation, cell survival, oxidative phosphorylation, mitochondrial dysfunction, and protein ubiquitination pathways. An age-related increase in genes for antigen presentation and IL-4 signaling was evident only in region CA1 suggesting that CA1 may be more sensitive to the effects of age, at least with regard to processes that increase the expression of genes related to immune responses (Wang et al., 2009).

Similarly, regional specificity was observed for CR influences, such that regions CA1 and CA3 exhibited altered LTP signaling; however, no gene changes were found to be common between the two regions. Several kinases were upregulated in CR animals including calcium/calmodulin-dependent protein kinase IV (CAMK4) in the CA1 region and cAMP dependent protein kinase (PKA) and mitogen-activated protein kinase kinase 1 (MAP2K1) in CA3; protein kinase C gamma and protein kinase C beta increased in CA3 and CA1, respectively. Similarly, calcium/calmodulin dependent protein kinase II (CaMKII) alpha was upregulated in CA3 and CaMKII gamma was upregulated in CA1. In region CA3, the catalytic and regulatory subunits for the phosphatase calcineurin (PPP3CA, PPP3CB), were down and upregulated, respectively. In the CA1 region, alpha-amino-3-hydroxy-5-methyl-4-isoxazole propionate selective glutamate receptor (GRIA2) receptor was upregulated and the NMDA receptor associated protein 1 (GRINA) increased in CA3. The results are consistent with research indicating that CR can improve synaptic plasticity in the hippocampus and suggest the mechanism varies between regions.

Table 3 illustrates the directional changes in genes that were altered in at least two of the three regions for the IGF-1, PI3K/AKT, P53, apoptosis, oxidative phosphorylation, mitochondrial dysfunction, and protein ubiquitination pathways. Several pathways share common molecular members. In some cases, these molecules were similarly influenced across regions during aging; however, notable differences were observed for CR influences.

### 3.3. Apoptosis and cell survival pathways

Pathways pertinent to apoptosis and viability or cell survival, which share several common molecular members, were found to be altered by aging including IGF-1, PI3K/AKT, P53, and apoptosis signaling (Table 3). In general, aging increased signaling molecules for apoptosis. Gene enrichment was observed for the P53 pathway

Please cite this article in press as: Zeier, Z., et al., Gene expression in the hippocampus: Regionally specific effects of aging and caloric restriction. Mech. Ageing Dev. (2010), doi:10.1016/j.mad.2010.10.006

**Table 2**
Pathways altered by caloric restriction or aging in the hippocampus.

| Aging | | | | Caloric Restriction | | | |
|---|---|---|---|---|---|---|---|
| Pathway | P | Ratio | FC | Pathway | P | Ratio | FC |
| CA1 | | | | | | | |
| Estrogen Receptor Signaling | 0.000567 | 0.178 | +18, −3 | Synaptic Long Term Potentiation | 0.00635 | 0.054 | +5, −1 |
| NRF2-mediated Oxidative Stress Response | 0.000586 | 0.167 | +24, −6 | Neuregulin Signaling | 0.00927 | 0.055 | +2, −3 |
| Huntington's Disease Signaling | 0.000994 | 0.147 | +29, −5 | Hepatic Fibrosis/Hepatic Stellate Cell Activation | 0.0105 | 0.046 | +4, −2 |
| IL-4 Signaling | 0.00322 | 0.191 | +11, −2 | Hypoxia Signaling in the Cardiovascular System | 0.0157 | 0.056 | +0, −4 |
| Apoptosis Signaling | 0.00359 | 0.184 | +13, −3 | Notch Signaling | 0.018 | 0.073 | +1, −2 |
| Insositol Phosphate Metabolism | 0.0137 | 0.121 | +6, −5 | | | | |
| Antigen presentation | 0.0169 | 0.154 | +6, −0 | | | | |
| IGF-1 Signaling | 0.0204 | 0.163 | +12, −3 | | | | |
| p53 Signaling | 0.022 | 0.149 | +12, −1 | | | | |
| CA3 | | | | | | | |
| p53 Signaling | 0.00446 | 0.138 | +11, −1 | Protein Ubiquitination Pathway | 0.00108 | 0.119 | +16, −8 |
| Hypoxia Signaling in the Cardiovascular System | 0.0048 | 0.155 | +10, −1 | IGF-1 Signaling | 0.00116 | 0.163 | +12, −3 |
| Parkinson's signaling | 0.0115 | 0.235 | +4, −0 | ERK/MAPK Signaling | 0.00402 | 0.122 | +16, −6 |
| PI3K/AKT signaling | 0.0168 | 0.113 | +10, −4 | Hypoxia Signaling in the Cardiovascular System | 0.00494 | 0.155 | +8, −3 |
| Biosynthesis of Steroids | 0.0309 | 0.039 | +2, −3 | Synaptic Long Term Potentiation | 0.0109 | 0.135 | +12, −3 |
| Protein Ubiquitinatioin | 0.0326 | 0.094 | +17, −2 | Cardiac $\beta^2$-adrenergic Signaling | 0.012 | 0.115 | +13, −2 |
| Amyotrophic Lateral Sclerosis Signaling | 0.0389 | 0.107 | +8, −3 | Insulin Receptor Signaling | 0.0138 | 0.12 | +14, −2 |
| | | | | Oxidative Phosphorylation | 0.0155 | 0.095 | +9, −6 |
| | | | | Chemokine Signaling | 0.0166 | 0.147 | +9, −2 |
| | | | | Glucocorticoid Receptor Signaling | 0.017 | 0.095 | +14, −2 |
| | | | | PI3K/AKT Signaling | 0.0186 | 0.113 | +12, −2 |
| DG | | | | | | | |
| PI3K/AKT signaling | 0.000293 | 0.113 | +10, −4 | Oxidative Phosphorylation | 0.00389 | 0.133 | +14, −7 |
| Oxidative Phosphorylation | 0.0019 | 0.082 | +12, −1 | IL-2 Signaling | 0.0108 | 0.208 | +8, −3 |
| Mitochondrial Dysfunction | 0.00251 | 0.073 | +10, −2 | PTEN Signaling | 0.0154 | 0.163 | +7, −8 |
| Ubiquinone Biosynthesis | 0.00416 | 0.067 | +7, −3 | Estrogen Receptor Signaling | 0.0203 | 0.144 | +8, −9 |
| Ceramide Signaling | 0.0115 | 0.101 | +4, −4 | EGF Signaling | 0.0214 | 0.191 | +6, −3 |
| P53 Signaling | 0.0165 | 0.092 | +7, −1 | Nucleotide Excision Repair Pathway | 0.0254 | 0.2 | +1, −6 |
| | | | | GM-CSF Signaling | 0.0339 | 0.177 | +6, −5 |
| Hippocampus | | | | | | | |
| Antigen Presentation Pathway | 0.0000729 | 0.308 | +12, −0 | Protein Ubiquitination Pathway | 0.0018 | 0.218 | +18, −26 |
| Mitochondrial Dysfunction | 0.000192 | 0.2 | +26, −7 | GM-CSF Signaling | 0.008 | 0.29 | +11, −7 |
| NRF2-mediated Oxidative Stress Response | 0.00157 | 0.244 | +38, −6 | Nucleotide Excision Repair Pathway | 0.0205 | 0.286 | +2, −8 |
| Amyloid Processing | 0.002 | 0.346 | +15, −3 | Synaptic Long Term Potentiation | 0.021 | 0.243 | +19, −8 |
| Integrin Signaling | 0.00499 | 0.24 | +34, −12 | Antigen Presentation Pathway | 0.066 | 0.179 | +1, −6 |
| Huntington's Disease Signaling | 0.0063 | 0.211 | +42, −7 | | | | |
| Ubiquinone Biosynthesis | 0.00755 | 0.144 | +13, −2 | | | | |
| Protein Ubiquitination Pathway | 0.00937 | 0.208 | +32, −10 | | | | |

Pathways significantly altered ($p$) by caloric restriction or aging, the ratio of significantly altered pathway genes to total pathway genes members, and the number of genes in the corresponding pathway that were upregulated (+FC) or downregulated (−FC).

in each region (Table 2) and several apoptosis promoting molecules exhibited increased expression in all three regions including p53, BAX, and ACIN1 (Table 3). Differences in expression, particularly between CA1 and the DG were also observed (Table 3), with CA1 exhibiting increased expression of additional p53/apoptosis signaling regulators (BAI1, CASP9, IHPK2, JUN, SFN). In the case of cell survival pathways, aging was associated with gene enrichment for the PI3K/AKT signaling pathway in CA3 and the DG and for IGF-1 signaling in CA1 (Table 2). In addition, AKT, which has anti-apoptotic actions, was increased in all regions (Table 3).

CR influenced cell survival pathways, particularly in region CA3 and the DG. As such, gene enrichment reached significance in region CA3 for IGF-1, insulin, PI3K/AKT, and ERK/MAPK signaling (Table 2). CR reversed an age-related increased expression of the gene encoding the pro-apoptotic molecule, BAX, and increased expression of anti-apoptosis molecule BIRC2, in area CA3 and the DG (Table 3). Interestingly, the expression of genes in these apoptotic and cell survival pathways exhibited minimal CR effects in region CA1 (Table 3). Thus, CR appears to promote cell survival signaling, particularly in regions CA3, while cell survival pathways in region CA1 may be less responsive to CR.

### 3.4. Mitochondria and oxidative phosphorylation

Aging was associated with an enrichment of genes related to mitochondrial dysfunction across the hippocampus when all regions were combined and specifically in the DG when individual regions were considered (Table 2). The mitochondrial dysfunction pathway shares common molecules with oxidative phosphorylation, and oxidative phosphorylation was influenced by CR in region CA3 and the DG (Table 2). In examining genes that were common across regions, it is clear that the three regions were influenced in the same direction during aging, and that the CA1 region was less responsive to CR (Table 3).

Please cite this article in press as: Zeier, Z., et al., Gene expression in the hippocampus: Regionally specific effects of aging and caloric restriction. Mech. Ageing Dev. (2010), doi:10.1016/j.mad.2010.10.006

**Table 3**
Regionally distinct treatment effects.

| Molecule | Age Effect | | | Diet Effect | | | Pathways | | | |
|---|---|---|---|---|---|---|---|---|---|---|
| | CA1 | CA3 | DG | CA1 | CA3 | DG | IGF | AKT | P53 | Apoptosis |
| | IGF1-PI3K/AKT and P53-Apoptosis | | | | | | | | | |
| ACIN1 | 1.62 | 1.53 | 1.54 | NS | NS | NS | | | | X |
| AKT1 | 1.61 | 1.53 | 1.46 | NS | 1.32 | 1.33 | X | X | X | |
| BAI1 | 1.39 | 1.61 | NS | NS | 1.33 | 1.4 | | | X | |
| BAX | 1.71 | 1.81 | 1.93 | NS | −1.47 | −1.44 | | | X | X |
| BIRC2 | −1.36 | NS | NS | NS | 1.29 | 1.26 | | | | X |
| CAPNS1 | 1.42 | NS | 1.41 | NS | NS | NS | | | | X |
| CASP9 | 1.24 | 1.22 | NS | NS | NS | NS | X | | | X |
| CTNNB1 | NS | 1.27 | 1.24 | NS | −1.28 | −1.28 | | X | X | |
| GRB2 | −3.17 | −3.45 | −2.09 | NS | NS | NS | X | X | | |
| IGF1R | NS | NS | NS | 1.73 | 1.68 | 1.39 | X | | | |
| IHPK2 | 1.87 | 1.61 | NS | NS | 1.35 | 1.5 | | | X | |
| JUN | 1.77 | 1.7 | NS | NS | NS | NS | X | | X | |
| NFKBIB | 1.55 | 1.38 | 1.45 | NS | NS | NS | | X | | X |
| P53 | 2.11 | 2.02 | 1.89 | NS | NS | NS | | X | X | X |
| PIK3CA | NS | NS | NS | NS | 1.17 | −1.55 | X | X | X | |
| PIK3R2 | 1.98 | −3.13 | −3.16 | NS | 2.75 | 3.88 | X | X | X | |
| PPKAR1B | NS | NS | NS | NS | 1.14 | 1.23 | X | | | |
| PRKACB | −4.41 | −3.35 | −2.65 | NS | 2.66 | 2.89 | X | | | |
| SFN | 1.65 | 1.75 | NS | NS | NS | 1.32 | X | X | X | |
| YWHAB | 1.47 | 1.46 | 1.43 | NS | NS | NS | X | X | | |
| | Oxidative Phosphorylation and Mitochondrial Dysfunction | | | | | | OX-Phos | | Myto-Dys | |
| ATP5D | 1.26 | 1.23 | 1.21 | NS | NS | NS | X | | | |
| ATP6V0A1 | 1.59 | 1.49 | NS | NS | 1.37 | 1.5 | X | | | |
| ATP6V0A2 | 1.37 | NS | 1.36 | NS | NS | NS | X | | | |
| ATP6V0B | NS | NS | NS | NS | 6.38 | 1.24 | X | | | |
| ATP6V0D1 | NS | NS | NS | NS | 1.15 | 1.23 | X | | | |
| ATP6V1B2 | NS | NS | NS | NS | 1.17 | 1.22 | X | | | |
| ATP6V1G2 | NS | NS | NS | NS | 1.12 | 1.18 | X | | | |
| CASP9 | 1.24 | 1.22 | NS | NS | NS | NS | | | X | |
| COX5B | NS | 1.16 | 1.14 | NS | NS | NS | X | | X | |
| COX7B | NS | 1.25 | 1.31 | NS | −1.38 | −1.36 | X | | X | |
| GPX4 | 1.21 | NS | 1.23 | NS | NS | NS | | | X | |
| HCG25731 | NS | NS | NS | NS | −1.09 | 1.12 | X | | | |
| IHPK2 | 1.87 | 1.61 | NS | NS | 1.35 | 1.5 | X | | | |
| MAP2K4 | −1.24 | NS | −1.27 | NS | NS | NS | | | X | |
| NDUFA7 | −2.3 | −1.78 | NS | NS | 1.9 | 2.87 | X | | X | |
| NDUFS8 | 1.38 | 1.35 | 1.39 | NS | NS | NS | X | | X | |
| NDUFV3 | 1.53 | 1.58 | 1.44 | NS | −1.26 | −1.59 | X | | X | |
| UGCRQ | 1.32 | 1.28 | NS | NS | NS | NS | X | | | |
| UQCRC1 | NS | 1.15 | 1.17 | NS | NS | 1.14 | X | | X | |
| | Protein Ubiquitination | | | | | | | | | |
| ANAPC2 | 1.36 | 1.38 | 1.44 | NS | NS | NS | | | | |
| ANAPC5 | NS | 1.15 | 1.13 | NS | NS | NS | | | | |
| BAG1 | NS | 1.38 | 1.27 | NS | −1.34 | −1.23 | | | | |
| BIRC2 | −1.36 | NS | NS | NS | 1.29 | 1.26 | | | | |
| BTRC | 1.67 | 1.72 | 1.75 | NS | NS | NS | | | | |
| FZR1 | 1.54 | 1.42 | 1.53 | NS | NS | 1.33 | | | | |
| PSMA3 | NS | NS | NS | NS | −1.19 | −1.26 | | | | |
| PSMB5 | NS | 1.17 | 1.21 | NS | NS | NS | | | | |
| PSMD14 | NS | NS | NS | NS | 1.64 | −1.34 | | | | |
| STUB1 | NS | NS | 1.17 | NS | 1.14 | 1.24 | | | | |
| TAP2 | 5.51 | 4.83 | NS | NS | NS | −3.11 | | | | |
| THOP1 | 1.93 | 1.88 | 1.68 | NS | NS | NS | | | | |
| UBA1 | 1.37 | 1.26 | NS | NS | 1.2 | 1.4 | | | | |
| UBE2D2 | NS | 1.38 | 1.57 | NS | 2.2 | 1.4 | | | | |
| UBE2J1 | 1.31 | 1.32 | NS | NS | NS | NS | | | | |
| UBE2Q1 | NS | 1.17 | NS | −1.37 | −1.22 | NS | | | | |
| UBE2S | 1.67 | 1.94 | 1.95 | NS | NS | NS | | | | |
| UBE2V1 | NS | NS | NS | NS | 1.1 | 1.18 | | | | |
| UCHL3 | NS | NS | NS | NS | −1.16 | −1.15 | | | | |
| USO1 | −1.35 | NS | −1.25 | NS | NS | NS | | | | |
| USP11 | NS | NS | NS | NS | 1.17 | 1.29 | | | | |
| USP22 | NS | NS | NS | NS | 1.73 | 1.53 | | | | |
| USP5 | 1.27 | 1.21 | NS | NS | 1.28 | 1.33 | | | | |

Numbers represent significant fold change values; those that were not significant (NS) are indicated. Functional categories with multiple pathways indicate molecular inclusion (X).

Please cite this article in press as: Zeier, Z., et al., Gene expression in the hippocampus: Regionally specific effects of aging and caloric restriction. Mech. Ageing Dev. (2010), doi:10.1016/j.mad.2010.10.006

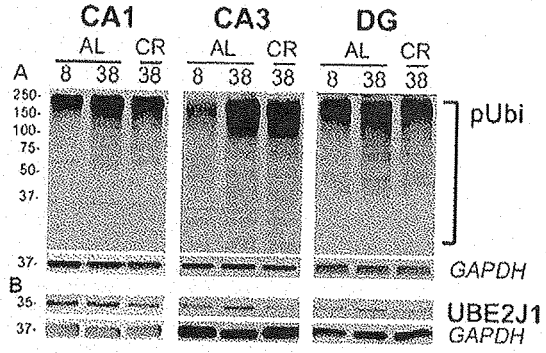


**Fig. 2.** Polyubiquitination of proteins in the hippocampus. (A) Western blot analysis of total protein (20 μg/lane) from CA1, CA3, and DG regions of the hippocampi of 8 and 38 mo old rats fed AL and 38 mo old rats on 40% CR diet ($n = 3$ per group) probed with an anti-ubiquitin antibody. Slow migrating poly-ubiquitinated (pUbi) protein substrates are marked by a square bracket. (B) Staining against the ubiquitin ligase family member (UBE2J1). GAPDH is shown as a protein loading control. Molecular mass is kDA, on the left.

### 3.5. Protein ubiquitination

Table 2 indicates that the enrichment of genes for protein ubiquitination associated with aging and CR, which was observed for analysis across all regions, was also observed for region CA3. Furthermore, both conditions were mainly associated with an increase in expression, with 17 genes increased during aging and 16 genes increased in CA3 of older CR animals relative to age matched AL animals. Closer examination of the genes that were altered in at least two of the three regions (Table 3) indicates that aging is associated with an increase in the expression of genes involved in the degradation of antigens (PSMB5, TAP2, THOP1), and genes for proteins that mediate the covalent attachment of ubiquitin to other proteins (UBE2J1, UBE2Q1, UBE2S, BTRC), including those for the E3 ubiquitin ligase of the anaphase promoting complex (ANAPC2, ANAPC5, FZR1). In contrast, CR was associated with increased expression of deubiquitinating enzymes (PSMD14, USP11, USP22, USP5). Finally, age and CR effects were observed for proteins that mediate the interaction between chaperone activity and ubiquitination of misfolded proteins (BAG1, STUB1). Importantly, very few genes exhibited a shift in the opposite direction due to aging and CR, rather it appears that there is an increase in expression for ubiquitinating and deubiquitinating molecules, respectively.

To assess the function of the ubiquitin-proteosome pathway, we analyzed the degree of polyubiquitinated substrates, as well as the expression level of an ubiquitin-conjugating enzyme (UBE2J1) ($n = 3$ per group). In general, the level of polyubiquitinated proteins was increased with age and decreased in CR animals for each hippocampal region (Fig. 2). Densitometric quantification of western blots (Table 4) indicated that, across all regions of the hippocampus, there was a tendency for an increase in the expression of polyubiquitinated proteins (1.31 fold change, $p = 0.066$). In addition, the expression level of UBE2J1 was reduced in CR animals in all regions of the hippocampus (−1.83-fold change, $p < 0.005$) and this decrease was significant for region CA3 (38 mo AL vs 38 mo CR: −2.94-fold change, $p < 0.01$).

Consistent with an age-related increase in polyubiquitinated proteins, immunolabeling of hippocampal sections exhibited

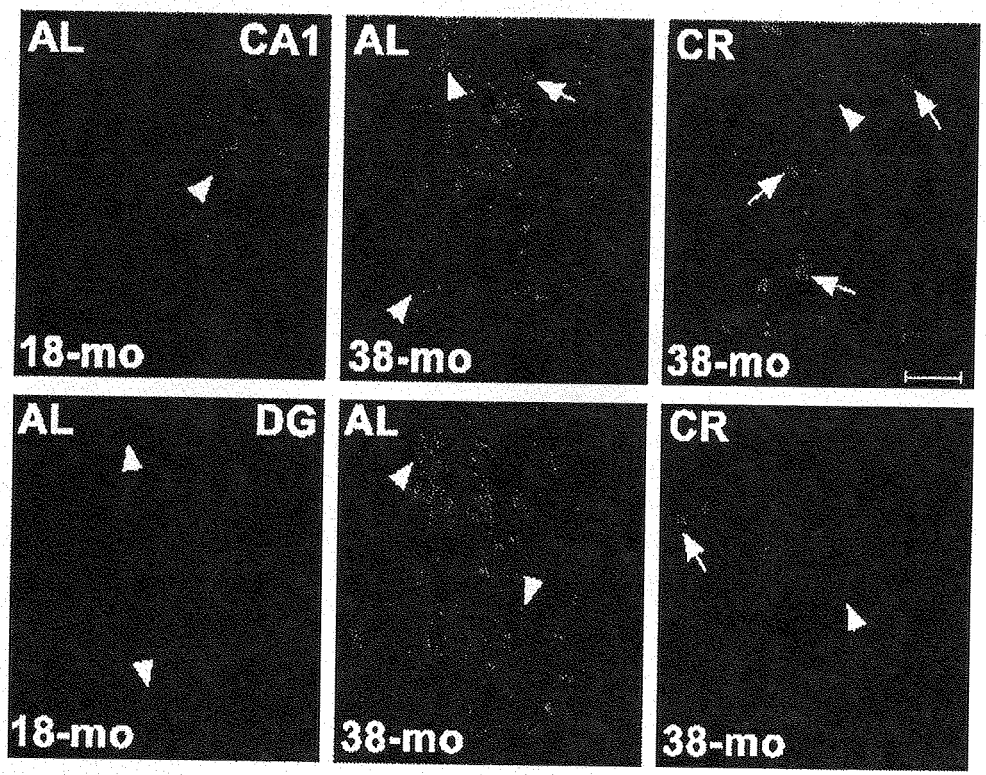


**Fig. 3.** Immunofluorescence showing ubiquitinated inclusions (red) in CA1 (top row, 60×) and DG (bottom row, 60×) regions for 18 mo AL (left column), 38 mo AL (center column) and 38 mo CR (right column). Nuclei were stained with a Hoechst (blue). There appears to be more ubiquitin staining in 38 AL compared to 18 AL and the ubiquitin was diffuse (arrow heads) and distributed throughout the cell body. In comparison, overall ubiquitin-like immunoreactivity appears reduced by CR and more focal, often limited to inclusions (arrows) adjacent to nuclei. The calibration bar is 10 μM.

Please cite this article in press as: Zeier, Z., et al., Gene expression in the hippocampus: Regionally specific effects of aging and caloric restriction. Mech. Ageing Dev. (2010), doi:10.1016/j.mad.2010.10.006

**Table 4**
Western blot analysis of stress response and ubiquitination.

| Antigen | CA1 | | | | CA3 | | | | DG | | | | All | | | |
|---|---|---|---|---|---|---|---|---|---|---|---|---|---|---|---|---|
| | AGE | | CR | | AGE | | CR | | AGE | | CR | | AGE | | CR | |
| | FC | P | FC | P | FC | P | FC | P | FC | P | FC | P | FC | P | FC | P |
| HSP90 | 1.21 | NS | −1.95 | 0.089 | 1.23 | NS | −1.64 | 0.098 | 1.21 | NS | −1.76 | 0.066 | 1.22 | NS | −1.77 | 0.001 |
| HSP70 | 1.19 | NS | −1.21 | NS | −1.05 | NS | −1.50 | NS | −1.06 | NS | −1.44 | NS | 1.03 | NS | −1.35 | NS |
| HSP40 | 1.15 | NS | −1.15 | NS | −1.04 | NS | −1.42 | NS | 1.04 | NS | −1.15 | NS | 1.05 | NS | −1.22 | NS |
| HSP27 | 27.03 | 0.003 | 1.15 | NS | 48.12 | 0.001 | 1.07 | NS | 12.66 | 0.036 | −1.38 | NS | 29.28 | 0.001 | 1.05 | NS |
| pUbi | 1.24 | NS | −1.13 | NS | 1.47 | 0.081 | −1.01 | NS | 1.24 | NS | 1.04 | NS | 1.31 | 0.066 | −1.03 | NS |
| UBE2J | −1.04 | NS | −1.55 | NS | 1.09 | NS | −2.94 | 0.009 | 1.02 | NS | −1.49 | NS | 1.02 | NS | −1.83 | 0.005 |

The fold change for age represents comparisons between 8 mo-AL and 38 mo-AL rats. The fold change for CR represents comparisons between 38 mo-AL and 38 mo-CR rats. NS: not significant.

strong ubiquitin-like reactivity (red) in the hippocampus from a 38 mo AL relative to 18 mo AL animal (Fig. 3). In samples from the AL animal, the ubiquitin was diffuse and distributed throughout the cell body, likely reflecting cytosolic localization. In comparison, it appears that overall ubiquitin-like immunoreactivity was reduced by CR and was more focal, often limited to inclusions adjacent to nuclei (blue).

### *3.6. CR effects that directly oppose aging effects are associated with stress responses*

In addition to compensatory effects of CR, we sought to determine whether CR can directly counteract age effects on specific genes and biological processes, therefore, we examined the genes that were significantly altered during aging and CR, and

**Table 5**
Pathways associated with genes oppositely affected by aging and CR.

| Pathways | *p*-value | Molecules |
|---|---|---|
| CA1 | | |
| Hypoxia Signaling in the Cardiovascular System | 0.027 | NFKBIE (1.4, −1.2), UBE2L6 (1.7, −1.4) |
| CA3 | | |
| p53 Signaling | 0.001 | PRKDC (1.4, −1.3), PIK3R2 (−3.1, 2.8), BAX (1.8, −1.4), CTNNB1 (1.3, −1.3) |
| RAR Activation | 0.010 | PRKACB (−3.4, 2.7), NSD1 (1.5, −1.4), RDH10 (−1.2, 1.2), RDH11 (1.3, −1.2), PIK3R2 (−3.1, 2.8) |
| Oxidative Phosphorylation | 0.016 | COX7B (−1.3, 1.4), ATP5E (1.2, −1.2), NDUFV3 (1.6, −1.3), NDUFA7 (−1.8, 1.9), UQCRQ (1.3, −1.3) |
| Glucocorticoid Receptor Signaling | 0.020 | PRKACB (−3.4, 2.7), HSP90AB1 (−15.7, 2.5), BAG1 (1.4, −1.3), TAF5L (1.2, −1.2), PIK3R2 (−3.1, 2.8), POLR2I (1.4, −1.3) |
| N-Glycan Biosynthesis | 0.023 | MAN2A2 (1.5, −1.5), DPM2 (1.2, 1.2) |
| Mitochondrial Dysfunction | 0.044 | COX7B (−1.3, 1.4), NDUFV3 (1.6, −1.3), NDUFA7 (−1.8, 1.9) |
| DG | | |
| p53 Signaling | 0.002 | PIK3R2 (−3.2, 3.9), BAX (1.9, −1.5), CTNNB1 (1.2, −1.3) |
| Glucocorticoid Receptor Signaling | 0.010 | PRKACB (−2.6, 2.9), HSP90AB1 (−10.7, 9.5), BAG1 (1.3, −1.2), POLR2J (1.3, −1.2), PIK3R2 (−3.2, 3.9) |
| Oxidative Phosphorylation | 0.017 | ATP7B (−2.1, 1.7), COX7B (1.3, −1.4), NDUFV3 (1.4, −1.3) |
| Nucleotide Excision Repair Pathway | 0.024 | XPC (−1.7, 2.5), POLR2J (1.3, −1.2) |
| Hippocampus | | |
| Oxidative Phosphorylation | 0.004 | ATP5E (1.2, −1.1), ATP6V1B2 (−1.1, 1.1), COX15 (1.5, −1.4), COX5B (1.2, −1.2), COX6C (−1.5, 1.9), COX7B (1.3, −1.3), FAM63B (−3.4, 2.7), IP6K2 (−1.2, 1.1), NDUFA1 (1.1, −1.1), NDUFA12 (1.1, −1.1), NDUFA7 (−2.0, 1.9), NDUFB10 (1.3, −1.1), NDUFB4 (1.1, −1.1), NDUFS5 (1.2, −1.1), NDUFV3 (1.5, −1.4), UQCRQ (1.3, −1.2) |
| FcgRIIB Signaling in B Lymphocytes | 0.007 | BTK (2.1, −1.8), FCGR2B (1.9, −1.6), MAPK8 (−1.1, 1.2), MRAS (1.3, −1.3), PIK3CA (1.4, −1.4), PIK3R2 (−3.3, 2.4), SOS1 (−1.2, 1.3) |
| Antigen Presentation Pathway | 0.010 | B2M (1.3, −1.2), CANX (1.1, −1.1), HLA-DQA1 (4.2, −2.6), HLA-DRB1 (4.9, −3.1), TAP2 (4.7, −2.3) |
| Ubiquinone Biosynthesis | 0.012 | NDUFA1 (1.1, −1.1), NDUFA12 (1.1, −1.1), NDUFA7 (−2.0, 1.9), NDUFB10 (1.3, −1.1), NDUFB4 (1.1, −1.1), NDUFS5 (1.2, −1.1), NDUFV3 (1.5, −1.4), EDF1 (1.4, −1.1) |
| Mitochondrial Dysfunction | 0.020 | NDUFA1 (1.1, −1.1), NDUFA12 (1.1, −1.1), NDUFA7 (−2.0, 1.9), NDUFB10 (1.3, −1.1), NDUFB4 (1.1, −1.1), NDUFS5 (1.2, −1.1), NDUFV3 (1.5, −1.4), COX15 (1.5, −1.4), COX5B (1.2, −1.2), COX6C (−1.5, 1.9), COX7B (1.3, −1.3), MAPK8 (−1.1, 1.2), GPX7 (1.2, −1.2), PSEN1 (1.3, −1.3) |
| Dendritic Cell Maturation | 0.022 | B2M (1.3, −1.2), CANX (1.1, −1.1), FCGR2A (1.2, −1.2), FCGR2B (1.9, −1.6), HLA-DQA1 (4.2, −2.6), HLA-DRB1 (4.9, −3.1), IFNAR1 (1.5, −1.3), IRF8 (1.6, −1.6), MAPK8 (−1.1, 1.2), PIK3CA (1.4, −1.4), PIK3R2 (−3.3, 2.4), STAT2 (1.6, −1.2), TREM2 (1.9, −1.5), TYROBP (2.3, −1.4) |
| Lipid Antigen Presentation by CD1 | 0.023 | B2M (1.3, −1.2), PDIA3 (1.3, −1.2) |
| Pyrimidine Metabolism | 0.034 | APOBEC1 (1.6, −1.6), DTYMK (−2.1, 2.1), NME3 (−1.1, 1.1), NME4 (1.3, −1.4), NME6 (1.4, −1.4), POLD4 (1.4, −1.5), POLR2F (1.3, −1.2), POLR2J (1.3, −1.2), POLR3D (1.2, −1.2), POLR3F (−1.5, 1.6), POLR3H (1.2, −1.2), POLRMT (−1.3, 1.5), RPUSD4 (1.2, −1.2), TRUB2 (1.3, −1.2) |
| NRF2-mediated Oxidative Stress Response | 0.047 | ACTA1 (1.3, −1.2), DNAJC17 (1.3, −1.3), DNAJC4 (1.4, −1.1), EIF2AK3 (1.2, −1.2), ERP29 (1.3, −1.2), FTL (1.3, −1.1), GSTA1 (1.2, −1.1), HMOX1 (1.4, −1.4), MAPK8 (−1.1, 1.2), MGST1 (1.3, −1.2), MRAS (1.3, −1.3), PIK3CA (1.4, −1.4), PIK3R2 (−3.3, 2.4), PPIB (1.2, −1.1), SCARB1 (1.3, −1.2), SLC35A2 (1.4, −1.2) |

The fold change values for aging followed by CR are indicated in the brackets. Some molecules are associated with multiple pathways.

Please cite this article in press as: Zeier, Z., et al., Gene expression in the hippocampus: Regionally specific effects of aging and caloric restriction. Mech. Ageing Dev. (2010), doi:10.1016/j.mad.2010.10.006

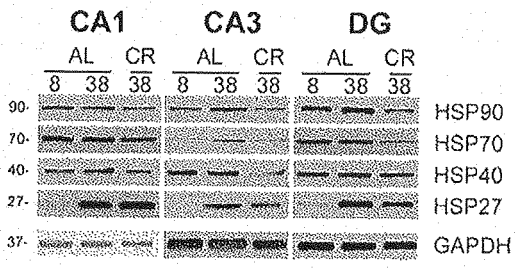


**Fig. 4.** Expression of heat shock proteins (HSP90, HSP70, HSP40, HSP27) in three regions of the hippocampus from 8 or 38 mo rats fed AL or CR diet ($n = 3$ per group). Note the increased expression of the small heat shock protein HSP27 in samples from the older animals. GAPDH is shown as a protein loading control. Molecular mass is kDa, on the left.

whose expression was oppositely affected by the two treatments. In the CA1, CA3, and DG regions of the hippocampus there were 95, 330, and 247 probe sets sensitive to both aging and CR, respectively (Fig. 1). A large majority of these overlapping probe sets were oppositely affected by aging and CR. Across all regions of the hippocampus, 1191 probe sets were significantly, and oppositely affected by aging and CR (Fig. 1). The probe sets that were oppositely affected by aging and CR, were submitted to IPA to determine enrichment in functional pathways. Table 5 provides the pathways and genes that exhibited significant and opposite alterations in each region. When all regions were considered together, pathways linked to immune responses were revealed including antigen presentation, signaling in B lymphocytes, and dendritic cell maturation. In addition, a significant enrichment of genes was observed for mitochondrial dysfunction and the metabolic pathway for oxidative phosphorylation. IPA analysis within individual regions indicated significant functional enrichment of genes for oxidative phosphorylation in region CA3 and the DG. In addition, we observed regional differences in several pathways involved in responding to stress, including hypoxia signaling in region CA1, p53, and glucocorticoid receptor signaling in CA3 and the DG, and nucleotide excision repair in the DG.

For assessment of the stress response, we measured the expression levels of several heat shock proteins (HSP) including HSP90, HSP70, HSP40, and HSP27 using western blots (Fig. 4). HSPs are induced in response to environmental and pathophysiological stressors, including aging (Kalmar and Greensmith, 2009; Morimoto, 1998). Previous work indicates that the level of HSP expression increases in the hippocampus during aging (Calabrese et al., 2004; Di Domenico et al., 2010; Ghi et al., 2009), and caloric restriction is associated with reduced constitutive HSP expression (for review see Kalmar and Greensmith, 2009). There was a tendency ($p < 0.1$) for age or CR effects within specific regions, which reached significance when examined across all regions, such that aging was associated with upregulation of HSP27 and HSP90 expression was decreased by CR (Table 4, Fig. 4).

## 4. Discussion

In the present study, we have investigated gene expression in the hippocampus, a brain region that is critical for learning and memory and highly sensitive to aging. Our study was designed to determine whether CR had similar effects in three closely linked regions of the hippocampus and whether CR would act on genes related to biological markers of aging in the hippocampus. Our data revealed several aspects of aging and CR which were common across regions and others that were unique to the CA1, CA3, and DG regions.

Before, considering the interpretation of the results, it is important to recognize the limitations of the study. First, age-related gene changes were examined between 18 and 28 mo and not all gene changes are monotonic with age (Blalock et al., 2003; Xu et al., 2007). It has been suggested that changes in expression from young to middle-age might reflect processes for compensation of increasing stress (Aenlle et al., 2009; Blalock et al., 2003). For example, increased transcription associated with oxidative stress begins in middle-age; however, expression of antioxidant defenses may decline with advanced age (Aenlle et al., 2009; Blalock et al., 2003; Colombrita et al., 2003; Rao et al., 1990; Tsay et al., 2000). Second, due to the limited availability of CR animals at specific ages, the protein assays involved different ages; 8–38 mo for western blots and 18 to 38 mo for immunocytochemistry. Despite the use of different ages, the results from the protein assays support the findings of the gene arrays, indicating aging is associated with increased cellular stress and CR altered protein ubiquitination.

While the western blots indicated changes in HSP expression, the specific HSP genes were not necessarily detected in our array studies. Other researchers have noted that the correlation of mRNA and protein is weak at best (Greenbaum et al., 2003; Gygi et al., 1999; Maier et al., 2009). For the current study, the difference is likely due to the strictness of the statistical filtering, which will limit the number of genes to be examined. Further, the polyclonal antibodies used in the protein expression analysis detect total protein and are not isoform or subunit specific. Finally, the transcription of HSP genes is negatively regulated by expression of heat shock proteins, such that gene expression will be balanced by the level of stress and the level of HSP expression (Morimoto, 1998). Thus, gene changes are likely to provide makers indicating which pathways are important to consider; however, protein expression and the function of the pathway will be determined by several factors including protein translation and degradation processes.

Consistent with previous microarray research on neural tissue, we observed that aging was associated with expression of markers for mitochondrial dysfunction, oxidative phosphorylation, inflammation and oxidative stress (Aenlle et al., 2009; Blalock et al., 2003; Erraji-Benchekroun et al., 2005; Prolla, 2002; Weindruch et al., 2002). While relatively few genes were influenced in the opposite direction by age and CR, the results indicate that CR can reduce some of the markers of aging. Across the three regions, CR had opposing effects for genes related to oxidative phosphorylation, mitochondrial dysfunction, antigen presentation, and the response to oxidative stress. In particular, across the hippocampus, upregulation and downregulation was observed for antigen presentation due to aging and CR, respectively. The gene expression changes for the regionally combined analysis likely reflect the well described increase in microglia activation during aging, which can be reversed by CR (Morgan et al., 2007; Wu et al., 2008). However, it should be pointed out that changes in the immune response may reflect downstream responses to aging mechanisms and compensatory processes mediated by CR.

Other pathways exhibited effects of age and CR which were not necessarily opposite; rather CR induced offsetting or compensatory changes to counterbalance aging. When all regions were combined, effects of age and CR were prominent for the protein ubiquitination pathway (Table 2); however, the two conditions did not have the opposite effect on gene expression (Tables 2 and 3). Rather, the microarray data indicated that, aging was associated an upregulation of genes in this pathway, particularly for ubiquitin conjugating enzymes. The increase in expression of genes for ubiquitin conjugating enzymes and diffuse ubiquitin-like immunoreactivity within hippocampal cells is consistent with the age-related increase in ubiquinated proteins observed in a number of tissues, and is thought to result from proteasome inhibition (Ding et al., 2006; Grune, 2000; Szweda et al., 2003; Yang et al., 2008). CR was marked by an overall downregulation of gene expression in the protein ubiquitination pathway, but an upregulation of

Please cite this article in press as: Zeier, Z., et al., Gene expression in the hippocampus: Regionally specific effects of aging and caloric restriction. Mech. Ageing Dev. (2010), doi:10.1016/j.mad.2010.10.006

Kalmar, B., Greensmith, L., 2009. Induction of heat shock proteins for protection against oxidative stress. Adv. Drug Deliv. Rev. 61, 310–318.
Kasahara, J., Fukunaga, K., Miyamoto, E., 2001. Activation of calcium/calmodulin-dependent protein kinase IV in long term potentiation in the rat hippocampal CA1 region. J. Biol. Chem. 276, 24044–24050.
Katare, R.G., Kakinuma, Y., Arikawa, M., Yamasaki, F., Sato, T., 2009. Chronic intermittent fasting improves the survival following large myocardial ischemia by activation of BDNF/VEGF/PI3K signaling pathway. J. Mol. Cell Cardiol. 46, 405–412.
Knowles, W.D., 1992. Normal anatomy and neurophysiology of the hippocampal formation. J. Clin. Neurophysiol. 9, 252–263.
Lein, E.S., Zhao, X., Gage, F.H., 2004. Defining a molecular atlas of the hippocampus using DNA microarrays and high-throughput in situ hybridization. J. Neurosci. 24, 3879–3889.
Li, C., Wong, W.H., 2001. Model-based analysis of oligonucleotide arrays: expression index computation and outlier detection. Proc. Natl. Acad. Sci. U. S. A. 98, 31–36.
Li, M., Shin, Y.H., Hou, L., Huang, X., Wei, Z., Klann, E., Zhang, P., 2008. The adaptor protein of the anaphase promoting complex Cdh1 is essential in maintaining replicative lifespan and in learning and memory. Nat. Cell Biol. 10, 1083–1089.
Lu, F.M., Hawkins, R.D., 2006. Presynaptic and postsynaptic Ca(2+) and CamKII contribute to long-term potentiation at synapses between individual CA3 neurons. Proc. Natl. Acad. Sci. U. S. A. 103, 4264–4269.
Lynch, C.D., Lyons, D., Khan, A., Bennett, S.A., Sonntag, W.E., 2001. Insulin-like growth factor-1 selectively increases glucose utilization in brains of aged animals. Endocrinology 142, 506–509.
Maier, T., Guell, M., Serrano, L., 2009. Correlation of mRNA and protein in complex biological samples. FEBS Lett. 583, 3966–3973.
Mattson, M.P., Duan, W., Wan, R., Guo, Z., 2004. Prophylactic activation of neuroprotective stress response pathways by dietary and behavioral manipulations. NeuroRx 1, 111–116.
Mattson, M.P., Guthrie, P.B., Kater, S.B., 1989. Intrinsic factors in the selective vulnerability of hippocampal pyramidal neurons. Prog. Clin. Biol. Res. 317, 333–351.
Mattson, M.P., Wan, R., 2005. Beneficial effects of intermittent fasting and caloric restriction on the cardiovascular and cerebrovascular systems. J. Nutr. Biochem. 16, 129–137.
McBain, C.J., 2008. Differential mechanisms of transmission and plasticity at mossy fiber synapses. Prog. Brain Res. 169, 225–240.
McEwen, B.S., 2001. Plasticity of the hippocampus: adaptation to chronic stress and allostatic load. Ann N Y Acad Sci 933, 265–277.
Morgan, T.E., Wong, A.M., Finch, C.E., 2007. Anti-inflammatory mechanisms of dietary restriction in slowing aging processes. Interdiscip Top Gerontol 35, 83–97.
Morimoto, R.I., 1998. Regulation of the heat shock transcriptional response: cross talk between a family of heat shock factors, molecular chaperones, and negative regulators. Genes Dev 12, 3788–3796.
Naik, M.U., Benedikz, E., Hernandez, I., Libien, J., Hrabe, J., Valsamis, M., Dow-Edwards, D., Osman, M., Sacktor, T.C., 2000. Distribution of protein kinase Mzeta and the complete protein kinase C isoform family in rat brain. J Comp Neurol 426, 243–258.
Nie, T., McDonough, C.B., Huang, T., Nguyen, P.V., Abel, T., 2007. Genetic disruption of protein kinase A anchoring reveals a role for compartmentalized kinase signaling in theta-burst long-term potentiation and spatial memory. J Neurosci. 27, 10278–10288.
Ormerod, B.K., Palmer, T.D., Caldwell, M.A., 2008. Neurodegeneration and cell replacement. Philos Trans R Soc Lond B Biol Sci 363, 153–170.
Patrick, G.N., 2006. Synapse formation and plasticity: recent insights from the perspective of the ubiquitin proteasome system. Curr Opin Neurobiol. 16, 90–94.
Patrylo, P.R., Williamson, A., 2007. The effects of aging on dentate circuitry and function. Prog. Brain Res. 163, 679–696.
Pawluski, J.L., Brummelte, S., Barha, C.K., Crozier, T.M., Galea, L.A., 2009. Effects of steroid hormones on neurogenesis in the hippocampus of the adult female rodent during the estrous cycle, pregnancy, lactation and aging. Front. Neuroendocrinol. 30, 343–357.
Paz Gavilan, M., Vela, J., Castano, A., Ramos, B., del Rio, J.C., Vitorica, J., Ruano, D., 2006. Cellular environment facilitates protein accumulation in aged rat hippocampus. Neurobiol. Aging 27, 973–982.
Pitsikas, N., Algeri, S., 1992. Deterioration of spatial and nonspatial reference and working memory in aged rats: protective effect of life-long calorie restriction. Neurobiol. Aging 13, 369–373.
Prolla, T.A., 2002. DNA microarray analysis of the aging brain. Chem. Senses 27, 299–306.
Rangaraju, S., Hankins, D., Madorsky, I., Madorsky, E., Lee, W.H., Carter, C.S., Leeuwenburgh, C., Notterpek, L., 2009. Molecular architecture of myelinated peripheral nerves is supported by caloric restriction with aging. Aging Cell 8, 178–191.
Rao, G., Xia, E., Richardson, A., 1990. Effect of age on the expression of antioxidant enzymes in male Fischer F344 rats. Mech. Ageing Dev. 53, 49–60.
Rosenzweig, E.S., Barnes, C.A., 2003. Impact of aging on hippocampal function: plasticity, network dynamics, and cognition. Prog. Neurobiol. 69, 143–179.
Selman, C., Kerrison, N.D., Cooray, A., Piper, M.D., Lingard, S.J., Barton, R.H., Schuster, E.F., Blanc, E., Gems, D., Nicholson, J.K., Thornton, J.M., Partridge, L., Withers, D.J., 2006. Coordinated multitissue transcriptional and plasma metabonomic profiles following acute caloric restriction in mice. Physiol. Genom. 27, 187–200.
Sivakumaran, S., Mohajerani, M.H., Cherubini, E., 2009. At immature mossy-fiber-CA3 synapses, correlated presynaptic and postsynaptic activity persistently enhances GABA release and network excitability via BDNF and cAMP-dependent PKA. J. Neurosci. 29, 2637–2647.
Spindler, S.R., Dhahbi, J.M., 2007. Conserved and tissue-specific genic and physiologic responses to caloric restriction and altered IGFI signaling in mitotic and postmitotic tissues. Annu. Rev. Nutr. 27, 193–217.
Swindell, W.R., 2008. Comparative analysis of microarray data identifies common responses to caloric restriction among mouse tissues. Mech. Ageing Dev. 129, 138–153.
Szweda, P.A., Camouse, M., Lundberg, K.C., Oberley, T.D., Szweda, L.I., 2003. Aging, lipofuscin formation, and free radical-mediated inhibition of cellular proteolytic systems. Ageing Res. Rev. 2, 383–405.
Terao, A., Apte-Deshpande, A., Dousman, L., Morairty, S., Eynon, B.P., Kilduff, T.S., Freund, Y.R., 2002. Immune response gene expression increases in the aging murine hippocampus. J. Neuroimmunol. 132, 99–112.
Tsay, H.J., Wang, P., Wang, S.L., Ku, H.H., 2000. Age-associated changes of superoxide dismutase and catalase activities in the rat brain. J. Biomed. Sci. 7, 466–474.
Tydlacka, S., Wang, C.E., Wang, X., Li, S., Li, X.J., 2008. Differential activities of the ubiquitin-proteasome system in neurons versus glia may account for the preferential accumulation of misfolded proteins in neurons. J. Neurosci. 28, 13285–13295.
Wang, X., Zaidi, A., Pal, R., Garrett, A.S., Braceras, R., Chen, X.W., Michaelis, M.L., Michaelis, E.K., 2009. Genomic and biochemical approaches in the discovery of mechanisms for selective neuronal vulnerability to oxidative stress. BMC Neurosci. 10, 12.
Weindruch, R., Kayo, T., Lee, C.K., Prolla, T.A., 2002. Gene expression profiling of aging using DNA microarrays. Mech. Ageing Dev. 123, 177–193.
Weindruch, R., Naylor, P.H., Goldstein, A.L., Walford, R.L., 1988. Influences of aging and dietary restriction on serum thymosin alpha 1 levels in mice. J. Gerontol. 43, B40–42.
Wu, P., Shen, Q., Dong, S., Xu, Z., Tsien, J.Z., Hu, Y., 2008. Calorie restriction ameliorates neurodegenerative phenotypes in forebrain-specific presenilin-1 and presenilin-2 double knockout mice. Neurobiol. Aging 29, 1502–1511.
Xu, X., Zhan, M., Duan, W., Prabhu, V., Brenneman, R., Wood, W., Firman, J., Li, H., Zhang, P., Ibe, C., Zonderman, A.B., Longo, D.L., Poosala, S., Becker, K.G., Mattson, M.P., 2007. Gene expression atlas of the mouse central nervous system: impact and interactions of age, energy intake and gender. Genome Biol. 8, R234.
Yang, S., Liu, T., Li, S., Zhang, X., Ding, Q., Que, H., Yan, X., Wei, K., Liu, S., 2008. Comparative proteomic analysis of brains of naturally aging mice. Neuroscience 154, 1107–1120.
Zalutsky, R.A., Nicoll, R.A., 1990. Comparison of two forms of long-term potentiation in single hippocampal neurons. Science 248, 1619–1624.

Please cite this article in press as: Zeier, Z., et al., Gene expression in the hippocampus: Regionally specific effects of aging and caloric restriction. Mech. Ageing Dev. (2010), doi:10.1016/j.mad.2010.10.006

Development/Plasticity/Repair

# Intracellular Redox State Alters NMDA Receptor Response during Aging through $Ca^{2+}$/Calmodulin-Dependent Protein Kinase II

**Karthik Bodhinathan, Ashok Kumar, and Thomas C. Foster**
Department of Neuroscience, McKnight Brain Institute, University of Florida, Gainesville, Florida 32610

The contribution of the NMDA receptors (NMDARs) to synaptic plasticity declines during aging, and the decline is thought to contribute to memory deficits. Here, we demonstrate that an age-related shift in intracellular redox state contributes to the decline in NMDAR responses through $Ca^{2+}$/calmodulin-dependent protein kinase II (CaMKII). The oxidizing agent xanthine/xanthine oxidase (X/XO) decreased the NMDAR-mediated synaptic responses at hippocampal CA3–CA1 synapses in slices from young (3–8 months) but not aged (20–25 months) rats. Conversely, the reducing agent dithiothreitol (DTT) selectively enhanced NMDAR response to a greater extent in aged hippocampal slices. The enhancement of NMDAR responses facilitated induction of long-term potentiation in aged but not young animals. The DTT-mediated growth in the NMDAR response was not observed for the AMPA receptor-mediated synaptic responses. A similar increase was observed by intracellular application of the membrane-impermeable reducing agent, L-glutathione (L-GSH), through the intracellular recording pipette, indicating that the increased NMDAR response was dependent on intracellular redox state. DTT enhancement of the NMDAR response was dependent on CaMKII activity and was blocked by the CaMKII inhibitor—myristoylated autocamtide-2-related inhibitory peptide (myr-AIP)—but not by inhibition of the activity of protein phosphatases—PP1 and calcineurin (CaN/PP2B) or protein kinase C. CaMKII activity assays established that DTT increased CaMKII activity in CA1 cytosolic extracts in aged but not in young animals. These findings indicate a link between oxidation of CaMKII during aging, a decline in NMDAR responses, and altered synaptic plasticity.

## Introduction

The NMDA receptor (NMDAR) is a major source of $Ca^{2+}$ influx into the postsynaptic neuron during the induction of LTP at hippocampal CA3–CA1 synapses (Bliss and Collingridge, 1993). CA1 region-specific knock-out of the NR1 subunit of the NMDAR abolishes LTP, in addition to impairing spatial memory (Tsien et al., 1996). Aged, memory impaired animals exhibit deficits in LTP induction. Importantly, the NMDAR component of the synaptic response is decreased in aged animals (Barnes et al., 1997; Billard and Rouaud, 2007), suggesting that age-related LTP and memory deficits are due to a decrease in the NMDAR-mediated component of synaptic transmission (Foster, 1999, 2007; Rosenzweig and Barnes, 2003), also referred to here as "NMDAR hypofunction." Numerous studies indicate that NMDARs contribute less $Ca^{2+}$ to the induction of LTP in the area CA1 of aged hippocampus, when compared to the young hippocampus (Norris et al., 1998a; Shankar et al., 1998; Boric et al., 2008). However, it is unclear what age-related mechanism underlies the NMDAR hypofunction.

Received Nov. 5, 2009; revised Dec. 17, 2009; accepted Dec. 22, 2009.
This work was supported by the Evelyn F. McKnight Brain Research Foundation, National Institutes of Health Grants AG014979 and MH059891 to T.C.F., and a University of Florida Alumni fellowship to K.B.
Correspondence should be addressed to Dr. Thomas C. Foster, Department of Neuroscience, McKnight Brain Institute, University of Florida, P.O. Box 100244, Gainesville, FL 32610-0244. E-mail: foster@mbi.ufl.edu.
DOI:10.1523/JNEUROSCI.5485-09.2010
 0270-6474/10/301914-11$15.00/0

Age-related alterations that may contribute to the NMDAR deficits include altered subunit expression, composition, and splice forms (Magnusson et al., 2005, 2006). However, there is a debate concerning whether NMDAR subunit expression decreases at hippocampal CA3–CA1 synapses (Foster, 2002). In addition, it is possible that functional differences are related to posttranslational modifications associated with oxidation or phosphorylation state rather than number and/or type of receptor subunits (Foster, 2007). Previous research examining the ability of reducing and oxidizing (redox) agents to modulate NMDAR activity in cell cultures and in tissue from neonates suggests that redox state is an important determinant of NMDAR function (Aizenman et al., 1989, 1990; Bernard et al., 1997; Choi and Lipton, 2000; Choi et al., 2001), possibly through oxidation of extracellular cysteine residues on the NMDAR (Lipton et al., 2002). Intracellular signaling molecules that affect NMDAR function are also sensitive to redox state. The aged brain exhibits an increase in oxidative damage (Foster, 2006; Poon et al., 2006), and a decrease in redox buffering capacity (Parihar et al., 2008); however, the effect of redox state on NMDAR function during aging has not been examined.

The current studies confirm that the NMDAR-mediated synaptic potentials are decreased at CA3–CA1 synapses of the aged hippocampus. We now provide evidence that the age-related decline in NMDAR-mediated synaptic responses and impaired induction of LTP in area CA1 of the hippocampus are related to the intracellular redox state. NMDAR responses were modified by

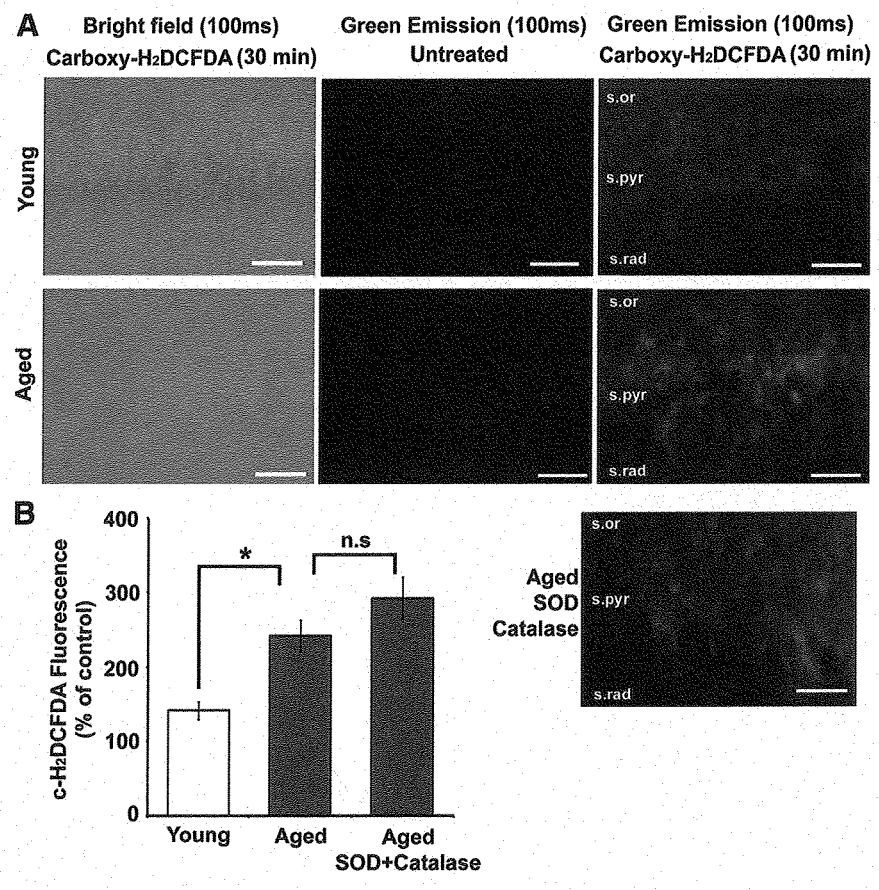


**Figure 1.** Enhanced ROS production is observed in hippocampal tissue from aged rats. ***A***, Indicated above each image column are the imaging conditions (bright field or green emission) and the exposure time (100 ms) for hippocampal slices that were either untreated or treated (Carboxy-$H_2$DCFDA) with the dye. The rows are images of the CA1 region of young (top row) and aged (second row) hippocampal slices. The lowermost image is a Carboxy-$H_2$DCFDA-treated slice from an aged animal, which was incubated with SOD + catalase. The various layers of hippocampal area CA1—stratum radiatum (s.rad), stratum pyramidale (s.pyr), and stratum oriens (s.or)—are indicated in the last set of images. Scale bars, 50 $\mu$m. ***B***, Quantification of the mean fluorescence intensity generated by the oxidation of c-$H_2$DCFDA (c-$H_2$DCFDA Fluorescence) from young ($n = 3$) (open bar), aged ($n = 3$), and SOD + catalase-exposed aged ($n = 3$) (gray bars) hippocampal slices expressed as percentage of fluorescence in untreated (control) slices from the same animal. In this and subsequent figures, error bars represent SEM, asterisks indicate significant difference between the groups indicated, and n.s indicates no significant difference.

redox agents in an age-dependent manner. However, using a combination of extracellular and intracellular recordings with the relatively membrane-impermeable L-glutathione (L-GSH), we found that intracellular redox state mediates that age-dependent shift in NMDAR responses. Furthermore, we demonstrate that the mechanism for the age-dependent redox modulation of NMDARs involves $Ca^{2+}$/calmodulin-dependent protein kinase II (CaMKII) activity. These findings establish age-related changes in the redox state as a mechanism for the decrease in NMDAR response.

## Materials and Methods

*Animals.* Procedures involving animals have been reviewed and approved by the Institutional Animal Care and Use Committee and were in accordance with guidelines established by the United States Public Health Service Policy on Human Care and Use of Laboratory Animals. Male Fischer 344 rats, young (3–8 months) and aged (20–25 months), were obtained from National Institute on Aging colony at Harlan Sprague Dawley. All animals were group housed (2 per cage), maintained on a 12:12 h light schedule, and provided *ad libitum* access to food and water.

*Hippocampal slice preparation.* The animals were deeply anesthetized using isoflurane (Webster) and decapitated with a guillotine (MyNeurolab). The brains were rapidly removed and hippocampi were dissected. Hippocampal slices (~400 $\mu$m) were cut parallel to the alvear fibers using a tissue chopper (Mickle Laboratory Engineering). The slices were incubated in a holding chamber (at room temperature) with artificial CSF (ACSF). The ACSF consisted of the following (in mM): NaCl 124, KCl 2, $KH_2PO_4$ 1.25, $MgSO_4$ 2, $CaCl_2$ 2, $NaHCO_3$ 26, and D-glucose 1. The ACSF was bubbled with 95% $O_2$ and 5% $CO_2$ for 20 min before measurement of pH. The pH was adjusted to 7.4 using 1–2 drops of 10 M NaOH in 4 L of ACSF. At least 30 min before recording, slices were transferred to a standard interface recording chamber (Warner Instrument). The chamber was continuously perfused with oxygenated ACSF at the rate of 2 ml/min, and the temperature was maintained at 30 ± 0.5°C.

*Electrophysiological recordings.* Extracellular field EPSPs (fEPSP) from stratum radiatum of the CA1 region of the hippocampus were recorded using glass micropipettes (4–6 MΩ) filled with recording medium (ACSF). Two concentric bipolar stimulating electrodes (outer pole: stainless steel, 200 $\mu$m diameter; inner pole: platinum/iridium, 25 $\mu$m diameter) (FHC) were localized to the middle of the stratum radiatum to stimulate CA3 inputs onto CA1. Diphasic stimulus pulses of 100 $\mu$s duration were delivered by a stimulator (SD9 Stimulator; Grass Instrument) and alternated between the two pathways such that each pathway was activated at 0.033 Hz. The signals were amplified, filtered between 1 Hz and 1 kHz, and stored on a computer disk for off-line analysis. Two cursors were placed to cover the initial descending phase of the waveform and the maximum negative slope (in millivolts per millisecond) of the fEPSP and NMDAR-fEPSP was determined by a computer algorithm that determined the maximum change across a set of 20 consecutively recorded points (20 kHz sampling frequency) between the two cursors. In a few cases, two cursors were placed to cover the entire waveform, and the maximum amplitude (in millivolts) of the NMDAR-fEPSP and NMDAR-mediated intracellular EPSP was determined by a computer algorithm that calculated the valley voltage from zero (for NMDAR-fEPSP) or the maximum voltage from zero (for NMDAR-mediated intracellular EPSP) between the cursors.

For measuring the paired-pulse ratio, paired pulses were delivered through a single stimulating electrode at varying inter pulse intervals. The first pulse was set to elicit 50% of the maximal fEPSP. The various inter pulse intervals between successive pulses were 50 ms, 100 ms, 150 ms, and 200 ms. The ratio of the maximum negative slope of the second pulse to the slope of the first pulse was computed as the paired-pulse ratio. To measure changes in the presynaptic fiber volley (PFV) upon application of dithiothreitol (DTT) and xanthine/xanthine oxidase (X/XO), the average PFV amplitudes from the last 5 min of drug application were normalized to the average PFV amplitude recorded during the baseline.

For induction of LTP, the stimulation intensity was set to elicit 50% of the maximal fEPSP. After stable baseline recording at 0.033 Hz for at least 20 min, high-frequency stimulation (HFS) was delivered to the pathway at 100 Hz for 1 s (100 pulses) at the baseline stimulus intensity, and recorded for 60 min after HFS. A simultaneously recorded control (non-HFS) pathway received the test stimulus but not the HFS. In some cases, the slices were preincubated with the reducing agent DTT for at least 45

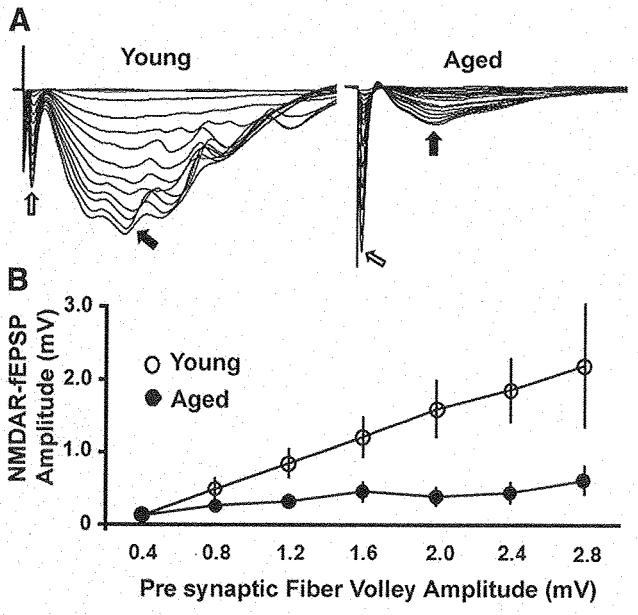


**Figure 2.** NMDAR-mediated synaptic potentials (NMDAR-fEPSP) are reduced in area CA1 of the hippocampus during aging. ***A***, Representative traces of NMDAR-fEPSPs obtained at consecutively higher stimulus intensities from the young (left) and aged (right) animals. Open and filled arrows indicate the PFV and NMDAR-fEPSP, respectively. As observed in the traces, the aged animals exhibit a markedly reduced NMDAR-mediated synaptic potential. ***B***, Plot of the mean NMDAR-fEPSP amplitude versus the PFV amplitude (at 0.4 mV binning width). The aged animals (filled circles) ($n = 6$) exhibited reduced NMDAR-fEPSP when compared to the young animals (open circles) ($n = 5$).

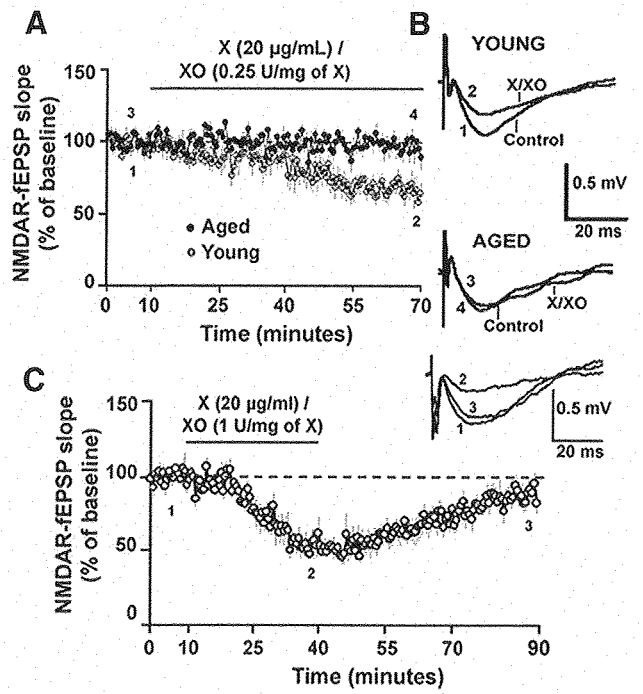


**Figure 3.** The oxidizing agent X/XO decreases NMDAR-mediated synaptic potentials in young animals but not in aged animals. ***A***, Time course of the change in the normalized NMDAR-fEPSP slope in the aged (filled circles) ($n = 7$) and in the young (open circles) ($n = 5$) animals following application of X/XO [20 µg/ml/(0.25 U/mg xanthine)] for 60 min. ***B***, Representative traces (average of 5 traces under each condition) illustrating the change in the NMDAR-fEPSP in the young (top) and aged (bottom) animals under control conditions and at the end of a 60 min application of X/XO. Calibration: 20 ms, 0.5 mV. ***C***, Time course of the change in the normalized NMDAR-fEPSP slope in the young animals ($n = 5$) following application of X/XO [20 µg/ml/(1 U/mg xanthine)] for 30 min and followed by a washout for 50 min. The inset illustrates the average of 5 traces obtained during the indicated time points: baseline (1), under X/XO (2), and upon washout (3). Calibration: 20 ms, 0.5 mV.

min before delivering the HFS. The average fEPSP slope corresponding to the last 5 min from each pathway was used to compare changes in synaptic strength relative to the baseline.

To obtain the NMDAR-mediated field EPSP (NMDAR-fEPSP) of CA3–CA1 synaptic transmission, slices were incubated in ACSF containing low extracellular $Mg^{2+}$ (0.5 mM), 6,7-dinitroquinoxaline-2,3-dione (DNQX, 30 µM), and picrotoxin (PTX, 10 µM). In each case, the baseline response was collected for at least 10 min before experimental manipulations (drug application). Changes in the transmission properties of the synapses, induced by drug application, were calculated as percentage change from the averaged baseline responses.

To obtain the NMDAR-mediated intracellular synaptic potentials from CA1 pyramidal neurons, slices were incubated in ACSF containing low extracellular $Mg^{2+}$, DNQX, and PTX as described above. Sharp microelectrodes were pulled from thin walled (1 mm) borosilicate capillary glass using a Flaming/Brown horizontal micropipette puller (Sutter Instruments). Microelectrode tips were filled with 3 M potassium acetate and in some cases included reduced L-GSH (0.7–1.4 mM). The microelectrode resistances ranged from 42 to 55 MΩ and 39 to 50 MΩ for 3 M potassium acetate- and 3 M potassium acetate + L-GSH-containing microelectrodes, respectively. Microelectrodes were visually positioned in the CA1 pyramidal cell layer using a dissecting microscope (SZH10, Optical Elements), and a bipolar stimulating electrode was positioned to stimulate the CA3 afferents onto CA1 pyramidal neurons. On cell entry, positive or negative current was applied to clamp the neuronal membrane potential at −65 mV. Only neurons with a resting membrane potential less than −59 mV, an input resistance >23 MΩ, and an action potential amplitude rising ≥78 mV from the point of spike initiation were included in the analysis. The mean resting membrane potential and holding current was −63 ± 2 mV, −0.07 ± 0.15 nA for the control cells and −63 ± 2 mV, 0.07 ± 0.18 nA for the L-GSH-injected neurons. Inclusion of L-GSH in the pipette had no significant effect on the resting membrane potential, holding current, input resistance, action potential amplitude, or the microelectrode resistance. Diphasic stimulus pulses of 100 µs duration were delivered at 0.033 Hz, and the stimulation intensity was adjusted to elicit an intracellular NMDAR synaptic response, which was below action potential threshold. Baseline response recording began within 3 min after cell entry.

All the drugs were prepared according to the manufacturer's specifications and ultimately dissolved in ACSF before bath application on the slices. 6,7-Dinitroquinoxaline-2,3(1*H*,4*H*)-dione (DNQX) (Sigma); 4-[(2*S*)-2-[(5-isoquinolinylsulfonyl)methylamino]-3-oxo-3-(4-phenyl-1-piperazinyl)propyl]phenyl isoquinolinesulfonic acid ester (KN-62), okadaic acid (OA) (Tocris Bioscience), and FK-506 (LC Laboratories) were initially dissolved in a small amount of dimethyl sulfoxide (DMSO; Sigma) and diluted in ACSF to a final DMSO concentration of <0.01% and to final DNQX, KN-62, OA, and FK-506 concentrations of 30, 10, 1, and 10 µM, respectively. Picrotoxin (PTX; Tocris Bioscience) and 5,5′-dithiobis(2-nitrobenzoic acid) (DTNB; Sigma) were initially dissolved in a small amount of ethanol and diluted in ACSF to a final ethanol concentration of 0.0001% and to final PTX and DTNB concentrations of 10 µM and 0.5 mM, respectively. Xanthine (Calbiochem) was initially dissolved in a small amount of 0.1N NaOH and finally dissolved in ACSF whose pH was readjusted to 7.4 using 10N hydrochloric acid. DTT, DL-2-amino-5-phosphonovaleric acid (AP-5), reduced L-GSH (Sigma), (±)-1-(5-isoquinolinesulfonyl)-2-methylpiperazine dihydrochloride (H-7) (Tocris Bioscience), bisindolylmaleimide I (Bis-I), myristoylated autocamtide-2-related inhibitory peptide (myr-AIP) (Calbiochem), and xanthine oxidase (Roche Diagnostics) were directly dissolved in ACSF. DMSO control studies were interleaved with experiments using DMSO as vehicle.

*Measurement of reactive oxygen species levels in the hippocampal slices.* Hippocampal slices were incubated for 30 min in ACSF containing a 10 µM concentration of the reactive oxygen species (ROS) detection reagent 5-(and-6)-carboxy-2′,7′-dichlorodihydrofluorescein diacetate

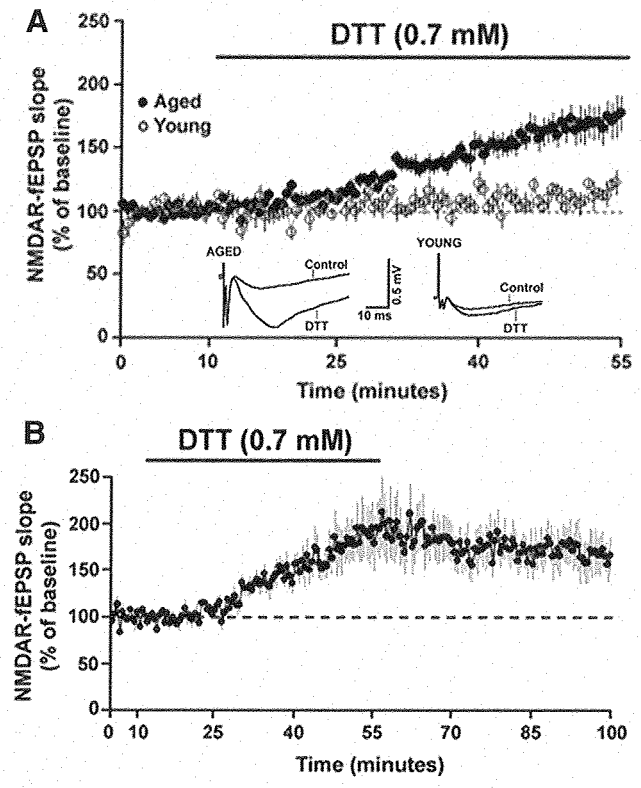


**Figure 4.** The reducing agent DTT increases NMDAR-mediated synaptic responses to a greater extent in aged than in the young animals. ***A***, Time course of the change in the normalized NMDAR-fEPSP slope in the aged (filled circles) ($n = 16$) and young (open circles) ($n = 5$) animals following application of DTT for 45 min. Inset, Representative traces (average of 5 consecutive traces under each condition) illustrating the change in NMDAR-fEPSP in the presence of DTT in an aged (top) and a young animal. Calibration: 10 ms, 0.5 mV. ***B***, Time course of the change in the normalized NMDAR-fEPSP slope in aged animals (filled circles) ($n = 5$) upon application of DTT for 45 min followed by a washout for 45 min.

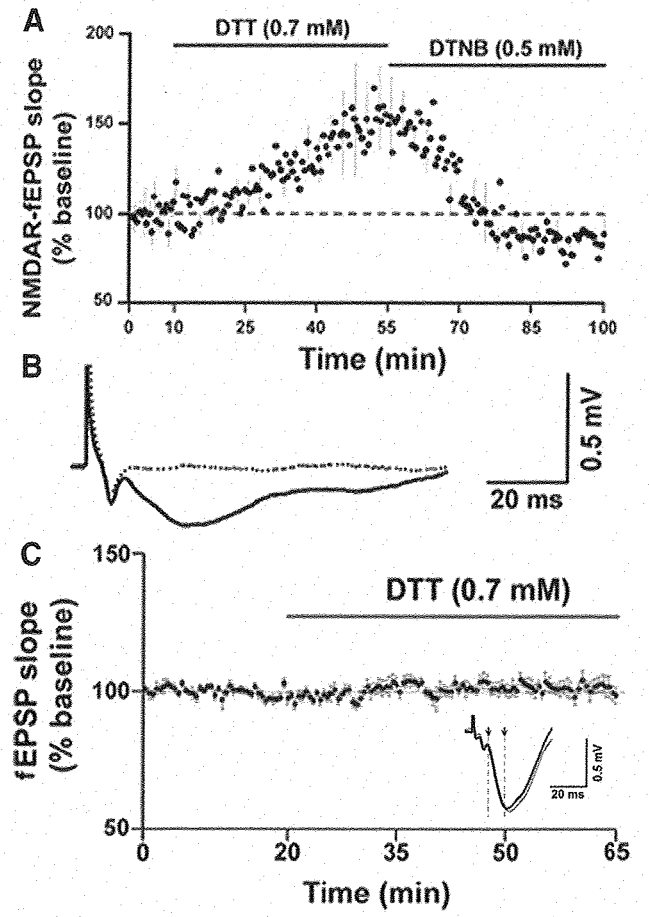


**Figure 5.** The effect of DTT on the NMDARs involves cysteine residues. ***A***, Time course of the change in the normalized NMDAR-fEPSP slope in aged animals ($n = 4$) in response to the bath application of DTT followed by DTNB. The increase in NMDAR-mediated synaptic responses by DTT was decreased by the oxidizing agent DTNB. Error bar in ***A*** is indicated for every fourth point, for purposes of clarity. ***B***, Representative traces (average of 5 consecutive traces) of the NMDAR-fEPSP recorded under control conditions (solid black trace) and upon application of 100 $\mu$M AP-5 (dashed black trace) for at least 30 min. ***C***, DTT does not affect the AMPAR function of aged animals. Time course of the change in fEPSP upon application of DTT for 45 min in aged hippocampal slices ($n = 10$). Inset, Representative traces (average of 5 consecutive traces) of the fEPSP recorded under control conditions (black trace) and after application of DTT for 45 min (gray trace). The downward-pointing arrows and cursors indicate the 15 ms time window, where the initial descending phase of the fEPSP is predominantly mediated by AMPARs. Calibration: 20 ms, 0.5 mV.

(c-$H_2$DCFDA; Invitrogen). Slices incubated for 30 min in absence of c-$H_2$DCFDA were used to detect background or autofluorescence. Following incubation, fluorescent images were obtained with an Axiovert 40 CFL fluorescent microscope and Axiocam digital CCD camera (Carl Zeiss). Fluorescence intensity was quantified as follows: fluorescent microscope was used to obtain images under uniform exposure time and intensity. The images were then converted to grayscale images in Adobe Photoshop 5.5; the resulting images were quantified by densitometry analysis using ImageJ software (http://rsbweb.nih.gov/ij). An area of ~225 $\mu$m along the medial–lateral axis and 187.5 $\mu$m along the anterior–posterior axis, centered on the CA1 pyramidal neurons was selected for analysis of fluorescence intensity. The mean gray value intensities obtained from the aged and young animals are represented as the mean fluorescence intensities. The mean fluorescence intensity from the dye-exposed slices is normalized to the mean fluorescence intensity obtained from dye-unexposed slices (harvested from the same animal) using the following relationship:

$$\text{Mean c-H}_2\text{DCFDA fluorescence (\% of control)} = [(F_s - F_c)/F_c] \times 100,$$

where Fs and Fc are the mean fluorescence intensities obtained from dye-exposed and dye-unexposed slices, respectively.

*CaMKII activity.* Hippocampi were isolated from aged F344 rats as described above. CA1 region was separated from the rest of the hippocampus, collected in an Eppendorf tube, flash frozen in liquid nitrogen, and stored at −80°C. The frozen CA1 tissue samples were placed in a Dounce homogenizer containing 1 ml of the homogenization buffer (sucrose, 1 M Tris, pH 7.5, 1 M KCl, protease inhibitor, protein phosphatase 1 inhibitor, protein phosphatase 2 inhibitor, 100 mg/ml sodium butyrate, and 0.1 M phenylmethylsulfonyl fluoride; all prepared in distilled $H_2O$) and homogenized using at least six strokes of the pestle. Homogenates were centrifuged at 7700 × *g* for 10 min at 4°C. The supernatant (containing the cytosolic fraction) was carefully isolated and stored at −80°C. Protein concentrations of the cytosolic fractions were determined using the BCA assay method (Pierce). CaMKII activity in the cytosolic fraction was measured using the CaMKII assay kit (CycLex). Briefly, uniform amount of cytosolic extracts (protein concentration = 2.0 $\mu$g per well) were loaded onto microtiter wells coated with a specific peptide substrate for CaMKII—Syntide-2, along with kinase reaction buffer with or without $Ca^{2+}$/calmodulin. Purified CaMKII (30 mU per reaction; CycLex) was used as positive control and cytosolic extracts incubated with EGTA + myr-AIP (CaMKII-specific peptide inhibitor) were used as negative control to obtain a measure of comparison for the CaMKII activity in the DTT-treated and untreated cytosolic extracts. CaMKII activity is expressed as spectral absorbance units at 450 nm, normalized to the control.

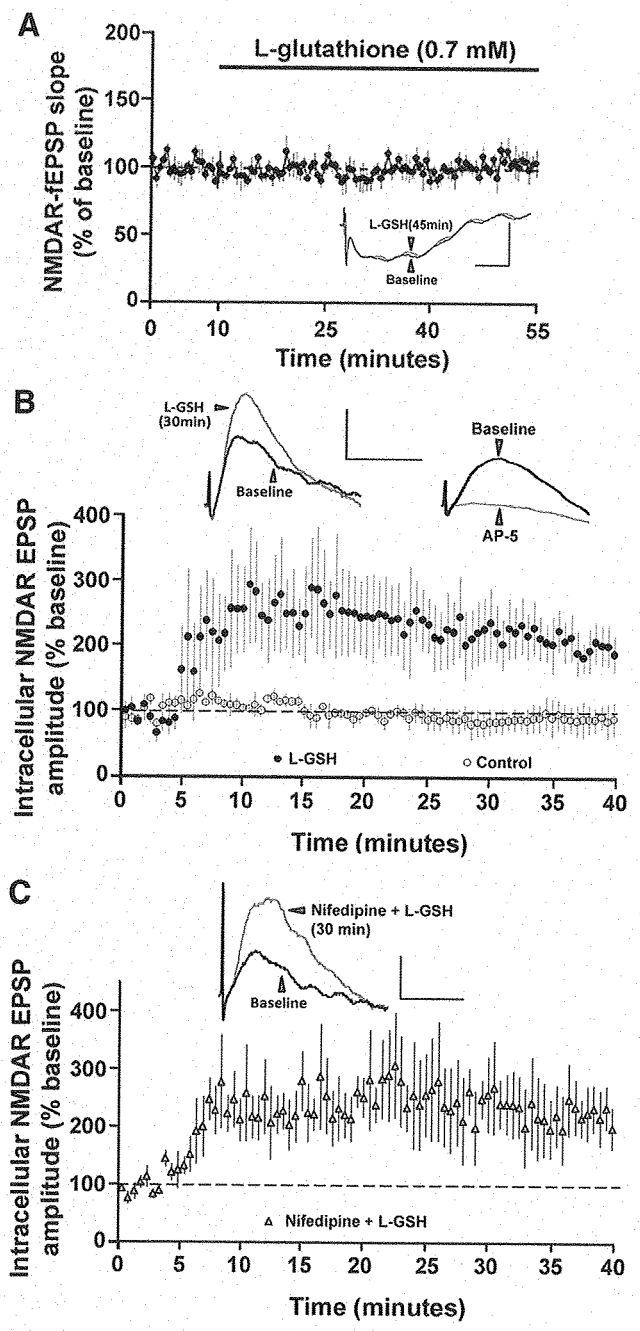


**Figure 6.** Intracellular, but not extracellular, application of L-GSH enhances NMDAR-mediated synaptic responses in aged animals. ***A***, Time course of the normalized NMDAR-fEPSP slope in the aged animals ($n = 6$) in response to extracellular application of the L-GSH. Inset, Overlay of the means of five consecutive responses during the baseline (black trace) and 45 min after application of L-GSH (gray trace). Calibration: 20 ms, 0.5 mV. ***B***, Time course of the normalized NMDAR-mediated intracellular EPSP amplitude in the aged animals obtained under control conditions (open circles, $n = 3$) or with L-GSH in the recording pipette (filled circles, $n = 6$). Left inset, Overlay of means from five consecutive responses obtained intracellularly during baseline (black trace) and 30 min after impalement (gray trace). Right inset, Overlay of means from five consecutive traces obtained intracellularly during baseline (black trace) and 25 min after application of AP-5 (gray trace). ***C***, Time course of normalized NMDAR-mediated intracellular EPSP amplitude obtained with nifedipine in the ACSF and L-GSH in the recording pipette (filled triangles, $n = 3$). Inset, Overlay of means from five consecutive responses obtained intracellularly during baseline (black trace) and 30 min after impalement (gray trace). Calibration (in ***B***, ***C***): 40 ms, 2 mV.

*Statistical analysis.* All statistical analyses were performed using StatView 5.0 (SAS Institute). Student's $t$ tests were used to examine for differences between treatments with significance set at $p < 0.05$. For tests involving more than one factor, ANOVA was used, followed by Fisher's protected least significant difference (PLSD) *post hoc* analysis to localize differences. In general only one or two slices per animal were used for a given experimental condition; although, several conditions could be examined using slices from the same animal. Therefore, where stated, $n$ represents the number of slices used in each experiment, unless stated as the number of animals, in which case we used only one slice from each animal. To ensure the reliability of our main effect (increased NMDAR responses following DTT application in aged animals), experiments involving DTT application alone were interleaved with experiments involving kinase/phosphatase inhibitors, DTNB and AP-5, resulting in a relatively large number of slices ($n = 16$) for this experiment.

## Results

### Oxidation decreases NMDAR responses in an age-dependent manner

The ROS detection reagent c-$H_2$DCFDA was used to evaluate differential rates of ROS production in hippocampal slices from young and aged animals (Fig. 1*A*,*B*). Dye-unexposed slices (aged control: 36.14 ± 4.42%, $n = 3$ animals; young control: 31.97 ± 3.16%, $n = 3$ animals) showed no significant difference in fluorescence across the age groups and were used to normalize the fluorescence intensity obtained from c-$H_2$DCFDA-treated slices. Incubation of the hippocampal slices from young and aged animals with c-$H_2$DCFDA for 30 min resulted in significantly (unpaired $t$ test; $p < 0.05$) enhanced fluorescence in aged animals (242.19 ± 20.96%, $n = 3$ animals) when compared to young animals (141.61 ± 11.78%, $n = 3$ animals). To exclude possible ROS outside the cells, aged hippocampal slices were incubated with superoxide dismutase (SOD; 121 U/ml) and catalase (260 U/ml) during the 30 min before imaging. There was no significant difference ($p > 0.05$) in the c-$H_2$DCFDA fluorescence observed between the SOD/catalase-exposed (292.388 ± 28.04%, $n = 3$) and unexposed aged hippocampal slices.

The NMDAR-mediated field EPSPs (NMDAR-fEPSPs) were studied to assess changes in the NMDAR response in hippocampal slices from young and aged animals. We confirmed that the NMDAR-mediated synaptic transmission decreases in the area CA1 of the hippocampus during aging. The stimulation-evoked PFV is an indicator of the level of axon activation that gives rise to the NMDAR-fEPSP (Fig. 2*A*). To examine the relationship between PFV amplitude and the amplitude of the NMDAR-fEPSP across age groups, the PFV amplitude was separated into 0.4 mV bins and plotted against the corresponding NMDAR-fEPSP amplitude obtained from the aged and the young animals (Fig. 2*B*). An ANOVA revealed that the amplitude of the NMDAR-fEPSP was reduced in the aged animals ($n = 6$ animals) when compared to young animals ($n = 5$ animals) ($F_{(1,47)} = 27.47$, $p < 0.0001$). The maximum amplitude of the NMDAR-fEPSP was 0.73 ± 0.14 mV and 2.87 ± 0.9 mV in aged and young animals, respectively.

For subsequent studies, the stimulation intensity was set to evoke a response that was 30% to 50% of the maximal NMDAR-fEPSP, and the slope of the NMDAR-fEPSP was measured before and after pharmacological manipulations. To test the hypothesis that the decrease in the NMDAR response was related to oxidizing conditions X/XO, an enzyme substrate combination that produces two types of ROS—superoxide anion and hydrogen peroxide—was applied to hippocampal slices of young and aged animals. Paired $t$ test revealed that application of X/XO [20 μg/ml/(0.25 U/mg xan-

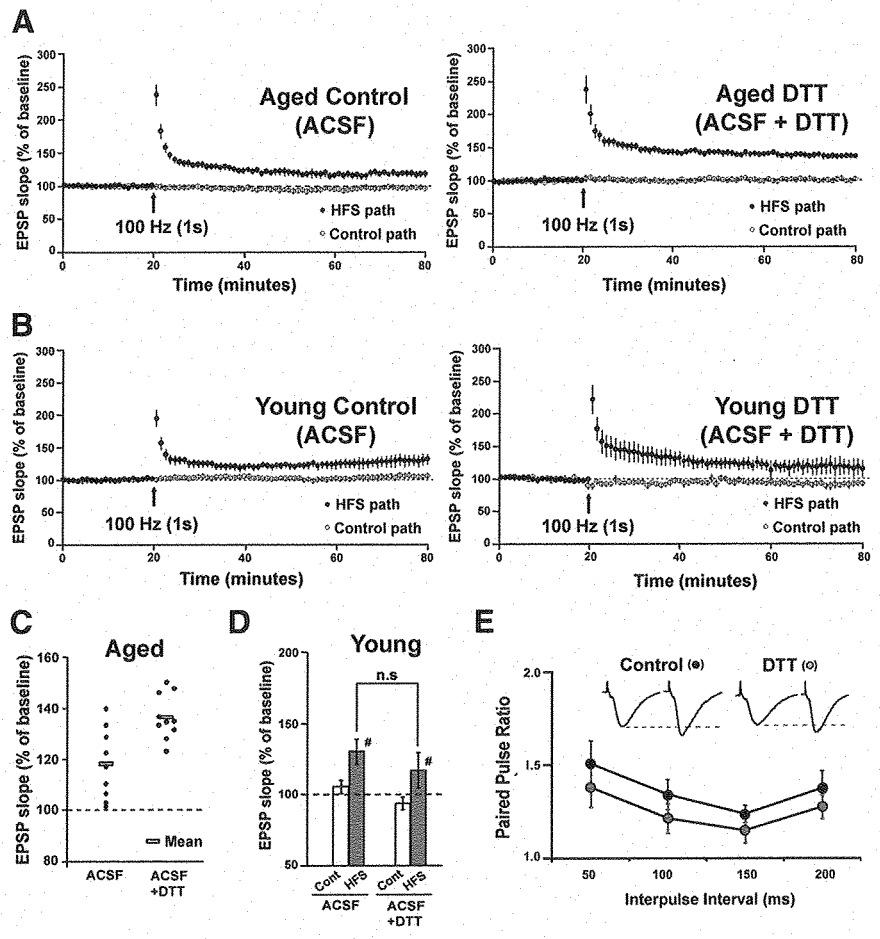


**Figure 7.** DTT enhances LTP in hippocampal area CA1 of aged animals. ***A***, Time course for the expression of LTP recorded in hippocampal slices from aged animals. Slices were bathed in control ACSF ($n = 9$) or ACSF containing DTT ($n = 10$) for at least 45 min before HFS. Baseline stimulation was applied to a control pathway (open circles) and to a second pathway that received HFS (100 Hz, 1 s) (filled circles). Arrows denote HFS delivery. For purpose of clarity, each point represents the mean of two consecutive responses. ***B***, Time course for the expression of LTP recorded in hippocampal slices from young animals. Slices were bathed in control ACSF ($n = 6$) (left) or ACSF containing DTT ($n = 5$) (right) for at least 45 min before HFS. Baseline stimulation was applied to a control pathway (open circles) and to a second pathway that received HFS (100 Hz, 1 s) (filled circles). Arrows denote HFS delivery. ***C***, Distribution of the LTP magnitude for individual slices from aged animals bathed in control ACSF and ACSF + DTT. The rectangular boxes indicate the mean of each group. ***D***, Quantification of the mean percentage change in the fEPSP slope recorded from the control (Cont) and HFS (HFS) pathways from young slices bathed in ACSF or ACSF + DTT. ***E***, Plot of the paired-pulse ratio obtained under control conditions (black circles) and after 45 min bath application of DTT (gray circles) for four interpulse intervals (50, 100, 150, 200 ms). Inset: Responses obtained upon paired pulse stimulation (average of 5 consecutive traces; 50 ms interpulse interval) under control conditions and under DTT application.

thine)] for 60 min, significantly decreased the slope of the NMDAR-fEPSP from the baseline levels in the young ($p < 0.01$) but not in the aged animals. Furthermore, application of X/XO significantly ($F_{(1,10)} = 15.49$, $p < 0.01$) decreased the NMDAR-fEPSP slope to a greater extent in the young animals (66.37 ± 7.04%, $n = 5$), when compared to the aged animals (96.41 ± 6.14%, $n = 7$) (Fig. 3*A*,*B*). Paired *t* test on the percentage change in the PFV indicated no effect ($p > 0.05$) of X/XO (young: 95.16 ± 8.29; aged: 108.23 ± 19.44). The effect of ROS on the NMDAR response of young animals was reversible, such that even in the presence of a higher concentration of xanthine oxidase [X/XO: 20 μg/ml/(1 U/mg xanthine)], which decreased the NMDAR-mediated synaptic response to 54.21 ± 5.79%, the response recovered to 88.11 ± 5.41% of the baseline ($n = 5$) following a 50 min washout (Fig. 3*C*).

### Reducing agents enhance NMDAR responses in an age-dependent manner

The age-dependent sensitivity of NMDAR-fEPSP to oxidizing conditions suggests that components of the NMDAR signaling system are initially oxidized to a greater extent in aged animals. Furthermore, the recovery of the NMDAR-fEPSP following washout indicates that young animals possess sufficient antioxidant and/or redox buffering capacity to absorb the excess oxyradical production. To test whether the decline in the NMDAR response in aged animals might be due to the age-dependent increase in the formation of disulfide linkages on the cysteine residues, the reducing agent DTT was applied to hippocampal slices. DTT can reduce the disulfide bonds on proteins into free thiols, thus partially reversing the effect of oxidative stress. Paired *t* test revealed that DTT significantly enhanced the slope of the NMDAR-fEPSP from the baseline levels in both the aged ($p < 0.0001$) and young ($p < 0.05$) animals. However, bath application of DTT (0.7 mM, 45 min) significantly ($F_{(1,19)} = 5.49$, $p < 0.05$) increased the slope of the NMDAR-fEPSP to a greater extent in the aged animals (171.38 ± 13.26%, $n = 16$) when compared to young animals (114.55 ± 4.41%, $n = 5$) (Fig. 4*A*). Paired *t* test on the PFV amplitude before and after application of DTT confirmed no change ($p > 0.05$) in the PFV amplitude for aged (102.81 ± 3.84) and young (97.08 ± 5.41) animals, indicating that the effect of DTT on the NMDAR-mediated response was not due to changes in excitability and/or the number of axons activated. The enhancement of the NMDAR-fEPSP in the aged animals was maintained (167.32 ± 20.91%, $n = 5$) following a 45 min washout of DTT (Fig. 4*B*).

To test whether the NMDAR-fEPSP in aged animals was indeed affected by the redox environment, the oxidizing agent DTNB was applied subsequent to the DTT-mediated enhancement of the NMDAR response in aged animals. Bath application of DTNB (0.5 mM, 45 min) significantly decreased ($p < 0.05$) the DTT-mediated increase in NMDAR-fEPSP in aged animals, such that the NMDAR-fEPSP slope was 86.49 ± 5.54% ($n = 4$) of the baseline (Fig. 5*A*). A repeated-measures ANOVA comparing the mean NMDAR-fEPSP slope corresponding to the last 5 min under each condition indicated a significant ($F_{(2,9)} = 6.24$, $p < 0.05$) difference. *Post hoc* analysis revealed that the NMDAR-fEPSP slope was significantly ($p < 0.05$) increased under DTT compared to baseline and DTNB ($p < 0.05$), and no significant difference was observed between the NMDAR-fEPSP slopes in the baseline and under DTNB. Finally, the NMDAR-fEPSP was abolished by application of AP-5 (Fig. 5*B*), indicating that the response was dependent on NMDARs.

To further examine the specificity of the DTT effects, slices were bathed in normal ACSF and the AMPA receptor (AMPAR) component was recorded as the initial descending phase of the synaptic response. Application of DTT did not affect the AMPAR component of the synaptic response such that responses were 101.63 ± 2.89% ($n = 10$) of the baseline after application of DTT for 45 min (Fig. 5C). This confirms previous reports that DTT does not influence AMPAR function (Gozlan et al., 1995; Abele et al., 1998). Together, the results indicate that oxidation of sulfhydryl groups can rapidly regulate responsiveness of NMDARs, and that an age-related reduction in the NMDAR response is linked to the redox environment.

### Intracellular redox status contributes to age-related differences in NMDAR synaptic responses

Previous research indicates that L-GSH is a cellular reducing agent that protects hippocampal neurons against oxidative stress (Shin et al., 2005; Shih et al., 2006; Yoneyama et al., 2008). However, L-GSH is relatively membrane impermeable such that exogenous application of L-GSH is not effective in increasing intracellular free thiols when compared to DTT (Mazor et al., 1996; Zou et al., 2001; Susankova et al., 2006). Extracellular application of the reduced form of L-GSH (0.7 mM, 45 min) did not alter NMDAR-fEPSP in the aged animals (104.83 ± 8.39%, $n = 6$) (Fig. 6A). In contrast to the extracellular application, inclusion of the reduced form of L-GSH (0.7 mM to 1.4 mM) in the intracellular recording pipette significantly ($F_{(1,6)} = 6.87$, $p < 0.05$) enhanced the amplitude of the NMDAR-mediated synaptic potentials (203.90 ± 31.38%, $n = 5$) in single hippocampal CA1 pyramidal neurons from aged hippocampus when compared to age-matched control cells (91.55 ± 22.94%, $n = 3$), for which L-GSH was not included in the intracellular recording pipette (Fig. 6B). Finally, intracellular delivery of L-GSH in the presence of nifedipine (10 μM) continued to enhance the amplitude of the NMDAR-mediated synaptic potentials (223.54 ± 46.56%, $n = 3$) (Fig. 6C), suggesting that the DTT effect is not due to differences in L-channel activity. The fact that intracellular delivery of glutathione enhanced the NMDAR response provides strong evidence for intracellular redox status as a mechanism for the age-associated modulation of NMDAR function.

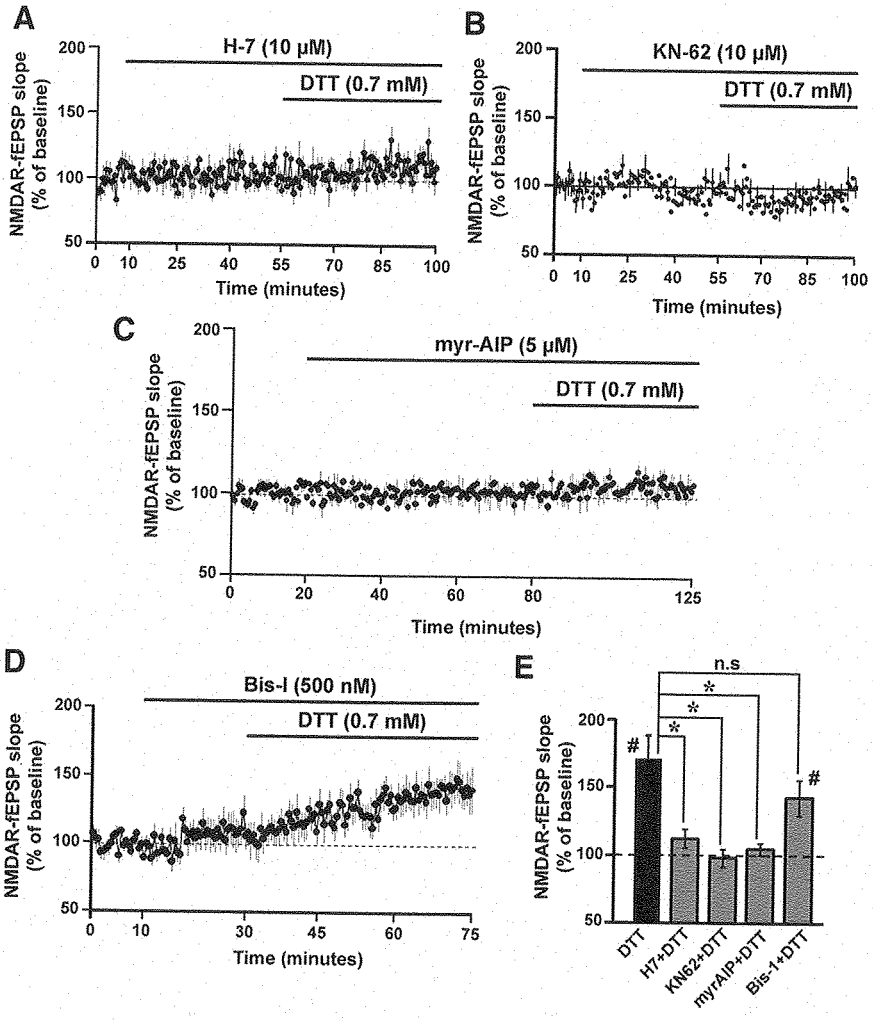


**Figure 8.** CaMKII involvement in the DTT-mediated enhancement of NMDAR synaptic responses in aged animals. ***A–D***, Time course of the change in the normalized NMDAR-fEPSP slope in the aged animals that were incubated with the broad spectrum Ser/Thr kinase inhibitor H-7 dihydrochloride (10 μM, $n = 7$) (***A***), the CaMK inhibitor KN-62 (10 μM, $n = 5$) (***B***), the specific CaMKII inhibitor myr-AIP (5 μM, $n = 4$) (***C***), or the PKC inhibitor Bis-I (500 nM, $n = 6$) (***D***) before and during DTT application. ***E***, Quantification of the mean percentage change in the NMDAR-fEPSP slope for aged animals under DTT alone (filled bar), and DTT applied in the presence of H-7, KN-62, myr-AIP, and Bis-I (gray bars). An asterisk indicates a significant difference ( $p < 0.05$) between the increases observed in presence of DTT alone and DTT applied in the presence of H-7, KN-62, myr-AIP, and Bis-I. A pound sign indicates a significant ( $p < 0.05$) increase in the response relative to baseline level of 100%, following DTT application.

### Reducing conditions enhance LTP in region CA1 of aged hippocampus

For studies on LTP and paired-pulse facilitation, slices were bathed in normal ACSF to record the AMPAR and NMDAR component of the synaptic response. LTP was induced by a single episode of high-frequency stimulation (HFS; 100 Hz, 1 s). The magnitude of LTP was significantly ($F_{(1,17)} = 12.14$, $p < 0.01$) greater in aged hippocampal slices preincubated with DTT for 45 min (136.53 ± 2.77%; $n = 10$), when compared to the aged controls not exposed to DTT (118.15 ± 4.63%; $n = 9$) (Fig. 7A,C). In contrast, there was no difference in the levels of HFS-induced LTP between young controls (130.17 ± 8.64%; $n = 6$) and the young slices exposed to DTT (117.09 ± 12.24%; $n = 5$) (Fig. 7B,D). Thus, reducing conditions enhance NMDAR responses and the magnitude of LTP only in aged animals. Furthermore, examination of paired pulses delivered at varying interpulse intervals ($\Delta t = 50$ ms, 100 ms, 150 ms, 200 ms), under control conditions and 45 min after the bath application of DTT indicated no effect of treatment across the four interpulse intervals (Fig. 7E).

### CaMKII contributes to DTT-mediated enhancement of NMDAR responses in aged animals

NMDAR function is controlled by several intracellular kinases (Ben-Ari et al., 1992; Westphal et al., 1999; Li et al., 2001). Fur-

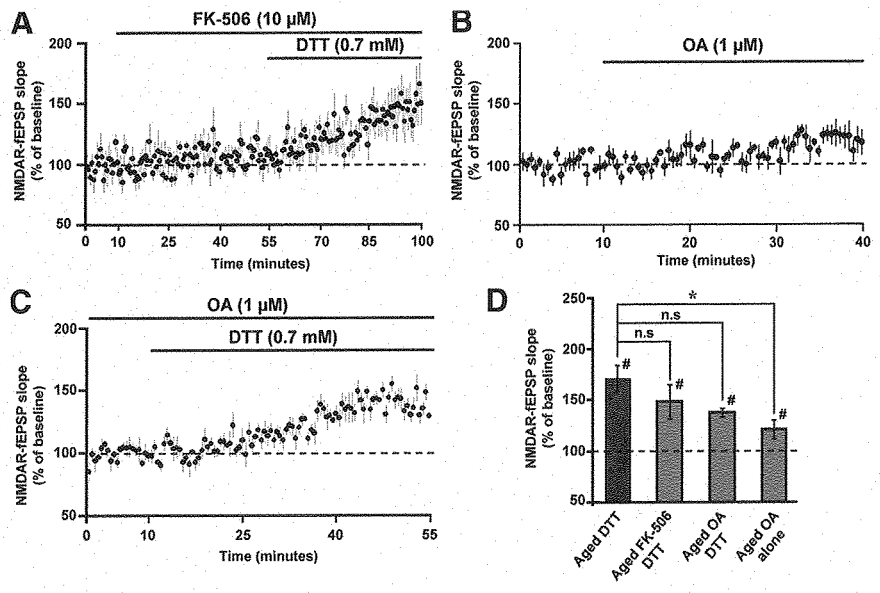


**Figure 9.** Calcineurin and PP1 are not involved in the DTT-mediated enhancement of NMDAR synaptic responses in aged animals. ***A***, Time course of the increase in the NMDAR-fEPSP slope in slices from aged animals that were incubated with FK-506 (10 μM), 45 min before and during the application of DTT ($n = 5$). ***B***, The NMDAR-fEPSP slope exhibited a modest increase (121.46 ± 9.19%) following a 30 min incubation with OA (1 μM) ($n = 5$). ***C***, Following stabilization of the response in OA, the baseline was recalculated. The figure illustrates the time course for the increase in the renormalized NMDAR-fEPSP slope following application of DTT ($n = 5$). ***D***, Quantification of the mean percentage change in the NMDAR-fEPSP slope for aged animals under DTT alone (filled bar) and in the presence of FK-506 + DTT, OA + DTT, and OA alone (gray bars).

thermore, the enzymatic activity of these kinases can be regulated by the reduction and oxidation of the cysteine residues located in their structure (Raynaud et al., 1997; Griendling et al., 2000; Knapp and Klann, 2000). To test whether serine/threonine (Ser/Thr) kinases were involved in the DTT-mediated increase of the NMDAR response, the broad-spectrum and membrane-permeable Ser/Thr kinase inhibitor H-7 was bath applied before and during the application of DTT. In the presence of H-7 (10 μM, 45 min), DTT application failed to produce the robust increase (one-group $t$ test; $p > 0.05$) in the NMDAR-fEPSP slope (111.86 ± 6.92%, $n = 7$) from the baseline levels (Fig. 8*A*). Similarly, bath application of the CaMK inhibitor KN-62 (10 μM, 45 min) (Tokumitsu et al., 1990), before and during the application of DTT, blocked (97.9 ± 7.98%, $n = 5$) the DTT-mediated increase in NMDAR-fEPSP in aged animals (Fig. 8*B*). Finally, the specific inhibitor of CaMKII, myr-AIP (5 μM, 60 min), which was bath applied before and during the application of DTT, effectively blocked (104.48 ± 4.29%, $n = 4$) the DTT-mediated increase in NMDAR-fEPSP in aged animals (Fig. 8*C*). In contrast, the membrane-permeable PKC inhibitor, Bis-I (500 nM, 45 min) (Knapp and Klann, 2002) failed to block the DTT-mediated increase in the NMDAR-fEPSP (142.58 ± 13.06%, $n = 6$) (Fig. 8*D*). An ANOVA comparison of the effect of DTT in the presence and absence of the kinase inhibitors, indicated a significant effect of kinase inhibitors on the DTT effect in aged animals ($F_{(4,33)} = 5.85$, $p < 0.01$). *Post hoc* comparisons indicated that the DTT-mediated increase in the NMDAR response was blocked by H-7, myr-AIP, and KN-62 but not Bis-I (Fig. 8*E*). Finally, $t$ tests indicated no effect of 0.01% DMSO (96.38 ± 7.64, $n = 5$) or kinase inhibition per se (H-7: 103.01 ± 4.21%, $n = 7$; KN-62: 96.23 ± 8.3%, $n = 5$; myr-AIP: 100.52 ± 4.42%, $n = 4$; Bis-I: 110.72 ± 11.44%, $n = 6$) on the baseline NMDAR-fEPSP slope in aged animals.

The activity of Ser/Thr phosphatases, such as calcineurin (CaN) and protein phosphatase 1 (PP1), is thought to contribute to altered synaptic plasticity during aging (Foster et al., 2001). Furthermore, phosphatase activity decreases NMDAR function (Lieberman and Mody, 1994; Wang et al., 1994). To test whether DTT effects were mediated by CaN, the CaN inhibitor FK-506 (10 μM) (Norris et al., 2010) was bath applied 45 min before and during the application of DTT on aged hippocampal slices. Application of FK-506 per se did not affect the NMDAR-fEPSP slope (109.61 ± 9.16%, $n = 5$). Importantly, FK-506 failed to block the DTT-mediated increase in the NMDAR response in aged animals such that the NMDAR-fEPSP slope increased to 148.61 ± 16.42% ($n = 5$) (Fig. 9*A*,*C*).

To examine the role of PP1, the PP1 inhibitor OA (1 μM, 30 min) (Schnabel et al., 2001) was applied before and during application of DTT to aged hippocampal slices. Application of OA significantly increased the NMDAR-fEPSP slope during the baseline recording period (121.46 ± 9.19%, $n = 5$, $p < 0.05$). Therefore, a new stable baseline was recorded before the application of DTT. Relative to the new baseline, DTT increased the NMDAR-fEPSP slope (137.89 ± 3.99%, $n = 5$) in the presence of OA (Fig. 9*B*,*C*). An ANOVA comparing the effect of DTT in the presence and absence of the phosphatase inhibitors, indicated no significant difference ($F_{(2,15)} = 1.37$, $p > 0.05$) (Fig. 9*D*).

To determine whether DTT was directly influencing CaMKII activity, cytosolic extracts from CA1 region of the hippocampus from aged and young animals were assayed for CaMKII activity by examining the phosphorylation of the synthetic peptide, syntide-2, in the presence and absence of DTT. Relative to baseline control levels, cytosolic CaMKII activity was significantly enhanced ($p < 0.05$) in the presence of 0.7 mM (113.11 ± 3.47%, $n = 3$) and 1.4 mM (120.46 ± 3.14%, $n = 3$) DTT in the aged CA1 cytosolic extracts (Fig. 10*A*). Higher levels of DTT (2.8 mM) resulted in a decrease in CaMKII activity, presumably due to denaturation of the enzyme. In contrast to the effect observed in aged animals, DTT had either no effect or decreased CaMKII activity in CA1 cytosolic extracts from young animals (Fig. 10*B*). In both age groups, the CaMKII activity was inhibited ($p < 0.05$) by the addition of calcium chelator EGTA (2 mM) and a CaMKII-specific peptide inhibitor myr-AIP (10 μM) (aged: 5.36 ± 2.85%, $n = 3$; young: 19.99 ± 9.01%, $n = 3$).

One possibility is that DTT was acting on the CaMKII activity regulator calmodulin (CaM). In this case, the effect of DTT on CaMKII activity may have been reduced by the addition of exogenous and unoxidized CaM. To test this idea the assay was repeated in the absence of exogenously added CaM. The CaMKII activity from aged CA1 cytosolic extract in the presence of 0.7 mM DTT, in the absence of exogenous CaM (112.11 ± 3.91%, $n = 3$), was not enhanced beyond that observed following addition of exogenous CaM, suggesting that DTT effects were not mediated by reducing cysteines on CaM. Finally, addition of DTT to purified CaMKII (CycLex) decreased CaMKII activity ($p < 0.05$) (0.7 mM DTT: 86.62 ± 6.04%, $n = 3$; 1.4 mM DTT: 70.72 ±

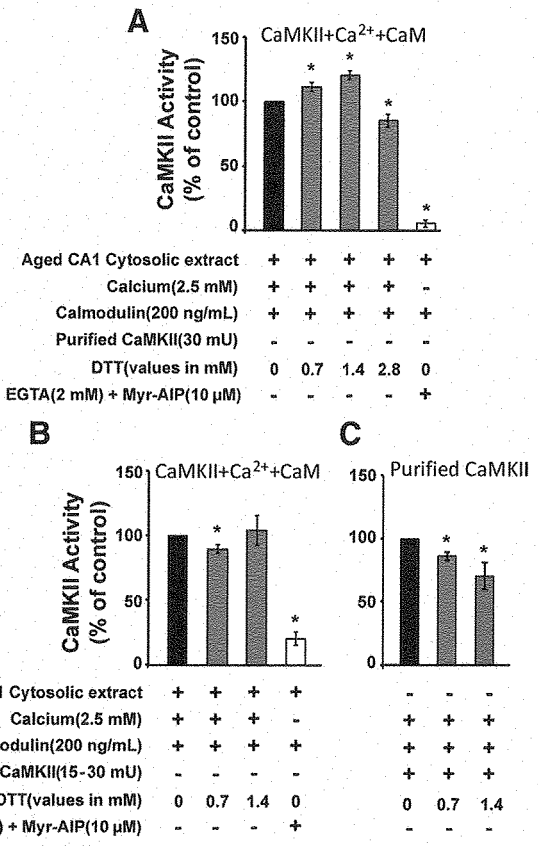


**Figure 10.** DTT enhances CaMKII activity in aged but not in young hippocampal CA1 cytosolic extracts. ***A***, CaMKII activity measured from the hippocampal CA1 cytosolic extracts of aged F344 rats. CaMKII activity is represented as percentage of control activity (black bars) in the presence of exogenous calmodulin. CaMKII activity was significantly enhanced in the presence of 0.7 mM and 1.4 mM DTT (gray bars) and was blocked by the addition of EGTA (2 mM) + myr-AIP (10 $\mu$M) (white bars). ***B***, Addition of 0.7 mM and 1.4 mM DTT did not increase CaMKII activity in hippocampal CA1 cytosolic extracts of young F344 rats. ***C***, Addition of 0.7 and 1.4 mM DTT decreased the activity of purified CaMKII. An asterisk indicates a significant difference ( $p < 0.05$) from respective controls. Plus and minus represent the presence and absence (respectively) of the indicated component in the reaction mix.

18.58%, $n = 3$) (Fig. 10*C*), indicating that the DTT effects were specific for CaMKII present in the aged CA1 cytosolic extracts.

## Discussion

### Intracellular redox state contributes to "NMDAR hypofunction" in the aged hippocampus

Previous work demonstrates that NMDAR responses are reduced in the area CA1 of the hippocampus of aged rat brain (Barnes et al., 1997; Billard and Rouaud, 2007), possibly due to altered receptor function (Cady et al., 2001). We confirmed an age-related decrease in the NMDAR response and demonstrate age-dependent effects of redox modulators on the NMDAR response. Our results reveal a role for intracellular redox state in contributing to the age-related decline in NMDAR-mediated synaptic responses and impaired induction of LTP in area CA1 of the hippocampus. The effects of DTT application were specific for aged animals and not observed for young animals. Furthermore, the DTT-mediated increase in the NMDAR response was not associated with a change in the PFV, was not mimicked for the AMPAR-mediated response (Fig. 5*D*) and was not blocked by nifedipine, suggesting the effect was not due to a general influence on cell excitability. Finally, the manner in which DTT affects the NMDAR response was specific to the intracellular redox state and the activity of CaMKII. Thus, we establish a mechanism that links general theories of aging (i.e., oxidative stress and redox state) with biological markers of age-related cognitive decline, reduced NMDAR responses, and impaired LTP.

The redox state of the extracellular cysteine residues of the NMDARs have been implicated in regulating the NMDAR function in cell cultures and neonatal animals (Aizenman et al., 1989, 1990; Bernard et al., 1997; Choi and Lipton, 2000; Choi et al., 2001). In contrast, our results are consistent with recent work in hippocampal cell cultures indicating a decrease in the intracellular redox ratio during aging, due in part to a deficit in intracellular GSH (Parihar et al., 2008). Specifically, we observed that intracellular but not extracellular application of L-GSH enhanced the NMDAR response in the aged neurons, indicating that the age-related decrease in NMDAR function is due to a shift in redox state of the intracellular compartment.

### CaMKII-dependent mechanism for altered NMDAR responses in aged animals

The DTT-mediated enhancement of NMDAR responses was specific to CaMKII activity. CaMKII inhibitors, myr-AIP and KN-62, blocked the DTT-mediated enhancement of the NMDAR response in aged animals. The DTT effects were not blocked by inhibition of PKC or phosphatases—CaN and PP1. The results point to CaMKII as a critical link between the intracellular redox state and the decrease in the NMDAR response. The role of CaMKII was confirmed by enzyme activity assays, which established that DTT increased CaMKII activity only in CA1 cytosolic extracts of aged animals. DTT did not increase CaMKII activity in samples from young animals or in purified CaMKII.

Oxidation of methionine residues on CaM has been reported to decrease the ability of CaM to activate CaMKII (Robison et al., 2007). Our results are not likely due to CaM methionine oxidation since DTT selectively reduces cysteine residues (Ciorba et al., 1997; Cai and Sesti, 2009; Long et al., 2009). In addition, DTT had equivalent effects in activating CaMKII, regardless of whether exogenous CaM was added to the reaction. The results indicate that oxidation of CaMKII, rather than CaM, underlies the reduction in kinase activity and are consistent with a recent report demonstrating that oxidative stress induced by ischemia results in disulfide linkages on the cysteine residues of CaMKII, which decrease kinase activity (Shetty et al., 2008). While the data provide a link between age-related changes in intracellular redox state, CaMKII activity, and NMDAR function, the exact mechanism through which CaMKII regulates the NMDAR response remains to be determined. In addition to regulating phosphorylation state of proteins, including glutamate receptors, synaptic CaMKII participates in protein–protein interactions with several proteins localized to the dendritic spine, which could ultimately alter NMDAR location and function (Lisman et al., 2002; Robison et al., 2005). Indeed, reduced CaMKII activity is associated with a specific decrease in synaptic NMDARs and decreased LTP (Gardoni et al., 2009).

In addition to a role for CaMKII, we observed that PP1 inhibition resulted in a modest increase in the NMDAR-fEPSP in aged hippocampal neurons. Age differences in the NMDAR response, which depend on kinase/phosphatase activity, are reminiscent of the age-dependent effects of kinase and phosphatase inhibitors on the rapid component of synaptic transmission mediated by AMPARs (Norris et al., 1998b; Hsu et al., 2002; Foster, 2007) and suggest that PP1 activity contributes to a reduction in AMPAR and NMDAR components of synaptic transmission (Foster et al., 2001; Morishita et al.,

2005), a characteristic specific to senescent CA1 synapses (Rosenzweig and Barnes, 2003). Our results indicate that a shift in the intracellular redox state during aging may cause or magnify the imbalance in the kinase/phosphatase activity, favoring phosphatases (Foster, 2007).

Finally, NMDAR function is critical to the induction of LTP, and we observed that DTT improved LTP in hippocampal area CA1 in the aged animals. The interaction of NMDARs with CaMKII has been proposed as a model of memory (Lisman et al., 2002) and recent work indicates that disruption of the interaction between CaMKII and NMDAR impairs the induction of LTP and spatial learning (Zhou et al., 2007). We have provided evidence to indicate that an age-related shift in redox state is a biological mechanism that can progressively inhibit NMDAR function in the hippocampus during senescence. Together, the results suggest that age-related changes in the redox state contributes to a decline in CaMKII activity, which ultimately leads to a decline in the NMDAR response. The outcome of such senescent mechanisms is an alteration in the synaptic plasticity at the CA3–CA1 synapses that contributes to the age-related cognitive decline.

## References


Abele R, Lampinen M, Keinänen K, Madden DR (1998) Disulfide bonding and cysteine accessibility in the alpha-amino-3-hydroxy-5-methylisoxazole-4-propionic acid receptor subunit GluRD. Implications for redox modulation of glutamate receptors. J Biol Chem 273:25132–25138.

Aizenman E, Lipton SA, Loring RH (1989) Selective modulation of NMDA responses by reduction and oxidation. Neuron 2:1257–1263.

Aizenman E, Hartnett KA, Reynolds IJ (1990) Oxygen free radicals regulate NMDA receptor function via a redox modulatory site. Neuron 5:841–846.

Barnes CA, Rao G, Shen J (1997) Age-related decrease in the N-methyl-D-aspartateR-mediated excitatory postsynaptic potential in hippocampal region CA1. Neurobiol Aging 18:445–452.

Ben-Ari Y, Aniksztejn L, Bregestovski P (1992) Protein kinase C modulation of NMDA currents: an important link for LTP induction. Trends Neurosci 15:333–339.

Bernard CL, Hirsch JC, Khazipov R, Ben-Ari Y, Gozlan H (1997) Redox modulation of synaptic responses and plasticity in rat CA1 hippocampal neurons. Exp Brain Res 113:343–352.

Billard JM, Rouaud E (2007) Deficit of NMDA receptor activation in CA1 hippocampal area of aged rats is rescued by D-cycloserine. Eur J Neurosci 25:2260–2268.

Bliss TV, Collingridge GL (1993) A synaptic model of memory: long-term potentiation in the hippocampus. Nature 361:31–39.

Boric K, Muñoz P, Gallagher M, Kirkwood A (2008) Potential adaptive function for altered long-term potentiation mechanisms in aging hippocampus. J Neurosci 28:8034–8039.

Cady C, Evans MS, Brewer GJ (2001) Age-related differences in NMDA responses in cultured rat hippocampal neurons. Brain Res 921:1–11.

Cai SQ, Sesti F (2009) Oxidation of a potassium channel causes progressive sensory function loss during aging. Nat Neurosci 12:611–617.

Choi YB, Lipton SA (2000) Redox modulation of the NMDA receptor. Cell Mol Life Sci 57:1535–1541.

Choi Y, Chen HV, Lipton SA (2001) Three pairs of cysteine residues mediate both redox and $Zn^{2+}$ modulation of the nmda receptor. J Neurosci 21:392–400.

Ciorba MA, Heinemann SH, Weissbach H, Brot N, Hoshi T (1997) Modulation of potassium channel function by methionine oxidation and reduction. Proc Natl Acad Sci U S A 94:9932–9937.

Foster TC (1999) Involvement of hippocampal synaptic plasticity in age-related memory decline. Brain Res Brain Res Rev 30:236–249.

Foster TC (2002) Regulation of synaptic plasticity in memory and memory decline with aging. Prog Brain Res 138:283–303.

Foster TC (2006) Biological markers of age-related memory deficits: treatment of senescent physiology. CNS Drugs 20:153–166.

Foster TC (2007) Calcium homeostasis and modulation of synaptic plasticity in the aged brain. Aging Cell 6:319–325.

Foster TC, Sharrow KM, Masse JR, Norris CM, Kumar A (2001) Calcineurin links $Ca^{2+}$ dysregulation with brain aging. J Neurosci 21:4066–4073.

Gardoni F, Mauceri D, Malinverno M, Polli F, Costa C, Tozzi A, Siliquini S, Picconi B, Cattabeni F, Calabresi P, Di Luca M (2009) Decreased NR2B subunit synaptic levels cause impaired long-term potentiation but not long-term depression. J Neurosci 29:669–677.

Gozlan H, Khazipov R, Diabira D, Ben-Ari Y (1995) In CA1 hippocampal neurons, the redox state of NMDA receptors determines LTP expressed by NMDA but not by AMPA receptors. J Neurophysiol 73:2612–2617.

Griendling KK, Sorescu D, Lassègue B, Ushio-Fukai M (2000) Modulation of protein kinase activity and gene expression by reactive oxygen species and their role in vascular physiology and pathophysiology. Arterioscler Thromb Vasc Biol 20:2175–2183.

Hsu KS, Huang CC, Liang YC, Wu HM, Chen YL, Lo SW, Ho WC (2002) Alterations in the balance of protein kinase and phosphatase activities and age-related impairments of synaptic transmission and long-term potentiation. Hippocampus 12:787–802.

Knapp LT, Klann E (2000) Superoxide-induced stimulation of protein kinase C via thiol modification and modulation of zinc content. J Biol Chem 275:24136–24145.

Knapp LT, Klann E (2002) Potentiation of hippocampal synaptic transmission by superoxide requires the oxidative activation of protein kinase C. J Neurosci 22:674–683.

Li BS, Sun MK, Zhang L, Takahashi S, Ma W, Vinade L, Kulkarni AB, Brady RO, Pant HC (2001) Regulation of NMDA receptors by cyclin-dependent kinase-5. Proc Natl Acad Sci U S A 98:12742–12747.

Lieberman DN, Mody I (1994) Regulation of NMDA channel function by endogenous Ca(2+)-dependent phosphatase. Nature 369: 235–239.

Lipton SA, Choi YB, Takahashi H, Zhang D, Li W, Godzik A, Bankston LA (2002) Cysteine regulation of protein function—as exemplified by NMDA-receptor modulation. Trends Neurosci 25:474–480.

Lisman J, Schulman H, Cline H (2002) The molecular basis of CaMKII function in synaptic and behavioural memory. Nat Rev Neurosci 3:175–190.

Long LH, Liu J, Liu RL, Wang F, Hu ZL, Xie N, Fu H, Chen JG (2009) Differential effects of methionine and cysteine oxidation on [Ca2+] i in cultured hippocampal neurons. Cell Mol Neurobiol 29:7–15.

Magnusson KR, Bai L, Zhao X (2005) The effects of aging on different C-terminal splice forms of the zeta1(NR1) subunit of the N-methyl-d-aspartate receptor in mice. Brain Res Mol Brain Res 135:141–149.

Magnusson KR, Kresge D, Supon J (2006) Differential effects of aging on NMDA receptors in the intermediate versus the dorsal hippocampus. Neurobiol Aging 27:324–333.

Mazor D, Golan E, Philip V, Katz M, Jafe A, Ben-Zvi Z, Meyerstein N (1996) Red blood cell permeability to thiol compounds following oxidative stress. Eur J Haematol 57:241–246.

Morishita W, Marie H, Malenka RC (2005) Distinct triggering and expression mechanisms underlie LTD of AMPA and NMDA synaptic responses. Nat Neurosci 8:1043–1050.

Norris CM, Halpain S, Foster TC (1998a) Reversal of age-related alterations in synaptic plasticity by blockade of L-type $Ca^{2+}$ channels. J Neurosci 18:3171–3179.

Norris CM, Halpain S, Foster TC (1998b) Alterations in the balance of protein kinase/phosphatase activities parallel reduced synaptic strength during aging. J Neurophysiol 80:1567–1570.

Norris CM, Blalock EM, Chen KC, Porter NM, Thibault O, Kraner SD, Landfield PW (2010) Hippocampal 'zipper' slice studies reveal a necessary role for calcineurin in the increased activity of L-type Ca(2+) channels with aging. Neurobiol Aging 31:328–338.

Parihar MS, Kunz EA, Brewer GJ (2008) Age-related decreases in NAD(P)H and glutathione cause redox declines before ATP loss during glutamate treatment of hippocampal neurons. J Neurosci Res 86:2339–2352.

Poon HF, Calabrese V, Calvani M, Butterfield DA (2006) Proteomics analyses of specific protein oxidation and protein expression in aged rat brain and its modulation by L-acetylcarnitine: insights into the mechanisms of action of this proposed therapeutic agent for CNS disorders associated with oxidative stress. Antioxid Redox Signal 8:381–394.

Raynaud F, Evain-Brion D, Gerbaud P, Marciano D, Gorin I, Liapi C, Anderson WB (1997) Oxidative modulation of cyclic AMP-dependent protein kinase in human fibroblasts: possible role in psoriasis. Free Radic Biol Med 22:623–632.

Robison AJ, Bass MA, Jiao Y, MacMillan LB, Carmody LC, Bartlett RK, Colbran RJ (2005) Multivalent interactions of calcium/calmodulin-dependent pro-

tein kinase II with the postsynaptic density proteins NR2B, densin-180, and alpha-actinin-2. J Biol Chem 280:35329–35336.

Robison AJ, Winder DG, Colbran RJ, Bartlett RK (2007) Oxidation of calmodulin alters activation and regulation of CaMKII. Biochem Biophys Res Commun 356:97–101.

Rosenzweig ES, Barnes CA (2003) Impact of aging on hippocampal function: plasticity, network dynamics, and cognition. Prog Neurobiol 69:143–179.

Schnabel R, Kilpatrick IC, Collingridge GL (2001) Protein phosphatase inhibitors facilitate DHPG-induced LTD in the CA1 region of the hippocampus. Br J Pharmacol 132:1095–1101.

Shankar S, Teyler TJ, Robbins N (1998) Aging differentially alters forms of long-term potentiation in rat hippocampal area CA1. J Neurophysiol 79:334–341.

Shetty PK, Huang FL, Huang KP (2008) Ischemia-elicited oxidative modulation of Ca2+/calmodulin-dependent protein kinase II. J Biol Chem 283:5389–5401.

Shih AY, Erb H, Sun X, Toda S, Kalivas PW, Murphy TH (2006) Cystine/glutamate exchange modulates glutathione supply for neuroprotection from oxidative stress and cell proliferation. J Neurosci 26:10514–10523.

Shin EJ, Suh SK, Lim YK, Jhoo WK, Hjelle OP, Ottersen OP, Shin CY, Ko KH, Kim WK, Kim DS, Chun W, Ali S, Kim HC (2005) Ascorbate attenuates trimethyltin-induced oxidative burden and neuronal degeneration in the rat hippocampus by maintaining glutathione homeostasis. Neuroscience 133:715–727.

Susankova K, Tousova K, Vyklicky L, Teisinger J, Vlachova V (2006) Reducing and oxidizing agents sensitize heat-activated vanilloid receptor (TRPV1) current. Mol Pharmacol 70:383–394.

Tokumitsu H, Chijiwa T, Hagiwara M, Mizutani A, Terasawa M, Hidaka H (1990) KN-62, 1-[N,O-bis(5-isoquinolinesulfonyl)-N-methyl-L-tyrosyl]-4-phenylpiperazi ne, a specific inhibitor of Ca2+/calmodulin-dependent protein kinase II. J Biol Chem 265:4315–4320.

Tsien JZ, Huerta PT, Tonegawa S (1996) The essential role of hippocampal CA1 NMDA receptor-dependent synaptic plasticity in spatial memory. Cell 87:1327–1338.

Wang LY, Orser BA, Brautigan DL, MacDonald JF (1994) Regulation of NMDA receptors in cultured hippocampal neurons by protein phosphatases 1 and 2A. Nature 369:230–232.

Westphal RS, Tavalin SJ, Lin JW, Alto NM, Fraser ID, Langeberg LK, Sheng M, Scott JD (1999) Regulation of NMDA receptors by an associated phosphatase-kinase signaling complex. Science 285:93–96.

Yoneyama M, Nishiyama N, Shuto M, Sugiyama C, Kawada K, Seko K, Nagashima R, Ogita K (2008) In vivo depletion of endogenous glutathione facilitates trimethyltin-induced neuronal damage in the dentate gyrus of mice by enhancing oxidative stress. Neurochem Int 52:761–769.

Zhou Y, Takahashi E, Li W, Halt A, Wiltgen B, Ehninger D, Li GD, Hell JW, Kennedy MB, Silva AJ (2007) Interactions between the NR2B receptor and CaMKII modulate synaptic plasticity and spatial learning. J Neurosci 27:13843–13853.

Zou CG, Agar NS, Jone GL (2001) Oxidative insult in sheep red blood cells induced by T-butyl hydroperoxide: the roles of glutathione and glutathione peroxidase. Free Radic Res 34:45–56.

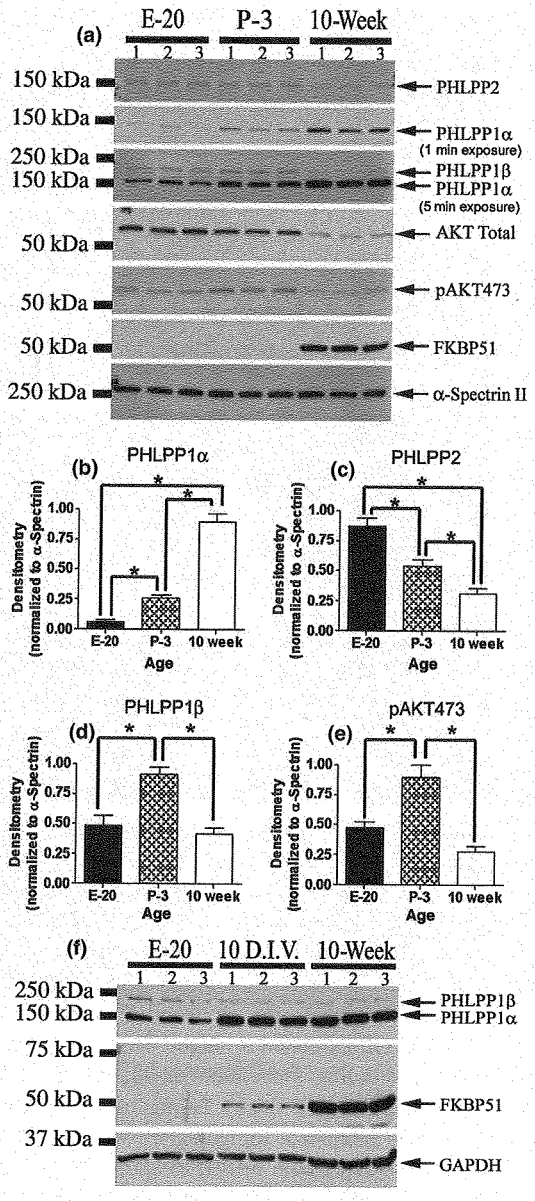


**Fig. 5** Developmental changes in PHLPP and AKT levels in the hippocampus. (a) Western blots showing protein changes in the level of PHLPP2, PHLPP1α, PHLPP1β, AKT total, pAKT473, FKBP51, and α-Spectrin II during early hippocampal development (E-20 = embryonic day 20; P-3 = postnatal day 3; 10-week = 10-week-old male adult hippocampal tissue; $n$ = 3/age). α-Spectrin II levels did not vary across the developmental ages examined and therefore was used as a loading control. Densitometry measures for expression of (b) PHLPP1α (c) PHLPP2 (d) PHLPP1β, and (e) pAKT473 during development. (f) FKBP51 is a critical regulator of PHLPP/AKT interaction. Western blots show 10 DIV hippocampal neurons express FKBP51. Further, PHLPP1α levels are much higher, and PHLPP1β levels are lower, in 10 DIV neurons compared to embryonic tissue, consistent with cultured neurons showing an adult phenotype.

neurons and compared to embryonic day 20- and 10-week-old adult hippocampi (Fig. 5f). Cultured hippocampal neurons expressed far higher levels of PHLPP1α and lower levels of PHLPP1β/SCOP compared to E20 hippocampi, consistent with adult PHLPP1 levels. In addition, FKPBP51 was clearly present in cultured neurons; although, the expression level was lower compared to adult tissue extracts. Higher levels of FKBP51protein in adult extracts may be because of increased FKBP51 expression and accumulation during maturation. Alternatively, glial cells may express high levels of FKBP51protien in the adult brain, explaining intense FKBP51 immunoreactivity in adult extracts. Together, the data demonstrate PHLPP proteins show a distinct pattern of protein expression at each stage of development, and suggest each PHLPP protein serves a unique function in the developing hippocampus. Moreover, our results confirm *in vitro* embryonic hippocampal neurons are representative of an adult phenotype, with respect to PHLPP protein levels, and express relevant PHLPP regulators. Therefore, *in vitro* neurons can be used to investigate neuronal PHLPP signaling mechanisms.

### PHLPP1 inhibits AKT signaling in hippocampal neurons

To elucidate the function of PHLPP1 in hippocampal neurons, we selectively knocked down either PHLPP1β/SCOP alone or PHLPP1α and PHLPP1β/SCOP together, and examined the activity of key kinases following stimulation with IGF-1. Previous work indicates that acute application of brain-derived neurotrophic factor to hippocampal neurons caused rapid degradation and a reduction in the levels of PHLPP1β/SCOP(Shimizu *et al.* 2007). To insure that a decline in PHLPP1β/SCOP or PHLPP1α was because of our shRNA treatment, rather than IGF-1 application, we measured PHLPP1β/SCOP and PHLPP1α levels in neurons transduced with a non-targeting shRNA and treated for 20 min with 100 ng/mL IGF-1. While pAKT437 ($p < 0.0001$), pAKT308 ($p < 0.0001$), and pERK2 ($p = 0.03$) were all significantly increased (Fig. 6a), IGF-1 stimulation had no effect on PHLPP1α or PHLPP1β/SCOP levels (Fig. 6b and c). Therefore, decreased levels of PHLPP1α and PHLPP1β/SCOP in our paradigm are because of targeting shRNA's and not proteolytic degradation induced by brief stimulation with IGF-1.

Pleckstrin homology and leucine rich repeat protein phosphatase 1β/SCOP was selectively knocked down by PHLPP1β/SCOP targeting shRNA, in 10 DIV hippocampal cultures (Fig. 7a–c). Cultures were transduced at both 0 DIV and 7 DIV with a non-targeting shRNA or selective PHLPP1β/SCOP targeting shRNA. At 10 DIV cultures were stimulated with 100 ng/mL IGF-1 for 20 min and subsequently analyzed for changes in the phosphorylation status of AKT, PKCα, and ERK. Loss of PHLPP1β/SCOP caused a dramatic increase in pERK levels (Fig. 8a–c), indicating PHLPP1β/SCOP negatively regulates Ras/MAP/ERK

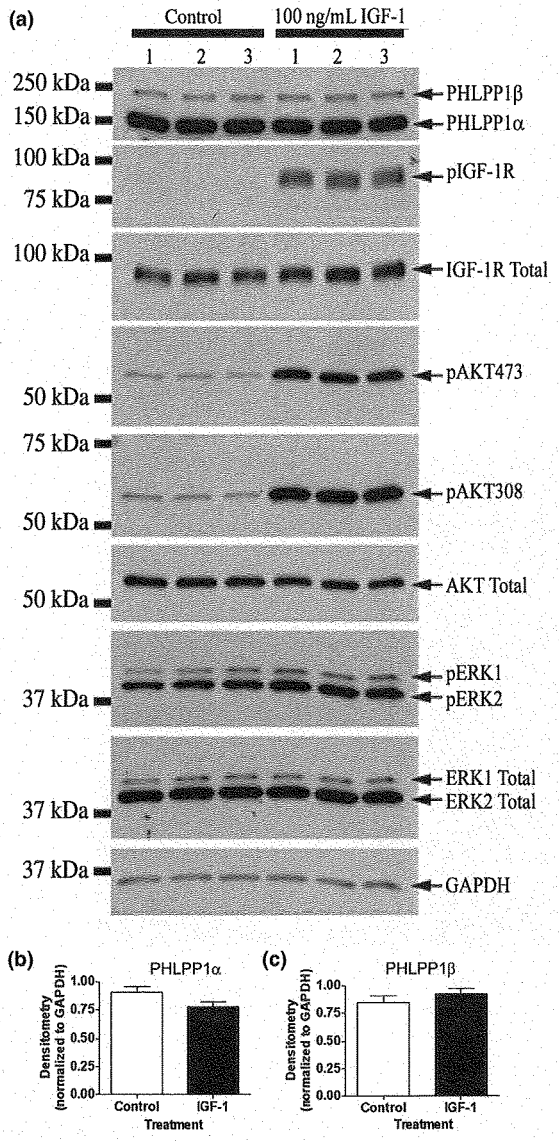


**Fig. 6** Acute treatment of IGF-1 does not alter PHLPP1 levels. Hippocampal neurons were transduced with lentivirus containing non-targeting shRNA and treated with or without 100 ng/mL IGF-1 for 20 min. (a) Western blots show increases in the level of pIGF-1R, pAKT473, pAKT308, and pERK. Stimulation of hippocampal neurons did not affect the level of either (b) PHLPP1α or (c) PHLPP1β ($n = 3$ for all graphs).

signaling. This finding is consistent with reports that overexpression of PHLPP1β/SCOP in hippocampal neurons robustly decreases ERK signaling. However, phosphorylated AKT (Fig. 9a, c and d) and PKCα (Fig. 10a and d) were significantly decreased; indicating PHLPP1β/SCOP positively regulates these signaling kinases. The shift in protein phosphorylation was also observed under steady state conditions. Examination of proteins after a 2-h serum starvation, in the absence of IGF-1 stimulation, confirmed decreased AKT/PKC phosphorylation and increased ERK phosphorylation in PHLPP1β/SCOP knockdown neurons (Figure S5). The results support the idea that PHLPP1β/SCOP alters the basal activity of AKT, PKC, and ERK kinases.

To verify that knock down of PHLPP1β/SCOP resulted in decreased activation of AKT and PKCα, we measured total levels of PKCα and FOXO3a. By inducing FOXO3a nuclear to cytoplasmic export and subsequent degradation (Plas and Thompson 2003), AKT negatively regulates the pro-death protein FOXO3a. Therefore, down-regulation of phosphorylated AKT would predict increased total levels of FOXO3a. Consistent with AKT's inhibition of FOXO3a signaling, total levels of FOXO3a were significantly increased in PHLPP1β/SCOP knockout neurons (Fig. 9a and f). Phosphorylation at pPKCα657 stabilizes PKCα levels (Bornancin and Parker 1997). Therefore, our results on phosphorylated PKC would predict a robust decrease in total PKCα levels, which was found to be the case (Fig. 10a and c). Moreover, longer exposures of pPKCα657 blots indicate a higher migrating band similarly affected by knockdown of PHLPP1β/SCOP and not observed in PKCα total blots (asterisks in Fig. 10a and b). Given the homology of the Ser657 PKCα hydrophobic phosphorylation site on other PKCs, the upper band may be the pPKCα657 antibody cross-reacting with other PKC isoforms. Therefore, additional PKC proteins may also be regulated by PHLPP1 protein levels.

Because the mRNA sequence for PHLPP1α is also contained in the PHLPP1β/SCOP mRNA, targeting PHLPP1α through shRNA techniques also inhibits PHLPP1β/SCOP, resulting in a general PHLPP1 knockdown (designated PHLPP1α/β knockout (KO) samples). Hippocampal neurons were transduced at both 0 DIV and 7 DIV with a non-targeting shRNA or two shRNA's targeting predicted coding regions within the middle of rat PHLPP1 mRNA. At 10 DIV, cultures were treated with 100 ng/mL IGF-1 for 20 min, and subsequently analyzed for changes in the phosphorylation status of AKT, PKCα, and ERK. We observed an approximately 90% knockdown of PHLPP1β/SCOP and 30–40% knockdown of PHLPP1α (Fig. 7d–f). To further verify knockdown, immunofluorescence of PHLPP1α was analyzed in 10 DIV neurons either transduced with a non-targeting shRNA (Fig. 7g–i) or the PHLPP1 targeting shRNA's (Fig. 7j–l). Consistent with the western blot results, PHLPP1α signal (Red Staining) is dramatically reduced in neurons transduced with PHLPP1 targeting shRNA's. Importantly, even moderate knockdown of PHLPP1 induced a robust increase in the phosphorylated levels of pAKT473 (~ 40% increase/Fig. 9b and g) and pAKT308 (~ 50% increase/Fig. 9b and h). On the other hand total AKT levels showed a mild decrease (Fig. 9b and i). Moreover, the results on pAKT are confirmed by changes in the level of FOXO3a total. FOXO3a was significantly decreased in PHLPP1 knockdown neurons (Fig. 9b and j). No significant differences in the

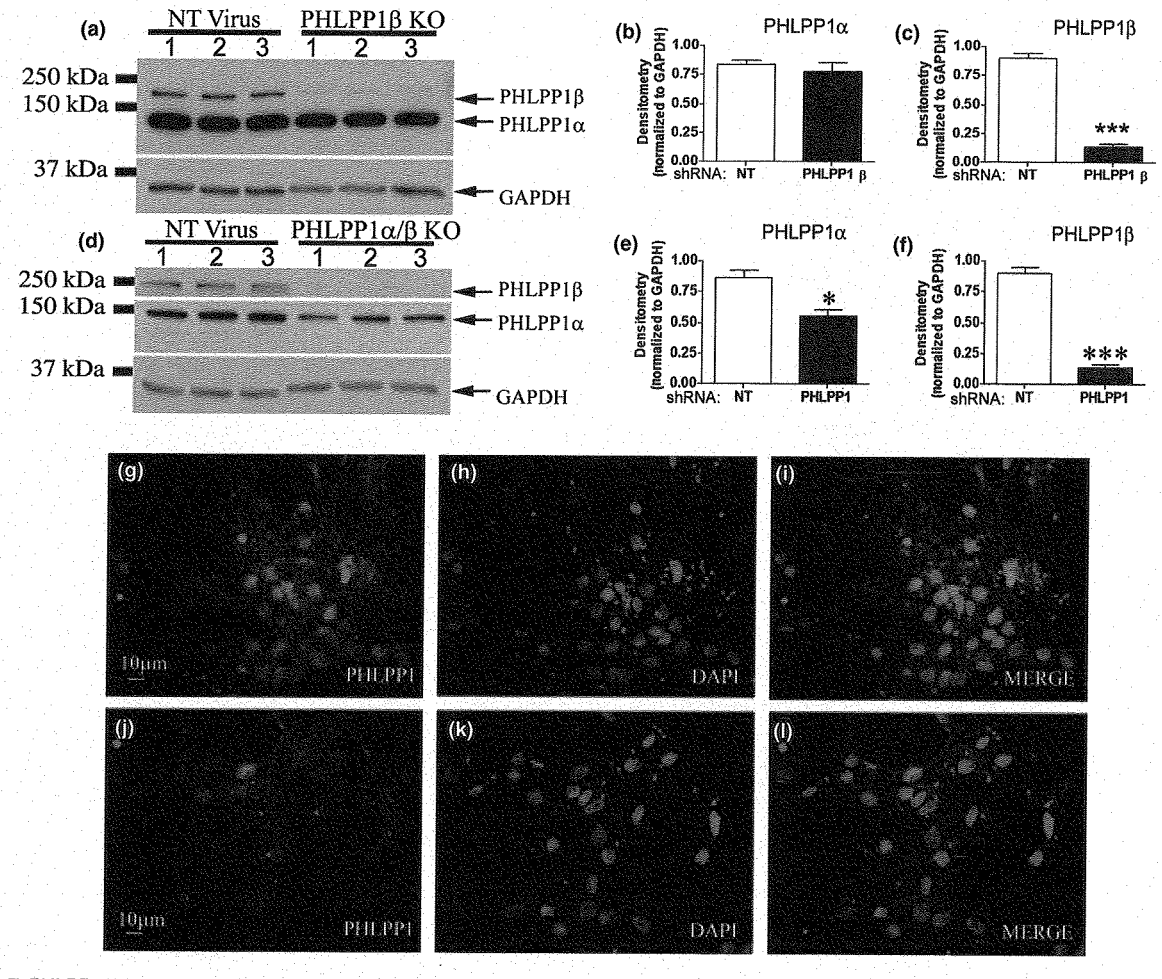


**Fig. 7** PHLPP1β and PHLPP1 knockdown in hippocampal neurons. Hippocampal neurons were transduced with lentivirus containing either a non-targeting shRNA (NT Virus), a shRNA virus targeting PHLPP1β (PHLPP1β KO), or shNRA's targeting both PHLPP1α/β (PHLPP1 KO) and treated with 100 ng/mL IGF-1 for 20 min. (a) Representative western blots ($n = 3$) showing effect of shRNA on PHLPP1β levels. (b and c) Densitometry of western blots ($n = 6$) show protein levels of PHLPP1β, but not PHLPP1α, is significantly decreased. (d) Representative western blots ($n = 3$) showing effect of shRNA's on PHLPP1 levels. (e and f) Densitometry of western blots ($n = 6$) show both PHLPP1β and PHLPP1α are significantly decreased. Knockdown of PHLPP1α was verified by immunofluorescence. (g–i) 10 DIV hippocampal neurons transduced with the non-targeting shRNA show a high level of PHLPP1 staining (RED) which predominantly localizes to the nucleus. (j–l) PHLPP1 staining is decreased in neurons transduced with PHLPP1α/β targeting shRNA's. Data are significant at $^*p < 0.05$, $^{***}p < 0.0001$.

level of pPKCα657 and PKCα total levels were observed following knockdown of PHLPP1 (Fig. 10b, e and f). In addition, decreasing PHLPP1 levels caused a robust increase in the levels of phosphorylated ERK1 but significantly decreased ERK1 total levels (Fig. 8d–f). Together, the data indicate that PHLPP1α inhibits the AKT pathway in hippocampal neurons.

## Discussion

Pleckstrin homology and leucine rich repeat phosphatase proteins are novel regulators of multiple cell signaling pathways. Studies using non-neuronal culture models indicate PHLPP1 inhibits the kinases AKT and PKCα (Gao *et al.* 2005; Brognard *et al.* 2007; Hirano *et al.* 2009). However, it has not been directly shown PHLPP1 can inhibit AKT and PKCα in neurons. Multiple CNS diseases are linked to dysregulation of neuronal AKT. Validation that PHLPP proteins are in fact AKT regulators in the brain is an important advancement in our understanding of the underlying biochemical mechanisms controlling CNS AKT signaling.

The results of the current study provide unique evidence for a divergence in the function of PHLPP1α and PHLPP1β/SCOP splice variants, and suggest that PHLPP1α plays a major role in regulating AKT signaling in neurons. As PHLPP1β/SCOP possesses some of the same regulatory

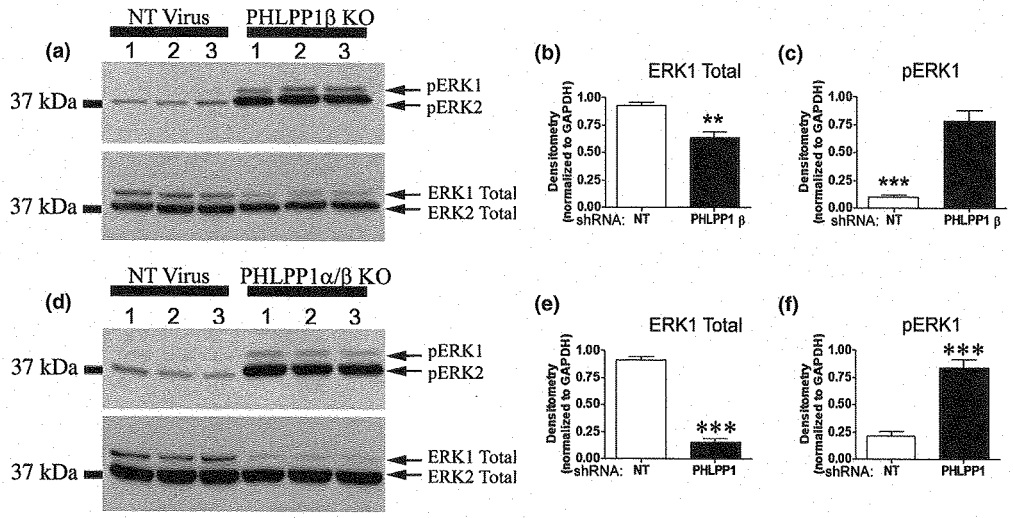


**Fig. 8** Effect of PHLPP1β and PHLPP1 knockdown on ERK phosphorylation. Hippocampal neurons transduced with lentivirus containing either a non-targeting shRNA (NT Virus), a shRNA virus targeting PHLPP1β (PHLPP1β KO), or shNRA's targeting both PHLPP1α/β (PHLPP1 KO) and treated with 100 ng/mL IGF-1 for 20 min. (a and d) Representative western blots ($n = 3$) show the effect of knockdown on ERK phosphorylation. (b and c) Densitometry of western blots ($n = 6$) show PHLPP1β knockdown reduces ERK1 total levels but increases phosphorylated ERK levels. (e and f) Densitometry of western blots ($n = 6$) show knockdown of PHLPP1 also reduces ERK1 total levels and increases ERK1 phosphorylation. Data are significant at $^{**}p < 0.001$, $^{***}p < 0.0001$.

domains as PHLPP1α, it is thought PHLPP1β/SCOP may regulate AKT and PKCα, in addition to ERK (Shimizu *et al.* 2010). Here, we report, for the first time, significant functional differences in the role of PHLPP1 splicoforms for regulating the AKT and PKC signaling pathways in neurons. The difference was revealed by comparing the effects of knockdown of both PHLPP1α and PHLPP1β/SCOP, relative to knockdown of PHLPP1β/SCOP alone (Figs 7–10). Knockdown of both phosphatases results in the expected increase in pAKT473, consistent with previous studies in cancer cells (Gao *et al.* 2005). Quite the opposite was observed following selective knockdown of PHLPP1β/SCOP, which significantly reduced pAKT473, pAKT308, and pPKCα657 in hippocampal neurons. Similarly, the decrease in pPKCα657 and total PKCα levels observed following knockdown of PHLPP1β/SCOP was not observed following knockdown of PHLPP1α/β, consistent with the idea that PHLPP1α and PHLPP1β/SCOP have opposing influences on some signaling pathways. In contrast, PHLPP1α/β KO, like PHLPP1β/SCOP KO, reduced total ERK1 and increased pERK expression. Together, the results suggest that PHLPP1α exhibits greater control over the AKT signaling pathway and PHLPP1β/SCOP has effects opposite PHLPP1α on AKT and PKCα, while acting as the primarily regulator of the Ras/MAP/ERK signaling pathway. Finally, the decreased AKT/PKC phosphorylation and increased ERK phosphorylation was observed under steady state conditions in PHLPP1β/SCOP knockdown neurons (Figure S5) indicating that PHLPP1β/SCOP contributes to the basal activation of AKT, PKC, and ERK kinases.

The fact PHLPP1α and PHLPP1β/SCOP have divergent effects on AKT and PKC signaling, may help explain why over-expressing PHLPP1α in HEK293-FT cells results in a massive increase in PHLPP1β/SCOP levels. That is, expression of PHLPP1β/SCOP may be altered in order to adjust PHLPP1α actions on AKT activity. This balance in PHLPP1 splice variants is reflected by hippocampal differences in the level of PHLPP proteins in region CA1 and CA3. Specifically, PHLPP1α is significantly lower in the CA3 and PHLPP1β/SCOP tends to be lower in this region as well. However, many signaling pathways are affected by selective PHLPP1β/SCOP knockdown, thus it is not certain which pathway mitigates this cross-talk. Moreover, because we over-expressed PHLPP1α and knocked down PHLPP1α/β in HEK293-FT cells to verify the quality of the antibodies used in our work, we had the opportunity to determine if PHLPP1 regulates AKT, PKC, and ERK in HEK293-FT cells in a manner similar to neurons. Intriguingly, we did not observe the same role of PHLPP1 proteins in regulating AKT, PKC, and ERK signaling in HEK293-FT cells, compared to hippocampal neurons (Figures S6 and S7). Knockdown of PHLPP1 had no effect on the phosphorylated levels of AKT or ERK; however, a mild (although significant) increase in pPKCα657 levels was observed. In addition, over-expression of PHLPP1α robustly increased pERK levels and tended to increase pAKT473 levels. While we cannot explain the differential regulation of PHLPP1 proteins on cell signaling pathways in HEK393-FT cells, our findings are in agreement with work by Qiao and colleagues. These authors recently examined PHLPP

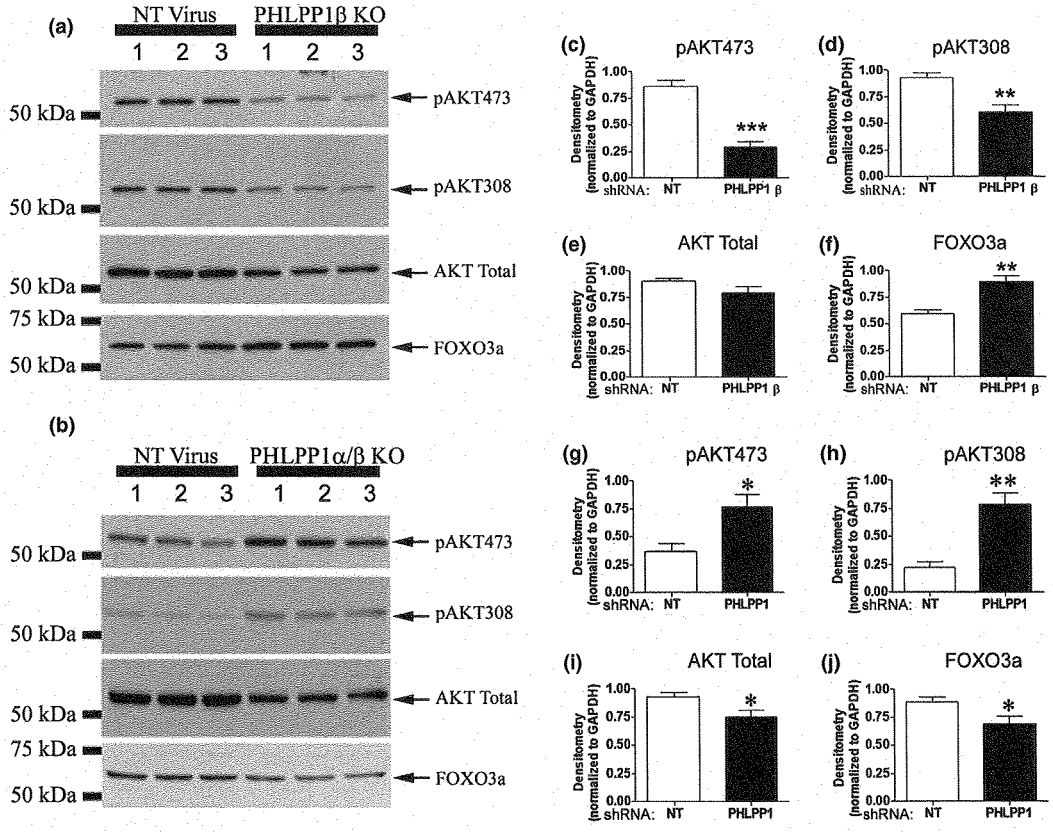


**Fig. 9** Effect of PHLPP1β and PHLPP1 knockdown on AKT signaling. Hippocampal neurons transduced with lentivirus containing either a non-targeting shRNA (NT Virus), a shRNA virus targeting PHLPP1β (PHLPP1β KO), or shNRA's targeting both PHLPP1α/β (PHLPP1 KO) and treated with 100 ng/mL IGF-1 for 20 min. (a and b) Representative western blots ($n = 3$) show the effect of knockdown on AKT phosphorylation and the AKT target substrate FOXO3a. (c–e) Densitometry of western blots ($n = 6$) show PHLPP1β knockdown significantly reduces AKT phosphorylation at Ser473 and Thr308. No change in AKT total levels was observed. (f) Densitometry ($n = 6$) shows FOXO3a is significantly increased in PHLPP1β knockdown neurons, consistent with reduced AKT activity. (g–i) Densitometry of western blots ($n = 6$) show PHLPP1 knockdown significantly increases AKT phosphorylation at Ser473 and Thr308. In addition AKT total levels are significantly decreased. (j) Densitometry ($n = 6$) shows FOXO3a is significantly decreased in PHLPP1 knockdown neurons, consistent with increased AKT activity. Data are significant at $^{*}p < 0.05$, $^{**}p < 0.001$, $^{***}p < 0.0001$.

signaling in multiple cell types. In some cells, including those of a breast cancer lineage, AKT activation is inhibited by over-expression of PHLPP proteins. However, over-expression of PHLPP proteins in many other cell types, including HEK293-T cells, did not alter AKT phosphorylation (Qiao *et al.* 2010). It is conceivable that HEK293 cells do not express crucial adapter proteins required for PHLPP1 regulation of AKT.

In addition to knockdown experiments, characterization of PHLPP proteins in the brain reveal several significant findings which underscore the potential importance of the PHLPP1α splice variant in regulation of neuronal AKT. First, developmental studies reveal the PHLPP1α isoform accumulates over development and expression in the adult is greatly increased relative to PHLPP1β/SCOP and PHLPP2. Interestingly, the abrupt increase in PHLPP1α expression is associated with a decrease in AKT activity during development. A recent study found overactivation of AKT during development disrupts normal neuronal growth and may contribute to mental illness (Kim *et al.* 2009). Our results suggest that PHLPP1α contributes to the stringent regulation of AKT activity, which is critical for normal CNS growth during maturation. It would be interesting to learn if changes in PHLPP1α activity accompany changes in AKT activity in models of CNS disease.

In addition to developmental studies, subcellular fractionation experiments using adult hippocampal tissue reveal an important aspect of PHLPP1α regulation. While PHLPP1β/SCOP and PHLPP2 predominantly localize to the cytoplasmic/plasma membrane fraction, PHLPP1α is highly abundant in the nucleus and nuclear membrane. The latter finding is supported by intense nuclear and perinuclear immunofluorescent staining of PHLPP1α in cultured hippocampal neurons. The importance of this observation relates to AKT's

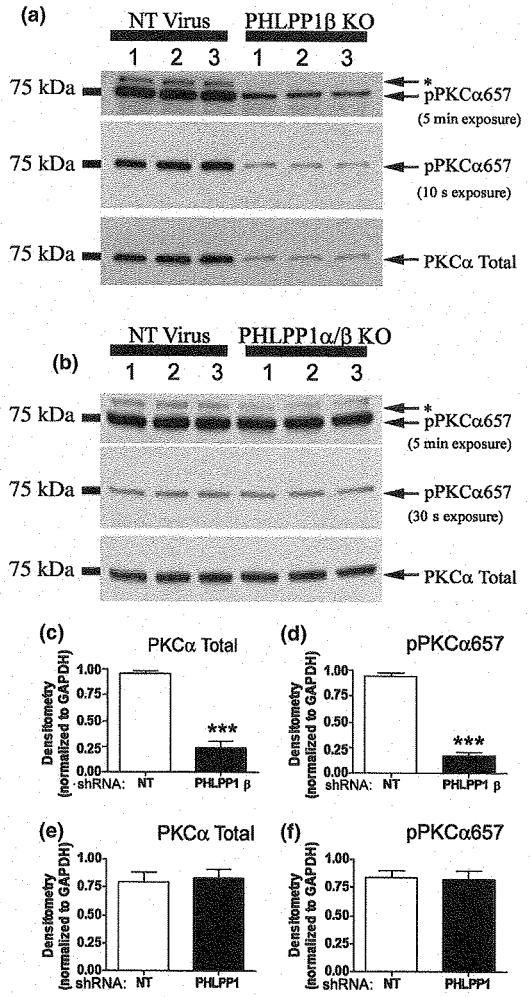


**Fig. 10** Effect of PHLPP1β and PHLPP1 knockdown on PKC phosphorylation. Hippocampal neurons transduced with lentivirus containing either a non-targeting shRNA (NT Virus), a shRNA virus targeting PHLPP1β (PHLPP1β KO), or shNRA's targeting both PHLPP1α/β (PHLPP1 KO) and treated with 100 ng/mL IGF-1 for 20 min. (a and b) Representative western blots ($n = 3$) show the effect of knockdown on PKC phosphorylation. (c and d) Densitometry of western blots ($n = 6$) show PHLPP1β knockdown significantly reduces PKC total levels and phosphorylation at Ser657. (e and f) Densitometry of western blots ($n = 6$) show PHLPP1 knockdown does not alter PKC total levels or phosphorylation. Data are significant at ***$p < 0.0001$.

well elucidated mechanisms of action. Specifically, activation of AKT by phosphorylation at Thr308 and Ser473 elicits a rapid and robust translocation of AKT into the nucleus. Once in the nuclear compartment AKT targets multiple substrates for phosphorylation, including FOXO3a, and thereby promotes survival signaling mechanisms (Zheng *et al.* 2002). The finding that PHLPP1α is the primary PHLPP protein within the nuclear compartment, suggests that PHLPP1α alone is positioned to turn off AKT once activated. Therefore, nuclear PHLPP1α, rather than the predominately cytoplasmic PHLPP1β/SCOP or PHLPP2, is poised to regulate nuclear AKT activity in neurons.

Finally, our characterization of PHLPP proteins reveal among different CNS cell types, PHLPP1α is primarily confined to neurons (Fig. 3). This ostensibly trite finding, in fact, may be one of the more intriguing and important discoveries within this work. Searching for methods to selectively increase AKT activity in neurons but not the supporting glia has been a continuous yet unsuccessful enterprise. Increasing AKT globally is decidedly undesirable because of the increased risk for developing peripheral or CNS cancers. This concern was highlighted in a recent review suggesting the hypoactivity of the AKT signaling cascade contributes to the development of schizophrenia (Kalkman 2006). At the same time, decreased AKT activity might explain the reduced risk for developing cancer in the schizophrenic population (Barak *et al.* 2005; Levav *et al.* 2007). Therefore, the author predicts using pharmacological interventions to increase CNS AKT activity may be a good strategy to prevent or reduce mental illness but increases the risk of developing CNS tumors as a consequence to AKT mediated therapies (Kalkman 2006). Together our results show that (i) PHLPP1α is primarily present in neurons and (ii) a potent AKT inhibitor in neurons, it is possible that inhibition of PHLPP1α with small molecule inhibitors may be a useful strategy to increase neuronal AKT levels while side-stepping the associated risk of developing gliomas. In addition, the comparatively low levels of PHLPP1α in multiple organs outside the brain may also help to reduce other side effects potentially caused by increased AKT activity. As PHLPP research advances its likely selective agonists and antagonists will become available, allowing the hypothesis to be put to the test.

As interest in PHLPP proteins for treatment of human disease mounts, our results for a divergence in the function of PHLPP1α and PHLPP1β/SCOP provide insight into potential therapeutic strategies. In cancer therapy, where activated AKT needs to be reduced, enhancing PHLPP1α signaling while reducing PHLPP1β/SCOP signaling might be more effective. Alternatively, in neurodegenerative disease where increased AKT activity is desired, the opposite strategy could apply. Consistent with the idea that targeting PHLPP1 proteins may improve outcomes in neurodegenerative disease, recent work inversely correlates decreased PHLPP1α levels with increased pAKT473 levels and reduced cell death in the striatum in Huntington's Disease mouse models (Saavedra *et al.* 2010). Moreover, decreased PHLPP1 levels in the putamen are observed in samples taken from Huntington's Disease patients, suggesting the PHLPP1/AKT axis is important in human disease.

Our finding that different PHLPP1 splice variants serve different functions also dovetails well with recent advances in PHLPP research. The first published report of a PHLPP1

knockout animal was recently described (Masubuchi *et al.* 2010). In the context of this new animal model, our observations on PHLPP1 splice variants are particularly important because they highlight subtleties in the dual regulation and interaction between PHLPP1α and PHLPP1β/SCOP which may otherwise be overlooked. Complete PHLPP1 gene knockout may hide effects caused by loss of PHLPP1β/SCOP and preferentially reveal PHLPP1α's influence on cell signaling. In our system, the effect of PHLPP1β/SCOP knockdown on AKT and PKCα was reversed and lost, respectively, when PHLPP1α was simultaneously knocked down; this finding indicates PHLPP1α's effects on the AKT and PKCα pathways are dominant to PHLPP1β/SCOP's when both our reduced; such is the case with the PHLPP1 KO mouse. Nevertheless, this animal model promises exciting new data and will help elucidate the roles PHLPP1 plays in the body, as well as, determine what consequences dysfunctional PHLPP1 signaling has on behavior.

In conclusion our results indicate PHLPP1α and PHLPP1β/SCOP do not serve the same function for regulation of AKT, PKC, or ERK signaling in hippocampal neurons. PHLPP1α inhibits AKT and PKC signaling in neurons. Alternatively, PHLPP1β/SCOP is important for the normal activation of AKT and PKC signaling but plays a dominant role in inhibiting the ERK pathway in neurons. The demonstration that PHLPP1α is highly abundant in neurons is a major advance in understanding potential strategies to increase neuronal AKT in diseased neurons. While work here points to PHLPP1α is a potent regulator of AKT in neurons, future studies will need to define PHLPP2's contribution to AKT regulation in neurons. Although, PHLPP2 appears to be less abundant, no broad conclusions can be made as to the potential importance of PHLPP2 for AKT regulation. It is possible the phosphatase activity of PHLPP2 is differently regulated relative to PHLPP1α and could provide another level of cell signaling regulation. In agreement with this possibility, PHLPP1β/SCOP expression in neurons is far lower than PHLPP1α, and yet PHLPP1β/SCOP is a major regulator of ERK phosphorylation.

## Acknowledgements

This research was supported by the NIH: (i) RO1-AG014979, (ii) RO1-MH059891 and (iii) Evelyn F. McKnight Brain Research Grant. The authors declare that they have no conflict of interest.

## Supporting information

Additional Supporting Information may be found in the online version of this article:

**Figure S1.** Validation of hippocampal cell culture.

**Figure S2.** Cayman PHLPP1 antibody detects PHLPP1α.

**Figure S3.** Enhanced image of astrocyte & neurons.

**Figure S4.** PHLPP1 brain immunofluorescence, control and CA1 228-ms exposure.

**Figure S5.** Neuronal PHLPP1β knockdown alters basal activation of AKT, PKC, and ERK kinases.

**Figure S6.** Effect of PHLPP1 knockdown to alter AKT, PKC, and ERK activation in HEK293-FT cells.

**Figure S7.** Effect of PHLPP1α over-expression to alter AKT, PKC, and ERK activation in HEK293-FT cells.

As a service to our authors and readers, this journal provides supporting information supplied by the authors. Such materials are peer-reviewed and may be re-organized for online delivery, but are not copy-edited or typeset. Technical support issues arising from supporting information (other than missing files) should be addressed to the authors.

## References

Barak Y., Achiron A., Mandel M., Mirecki I. and Aizenberg D. (2005) Reduced cancer incidence among patients with schizophrenia. *Cancer* **104**, 2817–2821.

Beaulieu J. M., Gainetdinov R. R. and Caron M. G. (2009) Akt/GSK3 signaling in the action of psychotropic drugs. *Annu. Rev. Pharmacol. Toxicol.* **49**, 327–347.

Bornancin F. and Parker P. J. (1997) Phosphorylation of protein kinase C-alpha on serine 657 controls the accumulation of active enzyme and contributes to its phosphatase-resistant state. *J. Biol. Chem.* **272**, 3544–3549.

Brewer G. J., Torricelli J. R., Evege E. K. and Price P. J. (1993) Optimized survival of hippocampal neurons in B27-supplemented Neurobasal, a new serum-free medium combination. *J. Neurosci. Res.* **35**, 567–576.

Brognard J., Sierecki E., Gao T. and Newton A. C. (2007) PHLPP and a second isoform, PHLPP2, differentially attenuate the amplitude of Akt signaling by regulating distinct Akt isoforms. *Mol. Cell* **25**, 917–931.

Colin E., Regulier E., Perrin V., Durr A., Brice A., Aebischer P., Deglon N., Humbert S. and Saudou F. (2005) Akt is altered in an animal model of Huntington's disease and in patients. *Eur. J. Neurosci.* **21**, 1478–1488.

Dickey C. A., Koren J., Zhang Y. J. *et al.* (2008) Akt and CHIP coregulate tau degradation through coordinated interactions. *Proc. Natl Acad. Sci. USA* **105**, 3622–3627.

Franke T. F. (2008) PI3K/Akt: getting it right matters. *Oncogene* **27**, 6473–6488.

Gao T., Furnari F. and Newton A. C. (2005) PHLPP: a phosphatase that directly dephosphorylates Akt, promotes apoptosis, and suppresses tumor growth. *Mol. Cell* **18**, 13–24.

Gao T., Brognard J. and Newton A. C. (2008) The phosphatase PHLPP controls the cellular levels of protein kinase C. *J. Biol. Chem.* **283**, 6300–6311.

Gines S., Ivanova E., Seong I. S., Saura C. A. and MacDonald M. E. (2003) Enhanced Akt signaling is an early pro-survival response that reflects N-methyl-D-aspartate receptor activation in Huntington's disease knock-in striatal cells. *J. Biol. Chem.* **278**, 50514–50522.

Gysin S. and Imber R. (1997) Phorbol-ester-activated protein kinase C-alpha lacking phosphorylation at Ser657 is down-regulated by a mechanism involving dephosphorylation. *Eur. J. Biochem.* **249**, 156–160.

Hirano I., Nakamura S., Yokota D., Ono T., Shigeno K., Fujisawa S., Shinjo K. and Ohnishi K. (2009) Depletion of Pleckstrin homology domain leucine-rich repeat protein phosphatases 1 and 2 by

Bcr-Abl promotes chronic myelogenous leukemia cell proliferation through continuous phosphorylation of Akt isoforms. *J. Biol. Chem.* **284**, 22155–22165.

Humbert S., Bryson E. A., Cordelieres F. P., Connors N. C., Datta S. R., Finkbeiner S., Greenberg M. E. and Saudou F. (2002) The IGF-1/Akt pathway is neuroprotective in Huntington's disease and involves Huntingtin phosphorylation by Akt. *Dev. Cell* **2**, 831–837.

Jackson T. C., Rani A., Kumar A. and Foster T. C. (2009) Regional hippocampal differences in AKT survival signaling across the lifespan: implications for CA1 vulnerability with aging. *Cell Death Differ.* **16**, 439–448.

Kalkman H. O. (2006) The role of the phosphatidylinositide 3-kinase-protein kinase B pathway in schizophrenia. *Pharmacol. Ther.* **110**, 117–134.

Kanan Y., Matsumoto H., Song H., Sokolov M., Anderson R. E. and Rajala R. V. (2010) Serine/threonine kinase akt activation regulates the activity of retinal serine/threonine phosphatases, PHLPP and PHLPPL. *J. Neurochem.* **113**, 477–488.

Kim J. Y., Duan X., Liu C. Y., Jang M. H., Guo J. U., Pow-anpongkul N., Kang E., Song H. and Ming G. L. (2009) DISC1 regulates new neuron development in the adult brain via modulation of AKT-mTOR signaling through KIAA1212. *Neuron* **63**, 761–773.

Lee H. K., Kumar P., Fu Q., Rosen K. M. and Querfurth H. W. (2009) The insulin/Akt signaling pathway is targeted by intracellular beta-amyloid. *Mol. Biol. Cell* **20**, 1533–1544.

Levav I., Lipshitz I., Novikov I., Pugachova I., Kohn R., Barchana M., Ponizovsky A. and Werner H. (2007) Cancer risk among parents and siblings of patients with schizophrenia. *Br. J. Psychiatry* **190**, 156–161.

Masubuchi S., Gao T., O'Neill A., Eckel-Mahan K., Newton A. C. and Sassone-Corsi P. (2010) Protein phosphatase PHLPP1 controls the light-induced resetting of the circadian clock. *Proc. Natl Acad. Sci. USA* **107**, 1642–1647.

Pei H., Li L., Fridley B. L., Jenkins G. D., Kalari K. R., Lingle W., Petersen G., Lou Z. and Wang L. (2009) FKBP51 affects cancer cell response to chemotherapy by negatively regulating Akt. *Cancer Cell* **16**, 259–266.

Plas D. R. and Thompson C. B. (2003) Akt activation promotes degradation of tuberin and FOXO3a via the proteasome. *J. Biol. Chem.* **278**, 12361–12366.

Qiao M., Wang Y., Xu X. *et al.* (2010) Mst1 is an interacting protein that mediates PHLPPs' induced apoptosis. *Mol. Cell* **38**, 512–523.

Saavedra A., Garcia-Martinez J. M., Xifro X., Giralt A., Torres-Peraza J. F., Canals J. M., Diaz-Hernandez M., Lucas J. J., Alberch J. and Perez-Navarro E. (2010) PH domain leucine-rich repeat protein phosphatase 1 contributes to maintain the activation of the PI3K/Akt pro-survival pathway in Huntington's disease striatum. *Cell Death Differ.* **17**, 324–335.

Semple-Rowland S. L., Eccles K. S. and Humberstone E. J. (2007) Targeted expression of two proteins in neural retina using self-inactivating, insulated lentiviral vectors carrying two internal independent promoters. *Mol. Vis.* **13**, 2001–2011.

Shimizu K., Mackenzie S. M. and Storm D. R. (2010) SCOP/PHLPP and its functional role in the brain. *Mol. Biosyst.* **6**, 38–43.

Shimizu K., Okada M., Takano A. and Nagai K. (1999) SCOP, a novel gene product expressed in a circadian manner in rat suprachiasmatic nucleus. *FEBS Lett.* **458**, 363–369.

Shimizu K., Okada M., Nagai K. and Fukada Y. (2003) Suprachiasmatic nucleus circadian oscillatory protein, a novel binding partner of K-Ras in the membrane rafts, negatively regulates MAPK pathway. *J. Biol. Chem.* **278**, 14920–14925.

Shimizu K., Phan T., Mansuy I. M. and Storm D. R. (2007) Proteolytic degradation of SCOP in the hippocampus contributes to activation of MAP kinase and memory. *Cell* **128**, 1219–1229.

Thiselton D. L., Vladimirov V. I., Kuo P. H. *et al.* (2008) AKT1 is associated with schizophrenia across multiple symptom dimensions in the Irish study of high density schizophrenia families. *Biol. Psychiatry* **63**, 449–457.

Timmons S., Coakley M. F., Moloney A. M. and O' Neill C. (2009) Akt signal transduction dysfunction in Parkinson's disease. *Neurosci. Lett.* **467**, 30–35.

Xiromerisiou G., Hadjigeorgiou G. M., Papadimitriou A., Katsarogiannis E., Gourbali V. and Singleton A. B. (2008) Association between AKT1 gene and Parkinson's disease: a protective haplotype. *Neurosci. Lett.* **436**, 232–234.

Yu H. S., Kim S. H., Park H. G., Kim Y. S. and Ahn Y. M. (2010) Activation of Akt signaling in rat brain by intracerebroventricular injection of ouabain: a rat model for mania. *Prog. Neuropsychopharmacol. Biol. Psychiatry* **34**, 888–894.

Zheng W. H., Kar S. and Quirion R. (2002) Insulin-like growth factor-1-induced phosphorylation of transcription factor FKHRL1 is mediated by phosphatidylinositol 3-kinase/Akt kinase and role of this pathway in insulin-like growth factor-1-induced survival of cultured hippocampal neurons. *Mol. Pharmacol.* **62**, 225–233.

# Redox Sensitive Calcium Stores Underlie Enhanced After Hyperpolarization of Aged Neurons: Role for Ryanodine Receptor Mediated Calcium Signaling

**Karthik Bodhinathan, Ashok Kumar and Thomas C. Foster**

*J Neurophysiol* 104:2586-2593, 2010. First published 8 September 2010; doi:10.1152/jn.00577.2010

*J Neurophysiol* 104: 2586–2593, 2010.
First published September 8, 2010; doi:10.1152/jn.00577.2010.

# Redox Sensitive Calcium Stores Underlie Enhanced After Hyperpolarization of Aged Neurons: Role for Ryanodine Receptor Mediated Calcium Signaling

**Karthik Bodhinathan, Ashok Kumar, and Thomas C. Foster**
*Department of Neuroscience, McKnight Brain Institute, University of Florida, Gainesville, FL 32610*

Submitted 29 June 2010; accepted in final form 2 September 2010

**Bodhinathan K, Kumar A, Foster TC.** Redox sensitive calcium stores underlie enhanced afterhyperpolarization of aged neurons: role for ryanodine receptor mediated calcium signaling. *J Neurophysiol* 104: 2586–2593, 2010. First published September 8, 2010; doi:10.1152/jn.00577.2010. A decrease in the excitability of CA1 pyramidal neurons contributes to the age related decrease in hippocampal function and memory decline. Decreased neuronal excitability in aged neurons can be observed as an increase in the $Ca^{2+}$-activated $K^+$- mediated post burst afterhyperpolarization (AHP). In this study, we demonstrate that the slow component of AHP (sAHP) in aged CA1 neurons (aged-sAHP) is decreased ~50% by application of the reducing agent dithiothreitol (DTT). The DTT-mediated decrease in the sAHP was age specific, such that it was observed in CA1 pyramidal neurons of aged (20–25 mo), but not young (6–9 mo) F344 rats. The effect of DTT on the aged-sAHP was blocked following depletion of intracellular $Ca^{2+}$ stores (ICS) by thapsigargin or blockade of ryanodine receptors (RyRs) by ryanodine, suggesting that the age-related increase in the sAHP was due to release of $Ca^{2+}$ from ICS through redox sensitive RyRs. The DTT-mediated decrease in the aged-sAHP was not blocked by inhibition of L-type voltage gated $Ca^{2+}$ channels (L-type VGCC), inhibition of Ser/Thr kinases, or inhibition of the large conductance BK potassium channels. The results add support to the idea that a shift in the intracellular redox state contributes to $Ca^{2+}$ dysregulation during aging.

afterhyperpolarization, aging, oxidative stress, redox state, neuronal excitability, ryanodine receptor, hippocampus

## INTRODUCTION

An age-related decline in hippocampus-dependent memory is thought to result from dysregulation of $Ca^{2+}$-dependent processes in CA1 pyramidal neurons including synaptic plasticity and neuronal excitability (Burke and Barnes 2010; Foster 2007, 1999; Kumar et al. 2009; Magnusson et al. 2010; Oh et al. 2010). One of the well characterized markers of aging in CA1 pyramidal neurons is an increase in the slow component of the $Ca^{2+}$ activated, $K^+$ - mediated afterhyperpolarization (sAHP) (Disterhoft et al. 1996; Kumar and Foster 2007; Kumar and Foster 2002, 2004; Landfield and Pitler 1984; Matthews et al. 2009; Moyer et al. 1992; Thibault et al. 2007; Tombaugh et al. 2005).

The exact mechanism that underlies the age-related increase in sAHP is unknown. The increase in sAHP may be due to altered $Ca^{2+}$ regulation, including an increase in L-type voltage gated $Ca^{2+}$ channels (L-type VGCC) (Thibault and Landfield 1996; Veng and Browning 2002), increased release of $Ca^{2+}$ from intracellular $Ca^{2+}$ stores (ICS) (Gant et al. 2006; Kumar and Foster 2004), or an increase in the function or density of $K^+$ channels that mediate the sAHP (Power et al. 2001; Power et al. 2002). Importantly, aging is associated with increased oxidative stress that could influence the highly redox sensitive ryanodine receptor (RyR), which regulates $Ca^{2+}$ release from the ICS (Bull et al. 2008; Eager and Dulhunty 1998; Hidalgo et al. 2004; Huddleston et al. 2008). Moreover, aged neurons are characterized by a decrease in their redox buffering capacity (Bodhinathan et al. 2010; Parihar et al. 2008) and recent work from our lab demonstrates that the shift in redox state contributes to decreased N-methyl D-aspartate receptor (NMDAR) function involving altered CaMKII activity in CA1 neurons from aged animals (Bodhinathan et al. 2010). Based on these observations, we tested the hypothesis that the redox state of the aged neuron contributes to the increase in sAHP (Foster 2007; Kumar et al. 2009).

The results reveal that the sAHP is decreased by the reducing agent dithiothreitol (DTT) in an age-dependent manner. Application of ryanodine, to block RyRs, prevented the DTT-mediated decrease of sAHP in the aged neurons. Depletion of ICS by the application of thapsigargin also blocked the DTT effect on aged-sAHP. The DTT-mediated decrease in the aged-sAHP was independent of the activity of L-type VGCC or Ser/Thr kinase activity. Finally, inhibition of large conductance potassium (BK) channel activity did not influence the DTT-mediated decrease in the aged-sAHP. The results point to an ICS-dependent and RyR-mediated mechanism that links altered redox state during aging with the enhanced sAHP in CA1 pyramidal neurons. Reversal of the redox state of aged hippocampal CA1 pyramidal neurons is a potential target to ameliorate $Ca^{2+}$ dysregulation, decrease sAHP, and restore normal functionality in aged neurons.

## METHODS

### *Animals*

Procedures involving animals have been reviewed and approved by the Institutional Animal Care and Use Committee and were in accordance with guidelines established by the U.S. Public Health Service Policy on Human Care and Use of Laboratory Animals. Male Fischer 344 rats, young (3–8 mo) and aged (20–25 mo), were obtained from National Institute on Aging colony at Harlan Sprague Dawley Inc (Indianapolis, IA). All animals were group housed (2 per cage), and maintained on a 12:12 h light schedule, and provided *ad lib* access to food and water.

### *Hippocampal slice preparation*

The animals were deeply anesthetized using isoflurane (Webster, Sterling, MA) and decapitated with a guillotine (MyNeurolab, St Louis, MO). The brains were rapidly removed and hippocampi were

Address for reprint requests and other correspondence: Thomas C. Foster, Ph.D., Department of Neuroscience, McKnight Brain Institute, University of Florida, PO Box 100244, Gainesville, FL 32610-0244, USA., Phone (352) 392-4359, Fax (352) 392-8347, (E-mail: foster@mbi.ufl.edu).

TABLE 1. *Physiological properties of CA1 pyramidal neurons recorded from young and aged rats*

| | IR, MΩ | RMP, mV | Sp Amp, mV |
|---|---|---|---|
| Young ($n$ = 12) | 37.0 ± 2.5 | −62.8 ± 1.5 | 80.6 ± 1.9 |
| Aged ($n$ = 40) | 37.8 ± 1.1 | −61.9 ± 0.6 | 82.8 ± 0.7 |

The values for input resistance (IR), resting membrane potential (RMP), and spike amplitude (Sp Amp) are indicated as mean ± SE. The number in parentheses indicates the number of cells from the young and aged animals.

dissected. Hippocampal slices (~400 μm) were cut parallel to the alvear fibers using a tissue chopper (Mickle Laboratory Engineering Co, Surrey, UK). The slices were incubated in a holding chamber (at room temperature) with artificial cerebrospinal fluid (ACSF) containing (in mM): NaCl 124, KCl 2, $KH_2PO_4$ 1.25, $MgSO_4$ 2, $CaCl_2$ 2, $NaHCO_3$ 26, and D-glucose 10. ≥30 min before recording, slices were transferred to a standard interface recording chamber (Warner Instrument, Hamden, CT). In some experiments, the $Ca^{2+}$ of the ACSF was raised to 4 mM. The chamber was continuously perfused with oxygenated ACSF (95%-$O_2$-5%-$CO_2$) at the rate of 2 mL/min. The pH and temperature were maintained at 7.4 and 30 ± 0.5°C (maintained using the automatic temperature controller TC-324B; Warner Instrument, Hamden, CT), respectively.

### *Intracellular electrophysiological recordings*

Intracellular recordings were performed on CA1 pyramidal neurons to record the sAHP as previously described (Kumar and Foster 2004).

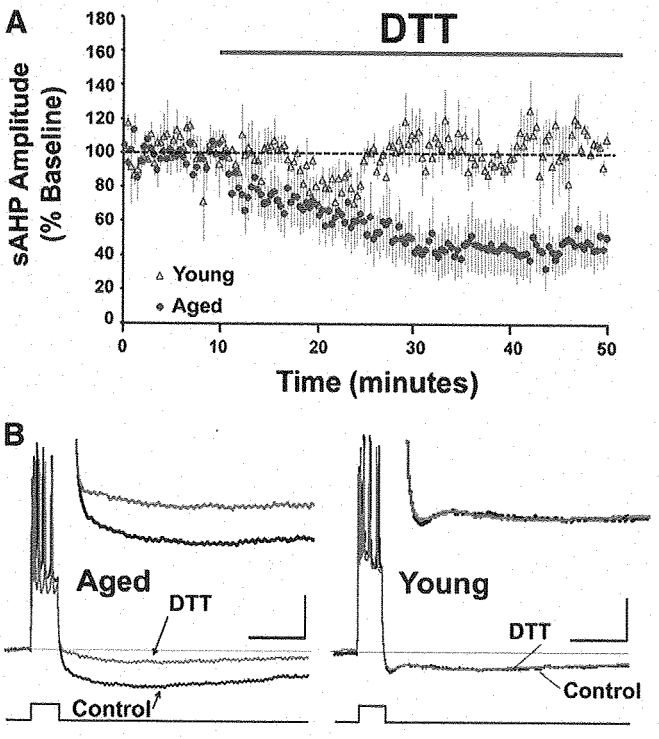


FIG. 1. Age-dependent reduction in the sAHP by DTT. (*A*) Time course of the change in the normalized sAHP amplitude in the aged (filled circles) ($n$ = 5) and young (open triangles) animals ($n$ = 3), following application of DTT for 40 min. (*B*) Representative traces illustrating the change in the AHP of aged (*left*) and young (*right*) animals under control conditions and at the end of 40 min application of DTT. The line beneath the traces indicates the onset and offset of the step current used to elicit a train of 5 action potentials. In this and subsequent figures, the faint line within the traces represents the baseline. Calibration bars: 200 ms, 10 mV. *Inset*: Magnified representation of change in the aged and young AHP under control condition, and 40 min after DTT application.

TABLE 2. *DTT effect on absolute sAHP amplitude from young and aged rats*

| | sAHP amplitude, mV | Holding current, nA | |
|---|---|---|---|
| | | Range | Mean ± SE |
| Young Control ($n$ = 12) | 4.23 ± 0.17 | −0.8 to +0.4 | −0.183 ± 0.114 |
| Young DTT ($n$ = 3) | 4.38 ± 0.15 | −0.2 to +0.1 | −0.067 ± 0.088 |
| Aged Control ($n$ = 40) | 6.44 ± 0.32 | −0.7 to +0.7 | −0.083 ± 0.051 |
| Aged DTT ($n$ = 5) | 3.70 ± 0.78 | −0.2 to +0.2 | 0.032 ± 0.078 |

The values for sAHP amplitude are indicated as mean ± S.E. The number in parentheses indicates the number of cells from the young and aged animals. The values of the holding. currents are presented as range and mean ± S.E.

Sharp microelectrodes were pulled from thin walled (1 mm) borosilicate capillary glass using a Flaming/Brown horizontal micropipette puller (Sutter Instruments, San Rafael, CA). The microelectrode resistances ranged from 38 to 90 MΩ when filled with 3 M potassium acetate. Microelectrodes were visually positioned in the CA1 pyramidal cell layer using a dissecting microscope (SZH10, Optical Elements Corp, Washington, DC). The signals were amplified using an Axoclamp 2B amplifier (Axon Instruments, Union City, CA), and sampled in continuous bridge mode at 5 kHz, and stored on a computer disk for off-line analysis (Data Wave Technologies).

Only neurons with a resting membrane potential (RMP) more hyperpolarized than −57 mV, and an input resistance >20 MΩ, and action potential amplitude rising ≥70 mV from the point of spike initiation were included in the analysis as described earlier (Kumar and Foster 2004). On cell entry, positive or negative current was applied to hold the neuron at the holding membrane potential (HMP) of −63 mV for the rest of the experiment. Voltage deflection resulting from hyperpolarizing current (1.0 nA) was used to determine the input

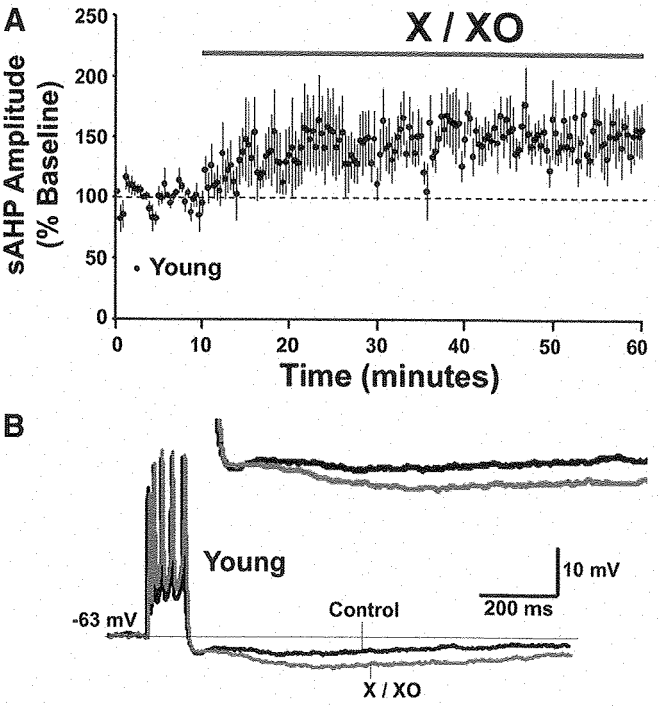


FIG. 2. Oxidizing agent decreases sAHP in young animals. (*A*) Time course of the change in the normalized sAHP amplitude in young animals ($n$ = 5), following application of X/XO for 50 min. (*B*) Representative traces illustrating the change in the AHP for a young animal under control conditions (black trace) and at the end of 50 min application of X/XO (gray trace). Calibration bars: 200 ms, 10 mV. *Inset*: Magnified representation of change in the young AHP under control condition, and 50 min after X/XO application.

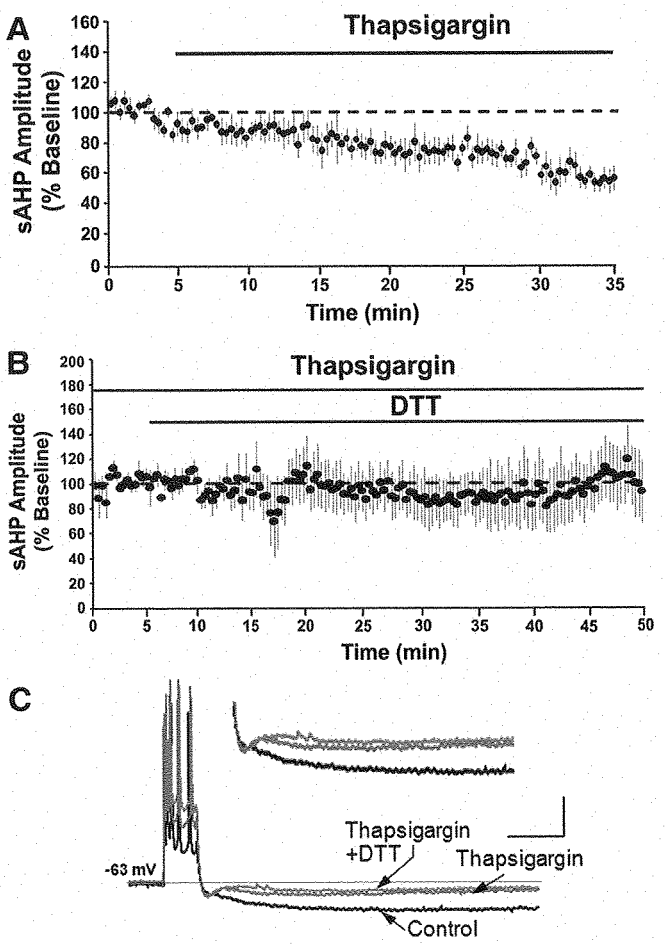


FIG. 3. Intracellular $Ca^{2+}$ stores underlie DTT-mediated decrease in aged-sAHP. (*A*) Time course of the change in the normalized sAHP amplitude in the aged animals on application of thapsigargin ($n = 7$). (*B*) Time course of change in the normalized sAHP amplitude in cells ($n = 4$) incubated with thapsigargin prior to and during DTT application. (*C*) Representative traces illustrating the AHP of aged animals under control condition (black trace), and at the end of 40 min application of thapsigargin (gray trace) and at the end of 50 min application of thapsigargin+DTT (gray trace). Calibration bars: 200 ms, 10 mV. *Inset*: Magnified representation of change in the aged AHP under control condition, thapsigargin, and thapsigargin + DTT.

resistance. Depolarizing current pulses (0.1–1.0 nA, 100 ms duration) were delivered every 20 s through the microelectrode to elicit sodium spike bursts containing a train of 5 action potentials.

The AHPs in the control and in the experimental conditions were elicited at the constant HMP of −63 mV, by manually clamping the membrane potential with DC current injection not exceeding ±1 nA. The sAHP amplitude was measured as the difference between the average membrane potential recorded during the 100-ms period immediately preceding the onset of the depolarizing current, and the average membrane potential recorded over a 100 ms window spanning the 400–500 ms after the offset of the depolarizing current pulse. The amplitude of the sAHP was compared before and during drug administration in the same neuron.

All drugs were prepared according to the manufacturer's specifications and ultimately dissolved in ACSF prior to bath application on the hippocampal slices. Nifedipine (Sigma, St. Louis, MO) and paxilline (Tocris Bioscience, Ellisville, MO) were initially dissolved in a small amount of dimethyl sulfoxide (DMSO; Sigma, St. Louis, MO) and diluted in ACSF to a final DMSO concentration of <0.01% and to a final nifedipine, paxilline concentration of 10 μM. Xanthine (20 μg/ml) (Calbiochem) was initially dissolved in a small amount of 0.1N NaOH and finally dissolved in ACSF. DTT (0.7 mM), thapsigargin (1 μM) (Sigma, St. Louis, MO), ryanodine (20 μM) (Calbiochem, San Diego, CA), (±)-1-(5-Isoquinolinesulphonyl)-2-methylpiperazine dihydrochloride (H-7, 10 μM) (Tocris Bioscience, Ellisville, MO), and xanthine oxidase (0.25 U/mg xanthine, Roche Diagnostics, Indianapolis, IN) were directly dissolved in ACSF.

### *Statistical analysis*

All statistical analyses were performed using Stat View 5.0 (SAS Institute Inc, NC). Student's *t*-test were used to examine for differences between treatments or groups with significance set at $P < 0.05$. Paired Student's *t*-test were used to analyze the effect of treatment before and after application of drugs and unpaired Student's *t*-test were used to examine the effect of treatments between age groups. Where stated, n represents the number of slices used in each experiment. All data are reported as group mean ± standard error of mean (SEM). In general only one or two slices per animal were employed for a given experimental condition; although, several conditions could be examined using slices from the same animal.

## RESULTS

### *Age dependent decrease in the sAHP following DTT application*

To study the effects of altered redox state on the aged-sAHP, the reducing agent DTT was applied to aged and young hippocampal CA1 pyramidal neurons while continuously recording the sAHP. In confirmation of previous reports (Kumar and Foster 2007; Kumar and Foster 2004; Landfield and Pitler 1984; Matthews et al. 2009; Moyer et al. 2000; Moyer et al. 1992; Power et

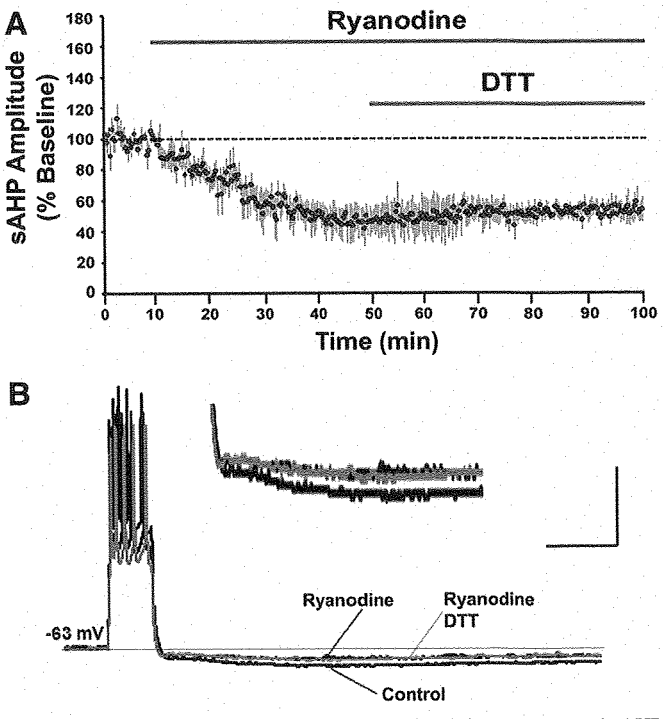


FIG. 4. RyR blockade inhibits the DTT-mediated decrease in aged-sAHP. (*A*) Time course of the change in the normalized sAHP amplitude recorded from aged animals that were incubated with the ryanodine receptor antagonist ryanodine ($n = 4$) followed by the application of DTT. (*B*) Representative traces illustrating the change in the AHP of aged animals under control condition (black trace), at the end of a 40 min application of ryanodine (black trace), and at the end of 50 min application of ryanodine+DTT (gray trace). Calibration bars: 200 ms, 20 mV. *Inset*: Magnified representation of change in the aged AHP under control condition, ryanodine, and ryanodine + DTT.

al. 2002; Tombaugh et al. 2005) the sAHP was significantly ($P < 0.05$) increased in aged (6.44 ± 0.32 mV, $n = 40$) relative to young CA1 pyramidal neurons (4.23 ± 0.17 mV, $n = 12$). The properties of the CA1 pyramidal neurons recorded from the young and aged animals are indicated in Table 1. In a subset of these neurons, after a stable baseline recording for 10 min, DTT was applied for 40 min. Application of DTT significantly ($P < 0.05$) decreased the sAHP amplitude from the baseline levels in the aged (48 ± 14% of baseline, $n = 5$), but not in the young animals (105 ± 10%, $n = 3$) (Fig. 1, *A* and *B*).

As such, the sAHP amplitude in aged following DTT application was similar to that observed in young animals (Table 2). The DC holding current required to maintain the membrane potential at −63 mV was similar for baseline recording and 45 min after DTT application (Table 2) indicating that the DTT-mediated reduction in sAHP was not associated with altered membrane properties. Finally, application of xanthine/xanthine oxidase (X/XO) to hippocampal slices from young animals increased the AHP in 4 out of 5 cells resulting in an overall significant increase in the sAHP amplitude (150 ± 21% of the baseline, $n = 5$) (Fig. 2, *A* and *B*). The results point to a link between altered redox state and the increased sAHP amplitude in aged neurons.

### *DTT-mediated decrease in aged-sAHP involves intracellular $Ca^{2+}$ stores and ryanodine receptors*

To test the hypothesis that the DTT-mediated decrease in the aged-sAHP was due to decreased $Ca^{2+}$ mobilization from ICS, thapsigargin was applied prior to and during the application of DTT to aged hippocampal slices. Application of thapsigargin for 30 min significantly decreased ($P < 0.05$) the amplitude of aged-sAHP to 58 ± 8% ($n = 7$) of the baseline levels (Fig. 3*A*). In a subset of these cells ($n = 4$), a new baseline was established and DTT was applied in the presence of thapsigargin. Application of DTT for 50 min failed to decrease the aged-sAHP amplitude (104 ± 23%) (Fig. 3, *B* and *C*). The results suggest that ICS provide a redox sensitive $Ca^{2+}$ source that contributes to the age-related increase in the sAHP.

RyRs mobilize $Ca^{2+}$ from the ICS and are highly redox sensitive. To test whether RyRs were involved in the DTT-mediated decrease in aged-sAHP, RyRs were blocked by ryanodine prior to and during the application of DTT. Application of ryanodine for 40 min, significantly ($P < 0.05$) decreased the aged-sAHP amplitude to 47 ± 10% ($n = 4$). Application of DTT for 50 min failed to further decrease the aged-sAHP amplitude such that it was 54 ± 7% ($n = 4$) of the original baseline (Fig. 4, *A* and *B*).

Both DTT (Fig. 1) and ryanodine (Fig. 4) decreased the aged-sAHP to ~50% of baseline. The similar magnitude of the response for the two conditions raises the possibility of a "floor effect" of ryanodine, which may have masked DTT influences on the sAHP. To address this issue, the sAHP of aged neurons was enhanced by increasing the extracellular $Ca^{2+}$ concentration from 2 mM to 4 mM. Increasing the extracellular $Ca^{2+}$ to 4 mM increased the sAHP almost two fold, from 6.71 ± 0.79

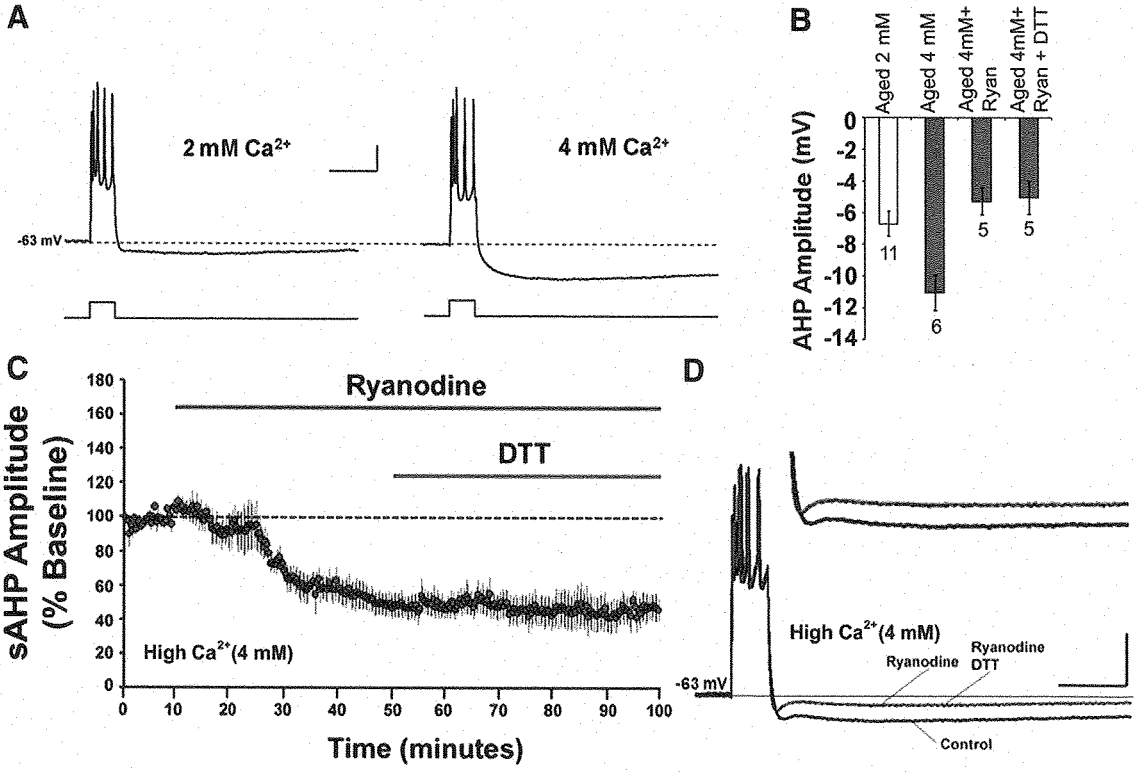


FIG. 5. RyR blockade inhibits the DTT-mediated decrease in aged-sAHP when the AHP is increased by increasing $Ca^{2+}$ in the recording medium. (*A*) Representative traces illustrating the AHP from aged neurons recorded under conditions of 2 mM or 4 mM $Ca^{2+}$ in the ACSF. Calibration bars: 200 ms, 10 mV. (*B*) Quantification of the mean sAHP amplitude in aged neurons recorded under 2 mM $Ca^{2+}$ ($n = 11$, open bar), under 4 mM $Ca^{2+}$ ($n = 6$), under 4 mM $Ca^{2+}$ with ryanodine ($n = 5$), and under 4 mM $Ca^{2+}$ with ryanodine + DTT ($n = 5$); all values under 4 mM $Ca^{2+}$ are represented as filled bars. (*C*) Time course of the change in the normalized sAHP amplitude recorded in 4 mM ACSF from aged animals and incubated with ryanodine ($n = 5$) prior to and during DTT application. (*D*) Representative traces illustrating the AHP of aged animals under control condition, and at the end of a 40 min application of ryanodine and at the end of 50 min application of ryanodine + DTT. Calibration bars: 200 ms, 20 mV. *Inset*: Magnified representation of change in the aged AHP (4 mM $Ca^{2+}$) under control condition, ryanodine, ryanodine + DTT.

mV ($n = 11$) to 11.06 ± 1.09 mV ($n = 6$) (Fig. 5, *A* and *B*). In five cells, a baseline was recorded in 4 mM $Ca^{2+}$, followed by application of ryanodine for 40 min, which was then followed by the application of DTT for 50 min (Fig. 5*C*). Application of ryanodine decreased ($P < 0.05$) the aged-sAHP amplitude to 53 ± 6% (5.31 ± 0.86 mV) and application of DTT for 50 min failed to further decrease the aged-sAHP amplitude (51 ± 7%, 5.06 ± 1.05 mV) of the original baseline (Fig. 5, *B–D*). Thus DTT failed to reduce the sAHP amplitude under high $Ca^{2+}$ and ryanodine application, despite the fact that sAHP amplitude was similar to the baseline under normal 2 mM $Ca^{2+}$ conditions (Fig. 5*B*). The results indicate that the ryanodine blockade of the DTT-mediated decrease in the sAHP was not due to a floor effect of the sAHP during ryanodine application. Rather, these data suggest that the DTT effect on sAHP in aged animals is mediated by RyRs.

Finally, application of DTT for 40 min, decreased the aged-sAHP amplitude to 44 ± 7% ($n = 4$) of the baseline (similar to that observed in Fig. 1). In two of these cells, application of ryanodine for 40 min failed to further decrease the aged-sAHP amplitude such that it was 55 ± 6% ($n = 2$) of the original baseline. In the other two cells, application of thapsigargin also failed to further decrease the aged-sAHP amplitude such that it was 41 ± 8% ($n = 2$) of the original baseline. This suggests that application of DTT occluded the effect of ryanodine and thapsigargin on the aged-sAHP amplitude.

### *DTT-mediated reduction in the aged-sAHP is independent of L-type VGCCs*

L-type VGCCs are another major source of $Ca^{2+}$ for the sAHP. To test the hypothesis the DTT-mediated decrease in the aged-sAHP involves the L-type VGCC, nifedipine was applied prior to and during the application of DTT to aged hippocampal slices (Fig. 6*A*). Application of nifedipine for 20 min decreased the sAHP to 68 ± 4% ($n = 5$) of the baseline. Subsequent application of DTT for 30 min further decreased the amplitude of aged-sAHP to 34 ± 4% ($n = 5$) of the original baseline. The results suggest that the effects of nifedipine and DTT may be independent. In fact, using the sAHP responses recorded in nifedipine (bath application for ≥20 min) as the baseline, application of DTT decreased the amplitude of the aged-sAHP to 48 ± 6% ($P < 0.05$; $n = 6$) (Fig. 6*B*), a decrease comparable to that observed following DTT application in the absence of nifedipine (Fig. 6*B*). The activity of BK channels is sensitive to oxidation (DiChiara and Reinhart 1997). Moreover, an increase in BK channel activity can reduce the sAHP amplitude by decreasing the action potential spike width (Giese et al. 1998; Murphy et al. 2004; Shao et al. 1999). To test the hypothesis that the DTT-mediated decrease in aged-sAHP involves the BK channels, paxilline was first applied to inhibit BK channel activity (Sanchez and McManus 1996). Aged hippocampal slices were incubated in paxilline for ≥60 min prior to recording the sAHP and applying DTT. Paxilline failed to block the DTT-mediated decrease in aged-sAHP, such that DTT application was still able to decrease the amplitude of the aged-sAHP to 28 ± 11% ($n = 3$) of the baseline (Fig. 7, *A* and *B*). Furthermore, the DTT-mediated decrease in the presence of paxilline was not significantly ($P > 0.05$) different from the decrease observed in the presence of DTT alone.

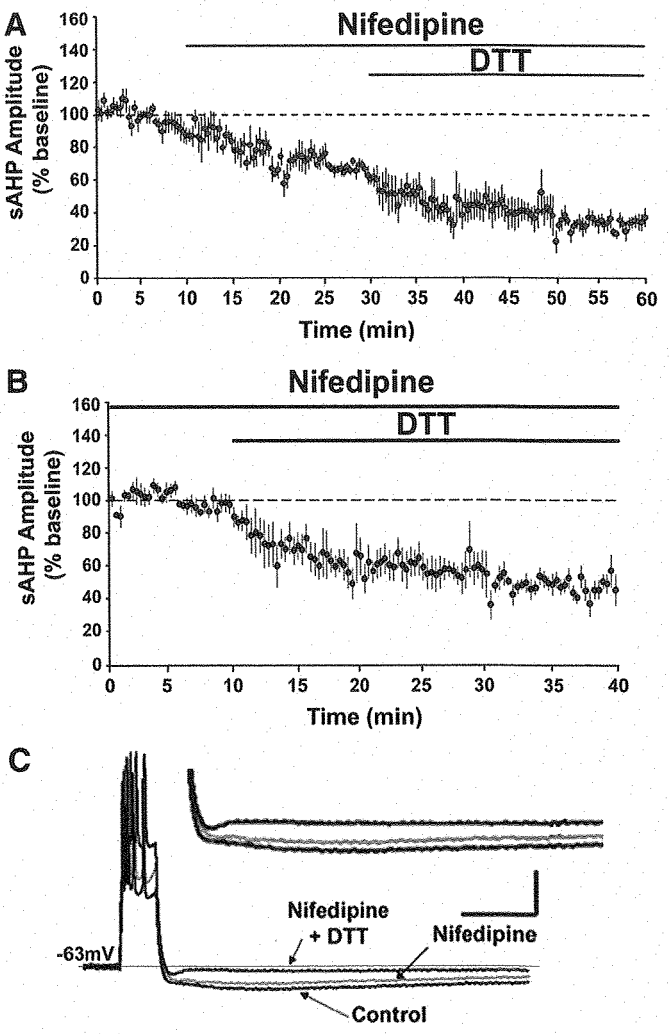


FIG. 6. DTT-mediated decrease is independent of L-type $Ca^{2+}$ channel function. (*A*) Time course of the change in the normalized sAHP amplitude recorded from aged animals that were incubated with nifedipine ($n = 4$), followed by application of DTT. (*B*) Time course of the change in the normalized sAHP amplitude in the aged animals that were incubated with nifedipine ($n = 6$) for ≥45 min prior to the application of DTT for 30 min. Calibration bars: 200 ms, 10 mV. (*C*) Representative traces illustrating the change in the AHP of aged animals under control condition (black trace), and at the end of a 20 min application of nifedipine (gray trace) and at the end of 30 min application of nifedipine+DTT (black trace). *Inset*: Magnified representation of change in the aged AHP under control condition, nifedipine, and nifedipine + DTT.

Serine/threonine kinases provide another potential mechanism for regulating RyRs and the $K^+$ channels that mediate the sAHP. Protein kinase A increases the activity of cardiac RyRs (RyR subtype 2) (Danila and Hamilton 2004; Morimoto et al. 2009; Xiao et al. 2007; Yoshida et al. 1992), and kinase activity inhibits the sAHP (Madison and Nicoll 1986; Malenka et al. 1986; Melyan et al. 2002; Muller et al. 1992; Pedarzani and Storm 1993). To test whether the changes in kinase activity underlie the decrease in sAHP of aged neurons on application of DTT, the broad spectrum serine/threonine kinases inhibitor H-7 was applied prior to and during the application of DTT. Aged hippocampal slices were incubated with H-7 for ≥60 min before recording the sAHP. In the presence of H-7, application of DTT significantly ($P < 0.05$) decreased the aged-sAHP to 53 ± 14% ($n = 3$) of the baseline (Fig. 8*A*). The

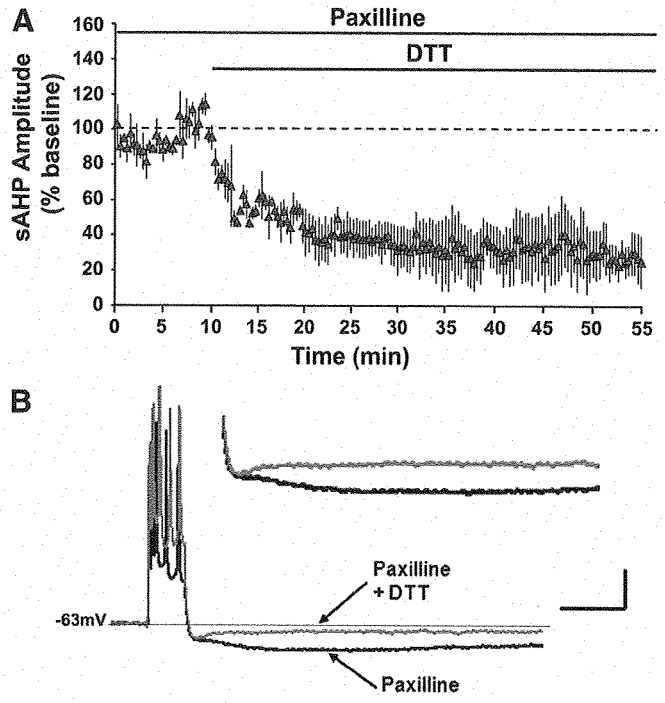


FIG. 7. DTT effects on aged-sAHP are independent of BK channel function. (*A*) Time course of the change in the normalized sAHP amplitude in the aged animals (filled triangles) that were incubated with paxilline ($n = 3$) for ≥60 min prior to DTT application. (*B*) Representative traces illustrating the change in the AHP of aged animals under paxilline (black trace), and at the end of 45 min under paxilline+DTT (gray trace). Calibration bars: 200 ms, 10 mV. *Inset*: Magnified representation of change in the aged AHP under paxilline, and paxilline + DTT.

results suggest that DTT is not altering the sAHP through modulation of kinase activity.

Figure 8*B* summarizes the change in the sAHP amplitude of aged CA1 neurons following DTT application in the presence of various inhibitors. In each case, the response was normalized to the preDTT baseline. Treatments that blocked $Ca^{2+}$ release from ICS (thapsigargin, ryanodine) blocked the DTT-mediated reduction in the sAHP. However the DTT-mediated reduction in sAHP was not blocked in the presence of nifedipine, paxilline, or H-7. Consistent with previous reports, we observed ~50% and ~30% reduction in sAHP amplitude on application of ryanodine (Gant et al. 2006; Kumar and Foster 2004) and nifedipine (Disterhoft et al. 2004; Power et al. 2002) respectively.

## DISCUSSION

The results demonstrate a link between the age-related increase in the sAHP and redox state, through the release of $Ca^{2+}$ from ICS. A shift in $Ca^{2+}$ regulation and altered $Ca^{2+}$ channel function is a characteristic of aging CA1 neurons (Burke and Barnes 2010; Foster 2007, 1999; Gant et al. 2006; Hemond and Jaffe 2005; Kumar et al. 2009; Landfield and Pitler 1984; Magnusson et al. 2010; Oh et al. 2010; Thibault et al. 2001; Thibault and Landfield 1996). Recently, we demonstrated that DTT could reverse an age-related decrease in NMDA receptor function in region CA1 (Bodhinathan et al. 2010). In the current study, the reducing agent, DTT, decreased the sAHP in aged, but not in young CA1 neurons. The data are consistent with the altered redox buffering in aged animals as a mechanism contributing to $Ca^{2+}$ dysregulation and electrophysiological changes observed in aged neurons.

Redox modulation has been observed for several ion channels including $K^+$ and $Ca^{2+}$ channels (Chiamvimonvat et al. 1995; DiChiara and Reinhart 1997; Hidalgo et al. 2004; Ruppersberg et al. 1991; Stephens et al. 1996), which could contribute to the sAHP. The identity of the $K^+$ channel that underlies the sAHP is unknown (Furuichi et al. 1994; Sah and Faber 2002); however, the amplitude to the sAHP is reduced by activation of Ser/Thr kinases, including PKA (Madison and Nicoll 1986; Pedarzani and Storm 1993), CaMKII (Muller et al. 1992), and PKC (Malenka et al. 1986). In the current study, the broad spectrum Ser/Thr kinase inhibitor H-7 had no influence on the DTT-mediated decrease in aged-sAHP, indicating that the reduction was not mediated through kinase activity.

In the case of $K^+$ channels, previous reports indicate that cysteine specific oxidation decreases BK channel activity (Tang et al. 2001; Tang et al. 2004), and that the reducing agent

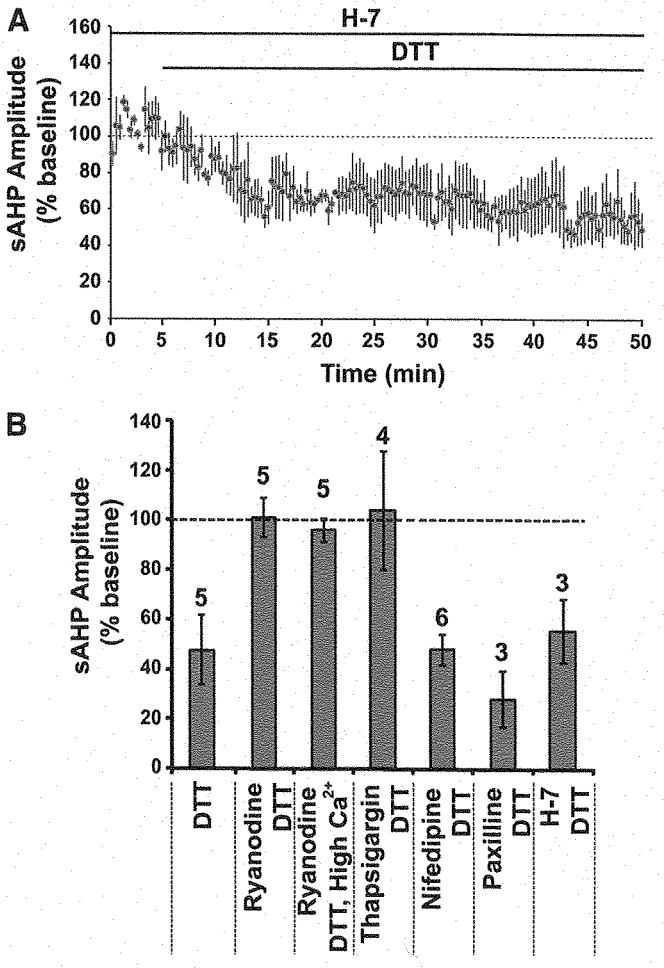


FIG. 8. Ser/Thr kinase activity does not mediate DTT effects on aged-sAHP. (*A*) Time course of the change in the normalized sAHP amplitude in the aged animals that were incubated with the broad spectrum Ser/Thr kinase inhibitor H-7 ($n = 3$) for ≥60 min prior to DTT application. (*B*) Summary diagram representing the mean percent change in the sAHP amplitude of aged neurons following DTT application under various conditions (*filled bars*). In each case, the response represents the percent change relative to the preDTT application baseline (dashed line). The numbers above each bar represents the number of neurons recorded in each condition.

DTT increases BK channel activity (DiChiara and Reinhart 1997). The BK channels are involved in repolarization of action potential, and an increase in BK channel activity will reduce the width of the action potential (Shao et al. 1999). Moreover, a decrease in the spike width can decrease the sAHP, by limiting the duration of depolarization-induced $Ca^{2+}$ entry through L-type VGCCs (Giese et al. 1998; Murphy et al. 2004). Thus DTT could be acting on the BK channels to decrease L-type VGCC activity and the sAHP amplitude. However, several pieces of evidence suggest that this might not be the case. First, blockade of BK channels with paxilline did not block the DTT-mediated decrease in aged-sAHP. Second, blockade of VGCC's with nifedipine did not influence the DTT-mediated decrease in aged-sAHP. Finally, the fast AHP, which is mediated by the BK channel, is not altered with age (Matthews et al. 2009).

The amplitude of the sAHP is dependent on the level of cytosolic $Ca^{2+}$. L-type VGCCs play a role in determining the amplitude of the sAHP (Landfield and Pitler 1984; Moyer et al. 1992; Norris et al. 1998) and contribute to the increase in the sAHP during aging (Thibault and Landfield 1996; Veng and Browning 2002). However, it does not appear that the DTT-mediated reduction in the aged-sAHP is acting through L-channels. The DTT-mediated reduction in the sAHP was larger than that observed for L-channel blockade, and was specific to aged animals. Previous research indicates that the decrease in the sAHP following blockade of L-channels is quantitatively larger in aged animals; however, the percent decrease (~30%) is similar across ages, suggesting other mechanisms contribute to the age-related increase in the sAHP amplitude in aged animals (Disterhoft et al. 2004; Power et al. 2002). In the present study, blockade of the L-channel reduced the aged-sAHP ~30%, consistent with previous reports (Norris et al. 1998; Power et al. 2002). Regardless of L-channel function, DTT reduced the aged-sAHP by ~50% and the effect of DTT was specific to aged animals. The results suggest that DTT is acting on mechanisms other than the L-channel, which may mediate the age-related increase in the sAHP.

### *RyR and redox state dependent effects on sAHP*

Release of $Ca^{2+}$ from ICS through RyR activation, plays a role in determining the sAHP amplitude (Borde et al. 2000; Davies et al. 1996; Sah and McLachlan 1991; Usachev et al. 1993; van de Vrede et al. 2007) and $Ca^{2+}$ from ICS contributes to altered physiology during aging (Gant et al. 2006; Kumar and Foster 2004, 2005). In addition, the RyRs are highly redox sensitive (Bull et al. 2008), such that oxidation of the cysteine residues increases the $Ca^{2+}$ sensitivity and activity of RyR (Eager and Dulhunty 1998; Hidalgo et al. 2004; Huddleston et al. 2008). In the present study, the DTT-mediated decrease in the sAHP was blocked on depletion of ICS by thapsigargin or blockade of RyRs by ryanodine, indicating the involvement of ICS and RyRs in the decreased $Ca^{2+}$ mobilization by DTT application. Together, the results suggest that the increase in the sAHP in aged neurons is related to redox sensitive $Ca^{2+}$ mobilization from the ICS through the RyRs.

Treatments that modify intracellular redox state may provide a novel therapeutic strategy to restore $Ca^{2+}$ homeostasis in the aged neurons. Interestingly, a learning mediated decrease in the sAHP is observed in aged memory-unimpaired rats (Matthews et al. 2009; Moyer et al. 2000; Murphy et al. 2006; Tombaugh et al. 2005). Future research should include an examination of a learning induced shift in redox state (Shvets-Teneta-Gurii et al. 2007) as a possible mechanism mediating the decrease in the sAHP of memory unimpaired animals.

## GRANTS

This work was supported by, the Evelyn F. McKnight Brain Research Foundation, National Institutes of Health Grant AG014979 and MH059891 to TCF, a UF Alumni fellowship to K. Bodhinathan.

## DISCLOSURES

No conflicts of interest, financial or otherwise, are declared by the author(s).

## REFERENCES

**Bodhinathan K, Kumar A, Foster TC.** Intracellular redox state alters NMDA receptor response during aging through $Ca^{2+}$/calmodulin-dependent protein kinase II. *J Neurosci* 30: 1914–1924, 2010.

**Borde M, Bonansco C, Fernandez de Sevilla D, Le Ray D, Buno W.** Voltage-clamp analysis of the potentiation of the slow $Ca^{2+}$-activated $K^+$ current in hippocampal pyramidal neurons. *Hippocampus* 10: 198–206, 2000.

**Bull R, Finkelstein JP, Galvez J, Sanchez G, Donoso P, Behrens MI, Hidalgo C.** Ischemia enhances activation by $Ca^{2+}$ and redox modification of ryanodine receptor channels from rat brain cortex. *J Neurosci* 28: 9463–9472, 2008.

**Burke SN, Barnes CA.** Senescent synapses and hippocampal circuit dynamics. *Trends Neurosci* 33: 153–161, 2010.

**Chiamvimonvat N, O'Rourke B, Kamp TJ, Kallen RG, Hofmann F, Flockerzi V, Marban E.** Functional consequences of sulfhydryl modification in the pore-forming subunits of cardiovascular $Ca^{2+}$ and $Na^+$ channels. *Circ Res* 76: 325–334, 1995.

**Danila CI, Hamilton SL.** Phosphorylation of ryanodine receptors. *Biol Res* 37: 521–525, 2004.

**Davies PJ, Ireland DR, McLachlan EM.** Sources of $Ca^{2+}$ for different Ca(2+)-activated $K^+$ conductances in neurones of the rat superior cervical ganglion. *J Physiol* 495( Pt 2):353–366, 1996.

**DiChiara TJ, Reinhart PH.** Redox modulation of hslo $Ca^{2+}$-activated $K^+$ channels. *J Neurosci* 17: 4942–4955, 1997.

**Disterhoft JF, Thompson LT, Moyer JR, Jr, Mogul DJ.** Calcium-dependent afterhyperpolarization and learning in young and aging hippocampus. *Life Sci* 59: 413–420, 1996.

**Disterhoft JF, Wu WW, Ohno M.** Biophysical alterations of hippocampal pyramidal neurons in learning, ageing and Alzheimer's disease. *Ageing Res Rev* 3: 383–406, 2004.

**Eager KR, Dulhunty AF.** Activation of the cardiac ryanodine receptor by sulfhydryl oxidation is modified by $Mg^{2+}$ and ATP. *J Membr Biol* 163: 9–18, 1998.

**Foster TC.** Calcium homeostasis and modulation of synaptic plasticity in the aged brain. *Aging Cell* 6: 319–325, 2007.

**Foster TC.** Involvement of hippocampal synaptic plasticity in age-related memory decline. *Brain Res Brain Res Rev* 30: 236–249, 1999.

**Furuichi T, Kohda K, Miyawaki A, Mikoshiba K.** Intracellular channels. *Curr Opin Neurobiol* 4: 294–303, 1994.

**Gant JC, Sama MM, Landfield PW, Thibault O.** Early and simultaneous emergence of multiple hippocampal biomarkers of aging is mediated by $Ca^{2+}$-induced $Ca^{2+}$ release. *J Neurosci* 26: 3482–3490, 2006.

**Giese KP, Storm JF, Reuter D, Fedorov NB, Shao LR, Leicher T, Pongs O, Silva AJ.** Reduced $K^+$ channel inactivation, spike broadening, and after-hyperpolarization in Kvbeta1.1-deficient mice with impaired learning. *Learn Mem* 5: 257–273, 1998.

**Hemond P, Jaffe DB.** Caloric restriction prevents aging-associated changes in spike-mediated $Ca^{2+}$ accumulation and the slow afterhyperpolarization in hippocampal CA1 pyramidal neurons. *Neuroscience* 135: 413–420, 2005.

**Hidalgo C, Bull R, Behrens MI, Donoso P.** Redox regulation of RyR-mediated $Ca^{2+}$ release in muscle and neurons. *Biol Res* 37: 539–552, 2004.

**Huddleston AT, Tang W, Takeshima H, Hamilton SL, Klann E.** Superoxide-induced potentiation in the hippocampus requires activation of ryanodine receptor type 3 and ERK. *J Neurophysiol* 99: 1565–1571, 2008.

**Kumar A, Bodhinathan K, Foster TC.** Susceptibility to calcium dysregulation during brain aging. *Frontiers in Aging Neuroscience* 1: 1–13, 2009.

**Kumar A, Foster T.** Environmental enrichment decreases the afterhyperpolarization in senescent rats. *Brain Res* 1130: 103–107, 2007.

**Kumar A, Foster TC.** 17beta-estradiol benzoate decreases the AHP amplitude in CA1 pyramidal neurons. *J Neurophysiol* 88: 621–626, 2002.

**Kumar A, Foster TC.** Enhanced long-term potentiation during aging is masked by processes involving intracellular calcium stores. *J Neurophysiol* 91: 2437–2444, 2004.

**Kumar A, Foster TC.** Intracellular calcium stores contribute to increased susceptibility to LTD induction during aging. *Brain Res* 1031: 125–128, 2005.

**Landfield PW, Pitler TA.** Prolonged $Ca^{2+}$-dependent afterhyperpolarizations in hippocampal neurons of aged rats. *Science* 226: 1089–1092, 1984.

**Madison DV, Nicoll RA.** Actions of noradrenaline recorded intracellularly in rat hippocampal CA1 pyramidal neurones, in vitro. *J Physiol* 372: 221–244, 1986.

**Magnusson KR, Brim BL, Das SR.** Selective vulnerabilities of N-methyl-D-aspartate (NMDA) receptors during brain aging. *Frontiers in Aging Neuroscience* 2: 1–15, 2010.

**Malenka RC, Madison DV, Andrade R, Nicoll RA.** Phorbol esters mimic some cholinergic actions in hippocampal pyramidal neurons. *J Neurosci* 6: 475–480, 1986.

**Matthews EA, Linardakis JM, Disterhoft JF.** The fast and slow afterhyperpolarizations are differentially modulated in hippocampal neurons by aging and learning. *J Neurosci* 29: 4750–4755, 2009.

**Melyan Z, Wheal HV, Lancaster B.** Metabotropic-mediated kainate receptor regulation of IsAHP and excitability in pyramidal cells. *Neuron* 34: 107–114, 2002.

**Morimoto S, J OU, Kawai M, Hoshina T, Kusakari Y, Komukai K, Sasaki H, Hongo K, Kurihara S.** Protein kinase A-dependent phosphorylation of ryanodine receptors increases $Ca^{2+}$ leak in mouse heart. *Biochem Biophys Res Commun* 390: 87–92, 2009.

**Moyer JR, Jr, Power JM, Thompson LT, Disterhoft JF.** Increased excitability of aged rabbit CA1 neurons after trace eyeblink conditioning. *J Neurosci* 20: 5476–5482, 2000.

**Moyer JR, Jr, Thompson LT, Black JP, Disterhoft JF.** Nimodipine increases excitability of rabbit CA1 pyramidal neurons in an age- and concentration-dependent manner. *J Neurophysiol* 68: 2100–2109, 1992.

**Muller W, Petrozzino JJ, Griffith LC, Danho W, Connor JA.** Specific involvement of Ca(2+)-calmodulin kinase II in cholinergic modulation of neuronal responsiveness. *J Neurophysiol* 68: 2264–2269, 1992.

**Murphy GG, Fedorov NB, Giese KP, Ohno M, Friedman E, Chen R, Silva AJ.** Increased neuronal excitability, synaptic plasticity, and learning in aged Kvbeta1.1 knockout mice. *Curr Biol* 14: 1907–1915, 2004.

**Murphy GG, Rahnama NP, Silva AJ.** Investigation of age-related cognitive decline using mice as a model system: behavioral correlates. *Am J Geriatr Psychiatry* 14: 1004–1011, 2006.

**Norris CM, Halpain S, Foster TC.** Reversal of age-related alterations in synaptic plasticity by blockade of L-type $Ca^{2+}$ channels. *J Neurosci* 18: 3171–3179, 1998.

**Oh MM, Oliveira FA, Disterhoft JF.** Learning and aging related changes in intrinsic neuronal excitability. *Frontiers in Aging Neuroscience* 2: 1–10, 2010.

**Parihar MS, Kunz EA, Brewer GJ.** Age-related decreases in NAD(P)H and glutathione cause redox declines before ATP loss during glutamate treatment of hippocampal neurons. *J Neurosci Res* 86: 2339–2352, 2008.

**Pedarzani P, Storm JF.** PKA mediates the effects of monoamine transmitters on the $K^+$ current underlying the slow spike frequency adaptation in hippocampal neurons. *Neuron* 11: 1023–1035, 1993.

**Power JM, Oh MM, Disterhoft JF.** Metrifonate decreases sI(AHP) in CA1 pyramidal neurons in vitro. *J Neurophysiol* 85: 319–322, 2001.

**Power JM, Wu WW, Sametsky E, Oh MM, Disterhoft JF.** Age-related enhancement of the slow outward calcium-activated potassium current in hippocampal CA1 pyramidal neurons in vitro. *J Neurosci* 22: 7234–7243, 2002.

**Ruppersberg JP, Stocker M, Pongs O, Heinemann SH, Frank R, Koenen M.** Regulation of fast inactivation of cloned mammalian IK(A) channels by cysteine oxidation. *Nature* 352: 711–714, 1991.

**Sah P, Faber ES.** Channels underlying neuronal calcium-activated potassium currents. *Prog Neurobiol* 66: 345–353, 2002.

**Sah P, McLachlan EM.** Ca(2+)-activated $K^+$ currents underlying the afterhyperpolarization in guinea pig vagal neurons: a role for Ca(2+)-activated $Ca^{2+}$ release. *Neuron* 7: 257–264, 1991.

**Sanchez M, McManus OB.** Paxilline inhibition of the alpha-subunit of the high-conductance calcium-activated potassium channel. *Neuropharmacology* 35: 963–968, 1996.

**Shao LR, Halvorsrud R, Borg-Graham L, Storm JF.** The role of BK-type $Ca^{2+}$-dependent $K^+$ channels in spike broadening during repetitive firing in rat hippocampal pyramidal cells. *J Physiol 521 Pt* 1: 135–146, 1999.

**Shvets-Teneta-Gurii TB, Troshin GI, Dubinin AG.** Local changes in the redox potential in the rabbit cerebral cortex accompanying the acquisition of a conditioned defensive reflex. *Neurosci Behav Physiol* 37: 481–487, 2007.

**Stephens GJ, Owen DG, Robertson B.** Cysteine-modifying reagents alter the gating of the rat cloned potassium channel Kv1.4. *Pfluegers* 431: 435–442, 1996.

**Tang XD, Daggett H, Hanner M, Garcia ML, McManus OB, Brot N, Weissbach H, Heinemann SH, Hoshi T.** Oxidative regulation of large conductance calcium-activated potassium channels. *J Gen Physiol* 117: 253–274, 2001.

**Tang XD, Garcia ML, Heinemann SH, Hoshi T.** Reactive oxygen species impair Slo1 BK channel function by altering cysteine-mediated calcium sensing. *Nat Struct Mol Biol* 11: 171–178, 2004.

**Thibault O, Gant JC, Landfield PW.** Expansion of the calcium hypothesis of brain aging and Alzheimer's disease: minding the store. *Aging Cell* 6: 307–317, 2007.

**Thibault O, Hadley R, Landfield PW.** Elevated postsynaptic $[Ca^{2+}]i$ and L-type calcium channel activity in aged hippocampal neurons: relationship to impaired synaptic plasticity. *J Neurosci* 21: 9744–9756, 2001.

**Thibault O, Landfield PW.** Increase in single L-type calcium channels in hippocampal neurons during aging. *Science* 272: 1017–1020, 1996.

**Tombaugh GC, Rowe WB, Rose GM.** The slow afterhyperpolarization in hippocampal CA1 neurons covaries with spatial learning ability in aged Fisher 344 rats. *J Neurosci* 25: 2609–2616, 2005.

**Usachev Y, Shmigol A, Pronchuk N, Kostyuk P, Verkhratsky A.** Caffeine-induced calcium release from internal stores in cultured rat sensory neurons. *Neuroscience* 57: 845–859, 1993.

**van de Vrede Y, Fossier P, Baux G, Joels M, Chameau P.** Control of IsAHP in mouse hippocampus CA1 pyramidal neurons by RyR3-mediated calcium-induced calcium release. *Pfluegers* 455: 297–308, 2007.

**Veng LM, Browning MD.** Regionally selective alterations in expression of the alpha(1D) subunit (Ca(v)1.3) of L-type calcium channels in the hippocampus of aged rats. *Brain Res Mol Brain Res* 107: 120–127, 2002.

**Xiao B, Tian X, Xie W, Jones PP, Cai S, Wang X, Jiang D, Kong H, Zhang L, Chen K, Walsh MP, Cheng H, Chen SR.** Functional consequence of protein kinase A-dependent phosphorylation of the cardiac ryanodine receptor: sensitization of store overload-induced $Ca^{2+}$ release. *J Biol Chem* 282: 30256–30264, 2007.

**Yoshida A, Ogura A, Imagawa T, Shigekawa M, Takahashi M.** Cyclic AMP-dependent phosphorylation of the rat brain ryanodine receptor. *J Neurosci* 12: 1094–1100, 1992.

# CONTACT INFORMATION

**David S. Guzick, M.D.**
Senior Vice President for Health Affairs
President, UF&Shands Health System
PO Box 100014
Gainesville, FL 32610-0014
352-733-1700

**Michael L. Good, M.D.**
Dean, College of Medicine
University of Florida
PO Box 100215
Gainesville, FL 32610-0215
352-273-7500

**Tetsuo Ashizawa, M.D.**
Executive Director, McKnight Brain Institute
Chairman & The Melvin Greer Professor of Neurology
Department of Neurology, UF College of Medicine
100 S. Newell Drive, Room L3-100
PO Box 100236
Gainesville, FL 32610-0236
352-273-5550

**Marco Pahor, M.D.**
Professor and Chair, Department of Aging and Geriatric Research
Director, Institute on Aging
1329 SW 16th Street, Room 5263
PO Box 100107
Gainesville, FL 32610-0107
352-265-7227

**Thomas C. Foster, Ph.D.**
Professor of Neuroscience
McKnight Chair for Research on Aging and Memory
Investigator, McKnight Brain Institute
PO Box 100244
Gainesville, FL 32610-0244
352-392-4359

**Mary Ann Kiely**
Associate Vice President for Development, UFHSC
Vice President for Development, Shands HealthCare
PO Box 100014
Gainesville, FL 32610-0014
352-273-9620